UNIVERSITAT DE BARCELONA

Metal catalysed asymmetric C–C bond forming reactions

Oriol Galeote Martin

UNIVERSITAT DE BARCELONA

Metal catalysed C–C bond forming reactions

Oriol Galeote Martin

Programa de Doctorat de Química Orgànica

Metal catalysed C–C bond forming reactions

Oriol Galeote Martin

Supervised by

Prof. Pedro Romea García

Prof. Fèlix Urpí Tubella

Secció de Química Orgànica

Departament de Química Inorgànica i Química Orgànica

Facultat de Química

Universitat de Barcelona

UNIVERSITAT DE BARCELONA

This thesis was performed from February 2021 to September 2024 in the section of Organic Chemistry of the Department of Inorganic and Organic Chemistry of the University of Barcelona. The work has been carried out with the financial support of the “Ministerio de Ciencia e Innovación (Projects PID2021-126251NB-I00 and PGC2018- 093863-B-C21) and with the support of “ajuts per a la contractació de personal investigador predoctoral en formació” (FI 2021) fellowship.

Acknowledgments

Agrair als meus tutors Fèlix i Pere per donar-me l'oportunitat de realitzar aquesta tesi. Durant tot aquest temps he sentit que he tingut la llibertat d'escollir la recerca que fèiem i alhora sempre heu estat disposats a ajudar en qualsevol moment, he tingut la sort de tenir uns grans tutors de Tesi dels que he pogut aprendre molt.

Gracias a toda mi familia, especialmente a mis yayos, Joaquin y Piedad, por todo lo que habéis hecho por mí, durante todo este tiempo y por cuidar tanto de mí. También a mi madre y a mi hermana, Montse y Ana, os aprecio mucho a todos y he conseguido llegar hasta aquí gracias a vosotros.

Δgradecer a Clara, una persona genial que siempre ha estado a mi lado apoyándome en todo, siempre atenta a cualquier cosa que necesitara, y espero que siempre sea así. Desde que te conozco siempre has sido uno de los pilares más importantes de mi vida y sé que eso no va a cambiar. Nunca olvides lo genial que eres y espero estar siempre a tu lado.

Agradecer también a Araceli, una persona que siempre me ha apoyado en todo lo que he necesitado, y que cualquier cosa que me pasa siempre ha estado ahí. Eres un gran pilar en mi vida y eres una gran persona y una gran química, llegarás tan lejos como te propongas.

Gracias a todos mis amigos, Rubén, Jose, Arnau (Δ), Sara, Alba. Muchas gracias por todos los momentos que hemos pasado juntos, antes y durante el PhD. I los que aún quedan. Habéis sido un gran soporte y estoy muy orgulloso de tener unos amigos tan buenos como vosotros. Agradecer también a mis amigos y compañeros, Isaac, Iván, Aleix y Pol, por todos los momentos que hemos pasado juntos. También un agradecimiento a Sergi por las tardes que hemos pasado. Agradecer también a Gara i Daiana, que pese a todo fueron un gran pilar durante gran parte de mi tesis.

I want to thank all people I have met in Mülheim and that helped me during my stay. I want to start with Prof. Benjamin List, for the great opportunity given to me to work in his group, a great person who made me feel like home and part of the group from the first moment, always open to everybody, I have learnt a lot from you. Another special

mention for Benni, one of the best persons I've ever met and a great chemist, I'm sure you will reach whatever you propose. Thank you for all the people I've met, Jan, Niski, Markus, Bruni, Mathias, Manuel, Luc, Wencke, Chandra and all the team. These months were a beautiful period that I will never forget. Una menció especial per Marian, que vas ajudarme molt en els moments que tenia més dubtes. A special mention to Alexandra, who was crucial managing my German landlords.

I want to thank also all my international students that helped me in the projects, Lena and Vanessa for its hard work and great order, and to Evan for all the moments we spent together, including the vermouths, the Newcastle games or the trips to the immigration office. I have seen you grow a lot as a chemist and I am very proud of you. A special mention to Luke, who did not work in my projects directly, but he has support me a lot, always open to learn and share his knowledge with a big smile, I hope the best for you!

A Gabriela por su gran esfuerzo durante su TFM, contribuyendo a una de las partes más complicadas del proyecto. No solo encontré una muy buena química sino una gran amiga. ¡Estoy seguro de que todo te irá genial!

A todos los que han pasado por FUT. A Stuart por ser mi mentor desde el principio, he aprendido mucho de ti. A Marina por su constante alegría. A Miquel un gran compañero siempre dispuesto a ayudar, y crear conciertos en el laboratorio! A Edu por todos los momentos compartidos, las conversaciones de química y los consejos. Hemos pasado muchos momentos juntos y se que te irá muy bien! A Xènia por ser una persona muy abierta y agradable desde el principio, con una motivación extraordinaria. Te irá muy bien todo! A Joan, que aunque breve me ha hecho pasar grandes momentos en el lab (y en su twitter). Una mención especial a Elias, que aunque no pudiste seguir el tiempo que pasamos fue genial! Y finalmente a todos los que han ido pasando por FUT durante estos años. Mención especial a Toñi por todas las mañanas que nos encontrábamos en el lab.

En definitiva, agradecer a todos aquellos que han pasado por mi vida durante estos años, ha sido un periodo muy importante para mí y me habéis ayudado a crecer y avanzar.

You won’t enjoy cava anymore when you return to Barcelona.

Benjamin List

Science is the progressive approach of mankind to the real world.

Max Planck

GENERAL INTRODUCTION

Table of contents

1 Organic synthesis

"Chemical synthesis always has some elements of planning in it. But, the planning should never be too rigid. Because, in fact, the specific objective which the synthetic chemist uses as the excuse for his activity is often not of special importance in the general sense; rather, the important things are those that he finds out in the course of attempting to reach his objective." R. B. Woodward

These words are credited to the Nobel laureate R. B. Woodward, which summarize the symbiotic nature between the development of organic chemistry and the aspiration of chemists to synthesize increasingly more intricate molecules. The origins of organic synthesis can be traced back to Wöhler's urea synthesis in 1828.[1] Since that milestone, a plethora of novel transformations have emerged, furnishing chemists with a wide array of tools to synthesize complex molecules whilst enhancing the efficiency of such processes.

The advances achieved by synthetic chemists have elevated total synthesis to the forefront of 21st-century natural sciences, serving as a seed for the development of various disciplines (Figure 1). The ability to synthesize new molecules efficiently has played a pivotal role in uncovering new biological phenomena, such as biochemical pathways and the elucidation of the structures of natural products. Additionally, it has significantly impacted industry by facilitating the development of numerous medicines, nutritional products, cosmetics, and has even emerged as a new field in materials science.

Indeed, the journey of discovery in organic chemistry is far from over, and there is still much ground to be covered. Nowadays, the improved reaction efficiency through catalytic transformations, the development of asymmetric methods, and pioneering more environmentally friendly green chemical transformations are in the forefront of organic chemistry. By pushing the boundaries of knowledge and innovation in these areas, organic synthesis continues to play a crucial role in shaping the future of science and technology.

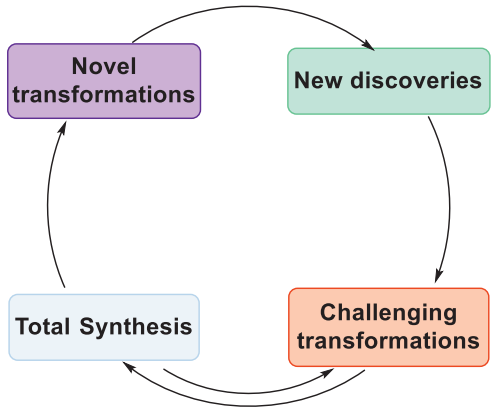

Figure 1. Cooperative relation between different areas.

2 Chirality

Chirality is defined by the impossibility of superimposing the mirror image of a certain object onto itself. This idea extends to the realm of chemistry, wherein a molecule is considered chiral if it can be distinguished from its mirror image. Lord Kelvin stated in 1893 a definition for chirality that it is still used in our days: "I call any geometrical figure, or group of points, 'chiral', and say that it has chirality if its image in a plane mirror, ideally realized, cannot be brought to coincide with itself."[2]

A chiral molecule and its mirror image are termed enantiomers, possessing the same physical properties aside from the optical rotation of polarized light. This rotation occurs in opposite directions for each enantiomer, a phenomenon initially observed by Biot in 1832.[3] Years later, in 1848, Louis Pasteur achieved the resolution of tartaric acid enantiomers by manually separating its chiral crystals.[4]

Enantiopure compounds hold a prominent position across various fields, with particular emphasis on biological systems. All known biological systems are formed by a large amount of homochiral molecules such as the series of *D*-sugars or *L*-amino acids amongst a large variety of chiral unrelated compounds. The origin of homochirality in all living organisms remains elusive, yet it plays a pivotal role in molecular recognition across diverse biological mechanisms, typically rendering only one enantiomer biologically valuable.

In the pharmaceutical market, approximately 50% of medicines are chiral and half of them are administered as enantiopure compounds. The

utilization of chiral drugs in its racemic form presents a plethora of disadvantages.[5,6] Typically, the two enantiomers present different roles within the organism and can act completely different. For instance, *L*-Dopa proves to be a powerful treatment for Parkinson disease, while its *D*-counterpart is toxic and causes agranulocytosis. Another case in point is the application of (*S,S*)-ethambutol treatment of tuberculosis, where its *meso* form (*R,S*)-ethambutol and the enantiomer (*R,R*)-ethambutol can lead to optic neuritis, potentially resulting in blindness. Additionally, a prominent effect is observed in (*S*)-methamphetamine which is often used as a recreational drug while its enantiomer (*R*)-methamphetamine is used as an active ingredient of some nasal decongestant (Figure 2).[7]

Other pair of enantiomers exhibit similar effects, but usually one enantiomer is more potent than the other one, even resulting in the ineffectiveness of the second. Although the administration of such drugs as a racemic mixture is usually considered safe, it remains undesirable for two reasons. Firstly, the less potent enantiomer provokes the necessity of increasing the overall dose to achieve the same effect. Secondly, the administration of an enantiopure compound may result in fewer side effects due to the removal of those associated with the less potent enantiomer.

Therefore, the enantioselective synthesis of the active enantiomer always represents a remarkable improvement, and the change from the administration of a racemic mixture to its enantiopure form is commonly referred as a chiral switch.[8] A case in point is observed with the racemic mixture citalopram, an antidepressant drug, and escitalopram which constitutes the pure and more potent (*S*)-enantiomer. Another widely used drug that adheres to this principle is esomeprazole, the (*S*)-enantiomer of omeprazole, which is employed to reduce stomach acidity by inhibiting the proton pump. (Figure 2).

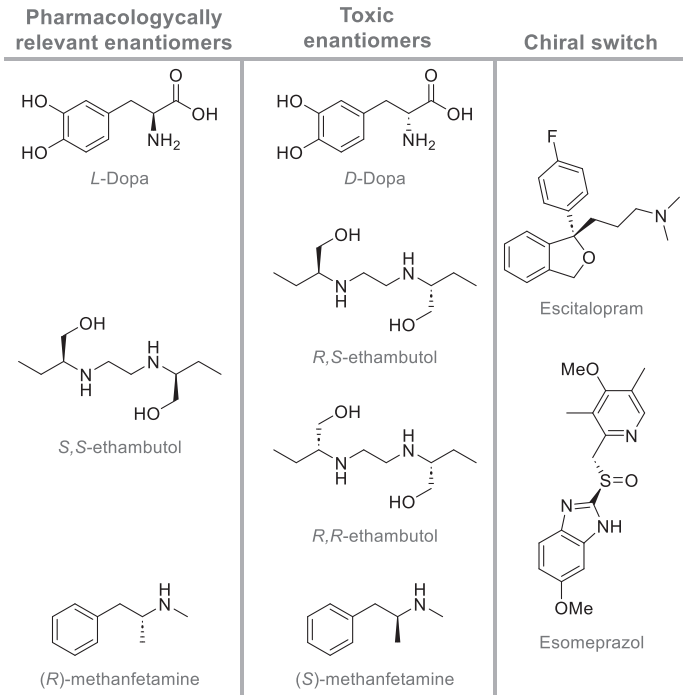

Figure 2. Enantiomers of different drugs.

In this context, the development of new methodologies enabling the stereocontrolled construction of new chiral elements represents a key challenge for organic synthesis, which serves as a pivotal instrument to gain access to novel types of molecules thereby facilitating the development of the aforementioned applications. Over the last decades, asymmetric catalysis has emerged as the most effective and sustainable tool to address such challenges.

3 Asymmetric catalysis

Traditionally, methods based on chiral resolutions or chiral auxiliaries were the most commonly employed for the asymmetric synthesis of chiral compounds. [9-16] Despite their importance and their high current value, the introduction of *atom economy* concept by Trost [17,18] represented a paradigm shift in organic synthesis. This simply states that an efficient transformation implies that most atoms in the starting materials have to be part of the resultant product, and the other reagents ideally should be used only in catalytic amounts, which encouraged to carry out chemical transformation under catalytic conditions.

Since then, organic chemists strive to develop asymmetric reactions under catalytic conditions, whether using enzymes (biocatalysis), organocatalysts, or metal catalysts.

3.1 Biocatalysis

The use of enzymes in asymmetric synthesis is commonly referred as biocatalysis. As early as 1894, Emil Fischer proposed the lock and key model, in which he already recognized that enzymes were chiral compounds, and as such, they can effectively differentiate between prochiral elements to generate chiral compounds in an enantioselective manner. [19,20]

Since then, enzymes have been widely used in catalytic transformations, due to their low toxicity, environmentally friendly conditions and remarkable selectivities.[21-24] Indeed, enzymes serve as highly specific catalysts, minimizing the formation of byproducts and leading to high yields in most cases.

While very powerful, biocatalytic approaches to asymmetric synthesis faces several challenges. A primarily issue lies in the specificity of most enzymes to their natural substrates. While this is very useful to perform reactions simultaneously, it is a drawback to devise widely applicable methods. Furthermore, they are usually unable to deliver the complementary enantiomer, since the enzyme with the opposite configuration is not accessible. Finally, the strictly narrow conditions that enzymes require, such as the use of water as solvent and its incompatibility to most organic solvents, a very narrow margin of temperatures and pH to be active, or the need for certain cofactors that act as "biological reagents" such as NADP, ATP or thiamine phosphates restrict their use in large scale processes.

Directed evolution has emerged as a solution to some of these problems, which consist of mimicking nature to obtain the desired enzyme with modifications that improve its performance by human selection. In this approach, the desired gene to code an enzyme is subjected to a mutagenic process in which a library of genes is formed. Then, these resultant genes are expressed in the corresponding modified enzymes which are screened in the objective reaction. The most successful variants are isolated, and the cycle is repeated. By repeating this cycle, a variant with much better efficiency than the wild-type one can be obtained, with the desired variants that were being sought in a fast process (Figure 3).

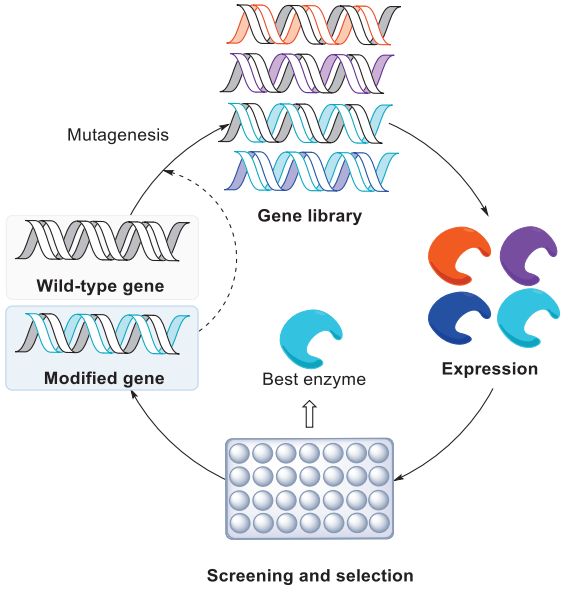

Figure 3. Directed evolution.

An example of an asymmetric biocatalytic transformation improved by directed evolution used on an industrial scale is the Baeyer-Villiger Monooxygenase CDX-003 (Scheme 1).[25,26] In this approach the BVMO enantioselectively oxidizes the sulphide to the corresponding sulfoxide, generating esomeprazole, a drug widely used to reduce stomach acid. The ketoreductase CDX-019 alongside with isopropanol allows the recovery of NADP cofactor, which is used in tiny amounts (Chem rev 2018, 118, 1-3). CDX-003, the desired variant, was developed after 41 mutations respect to the wild-type, which initially yielded the undesired isomer (*R*)-omeprazole in a 70% *ee*.

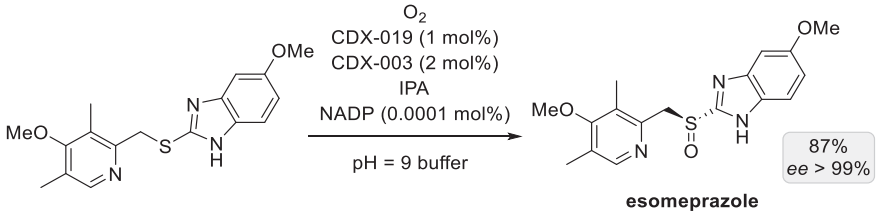

Scheme 1. Biocatalytic synthesis of esomeprazole.

3.2 Organocatalysis

Biocatalysis alongside with metal catalysed reactions, which will be covered in the next section, were the only transformations to create new asymmetric reactions until few decades ago. A new type of catalysis, known as organocatalysis, emerged in 2000. This type of catalysis takes advantage of the catalytic properties of small organic molecules without the need for complementary metals to trigger highly stereocontrolled transformations, thereby rendering enantiopure compounds. [27–31]

David MacMillan and Benjamin List were awarded the Nobel Prize in Chemistry 2021 "for the development of asymmetric organocatalysis" which started independently by two seminal contributions. [32,33]

Indeed, MacMillan reported the asymmetric Diels-Alder reaction of α,β-unsaturated aldehydes with dienes catalysed by a chiral imidazolidinone to obtain the *endo* adducts with a remarkable enantiomeric excess (Scheme 2).

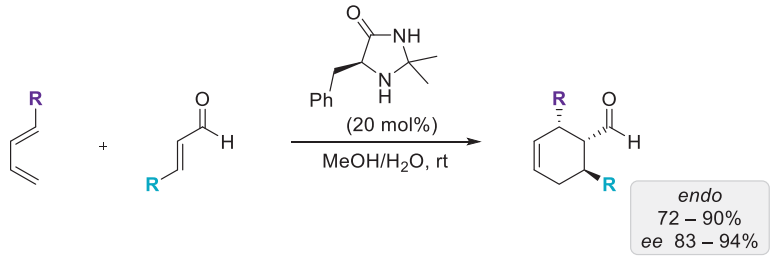

Scheme 2. Organocatalysed Diels-Alder reaction.

In parallel, Benjamin List disclosed the direct and asymmetric aldol reaction between acetone and aldehydes catalysed by the simple natural α-amino acid *L*-proline (Scheme 3). This methodology hinges on the double functionality of proline, that provides both the nucleophilic amino group and the acid-base functionality to act as a cocatalyst.

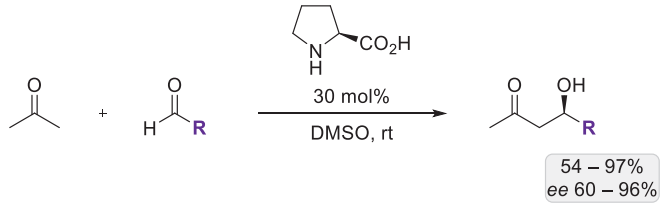

Scheme 3. Proline-catalysed aldol reaction.

Organocatalysis is nowadays a mature technology that has already reached industrial processes. A case in point is the industrial synthesis of Darunavir, an antiretroviral for the treatment of HIV that was approved by the

FDA in 2006. A key step of this synthetic sequence consists of a *L*-proline catalysed cross aldol reaction, which yields the required intermediate as a 80:20 diastereomeric mixture and 99% enantiomeric excess. An alternative route uses diphenylprolinol to give the aldol adduct in a 94:6 diastereomeric ratio and 99% enantiomeric excess. These two intermediates are further transformed into the final product darunavir (Scheme 4). [34,35]

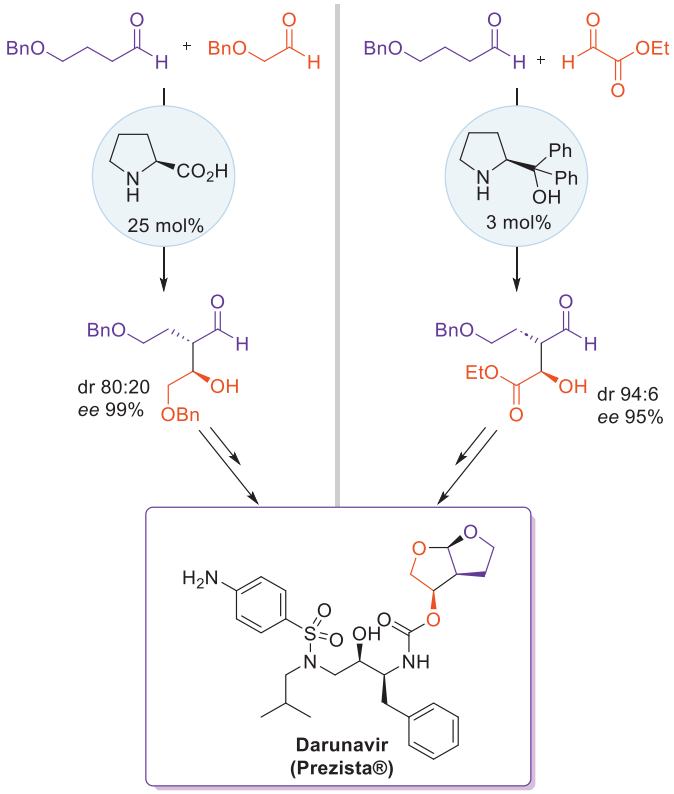

Scheme 4. Organocatalytic industrial-scale synthesis of darunavir.

3.3 Metal catalysis

The use of chiral metal complexes represents the third approach in asymmetric catalysis. As its name suggests, this takes advantage of the chemical activity of complexes coupled to the metal centre, the key reading element, and chiral small organic molecules or ligands, which provide suitable environment around the metal necessary to discriminate the pathway leading to a particular enantiomer.

The 2001 Nobel Prize of Chemistry was awarded to Knowles, Noyori and Sharpless for "their work on chirally catalysed hydrogenation and oxidation reactions". [36–39]

One of the first breakthroughs in this field was made by Knowles. In 1968, he developed an enantioselective hydrogenation method using a monodentate phosphine, which initially yielded low enantiomeric excess.[40] However, in 1975, Knowles improved this method by introducing a bidentate phosphine chiral complex, DIPAMP, which significantly enhanced enantioselectivity to over 90%.[41] These developments proved their utility by contributing to the industrial-scale production of *L*-Dopa, a crucial treatment for Parkinson's disease (Scheme 5, A).[42,43]

The introduction of BINAP ligand by Noyori in 1980 represented a second milestone (Scheme 5, B).[44–46] This C2 symmetric axially chiral diphosphine revolutionized asymmetric hydrogenation, achieving perfect enantioselectivity in the synthesis of phenylalanine derivatives from (*Z*)-(α-amido)cinnamic acids. The widespread adoption of this chiral ligand in various organic synthesis processes underscores its profound impact on the field.

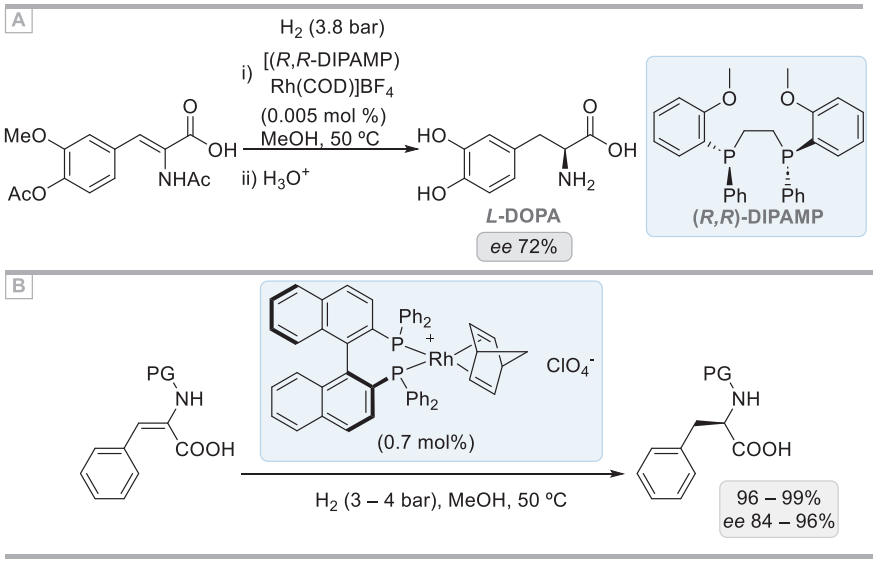

Scheme 5. Asymmetric reduction reactions.

These developments in asymmetric hydrogenation, along with further improvements, are currently recognized as one of the most versatile methods for the generation of chiral compounds at large scale, being present in several industrial transformations.[47]

In parallel, Sharpless also made significant contributions in asymmetric epoxidations (Scheme 6, A).[48] In 1980, he developed the first asymmetric variant of allylic alcohol epoxidation employing diethyl tartrate as chiral

ligand, and subsequently expanded the scope of asymmetric oxidation, using $(DHQ)_2PHAL$ and $(DHQD)_2PHAL$ ligands in the osmium-mediated dihydroxylation of olefins (Scheme 6, B).[49–51]

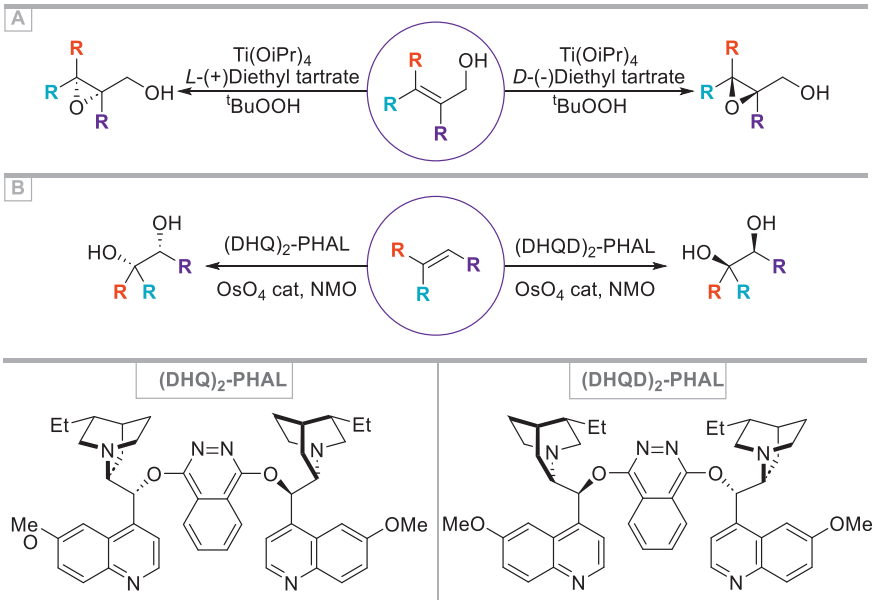

Scheme 6. Asymmetric oxidation of olefins.

Since these pioneering contributions, other chiral ligands for metal catalysed asymmetric transformations have arisen (Figure 4). [52–55] Amongst all of them, some privileged scaffolds, typically with C_2 symmetry, are the most employed ones, and high levels of enantioinduction have been achieved in manifold transformations such as Diels-Alder cycloadditions, aldol reactions, conjugate additions, Mannich-type reactions or allylic alkylations, amongst others.

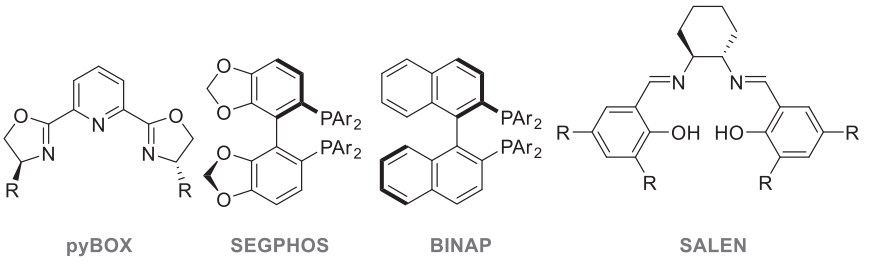

Figure 4. Privileged chiral ligands structures.

4 Mechanistic considerations

4.1 Activation modes

Asymmetric catalysts hinges on the differentiation of enantiotopic elements to selectively drive the reaction towards one enantiomer, which is achieved by the incorporation of chiral elements into the catalyst. Additionally, each catalyst possesses a particular mechanism in which the substrate is activated, accelerating the reaction rate. The mechanism of a catalyst can be classified in various categories, known as activation modes (Figure 5). [27,56,57]

One prevalent activation mode consists of the activation of a carbonyl compound by transforming it into an enamine intermediate, which efficiently reacts with the desired electrophile. A case in point is represented by a plethora of *L*-proline catalysed transformations such as aldol[32] or Mannich[58] reactions. Alternatively, a secondary amine also facilitates its condensation with aldehydes or ketones forming the corresponding iminium intermediate, increasing the electrophilicity of the substrate. [33,59,60]

A particular activation mode was introduced by MacMillan in 2007, in which the iminium ion formed was subjected to a single electron transfer (SET) oxidation to generate a radical intermediate, enabling access to homolytic reactivity. [61]

Another notable contribution pioneered by Jacobsen and Sigman was the development of a thiourea derived catalyst, which activated a carbonyl compound by the formation of hydrogen bonds.[62] This method has been extended to a plethora of new transformations based on the activation of various substrates by hydrogen bonds.[63–65]

Amongst all activation modes, acid catalysed transformations represent one of the most abundant strategies to activate the desired substrates due to its capacity to activate a wide array of substrates. Illustrative examples include the use of chiral highly acidic Brønsted acids such as chiral phosphoric acids, or the wide field of metal catalysed transformations, which commonly acts as chiral Lewis acidic species activating either the nucleophile, the electrophile or both simultaneously.[66–71]

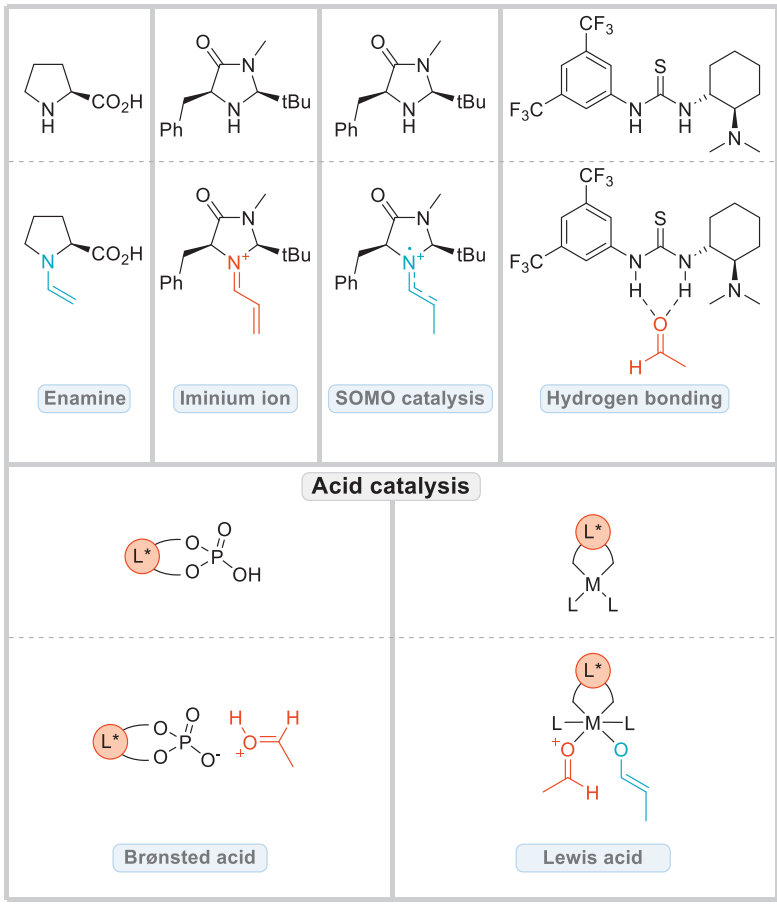

Figure 5. Activation modes of various transformations.

4.2 Acid catalysis

Most organic reactivity hinges on polar reactions in which a nucleophilic species reacts with an electrophilic counterpart. If the electrophile used is coordinated with a proton or a Lewis acid, the electron deficiency is increased, thus enhancing its reactivity. Based on this principle, the utilization of acids as catalysts represents a common method to catalyse organic reactions (Figure 6).

In general, phosphoric acids have a pK_a of 12–14 in acetonitrile, *N*-sulphonyl phosphoramides are more acidic with pK_a around 6–8 and sulfonyl imides around 5. These acids are very strong and can be compared with other widely used acids such as trifluoroacetic acid (TFA) or hydrobromic acid. [72]

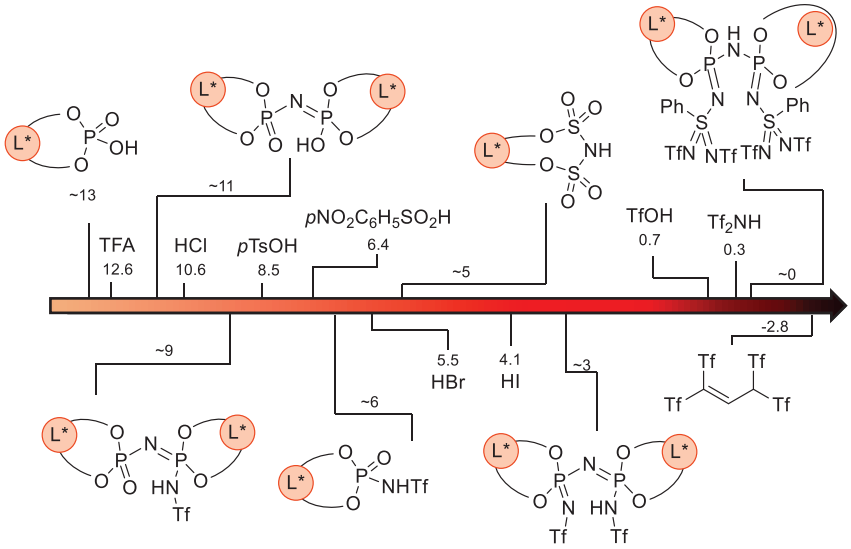

Figure 6. pKa scale of acids used in asymmetric catalysis.

List group has recently developed a new class of chiral Brønsted acid catalysts, imidodiphosphorimidates (IDPi).[72–76] They are BINOL-derived species with highly acidic centres confined by a bulky chiral microspace, which mimics enzymes as the confinement of the substrate to provide an excellent discrimination. Importantly, these catalysts can be fine-tuned by adjusting the 3,3´ positions of BINOL moiety, modifying the chiral space to adapt the desired substrate as well as its acidity, which depends on the imidodiphosphorimidate group. This combination of remarkable versatility coupled with an exceptional selectivity through confinement establishes IDPi as general catalysts for acidic transformations.

Embracing this approach, List and co-workers have been able to achieve unprecedented asymmetric transformations *via* the activation of highly inert substrates. Indeed, the strongly acidic character of IDPi generates highly reactive carbocation or oxocarbenium intermediates, which form an ion pair with the IDPi controlling the stereochemical outcome of the reaction.

IDPi are capable of activating substrates such as the simple olefins to form carbenium intermediates, which upon intramolecular addition furnished different tetrahydrofurans (Scheme 7, **A**).[77] They can also form norbornane derivatives *via* non-classical carbocations (Scheme 7, **B**),[78] oxocarbenium intermediates from tetrahydrofurans and tetrahydropirans (Scheme 7, **C**),[79] or active aldehydes to form oxocarbenium surrogates (Scheme 7, **D**).[80] The last reaction is particularly interesting because the product directly yields another aldehyde, which has a similar reactivity compared to the reagent.

However, the IDPi confinement achieves the discrimination between them, avoiding the otherwise typically oligomerization of the product.

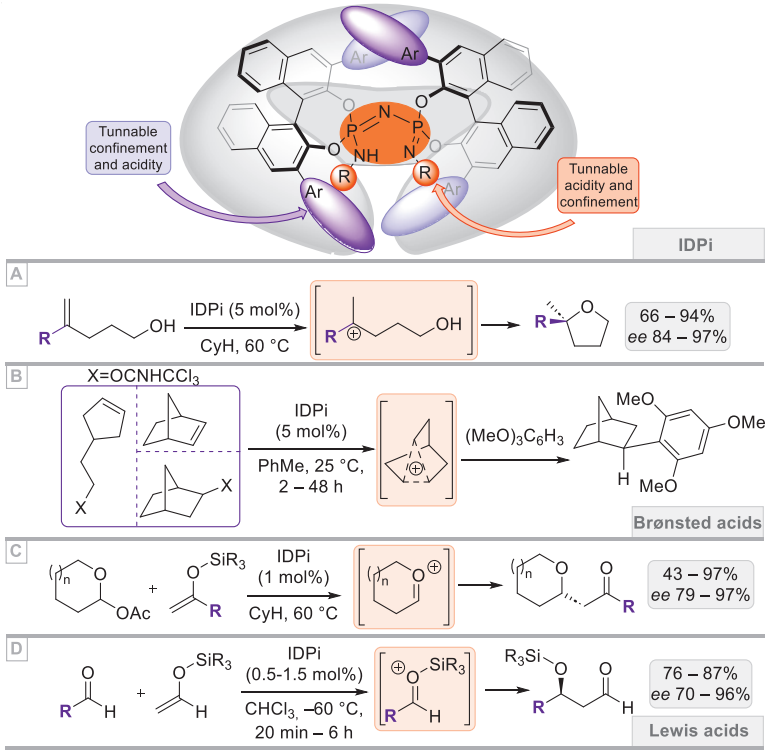

Scheme 7. IDPi catalysed transformations.

While acidity scales may assist in the choice of the appropriate catalyst to generate the cationic active intermediates, chemists still rely on their intuitive ability to distinguish among diverse substrates and predict potential reactivity between them. In order to gain a better understanding and efficiency, it is highly valuable to possess tools that facilitate fast and accurate predictions regarding the reactivity of different species.

4.3 Mayr parameters

In this context, Mayr established a scale to measure the electrophilicity and nucleophilicity of a wide range of compounds. Assuming that the kinetics of reactions depends on the electrophile and nucleophile independently, Mayr established Equation 1, and defined two parameters. The *N* parameter, which measures the nucleophilicity of a certain compound, and the slope parameter s_N, for which allyl trimethylsilane was established as the referent nucleophile with a s_N =1. For the electrophilic counterpart, only one parameter non solvent

dependant was necessary, E, for which bis(4-methoxyphenyl)methylium cation was established as the reference electrophile with a $E = 0$.[81,82]

$$\log k_{20\,°C} = s_N(E + N)$$

Equation 1. Mayr's equation.

Using this approach it has been established the E parameters for over three hundred electrophiles with a range between –30 to 8.[83–85] Also the N and s_N parameters have been determined for over one thousand nucleophiles with a range between –9 to 32.[86–89] This allows the quantification of the kinetic constant k of a large number of reactions and also permits organic chemists quantify and order the electrophilic and nucleophilic character of the species involved. As a general *rule of thumb* established by Mayr, if the $N + E > -5$, which means a $k = 10^{-5}$ $M^{-1}s^{-1}$, a reaction is expected to occur within one day. Contrarily, if the $N + E < 5$ the reaction will proceed too slowly (Figure 7). Deviations from Mayr correlations will appear in $N + E > 9$ ($k > 10^{10}$ $M^{-1}s^{-1}$), which is known as "*diffusion control conditions*". In this type of reactions, the rate determining step is not the formation of the adduct between the electrophile of the nucleophile, but rather the diffusion of the species through the reacting mixture, which favours the observation of side reactions and loss of selectivity in the desired reaction.

Mayr model has demonstrated a wide applicability and one of the main strengths is the ease of use. Noteworthily, this model does not consider the formation of the electrophile *in situ*, for example by a Lewis acid, if this is the rate-determining step, or the presence of side reactions that become faster than the formation of the Nucleophile-Electrophile adduct.

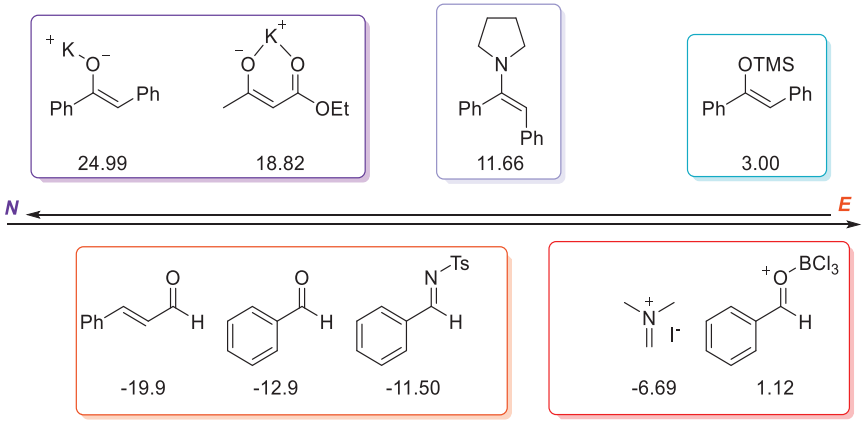

Figure 7. Mayr's nucleophilicity and electrophilicity scale.

Based on this scheme, enolates of alkaline metals, usually generated by strong bases such as LDA or LiHDMS, can react with neutral electrophiles such as primary alkyl halides by a S_N2 mechanism as demonstrated by Evans.[12] Contrarily, transition metal enolates such as titanium enolates can only react with alkyl halides favoured by S_N1 mechanism or activated electrophiles such as oxocarbenium compounds [13] or by radical mechanisms.[90–93] In this context, a general strategy relies on the activation of electrophilic species with a Lewis acid to generate the corresponding oxocarbenium, carbocation or iminium ion, facilitating their reaction with the appropriate nucleophile.

5 Stereodivergence

Despite the advancements highlighted above, achieving a complete control over both absolute and relative configuration in catalytic and asymmetric transformations remains a formidable challenge. Indeed, most methodologies aiming to synthesize two stereocentres in a single step can effectively control both the absolute and relative configuration, albeit only for one of the potential diastereomers.[94]

Therefore, the development of methodologies capable of obtaining any of the potential stereoisomers at will is highly desirable.[95,96] A case in point of such a challenge involves the synthesis of the antimalarial mefloquine, the (*R,S*) enantiomer of which induces psychotropic side effects. In 2013, Hall synthesized and evaluated all four stereoisomers for their medicinal applications (Scheme 8).[97] The synthesis relied on a tandem Pd-catalysed asymmetric isomerization and allylation step, yielding the *syn* stereoisomer. Unfortunately, the *anti* stereoisomer was not available, and two additional steps were required to invert the configuration of the alcohol, a process that could have been circumvented with the availability of a stereodivergent methodology.

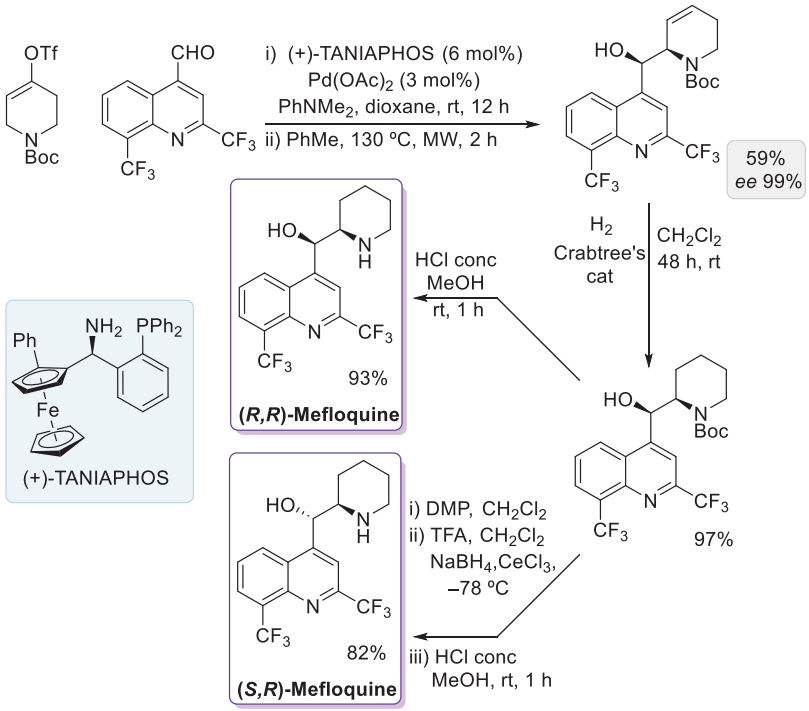

Scheme 8. Stereoselective synthesis of mefloquine isomers.

One of the main strategies for accessing all stereoisomers involves the use of slightly modified starting materials in a *pseudo*-stereodivergent approach. In enolate based reactions, the use of preformed silyl enol ethers with different geometry gives the opposite diastereoselectivity. However, a genuine catalytic stereodivergent approach does not require to change the starting material, just the catalyst.

Such a formidable challenge has been met by dual catalysis, which has emerged as a promising option for stereodivergent catalysis. Dual catalysis hinges on the activation of both the nucleophile and the electrophile with two distinct chiral catalysts, which facilitates the stereodivergent approach. The key feature of such approach is that each catalyst independently controls the stereocentre it activates, operating autonomously from the other.

For instance, Carreira and coworkers reported the stereodivergent α-allylation of hydratropaldehyde using the *pseudo*-enantiomers quinine and quinidine derivatives to activate the aldehyde through an enamine intermediate alongside with the chiral iridium phosphite complex which activates the allyl group (Scheme 9).[98] The four stereoisomers were prepared with excellent selectivities by only choosing the appropriate combination of ligands.

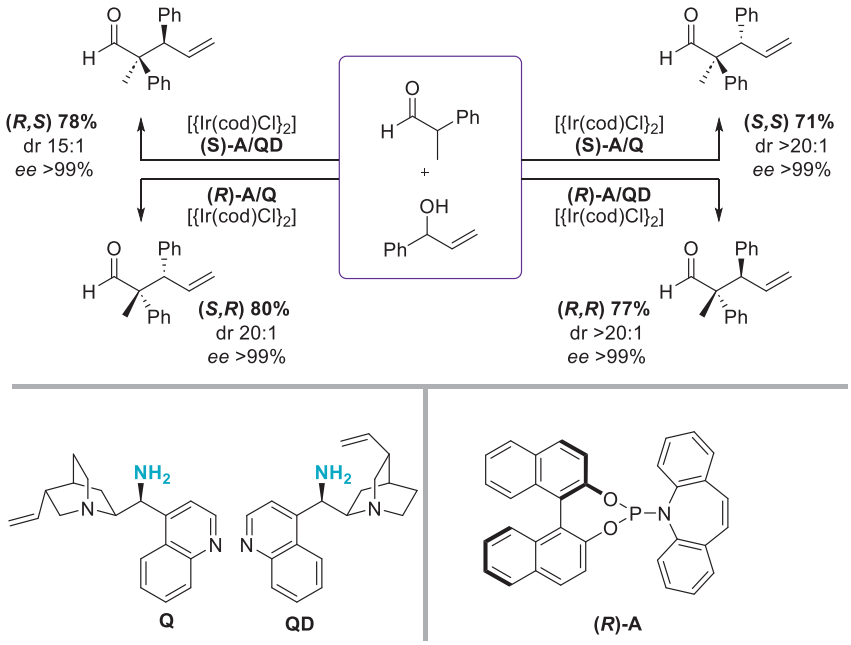

Scheme 9. Stereodivergent allylation of α-branched aldehydes.

An alternative strategy consists of the use of a tandem reaction. The initial stereocentre is created through an asymmetric reaction, followed by the installation of a second stereocentre by means of a catalyst-controlled diastereoselective reaction, subject to matching/mismatching effects. A particularly impressive example was reported by Buchwald and coworkers, who prepared all eight stereoisomers of a 1,3-aminoalcohol containing three stereocentres (Scheme 10).[99] Treatment of *E* or *Z* α,β-unsaturated ketone and combining it with the appropriate combination of the chiral diphosphines DTBM-SEGPHOS and DM-SEGPHOS, along with $Cu(OAc)_2$ to facilitate a hydrosilylation-hydroamination sequence, it is possible to produce all the potential stereoisomers in excellent selectivities and moderate yields.

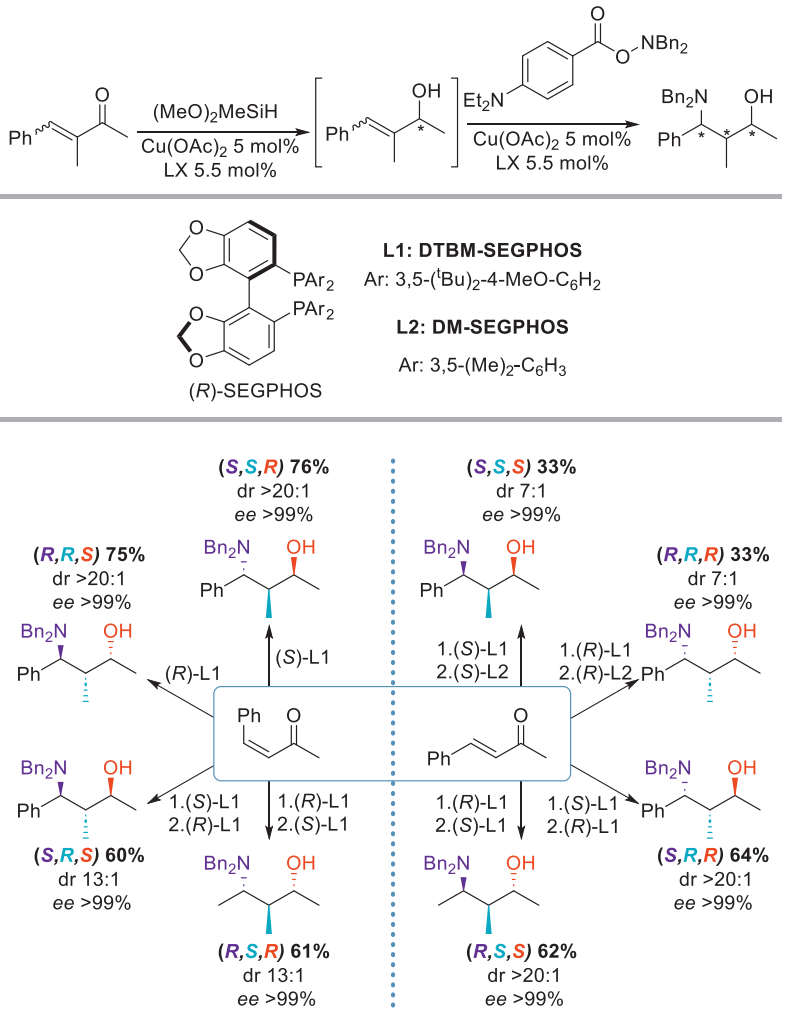

Scheme 10. Stereodivergent synthesis of 1,3-aminoalcohols.

6 C–C Bond forming reactions

One of the main challenges in modern organic chemistry lies in the stereocontrolled construction of C–C bonds. Unfortunately, there is a limited array of transformations capable of generating these bonds in a stereoselective manner. Therefore, the development of new methodologies in this area is highly desirable.

Several strategies have been used to generate new stereocentres while forging new C–C bonds, including allylation of carbonyl compounds, α-alkylations, additions to carbonyls, electron-deficient olefins, or cycloaddition

reactions (Figure 8). In this context, metal enolates from carbonyl compounds emerge as one of the most versatile nucleophiles for the stereocontrolled construction of C–C bonds.[94]

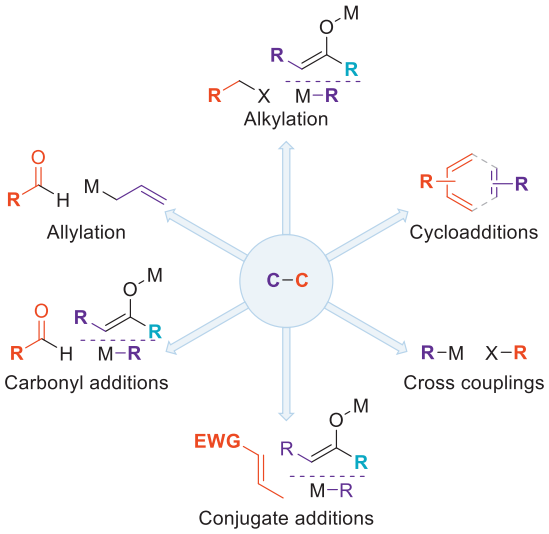

Figure 8. C–C bond forming reactions.

6.1 Carbonyl as nucleophiles

Depending on the electrophile used the reaction of the α-position of a carbonyl compound can be classified into different groups, standing out as the most important ones the aldol reaction, the Michael addition, the Mannich reaction and the α-alkylation, using aldehydes, electron-deficient olefins, imines or alkylating agents respectively (Figure 9).

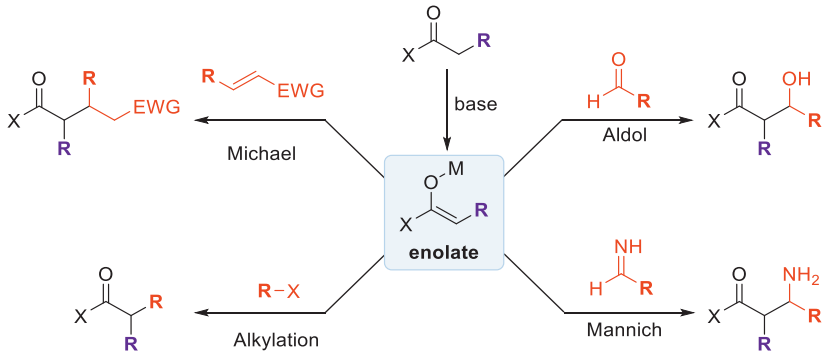

Figure 9. Reactions of metal enolates with different electrophiles.

Enolate geometry plays a pivotal role in determining the stereochemical outcome of such reactions. Therefore, the stereoselective

synthesis of either the (*E*)- or (*Z*)-enolate becomes essential. While certain substrates like acyclic ketones or esters are particularly challenging in this regard, substituted imides or thioderivatives have shown to be reliable substrates for generating the corresponding enolate with excellent stereocontrol.

Indeed, a very powerful strategy to control the enolate geometry takes advantage of some privileged platforms from which to carry out the asymmetric reaction, and finally remove them to obtain the desired functional group (Figure 10).Easily removable amides containing a chelating element are specially useful to generate the (*Z*)-enolate while simultaneously chelate the metal used to produce a rigid five or six-membered chelates. The most spread scaffolds include the Evans-like oxazolidinones and thiazolidinethiones,[100] 2,5-pyrrolidinones,[101–103] pyrazoles,[104–107] imidazoles[108] or 7-azaindolines.[109,110]

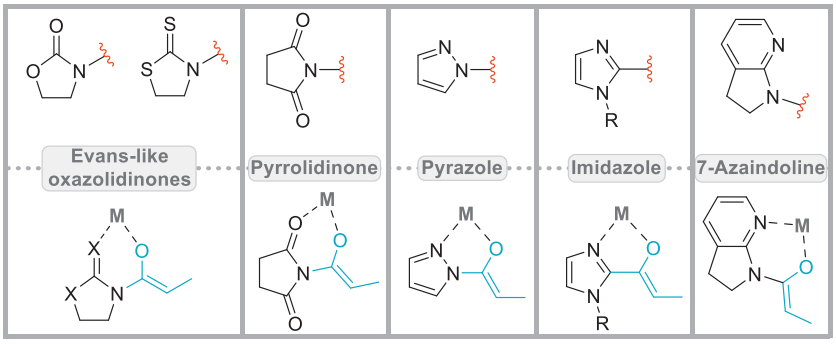

Figure 10. Platforms commonly used in asymmetric catalysis from carbonylic compounds.

Finally, the enolates represented in Figure 10 may undergo highly stereocontrolled reactions, which evolve through open or closed transition states.

6.2 Direct reactions

Classical approaches based on the reactivity of metal enolates rely on a two-step sequence. The first step involves the treatment of the carbonyl compound with either with a strong base or an appropriate combination of a Lewis acid and a tertiary amine to generate the required enolate. Once the nucleophilic intermediate is formed, addition of the electrophile permits the stereocontrolled construction of the carbon-carbon bond to take place. Such two-step sequence is known as *indirect* reaction.

Aiming to adhere to principles dictated by atom economy, *direct* reactions encompass catalytic transformations in which the latent nucleophile and the electrophile are subjected to the required conditions to form the enolate *in situ*, which is usually achieved by the combination of a Lewis acid and a tertiary amine, without affecting the electrophile (Scheme 11).[111] This approach enables the use of substoichiometric amounts of Lewis acids, facilitating the development of catalytic asymmetric processes.

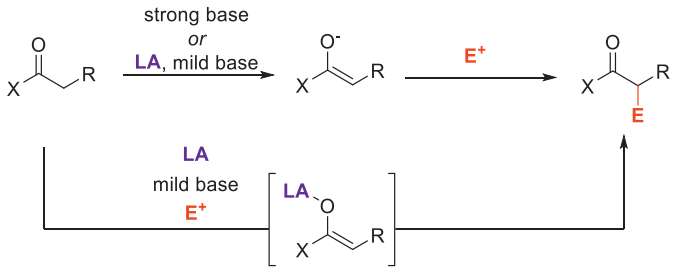

Scheme 11. Direct reactions.

6.2.1 Aldol additions

The first example of a direct aldol reaction was reported by Shibasaki, in which the heterobimetallic complex BINOL-La triggered the reaction of unmodified ketones with aldehydes (Scheme 12).[112]

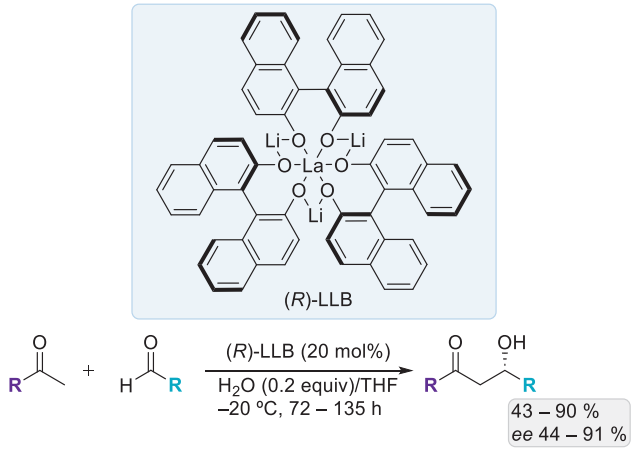

Scheme 12. Shibasaki's LLB direct aldol reaction.

Another prominent example of a direct aldol reaction was developed by Trost, which involves a bimetallic zinc complex with an engineered designed chiral ligand ProPhenol (Scheme 13).[113] This bimetallic species acts as a bifunctional catalyst, generating the enolate from unmodified aromatic

ketones and activating the aldehyde simultaneously to generate the aldol adduct in good yields and selectivities for most cases.

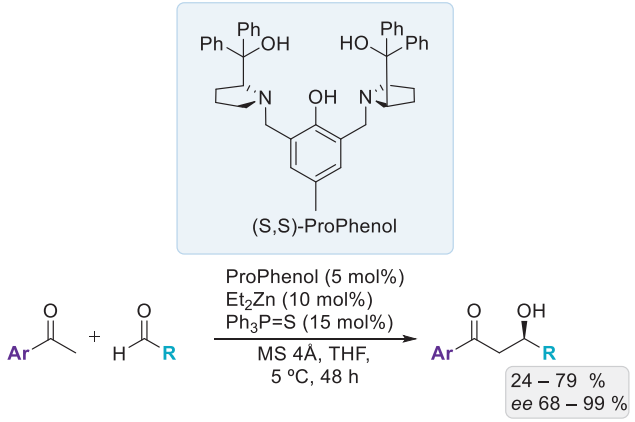

Scheme 13. Trost's ProPhenol catalysed direct aldol reaction.

These two seminal reports inspired several approaches towards the development of direct aldol addition reactions, which due to its potential and prevalence in several target molecules it persists as a field of great interest.

6.2.2 Michael addition

The asymmetric variant of the Michael addition experienced a rapid growth after the reports of Yamaguchi[114] and Shibasaki,[115] who used malonates as Michael donors and different enones as acceptors.

The rubidium salt of (*S*)-proline resulted a good catalyst for the asymmetric Michael additions of malonates to different enones, although only modest enantioselectivities were achieved (Scheme 14).

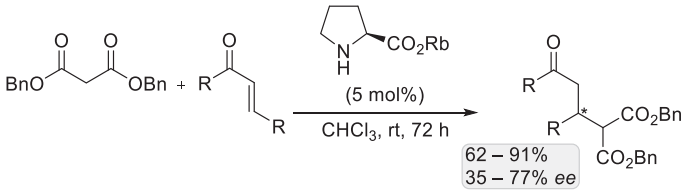

Scheme 14. Yamaguchi rubidium prolinate Michael reaction.

Shibasaki developed a series of heterobimetallic complexes, including (*R,R*)-ALB, which performed with excellent results on the Michael addition of benzyl malonate to cyclic enones, achieving excellent yields and enantioselectivities. Afterwards, this intermediate was used on the total synthesis of tubifolidine (Scheme 15).[116]

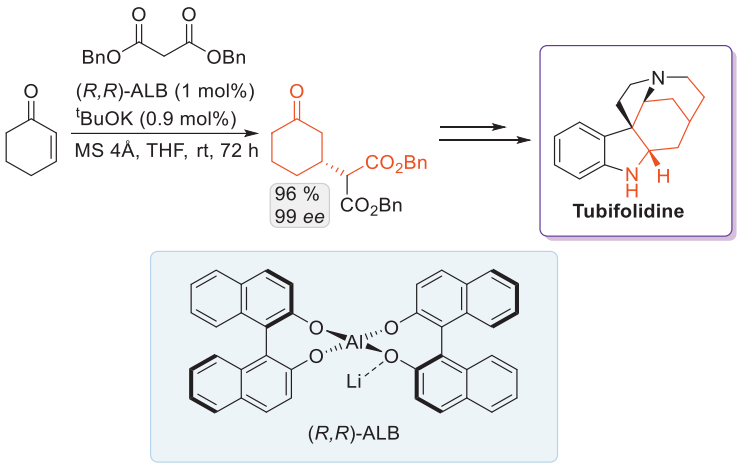

Scheme 15. Total synthesis of tubifolidine by a direct asymmetric Michael addition.

The wide variety of Michael donors, including but not restricted to carbonyl pronucleophiles, combined with the several existing possibilities as Michael acceptors makes this transformation one of the most versatile organic reactions. However, several challenges arise from this versatility, including the stereochemical control or regioselectivity towards the 1,2 addition in several substrates. Therefore, much effort is done to obtain novel highly selective methodologies with wide scopes to enable the exploitation of these transformations.

6.2.3 Mannich Reaction

Shibasaki reported the first direct asymmetric Mannich reaction using his heterobimetallic complexes. The initial reports resulted in only modest enantioselectivities.[117] However, further developments lead to the use of a combination of Et_2Zn alongside with (*S,S*)-Linked-BINOL ligands, which provided outstanding results for the *anti* Mannich adducts (Scheme 16).[118]

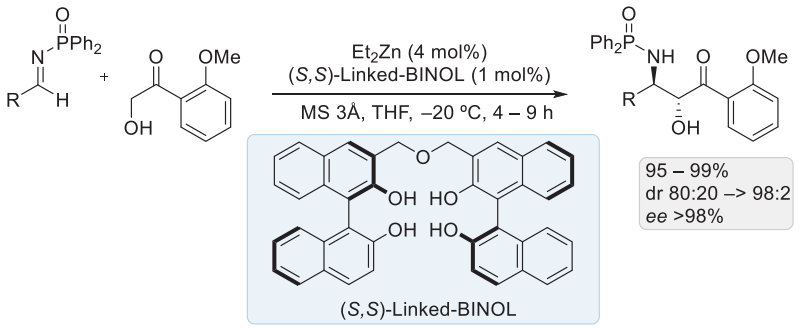

Scheme 16. Et_2Zn/Linked BINOL catalysed Mannich reaction.

Later, List [58] reported the first organocatalysed Mannich reaction based on his previous work on aldol reactions and Kobayashi's[119] three component Mannich addition. As shown in Scheme 17, the three component system consists of the pronucleophile carbonyl compound, the desired aldehyde and *p*-anisidine. In this system, the imine is formed *in situ*, and further reacts with the carbonyl nucleophile catalysed by the natural amino acid *L*-proline to furnish the *N*-PMP-protected *anti* Mannich adduct in good yields and remarkable stereocontrol.

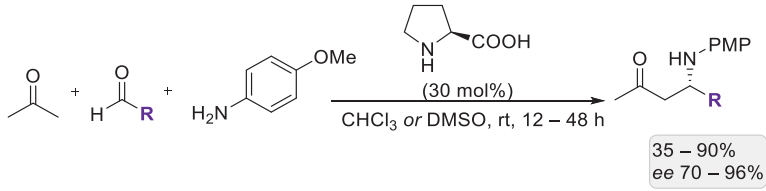

Scheme 17. *L*-Proline catalysed three component Mannich addition.

All these approaches paved the way towards the development of direct asymmetric Mannich additions. Unfortunately and despite significant efforts, several challenges remain unconquered, such as the use of non-precious metal catalysis or uncovering transformations with broader applicability.

7 References

(1) Cohen, P. S.; Cohen, S. M. Wöhler's Synthesis of Urea: How Do the Textbooks Report It? *J. Chem. Educ.* **1996**, *73* (9), 883.

(2) Lord Kelvin, P. R. S. The Molecular Tactics of a Crystal. **1894**.

(3) Biot, J. B. Mémoire Sur La Polarization Circulaire et Sur Ses Applications à La Chimie Organique. **1832**, 39–176.

(4) Pasteur, L. Sur Les Relations Qui Peuvent Exister Entre La Forme Cristalline, La Composition Chimique et Le Sens de La Polarisation Rotatoire. *Ann. Chim. Phys.* **1848**, *24* (1848), 442–459.

(5) McConathy, J.; Owens, M. J. Stereochemistry in Drug Action. *Prim. Care Companion J. Clin. Psychiatry* **2003**, *5* (2), 70–73.

(6) Caldwell, J. The Importance of Stereochemistry in Drug Action and Disposition. *J. Clin. Pharmacol.* **1992**, *32* (10), 925–929.

(7) Nguyen, L. A.; He, H.; Pham-Huy, C. Chiral Drugs: An Overview. *Int. J. Biomed. Sci.* **2006**, *2* (2), 85–100.

(8) Calcaterra, A.; D'Acquarica, I. The Market of Chiral Drugs: Chiral Switches versus de Novo Enantiomerically Pure Compounds. *J. Pharm. Biomed. Anal.* **2018**, *147*, 323–340.

(9) Corey, E. J.; Ensley, H. E. Preparation of an Optically Active Prostaglandin Intermediate via Asymmetric Induction. *J. Am. Chem. Soc.* **1975**, *97* (23), 6908–6909.

(10) Davies, S. G.; Fletcher, A. M.; Roberts, P. M.; Thomson, J. E. SuperQuat Chiral Auxiliaries: Design, Synthesis, and Utility. *Org. Biomol. Chem.* **2019**, *17* (6), 1322–1335.

(11) Evans, D. A.; Bartroli, J.; Shih, T. L. Enantioselective Aldol Condensations. 2. Erythro-Selective Chiral Aldol Condensations via Boron Enolates. *J. Am. Chem. Soc.* **1981**, *103* (8), 2127–2129.

(12) Evans, D. A.; Ennis, M. D.; Mathre, D. J. Asymmetric Alkylation Reactions of Chiral Imide Enolates. A Practical Approach to the Enantioselective Synthesis of Alpha-Substituted Carboxylic Acid Derivatives. *J. Am. Chem. Soc.* **1982**, *104* (6), 1737–1739.

(13) Evans, D. A.; Urpi, F.; Somers, T. C.; Clark, J. S.; Bilodeau, M. T. New Procedure for the Direct Generation of Titanium Enolates.

Diastereoselective Bond Constructions with Representative Electrophiles. *J. Am. Chem. Soc.* **1990**, *112* (22), 8215–8216.

(14) Evans, D. A.; Kaldor, S. W.; Jones, T. K.; Clardy, J.; Stout, T. J. Total Synthesis of the Macrolide Antibiotic Cytovaricin. *J. Am. Chem. Soc.* **1990**, *112* (19), 7001–7031.

(15) Oppolzer, W.; Kingma, A. J. Asymmetric Induction on Copper(I) Chloride Catalyzed 1,4-addition of Alkylmagnesium Chlorides to α,β -disubstituted (*E*)-enoylsultams and Subsequent Protonation. *Helv. Chim. Acta* **1989**, *72* (6), 1337–1345.

(16) Oppolzer, W.; Poli, G.; Kingma, A. J.; Starkemann, C.; Bernardinelli, G. Asymmetric Induction at C(β) and C(α) of *N*-Enoylsultams by Organomagnesium 1,4-Addition/Enolate Trapping. *Helv. Chim. Acta* **1987**, *70* (8), 2201–2214.

(17) Trost, B. M. Atom Economy–A Challenge for Organic Synthesis: Homogeneous Catalysis Leads the Way. *Angew. Chem. Int. Ed.* **1995**, *34* (3), 259–281.

(18) Trost, B. M. The Atom Economy–a Search for Synthetic Efficiency. *Science (1979)* **1991**, *254* (5037), 1471–1477.

(19) Fischer, E. Einfluss Der Configuration Auf Die Wirkung Der Enzyme. *Dtsch. Chem. Ges.* **1894**, *27* (3), 2985–2993.

(20) Fischer, E. Syntheses in the Purine and Sugar Group. *Nobel Lectures* **1902**.

(21) Bell, E. L.; Finnigan, W.; France, S. P.; Green, A. P.; Hayes, M. A.; Hepworth, L. J.; Lovelock, S. L.; Niikura, H.; Osuna, S.; Romero, E.; Ryan, K. S.; Turner, N. J.; Flitsch, S. L. Biocatalysis. *Nat. Rev. Methods Primers* **2021**, *1* (1), 46.

(22) Sheldon, R. A.; Brady, D. Broadening the Scope of Biocatalysis in Sustainable Organic Synthesis. *ChemSusChem* **2019**, *12* (13), 2859–2881.

(23) Theil, F. Lipase-Supported Synthesis of Biologically Active Compounds. *Chem. Rev.* **1995**, *95* (6), 2203–2227.

(24) Csuk, Rene.; Glaenzer, B. I. Baker's Yeast Mediated Transformations in Organic Chemistry. *Chem. Rev.* **1991**, *91* (1), 49–97.

(25) Hughes, G.; Lewis, J. C. Introduction: Biocatalysis in Industry. *Chem. Rev.* **2018**, *118* (1), 1–3.

(26) Wilson, R. Evolving BVMOs for Increasing the Yield and Purity of Enzyme Catalysed Oxidation. *Chim. Oggi – Chem. Today* **2015**, *33* (2), 7–10.

(27) MacMillan, D. W. C. The Advent and Development of Organocatalysis. *Nature* **2008**, *455* (7211), 304–308.

(28) Seayad, J.; List, B. Asymmetric Organocatalysis. *Org. Biomol. Chem.* **2005**, *3* (5), 719.

(29) Bertelsen, S.; Jørgensen, K. A. Organocatalysis—after the Gold Rush. *Chem. Soc. Rev.* **2009**, *38* (8), 2178.

(30) Dalko, P. I.; Moisan, L. In the Golden Age of Organocatalysis. *Angew. Chem. Int. Ed.* **2004**, *43* (39), 5138–5175.

(31) Notz, W.; Tanaka, F.; Barbas, C. F. Enamine-Based Organocatalysis with Proline and Diamines: The Development of Direct Catalytic Asymmetric Aldol, Mannich, Michael, and Diels–Alder Reactions. *Acc. Chem. Res.* **2004**, *37* (8), 580–591.

(32) List, B.; Lerner, R. A.; Barbas, C. F. Proline-Catalyzed Direct Asymmetric Aldol Reactions. *J. Am. Chem. Soc.* **2000**, *122* (10), 2395–2396.

(33) Ahrendt, K. A.; Borths, C. J.; MacMillan, D. W. C. New Strategies for Organic Catalysis: The First Highly Enantioselective Organocatalytic Diels–Alder Reaction. *J. Am. Chem. Soc.* **2000**, *122* (17), 4243–4244.

(34) Hayashi, Y.; Aikawa, T.; Shimasaki, Y.; Okamoto, H.; Tomioka, Y.; Miki, T.; Takeda, M.; Ikemoto, T. Research and Development of an Efficient Synthesis of a Key Building Block for Anti-AIDS Drugs by Diphenylprolinol-Catalyzed Enantio- and Diastereoselective Direct Cross Aldol Reaction. *Org. Process Res. Dev.* **2016**, *20* (9), 1615–1620.

(35) Mizhiritskii, M.; Marom, E. Process for the Preparation of Darunavir and Darunavir Intermediates. *WO2011092687A1* **2011**.

(36) Knowles, W. S. Asymmetric Hydrogenations (Nobel Lecture 2001). *Adv. Synth. Catal.* **2003**, *345* (1–2), 3–13.

(37) Knowles, W. S.; Sabacky, M. J.; Vineyard, B. D. Catalytic Asymmetric Hydrogenation. *Chem. Commun.* **1972**, *214* (1), 10.

(38) Sharpless, K. B. The Search for New Chemical Reactivity. *Nobel lectures* **2001**.

(39) Noyori, R. Asymmetric Catalysis: Science and Opportunities. *Nobel lectures* **2001**.

(40) Knowles, W. S.; Sabacky, M. J. Catalytic Asymmetric Hydrogenation Employing a Soluble, Optically Active, Rhodium Complex. *Chem. Commun.* **1968**, No. 22, 1445.

(41) Knowles, W. S.; Sabacky, M. J.; Vineyard, B. D.; Weinkauff, D. J. Asymmetric Hydrogenation with a Complex of Rhodium and a Chiral Bisphosphine. *J. Am. Chem. Soc.* **1975**, *97* (9), 2567–2568.

(42) Knowles, W. S. Asymmetric Hydrogenations – The Monsanto *L*-Dopa Process. *Asymmetric Catalysis on Industrial Scale* **2003**, 21–38.

(43) Knowles, W. S.; Sabacky, M. J.; Vineyard, B. D. *L*-Dopa Process and Intermediates. *US4005127A* **1977**.

(44) Miyashita, A.; Yasuda, A.; Takaya, H.; Toriumi, K.; Ito, T.; Souchi, T.; Noyori, R. Synthesis of 2,2'-Bis(Diphenylphosphino)-1,1'-Binaphthyl (BINAP), an Atropisomeric Chiral Bis(Triaryl)Phosphine, and Its Use in the Rhodium(I)-Catalyzed Asymmetric Hydrogenation of α-(Acylamino)Acrylic Acids. *J. Am. Chem. Soc.* **1980**, *102* (27), 7932–7934.

(45) Kitamura, M.; Ohkuma, T.; Tokunaga, M.; Noyori, R. Dynamic Kinetic Resolution in BINAP—Ruthenium(II) Catalyzed Hydrogenation of 2-Substituted 3-Oxo Carboxylic Esters. *Tetrahedron Asymmetry* **1990**, *1* (1), 1–4.

(46) Noyori, R.; Takaya, H. BINAP: An Efficient Chiral Element for Asymmetric Catalysis. *Acc. Chem. Res.* **1990**, *23* (10), 345–350.

(47) Blaser, H. U.; Spindler, F.; Studer, M. Enantioselective Catalysis in Fine Chemicals Production. *Appl. Catal.* **2001**, *221* (1–2), 119–143.

(48) Katsuki, T.; Sharpless, K. B. The First Practical Method for Asymmetric Epoxidation. *J. Am. Chem. Soc.* **1980**, *102* (18), 5974–5976.

(49) Sharpless, K. B.; Amberg, W.; Bennani, Y. L.; Crispino, G. A.; Hartung, J.; Jeong, K. S.; Kwong, H. L.; Morikawa, K.; Wang, Z. M. The Osmium-Catalyzed Asymmetric Dihydroxylation: A New Ligand Class and a Process Improvement. *J. Org. Chem.* **1992**, *57* (10), 2768–2771.

(50) Jacobsen, E. N.; Marko, Istvan.; Mungall, W. S.; Schroeder, Georg.; Sharpless, K. Barry. Asymmetric Dihydroxylation via Ligand-Accelerated Catalysis. *J. Am. Chem. Soc.* **1988**, *110* (6), 1968–1970.

(51) Kolb, H. C.; VanNieuwenhze, M. S.; Sharpless, K. B. Catalytic Asymmetric Dihydroxylation. *Chem. Rev.* **1994**, *94* (8), 2483–2547.

(52) Yoon, T. P.; Jacobsen, E. N. Privileged Chiral Catalysts. *Science (1979)* **2003**, *299* (5613), 1691–1693.

(53) Johnson, J. S.; Evans, D. a. Chiral Bis(Oxazoline) Copper(II) Complexes: Versatile Catalysts for Enantioselective Cycloaddition, Aldol, Michael, and Carbonyl Ene Reactions. *Acc. Chem. Res.* **2000**, *33* (6), 325–335.

(54) Shaw, S.; White, J. D. Asymmetric Catalysis Using Chiral Salen–Metal Complexes: Recent Advances. *Chem. Rev.* **2019**, *119* (16), 9381–9426.

(55) Cozzi, P. G. Metal–Salen Schiff Base Complexes in Catalysis: Practical Aspects. *Chem. Soc. Rev.* **2004**, *33* (7), 410–421.

(56) Rios, R.; Moyano, A. Activation Modes in Asymmetric Organocatalysis. *Stereoselective Organocatalysis* **2013**.

(57) Melchiorre, P.; Marigo, M.; Carlone, A.; Bartoli, G. Asymmetric Aminocatalysis—Gold Rush in Organic Chemistry. *Angew. Chem. Int. Ed.* **2008**, *47* (33), 6138–6171.

(58) List, B. The Direct Catalytic Asymmetric Three-Component Mannich Reaction. *J. Am. Chem. Soc.* **2000**, *122* (38), 9336–9337.

(59) Paras, N. A.; MacMillan, D. W. C. The Enantioselective Organocatalytic 1,4-Addition of Electron-Rich Benzenes to α,β-Unsaturated Aldehydes. *J. Am. Chem. Soc.* **2002**, *124* (27), 7894–7895.

(60) Brown, S. P.; Goodwin, N. C.; MacMillan, D. W. C. The First Enantioselective Organocatalytic Mukaiyama-Michael Reaction: A Direct Method for the Synthesis of Enantioenriched γ-Butenolide Architecture. *J. Am. Chem. Soc.* **2003**, *125* (5), 1192–1194.

(61) Jang, H.-Y.; Hong, J.-B.; MacMillan, D. W. C. Enantioselective Organocatalytic Singly Occupied Molecular Orbital Activation: The Enantioselective α-Enolation of Aldehydes. *J. Am. Chem. Soc.* **2007**, *129* (22), 7004–7005.

(62) Sigman, M. S.; Jacobsen, E. N. Schiff Base Catalysts for the Asymmetric Strecker Reaction Identified and Optimized from Parallel Synthetic Libraries. *J. Am. Chem. Soc.* **1998**, *120* (19), 4901–4902.

(63) Miller, S. J.; Copeland, G. T.; Papaioannou, N.; Horstmann, T. E.; Ruel, E. M. Kinetic Resolution of Alcohols Catalyzed by Tripeptides Containing

the *N*-Alkylimidazole Substructure. *J. Am. Chem. Soc.* **1998**, *120* (7), 1629–1630.

(64) Wenzel, A. G.; Jacobsen, E. N. Asymmetric Catalytic Mannich Reactions Catalyzed by Urea Derivatives: Enantioselective Synthesis of β-Aryl-β-Amino Acids. *J. Am. Chem. Soc.* **2002**, *124* (44), 12964–12965.

(65) Parvin, T.; Yadav, R.; Choudhury, L. H. Recent Applications of Thiourea-Based Organocatalysts in Asymmetric Multicomponent Reactions (AMCRs). *Org. Biomol. Chem.* **2020**, *18* (29), 5513–5532.

(66) Akiyama, T.; Mori, K. Stronger Brønsted Acids: Recent Progress. *Chem. Rev.* **2015**, *115* (17), 9277–9306.

(67) Lin, J.-S.; Wang, F.-L.; Dong, X.-Y.; He, W.-W.; Yuan, Y.; Chen, S.; Liu, X.-Y. Catalytic Asymmetric Radical Aminoperfluoroalkylation and Aminodifluoromethylation of Alkenes to Versatile Enantioenriched-Fluoroalkyl Amines. *Nature Commun.* **2017**, *8* (1), 14841.

(68) Terada, M. Chiral Phosphoric Acids as Versatile Catalysts for Enantioselective Transformations. *Synthesis (Stuttg)* **2010**, *2010* (12), 1929–1982.

(69) Uraguchi, D.; Terada, M. Chiral Brønsted Acid-Catalyzed Direct Mannich Reactions via Electrophilic Activation. *J. Am. Chem. Soc.* **2004**, *126* (17), 5356–5357.

(70) Akiyama, T.; Itoh, J.; Yokota, K.; Fuchibe, K. Enantioselective Mannich-Type Reaction Catalyzed by a Chiral Brønsted Acid. *Angew. Chem. Int. Ed.* **2004**, *43* (12), 1566–1568.

(71) Garcia-Garcia, P.; Lay, F.; Garcia-Garcia, P.; Rabalakos, C.; List, B. A Powerful Chiral Counteranion Motif for Asymmetric Catalysis. *Angew. Chem. Int. Ed.* **2009**, *48* (24), 4363–4366.

(72) Schreyer, L.; Properzi, R.; List, B. IDPi Catalysis. *Angew. Chem. Int. Ed.* **2019**, *58* (37), 12761–12777.

(73) Čorić, I.; List, B. Asymmetric Spiroacetalization Catalysed by Confined Brønsted Acids. *Nature* **2012**, *483* (7389), 315–319.

(74) Kaib, P. S. J.; Schreyer, L.; Lee, S.; Properzi, R.; List, B. Extremely Active Organocatalysts Enable a Highly Enantioselective Addition of Allyltrimethylsilane to Aldehydes. *Angew. Chem. Int. Ed.* **2016**, *55* (42), 13200–13203.

(75) Xie, Y.; Cheng, G. J.; Lee, S.; Kaib, P. S. J.; Thiel, W.; List, B. Catalytic Asymmetric Vinylogous Prins Cyclization: A Highly Diastereo- and Enantioselective Entry to Tetrahydrofurans. *J. Am. Chem. Soc.* **2016**, *138* (44), 14538–14541.

(76) Mayer, S.; List, B. Asymmetric Counteranion-Directed Catalysis. *Angew. Chem. Int. Ed.* **2006**, *45* (25), 4193–4195.

(77) Tsuji, N.; Kennemur, J. L.; Buyck, T.; Lee, S.; Prévost, S.; Kaib, P. S. J.; Bykov, D.; Farès, C.; List, B. Activation of Olefins via Asymmetric Brønsted Acid Catalysis. *Science (1979)* **2018**, *359* (6383), 1501–1505.

(78) Properzi, R.; Kaib, P. S. J.; Leutzsch, M.; Pupo, G.; Mitra, R.; De, C. K.; Song, L.; Schreiner, P. R.; List, B. Catalytic Enantiocontrol over a Non-Classical Carbocation. *Nature Chem.* **2020**, *12* (12), 1174–1179.

(79) Lee, S.; Kaib, P. S. J.; List, B. Asymmetric Catalysis via Cyclic, Aliphatic Oxocarbenium Ions. *J. Am. Chem. Soc.* **2017**, *139* (6), 2156–2159.

(80) Schreyer, L.; Kaib, P. S. J.; Wakchaure, V. N.; Obradors, C.; Properzi, R.; Lee, S.; List, B. Confined Acids Catalyze Asymmetric Single Aldolizations of Acetaldehyde Enolates. *Science (1979)* **2018**, *362* (6411), 216–219.

(81) Mayr, H.; Ofial, A. R. Kinetics of Electrophile-Nucleophile Combinations: A General Approach to Polar Organic Reactivity. *Pure Appl. Chem.* **2005**, *77* (11), 1807–1821.

(82) Mayr, H.; Ofial, A. R. Do General Nucleophilicity Scales Exist? *J. Phys. Org. Chem.* **2008**, *21* (7–8), 584–595.

(83) Appel, R.; Mayr, H. Quantification of the Electrophilic Reactivities of Aldehydes, Imines, and Enones. *J. Am. Chem. Soc.* **2011**, *133* (21), 8240–8251.

(84) Li, Z.; Jangra, H.; Chen, Q.; Mayer, P.; Ofial, A. R.; Zipse, H.; Mayr, H. Kinetics and Mechanism of Oxirane Formation by Darzens Condensation of Ketones: Quantification of the Electrophilicities of Ketones. *J. Am. Chem. Soc.* **2018**, *140* (16), 5500–5515.

(85) Mayr, H.; Kempf, B.; Ofial, A. R. π-Nucleophilicity in Carbon–Carbon Bond-Forming Reactions. *Acc. Chem. Res.* **2003**, *36* (1), 66–77.

(86) Timofeeva, D. S.; Mayer, R. J.; Mayer, P.; Ofial, A. R.; Mayr, H. Which Factors Control the Nucleophilic Reactivities of Enamines? *Chem. Eur. J.* **2018**, *24* (22), 5901–5910.

(87) Lucius, R.; Loos, R.; Mayr, H. Kinetic Studies of Carbocation-Carbanion Combinations: Key to a General Concept of Polar Organic Reactivity. *Angew. Chem. Int. Ed.* **2002**, *41* (1), 91–95.

(88) Corral-Bautista, F.; Appel, R.; Frickel, J. S.; Mayr, H. Quantification of Ion-Pairing Effects on the Nucleophilic Reactivities of Benzoyl- and Phenyl-Substituted Carbanions in Dimethylsulfoxide. *Chem. Eur. J.* **2015**, *21* (2), 875–884.

(89) Leonov, A.; Timofeeva, D.; Ofial, A.; Mayr, H. Metal Enolates – Enamines – Enol Ethers: How Do Enolate Equivalents Differ in Nucleophilic Reactivity? *Synthesis (Stuttg)* **2019**, *51* (05), 1157–1170.

(90) Kennington, S. C. D.; Gómez-Palomino, A.; Salomó, E.; Romea, P.; Urpí, F.; Font-Bardia, M. General and Stereoselective Aminoxylation of Biradical Titanium(IV) Enolates with TEMPO: A Detailed Study on the Effect of the Chiral Auxiliary. *Org. Biomol. Chem.* **2018**, *16* (26), 4807–4815.

(91) Gómez-Palomino, A.; Romea, P.; Urpí, F. Stereoselective Oxidation of Titanium(IV) Enolates with Oxygen. *Synthesis (Germany)* **2018**, *50* (14), 2721–2726.

(92) Pérez-Palau, M.; Sanosa, N.; Romea, P.; Urpí, F.; López, R.; Gómez-Bengoa, E.; Font-Bardia, M. Stereoselective Alkylation of Chiral Titanium(IV) Enolates with *Tert* -Butyl Peresters. *Org. Lett.* **2021**, *23* (22), 8852–8856.

(93) Gómez-Palomino, A.; Pérez-Palau, M.; Romea, P.; Urpí, F.; Del Olmo, M.; Hesse, T.; Fleckenstein, S.; Gómez-Bengoa, E.; Sotorríos, L.; Font-Bardia, M. Stereoselective Decarboxylative Alkylation of Titanium(IV) Enolates with Diacyl Peroxides. *Org. Lett.* **2020**, *22* (1), 199–203.

(94) Carreira, E. M.; Kvaerno, L. Classics in Stereoselective Synthesis. *Wiley-VHC* **2009**.

(95) Gao, J.; Bai, S.; Gao, Q.; Liu, Y.; Yang, Q. Acid Controlled Diastereoselectivity in Asymmetric Aldol Reaction of Cycloketones with Aldehydes Using Enamine-Based Organocatalysts. *Chemical Communications* **2011**, *47* (23), 6716.

(96) Krautwald, S.; Carreira, E. M. Stereodivergence in Asymmetric Catalysis. *J. Am. Chem. Soc.* **2017**, *139* (16), 5627–5639.

(97) Ding, J.; Hall, D. G. Concise Synthesis and Antimalarial Activity of All Four Mefloquine Stereoisomers Using a Highly Enantioselective

Catalytic Borylative Alkene Isomerization. *Angew. Chem. Int. Ed.* **2013**, *52* (31), 8069–8073.

(98) Krautwald, S.; Sarlah, D.; Schafroth, M. A.; Carreira, E. M. Enantio- and Diastereodivergent Dual Catalysis: α-Allylation of Branched Aldehydes. *Science (1979)* **2013**, *340* (6136), 1065–1068.

(99) Shi, S.-L.; Wong, Z. L.; Buchwald, S. L. Copper-Catalysed Enantioselective Stereodivergent Synthesis of Amino Alcohols. *Nature* **2016**, *532* (7599), 353–356.

(100) Chen, L.; Huang, P. Evans' Chiral Auxiliary-Based Asymmetric Synthetic Methodology and Its Modern Extensions. *Eur. J. Org. Chem.* **2024**, *27* (4).

(101) Jensen, K. B.; Gothelf, K. V.; Hazell, R. G.; Jørgensen, K. A. Improvement of TADDOLate–$TiCl_2$-Catalyzed 1,3-Dipolar Nitrone Cycloaddition Reactions by Substitution of the Oxazolidinone Auxiliary of the Alkene with Succinimide. *J. Org. Chem.* **1997**, *62* (8), 2471–2477.

(102) Minakata, S.; Ezoe, T.; Nakamura, K.; Ryu, I.; Komatsu, M. $Yb(OTf)_3$-Catalyzed 1,3-Dipolar Cycloaddition of Nitrone with Alkene; Switch in Diastereoselectivity by Solvent and Bidentate Auxiliary. *Tetrahedron Lett.* **1998**, *39* (29), 5205–5208.

(103) Zhao, B.-L.; Du, D.-M. Enantioselective Synthesis of Enol Lactones from Tandem Michael Addition/Lactonization Catalyzed by a Chiral Squaramide Catalyst. *Tetrahedron Asymmetry* **2014**, *25* (4), 310–317.

(104) Shen, H.-C.; Zhang, L.; Chen, S.-S.; Feng, J.; Zhang, B.-W.; Zhang, Y.; Zhang, X.; Wu, Y.-D.; Gong, L.-Z. Enantioselective Addition of Cyclic Ketones to Unactivated Alkenes Enabled by Amine/Pd(II) Cooperative Catalysis. *ACS Catal.* **2019**, *9* (2), 791–797.

(105) Wang, H.; Bai, Z.; Jiao, T.; Deng, Z.; Tong, H.; He, G.; Peng, Q.; Chen, G. Palladium-Catalyzed Amide-Directed Enantioselective Hydrocarbofunctionalization of Unactivated Alkenes Using a Chiral Monodentate Oxazoline Ligand. *J. Am. Chem. Soc.* **2018**, *140* (10), 3542–3546.

(106) Yuan, W.; Shi, B. Synthesis of Chiral Spirolactams via Sequential C–H Olefination/Asymmetric [4+1] Spirocyclization under a Simple Co^{II}/Chiral Spiro Phosphoric Acid Binary System. *Angew. Chem. Int. Ed.* **2021**, *60* (43), 23187–23192.

(107) Liu, Y.; Liu, Y.; Zhang, Z.; Yan, S.; Chen, K.; Shi, B. Divergent and Stereoselective Synthesis of β -Silyl-α-Amino Acids through Palladium-Catalyzed Intermolecular Silylation of Unactivated Primary and Secondary C–H Bonds. *Angew. Chem. Int. Ed.* **2016**, *128* (44), 14063–14066.

(108) Lauberteaux, J.; Pichon, D.; Baslé, O.; Mauduit, M.; Marcia de Figueiredo, R.; Campagne, J. Acyl-Imidazoles: A Privileged Ester Surrogate for Enantioselective Synthesis. *ChemCatChem* **2019**, *11* (23), 5705–5722.

(109) Kumagai, N.; Shibasaki, M. 7-Azaindoline Auxiliary: A Versatile Attachment Facilitating Enantioselective C-C Bond-Forming Catalysis. *Synthesis (Germany)* **2019**, *51* (1), 185–193.

(110) Zhang, Y.-P.; You, Y.; Yin, J.-Q.; Wang, Z.-H.; Zhao, J.-Q.; Yuan, W.-C. Progress in Catalytic Asymmetric Reactions with 7-Azaindoline as the Directing Group. *Molecules* **2023**, *28* (23), 7898.

(111) Trost, B. M.; Brindle, C. S. The Direct Catalytic Asymmetric Aldol Reaction. *Chem. Soc. Rev.* **2010**, *39* (5), 1600–1632.

(112) Yoshikawa, N.; Yamada, Y. M. A.; Das, J.; Sasai, H.; Shibasaki, M. Direct Catalytic Asymmetric Aldol Reaction. *J. Am. Chem. Soc.* **1999**, *121* (17), 4168–4178.

(113) Trost, B. M.; Ito, H. A Direct Catalytic Enantioselective Aldol Reaction via a Novel Catalyst Design. *J. Am. Chem. Soc.* **2000**, *122* (48), 12003–12004.

(114) Yamaguchi, M.; Shiraishi, T.; Hirama, M. A Catalytic Enantioselective Michael Addition of a Simple Malonate to Prochiral α,β -Unsaturated Ketoses and Aldehydes. *Angew. Chem. Int. Ed.* **1993**, *32* (8), 1176–1178.

(115) Sasai, H.; Arai, T.; Shibasaki, M. Catalytic Asymmetric Michael Reactions Promoted by a Lithium-Free Lanthanum-BINOL Complex. *J. Am. Chem. Soc.* **1994**, *116* (4), 1571–1572.

(116) Shimizu, S.; Ohori, K.; Arai, T.; Sasai, H.; Shibasaki, M. A Catalytic Asymmetric Synthesis of Tubifolidine. *J. Org. Chem.* **1998**, *63* (21), 7547–7551.

(117) Yamasaki, S.; Iida, T.; Shibasaki, M. Direct Catalytic Asymmetric Mannich Reaction of Unmodified Ketones: Cooperative Catalysis of an

AlLibis(Binaphthoxide) Complex and $La(OTf)_3 \cdot nH_2O$. *Tetrahedron* **1999**, *55* (29), 8857–8867.

(118) Matsunaga, S.; Kumagai, N.; Harada, S.; Shibasaki, M. Anti -Selective Direct Catalytic Asymmetric Mannich-Type Reaction of Hydroxyketone Providing β-Amino Alcohols. *J. Am. Chem. Soc.* **2003**, *125* (16), 4712–4713.

(119) Manabe, K.; Kobayashi, S. Mannich-Type Reactions of Aldehydes, Amines, and Ketones in a Colloidal Dispersion System Created by a Brønsted Acid–Surfactant-Combined Catalyst in Water. *Org. Lett.* **1999**, *1* (12), 1965–1967.

OBJECTIVES

Building upon the precedents discussed previously, asymmetric catalytic transformations are currently at the forefront of organic chemistry. In this context, this thesis aims to develop novel direct, catalytic and asymmetric methodologies to construct new carbon-carbon (C–C) bonds using metal enolates derived from abundant and non-toxic metals.

In **Chapter I**, the objective is to study new asymmetric aldol reactions. In a first approach, reactions between different achiral *N*-acyl-thioimides and aromatic aldehydes are assessed. This involves the propionate as well as the acetate aldol reaction. In a second approach, additions to more challenging α,β-unsaturated aldehydes are examined. Finally, additions to propargylic aldehydes are also evaluated in parallel with new cobalt and iron aldol addition processes.

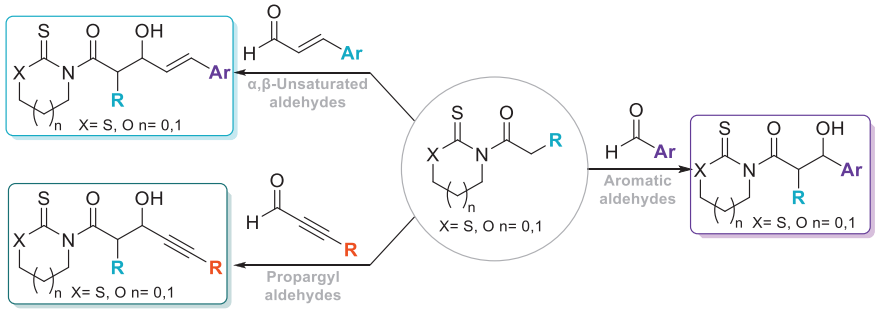

Scheme 18. Objectives of Chapter I.

In **Chapter II**, the focus is directed towards the regiocontrol additions to α,β-unsaturated aldehydes, optimizing the conditions for the obtention of both *syn* and *anti* Michael adducts in a diastereodivergent manner. Afterwards, the scope of this transformation is expanded to several α,β-unsaturated aldehydes and thioimides. Finally, more challenging extended Michael acceptors which involved the addition to α,β,γ,δ-unsaturated aldehydes are examined.

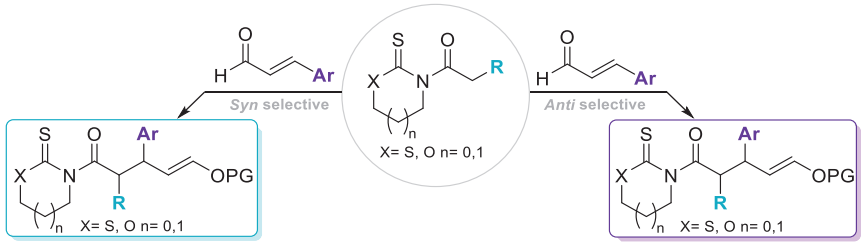

Scheme 19. Objectives of Chapter II.

In **Chapter III**, derivatization of the Michael adducts from the previously developed method is examined. The application of the resultant transformation to the synthesis tapentadol, a commercially available opioid, is described.

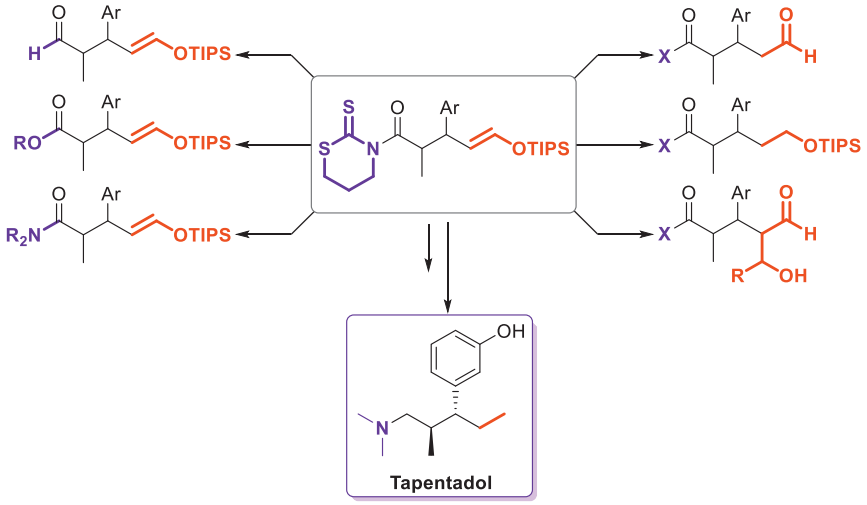

Scheme 20. Objectives of Chapter III.

In **Chapter IV**, summarized our efforts towards the development of Mannich-type reactions through activated iminium ions. Furthermore, preliminary studies towards 1,3-dipolar cycloaddition transformation between α,β-unsaturated thioimides and nitrones are presented.

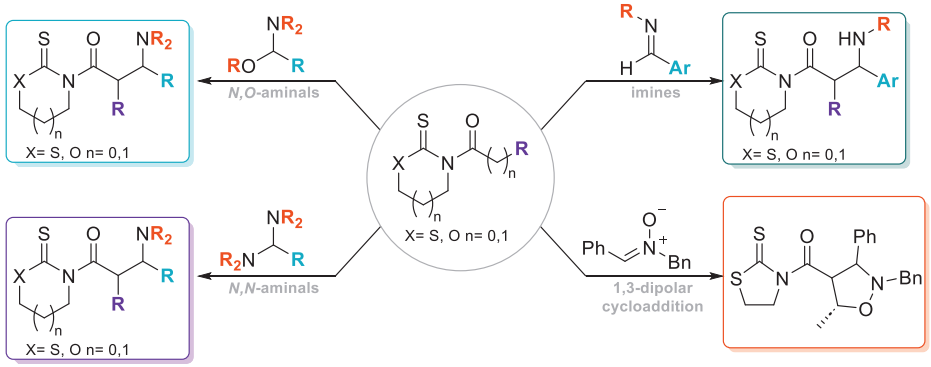

Scheme 21. Objectives of Chapter IV.

CHAPTER I

The aldol reaction

Table of contents

1 Introduction

The aldol reaction holds a prominent position amongst all organic transformations due to its capability to form new C-C bonds and install up to two new stereocenters. Importantly, the resultant β-hydroxy carbonyl compounds are prevalent motifs in a wide variety of natural products, which has made the aldol reaction a lingering topic of research. [1,2]

Indeed, since its discovery by Wurtz in 1872, several strategies have emerged to address the challenges inherent in these transformations. Key advancements include the introduction of preformed enolates in Mukaiyama reactions,[3–7] the development of stereocontrolled transformations based on chiral auxiliaries such as Evans oxazolidinones,[8] chiral ketones introduced by Paterson, or the development of catalytic asymmetric methods, amongst others (Figure 11).[9–20]

A particularly challenging variant involves the catalytic generation of the nucleophilic partner from the carbonylic reactant in the presence of the electrophilic aldehyde. The high efficiency of such approach, named direct reaction, has attracted much attention and triggered the development of a large number of methods, both in the organocatalytic and the metal catalytic arena.

In this context, the groundbreaking findings of Hajos-Parrish-Eder-Sauer-Wiechert on the intramolecular aldol reaction of an achiral triketone, catalysed by proline to yield an enantiomerically enriched bicyclic diketone, remained largely unexplored for three decades. [21] This changed when Barbas and List demonstrated the synthetic potential of intermolecular aldol reactions catalysed by proline and triggered the development of a variety of direct and organocatalytic aldol transformations.[22] Parallel to these achievements, the introduction of chiral metal catalysts such as [$LaLi_3$(BINOL)$_3$] (LLB) and ProPhenol by Shibasaki[23] and Trost[24] respectively, pioneered further advancements on direct aldol reactions through metal enolates.

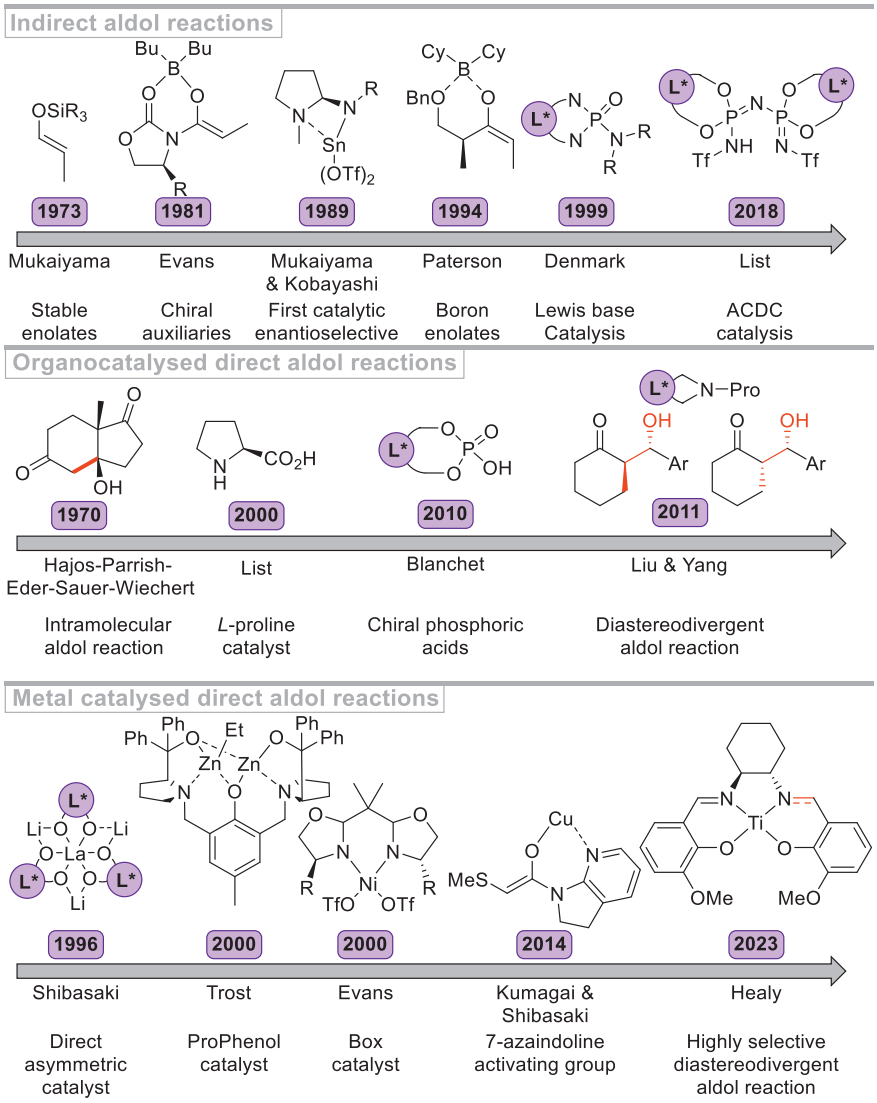

Figure 11. The development of the aldol reaction.

More than two decades from the first report by Shibasaki and the introduction of LLB catalyst, the direct asymmetric aldol reaction remains a significant challenge. Several of the reported methods provide access to the *syn* aldol adduct, while the *anti* adduct counterpart is usually elusive, which increases the interest towards the development of *anti* selective methodologies.[25]

One of the most efficient approaches towards the direct asymmetric aldol reactions was developed by Evans (Scheme 22). This relied on the

catalytic generation of the enolate combining *N*-acyl-thiazolidinethiones with chiral nickel(II) complexes in the presence of 2,6-lutidine, which upon reaction with the aldehyde furnished enantiomerically pure *syn* aldol adducts. Alternatively, aldol-like adducts derived from trimethyl orthoformate could be obtained by using other nickel catalysts in the presence of $BF_3{\cdot}OEt_2$. [26,27]

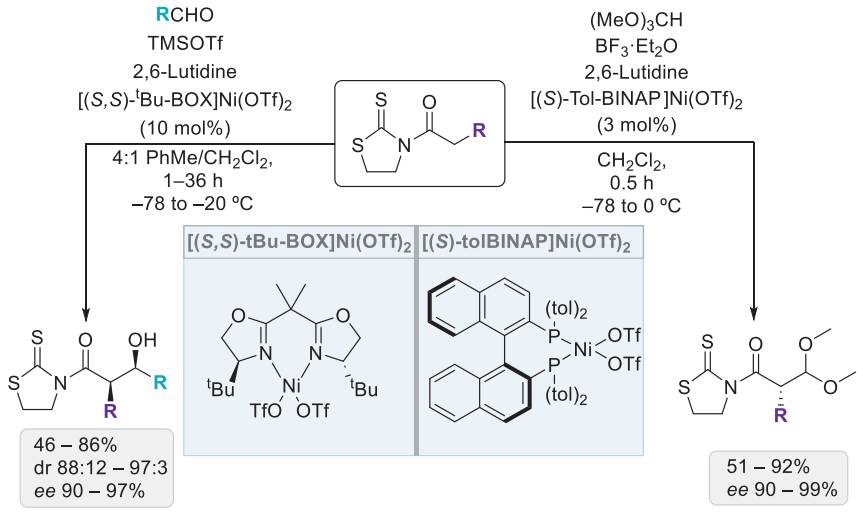

Scheme 22. Nickel(II) catalysed direct aldol type reactions.

Importantly, a further contribution from Sodeoka, which involved the use of nickel(II) chloride complex and its subsequent *in situ* activation by a silyl triflate.[28,29] This avoids the use of the highly moisture sensitive nickel(II) triflate complex, and facilitates the overall transformation, as proved in the α-fluorination of *N*-acyl-thiazolidinones shown in Scheme 23.

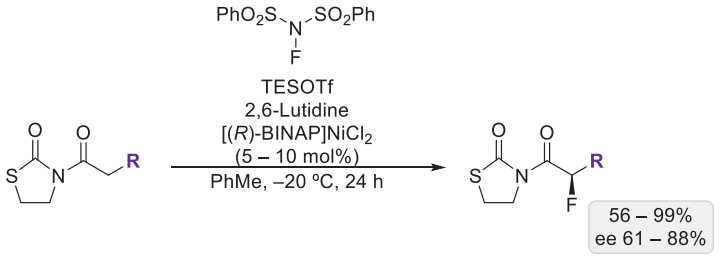

Scheme 23. *In situ* activation of nickel(II) chloride complex.

In turn, Kumagai and Shibasaki developed an asymmetric *syn* aldol reaction using *N*-acyl-7-azaindoline as the starting platform to carry out asymmetric aldol reactions with aromatic aldehydes, which furnishes the *syn* adducts in high yields and selectivities (Scheme 24). [30]

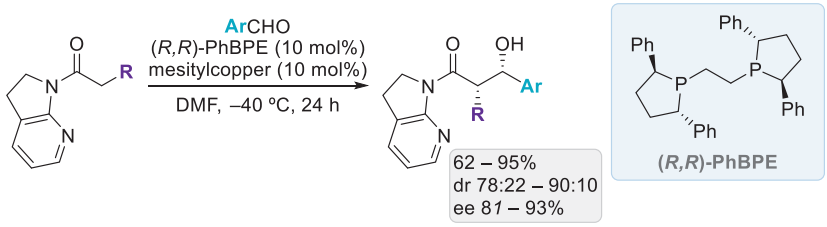

Scheme 24. Copper(I) catalysed *syn* aldol reaction.

Further developments of the direct aldol reaction of *N*-3-butenoyl-7-azaindolines with aromatic and aliphatic aldehydes have given access to the corresponding aldol adducts. Depending on the nature of the aldehyde and by choosing the appropriate combination of chiral ligand and phenolic additive, *syn* or *anti* relative configurations can be obtained in excellent yields and enantioselectivities (Scheme 25).[31] With these adducts in hand, the total syntheses of two different natural products with opposite relative stereochemistry, the blumiolide C and kainic acid were performed.

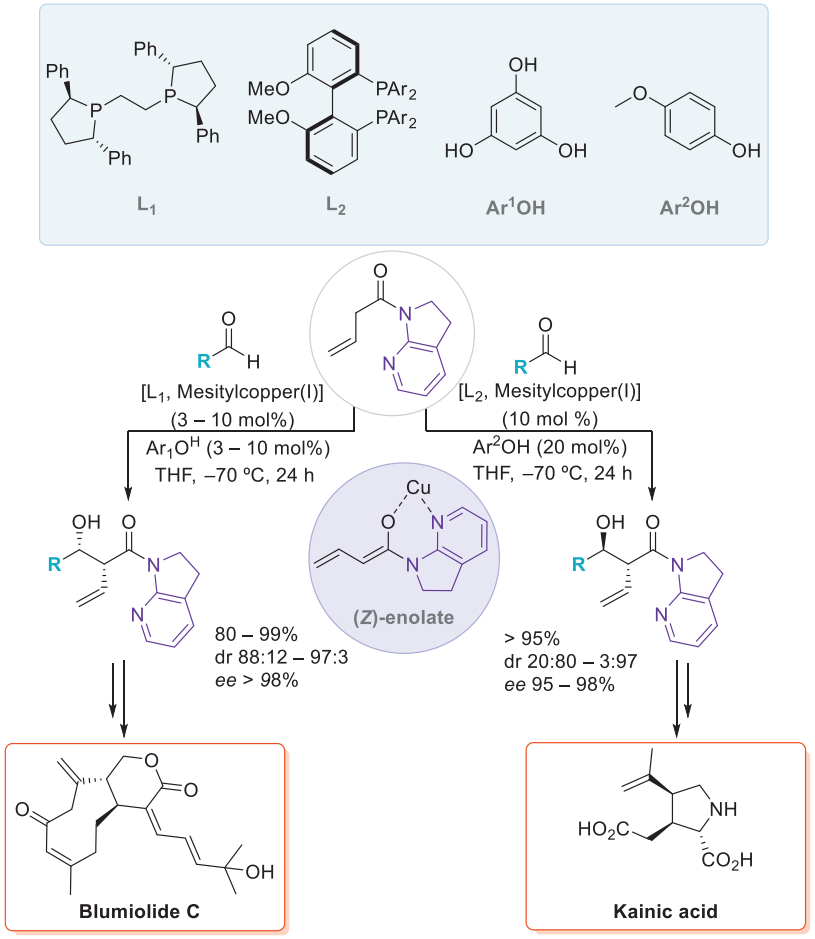

Scheme 25. Stereodivergent aldol addition of *N*-acyl-7-azaindolines.

In turn, Healy reported in 2023 an outstanding direct, asymmetric, and stereodivergent aldol reaction that provides access to all four possible stereoisomers from identical reactants (Scheme 26).[18] Indeed, simple treatment of malonic acid half thioesters with aldehydes in the presence of 10 mol% of salen or salalen-titanium complexes led to the *syn* or the *anti* aldol derivatives in a highly stereocontrolled manner. All in all, the choice of the titanium catalyst determines the stereochemical outcome of the reaction and proves the potential of metal enolates to undergo direct and enantioselective aldol reactions.

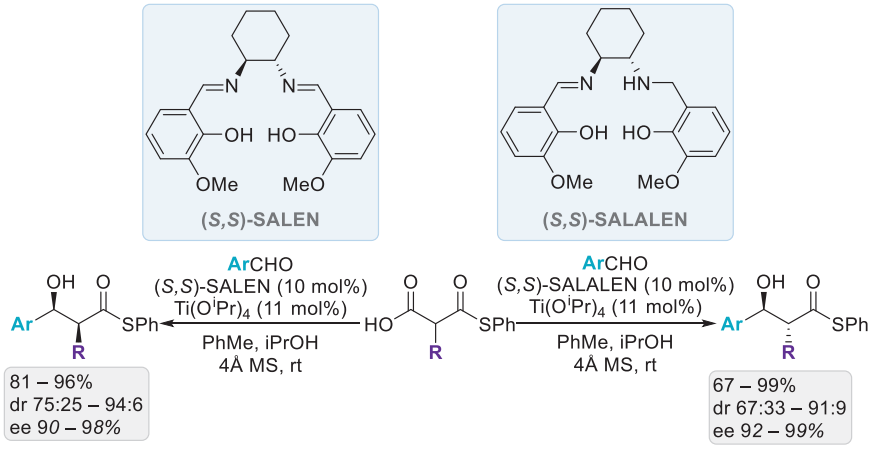

Scheme 26. Diastereodivergent aldol reaction.

In this context, and drawing upon the earlier contributions by Evans and Sodeoka, our research group has been working on the development of novel direct, catalytic, and asymmetric aldol reactions to yield protected aldol adducts. Using achiral thioimides as promising platforms to exclusively form the chelated metal (*Z*)-enolates, able to react with aldehydes and acetals activated by Lewis acids through open transition states in which the putative electrophile is an oxocarbenium species, the configuration of the resultant aldol adducts is governed by chiral nickel(II) complex.

Preliminary studies based on such an approach permitted our group to develop highly stereocontrolled silyl triflate mediated additions of different thioimides to trimethyl orthoformate catalysed by chiral nickel complexes. As a proof of concept, the anticonvulsant drug lacosamide was synthesized in only five steps taking advantage of this novel aldol-like reaction (Scheme 27).[32,33]

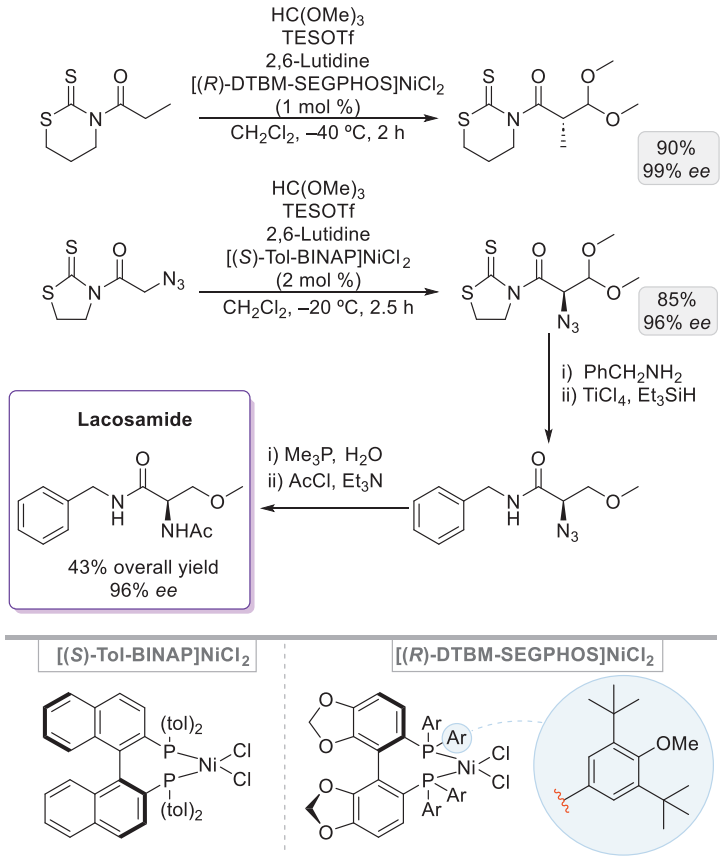

Scheme 27. Aldol like additions of trimethyl orthoformate.

Subsequently, the group initiated a project to investigate the simultaneous installation of two stereocenters. In this case, *N*-acyl-1,3-oxazinane-2-thiones were employed as pronucleophiles, TMSOTf serving as Lewis acid and 2-5 mol% [(*R*)-DTBM-SEGPHOS]$NiCl_2$ was utilized as catalyst. This approach resulted in the formation of *syn* aldol adducts protected as ethers in good yields and high selectivities (Scheme 28).[34]

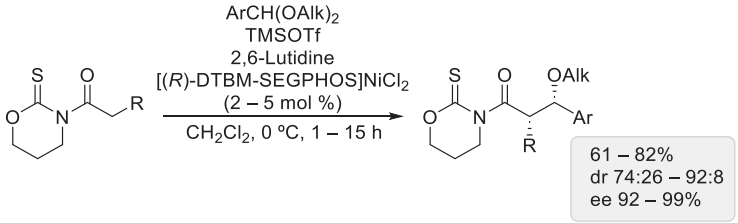

Scheme 28. Direct *syn* aldol-like reactions of acetals.

In parallel, a new strategy to gain access to the *anti*-aldol counterpart was devised. Studies carried out by Stuart Kennington in his PhD Thesis took advantage of the activation of aldehydes with bulky Lewis acids to obtain the *anti* protected aldol adducts in high yields and excellent selectivities (Scheme 29).[35,36]

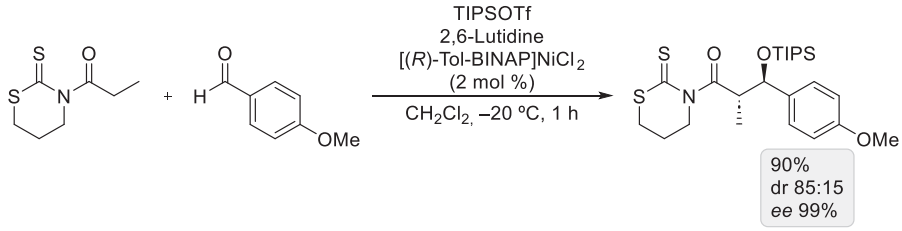

Scheme 29. Direct *anti* aldol reactions.

2 Towards wide scope aldol reactions

2.1 Studies on the *anti* aldol reaction from thioimides

The excellent results obtained in the *anti* selective aldol addition from *N*-propanoyl-1,3-thiazinane-2-thione summarized in Table 1. Aldehyde scope of the direct *anti* aldol reaction. served as the starting point of this Thesis. Building upon these results, we moved to analyse the impact of the substituents in the acyl group of the thiazinanethione.

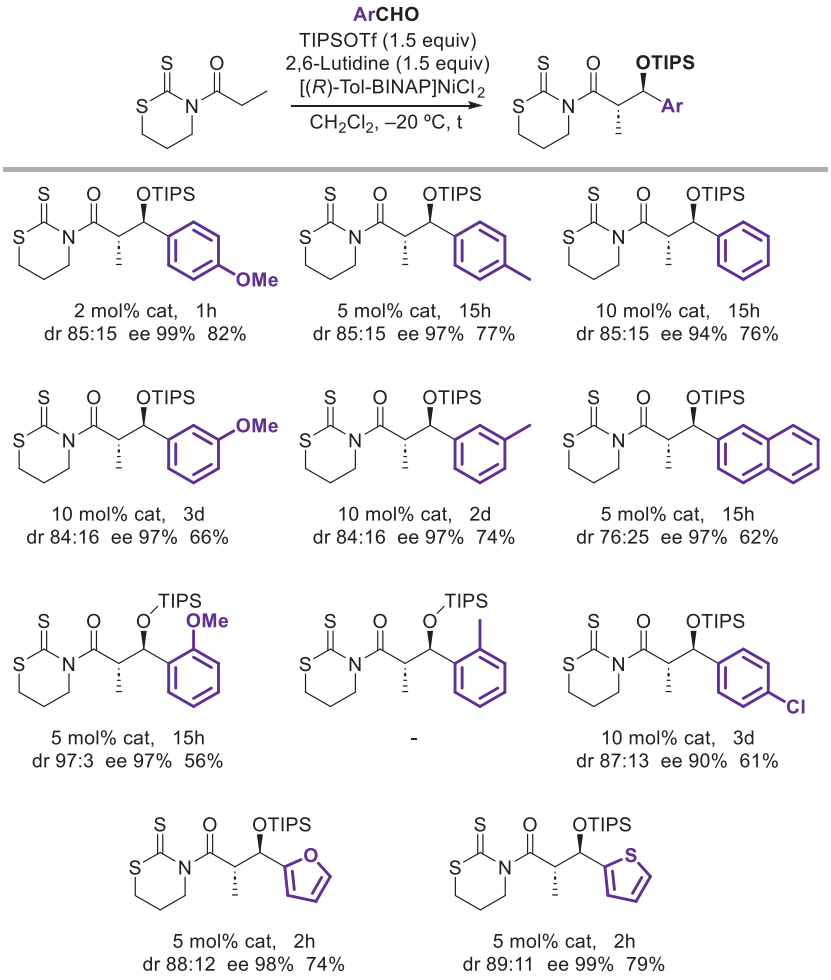

Table 1. Aldehyde scope of the direct *anti* aldol reaction.

Firstly, we required to synthesize the heterocycle in large quantities, so the two-step sequence to synthesize the 1,3-thiazinane-2-thione was scaled up to 120 mmol (Scheme 30). This started with the treatment of a solution of 3 amino-1-propanol in CH_2Cl_2 with chlorosulphonic acid at 0 °C to obtain 3-ammoniopropylsulphate in high yield (87%), effectively transforming the hydroxyl group into a good leaving group. Subsequently, the resultant sulphate was dissolved in ethanol, followed by the addition of carbon disulphide, which was reacted with a solution of KOH in water/ethanol to neutralize the ammonium group. After, heating the reaction mixture at 70 °C for 1 h results in the carbon disulphide forming a dithiocarbamate, which cyclize to form the desired 1,3 thiazinane-2-thione at large scale (120 mmol) and quite high yield (63%).[37]

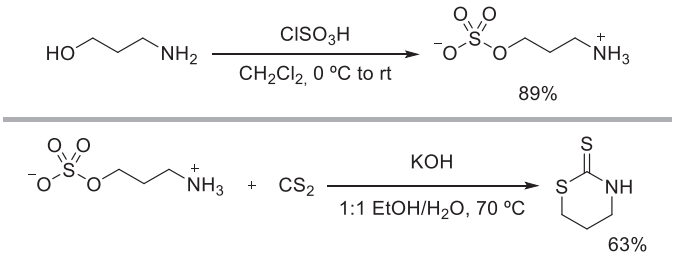

Scheme 30. Synthesis of 1,3-thiazinane-2-thione.

Following the synthesis of the heterocycle, the next step involved the synthesis of various *N*-acyl-1,3-thiazinane-2-thiones. These different derivatives were selected to assess the impact of bulkiness of the substituents, as well as the chemoselectivity of the overall transformation.

Two different methods were used to obtain the desired *N*-acyl-1,3-thiazinane-2-thiones **1**. Acyl chlorides were coupled to the thiazinanethione with Et_3N as a base (Table 2, protocol A), while carboxylic acids were coupled using carbodiimides and catalysed by DMAP (Table 2, protocol B). Alternatively, if the direct coupling using carbodiimides resulted in very low yields, the acid was derivatized with oxalyl chloride catalysed by DMF to yield the corresponding acyl chloride, after which the protocol A was followed. The products were purified by flash chromatography to afford the pure compound (22–84% yield).

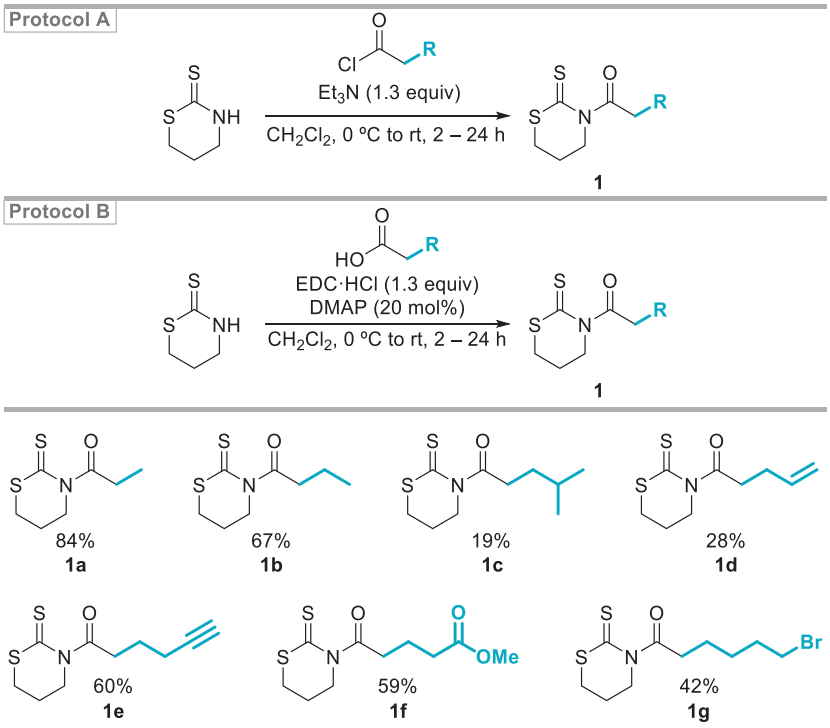

Table 2. Synthesis of *N*-acyl-1,3-thiazinane-2-thione.

Once prepared, the reaction of *N*-acyl-1,3-thiazinane-2-thiones with 4-methoxybenzaldehyde (**a**) was evaluated under the same conditions described in Table 3 to furnish the TIPS-protected *anti* aldol adducts. Each reaction was briefly optimized in terms of catalyst loading and time to achieve optimal results.

The TIPS-protected aldol adducts were successfully synthesised in most cases, with a remarkable excellent enantiomeric excess across all compounds. However, the diastereoselectivity, and consequently the yield, decreased when the steric hindrance increased, as shown in Table 3. Indeed, a significant loss of diastereoselectivity and yield was observed from **2aa** compared to compounds **2ba** and **2ca**. This trend was accompanied by a decrease in reaction rate, which forced an increase of catalyst loading from 2 mol% to 5 mol% in the latter example. Nevertheless, the tolerance to other functional groups was excellent, without a significant influence observed by the presence of some of the most common functional groups such as alkenes, alkynes, halides, or esters. Enantiomerically pure (*ee* 94–99%) protected *anti* adducts **2da**–**2ga** were isolated in good to high yields (62–76%).

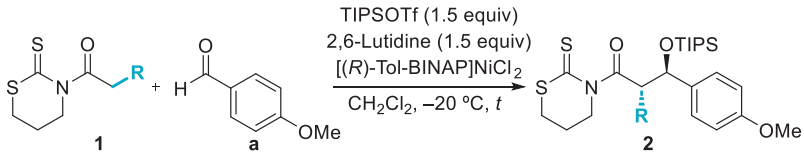

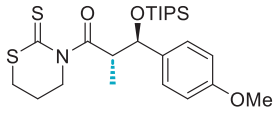

2aa
2 mol% cat, 1 h
dr 85:15 *ee* 99% 82%

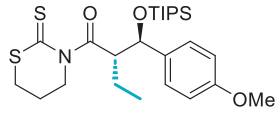

2ba
2 mol% cat, 2 h
dr 81:19 *ee* 99% 78%

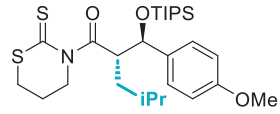

2ca
5 mol% cat, 2 h
dr 75:25 *ee* 99% 60%

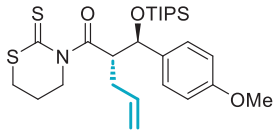

2da
2 mol% cat, 3 h
dr 81:19 *ee* 99% 76%

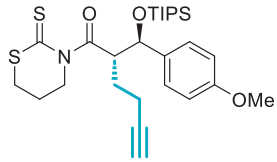

2ea
5 mol% cat, 5 h
dr 81:19 *ee* 98% 75%

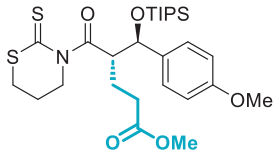

2fa
2 mol% cat, 3 h
dr 82:18 *ee* 94% 62%

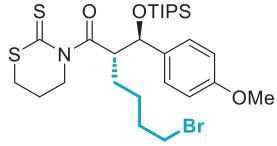

2ga
2 mol% cat, 15 h
dr 79:21 *ee* 99% 70%

Table 3. Thioimide scope of direct *anti* aldol reaction.

Once the scope of the reaction was firmly established, our group evaluated the displacement of the scaffold to obtain enantiomerically pure derivatives (Scheme 31).[36]

With this aim, these studies were carried out by Stuart Kennington in his Thesis, starting with the synthesis of different amides, including activated amides such as morfoline or Weinreb amide, was tested by nucleophilic displacement of the scaffold with the corresponding amine catalysed by 20 mol% of DMAP without detriment to the stereoselectivity. Furthermore, the absolute configuration of amide derived from (*S*)-α-Methylbenzylamine was assigned to the (2*S,* 3*S*) *via* X-ray analysis. To our pleasure, all these products were isolated in high yields (>80%), and even quantitative yield was achieved for the morpholine amide derivative. The aldol product can be reduced under mild conditions using $LiBH_4$ to furnish the corresponding alcohol in an 85%

yield. Esters can also be prepared by nucleophilic displacement using DMAP (20 mol%) as catalyst. Furthermore, the sodium enolate of ethyl acetate was used to obtain β-ketoesters with a remarkable 78% yield, which is a very powerful platform in enolate-based reactions.

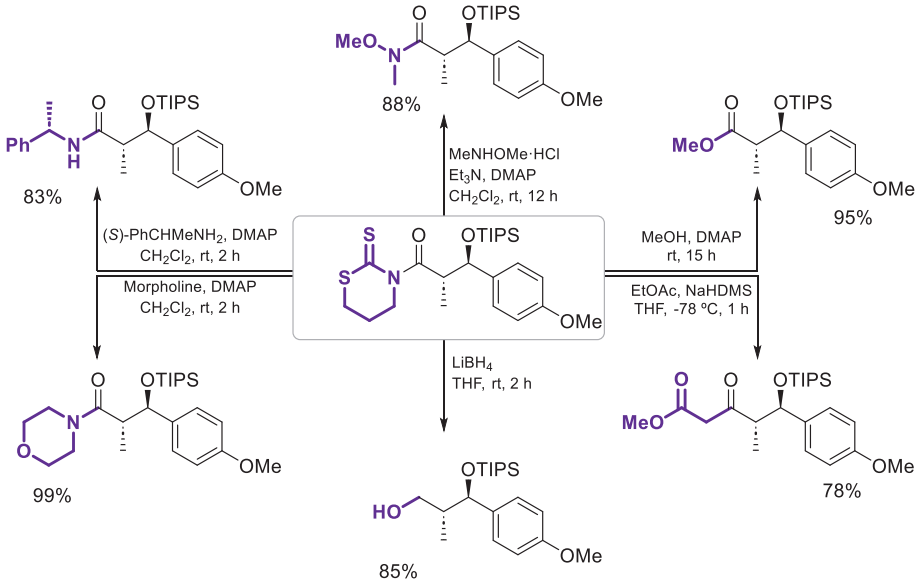

Scheme 31. Removal of the heterocycle.

2.2 Mechanistic studies

Theoretical calculations were carried out by Dr. Gabriel Aullón to shed light on a plausible mechanism compatible with the experimental data, which would be helpful for a better understanding of the experimental trends and suggest a transition state to account for the stereochemical outcome of the reaction.[36]

To initiate the study of the possible transition states, the molecular geometry of the enolate [{(*R*)-Tol-BINAP}Ni(thiazinanethione)]$^+$ was optimized in its singlet state. The most stable conformation represented in Figure 12 involves a slightly distorted square planar chelated nickel(II) enolate.

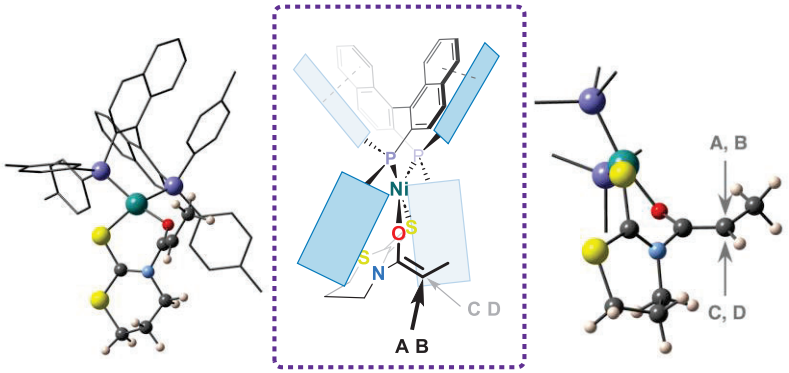

Figure 12. Optimized geometry of the nickel(II) enolate.

With this optimized geometry, the most favourable transition states leading to the different stereoisomers were analysed. The calculations were based on the previous enolate geometry combined with the oxocarbenium intermediate (TIPSO)CH(C_6H_4OMe)$^+$.

From the four transition states, A and C would lead to the *anti* diastereomers with opposite enantioselectivity, while B and D would lead to the *syn* diastereomers with opposite enantioselectivity (Figure 13). The results showed large energy difference (>2.2 kcal/mol) between the approach of the enolate from the *Re* face (Figure 13, transition states A and B) and that from the *Si* face (Figure 13, transition states C and D), therefore contributing the latter ones less than 1%, which accounted for the excellent enantioselectivity.

The diastereoselectivity was also explained by the energy difference between transition states A and B, which corresponds to a theoretical 68:32 ratio, in good agreement to the experimental ratio (*anti*/*syn* 85:15).

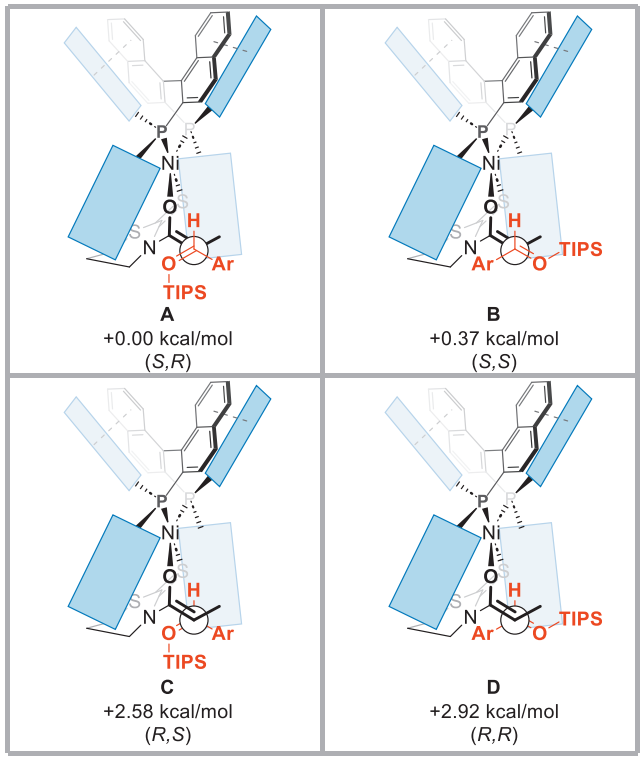

Figure 13. Transition states of the aldol addition.

An important detail to understand the energy order involves the additional stabilization through Van-der-Waals H···H interactions between the isopropyl groups of the silyl substituents and the thiazinanethione ring (distances <2.5 Å), which would explain the extra stability of transition state A and C over B and D respectively. As said, Ni(II) atom presents a close to a square-planar geometry, and it was found that D presents the most important destabilization through an interaction between the tolyl substituent of the phosphine and the aromatic group, forcing the TIPS group to adopt a near linear geometry far from ideal (132° in the free electrophile).

Therefore, we proposed the catalytic cycle, in which the nickel(II) chloride acts as a precatalyst, which is first activated by the silyl triflate to generate the true catalyst. This nickel(II) triflate complex chelates to the *N*-acyl-thiazinanethione, which acidifies the α-proton leading to its deprotonation by 2,6-lutidine to generate the enolate. Simultaneously, the silyl triflate activates the aldehyde, generating the oxocarbenium intermediate which reacts through an open transition state to produce the aldol adduct and regenerate the nickel catalyst (Scheme 32).

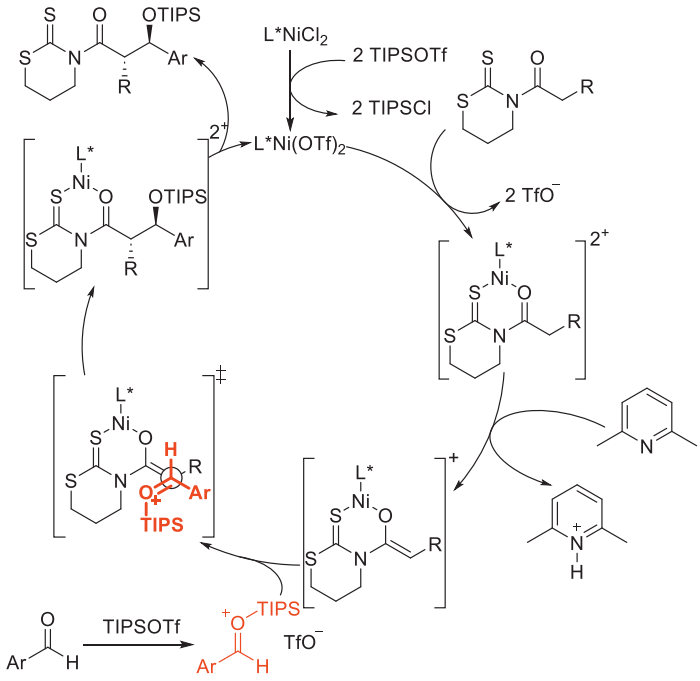

Scheme 32. Catalytic cycle of the aldol reaction.

In summary, the carbon-carbon bond forming step hinges on an open transition state, in which the Ni(II) adopts a close to square-planar geometry and one of the tolyl groups of the phosphine blocks the *Si* π-face of the resultant enolate formed, which explains the outstanding enantioselectivity obtained in all cases. In turn, the diastereoselectivity is defined by the attack through the *Re* or *Si* π-face of the oxocarbenium intermediate, and several weak interactions such as the Van-der-Waals stabilization between the trialkylsilyloxy group and the scaffold as well as distortions in the bond angles play a significant role in the π-facial differentiation.

3 Acetate aldol reaction

3.1 Introduction

Traditionally, acetate aldol reaction has received a special attention. Although it only generates one new stereocenter, the close energy of the transition states it can evolve through makes acetate aldol a particularly challenging reaction.[38] Indeed, well-developed methodologies for its propionate counterpart often fails in this type of enolates as in the case of Evans imide-derived boron enolates. One of the most successful approaches is based on the Mukaiyama aldol reaction with preformed silicon enolates promoted by chiral Lewis acids.[39] One of the first examples reported was by Mukaiyama and Kobayashi, who used a chiral diamine alongside with $Sn(OTf)_2$ in catalytic amounts (Scheme 33).[40] The power of this methodology was proved by the addition of the silyl ketene thioacetal to a chiral aldehyde, demonstrating that the inherent effect of the chiral group on the aldehyde had only a minimal impact on the stereochemical outcome, which was controlled by the chiral diamine.

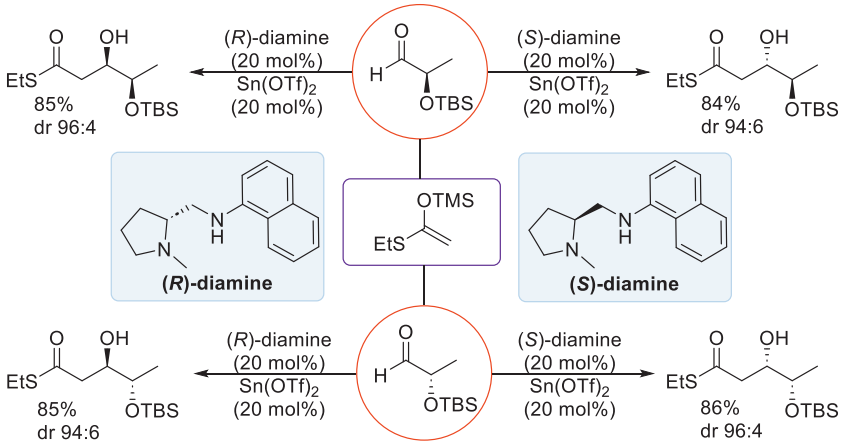

Scheme 33. Sn(II)-mediated acetate aldol reaction.

Much more recently, List showcased the potential of IDPi catalysts to activate substrates in highly stereoselective transformations proceeding through open transition states. A particular case of interest is the cross aldol reaction from aldehyde silyl enol ethers (Scheme 34).[41] This example is highly challenging due to the similar reactivity of the final product with the initial reagent, which usually leads to extensive levels of polimerization. The ability

of IDPi to distinguish between them resulted in the obtention of a single product with a remarkable enantioselectivity.

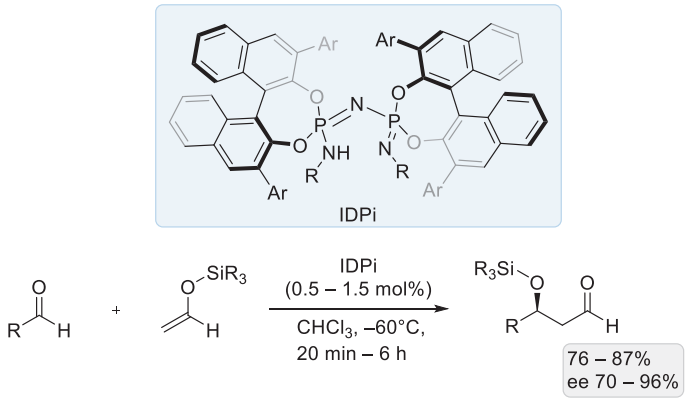

Scheme 34. IDPi organocatalysed acetate aldol reaction.

Parallel examples in direct reactions proceeding through metal enolates are scarce, Shibasaki's heterobimetallic compound LLB and Trost zinc ProPhenol were the two seminal reports in which the acetate aldol reaction was obtained in high enantioselectivities. (Scheme 12 and 13, general introduction). However, most reported methodologies suffers from poor selectivities or narrow scope.

In this context, we were interested in investigating the feasibility of aldol transformations with the acetate counterpart.

3.2 Optimization

Taking advantage of our own experience, we initiated the exploration of the acetate aldol addition by assessing the reaction of different thioimides with *p*-methoxybenzaldehyde (**a**) as a model substrate. The sterically hindered TIPSOTf was used as Lewis acid since it had proved to be crucial for the selectivity obtained in propionate aldol reactions.

Initial attempts included the reaction of **1h** with different chiral Ni(II) catalysts. Unfortunately the enantioselectivities turned out to be disappointingly poor, being the (*R*)-BIPHEP nickel complex the best catalyst (Table 4, entry 5), and the changes in both the binaphthyl moiety or the phosphine aromatic substituents did not significantly modified the selectivity (Table 4, entries 1–3, 5–6). The introduction of bulky substituents such as DTBM or the non-aromatic phosphine BPE (Table 4, entry 7) inhibited the reaction. Although increasing the temperature facilitated the formation of

aldol adduct as for DTBM-SEGPHOS, there was no stereocontrol at all (Table 4, entry 5).

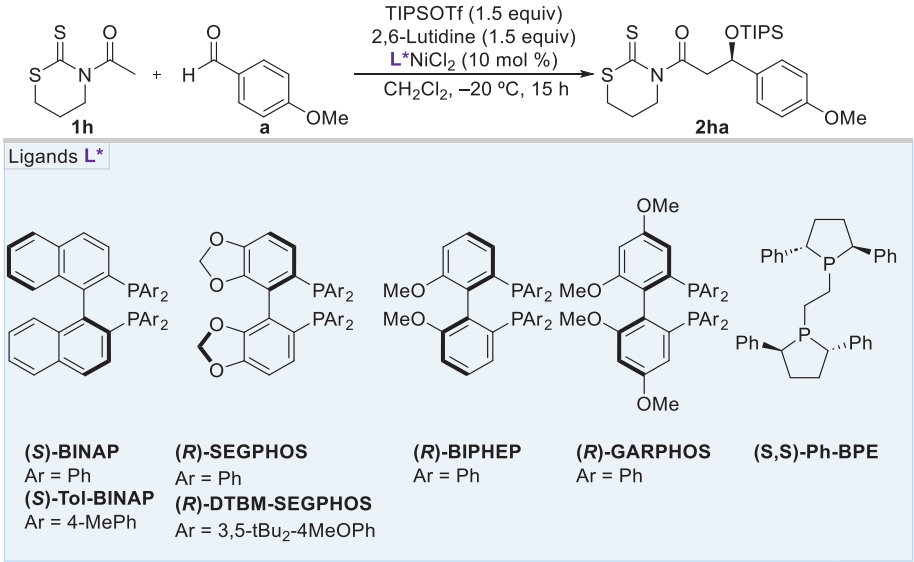

Entry	L*	Conv (%)[a]	Yield (%)[b]	*ee(%)*[c]
1	(*S*)-BINAP	72	-	30
2	(*S*)-Tol-BINAP	54	20	38
3	(*R*)-SEGPHOS	56	-	28
4	(*R*)-DTBM-SEGPHOS[d]	67	36	0
5	(*R*)-BIPHEP	98	-	42
6	(*R*)-GARPHOS	88	-	30
7	(*S,S*)-Ph-BPE	0	-	-

a) Established by ^{1}H NMR analysis. b) Isolated yield. c) Established by chiral HPLC analysis. d) 0 °C

Table 4. Chiral ligands screening with thiazinanethione.

Next, the thiazolidinthione **1i** was employed. The results were comparable to those of thiazinanethione **1h**. Modifications on both the binaphthyl structure and the aromatic substituents did not result in any significant improvement of the enantioselectivity, which remained poor around 38–44% *ee*. Particularly poor were the results with the bulky DTBM-SEGPHOS catalyst, which completely eliminate any facial discrimination, resulting in the formation of a racemic mixture of aldol adducts. Similarly to thiazinanethione, the (*R*)-BIPHEP nickel catalyst provided the best results (Table 5, entry 5).

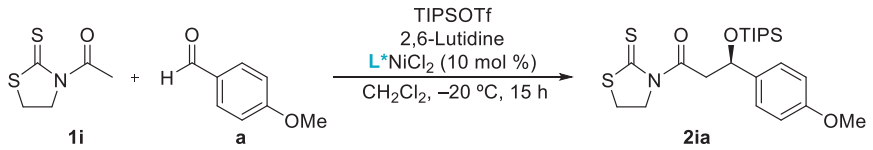

1i a 2ia

Entry	L*	Conv(%)[a]	Yield(%)[b]	*ee(%)*[c]
1	(*S*)-BINAP	54	-	42
2	(*S*)-Tol-BINAP	50	32	40
3	(*R*)-SEGPHOS	69	-	38
4	(*R*)-DTBM-SEGPHOS	80	-	0
5	(*R*)-BIPHEP	99	-	44
6	(*R*)-GARPHOS	89	-	42

a) Established by ^{1}H NMR analysis. b) Isolated yield. c) Established by chiral HPLC analysis.

Table 5. Chiral ligands screening with thiazolidinthione.

The substitution of the endocyclic sulphur with oxygen was also investigated by Vanessa Schmidt in her Erasmus thesis.[42] Unfortunately, enantioselectivities were poor in all cases, comparable to previous ones (Table 6, entries 4–7) or ever lower when oxazolidinethione **1j** were used (Table 6, entries 1–3). Both *N*-acetyl oxazinanethione **1k** and *N*-acetyl oxazolidinethione **1j** resulted in poor enantioselectivities, with similar results amongst all phosphines. Once again, the (*R*)-BIPHEP nickel catalyst provided the best results, although still not synthetically useful (Table 6, entry 6).

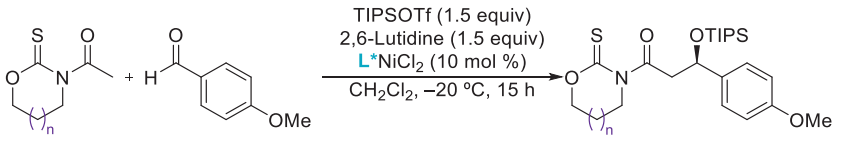

Entry	n	L*	Conv(%)[a]	Yield(%)[b]	*ee(%)*[c]
1	0	(*S*)-Tol-BINAP	95	93	28
2	0	(*R*)-BIPHEP	96	-	20
3	0	(*R*)-GARPHOS	82	69	7
4	1	(*S*)-BINAP	76	36	28
5	1	(*S*)-Tol-BINAP	62	20	40
6	1	(*R*)-BIPHEP	93	-	47
7	1	(*R*)-GARPHOS	70	54	40

a) Established by ^{1}H NMR analysis. b) Isolated yield. c) Established by chiral HPLC analysis.

Table 6. Chiral ligands screening with oxazinanethione and oxazolidinthione.

In summary, the acetate aldol reaction has proved to be a highly challenging transformation in which the differentiation of both π-faces of the aldehyde is significantly much more complicated than for the propionate counterparts. The present study indicates that the ring size and the change of the endocyclic heteroatom has no significant impact on the stereochemical outcome of the reaction. Moreover, none of the nickel catalyst from chiral phosphines, most of them based on C_2 symmetrical biarylic systems, have provided reasonably good enantioselectivities, being the [(*R*)-BIPHEP]$NiCl_2$ the most adequate among them.

At this point, it became evident that achieving high selectivities in acetate aldol reactions would require either designing a new catalytic system or developing a new platform to achieve such control. However, these objectives were out of the scope of this Thesis, and the acetate aldol reaction project was abandoned.

4 Other metal enolates for aldol reactions

In our quest to develop direct and stereocontrolled processes, we wondered if other metals could be the key for more efficient and successful catalysts. Most widely used catalysts are based on precious metals such as Pd, Pt, Ir, Ru. Unfortunately, the low abundancy of these metals renders them expensive and they usually present significant levels of toxicity. Therefore, there is a growing demand to replace these metals with more sustainable and less toxic alternatives such as 3d transition metals. Nickel has demonstrated to be highly successful in many catalysed reactions developed in our group, but we envisaged that other 3d metals might offer new options on catalysed transformations, including novel type of substrate activation.

4.1 Co catalysed aldol reactions

Cobalt catalysis represents an excellent complement to that supported by nickel. Indeed, nickel(II) complexes usually present a square planar geometry, typically observed in d^8 metal complexes. Whereas, cobalt(II) counterparts adopt a tetrahedral or octahedral geometry, greatly modifying the sterical demand of the ligands attached.

Additionally, cobalt catalysed transformations are uncommon, and just a few reports describe them on direct asymmetric aldol reactions. [43,44] The first example was reported independently by Duan[45] and Reiser,[46] in which *L*-proline combined with cobalt(II) salts acts as the catalytic species, albeit only modest levels of selectivity were achieved in most cases (Scheme 35).

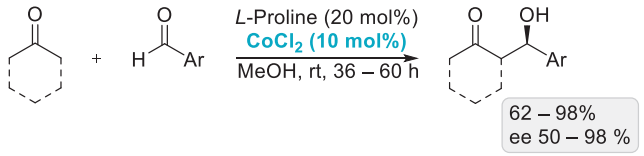

Scheme 35. Cobalt(II)-proline complex catalysed aldol reaction.

In this context, and considering that the development of a cobalt catalysed asymmetric direct aldol reactions could provide an excellent alternative to the nickel counterpart, we analysed different cobalt species as catalysts for the well-developed TESOTf-mediated aldol reaction described in Section 2 to test their catalytic potential.

The start of this project was grounded on the use of thiazolidinthione **1l** alongside with 4-methoxybenzaldehyde in the presence of TESOTf as the Lewis acid and 2,6-lutidine as the base. Initial trials were conducted at 0 °C for 16 h with a 20 mol% of catalyst loading. The obtained results are summarized in Table 7 revealed that $CoCl_2$ and $Co(OAc)_2$ were pretty active (Table 7, entries 2, 5). Surprisingly, they displayed higher activity compared to the nickel counterparts (Table 7, entries 1 and 4), which yielded a complex mixture of products in very low conversion and none of them being the aldol product. Cobalt(III) species such as CoF_3 were inactive leading only to the recovery of the starting materials (Table 7, entry 2). Other cobalt salts yielded complex mixtures of products, detecting the aldol adduct **3la** only in the $Co(acac)_2$ (Table 7, entry 6) although it was not possible to determine the diastereomeric outcome.

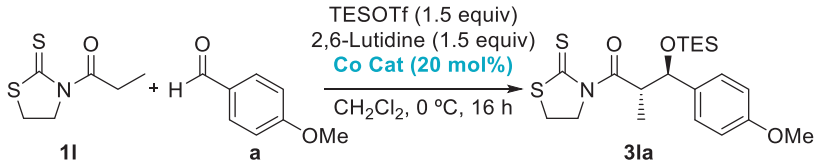

1l **a** **3la**

Entry	Catalyst	Conv(%)[a]	dr (*anti:syn*)[b]	Aldol adduct Detected[b]	Yield (%)[c]
1	$NiCl_2$	38	-	✗	Complex mixture
2	$CoCl_2$	72	59:41	✓	60
3	CoF_3	0	-	✗	-
4	$Ni(OAc)_2$	69	-	✗	0
5	$Co(OAc)_2$	80	70:30	✓	22
6	$Co(acac)_2$	23	-	✓	Complex mixture
7	$Co(NO_3)_2$	69	-	✗	Complex mixture
8	$CoSO_4$	76	-	✗	Complex mixture

a) Starting material recovered established by ^1H NMR analysis using methyl 4-nitrobenzoate as internal reference. b) Established by ^1H NMR analysis. c) NMR yield using methyl 4-nitrobenzoate as internal reference.

Table 7. Cobalt catalysed aldol reaction.

These results suggest that actually cobalt species could indeed serve as catalysts to generate the corresponding cobalt(II) enolates, which may exhibit higher activity than the corresponding nickel (II) enolates. With these results in mind, we introduced organic ligands in the structure with the objective of making cobalt complexes chiral and useful catalysts for asymmetric transformations

Our initial approach used achiral and readily available ligands, with a similar reactivity than their chiral counterparts. In this regard, we first chose triphenylphosphine, which should have a similar reactivity and catalyst stability as the chiral biarylphosphines counterparts. Additionally, we considered the Schiff base ligand SALEN, whose chiral counterparts are commercially available (Figure 14).

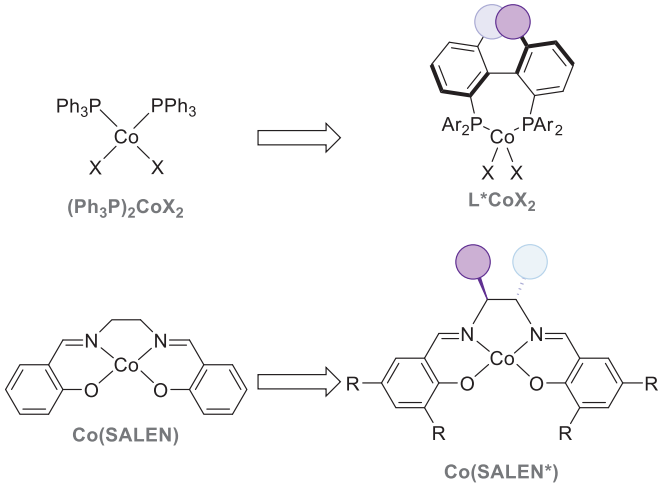

Figure 14. Chiral counterparts of SALEN and phosphine ligands.

To our delight, three commercially available cobalt species, including the Co(I) phosphine catalyst, gave good to high conversions and the desired aldol adducts were obtained in high yields (Table 8, entries 1–3). Surprisingly, the *in situ* preparation of the catalyst by adding $CoCl_2$ and PPh_3 resulted in the obtention of the complementary stereoisomer, albeit several byproducts appeared thus limiting the utility of the latter approach (Table 8, entry 4).

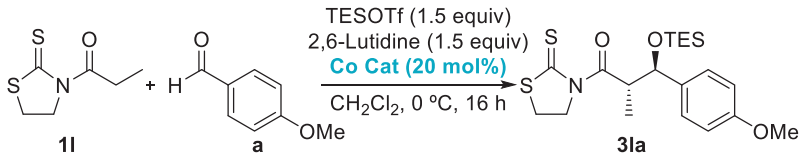

Entry	Catalyst	Conv (%)[a]	dr (*anti:syn*)[b]	Yield (%)[c]
1[47]	Co(SALEN)	92	70:30	90
2	$(Ph_3P)_3CoCl$	70	77:23	69
3	$(Ph_3P)_2CoCl_2$	76	71:29	66
4	$CoCl_2$ + 2 PPh_3	-	20:80	Complex mixture

a) Starting material recovered established by ^{1}H NMR analysis using methyl 4-nitrobenzoate as internal reference. b) Established by ^{1}H NMR analysis. c) NMR yield using methyl 4-nitrobenzoate as internal reference.

Table 8. Cobalt complex screening for the cobalt catalysed aldol reaction.

With these exciting results in hand, we proceeded to further optimize all these reactions. We initially analysed the impact of the catalyst loading and the concentration on the reaction kinetics while maintaining the lowest temperature to not compromise the reaction selectivity We found that the reaction could be carried out with just 10 mol% of cobalt catalyst at high concentration give the aldol adduct in >95% conversion in just 5 h at 0 °C.

Next, we analysed the reaction from different thioimides commonly used, substituting both the exocyclic and endocyclic heteroatom, as well as the ring size. Moving from five to six membered ring heterocycle **1a** enhanced the diastereoselectivity, albeit it reduced substantially the yield (Table 9, entries 4–6). Substitution of the endocyclic sulphur by oxygen in the five membered ring heterocycle **1m** leaded to degradation products with low yields of the aldol addition (Table 9, entries 7–9), while in the six membered ring **1n** leaded to extensive degradation (Table 9, entries 10–12). In turn, employing an exocyclic oxygen inhibited the reaction, and starting materials were recovered unchanged (Table 9, entries 13–15).

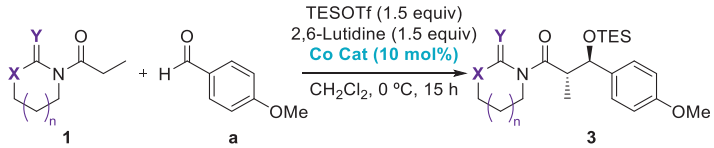

1 a 3

Entry	X,Y	N	Catalyst	Conv (%)[a]	dr (*anti:syn*)[b]	Yield (%)[c]
1	S,S	0	$(Ph_3P)_3CoCl$	70	77:23	69
2	S,S	0	$(Ph_3P)_2CoCl_2$	80	76:24	80
3[47]	S,S	0	$(SALEN)CoCl_2$	81	73:26	80
4	S,S	1	$(Ph_3P)_3CoCl$	74	96:4	36
5	S,S	1	$(Ph_3P)_2CoCl_2$	81	91:9	32
6[47]	S,S	1	$(SALEN)CoCl_2$	83	87:13	14
7	O,S	0	$(Ph_3P)_3CoCl$	100	-	0
8	O,S	0	$(Ph_3P)_2CoCl_2$	86	63:36	22
9[47]	O,S	0	$(SALEN)CoCl_2$	100	62:38	46
10	O,S	1	$(Ph_3P)_3CoCl$	100	-	0
11	O,S	1	$(Ph_3P)_2CoCl_2$	88	-	0
12[47]	O,S	1	$(SALEN)CoCl_2$	93	-	0
13	O,O	0	$(Ph_3P)_3CoCl$	0	-	-
14	O,O	0	$(Ph_3P)_2CoCl_2$	0	-	-
15	O,O	0	$(SALEN)CoCl_2$	0	-	-

a) Starting material recovered established by ^1H NMR analysis using methyl 4-nitrobenzoate as internal reference. b) Established by ^1H NMR analysis. c) NMR yield using methyl 4-nitrobenzoate as internal reference.

Table 9. Heterocycle optimization of cobalt catalysed reactions.

These results summarized in Table 9 clearly shows that cobalt complexes may trigger catalytic aldol reactions from five and six-membered ring thioimides. Unfortunately, they afford the *anti* aldol adduct and not the *syn* counterparts, which would be an ideal complement to the established method. However, the promising results from such substrates warrant further study involving the use of chiral cobalt complexes and a variety of Lewis acids.

4.2 Fe catalysed aldol reaction

Iron is the most abundant transition metal in earth and also the cheapest and most sustainable element to work with. Furthermore, life has adopted iron as an essential element in various biological systems, resulting in low toxicity and therefore allowing high concentrations (>1300 ppm) in pharmaceutical products, —a property that very few metal catalysts can achieve. Despite numerous efforts to replace precious metals with iron catalysts, the results have been very limited so far, proving the challenge of effectively implementing this metal in organic synthesis. In this context, we decided to explore iron as a catalyst in the direct aldol reaction, for which there are no precedents in the literature.

Following a similar strategy to that from the cobalt counterpart, the reaction was initially conducted with readily available iron salts, including the most common oxidation states. To our delight, the reaction with $FeCl_3$ yielded the corresponding aldol adduct with a promising 27% yield whereas $Fe(OAc)_2$ afforded a lower 14% yield (Table 10, entries 1–2). These firsts trials showed the potential of iron compounds to facilitate the aldol reaction.

Afterwards, we explored the use different additives to enhance the reactivity of the iron salts as well as to serve as well as a platform for the introduction of chirality. In this regard, we used diamines such as 1,10-phenantroline, 2,2'-bipyridine and 2,2'-biquinoline, alongside with triphenylphosphine. Diamines resulted in complex mixtures of products, none of them corresponding to the aldol adducts (Table 10, entries 3–6). In turn, introduction of triphenylphosphine in the iron(III) catalyst significantly reduced the reaction rate and decreased the stereoselectivity (Table 10, entry 7), although the combination of $Fe(OAc)_2$ and triphenylphosphine as ligand proved to be beneficial and gave a 67% of conversion and a promising 40% NMR yield.

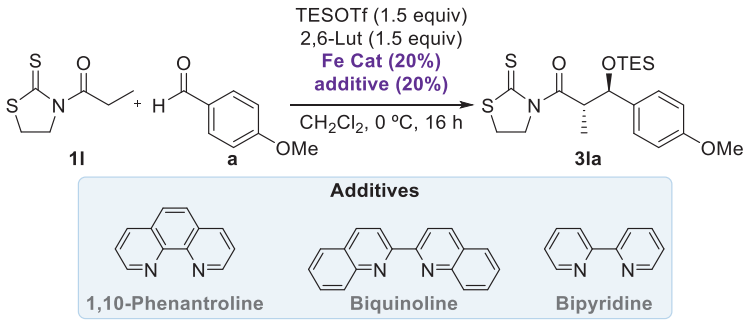

Entry	Catalyst	Additive	Conv (%)[a]	dr (*anti:syn*)[b]	Yield (%)[c]
1	$FeCl_3$	-	78	78:22	27
2	$Fe(OAc)_2$	-	49	78:22	14
3	$(Phen)FeCl_3$	-	61	-	0
4	$FeCl_3$	Phen	64	-	0
5	$FeCl_3$	Bipyridine	43	-	0
6	$FeCl_3$	Biquinoline	52	-	traces
7	$FeCl_3$	PPh_3	57	58:42	17
8	$Fe(OAc)_2$	PPh_3	67	55:45	40

a) Starting material recovered established by ^1H NMR analysis using methyl 4-nitrobenzoate as internal reference. b) Established by ^1H NMR analysis. c) NMR yield using methyl 4-nitrobenzoate as internal reference.

Table 10. Iron catalysed aldol reactions.

These very preliminary results just demonstrate that both $FeCl_3$ and $Fe(OAc)_2$ can effectively catalyse the aldol addition between thioimides **1** and activated aldehydes. Furthermore, phosphine ligand accelerates the reaction rate while preventing the formation of byproducts when combined with $Fe(OAc)_2$. Future studies should take into account these promising results and explore the impact of chiral ligands that have been employed in asymmetric transformations catalysed by iron complexes (Figure 15). These involve, bipyridine-based ligands have been successfully used at the asymmetric opening of ring epoxides, thia-Michael additions, cyclising aminofluorinations and asymmetric Mukaiyama aldol reactions. In turn, chiral diphosphines have been utilized in enantioconvergent Suzuki reactions, hydrogenations and hydrosilylation reactions.[48–51]

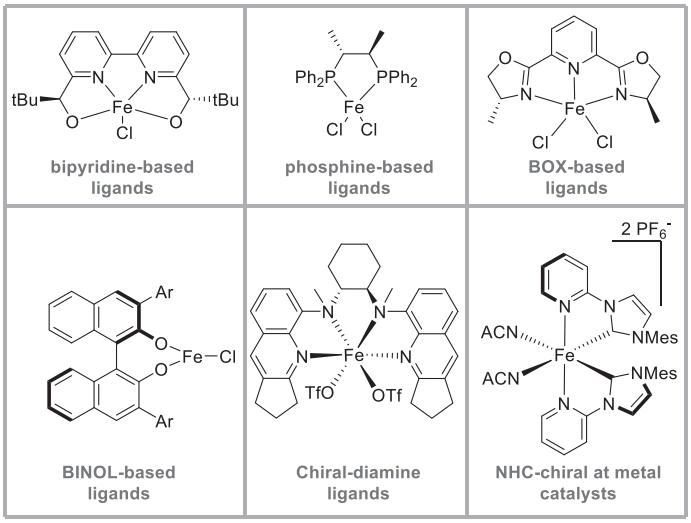

Figure 15. Iron chiral complexes.

5 Aldol reactions with α,β-unsaturated aldehydes

In parallel to these studies and aiming to expand the scope of the process, we evaluated the aldol reaction to α,β-unsaturated aldehydes due to its synthetic potential. Indeed, these reactions could furnish chiral γ,δ-unsaturated-β-hydroxy carbonyl compounds, which are among the most versatile building blocks in organic synthesis.[36]

Keeping in mind that addition of enolates to α,β-unsaturated aldehydes raises a regioselective problem, since the addition could take place not only towards the 1,2 position but also the 1,4 position, we decided to carry out a comprehensive optimization to find the appropriate conditions to achieve a highly regio- and stereoselective transformations.[2,25]

5.1 Aldol reactions with cinnamaldehyde

We started by optimizing the reaction conditions based on the ones developed previously for the *anti*-aldol addition to aromatic aldehydes, using commercially available (*E*)-cinnamaldehyde (**b**) as the model substrate. Preliminary results carried out by Stuart Kennington in his Thesis indicated that the reaction yielded mixtures of both aldol and Michael adducts.

First, we assessed the influence of the scaffold and the silyl triflate on the regio- and diastereoselectivity of the aldol reaction catalysed by $(Me_3P)_2NiCl_2$.

The results, summarized in Table 11, revealed that the regioselectivity is predominantly governed by the bulk of the silyl triflate, obtaining high selectivities towards the Michael adduct with bulky triflates such as TIPSOTf with ratios ranging from 28:72 up to 13:87, while the less bulky TMSOTf completely reverts the regioselectivity favouring the aldol addition with selectivities ranging from 73:27 up to 82:18. In contrast, the diastereoselectivity of the process is slightly affected by the Lewis acid employed, obtaining comparable results between all of them with the remarkable exception of the combination of **1m** with TMSOTf (entry 15), which lowers significantly the diastereomeric outcome.

In turn, the choice of the heterocycle had a lesser impact compared to the Lewis acid. Substitution the endocyclic sulphur atom by oxygen has a little influence in both the regioselectivity and the diastereoselectivity towards the aldol addition. Furthermore, the six-membered ring heterocycles afforded comparable results to the five membered counterparts.

In summary, optimal conditions to carry out the desired aldol addition involve using TMSOTf in combination with oxazinanethione **1n** (Table 11, entry 8), which showed the best regioselectivity towards the aldol product and an excellent diastereoselectivity.

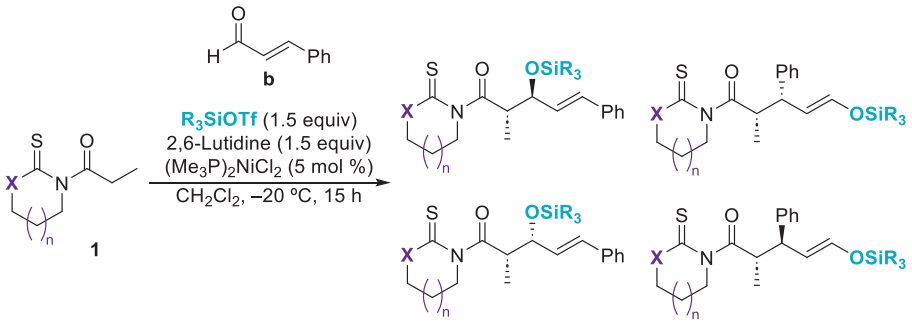

Entry	X	n	R_3SiOTf	t (h)	Conv (%)[a]	rr [a,b]	dr (1,2) [a,c]	dr (1,4) [a]
1[d]	S	1	TIPSOTf	5	93	15:85	-	81:19
2	S	1	TESOTf	5	88	44:56	84:16	78:22
3	S	1	TBSOTf	2	>99	67:33	76:24	78:22
4	S	1	TMSOTf	2	>95	74:26	80:20	80:20
5	O	1	TIPSOTf	5	94	27:73	-	80:20
6	O	1	TESOTf	5	94	62:38	95:5	65:35
7	O	1	TBSOTf	16	76	75:25	94:6	52:48
8[e]	O	1	TMSOTf	16	90	82:18	92:8	55:45
9	S	0	TIPSOTf	5	90	13:87	-	81:19
10	S	0	TESOTf	5	80	48:52	89:11	77:23
11	S	0	TMSOTf	2	>99	65:35	86:14	65:35
12	O	0	TIPSOTf	5	97	28:72	-	70:30
13	O	0	TESOTf	5	80	50:50	96:4	58:42
14	O	0	TBSOTf	5	85	52:48	90:10	50:50
15	O	0	TMSOTf	2	99	73:27	62:38	43:57

a) Established by ^1H NMR analysis. b) 1,2:1,4 ratio. c) Diastereomeric ratios from 1,2 adducts. d) Isolated yield. e) 43% isolated yield of TMS unprotected *anti* adduct.

Table 11. Lewis acid screening for the aldol reaction to (*E*)-cinnamaldehyde.

With these encouraging results in hand, we focused our attention on the chiral catalyst that should keep or even improve both the regio- and the diastereoselectivity with an excellent enantiocontrol.

Disappointingly, any of the commonly used chiral C_2 symmetric nickel(II) catalysts were effective (Table 12). The BIPHEP family (Table 12, entries 3–4) and the bulkier phosphines of the SEGPHOS family (Table 12, entries 6–7) gave very low conversions to the desired product **4nb** (<5%) and provided complex mixtures of subproducts, likely due to the nucleophilic addition of the exocyclic sulphur to cinnamaldehyde. In contrast, BINAP family (Table 12, entries 1–2), the less bulky SEGPHOS Table 12, entry 5) and the GARPHOS family (Table 12, entries 8–10) yielded almost equimolar mixtures of 1,2- and 1,4-adducts. Moreover, the diastereoselectivities were also lower than the ones obtained using the achiral $(Me_3P)_2NiCl_2$ catalyst.

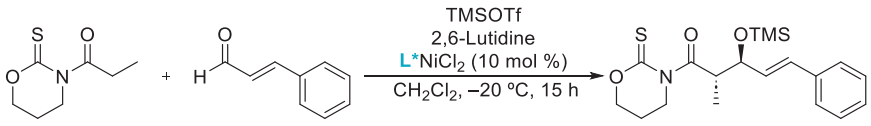

1n b 4nb

Entry	L*	Conv (%)[a]	rr (1,2:1,4)[a]	dr (*syn/anti*)[a,b]
1	(*S*)-BINAP	85	49:51	30:70
2	(*S*)-Tol-BINAP	40	50:50	28:72
3	(*R*)-BIPHEP	0	-	-
4	(*R*)-TM-BIPHEP	<5	-	-
5	(*R*)-SEGPHOS	67	43:57	33:67
6	(*R*)-DM-SEGPHOS	0	-	-
7	(*R*)-DTBM-SEGPHOS	<5	-	-
8	(*R*)-GARPHOS	64	46:54	31:69
9	(*R*)-DMM-GARPHOS	52	58:42	22:78
10	(*R*)-DTBM-GARPHOS	34	51:49	11:89

a) Established by ^{1}H NMR analysis. b) Diastereomeric ratio of aldol adduct

Table 12. Chiral ligand screening for the aldol reaction with cinnamaldehyde.

In a final attempt to obtain regioselectively the desired aldol addition we also explored the reaction of α-methyl-cinnamaldehyde (**c**). The reaction was conducted with two different catalysts. In this occasion the use of BINAP ligand (Table 13, entry 1) resulted exclusively in the formation of byproducts related to the exocyclic *S*-alkylation, while DTBM-SEGPHOS (Table 13, entry 2) afforded much better stereoselectivities, producing only one diastereomer albeit with a modest regioselectivity.

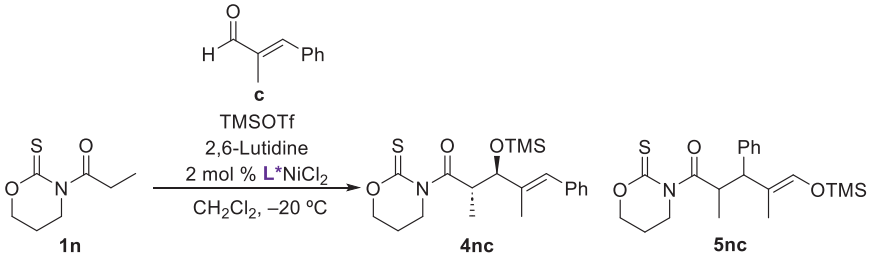

1n 4nc 5nc

Entry	L*	t (h)	Conv (%)[a]	rr (1,2:1,4)[a]	dr (major/minor)[a,b]
1	(*R*)-BINAP	2	0	-	-
2	(*R*)-DTBM-SEGPHOS	2	>95	65:35	>95

a) Established by ^{1}H NMR analysis. b) Diastereomeric ratio of aldol adduct.

Table 13. Chiral ligand screening for α-methyl α,β-unsaturated aldehydes.

These results improved those from cinnamaldehyde, albeit the regioselectivity was not synthetically useful, which led us to abandon the study of this transformation.

5.2 Aldol reaction with propargyl aldehydes

Propargyl aldehydes represent another class of α,β-unsaturated substrates that could give access to highly versatile products. Indeed, the resultant compounds might serve as useful substrates for reduction processes, facilitating formal aldol addition to non-aromatic aldehydes and undergo partial reductions to yield (*E*) or (*Z*) allylic alcohols.

As they also raise the intricate challenge of controlling simultaneously the regio-, diastereo- and enantioselectivities, we first used the optimized conditions to assess the feasibility of the reaction. Specifically, we used thiazinanethione **1a** alongside with phenylpropargyl aldehyde (**d**) and a combination of TIPSOTf as Lewis acid, 2,6-lutidine as the base and representative nickel(II) catalysts.

Unfortunately, complex mixtures of products containing both the 1,2 (**2ad**) and 1,4 adducts (**6**) were steadily obtained. Furthermore, a significant amount of exocyclic sulphur addition was detected, preferentially towards the 1,4 pathway forming **7** as the major product, but also obtaining a mixture of other several products. These results revealed that propargylic aldehydes were neither appropriate substrates for our purposes.

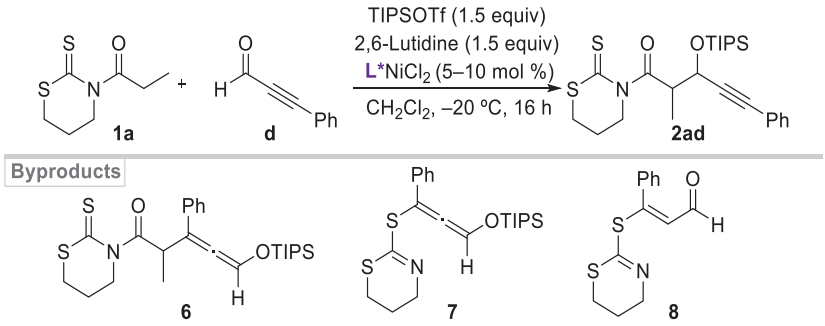

Entry	L*	Cat (mol %)	Conv (%)[a]	*S*-alkylation 7 (%)[a]
1	$(Me_3P)_2$	10	45	9
2	(*S*)-BINAP	5	82	26
3	(*R*)-DTBM-SEGPHOS	5	55	10

a) Established by ^{1}H NMR analysis.

Table 14. Aldol addition to phenylpropargyl aldehyde.

5.3 Nicholas–type aldol reaction with propargyl aldehydes

Given the difficulties encountered in controlling the aforementioned transformation, we decided to first protect the triple bond with $Co_2(CO)_8$, a strategy that had been already exploited by the group.[36,52] The role of the cobalt-protected species is twofold. First, it serves as a protecting group for the alkyne, avoiding the undesired 1,4 addition products; and secondly, it stabilizes the carbocation generated in the reaction mixture, which activates the propargylic position towards S_N1-type reactions (Scheme 36).[53,54] This approach, known as Nicholas-type reaction, has been a widely employed to produce and stabilize different types of carbocationic species.

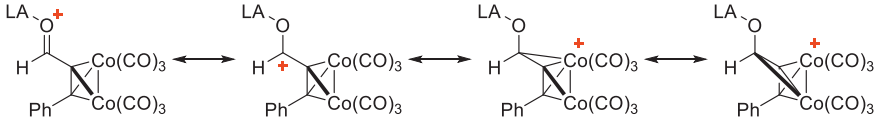

Scheme 36. Stabilization of carbocationic intermediates.

The cobalted propargyl aldehyde was readily synthesized in high yields by mixing $Co_2(CO)_8$ with propargyl aldehyde **d** at 0 °C in CH_2Cl_2 to give **e** in 93% yield after chromatographic purification (Scheme 37).

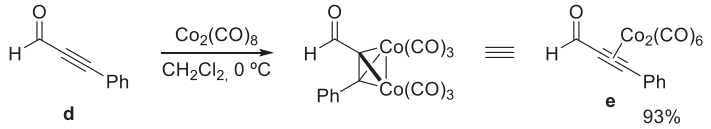

Scheme 37. Protection of propargyl aldehydes with dicobalt octacarbonyl.

A preliminary study by Stuart Kennington in his Thesis suggested that the combination of thiazolidinthione **1l** and TESOTf would be superior to that of the thiazinanethione **1a** and TIPSOTf counterpart, as the *S*-alkylation product is minimized. Based on this precedent, we examined the reaction under these conditions.

Initial trials indicated that the expected aldol adduct **3le** was obtained with good stereoselectivity, albeit in low yields. Different conditions were used to achieve complete conversion, as summarized in Table 15, which illustrated that long reaction times and high catalyst loadings resulted in lower yields, suggesting a possible product degradation under reaction conditions.

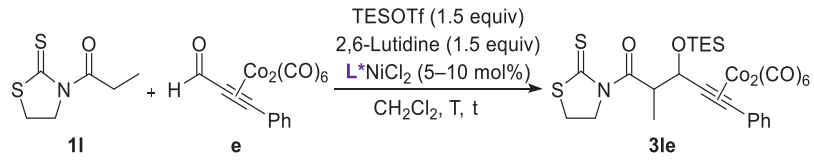

Entry	L*	Cat (%)	T (°C)	t (h)	Conv (%)[a]	dr (major/minor)[b]	yield[c]
1	(*R*)-DTBM-SEGPHOS	5	0	16	66	85:15	48
3	(*R*)-DTBM-SEGPHOS	10	0	16	100	87:13	(35),34
4	(*S*)-BINAP	10	0	16	100	78:22	-
6	(*R*)-DTBM-SEGPHOS	10	0	5	100	>97:3	(60),44
7	(*R*)-DTBM-SEGPHOS	10	-20	5	3	-	-
8	(*R*)-DTBM-SEGPHOS	7.5	0	5	100	>97:3	(60)

a) Starting material recovered established by ^{1}H NMR analysis using methyl 4-nitrobenzoate as internal reference. b) Established by ^{1}H NMR analysis. c) (NMR yield) isolated yield, using methyl 4-nitrobenzoate as internal reference.

Table 15. Catalyst optimization of the aldol addition to cobalted propargyl aldehydes.

With these results in hand, we assessed the impact of the heterocycle on the reaction outcome (Scheme 38). The reactions conducted with 6-membered ring heterocycles **1a** and **1n** resulted in the formation of a complex mixture of products. In contrast, the 5-membered counterparts afforded the protected aldol adducts without any detected byproducts, albeit with moderate yields. However, the lower selectivity of **1m** prompted us to discard this option in favour of **1l**.

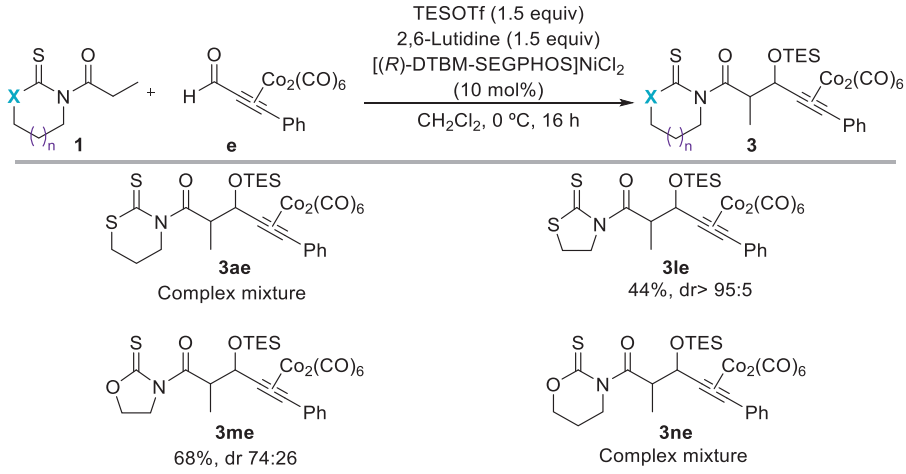

Scheme 38. Assessment of the scaffold.

Such puzzling results led us to launch a further scrutiny of the experimental conditions in an attempt to understand the key points of this aldol reactions. Unexpectedly, the reaction without the nickel complex yielded exclusively the aldol adduct **3le** without any byproducts, obtaining a full conversion and as a single diastereomer (Scheme 39).

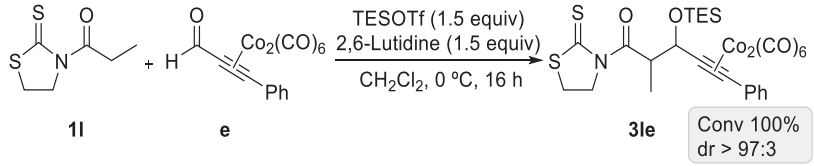

Scheme 39. Non-catalysed aldol addition to cobalted propargyl aldehydes.

This result suggests that the nickel catalyst was not responsible in the outcomes observed in all previous reactions, and consequently, the enantioselectivity was likely not being controlled as presumed. Subsequent analysis of the enantioselectivity of several batches of the resultant aldol adducts unveiled a very low enantiocontrol (0% *ee*).

The main hypothesis was that cobalt species formed in the synthesis or purification of the protected aldehyde could be the ones responsible of catalysing the aldol reaction without control of the selectivity. A careful purification of the cobalt protected aldehydes improved the results, but a significant contribution of the background reaction remained active, and overall the stereocontrol was still poor (7% *ee*). Finally, changes of the heterocycle and the Lewis acid turned to be unsuccessful, achieving higher enantioselectivities albeit with very low reproducibilities (47–77% *ee*).

In summary, and despite our efforts in the addition of nickel enolates from thioimides to a cobalted propargyl aldehyde, it proved to be troublesome due to undesired background reactions catalysed by cobalt salts.

6 Outline

Overall, Chapter I describes novel approaches towards direct asymmetric aldol reactions from thioimides catalysed by chiral nickel (II) complexes.

Indeed, a new method to furnish TIPS-protected *anti* aldol adducts has been successfully developed. This hinges on the use of the chiral [(*R*)-Tol-BINAP]$NiCl_2$, which provides high levels of stereocontrol with exceptional enantioselectivities, up to 99% *ee*. Remarkably, it has been established the high chemoselectivity of the method by analysis of a wide array of substrates.

Disappointingly, acetate aldol reactions proved to be challenging transformations, and the resultant products were obtained with poor enantioselectivities.

Unfortunately, parallel studies with α,β-unsaturated aldehydes have presented challenges in terms of regiocontrol, resulting in poor regioselectivities with trialkylsilyl triflates as Lewis acids. However, it has been found that less sterically demanding Lewis acids favours the 1,2 addition pathway, leading to the use of acetals as equivalents to activated aldehydes.

Interestingly, cobalt and iron complexes are promising candidates to develop more efficient catalytic methods. Indeed, preliminary studies open new pathways for the development of novel and sustainable catalysts to complement the reactivity based on nickel catalysts.

Finally, the reactivity of propargyl aldehydes and cobalted propargyl aldehydes also have been examined. Unfortunately, background processes without stereochemical control prevented us to attain successful results.

7 References

(1) Trost, B. M.; Brindle, C. S. The Direct Catalytic Asymmetric Aldol Reaction. *Chem. Soc. Rev.* **2010**, *39* (5), 1600–1632.

(2) Yamashita, Y.; Yasukawa, T.; Yoo, W. J.; Kitanosono, T.; Kobayashi, S. Catalytic Enantioselective Aldol Reactions. *Chem. Soc. Rev.* **2018**, *47* (12), 4388–4480.

(3) Mukaiyama, T.; Narasaka, K.; Banno, K. New Aldol Type Reaction. *Chem. Lett.* **1973**, *2* (9), 1011–1014.

(4) Mukaiyama, T.; Kobayashi, S.; Uchiro, H.; Shiina, I. Catalytic Asymmetric Aldol Reaction of Silyl Enol Ethers with Aldehydes by the Use of Chiral Diamine Coordinated Tin(II) Triflate. *Chem. Lett.* **1990**, *19* (1), 129–132.

(5) Kobayashi, S.; Furuya, M.; Ohtsubo, A.; Mukaiyama, T. Catalytic Asymmetric Aldol Reaction of the Silyl Enol Ether of Acetic Acid Thioester with Aldehydes Using Chiral Tin(II) Lewis Acid. *Tetrahedron Asymmetry* **1991**, *2* (7), 635–638.

(6) Mukaiyama, T.; Uchiro, H.; Kobayashi, S. Perfect Stereochemical Control in the Synthesis of *Syn*-α-Methyl-β-Hydroxy Thioesters by Asymmetric Aldol Reaction of Silyl Enol Ethers with Aldehydes. *Chem. Lett.* **1989**, *18* (6), 1001–1004.

(7) Mukaiyama, T.; Uchiro, H.; Kobayashi, S. An Efficient Chiral Promoter in the Aldol-Type Reaction. Chiral Diamine Coordinated Tin(II) Triflate–Dibutyltindiacetate Complex. *Chem. Lett.* **1989**, *18* (10), 1757–1760.

(8) Evans, D. A.; Bartroli, J.; Shih, T. L. Enantioselective Aldol Condensations. 2. Erythro-Selective Chiral Aldol Condensations via Boron Enolates. *J. Am. Chem. Soc.* **1981**, *103* (8), 2127–2129.

(9) Denmark, S. E.; Su, X.; Nishigaichi, Y.; Coe, D. M.; Wong, K.-T.; Winter, S. B. D.; Choi, J. Y. Synthesis of Phosphoramides for the Lewis Base-Catalyzed Allylation and Aldol Addition Reactions. *J. Org. Chem.* **1999**, *64* (6), 1958–1967.

(10) Gao, J.; Bai, S.; Gao, Q.; Liu, Y.; Yang, Q. Acid Controlled Diastereoselectivity in Asymmetric Aldol Reaction of Cycloketones with Aldehydes Using Enamine-Based Organocatalysts. *Chem. Commun.* **2011**, *47* (23), 6716–6718.

(11) Martínez-Castañeda, Á.; Poladura, B.; Rodríguez-Solla, H.; Concellón, C.; Del Amo, V. Direct Aldol Reactions Catalyzed by a Heterogeneous Guanidinium Salt/Proline System under Solvent-Free Conditions. *Org. Lett.* **2011**, *13* (12), 3032–3035.

(12) Evans, D. A.; Ennis, M. D.; Mathre, D. J. Asymmetric Alkylation Reactions of Chiral Imide Enolates. A Practical Approach to the Enantioselective Synthesis of Alpha-Substituted Carboxylic Acid Derivatives. *J. Am. Chem. Soc.* **1982**, *104* (6), 1737–1739.

(13) Schreyer, L.; Properzi, R.; List, B. IDPi Catalysis. *Angew. Chem. Int. Ed.* **2019**, *58* (37), 12761–12777.

(14) Kaib, P. S. J.; Schreyer, L.; Lee, S.; Properzi, R.; List, B. Extremely Active Organocatalysts Enable a Highly Enantioselective Addition of Allyltrimethylsilane to Aldehydes. *Angew. Chem. Int. Ed.* **2016**, *55* (42), 13200–13203.

(15) Mayer, S.; List, B. Asymmetric Counteranion-Directed Catalysis. *Angew. Chem. Int. Ed.* **2006**, *45* (25), 4193–4195.

(16) Garcia-Garcia, P.; Lay, F.; Garcia-Garcia, P.; Rabalakos, C.; List, B. A Powerful Chiral Counteranion Motif for Asymmetric Catalysis. *Angew. Chem. Int. Ed.* **2009**, *48* (24), 4363–4366.

(17) Pousse, G.; Cavelier, F. Le; Humphreys, L.; Rouden, J.; Blanchet, J. Brønsted Acid Catalyzed Asymmetric Aldol Reaction: A Complementary Approach to Enamine Catalysis. *Org. Lett.* **2010**, *12* (16), 3582–3585.

(18) Rahman, Md. A.; Cellnik, T.; Ahuja, B. B.; Li, L.; Healy, A. R. A Catalytic Enantioselective Stereodivergent Aldol Reaction. *Sci. Adv.* **2023**, *9* (11).

(19) Moser, D.; Schmidt, T. A.; Sparr, C. Diastereodivergent Catalysis. *JACS Au* **2023**, *3* (10), 2612–2630.

(20) Paterson, I.; Goodman, J. M.; Isaka, M. Aldol Reactions in Polypropionate Synthesis: High π-Face Selectivity of Enol Borinates from α-Chiral Methyl and Ethyl Ketones under Substrate Control. *Tetrahedron Lett.* **1989**, *30* (50), 7121–7124.

(21) Hajos, Z. G.; Parrish, D. R. Asymmetric Synthesis of Bicyclic Intermediates of Natural Product Chemistry. *J. Org. Chem.* **1974**, *39* (12), 1615–1621.

(22) List, B.; Lerner, R. A.; Barbas, C. F. Proline-Catalyzed Direct Asymmetric Aldol Reactions. *J. Am. Chem. Soc.* **2000**, *122* (10), 2395–2396.

(23) Sasai, H.; Arai, T.; Shibasaki, M. Catalytic Asymmetric Michael Reactions Promoted by a Lithium-Free Lanthanum-BINOL Complex. *J. Am. Chem. Soc.* **1994**, *116* (4), 1571–1572.

(24) Trost, B. M.; Ito, H. A Direct Catalytic Enantioselective Aldol Reaction via a Novel Catalyst Design. *J. Am. Chem. Soc.* **2000**, *122* (48), 12003–12004.

(25) Carreira, E. M.; Kvaerno, L. Classics in Stereoselective Synthesis. *Wiley-VHC* **2009**.

(26) Evans, D. A.; Thomson, B. J. Ni(II) Tol-BINAP-Catalyzed Enantioselective Orthoester Alkylations of *N*-Acylthiazolidinethiones. *J. Am. Chem. Soc.* **2005**, *127* (30), 10506–10507.

(27) Evans, D. A.; Downey, C. W.; Hubbs, J. L. Ni(II) Bis(Oxazoline)-Catalyzed Enantioselective *Syn* Aldol Reactions of *N*-Propionylthiazolidinethiones in the Presence of Silyl Triflates. *J. Am. Chem. Soc.* **2003**, *125* (29), 8706–8707.

(28) Suzuki, T.; Hamashima, Y.; Sodeoka, M. Asymmetric Fluorination of α-Aryl Acetic Acid Derivatives with the Catalytic System $NiCl_2$-Binap/R_3SiOTf/2,6-Lutidine. *Angew. Chem. Int. Ed.* **2007**, *46* (28), 5435–5439.

(29) Hamashima, Y.; Nagi, T.; Shimizu, R.; Tsuchimoto, T.; Sodeoka, M. Catalytic Asymmetric α-Chlorination of 3-Acyloxazolidin-2-One with a Trinary Catalytic System. *Eur. J. Org. Chem.* **2011**, No. 20–21, 3675–3678.

(30) Liu, Z.; Takeuchi, T.; Pluta, R.; Arteaga Arteaga, F.; Kumagai, N.; Shibasaki, M. Direct Catalytic Asymmetric Aldol Reaction of α-Alkylamides. *Org. Lett.* **2017**, *19* (3), 710–713.

(31) Takeuchi, T.; Kumagai, N.; Shibasaki, M. Direct Catalytic Asymmetric Aldol Reaction of α-Vinyl Acetamide. *J. Org. Chem.* **2018**, *83* (10), 5851–5858.

(32) Teloxa, S. F.; Kennington, S. C. D.; Camats, M.; Romea, P.; Urpí, F.; Aullón, G.; Font-Bardia, M. Direct, Enantioselective, and Nickel(II) Catalyzed Reactions of *N*-Azidoacetyl Thioimides with Trimethyl Orthoformate: A New Combined Methodology for the Rapid Synthesis of Lacosamide and Derivatives. *Chem. Eur. J.* **2020**, *26* (50), 11540–11548.

(33) Kennington, S. C. D.; Taylor, A. J.; Romea, P.; Urpí, F.; Aullón, G.; Font-Bardia, M.; Ferré, L.; Rodrigalvarez, J. Direct and Asymmetric Nickel(II)-Catalyzed Construction of Carbon-Carbon Bonds from N-Acyl Thiazinanethiones. *Org. Lett.* **2019**, *21* (1), 305–309.

(34) Mellado-Hidalgo, M.; Romero-Cavagnaro, E. A.; Nageswaran, S.; Puddu, S.; Kennington, S. C. D.; Costa, A. M.; Romea, P.; Urpí, F.; Aullón, G.; Font-Bardia, M. Protected *Syn* -Aldol Compounds from Direct, Catalytic, and Enantioselective Reactions of *N* -Acyl-1,3-Oxazinane-2-Thiones with Aromatic Acetals. *Org. Lett.* **2023**, *25* (4), 659–664.

(35) Kennington, S. C. D.; Teloxa, S. F.; Mellado-Hidalgo, M.; Galeote, O.; Puddu, S.; Bellido, M.; Romea, P.; Urpí, F.; Aullón, G.; Font-Bardia, M. Direct and Enantioselective Aldol Reactions Catalyzed by Chiral Nickel(II) Complexes. *Angew. Chem. Int. Ed.* **2021**, *60* (28), 15307–15312.

(36) Kennington, S. C. D. The Development of New, Direct and Asymmetric Ni(II) Catalysed Carbon-Carbon Bond Forming Reactions and Their Application to Total Synthesis. *PhD Thesis* **2020**, Universitat de Barcelona.

(37) Kennington, S. C. D. Synthesis and Acylation of 1,3-Thiazinane-2-Thione. *Org. Synth.* **2021**, *98*, 374–390.

(38) Palomo, C.; Oiarbide, M.; García, J. M. Current Progress in the Asymmetric Aldol Addition Reaction. *Chem. Soc. Rev.* **2004**, *33* (2), 65–75.

(39) Romea, P.; Urpí, F. Stereoselective Acetate Aldol Reactions. In *Modern Methods in Stereoselective Aldol Reactions*; Wiley-VCH, 2013; pp 1–81.

(40) Kobayashi, S.; Furuya, M.; Ohtsubo, A.; Mukaiyama, T. *Catalytic Asymmetric Aldol Reaction of the Silyl En01 Ether of Acetic Acid Thioester with Aldehydes Using Chiral Tin(II) Lewis Acid*; 1991; Vol. 2.

(41) Schreyer, L.; Kaib, P. S. J.; Wakchaure, V. N.; Obradors, C.; Properzi, R.; Lee, S.; List, B. Confined Acids Catalyze Asymmetric Single Aldolizations of Acetaldehyde Enolates. *Science (1979)* **2018**, *362* (6411), 216–219.

(42) Schmidt, V. Direct Asymmetric Aldol Reactions Catalysed by Chiral Ni(II)-Complexes. *Erasmus Thesis* **2023**, Universitat de Barcelona.

(43) Pellissier, H.; Clavier, H. Enantioselective Cobalt-Catalyzed Transformations. *Chem. Rev.* **2014**, *114* (5), 2775–2823.

(44) Pellissier, H. Enantioselective Cobalt-Catalysed Transformations. *Cobalt Catalysis in Organic Synthesis: Methods and Reactions. Chapter 10* **2020**.

(45) Wu, X.; He, C.; Wu, X.; Qu, S.; Duan, C. An L-Proline Functionalized Metallo-Organic Triangle as Size-Selective Homogeneous Catalyst for Asymmetry Catalyzing Aldol Reactions. *Chem. Commun.* **2011**, *47* (29), 8415.

(46) Karmakar, A.; Maji, T.; Wittmann, S.; Reiser, O. *L*-Proline/$CoCl_2$ - Catalyzed Highly Diastereo- and Enantioselective Direct Aldol Reactions. *Chem. Eur. J.* **2011**, *17* (39), 11024–11029.

(47) Davies-Howe, E. Direct and Enantioselective C–C Bond Forming Reactions Catalysed by 1st Row Transition Metals. *Erasmus Thesis* **2023**, Universitat de Barcelona.

(48) Morris, R. H. Exploiting Metal-Ligand Bifunctional Reactions in the Design of Iron Asymmetric Hydrogenation Catalysts. *Acc. Chem. Res.* **2015**, *48* (5), 1494–1502.

(49) Pellissier, H. Recent Developments in Enantioselective Iron-Catalyzed Transformations. *Coord. Chem. Rev.* Elsevier B.V. May 1, 2019, pp 1–31.

(50) Gopalaiah, K. Chiral Iron Catalysts for Asymmetric Synthesis. *Chem. Rev.* May 8, 2013, pp 3248–3296.

(51) Casnati, A.; Lanzi, M.; Cera, G. Recent Advances in Asymmetric Iron Catalysis. *Molecules*. MDPI AG September 1, 2020.

(52) Fernández-Valparís, J. Reacciones Directas y Estereoselectivas de N-Aciltioimidas Catalizadas Por Complejos de Níquel(II). Síntesis de derivados de La *Anti* ß-Hidroxitirosina. *PhD Thesis* **2018**, Universitat de Barcelona.

(53) Teobald, B. J. The Nicholas Reaction: The Use of Dicobalt Hexacarbonyl-Stabilised Propargylic Cations in Synthesis. *Tetrahedron* **2002**, *58* (21), 4133–4170.

(54) Nicholas, K. M.; Pettit, R. On the Stability of α-(Alkynyl)Dicobalt Hexacarbonyl Carbonium Ions. *J. Organomet. Chem* **1972**, *44* (1), 21–24.

CHAPTER II

The Michael reaction

Table of contents

1 Introduction

In 1887, Arthur Michael reported the conjugate addition of diethyl malonate to ethyl cinnamate in EtONa/EtOH. The resultant β-substituted ester was the first Michael adduct.[1] Such a simple addition of a nucleophile to an olefin activated with an electron withdrawing group heralded the development of one of the most important C–C bond-forming reactions, the 1,4- or Michael addition. Notable contributions to the field were due to Gilmann, who developed similar reactions with organocuprate reagents.[2] These organometallic compounds exhibit a remarkable predilection for additions to the β-position, thereby enriching the scope of conjugate addition reactions.

Since such seminal contributions, the landscape of Michael additions has undergone a profound development. Indeed, a plethora of new Michael acceptors and donors have emerged, greatly expanding the scope of the conjugate addition reactions.

Initially, the Michael reaction was developed in a two-step procedure, in which the first step involved the stoichiometric generation of the enolate, and the second step consisted of the addition of this enolate to the corresponding Michael acceptor in a process commonly referred to as an indirect Michael reaction.

The initial attempts to obtain new enantioenriched products were conducted using chiral auxiliaries such as Evans oxazolidinones.[3,4] Later, Kobayashi pioneered the development of asymmetric catalysis by using a BINOL-Ti complex.[5] Since then, other catalysts have been developed in this field, expanding the scope of this transformation (Figure 16).[6-8]

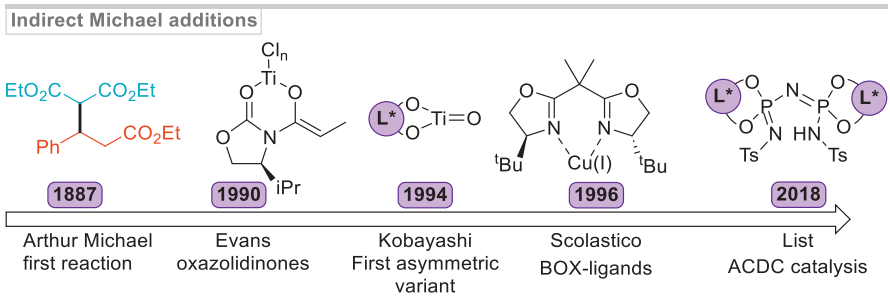

Figure 16. Milestones in the Michael reaction.

A highly desired transformation involves the *in situ* formation of the enolate and subsequent addition to the Michael acceptor, in which is known as a direct Michael reaction. This approach enables the catalytic generation of the enolate, thus increasing the overall atom economy of the transformation.[9,10]

Importantly, the first direct catalytic asymmetric variant appeared in 1975, when Wynberg pioneered the use of chiral chinchone alkaloids as catalysts.[11] Since the emergence of organocatalysis, several Michael reactions catalysed by small organic molecules, such thioureas and imidazolidinones developed by Takemoto and Macmillan respectively, have appeared. In parallel, metal-catalysed Michael additions were introduced by Brunner,[12] and further developed by Yamaguchi[13] using rubidium prolinate and Shibasaki[14] Al-BINOL (ALB) catalyst (Figure 17).[12,15-18]

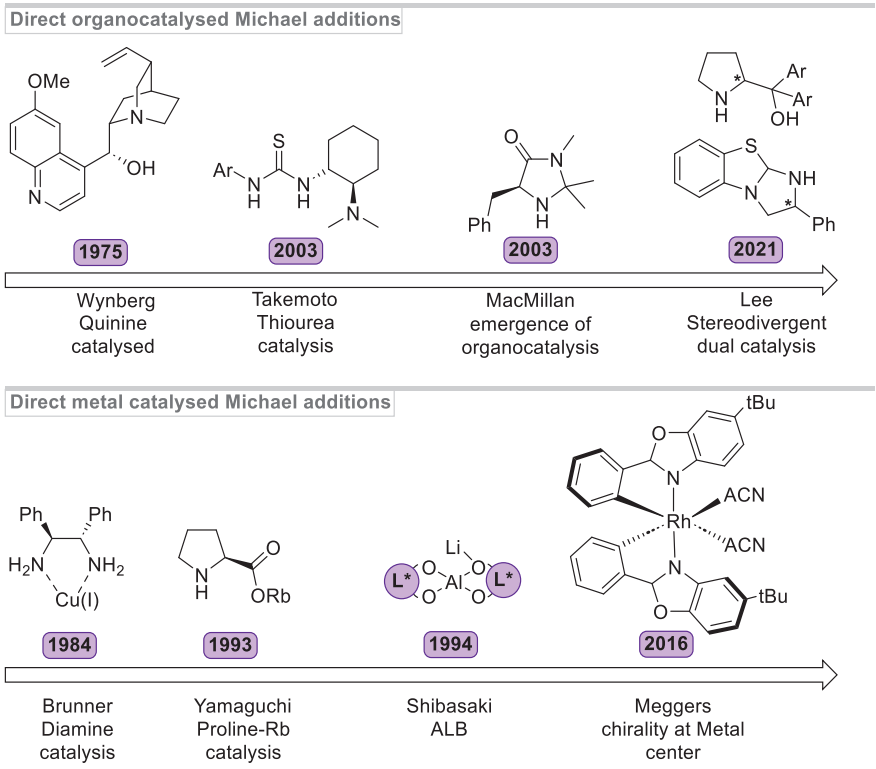

Figure 17. Direct Michael additions.

In this context, the increasing need for more efficient transformations has made the direct, asymmetric and catalytic addition of carbonyl nucleophiles to α,β-unsaturated carbonyl acceptors one of the most

interesting C–C bond forming reactions, since they provide access to valuable 1,5-dicarbonyl compounds with up to two new stereocenters. [19-21]

Unfortunately, one of the synthetically more valuable additions, which involve the use of α,β-unsaturated aldehydes remain underdeveloped. [20] This is due to the highly electrophilic character of aldehydes, which renders them prone to undergo 1,2 additions rather than the conjugate 1,4 additions.

To address the regioselectivity challenge arisen in these transformations, a common strategy hinges on organocatalytic approaches, thus avoiding the inherent activation of 1,2-position of metal catalysts. Typically, organocatalysts enhance the reactivity towards 1,4 position *via* iminium intermediates, facilitating the control of the regioselectivity of the process (Scheme 40).

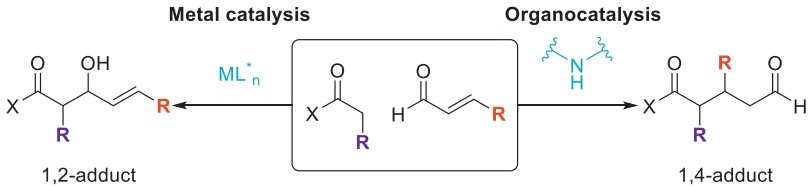

Scheme 40. Regioselectivity of the additions to α,β-unsaturated aldehydes.

The introduction of imidazolidinone catalyst by Macmillan enabled the participation of α,β-unsaturated aldehydes in Michael addition reactions. In this work, a silyloxy furane was reacted with different α,β-unsaturated aldehydes in the presence of imidazolidinone-DNBA salt *via* the formation of an iminium intermediate to give the corresponding *syn* Michael adducts in high yields (Scheme 41).[17]

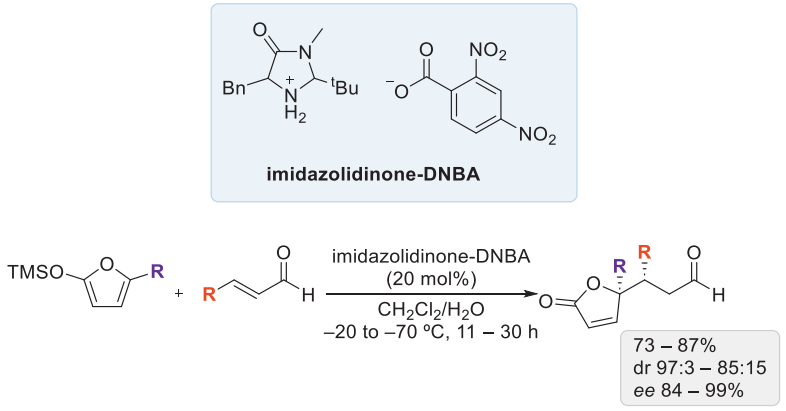

Scheme 41. Imidazolidinone catalysed Michael addition to α,β-unsaturated aldehydes.

Maruoka and coworkers devised an organocatalytic and regiodivergent approach to switch the selectivity by deactivating the inherent trend of iminium intermediates towards the 1,4 addition (Scheme 42). This was achieved by modifying the distance of the acid functionality. The proximity of this acid functionality in the diarylprolinol moiety effectively deactivates the iminium intermediate. Such deactivation of iminium pathway forces the activation of the aldehyde only by Brønsted acid catalysis, which consequently produces exclusively the 1,2 addition.[22]

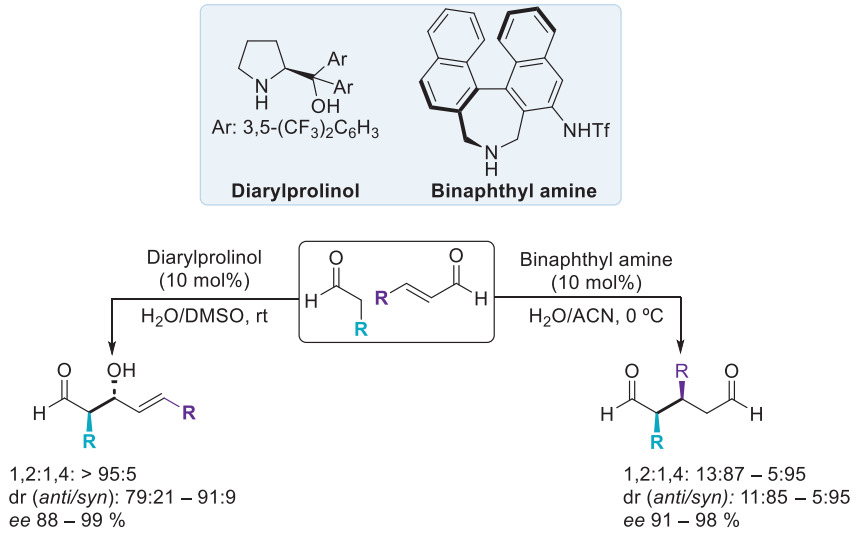

Scheme 42. Regiodivergent organocatalytic addition to α,β-unsaturated aldehydes.

In turn, Lee and coworkers developed a prominent reaction to form Michael adducts utilizing a stereodivergent approach through a dual catalytic system (Scheme 43).[18] In this method, highly acidic and labile esters pentafluorophenyl arylacetates, act as pronucleophiles, producing active species through reaction with the selected BTM catalyst. Upon reaction of the α,β-unsaturated iminium intermediate, the desired *syn* or *anti* enatiomerically pure 1,4 adduct is obtained.

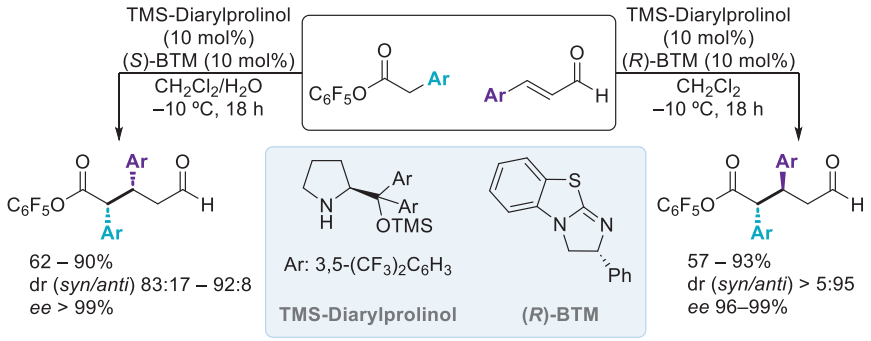

Scheme 43. Stereodivergent organocatalytic Michael addition to α,β-unsaturated aldehydes.

Although such approaches effectively produce 1,4 adducts in a regioselective manner, organocatalytic methods usually presents low reactivities, and only the most acidic pronucleophiles are capable of performing such transformations. On the other hand, there is a lack of metal-catalysed transformations to carry out such conjugate additions in a highly regio- and stereoselective manner.

In this context, we devised the possibility of using our thioimides as pronucleophiles to react them with α,β-unsaturated aldehydes, to activate the electrophilic partner and blocking the 1,2-addition in the carbonyl bond using bulky Lewis acids (Scheme 44).

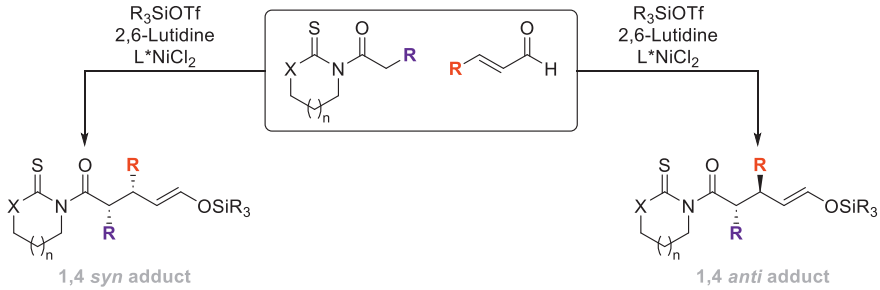

Scheme 44. Stereodivergent nickel(II) catalysed additions to α,β-unsaturated aldehydes.

2 Synthesis of α,β-unsaturated aldehydes

α,β-Unsaturated aldehydes were synthesized following a modified procedure reported by Ando,[23] which hinges on a one-pot Julia-Kocienski olefination. The synthesis of the 2,2-dimethoxyethyl 1-phenyl-1*H*-tetrazol-5-yl sulphone (PT sulphone) shown in Scheme 45 was scaled up to produce large amounts of product (>13 g). This synthesis consisted of a two-step process wherein the 1-phenyl-1*H*-tetrazole-5-thiol was coupled with bromoacetaldehyde dimethyl acetal in high yields, followed by oxidation of the resultant thioether to afford the desired PT sulphone (Scheme 45).

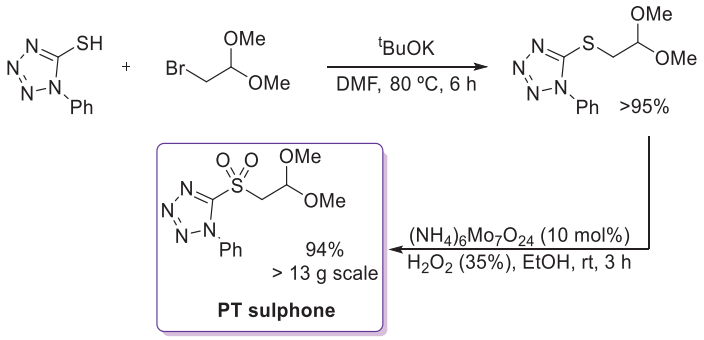

Scheme 45. Synthesis of the PT sulphone.

Next, a Julia-Kocienski olefination between that PT sulphone and the corresponding aldehyde, followed by an acid hydrolysis led to the desired α,β-unsaturated aldehydes **f–q** in good yields and excellent selectivities (Scheme 46).

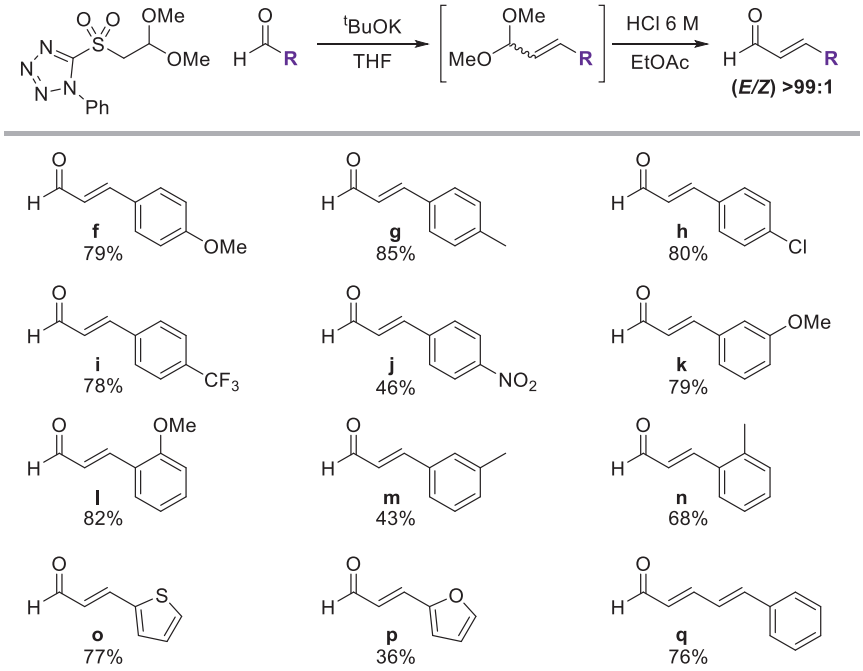

Scheme 46. Synthesis of aromatic α,β-unsaturated aldehydes.

Unfortunately, such a simple method was unsuitable for certain aldehydes. Thus, other approaches were required. For instance, (*Z*)-α-bromo-cinnamaldehyde **r** was synthesised following a literature procedure using an α-bromination of cinnamaldehyde (Scheme 47).[24]

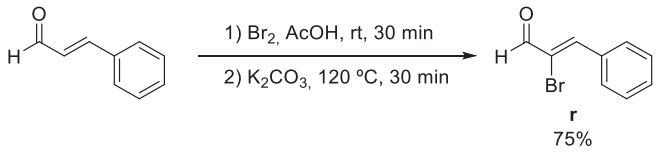

Scheme 47. Synthesis of (*Z*)-α-bromo-cinnamaldehyde.

In turn, (*E*)-iodoacrolein was synthesised by treatment of propiolaldehyde with NaI and 4 M H_2SO_4 (Scheme 48).[25] However, the resulting product was unstable upon exposure to air, necessitating its immediate utilization.

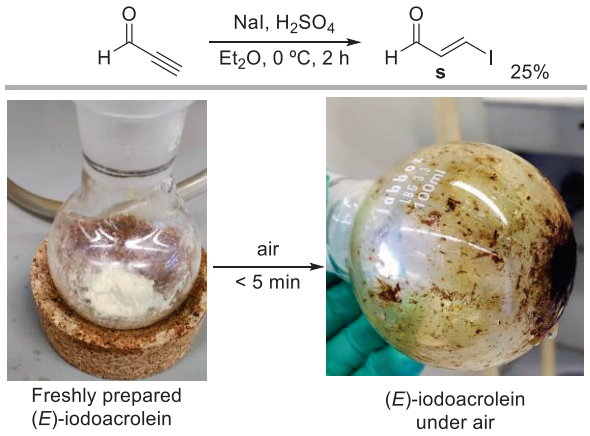

Scheme 48. Synthesis of (*E*)-iodoacrolein.

As an alternative, the slightly more stable (*Z*)-iodoacrolein was prepared via a two-step procedure.[26] As shown in Scheme 49, ethyl propiolate was treated with NaI in acetic acid at 70 °C to yield (*Z*)-ethyl-3-iodoacrylate. Subsequently, the resulting ester was reduced with DIBALH to afford the desired (*Z*)-iodoacrolein, which was utilized without further purification.

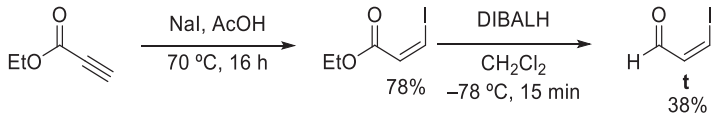

Scheme 49. Synthesis of (*Z*)-iodoacrolein.

Finally, the silylated α,β-unsaturated aldehyde **u** was synthesised in a three step sequence which involved the simultaneous silylation of the terminal alkyne and the alcohol of propargyl alcohol, followed by the hydrolysis of the resulting silyloxy group (Scheme 50).[27] Reduction of the acetylene to the (*E*)-allyl alcohol using RedAl® and oxidation of the resultant allylic alcohol with MnO_2 furnished the desired α,β-unsaturated aldehyde **u**.

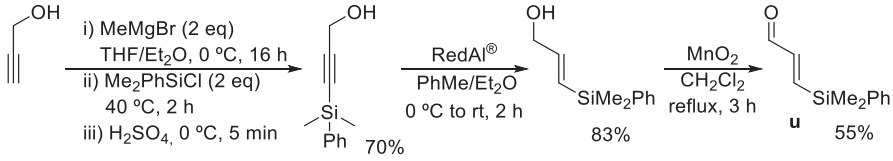

Scheme 50. Synthesis of (*E*)-3-(dimethylphenylsilyl)acrylaldehyde.

3 Results

3.1 Optimization

With the starting α,β-unsaturated aldehydes in hand, we initiated the development of a novel method to generate Michael adducts as a result of their reaction with chiral nickel enolates of thioimides to α,β-unsaturated aldehydes. As we have stated from the previous chapter (Table 10, Chapter I), increasing the steric bulk of silyl Lewis acid in the addition of thioimides to cinnamaldehyde, our α,β-unsaturated aldehyde model, significantly favoured the regioselectivity towards the Michael adduct, up to rr 13:87 using the most bulky TIPSOTf (Table 15, entries 1 and 9) while the least bulky TMSOTf provided the 1,2 adduct as the major product (Table 15, entries 4, 8, 11 and 15). Furthermore, our observations suggested that heterocycles containing a sulphur endocyclic adduct improved the regioselectivity towards the Michael product slightly (Table 15, entries 1, 5, 9 and 12).

In turn, six and five-membered scaffolds, thiazinanethione **1a** (Table 15, entries 1–4) and thiazolidinthione **1l** respectively (Table 15, entries 5–8), behave similarly, but the former usually reacted faster and the purification of the resultant product used to be easier. Consequently, the thiazinanethione **1a** was chosen as the optimal substrate to proceed with further optimization.

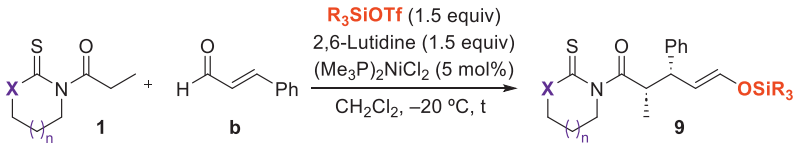

Entry	R_3SiOTf	1	X	n	t (h)	Conv (%)[a]	rr (1,2:1,4)[a]	dr (1,4)[a]
1	TIPSOTf	**1a**	S	1	5	93	15:85	81:19
2	TESOTf	**1a**	S	1	5	88	44:56	78:22
3	TBSOTf	**1a**	S	1	2	>99	67:33	78:22
4	TMSOTf	**1a**	S	1	2	>95	74:26	80:20
5	TIPSOTf	**1n**	O	1	5	94	27:73	80:20
6	TESOTf	**1n**	O	1	5	94	62:38	65:35
7	TBSOTf	**1n**	O	1	16	76	75:25	52:48
8	TMSOTf	**1n**	O	1	16	90	82:18	55:45
9	TIPSOTf	**1l**	S	0	5	90	13:87	81:19
10	TESOTf	**1l**	S	0	5	80	48:52	77:23
11	TMSOTf	**1l**	S	0	2	>99	65:35	65:35
12	TIPSOTf	**1m**	O	0	5	97	28:72	70:30
13	TESOTf	**1m**	O	0	5	80	50:50	58:42
14	TBSOTf	**1m**	O	0	5	85	52:48	50:50
15	TMSOTf	**1m**	O	0	2	99	73:27	43:57

a) Established by ^1H NMR.

Table 15. Optimization of auxiliary and Lewis acid.

Next, the impact of the solvent was evaluated. We employed [(*R*)-DTBM-SEGPHOS]$NiCl_2$ as catalyst because preliminary studies showed better results than [(*R*)-Tol-BINAP]$NiCl_2$ used in Chapter I.

To our pleasure, the use of this catalyst in CH_2Cl_2 enhanced the regioselectivity significantly towards adduct **9ab**, up to rr 98:2, while the diastereoselectivities remained high (Table 16, entry 1). The addition of large quantities of toluene slowed down the reaction rate (Table 16, entries 1–2 vs 3–4), but the 1,2-addition was completely supressed and the diastereoselectivity was substantially increased up to 88:12 (Table 16, entries 2–3). However, the solubility was troublesome in pure toluene and both conversion and diastereoselectivity were eroded (Table 16, entry 4). Substituting toluene by a non-polar solvent such as pentane resulted in the loss of diastereoselectivity (Table 16, entry 5), while the substitution of CH_2Cl_2 by 1,2-dichloroethane (DCE) had no discernible impact, maintaining the same selectivities with a slightly slower kinetics (Table 16, entry 6).

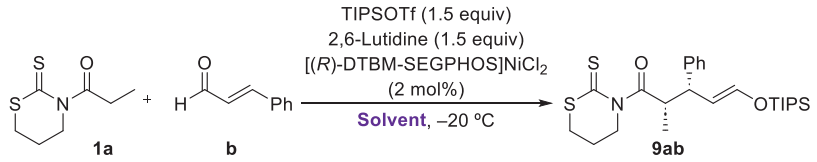

Entry	Solvent	t(h)	Conv (%)[a]	rr (1,2:1,4)[a]	dr (1,4)[a]	*syn* (%)[b]	*anti* (%)[b]
1	CH_2Cl_2	1	>97	98:2	79:21	70	19
2	PhMe/CH_2Cl_2 1:1	1	>97	>99:1	84:16	72	16
3	PhMe/CH_2Cl_2 4:1	5	>97	>99:1	88:12	80	11
4	PhMe	16	94	>99:1	84:16	-	-
5	Pentane/CH_2Cl_2 4:1	5	95	>99:1	76:24	-	-
6	PhMe/DCE 4:1	5	92	>99:1	87:13	-	-

a) Established by ^{1}H NMR analysis. b) Isolated yield.

Table 16. Optimization of the solvent.

Therefore, it was clear that the solvent had a significant impact on both the regio- and diastereoselectivity. Indeed, the *syn* Michael adduct **9ab** was the main product when the reaction was catalysed by [(*R*)-DTBM-SEGPHOS]$NiCl_2$ in 4:1 PhMe/CH_2Cl_2 (Table 17, entries 1–2). To our surprise, the diastereoselectivity also increased when [(*R*)-BINAP]$NiCl_2$ was used instead, but now the main product was the opposite diastereomer, the *anti* Michael adduct **9'ab** (Table 17, entries 3–4). Similar results were attained with [(*R*)-Tol-BINAP]$NiCl_2$ (Table 17, entries 5–6).

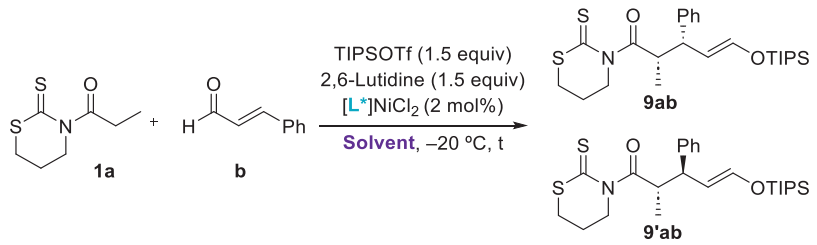

Entry	L*	Solvent	t (h)	Conv (%)[a]	rr (1,2:1,4)[a]	dr (*syn/anti*)[a]
1	(*R*)-DTBM-SEGPHOS	CH_2Cl_2	1	>97	98:2	79:21
2	(*R*)-DTBM-SEGPHOS	4:1 PhMe/CH_2Cl_2	5	>97	>99:1	88:12
3	(*R*)-BINAP	CH_2Cl_2	5	>97	97:3	51:49
4	(*R*)-BINAP	4:1 PhMe/CH_2Cl_2	5	>97	>99:1	15:85
5	(*R*)-Tol-BINAP	CH_2Cl_2	5	>97	98:2	60:40
6	(*R*)-Tol-BINAP	4:1 PhMe/CH_2Cl_2	5	>97	>99:1	15:85

a) Established by ^{1}H NMR analysis.

Table 17. Comparison of the selectivities with different catalysts and solvents.

With these exciting results in hand, we proceeded to analyse in depth the impact of the chiral ligand under the previous conditions on the regio-, diastereo-, and enantioselectivity of the reaction. With this aim, we assessed the reaction of the thiazinanethione **1a** with cinnamaldehyde catalysed by a wide range of chiral nickel(II) complexes containing commercially available atropoisomeric diphosphines shown in Table 18.

All four families of chiral biaryl phosphines (BIPHEP, GARPHOS, BINAP and SEGPHOS) provided the Michael adducts with a perfect regioselectivity (1:4/1:2 > 99:1) along with an amazing enantioselectivity (*ee* 99%). Therefore, diastereoselectivity remained as the main challenge.

Interestingly, the variation between these families was low and afforded a close range of diastereoselectivities (Table 18, entries 1, 3, 6 and 8). Contrarily, the aromatic substituent on the phosphine proved to be crucial in determining the main diastereomer. Indeed, phosphines containing small substituents rendered preferentially the *anti* diastereomer **9'ab** in selectivities up to 15:85 (Table 18, entries 1–4 and 6–9) while an increase of the steric hindrance of such aromatic substituents resulted in an increase towards the formation of the *syn* diastereomer **9ab** (Table 18, entries 4 and 10) In summary, the most significant differences are observed with DTBM aromatic substituents, which completely reverse the diastereoselectivity towards the preferential formation of the *syn* diastereomer **9ab** (Table 18, entries 5 and 10).

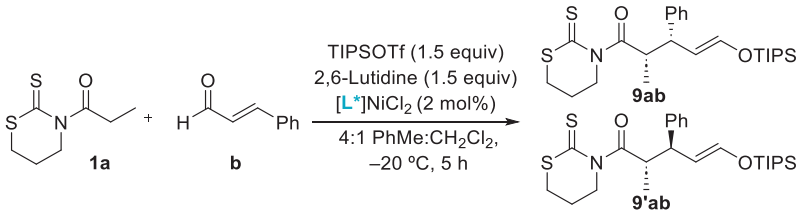

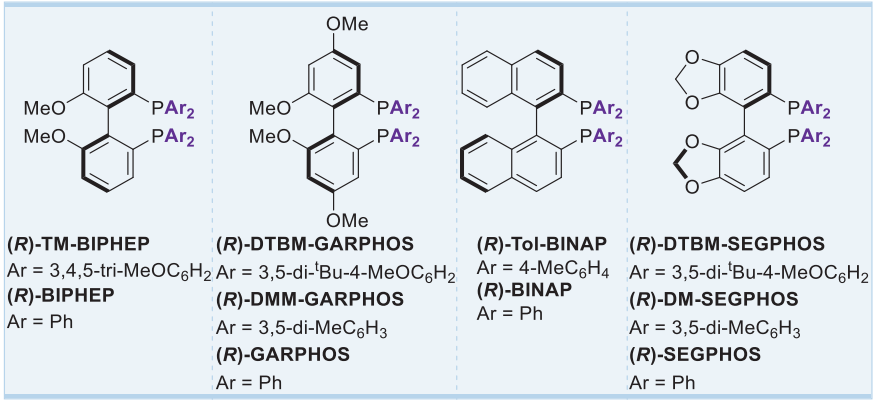

Entry	Ligand	Conv (%)[a]	rr (1,4:1,2)[a]	dr (*syn:anti*)[a]	*ee* major (%)[b]	*syn* (%)[c]	*anti* (%)[c]
1	*R*-BINAP	>99	>99:1	15:85	99	15	78
2	*R*-Tol-BINAP	>99	>99:1	15:85	99	15	75
3	*R*-SEGPHOS	>99	>99:1	19:81	99	19	74
4	*R*-DM-SEGPHOS	95	>99:1	31:69	99	26	52
5	*R*-DTBM-SEGPHOS	>97	>99:1	88:12	99	80	11
6	*R*-BIPHEP	>99	>99:1	23:77	99	23	75
7	*R*-TM-BIPHEP	16	>99:1	30:70	-	-	-
8	*R*-GARPHOS	>99	>99:1	20:80	-	19	79
9	*S*-DMM-GARPHOS	47	>99:1	13:87	-	-	-
10	*R*-DTBM-GARPHOS	90	>99:1	87:13	99	68	11

a) Established by ^{1}H NMR analysis. b) Established by chiral HPLC analysis. c) Isolated yield.

Table 18. Optimization of the ligand.

Therefore, this method offers a straightforward manner to achieve a stereodivergent approach, which provides access to all four stereoisomers by modification of the chiral ligand used (Scheme 51). Indeed, the (*R*)-DTBM-SEGPHOS leads to the (*S,R*) *syn* isomer while (*S*)- DTBM-SEGPHOS would yield the opposite (*R,S*) *syn* stereoisomer. In contrast, (*R*)-BINAP yields the (*S,S*) *anti* isomer while the (*S*)-BINAP counterpart furnishes the (*R,R*) adduct.

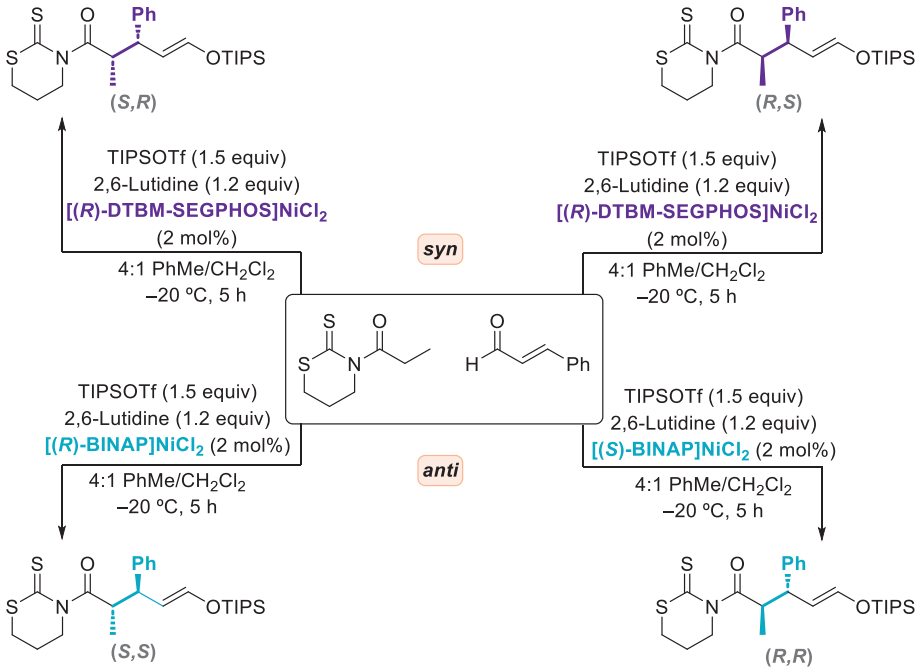

Scheme 51. Stereodivergent approach to all Michael adducts.

3.2 Other electrophiles

With these results in hand, we investigated parallel additions to other Michael acceptors commonly employed in conjugated additions, with the aim of expanding the scope of the method.

The addition to the chalcone under the experimental conditions previously optimized led to the obtention of a complex mixture, containing various isomers, including the (*E*) and (*Z*)- *syn* and *anti* adducts as well as the 1,2 addition product and the TIPS-deprotected 1,4 adduct (Scheme 52). In order to facilitate the analysis, different conditions to remove the silyl enol ether and substitute the scaffold were tried, but this only yielded complex mixtures.

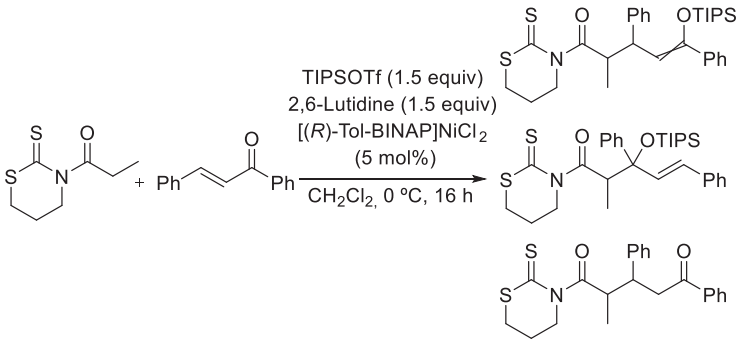

Scheme 52. Products towards the addition to chalcone.

We also analysed the feasibility of α,β-unsaturated esters as electrophiles. Model methyl cinnamate was subjected to the optimized conditions. However, the starting materials, both the thioimide and the methyl cinnamate, were recovered unmodified.

Finally, α,β-unsaturated nitro compounds were also examined. Unfortunately, treatment of the mixture of *N*-propanoyl-thiazinanethione and the β-nitrostyrene under optimized conditions did not yield any product. Instead, the starting materials remained unmodified, accompanied by minor impurities.

These negative results prove the sensitivity of the conjugate additions and the necessity to develop specific conditions for any Michael acceptor.

3.3 Aldehyde scope

At this point, we focused our attention on the effect of using different aldehydes in the presence of [(*R*)-DTBM-SEGPHOS]$NiCl_2$ as catalyst.

Firstly, we investigated the impact of the electronic effects of the aromatic ring (Table 19). The results proved that the regioselectivity towards the Michael addition remained excellent (>99:1) across all substrates, along with a consistent single enantiomer.

The main variations were observed in terms of diastereoselectivities. The most electron rich substrates exhibited fast kinetics and similar diastereoselectivities around 85:15. The placement of a moderate electronwithdrawing group at *para* position did not modify the diastereoselectivity but the catalyst loading had to be increased to 5 mol%. Stronger electronwithdrawing groups such as **i** and **j** required a 10 mol% catalyst loading and long reaction times to provide the corresponding *syn* Michael product **9ai** and **9aj** but in poorer diastereomeric ratios and

moderate to low yields. Noteworthily, the enantioselectivity of adduct **9ai** was not possible to determine due to a difficult separation of both diastereomers by either flash chromatography and chiral HPLC analysis.

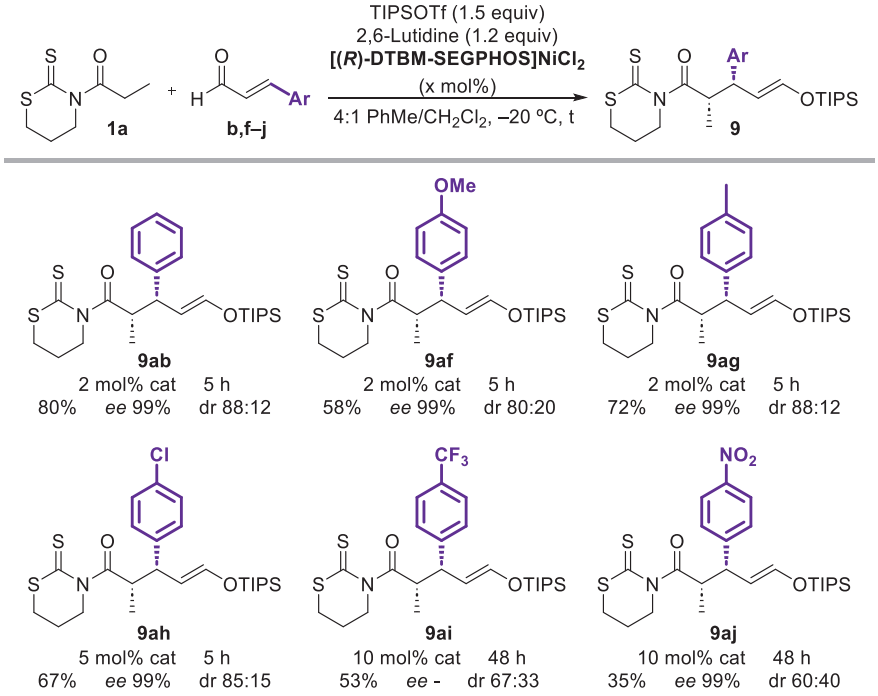

Table 19. *Syn* selective scope of *para* substituted α,β-unsaturated aldehydes.

These results prove the synthetic potential of the method, since even highly electron-poor substrates produced the desired Michael adduct. In any case, the electronic properties do not affect the regioselectivity and neither the enantioselectivity, which remained excellent across all substrates.

Next, with the collaboration of Lena Friedrich on her Erasmus thesis,[28] we investigated the impact of the substitution at different positions of the aromatic group (Table 20). We introduced a methoxy substituent in *ortho* and *meta* positions and compared it with the *para* substitution. Similarly, we examined the effect of methyl substitution. Noteworthily, the introduction of substituents in the *meta* position to form **9ak** and **9am** provided comparable results to those of substitutions on the *para* position **9af** and **9ag**, with selectivities around 85:15 and only the reaction to form 9am required an increase in catalyst loading to 5 mol%. In contrast, the introduction of substitutions in the *ortho* position to form **9al** and **9an** required an increase in catalyst loading or reaction time due to slower kinetics. Additionally, both

examples presented a higher diastereoselectivity, although the regioselectivity of **9al** was slightly eroded obtaining rr (1,2:1,4) 13:87.

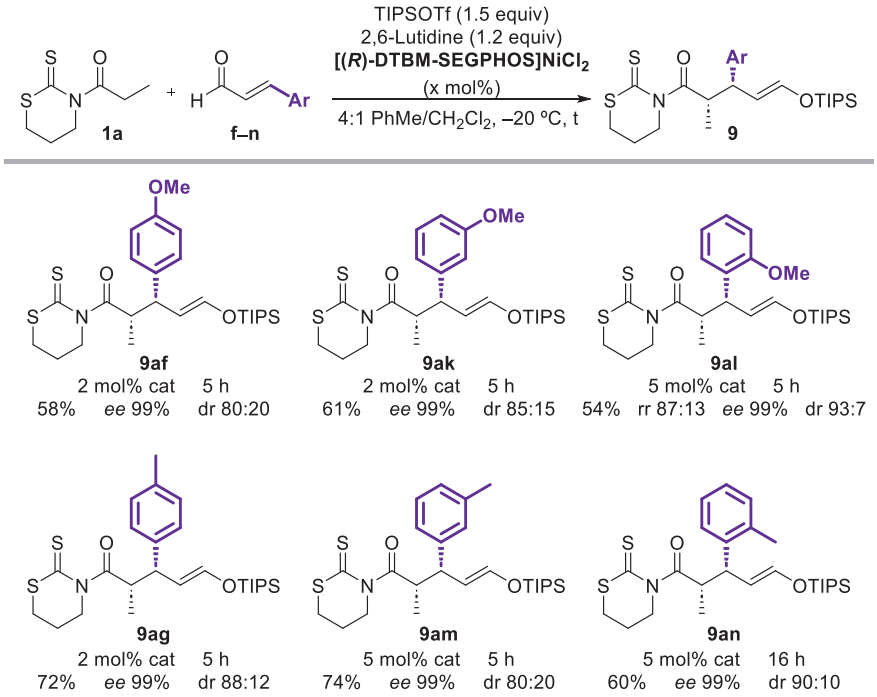

Table 20. Effect of the substitution on the aromatic ring on *syn* selective reactions.

Finally, other aromatic aldehydes were tested (Table 21). As the use of heterocycles represents a valuable approach for industrial purposes, due to the high prevalence of these substrates in commercial products, we investigated the reactions with two electron rich heterocycles **o** and **p**. These proved to be excellent substrates since they exhibited excellent regioselectivities and enantioselectivities (*ee* 99%), while high diastereoselectivities up to 94:6 provided excellent yields of the desired isomers **9ao** and **9ap**. It is worth mentioning that (*E*)-3-(2-furanyl)acrylaldehyde **p** proved to be slightly unstable and polymerized under the standard reaction conditions, which made necessary to increase the catalyst loading to accelerate the process.

A more challenging α,β,γ,δ–unsaturated aldehyde **q** was also examined. This substrate, being an extended Michael acceptor, contains an additional reactive centre at the δ position, thereby posing a new regioselective challenge. However, the reaction exhibited an excellent selectivity towards the β position while effectively controlling the enantioselectivity and afford the enantiomerically pure *syn* Michael adduct **9aq** in a remarkable 72% yield.

Finally, we also assessed the impact of incorporating substituents at the α-position of the aldehyde, such as a bromine or a methyl group. In both cases, the regio–, diastereo–, and enantioselectivities were outstanding, so the products **9ar** and **9ac** were isolated as a single isomer, which demonstrates the extraordinary potential of these substrates.

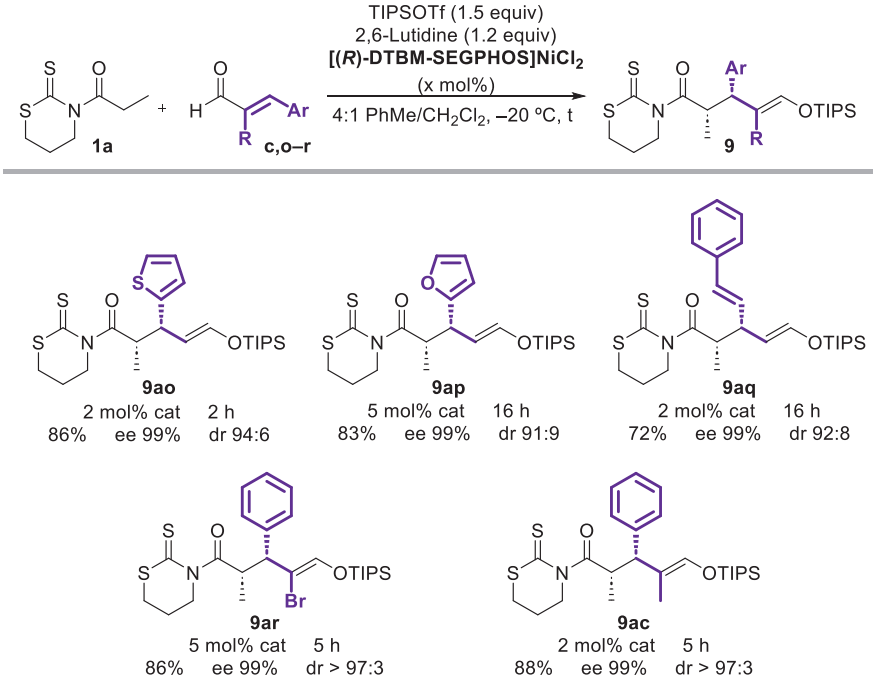

Table 21. *Syn* selective scope of other α,β-unsaturated aldehydes.

A parallel study was carried out with [(*R*)-BINAP]$NiCl_2$ complex. As for the former catalyst, we first examined the impact of electronically different substituents at *para* position (Table 22).

Strong electrondonor groups such as **f** slightly reduced the diastereoselectivity towards the *anti* isomer. However, the regioselectivity and enantioselectivity were not affected, and the corresponding *anti* Michael product **9'af** was isolated with a 50% yield in an enantiomerically pure form. In contrast to the (*R*)-DTBM-SEGPHOS counterpart, [(*R*)-BINAP]$NiCl_2$ tolerated better the most electron withdrawing substituents. Although increasing the catalyst to 10 mol% was unavoidable, the reaction with **i** provided comparable diastereoselectivities and yields in only 16 h, while the use of aldehyde **j** resulted in moderate diastereoselectivities and only 24 h of reaction were required. Unfortunately, the enantioselectivity of adduct **9'ai**

could not be determined because both stereoisomers could not be separated neither by flash chromatography nor chiral HPLC analysis.

In summary, the enantiomerically pure *anti* Michael products **9'** were isolated in 50–78% yield irrespective of the electronic character of the substrate in *para* position.

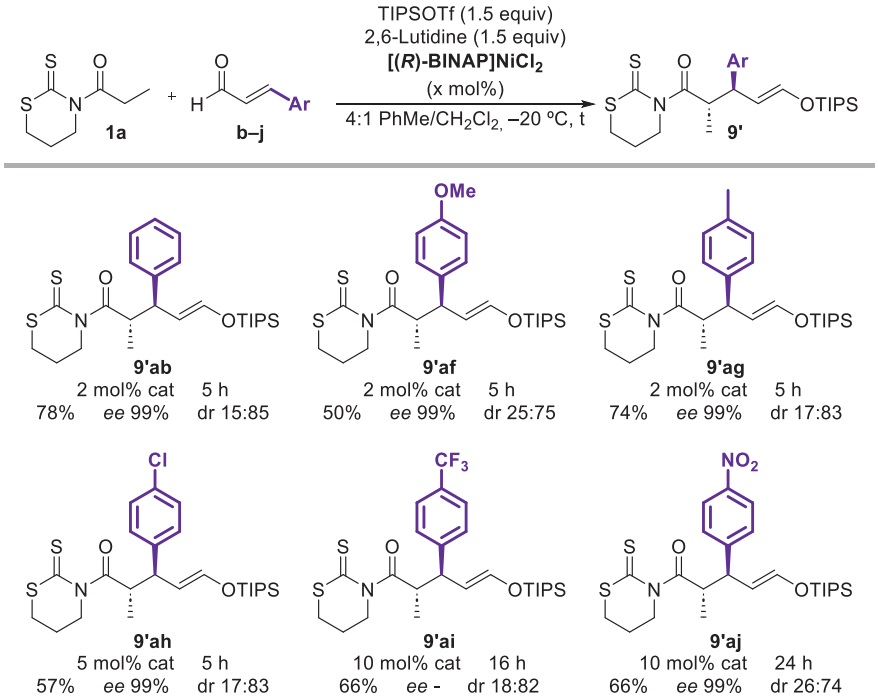

Table 22. *Anti* selective scope of *para* substituted α,β-unsaturated aldehydes.

Next, we assessed the effect of the substitution in *ortho* and *meta* positions compared to the *para* counterpart, as we had done for the *syn* adducts **9** (Table 23). Similarly, the regioselectivity and enantioselectivities were absolutely controlled, yielding enantiopure 1,4 adducts **9'**, while diastereoselectivity was the most affected parameter. Using aldehyde **k** resulted in a significantly increase in diastereoselectivity, achieving comparable results to other substrates, while ortho-substituted aldehyde **l** yielded comparable results of aldehyde **f**. Furthermore, the introduction of a methyl group in these positions were well-tolerated and similar results were obtained across all substrates, albeit reaction kinetics were slightly affected, necessitating an increase in catalyst loading to 5 mol% to afford adducts **9'am** and **9'an** (Table 23).

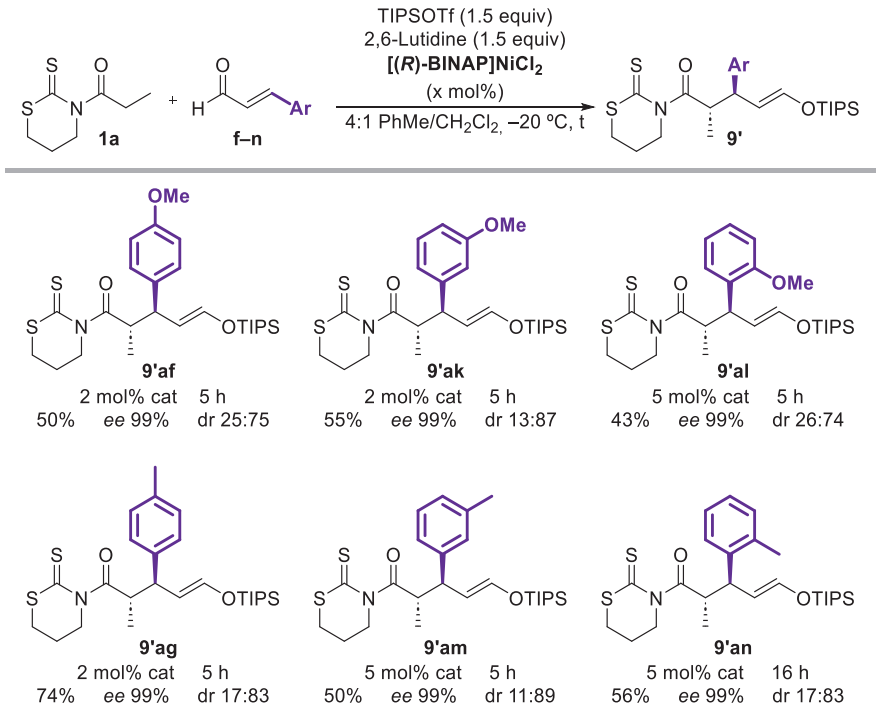

Table 23. Effect of the substitution on the aromatic ring on *anti* selective reactions.

Regarding the reactions with heteroaromatic aldehydes **o** and **p**, the regioselectivity and enantioselectivity were also outstanding, and only enantiopure 1,4 adducts were obtained (Table 24). Unfortunately, the diastereoselectivity suffered a significant detriment, leading to no control over the diastereoselectivity at –20 °C. Taking advantage of the high kinetics of these substrates, the reaction was carried out at –40 °C, which permitted us to obtain an acceptable dr (*syn*/*anti*) 26:74 to obtain **9'ao**. Unfortunately, the inherent instability of the furane counterpart **p** made this strategy unsuitable, and only a dr ~1:1 ratio was achieved.

The extended Michael acceptor α,β,γ,δ–unsaturated aldehyde **q** was not able to keep a complete regioselectivity as occurred with the former catalyst, and a rr (1,4:1,6) of 70:30 was obtained. However, high diastereoselectivities and enantioselectivities were maintained, obtaining an acceptable 49% yield.

Finally, the reactions with α-substituted aldehydes **r** and **c** were highly successful, since the regioselectivity was excellent, along with the enantioselectivity. In turn, high levels of diastereoselectivities (dr *syn/anti* 17:83) were achieved, particularly noteworthy for the **9'ac** adduct.

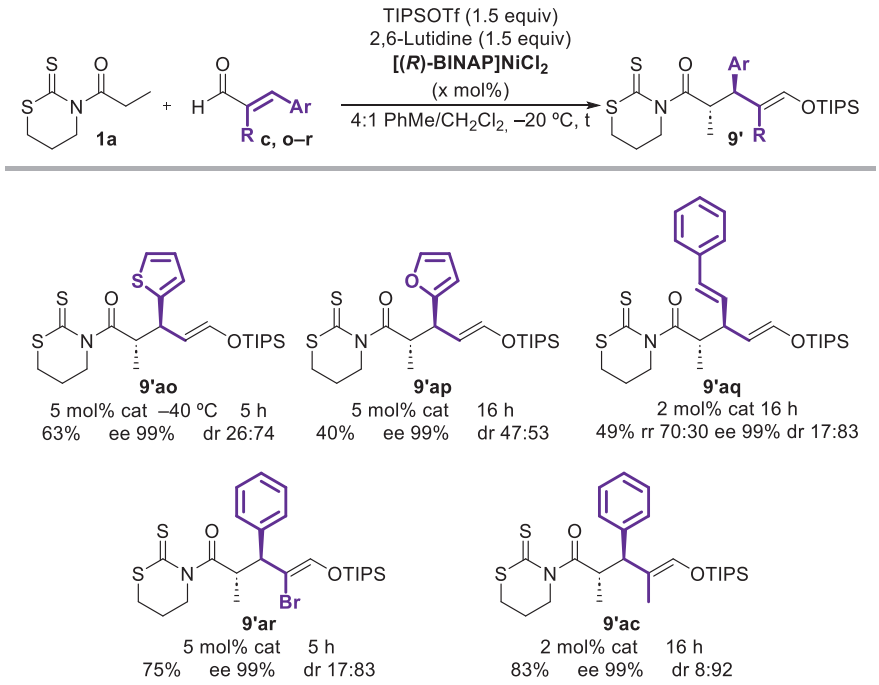

Table 24. *Anti* selective scope of other α,β-unsaturated aldehydes.

Up to this point, it has been demonstrated that this novel method shows a wide scope and a large array of aromatic α,β-unsaturated substrates, can undergo highly selective *syn* and *anti* Michael additions. The regioselectivity is in most cases excellent (rr > 99:1), the diastereoselectivity is consistently good, while the enantiocontrol is always outstanding (*ee* 99%).

3.4 *N*-Acyl-thiazinanethiones scope

The next step aimed to expand the reaction scope by utilizing *N*-acyl thiazinanethiones bearing different substituents at the acyl group and analysing their impact on the reaction, as well as the tolerance of other functional groups commonly employed in organic synthesis.

In this regard, with the collaboration of Gabriela Benedito in her Master thesis,[29] we first focused our attention towards the obtention of the *syn* Michael adducts using the [(*R*)-DTBM-SEGPHOS]$NiCl_2$ catalyst (Table 25). The results revealed that the reaction was highly sensitive to steric hindrance at the Cα position, which forced us to increase the catalyst loading to 10 mol%.

Indeed, the use of **1b** resulted in a drop in regioselectivity and diastereoselectivity, yielding a rr (1,2:1,4) 10:90 and dr (*syn/anti*) 76:24 for

adduct **9bb**. Bulky substituents at Cα such as **1p** and **1q** inhibited the reaction, leading to the recovery of the starting materials, while the use of the more acidic **1r** surprisingly furnished the *anti* adduct **9'rb** as the major diastereomer with a moderate selectivity dr (*syn/anti*) 35:65, considering such poor result, the enantioselectivity of this product was not checked.

The introduction of different functionalities such as a terminal alkyne, an ester or an azido, furnished the expected adducts **9eb**, **9fb** and **9ob** respectively without any interference associated to these functional groups in the reaction outcome, but these reactions required a 10 mol% of catalyst loading to reach full conversion. With regard to adduct **9eb** and **9fb**, they were obtained with slightly lower rr (1,2:1,4) 10:90, and additionally the adduct **9eb** diastereoselectivity was also slightly eroded with a dr (*syn/anti*) 71:29. As for adduct **9ob**, it was conducted with the thiazolidinethione instead of the thiazinanethione, because the preparation of the *N*-azidoacetyl-1,3-thiazinanethione was unfeasible due to its rapid degradation upon its formation. However, this modification did not affect in terms of selectivity, which afforded only the 1,4 adduct with a dr (*syn/anti*) 85:15. Noteworthy, all the reactions were tolerant in terms of enantioselectivity, obtaining a single enantiomer (99% *ee*) across all substrates.

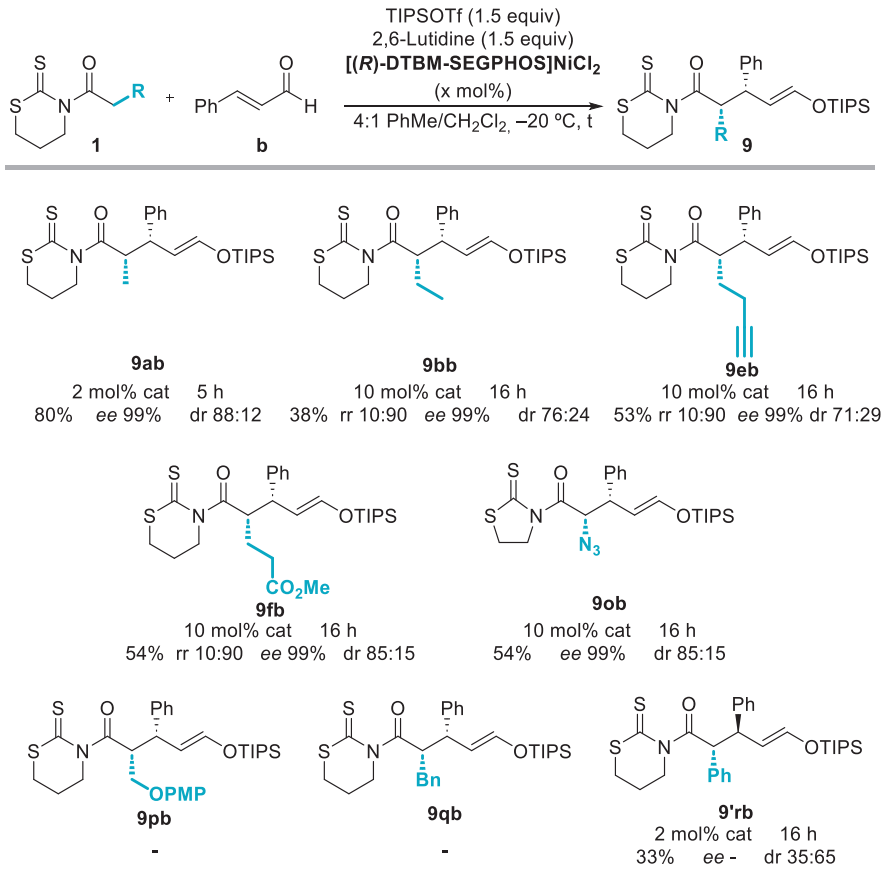

Table 25. *Syn* selective scope of *N*-acyl thiazinanethiones.

A parallel investigation was carried out with [(*R*)-BINAP]$NiCl_2$ counterpart, using identical substrates. The results shown in Table 26 revealed an enhanced tolerance towards the steric hindrance at the Cα position. Notably, the utilization of **1b** only required a 5 mol% of catalyst loading to achieve comparable results to **1a** counterpart. More bulky substituents also proved suitable and gave the corresponding *anti* adducts **9'pb** and **9'qb** with a remarkable stereocontrol, although ether **p** exhibited a detriment in regioselectivity obtaining a rr (1,2:1,4) 10:90. Furthermore, the more acidic **1r** also afforded the expected *anti* adduct in comparable results to the propionyl counterpart. Remarkably, the introduction of functional groups such as a terminal alkyne or an ester proved to be acceptable under reaction conditions and furnished the expected *anti* aldol adducts **9'eb 9'fb** smoothly. Unfortunately, azide-containing thioimide **1o** gave an equimolar mixture of diastereomers, although in good yield.

Finally, of particular note is the consistently excellent enantioselectivity observed, with a remarkable *ee* 99% observed across all formed adducts, thereby underscoring the exceptional control afforded by this methodology.

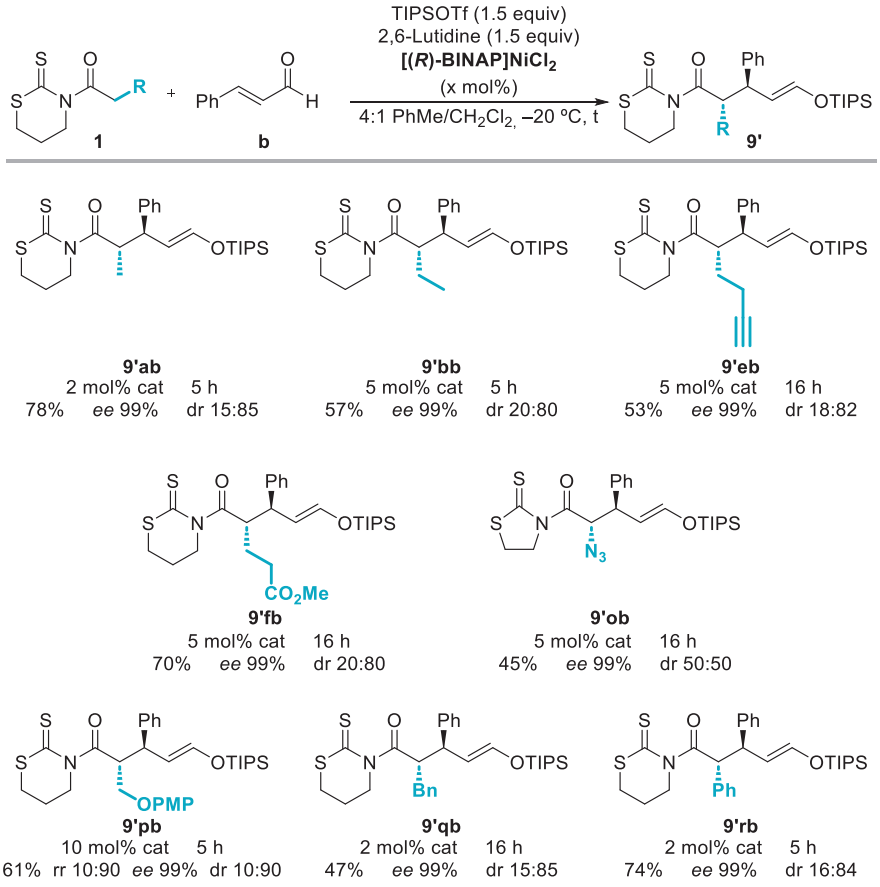

Table 26. *Anti* selective scope of *N*-acyl thiazinanethiones.

To determine the absolute configuration of both isomers, selected examples of the solid compounds were recrystallized from DCM/hexane. The resulting single crystals were analysed by X-ray crystallography by Mercè Font Bardia (Figure 18). The results showed that the adduct **9aj** and **9ar** corresponds to the *syn* 2*S*,3*R* isomer while the adduct 9'qb corresponds to the anti 2*S*,3*S* counterpart isomer.

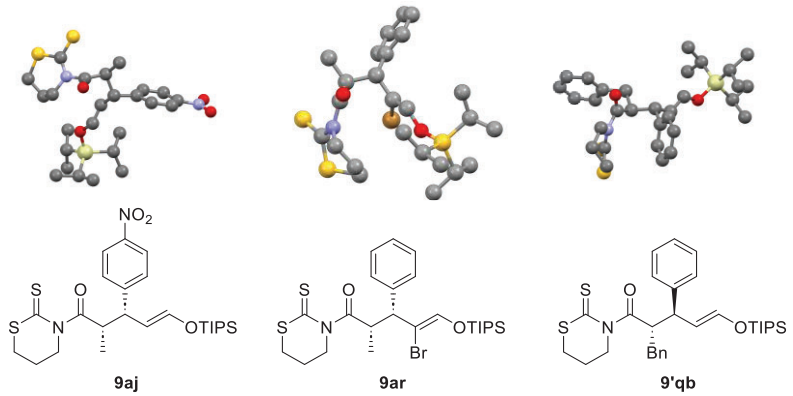

Figure 18. Crystal structures of selected compounds.

3.5 Limitations

The most important constraint of this novel Michael addition approach lies in the necessity of an aromatic moiety at the conjugated position of the aldehyde, since non-aromatic α,β-unsaturated aldehydes usually lead to low conversions, which may be attributed to the lack of aldehyde activation by the silyl triflate, owing the diminished stability of the oxocarbenium intermediate required (Table 27).

Initially, attempts were made to employ (*E*)-iodoacrolein **s** in the reaction. However, the starting material exhibited extreme instability and proved difficult to manipulate, undergoing extensive degradation within minutes as shown above in Scheme 48. Although the Michael addition was carried out, only a complex mixture of extensively degraded products was obtained. Therefore, we assayed the (*Z*)-aldehyde counterpart **t** which presented a higher stability. However, under reaction conditions the aldehyde partially isomerized to the (*E*)-counterpart **s**, which prompted the obtention of a complex mixture of products.

Other aldehydes lacking γ-CH were employed in order to avoid potential silyl enol ether side reactions. The introduction of a silyl substituent in γ-position resulted in the recovery of both the starting thioimide and the aldehyde **u** unaltered. Aldehydes possessing different functional groups at the γ-position did not provide better results. Indeed, the use of electron-withdrawing groups such as ethyl ester **v** was completely ineffective and produced the partial degradation of the aldehyde, while the starting thioimide was recovered. Even aldehydes with electron-donating groups such as dimethylamino **w** led to no conversion, with both the starting thioimide and the aldehyde being recovered.

Commercially available crotonaldehyde **y** was employed as the electrophile. However, only traces of some products could be found (< 5%) with the starting material predominantly recovered. Remarkably, the silyl enol ether of crotonaldehyde was not detected, which suggested that the lack of reaction may be attributed to the lack of aldehyde activation rather than to a deactivation *via* silyl enol ether formation. We also tested the reaction with methacrolein **z**, expecting that the less hindered β-position would enhance its reactivity while the absence at the γ-CH should mitigate potential alternate mechanism. Unfortunately, the expected adducts were neither obtained, and the starting thioimide was predominantly recovered. Additionally, products derived from the methacrolein were detected, which indicated that the aldehyde was degraded in the reaction mixture. We also used the chiral catalyst [(*R*)-BINAP]$NiCl_2$ which has proved to exhibit greater reactivity than the achiral counterpart in most reactions, but similar results were observed.

In summary, results summarised in Table 27 firmly established that the α,β-unsaturated aldehyde had to contain an aromatic group at the conjugated position.

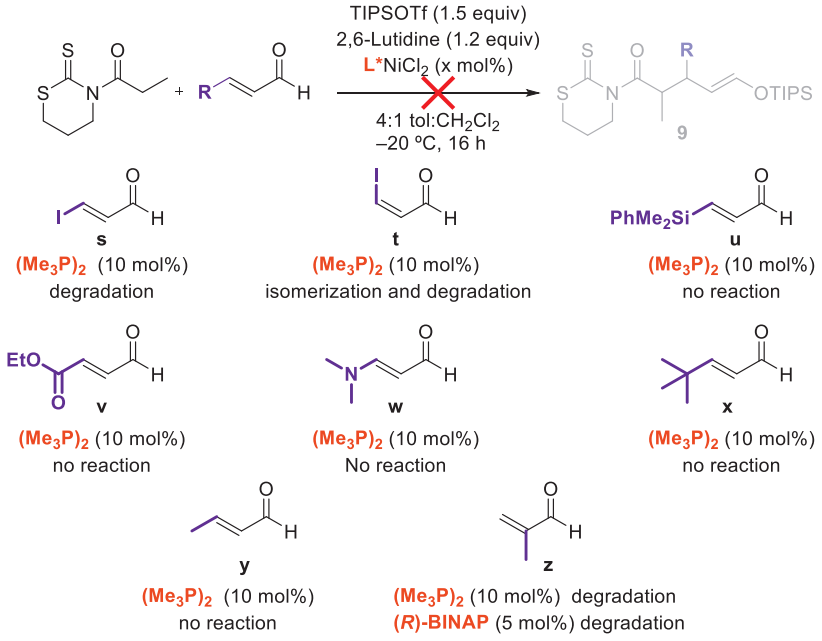

Table 27. Limitations on the Michael addition to α,β-unsaturated aldehydes.

3.6 1,6-Additions

α,β,γ,δ-Unsaturated aldehydes as electrophilic species are extremely challenging substrates due to the presence of three electrophilic centres, which increases the number of potential isomers. In general, metal-catalysed transformations show a high preference to the formation of 1,2 addition products, while most organocatalytic approaches strongly favour the 1,4 addition. Consequently, the acquisition of extended Michael adducts remains rare and scarce.

We had already established that the combination of aldehyde **q** with [BINAP]$NiCl_2$ as catalyst triggers the formation of a significant amount of 1,6 adducts **12** (Table 24). Thus, we hypothesized that it might be feasible to reoptimize the reaction conditions to favour the formation of 1,6 adducts over the 1,4 adducts.

Based on the aforementioned precedent, we explored the influence of the scaffold in this transformation. We tested different *N*-propanoyl thioimides, showing that only thioimide **1a** favours the 1,4 addition, while other substrates showed no control over the regioselectivity between β and δ positions (Table 28, entries 1–4). Additionally, we examined the outcome of the reaction using *N*-azidoacetyl thioimides, which would grant access to valuable α-amino acids (Table 28, entries 5–6). Unfortunately, both the regio as well as the diastereoselectivity were steadily poor and complex mixtures of isomers were obtained in all cases.

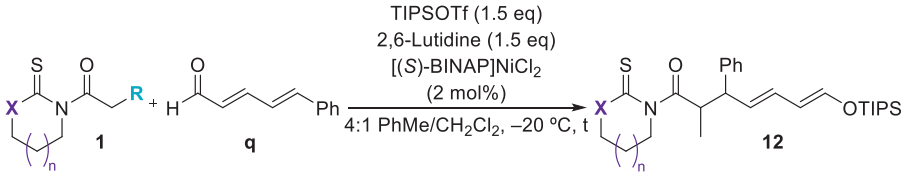

Entry	X	n	R	t(h)	Conv (%)[a]	rr (1,2:,1,4:1,6)[a]	dr (1,6)[a]
1	S	1	Me	1	>99	0:70:30	55:45
2	O	1	Me	0.5	>99	1:53:46	50:50
3	S	0	Me	0.5	>99	0:58:42	45:55
4	O	0	Me	0.5	>99	4:53:43	42:58
5	S	0	N_3	0.5	>99	1:53:46	44:56
6	O	0	N_3	0.5	>99	1:63:37	35:65

a) Determined by ^{1}H NMR analysis of the crude mixture.

Table 28. Study of the addition to α,β,γ,δ-unsaturated aldehydes.

Next, we investigated the impact of the Lewis acid in the addition of thiazolidinethione **1l** (Table 29). The results were moderate irrespective of Lewis acid, but we observed that less bulky triflates favours the formation of

the 1,2 addition without a significant improvement, which confirmed the importance of the steric hindrance of the triflate.

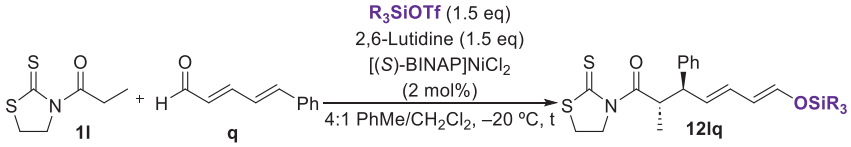

Entry	Lewis acid	t (h)	Conv (%)[a]	rr (1,2:,1,4:1,6)[a]	dr (1,6)[a]
1	TIPSOTf	1	>99	1:53:46	55:45
2	TESOTf	2	>99	10:63:27	34:66
3	TMSOTf	2	>99	39:35:26	37:63

a) Determined by ^{1}H NMR analysis of the crude mixture.

Table 29. Optimization of the Lewis acid.

Finally, we explored the impact of the chiral ligands and the solvent. The results suggests that BINAP can lead to very modest 1,6-regioselectivities and diastereoselectivities (Table 30, entries 1–2) while DTBM-SEGPHOS strongly favours the 1,4 addition (Table 30, entries 3–4). The addition of toluene as solvent enhanced significantly both the regioselectivity and diastereoselectivity for BINAP catalysed reactions, albeit useless approximately 2:1 mixtures rr and dr were obtained.

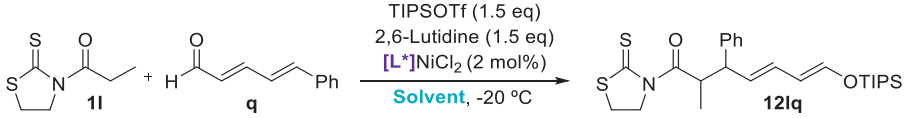

Entry	L*	Solvent	t (h)	Conv (%)[a]	rr (1,2:,1,4:1,6)[a]	dr (1,6)[a]
1	(*S*)-BINAP	CH_2Cl_2	0.5	>99	1:53:46	45:55
2	(*S*)-BINAP	PhMe:CH_2Cl_2 4:1	3	>99	7:32:61	39:61
3	(*R*)-DTBM-SEGPHOS	CH_2Cl_2	0.5	>99	0:84:16	39:61
4	(*R*)-DTBM-SEGPHOS	PhMe:CH_2Cl_2 4:1	3	>99	0:82:18	32:68

Table 30. Optimization of solvent and catalyst.

With these results in hand, the selective 1,6 conjugate addition turns out to be possible through the fine optimization of some parameters, being the most promising one the use of very bulky silyl triflates, although the exploration of different combinations of solvent/catalyst is required. Despite such promising conclusions and owing to the moderate selectivities obtained up to this point, this study was abandoned.

4 Mechanistic studies

Our investigation also extended to mechanistic insights into this novel transformation, aiming to elucidate the origins of the regioselectivity, the main transition states underlying the observed diastereoselectivity, and the outstanding enantioselectivity observed with both catalysts. These studies were carried out by Prof. Gabriel Aullón.

To initiate this investigation, theoretical calculations were conducted to determine the electronic effects that could account for the observed regioselectivity. Indeed, analysis of the LUMO of the [PhCH=CHCHOTIPS]$^+$ revealed that both 1,2 and 1,4 positions (C1 and C3) are actually electronically equivalent, suggesting an equal probability of attacking towards both positions (Figure 19). Therefore, the regioselectivity must be controlled mostly by sterical effects induced by the alkyl groups of the Lewis acid.

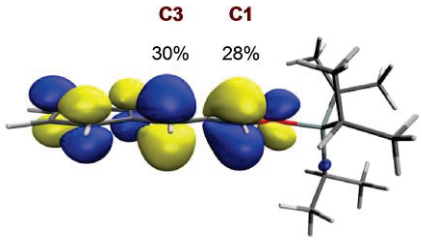

Figure 19. LUMO-orbital of the [PhCH=CHCHOTIPS]$^+$ adduct.

This observation aligns with the experimental data, wherein the use of less sterically hindered silyl triflates fails to properly control the regioselectivity of the reaction.

Subsequently, the most stable conformations of both [{(*R*)-BINAP}Ni(thiazinanethione)]$^+$ and [{(*R*)-DTBM-SEGPHOS} Ni(thiazinanethione)]$^+$ were examined (Figure 20). Interestingly, one of the aromatic substituents of the phosphine is placed on the *Si* π-face of the enolate in the four most stable conformations, thus blocking the attack towards this face (Figure 20). This explains the high levels of enantioselectivity observed and determines the absolute configuration of the Cα chiral centre. Additionally, these results accounts for the large alterations in selectivity observed when the aromatic substituents were modified during the optimization process, while the effect of the biarylic moiety modification was rather low.

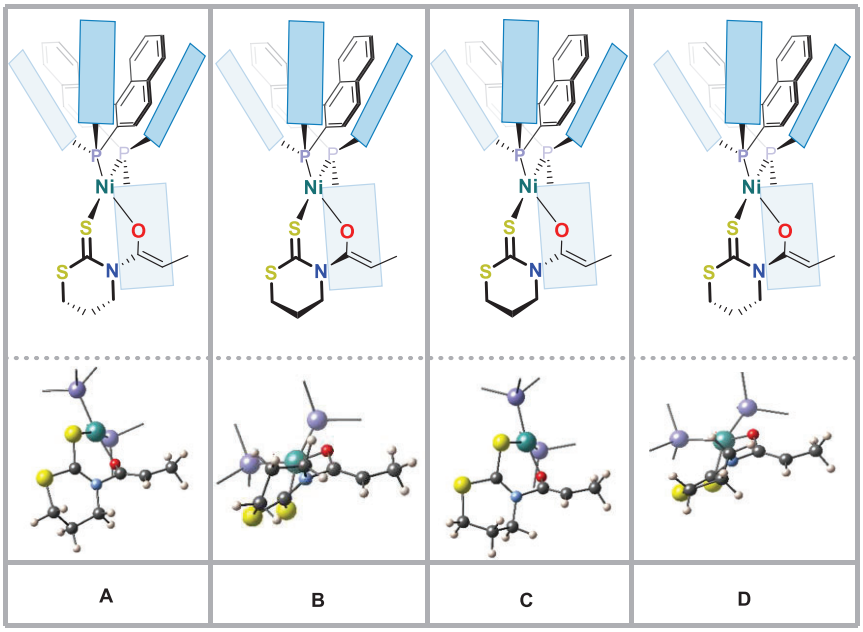

Figure 20. Geometries of the most stable enolate conformations.

With the optimized geometries in hand, the most stable transitions states for the Michael addition were evaluated. Sixteen different transition states were calculated, considering the four most stable conformations and the four more stable possible approaches (Figure 21).

Firstly, the transition states for [(*R*)-DTBM-SEGPHOS]$NiCl_2$ catalyst were explored. Interestingly, the most stable transition state involved the π-*Re* face of the enolate attacking the *Si* π-face of the aldehyde, positioning the bulky TIPS group towards the thiazinanethione. This configuration presented interactions between these two groups through Van der Waals forces, stabilizing the resulting intermediate. This approximation leads to the (*S,R*)–*syn* diastereomer, consistent with the experimental observations. Furthermore, the second most stable conformation, wherein π-*Re* face of the enolate engages the *Re* π-face of the aldehyde leads to the *anti* diastereomer, and exhibits an energy of +0.9 kcal/mol, which predicts a ratio *syn*/*anti* 85:15 at –20 °C, in good agreement with the experimental results (dr 88:12). Finally, other transition states present much higher energies (>2.2 kcal/mol), which avoids their effective participation on the reaction outcome, and thus explains the excellent enantioselectivity observed.

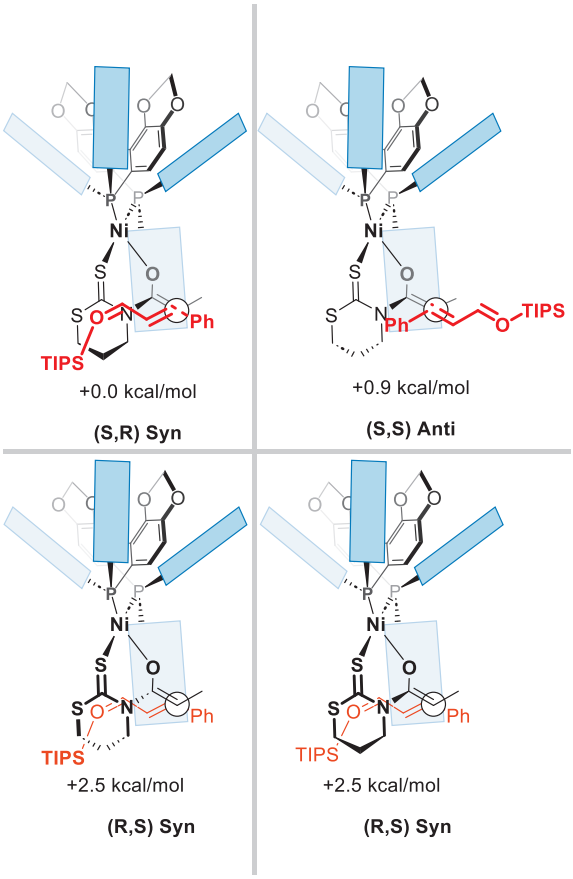

Figure 21. Transition states using [(*R*)-DTBM-SEGPHOS]$NiCl_2$ catalyst.

The same process was applied to the transition states catalysed by [(*R*)-BINAP]$NiCl_2$ (Figure 22). In this case, the most stable transition state resulted in the approach of the *Re* π-face of the enolate towards the *Re* π-face of the aldehyde, to provide the (*S,S*)–*anti* isomer, which matches perfectly with the experimental observations. However, the parallel transition state leading to the *syn* isomer presented an energy of +15.5 kcal/mol, which indicated that it would not participate in the reaction. This discrepancy does not align with the experimentally observed 15:85 diastereomeric ratio and suggests that other factor could come into play.

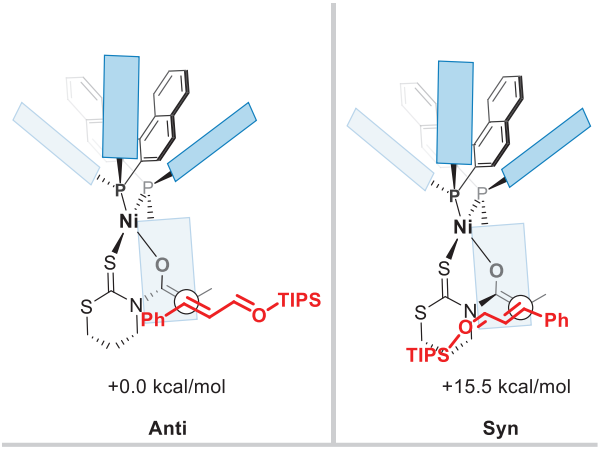

Figure 22. Transition states [(*R*)-BINAP]$NiCl_2$ catalyst.

The abovementioned transition states are consistent with a mechanism represented in Scheme 53. As shown, the nickel(II) chloride is activated to form the nickel(II) triflate complex, the real catalytic species. Then, it chelates the thioimide acidifying the Cα H. Then, the 2,6-lutidine deprotonates this species to form the nickel enolate. Simultaneously, the aldehyde is activated by the TIPSOTf. The resultant oxocarbenium intermediate approaches the enolate and reacts through either ***syn* TS** or ***anti* TS**, depending on the catalyst used. Finally, the release of the nickel catalyst gives the desired Michael adduct.

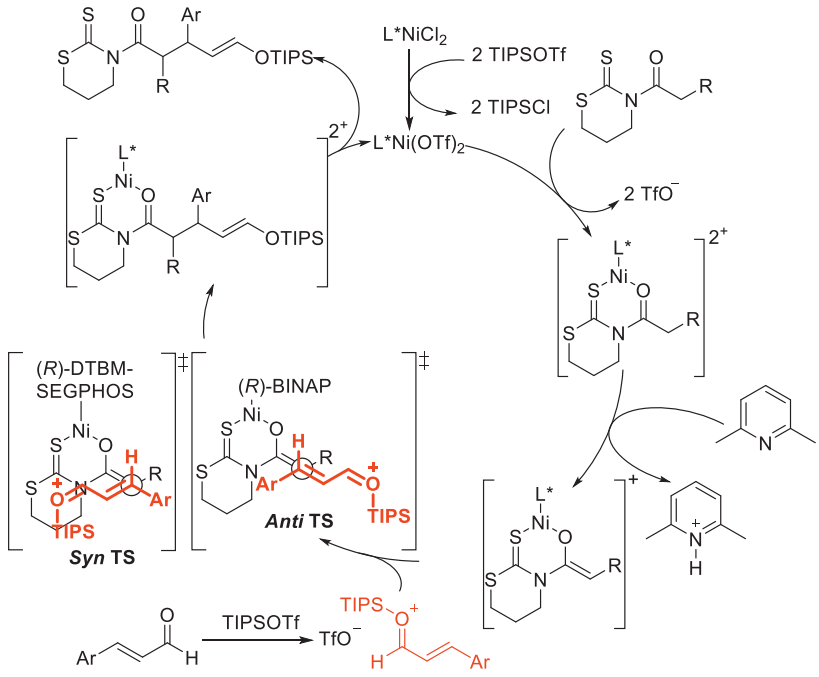

Scheme 53. Catalytic cycle of the Michael addition.

5 Outline

In summary, we have developed an unprecedented novel asymmetric Michael addition to α,β-unsaturated aldehydes catalysed by chiral nickel (II) complexes to get access to all possible stereocenters at will, through the simple modification of the chiral ligand of the catalyst. This method proved to be excellent in terms of regioselectivity, with most of substrates exhibiting a rr (1,2:1,4) exceeding >1:99. Remarkably, the enantioselectivity has emerged as one of the most robust aspects of this method, obtaining in all cases enantiopure compounds (99% *ee*).

The [(*R*)-DTBM-SEGPHOS]$NiCl_2$ has been established the most appropriate complex to obtain *syn* Michael adducts with high diastereoselectivities. Main limitations arise with strongly electron-poor substrates or the introduction of steric hindrance in the Cα position. Interestingly, the reaction with an α,β,γ,δ-unsaturated aldehyde showed an excellent regioselectivity and the adduct from the Cβ attack was isolated in excellent yield.

The results with [(*R*)-BINAP]$NiCl_2$ were excellent across most substrates, exhibiting a wider tolerance than the DTBM-SEGPHOS counterpart

in terms of reactivity. Main limitations of this catalyst affect the most electron rich substrates in which a slight loss in diastereoselectivity is observed.

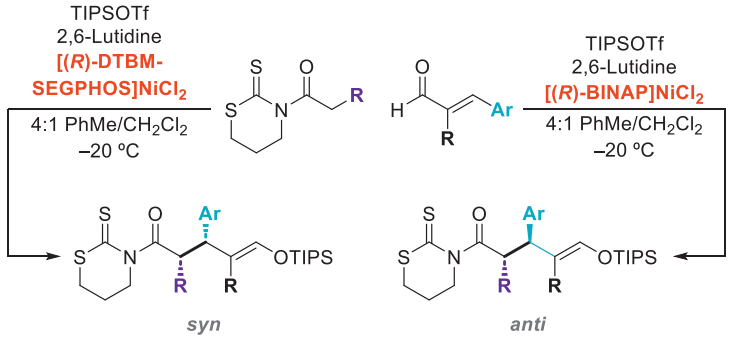

Scheme 54. Stereodivergent Michael addition catalysed by chiral nickel(II) complexes.

6 References

(1) Michael, A. Ueber Die Addition von Natriumacetessig- Und Natriummalonsäureäthern Zu Den Aethern Ungesättigter Säuren. *J. Prakt. Chem.* **1887**, *35* (1), 349–356.

(2) Gilman, H.; Jones, R. G.; Woods, L. A. The Preparation of Methylcopper and Some Observations on the Decomposition of Organocopper Compounds. *J. Org. Chem.* **1952**, *17* (12), 1630–1634.

(3) Evans, D. A.; Urpi, F.; Somers, T. C.; Clark, J. S.; Bilodeau, M. T. New Procedure for the Direct Generation of Titanium Enolates. Diastereoselective Bond Constructions with Representative Electrophiles. *J. Am. Chem. Soc.* **1990**, *112* (22), 8215–8216.

(4) Evans, D. A.; Bilodeau, M. T.; Somers, T. C.; Clardy, J.; Cherry, D.; Kato, Y. Enantioselective Michael Reactions. Diastereoselective Reactions of Chlorotitanium Enolates of Chiral *N*-Acyloxazolidinones with Representative Electrophilic Olefins. *J. Org. Chem.* **1991**, *56* (20), 5750–5752.

(5) Kobayashi, S.; Suda, S.; Yamada, M.; Mukaiyama, T. A Catalytic Asymmetric Michael Reaction of Silyl Enol Ethers with α,β-Unsaturated Ketones Using a Chiral Titanium Oxide. *Chem. Lett.* **1994**, *23* (1), 97–100.

(6) Bernardi, A.; Colombo, G.; Scolastico, C. Enantioselective Mukaiyama-Michael Reactions of 2-Carbomethoxy Cyclopentenone Catalyzed by Chiral Bis(Oxazoline)-Cu(II) Complexes. *Tetrahedron Lett.* **1996**, *37* (49), 8921–8924.

(7) Felker, I.; Pupo, G.; Kraft, P.; List, B. Design and Enantioselective Synthesis of Cashmeran Odorants by Using "Enol Catalysis." *Angew. Chem. Int. Ed.* **2015**, *54* (6), 1960–1964.

(8) Gatzenmeier, T.; Kaib, P. S. J.; Lingnau, J. B.; Goddard, R.; List, B. The Catalytic Asymmetric Mukaiyama–Michael Reaction of Silyl Ketene Acetals with α,β -Unsaturated Methyl Esters. *Angew. Chem. Int. Ed.* **2018**, *57* (9), 2464–2468.

(9) Trost, B. M. The Atom Economy–a Search for Synthetic Efficiency. *Science (1979)* **1991**, *254* (5037), 1471–1477.

(10) Trost, B. M. Atom Economy–A Challenge for Organic Synthesis: Homogeneous Catalysis Leads the Way. *Angew. Chem. Int. Ed.* **1995**, *34* (3), 259–281.

(11) Wynberg, H.; Helder, R. Asymmetric Induction in the Alkaloid-Catalysed Michael Reaction. *Tetrahedron Lett.* **1975**, *16* (46), 4057–4060.

(12) Brunner, H.; Hammer, B. Enantioselective Michael Additions with Optically Active Co^{II}/Diamine Catalysts. *Angew. Chem. Int. Ed.* **1984**, *23* (4), 312–313.

(13) Yamaguchi, M.; Shiraishi, T.; Hirama, M. A Catalytic Enantioselective Michael Addition of a Simple Malonate to Prochiral α,β -Unsaturated Ketoses and Aldehydes. *Angew. Chem. Int. Ed.* **1993**, *32* (8), 1176–1178.

(14) Sasai, H.; Arai, T.; Shibasaki, M. Catalytic Asymmetric Michael Reactions Promoted by a Lithium-Free Lanthanum-BINOL Complex. *J. Am. Chem. Soc.* **1994**, *116* (4), 1571–1572.

(15) Okino, T.; Hoashi, Y.; Takemoto, Y. Enantioselective Michael Reaction of Malonates to Nitroolefins Catalyzed by Bifunctional Organocatalysts. *J. Am. Chem. Soc.* **2003**, *125* (42), 12672–12673.

(16) Shen, X.; Huo, H.; Wang, C.; Zhang, B.; Harms, K.; Meggers, E. Octahedral Chiral-at-Metal Iridium Catalysts: Versatile Chiral Lewis Acids for Asymmetric Conjugate Additions. *Chem. Eur. J.* **2015**, *21* (27), 9720–9726.

(17) Brown, S. P.; Goodwin, N. C.; MacMillan, D. W. C. The First Enantioselective Organocatalytic Mukaiyama-Michael Reaction: A Direct Method for the Synthesis of Enantioenriched γ-Butenolide Architecture. *J. Am. Chem. Soc.* **2003**, *125* (5), 1192–1194.

(18) Kim, B.; Kim, Y.; Lee, S. Y. Stereodivergent Carbon-Carbon Bond Formation between Iminium and Enolate Intermediates by Synergistic Organocatalysis. *J. Am. Chem. Soc.* **2021**, *143* (1), 73–79.

(19) Carreira, E. M.; Kvaerno, L. Classics in Stereoselective Synthesis. *Wiley-VHC* **2009**.

(20) Zheng, K.; Liu, X.; Feng, X. Recent Advances in Metal-Catalyzed Asymmetric 1,4-Conjugate Addition (ACA) of Nonorganometallic Nucleophiles. *Chem. Rev.* **2018**, *118* (16), 7586–7656.

(21) Hui, C.; Pu, F.; Xu, J. Metal-Catalyzed Asymmetric Michael Addition in Natural Product Synthesis. *Chem. Eur. J.* Wiley-VCH Verlag March 23, 2017, pp 4023–4036.

(22) Kano, T.; Maruyama, H.; Sakamoto, R.; Maruoka, K. Regioselectivity Switch in Chiral Amine-Catalysed Asymmetric Addition of Aldehydes to Reactive Enals. *Chem. Commun.* **2015**, *51* (49), 10062–10065.

(23) Ando, K.; Watanabe, H.; Zhu, X. One-Pot Preparation of (*E*)-α,β-Unsaturated Aldehydes by a Julia–Kocienski Reaction of 2,2-Dimethoxyethyl PT Sulfone Followed by Acid Hydrolysis. *J. Org. Chem.* **2021**, *86* (9), 6969–6973.

(24) Allen, C. F. H.; Edens Jr, C. O. Phenylpropargyl Aldehyde. *Org. Synth.* **1945**, *25*, 92.

(25) Zheng, K.; Shen, D.; Hong, R. Biomimetic Synthesis of Lankacidin Antibiotics. *J. Am. Chem. Soc.* **2017**, *139* (37), 12939–12942.

(26) Paterson, I.; Paquet, T. Total Synthesis and Configurational Validation of (+)-Phorbaside A. *Org. Lett.* **2010**, *12* (9), 2158–2161.

(27) Schultz-Fademrecht, C.; Deshmukh, P. H.; Malagu, K.; Procopiou, P. A.; Barrett, A. G. M. Directed Ring-Closing Metathesis of Trienes by Silyl Substitution. *Tetrahedron* **2004**, *60* (35), 7515–7524.

(28) Friedrich, L. Enantioselective Michael Reactions of α,β-Unsaturated Aldehydes Catalysed by Chiral Ni(II) Complexes. *Erasmus Thesis* **2022**, Universitat de Barcelona.

(29) Benedito, G. Direct and Enantioselective Michael Addition to α,β-Unsaturated Aldehydes Catalyzed by Ni(II) Complexes. *Master Thesis* **2022**, Universitat de Barcelona.

CHAPTER III

Transformations of the Michael adducts. Total synthesis of Tapentadol

Table of contents

1 Introduction

In Chapter II, we have described a highly efficient stereodivergent Michael reaction, based on the direct and TIPSOTf-mediated addition of achiral thioimides to α,β-unsaturated aldehydes catalysed by chiral nickel(II) complexes. A remarkable feature of the method involves the use of an achiral heterocycle as a directing group. While this fragment serves as an effective platform for the C–C bond forming step, it is essential to devise mild methods for its removal and the subsequent conversion into a variety of functional groups.

Preliminary studies in our group had already documented experimental conditions for the removal of the thiazinanethione of aldol adducts to yield amides, carboxylic acids, as well as esters, ketones, aldehydes or alcohols (see Chapter I).[1] Such approaches have also been applied to other heterocycles shown in Figure 23.[2–4] The removal of the five or six-membered heterocycles is usually pretty similar, with those containing an endocyclic sulphur atom being slightly more reactive.

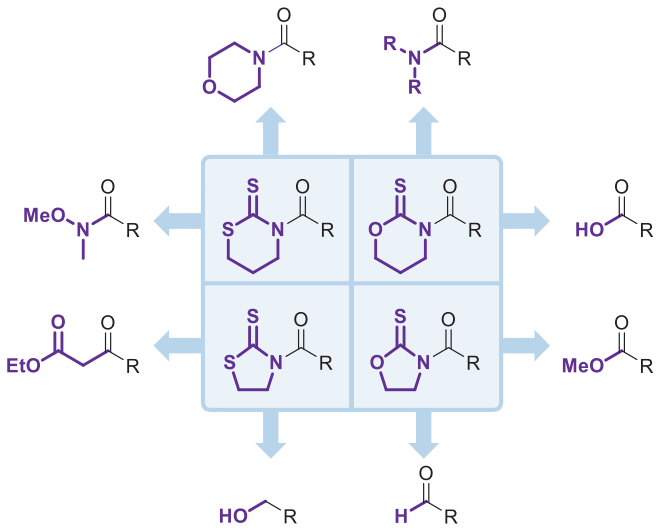

Figure 23. Derivatizations of *N*-acyl thioimides.

In this context and considering that the Michael adducts contain a particularly reactive site, the TIPS silyl enol ether, it was necessary to validate the abovementioned methods to deliver enantiomerically pure intermediates to be used in asymmetric synthesis. Furthermore, the silyl enol moiety could also be used to produce a new variety of intermediates. With the aim of

establishing appropriate conditions to fulfil such objectives, we carried out a comprehensive study of these transformations, which has been crucial for the asymmetric synthesis of tapentadol described on this Chapter.

2 Removal of the thiazinanethione heterocycle

2.1 Scale up of Michael adduct

We scaled-up the reaction to generate large amounts of the Michael adduct in order to facilitate the study. Indeed, the reaction catalysed by [(*R*)-DTBM-SEGPHOS]$NiCl_2$ was carried out at 10 mmol scale, which produced the desired enantiomerically pure adduct smoothly (Scheme 55). The conversion was complete, the diastereoselectivity remained high (dr 83:17) and the enantiomerically pure *syn* Michael adduct **9ab** was isolated with a 73% yield. Furthermore, a 12% of the *anti* diastereomer **9'ab** was also obtained.

As the diastereoselectivity was slightly poorer than that observed at 1 mmol scale (dr 83:17 vs 88:12) probably due to the exothermic nature of the reaction, cooling the bath initially at –40 °C was attempted. The diastereomeric ratio was increased to dr 88:12, but the final conversion reached only 70% in detriment of the overall yield. Thus, the previous conditions were considered good enough to obtain up to 5 g of the desired adduct.

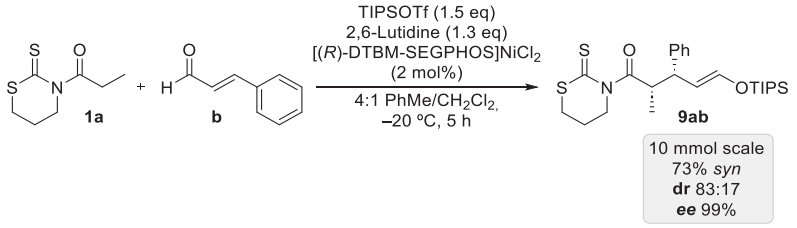

Scheme 55. Scale up of the asymmetric Michael addition.

2.2 Heterocycle displacement

We initiated this investigation by synthesizing a methyl ester, a common functional group useful for further reactions. The abundant prevalence of esters in natural and pharmaceuticals compounds is remarkable, which made their preparation synthetically strategic. Thus, a

mixture of the Michael adduct **9ab** and DMAP as nucleophilic catalyst in methanol at 0 °C was stirred overnight. Employing 10 mol% DMAP resulted in an 87% conversion over 16 h (Table 31, entry 1), so 20 mol% was required (Table 31, entry 2). The methyl ester **13** was obtained in quantitative yield, with the recovery of 90% of the heterocycle (Table 31, entry 3).

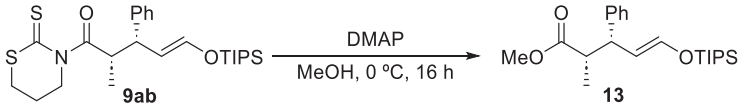

Entry	Scale (mmol)	DMAP (mol%)	Conv (%)[a]	Yield (%)[b]
1	0.1	10	87	-
2	0.1	20	100	-
3	0.5	20	100	99

a) Established by 1H NMR analysis. b) Isolated yield.

Table 31. Derivatization to methyl ester **13**.

Amides are also present in a wide variety of natural compounds and drugs, and are fundamental building blocks for entire research fields such as peptide synthesis. Additionally, morfoline amides are highly desirable intermediates in organic synthesis, owing to their facile transformation into carbonylic compounds.[5] Hence, the obtention of amides *via* heterocycle displacement was highly desirable.

Initially, methyl β-alaninate was used to generate amide **14** in the presence of Et_3N to neutralize the hydrochloride form of β-alaninate. Surprisingly, the displacement only proceeded with a 50% of conversion (Table 32, entry 1). Neither the introduction of DMAP nor the increase of methyl β-alaninate and Et_3N improved the conversion (Table 32, entries 2–3). To our pleasure, the use of CH_2Cl_2 instead of THF circumvented the problem, and a complete conversion was achieved along with a high yield (Table 32, entries 4–5).

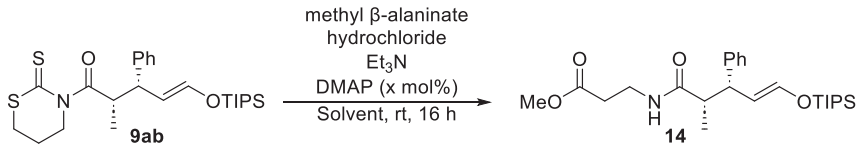

Entry	Scale (mmol)	β-alaninate·HCl (equiv)	Et_3N (equiv)	DMAP (mol%)	Solvent	Conv (%)[a]	Yield (%)[b]
1	0.1	1.25	1.5	-	THF	50	-
2	0.5	1.25	1.5	20	THF	50	-
3	0.1	2.5	3	20	THF	50	-
4	0.1	2.5	3	20	CH_2Cl_2	100	-
5	0.5	2.5	3	20	CH_2Cl_2	100	80

a) Established by ^1H NMR analysis. b) Isolated yield.

Table 32. Synthesis of a β-alanine amide **14**.

Furthermore, the Michael adduct was transformed into the morfoline amide under the optimized conditions used for methyl β-alaninate (Scheme 56). The adduct **9ab** was treated with morfoline and 20 mol% of DMAP to obtain amide **15** in 95% yield.

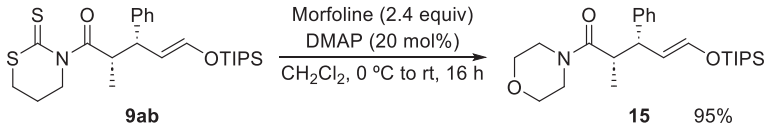

Scheme 56. Synthesis of morfoline amide **15**.

The thiazinanethione can also be eliminated by means of a reductive process. In this regard, the adduct **9ab** was converted into an alcohol employing $LiBH_4$. Remarkably, the reaction proved to be efficient, achieving complete conversion in only 2 h. Subsequent scale up to 3 mmol permitted us to isolate enantiomerically pure alcohol **16** in 93% yield (Scheme 57).

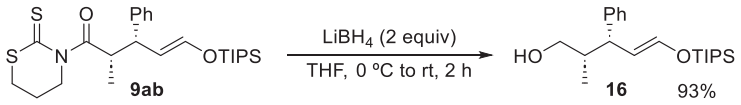

Scheme 57. Reduction to alcohol **16**.

The synthesis of the corresponding aldehyde **17** by treatment with DIBALH was also explored. On a first attempt, the conversion was not achieved, so the amount of DIBALH was increased, and the reaction time was extended with a limited success (Table 33, entries 1–3). Afterwards, DIBALH was added dropwise over 30 min, producing a significant increase in the conversion (Table 33, entry 4). Subsequently, the reaction was scaled up to 0.5 mmol to afford pure aldehyde **17** in 74% yield (Table 33, entry 5).

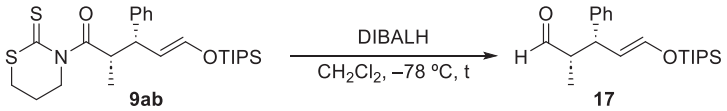

9ab **17**

Entry	Scale (mmol)	DIBALH (equiv)	t (h)	Conv (%)[a]	Yield (%)[b]
1	0.1	1.3	1	80	-
2	0.1	1.5	6	83	-
3	0.1	2	9	75	-
4	0.1	1.5[c]	4	90	-
5	0.5	1.7[c]	5	92	74

a) Established by ^{1}H NMR analysis. b) Isolated yield. c) slow addition of DIBALH over 30 min

Table 33. Reduction to aldehyde **17**.

2.3 Manipulation of the silyl enol ether

As mentioned previously, the resulting silyl enol ether is an attractive platform to carry out further transformations. To explore this reactivity, it was deemed prudent the previous removal of the heterocycle to form either an ester or an alcohol, which could be more suitable substrates for further transformations.

Initially, the alcohol derivative **16** was subjected to a catalytic hydrogenation process. Surprisingly, this proved to be a challenging substrate, as no conversion was observed under a variety of conditions. (Table 34, entries 1–7). Therefore, we moved to the ester derivative **13**, which proved to be an easy substrate towards the catalytic hydrogenation, furnishing the corresponding protected alcohol in quantitative yield (Table 34, entries 8–9).

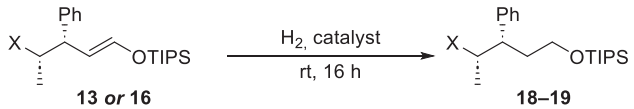

13 *or* 16 18–19

Entry	X	Product	Scale (mmol)	H_2 (bar)	Catalyst	mol%	Solvent	Conv (%)[a]	Yield(%)[b]
1	CH_2OH	**18**	0.1	1	Pd/C	10	EtOAc	0	-
2	CH_2OH	**18**	0.1	1	Pd/C	20	EtOAc	0	-
3	CH_2OH	**18**	0.1	1	Pd/C	20	MeOH	0	-
4	CH_2OH	**18**	0.1	1	Pd/C	20	EtOH	0	-
5	CH_2OH	**18**	0.1	1	$Rh(PPh_3)_3Cl_2$	20	EtOH	0	-
6	CH_2OH	**18**	0.1	5	Pd/C	10	EtOH	0	-
7	CH_2OH	**18**	0.1	5	Pt_2O	10	EtOH	0	-
8	COOMe	**19**	0.1	1	Pd/C	20	EtOH	100	99
9	COOMe	**19**	0.45	1	Pd/C	20	EtOH	100	99

a) Established by ^1H NMR analysis. b) Isolated yield.

Table 34. Hydrogenation of the silyl enol ether

The alcohol **16** containing the silyl enol ether was then converted into the corresponding aldehyde. Treatment of **16** with a 1 M solution of TBAF in THF furnished the aldehyde efficiently, which reacted with the hydroxyl group to form a cyclic acetal as a 1:1 mixture of diastereomers **20** in high yields (Scheme 58).

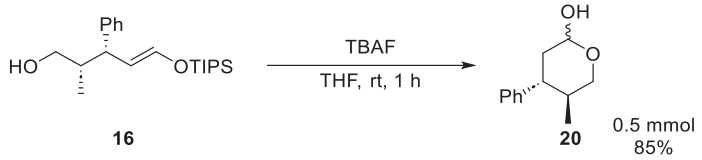

16 20

Scheme 58. Deprotection of the silyl enol ether.

2.4 An unexpected reaction.

The Mukaiyama aldol reaction holds a prominent position for the stereoselective formation of C–C bonds.[6] Therefore, we envisaged that our Michael adducts possessing a silyl enol ether could serve as a platform for stereocontrolled Mukaiyama-type transformations. In this context, we explored the feasibility of Mukaiyama-type transformations from our Michael adducts.

Benzaldehyde was chosen as a model substrate for the aldol addition, employing $BF_3{\cdot}Et_2O$ as a Lewis acid. Unexpectedly, the reaction furnished lactone **21** as the sole product with a full conversion and a 63% yield as a single diastereomer and the remaining aldehyde was fully recovered

unmodified (Scheme 59). In turn, the use of $TiCl_4$ produced only a complex mixture, including retro-Michael products.

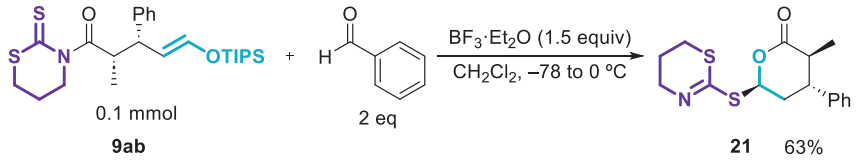

Scheme 59. An unexpected reaction.

Since the aldehyde seemed to be inactive, we repeated the reaction just using $BF_3{\cdot}Et_2O$. To our surprise, removal of the benzaldehyde resulted in the formation of a complex mixture of products, including the cyclized adduct **21** (Scheme 60). The conversion was incomplete and significant amounts of products from the retro-Michael **b** and **1a**, and free thiazinanethione were also detected. While modifying the protocol by introducing the starting material over a $BF_3{\cdot}Et_2O$ solution reduced the formation of most retro-Michael products, several subproducts persisted. These observations strongly suggest that the aldehyde plays a pivotal role, maybe as catalyst or promoter of the reaction.

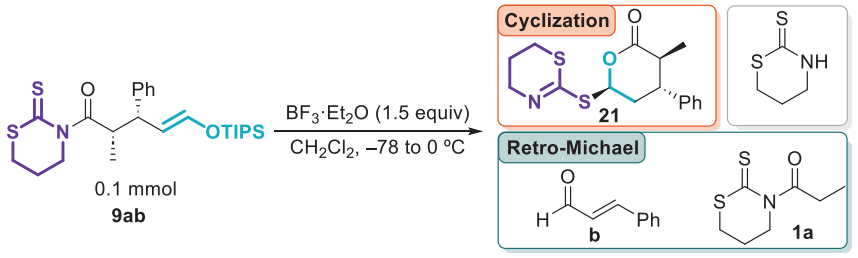

Scheme 60. Products obtained in the reaction.

Remarkably, the results at –78 or 0 °C were similar, which proved that the temperature has a negligible impact on the reaction outcome. Subsequently, aldehydes with different electronic properties were examined and compared to the reaction without the presence of any aldehyde (Table 35, entry 1). The results revealed that aldehydes containing electron donating substituents (Table 35, entries 2–3) partially inhibit the reaction, diminishing the reaction rate to afford a complex mixture with a high presence of retro-Michael products **1a** and **b** and deprotected adduct **22**. Conversely, neutral or electron withdrawing substituents proved to be beneficial, with benzaldehyde emerging as the optimal additive (Table 35, entries 4–5). Finally, the use of aliphatic aldehyde propanal did not bring any improvement (Table 35, entry 6).

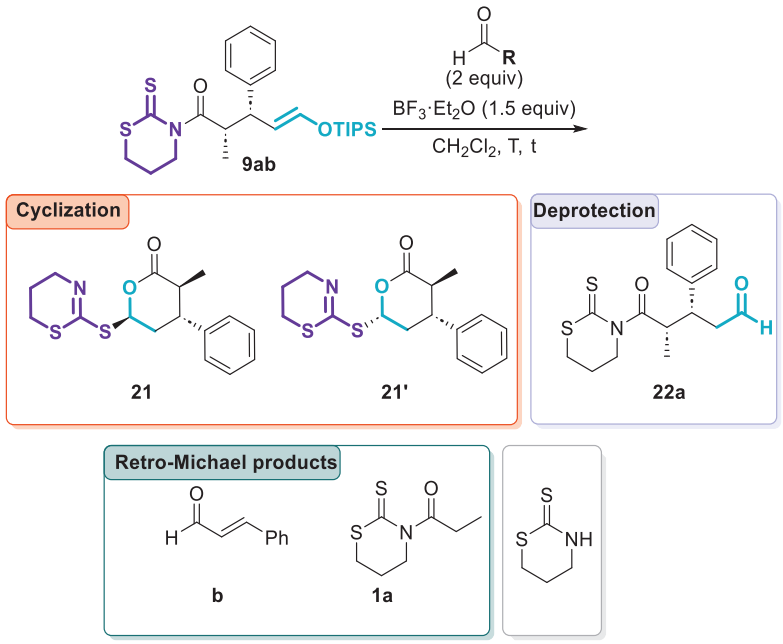

Entry	R	t (h)	T (°C)	Conv (%)[a]	Purity (%)[a,b]
1[c]	-	3	rt	96	56
2	4-MeO-C_6H_4	3	rt	83	Complex mixture
3	4-Me-C_6H_4	3	rt	92	40
4	Ph	3	rt	100	90
5	4-Cl-C_6H_4	3	rt	100	80
6	Et	4	0	70	44

a) Established by ^{1}H NMR analysis. b) Established by ^{1}H NMR comparing the ratio of product **21** vs all other subproducts. c) No aldehyde was used

Table 35. Aldehyde screening for the cyclization reaction.

Dilution proved advantageous in terms of both reaction rate and selectivity (Table 36, entries 1, 4–6), which suggested an intramolecular mechanism. Finally, treatment of a 0.01 M solution of adduct **9ab** with benzaldehyde and $BF_3{\cdot}OEt_2$ provided a 83% yield of lactone **21** (Table 36, entry 6).

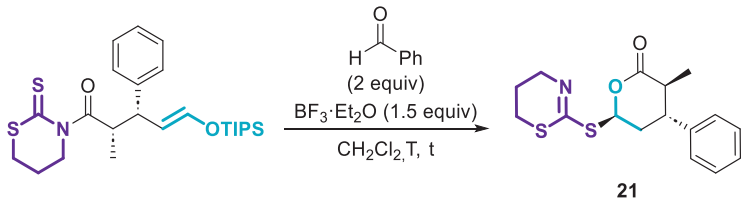

Entry	Scale (mmol)	Conc (M)	t (h)	T (°C)	Conv (%)[a]	Yield (%)[b]	Purity (%)[c]
1	0.1	0.07	3.5	–78 to 0	100	63	100
2	0.5	0.07	3	0 to rt	92	-	33
3	0.9	0.07	3	rt	95	-	58
4	0.2	0.04	3	0	100	-	91
5	0.1	0.01	1.5	0	100	-	91
6	0.5	0.01	1	0	95	83	100

a) Established by ^{1}H NMR analysis. b) Isolated yield. c) Established by ^{1}H NMR comparing the ratio of product **21** vs all other subproducts.

Table 36. Screening of the concentration.

This novel transformation was also evaluated for the *anti* counterpart **9'ab** to assess the formation of different stereoisomers (Scheme 61). On the contrary, the use of the (*R,R*)-isomer led to retro-Michael products, which demonstrated the key role of the relative configuration.

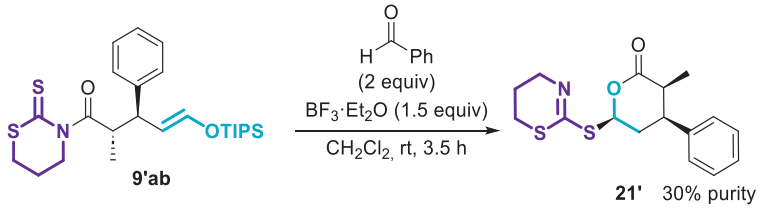

Scheme 61. Use of *anti* adduct for the cyclization reaction.

Based on the preceding results, we hypothesize that an initial step could involve the deprotection of silyl enol ether to generate the aldehyde. Indeed, a ^{19}F NMR analysis revealed the presence of TIPSF, indicating that $BF_3{\cdot}Et_2O$ may be responsible for its deprotection. Subsequently, the nucleophilic exocyclic sulphur could interact with the aldehyde, which in turn could attack the carbonyl amide in a highly ordered bicyclic transition state, with the Ph and the Me substituents located at equatorial positions (Scheme 62). In this mechanistic scheme, the aldehyde might act as a modulator of the Lewis acidity of BF_3, thereby either facilitating or hindering the deprotection step, and consequently influencing the reaction rate.

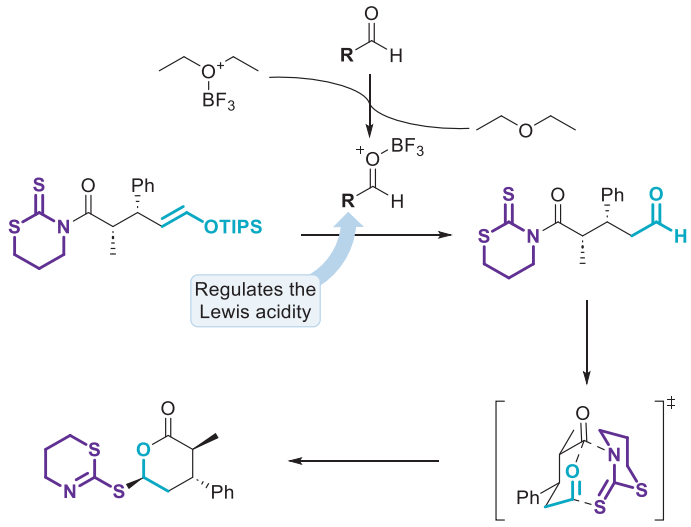

Scheme 62. Proposed mechanism of the cyclization reaction.

Keeping in mind our interest in new Mukaiyama-type reactions, and the influence of the heterocycle, we examined parallel reactions from TBDPS protected hydroxy derivative **23** (Table 37, entries 1–3) or morfoline amide **15** (Table 37, entry 4). Unfortunately and despite our efforts, we did not succeeded and simple deprotection of the silyl enol ether leading to the corresponding aldehyde was mostly observed.

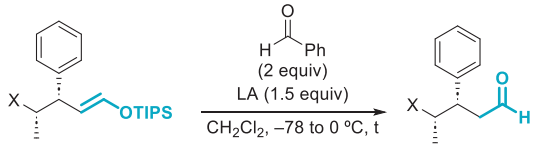

Entry	adduct	X	Scale (mmol)	Lewis acid	Aldehyde	t (h)	Conv (%)[a]	Yield (%)[b]
1	**23**	$CH_2OTBDPS$	0.1	$BF_3{\cdot}Et_2O$	PhCHO	3	100	62
2	**23**	$CH_2OTBDPS$	0.5	$BF_3{\cdot}Et_2O$	PhCHO	3	100	43
3	**23**	$CH_2OTBDPS$	0.1	$TiCl_4$	EtCHO	3	100	Complex mixture
4	**15**	$CON(CH_2CH_2)_2O$	0.1	$TiCl_4$	EtCHO	5	100	-

a) Established by ^1H NMR analysis. b) Isolated yield of aldehydes **22**.

Table 37. Trials to obtain the Mukaiyama-aldol adduct.

Methyl ester **13** was then used instead of the protected alcohol **23**. The reaction with $BF_3{\cdot}Et_2O$ resulted in the deprotection of the silyl enol ether,

exclusively generating the aldehyde **22d** (Table 38, entry 1). The substitution of the Lewis acid by $TiCl_4$ alongside with the use of propanal unexpectedly yielded the reduced cyclization product **24** as a single product. (Table 38, entry 2). Furthermore, the treatment of ester **13** with 30 mol% of $Sc(OTf)_3$ as Lewis acid in the presence of propanal excess furnished the cyclized adduct as a single product in 48 h, which demonstrates that this type of chemistry could be performed catalitycally (Table 38, entry 3).

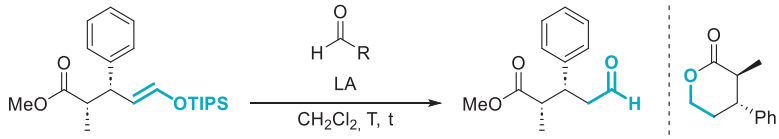

13 22d 24

Entry	Scale (mmol)	Lewis acid	R	t (h)	T (°C)	Conv (%)[a]	Major product
1	0.1	$BF_3{\cdot}Et_2O$	Ph	4	–78 to 0	100	**22c**
3	0.1	$TiCl_4$	Et	4	–78 to 0	100	**24**
4	0.5	$Sc(OTf)_3$	Et	48	rt	100	**24**

a) Established by ^1H NMR analysis.

Table 38. Obtention of the reduced cyclization product.

Due to the challenges encountered in such Mukaiyama-type reactions, the study was paused at this point. Nonetheless, further development of this novel reaction could be a great tool to generate enantiopure chiral lactones.

3 Total synthesis of Tapentadol

The development of novel transformations plays a pivotal role in organic synthesis as enables new and more efficient synthetic sequences.

In this context, we looked for different targets where our novel method could play a promising role (Figure 24). For instance, the installation of these two contiguous stereocentres in a diastereodivergent manner might be used to access cannabinoids moieties such as CBD or Δ^9-THC, psychoactive compounds able to interact with cannabinoid receptors, phenylpiperidines such as paroxetine, which strongly interacts with the nervous system, exhibiting morphine-like effects, antidepressants properties or acting as stimulants, or chebulinic acid, a natural product known for its hepatoprotective effects.

Finally, we envisaged that our Michael addition could be employed for the synthesis of tapentadol, a commercially available synthetic opioid for the treatment of intense pain management.[7–11]

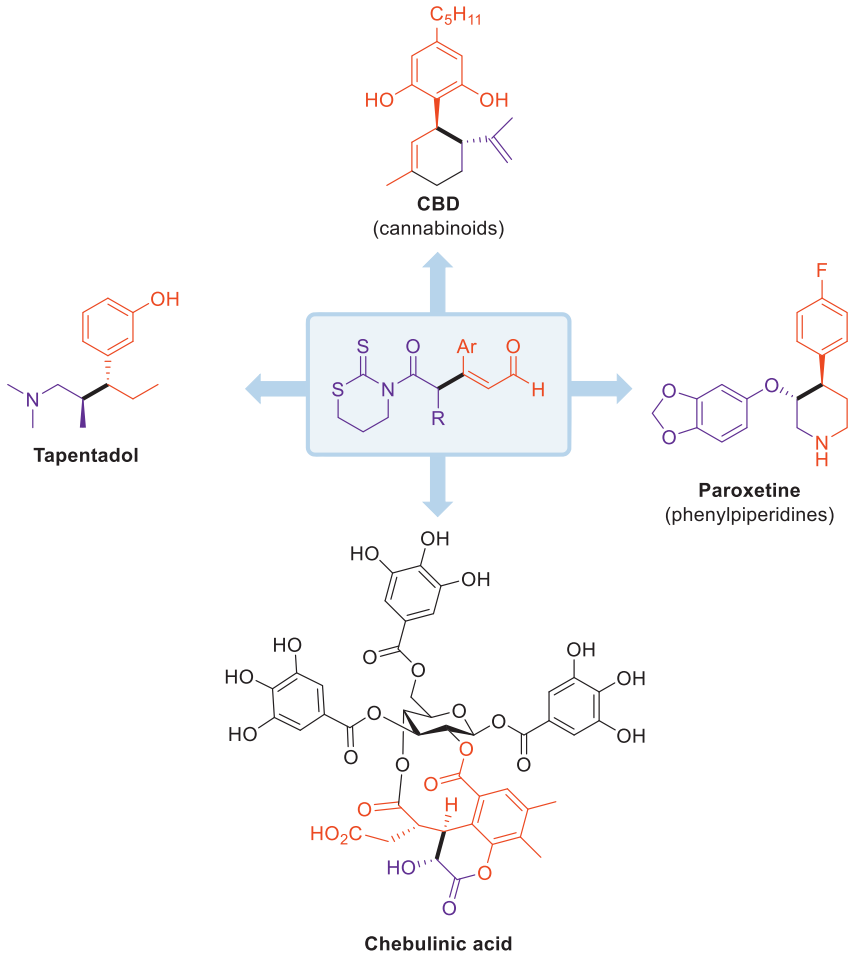

Figure 24. Potential applications of the asymmetric Michael addition.

3.1 Precedents

Tapentadol was developed by Grünenthal in 2001.[12] This molecule is a synthetic opioid which exhibits a dual mode of action, acting as agonist of the μ-opioid receptor and as a norephedrine reuptake inhibitor. Notably, it is slightly more potent than tramadol and oxycodone, with the added benefit of presenting less side effects. Such a profile makes tapentadol an appealing target, and not surprisingly, a few synthetic routes have already been reported.

There are primarly three types of approaches to the synthesis of this compound (Figure 25).[13] The first one consists of synthesizing a racemic mixture followed by an appropiate chiral resolution. The second approach

takes advantage of chiral auxiliaries to control the formation of the new stereocentres. The last one relies on the use of asymmetric catalysts to generate the new stereocentres.

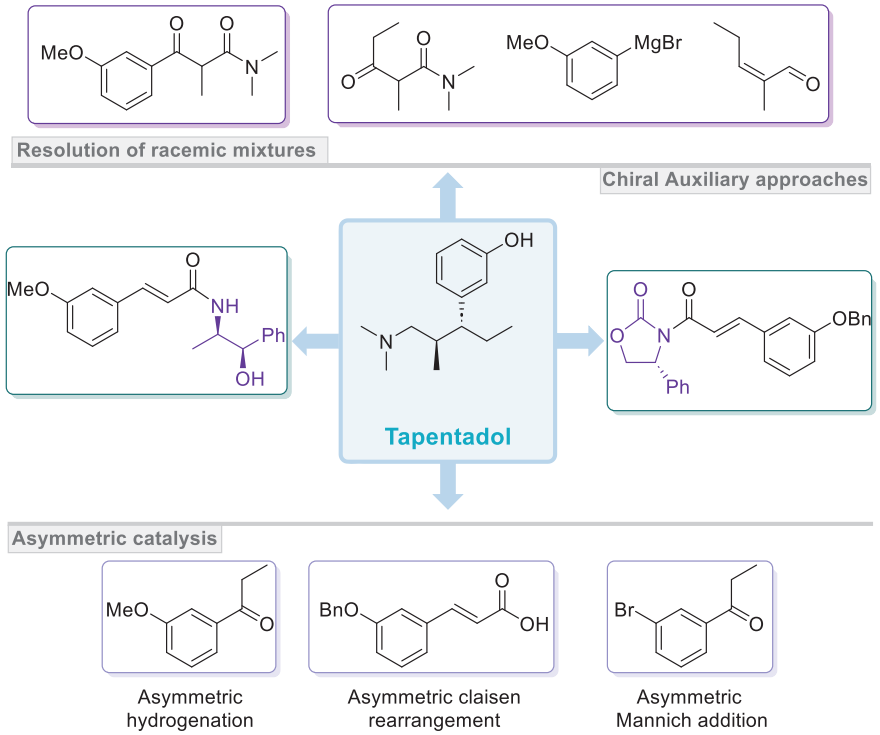

Figure 25. Precedent approaches towards tapentadol synthesis.

In 2012, Zhang et al[14] reported a synthesis of tapentadol based on the use of Evans oxazolidinones to control the configuration of the stereocentres (Scheme 63). They installed the first stereocentre by a stereocontrolled Michael addition of the organocuprate formed by EtMgBr and $CuBr{\cdot}Me_2S$, in the presence of $BF_3{\cdot}Et_2O$ as Lewis acid. Subsequent α-alkylation using NaHDMS and MeI afforded the second stereocentre with an excellent stereocontrol. After removal of the oxazolidinone, the reduction of the dimethylamide intermediate with $LiAlH_4$, followed by deprotection of the benzyl substituent by catalytic hydrogenation afforded tapentadol with an overall yield of 49% and 99% *ee* in ten steps.

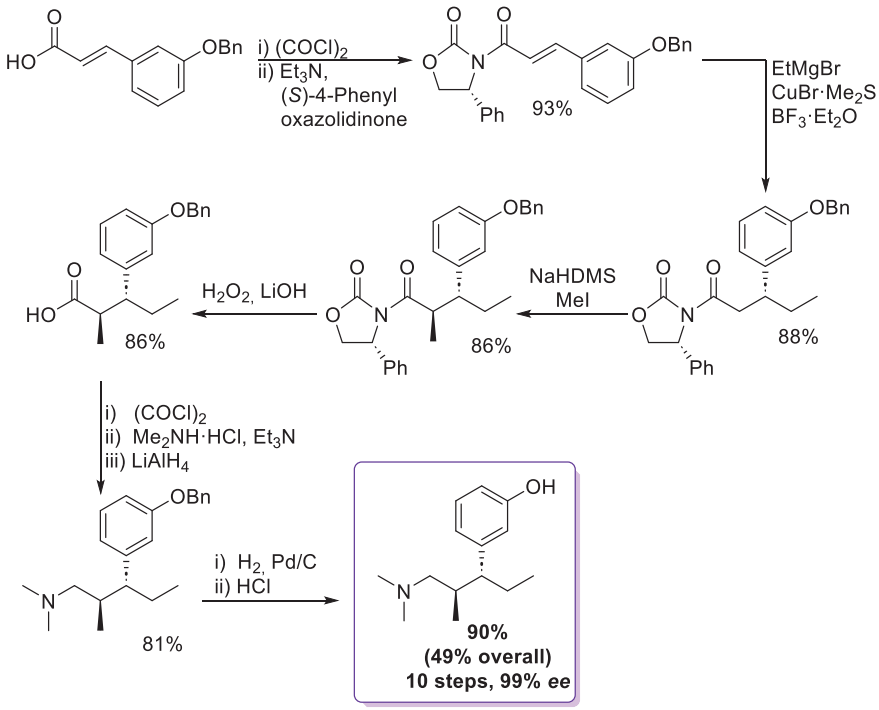

Scheme 63. Zhang synthesis of tapentadol.

A catalytic hydrogenation played a pivotal role in the synthesis of tapentadol by Mapi Pharma (Scheme 64).[15] The reduction of the (*Z*)-α,β-unsaturated amide, accessed prepared through a Horner-Wadsworth-Emmons olefination, produced the chiral amide in a 97% *ee*. Further reduction of the amide followed by demethylation yielded tapentadol in a 55% overall yield in five steps.

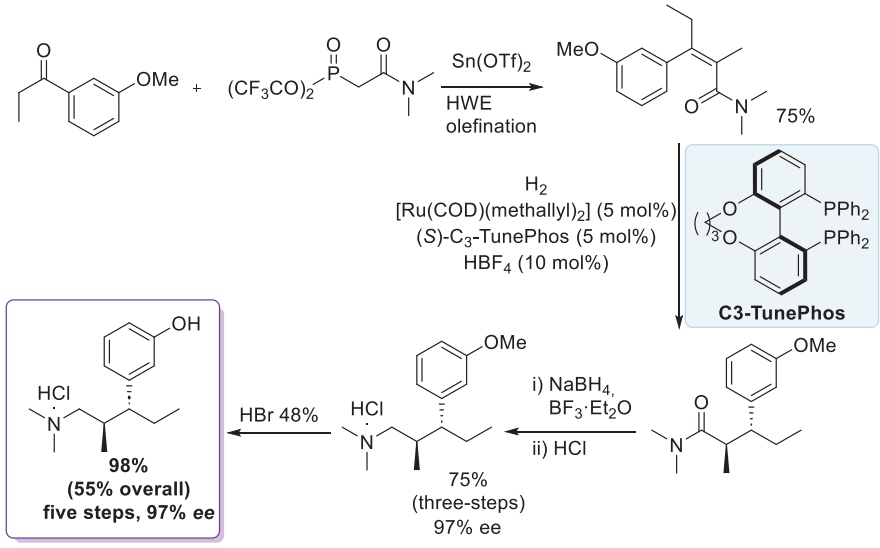

Scheme 64. Mapi Pharma tapentadol synthesis

An elegant synthesis was later described by scientists from Boehringer Ingelheim (Scheme 65).[16] Starting from the cinnamic acid derivative, its reduction to alcohol and subsequent conversion into an allylic ether followed by an isomerization catalysed by an iridium complex yielded the key intermediate. Then, a Ru-catalysed Claisen rearrangement introduced both stereocentres in a >95:5 dr and 93% *ee*. Subsequent reductive amination with Me_2NH and hydrogenation steps gave Tapentadol in 33% overall yield in eight steps.

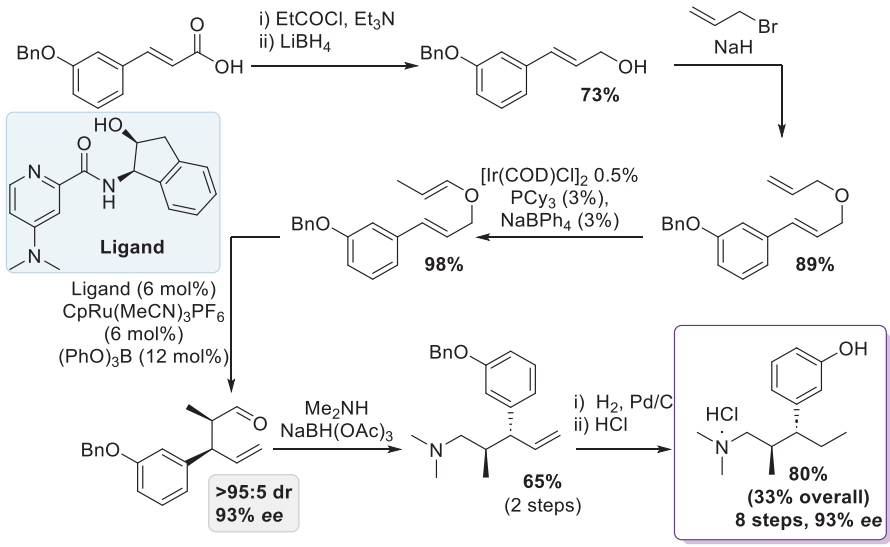

Scheme 65. Boehringer Ingelheim tapentadol synthesis.

An organocatalytic approach based on *L*-proline was pioneered by scientists from Shanghai Biobond Pharmaceutical (Scheme 66).[13,17] The key step consisted of a Mannich reaction of 1-(3-bromophenyl)propan-1-one with paraformaldehyde and dimethylamine catalysed by *L*-proline, which furnished enantiomerically pure (96% *ee*) β-amino ketone with a remarkable 85% yield. Then, a Wittig reaction and was conducted to generate the olefin, and subsequent Suzuki-type reaction facilitated the introduction of the hydroxyl group followed by hydrogenation of the olefin, which ultimately furnished Tapentadol in a 36% overall yield in seven steps.

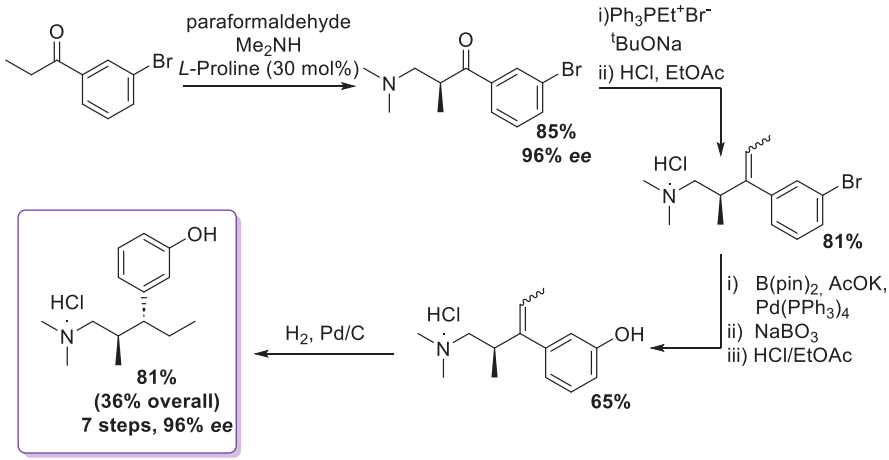

Scheme 66. Shangai Biobond Pharmaceutical tapentadol synthesis.

In summary, the stereocontrolled construction of the two stereocentres is a real challenge, and none of the approaches reported so far involved the use of a Michael addition reaction. Therefore, we envisaged that our Michael method might be able to install both stereocentres in a single step with excellent selectivities.

3.2 Synthesis of tapentadol *via* asymmetric Michael addition

The synthesis of tapentadol started using thioimide **1a** and aldehyde **k** to perform the asymmetric Michael reaction at 10 mmol scale catalysed by [(*S*)-BINAP]$NiCl_2$. The reaction proceeded as expected and the *anti* Michael adduct ***ent*-9'ak** (dr 19:81) was isolated with a 69% yield as a single enantiomer (Scheme 67).

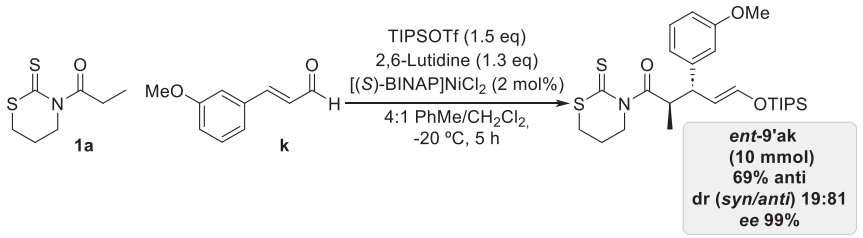

Scheme 67. Asymmetric Michael addition at multigram scale.

The heterocycle was efficiently removed employing $Me_2NH{\cdot}HCl$ with Et_3N in just 2 h in the presence of DMAP to furnish amide **25** quantitatively at 3 mmol (Scheme 68). The resultant product was pure enough and no chromatographic purification was required.

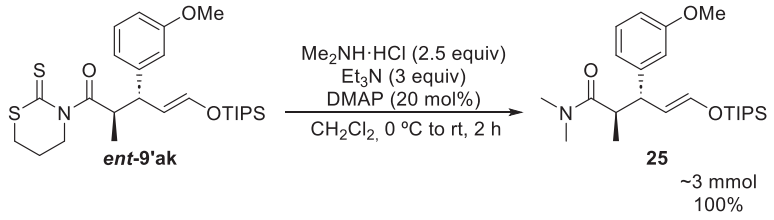

Scheme 68. Derivatization to dimethylamide **25**.

Next, the amide **25** was reduced with $LiAlH_4$ to the corresponding tertiary amine **26** with a 78% yield at 1 mmol scale (Scheme 69).

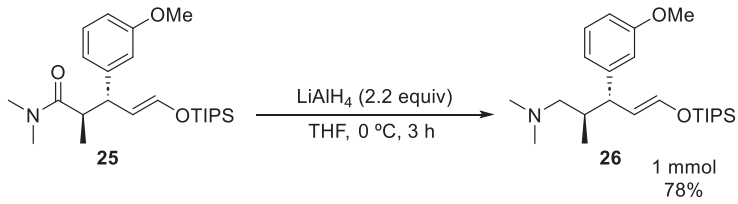

Scheme 69. Reduction to amine **26**.

Subsequently, the silyl protecting group was removed under mild conditions. Initially, TBAF was used but the appearance of several subproducts led us to discard this approach. Alternatively, the use of mild acidic conditions furnished the desired aldehyde **27** with excellent results (Scheme 70). Indeed, treatment of the silyl enol ether **26** with 1 M HCl at room temperature produced the desired aldehyde **27**, which was used without further purification.

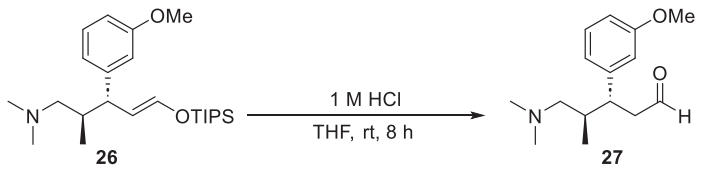

Scheme 70. Deprotection of the silyl enol ether **27**.

The previous aldehyde **27** was submitted to Wolff-Kishner reduction conditions to eliminate the carbonyl group. The aldehyde was first treated with hydrazine hydrate at 160 °C for 4 h. Then, the water generated and excess hydrazine was distilled by simply exposing the reaction mixture to the open atmosphere in which is known as Huang-Minlon modification.[18] Subsequently, addition of NaOH and stirring the mixture at 200 °C for 16 h afforded the amine **28**. Purification by column chromatography in SiO_2 deactivated with Et_3N resulted in significant amounts of product loss, whereas the purification by extractions afforded the pure product in 88% yield over the two previous steps (Scheme 71).

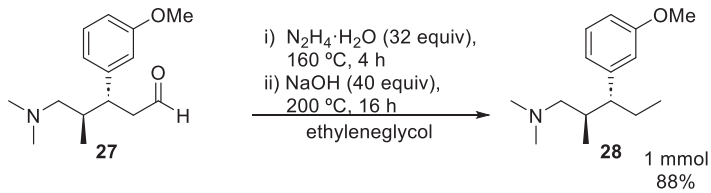

Scheme 71. Wolff-Kishner reduction to form amine **32**

The final step involved the deprotection of the methyl ether.[19] A solution of the previously prepared amine **28** in HBr 48% was heated to reflux temperature for 8 h to deliver the desired tapentadol with a remarkable 96% yield (Scheme 72).

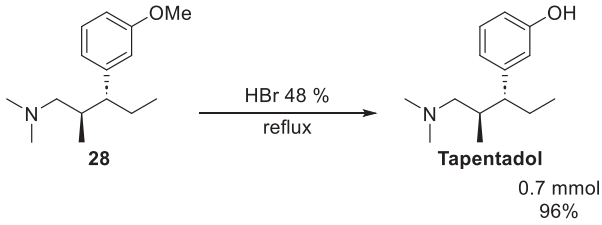

Scheme 72. Deprotection of methyl ether.

Overall, tapentadol was obtained in a six-step sequence with a 45% overall yield in its enantiopure form (*ee* 99%) with only two chromatographic purifications, which shows some advantages to other abovementioned synthesis (Scheme 73). The overall yield is superior to those of Shanghai Biobond Pharma (Scheme 66) and Boehringer Ingelheim (Scheme 65) comparable to the Zhang synthesis (Scheme 63) and slightly lower than Mapi Pharma synthesis (Scheme 64). Moreover, our synthesis includes simple experimental procedures and avoids the use of expensive metals such as rhodium, iridium, or difficult to handle Lewis acids such as $Sn(OTf)_2$ used in the synthesis by Boehringer Ingelheim and Mapi Pharma.

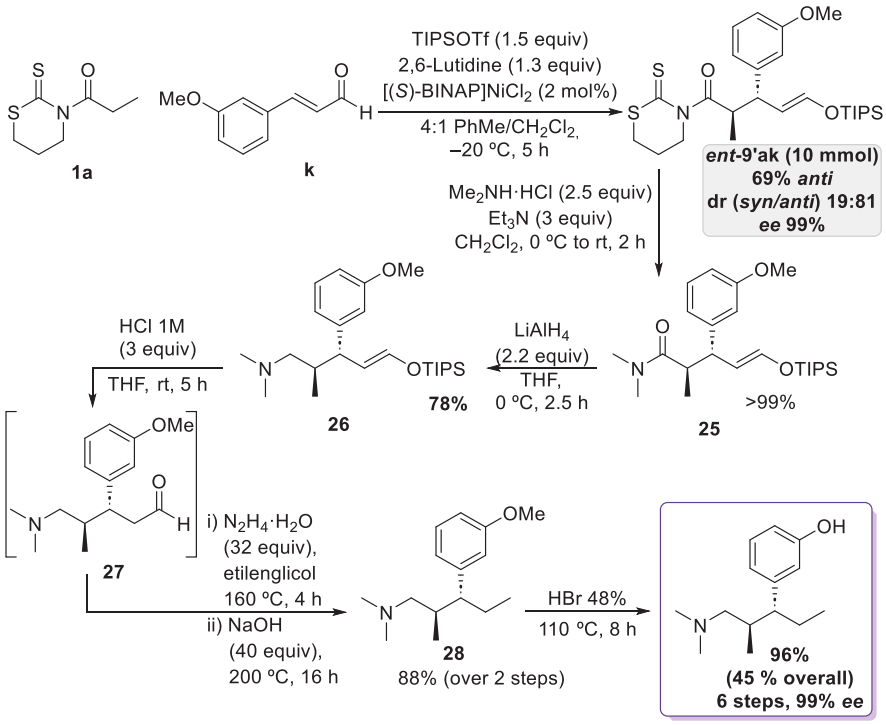

Scheme 73. Total synthesis of Tapentadol based on asymmetric *anti* Michael addition.

4 Outline

In summary, the resultant Michael adducts can be used to synthesize a large variety of enantiomerically pure intermediates by displacement and recovery of the heterocycle, including esters, amides, active amides such as morfoline amide, alcohols or aldehydes. Additionally, the silyl enol ether moiety serves as a second reactive point which can be employed in advanced transformations. Furthermore, a novel reaction was developed to obtain chiral enantioenriched lactones in high yields.

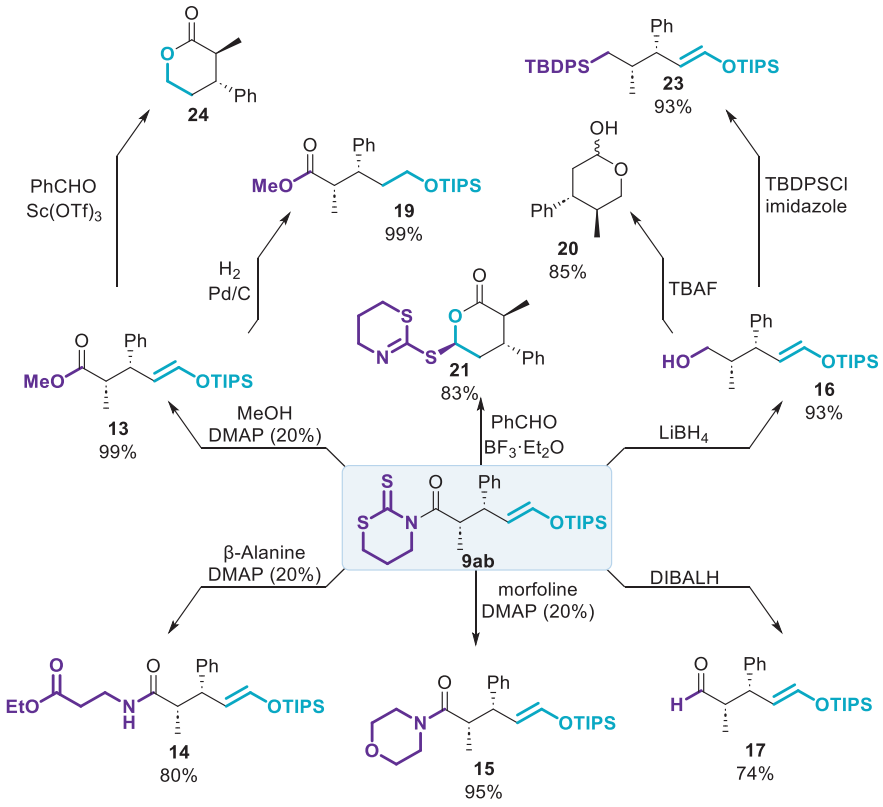

Scheme 74. Transformations of the Michael adduct.

Furthermore, the opioid (*R,R*)-tapentadol has been successfully synthesized, generating both stereocentres in a highly controlled manner. This useful drug has been synthesised in a six-step sequence with a 45% overall yield as a single enantiomer. Furthermore, readily accessible and commercially available reagents have been used in the subsequent steps after the asymmetric Michael addition and only two chromatographic purification steps are required, which increases the ease of use and scalability of the synthesis developed.

5 References

(1) Kennington, S. C. D.; Teloxa, S. F.; Mellado-Hidalgo, M.; Galeote, O.; Puddu, S.; Bellido, M.; Romea, P.; Urpí, F.; Aullón, G.; Font-Bardia, M. Direct and Enantioselective Aldol Reactions Catalyzed by Chiral Nickel(II) Complexes. *Angew. Chem. Int. Ed.* **2021**, *60* (28), 15307–15312.

(2) Mellado-Hidalgo, M.; Romero-Cavagnaro, E. A.; Nageswaran, S.; Puddu, S.; Kennington, S. C. D.; Costa, A. M.; Romea, P.; Urpí, F.; Aullón, G.; Font-Bardia, M. Protected *Syn* -Aldol Compounds from Direct, Catalytic, and Enantioselective Reactions of *N* -Acyl-1,3-Oxazinane-2-Thiones with Aromatic Acetals. *Org. Lett.* **2023**, *25* (4), 659–664.

(3) Teloxa, S. F.; Kennington, S. C. D.; Camats, M.; Romea, P.; Urpí, F.; Aullón, G.; Font-Bardia, M. Direct, Enantioselective, and Nickel(II) Catalyzed Reactions of *N*-Azidoacetyl Thioimides with Trimethyl Orthoformate: A New Combined Methodology for the Rapid Synthesis of Lacosamide and Derivatives. *Chem. Eur. J.* **2020**, *26* (50), 11540–11548.

(4) Kennington, S. C. D.; Taylor, A. J.; Romea, P.; Urpí, F.; Aullón, G.; Font-Bardia, M.; Ferré, L.; Rodrigalvarez, J. Direct and Asymmetric Nickel(II)-Catalyzed Construction of Carbon-Carbon Bonds from N-Acyl Thiazinanethiones. *Org. Lett.* **2019**, *21* (1), 305–309.

(5) Martín, R.; Romea, P.; Tey, C.; Urpí, F.; Vilarrasa, J. Simple and Efficient Preparation of Ketones from Morpholine Amides. *Synlett* **2000**, *12* (12), 1414–1416.

(6) Kennington, S. C. D.; Costa, A. M.; Romea, P.; Urpí, F. Chapter 1.02: Diastereoselective Aldol Reactions. *Comprehensive chirality 2nd Ed; Cossy, J. Ed in Elsevier:Academic Press* **2024**, 9–51.

(7) Hoy, S. M. Tapentadol Extended Release. *Drugs* **2012**, *72* (3), 375–393.

(8) Wiffen, P. J.; Derry, S.; Naessens, K.; Bell, R. F. Oral Tapentadol for Cancer Pain. *Cochrane Database Syst. Rev.* **2015**, *2020* (10).

(9) Santos, J.; Alarcão, J.; Fareleira, F.; Vaz Carneiro, A.; Costa, J. Tapentadol for Chronic Musculoskeletal Pain in Adults. *Cochrane Database Syst. Rev.* **2015**, *2020* (5).

(10) Tzschentke, T. M.; Christoph, T.; Kögel, B.; Schiene, K.; Hennies, H.-H.; Englberger, W.; Haurand, M.; Jahnel, U.; Cremers, T. I. F. H.; Friderichs, E.; De Vry, J. (–)-(1*R*,2*R*)-3-(3-Dimethylamino-1-Ethyl-2-Methyl-

Propyl)-Phenol Hydrochloride (Tapentadol HCl): A Novel μ-Opioid Receptor Agonist/Norepinephrine Reuptake Inhibitor with Broad-Spectrum Analgesic Properties. *J. Pharmacol. Exp. Ther.* **2007**, *323* (1), 265–276.

(11) Freo, U.; Romualdi, P.; Kress, H. G. Tapentadol for Neuropathic Pain: A Review of Clinical Studies. *J. Pain Res.* **2019**, *12*, 1537–1551.

(12) Buschmann, H.; Strassburger, W.; Friderichs, E. 1-Phenyl-3-Dimethylaminopropane Compounds with a Pharmacological Effects. *US6248737B1* **2001**.

(13) Graczyk, P. P.; Zbrojkiewicz, O.; Nerdinger, S. Evolution of Synthetic Routes towards Homochiral Tapentadol. *Tetrahedron:Asymmetry* **2017**, *28* (3), 387–400.

(14) Zhang, Q.; Li, J. F.; Tian, G. H.; Zhang, R. X.; Sun, J.; Suo, J.; Feng, X.; Fang, D.; Jiang, X. R.; Shen, J. S. A Practical and Enantioselective Synthesis of Tapentadol. *Tetrahedron:Asymmetry* **2012**, *23* (8), 577–582.

(15) Marom, E.; Mizhiritskii, M. Intermediate Compounds and Process for the Preparation of Tapentadol and Related Compounds. *WO2011080736A1* **2011**.

(16) Fandrick, D. R.; Rodriguez, S.; Yang, B.-S. Stereoselective Synthesis of Tapentadol and Its Salts. *WO2013090161A1* **2013**.

(17) Liu, Z.; Gao, H.; Bi, P.; Zhou, J.; Qiu, W. Method for Synthesizing Tapentadol Hydrochloride. *CN104803861B* **2015**.

(18) Huang-Minlon. A Simple Modification of the Wolff-Kishner Reduction. *J. Am. Chem. Soc.* **1946**, *68* (12), 2487–2488.

(19) Zhang, Q.; Zhu, M.; Zi, W. Synergizing Palladium with Lewis Base Catalysis for Stereodivergent Coupling of 1,3-Dienes with Pentafluorophenyl Acetates. *Chem* **2022**, *8* (10), 2784–2796.

CHAPTER IV

The Mannich Reaction

Table of contents

1 Introduction

β-Amino carbonyl motifs represent a highly versatile building block in organic synthesis, with a plethora of bioactive compounds featuring them. Despite their significance, β-amino carbonyl compounds are less frequently encountered in the literature compared to their β-hydroxy carbonyl counterparts, primarily due to the reduced electrophilicity of imines. Indeed, the classical Mannich reaction, first described by Carl Mannich in 1912, provides a direct method for synthesizing such β-amino carbonyl motifs, based on the utilization of a trinary system comprising an enolizable carbonyl compound, an aldehyde, and a primary or secondary amine (Scheme 75).

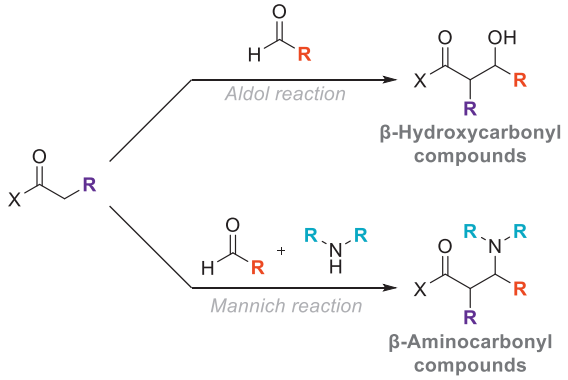

Scheme 75. Aldol and Mannich reactions.

The first asymmetric variants of the Mannich reaction were reported by Kobayashi using a chiral zirconium-BINOL catalyst in a Mukaiyama-type transformation. Later, List introduced the first three-component direct asymmetric Mannich reaction catalysed by the simple amino acid *L*-proline, applying the concept of organocatalysis to the field of Mannich reactions. In turn, a parallel contribution by Jørgensen described the direct addition of α-ketoesters to α-iminoesters catalysed by a BOX-copper(II) complex. Since then, the field of asymmetric catalysis has been steadily growing, with numerous catalysts being developed to efficiently facilitate Mannich additions. The most significant approaches are illustrated in Figure 26.[1–16]

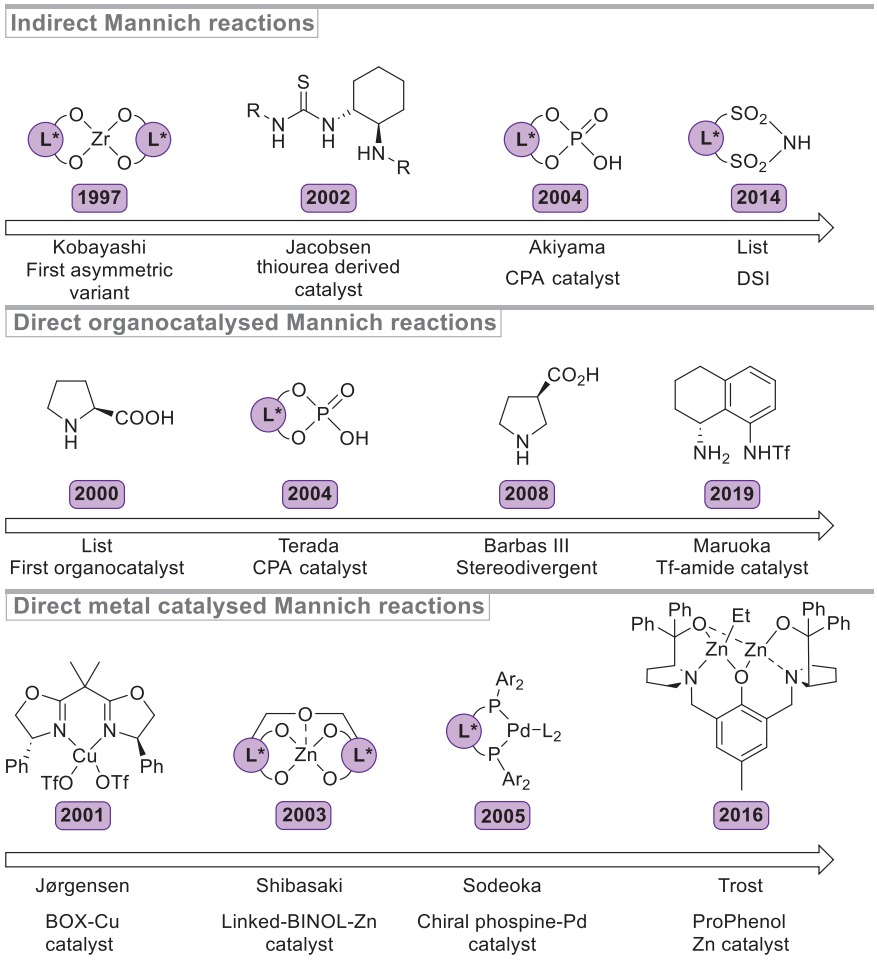

Figure 26. The development of the Mannich addition.

1.1 Activation of C=N bond

The Mannich reaction is one of the most potent methods to obtain β-amino carbonyl compounds, which are key structural motifs in a plethora of compounds. Furthermore, these motifs are also key precursors of β-lactams, one of the most important class of antibiotics.

In spite of such a central position, the Mannich reaction is underdeveloped compared to its carbonylic counterpart, the aldol reaction. This disparity can be attributed to the lower electrophilicity of C=N bond compared to the C=O, which makes it a more challenging reaction. A common strategy to surpass this electrophilic barrier involves the attachment of electron withdrawing substituents to the nitrogen atom, thus enhancing the electrophilicity of the carbon-nitrogen double bond. An illustrative

demonstration is the electrophilicity parameters of different C=N bond determined by Mayr. Compared to the benzaldehyde, even imines with electron withdrawing substituents such as *N*-diphenylphosphinic (Dpp) or Boc are still less reactive, while only electron withdrawing groups such as Ts are capable of reaching similar reactivities (Figure 27).

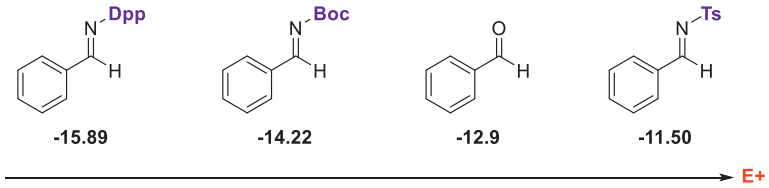

Figure 27. Electrophilicity parameters of imines and benzaldehyde

Interestingly, an added advantage of using these imine-activating groups is that, once the Mannich addition is complete, most of these groups act as protecting groups of the resultant amine, thus increasing the value of the Mannich adducts (Scheme 76).

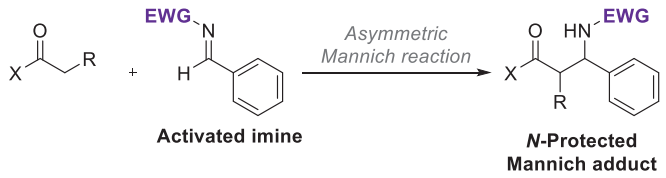

Scheme 76. Activating and protecting role of the electron withdrawing substituent.

1.2 Direct asymmetric Mannich reaction

Several approaches have been reported for the direct asymmetric Mannich addition. In the realm of metal-catalysed transformations, most Mannich additions furnish the *syn* adducts,[17-21] as exemplified in the process developed by Jørgensen. In this study, α-ketoesters reacted with *N*-tosyl-α-imino esters in the presence of a copper(II) complex to yield the corresponding *syn* Mannich adducts in high yields and selectivities (Scheme 77).

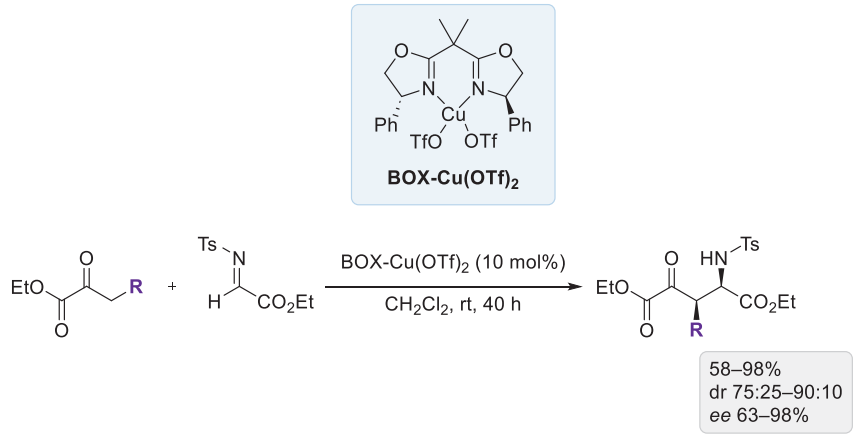

Scheme 77. Copper(II) catalysed Mannich addition.

More recently, Kumagai and Shibasaki reported the reaction of *N*-α-benzyloxyacetyl-7-azaindolines with *N*-Boc aromatic imines in the presence of a copper(I) catalyst to furnish stereoselectively *syn* Mannich adducts in high yields. (Scheme 78). [22]

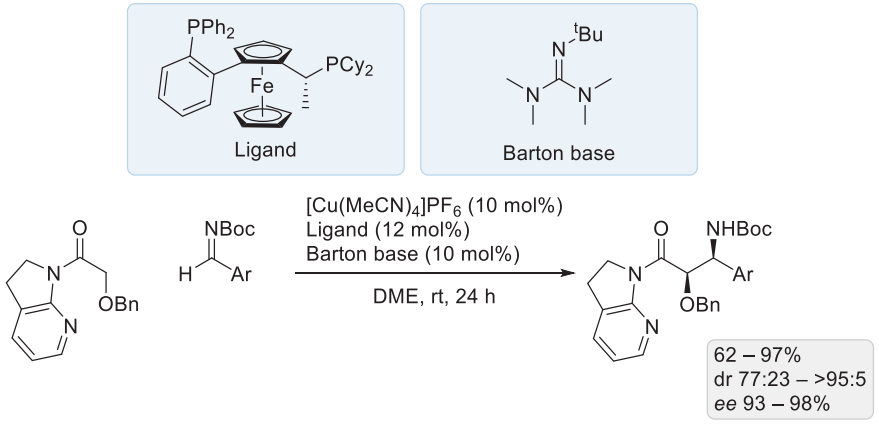

Scheme 78. Copper(I) catalysed Mannich addition.

Non-activated imines can also be used in Mannich reactions provided that the metal enolates are highly nucleophilic. A case in point involves the direct reaction of esters to non-activated imines catalysed by a strong potassium chiral base reported by Kobayashi. In this approach, a strongly nucleophilic potassium enolate is formed, which reacts with the unactivated imine while the stereochemical outcome of the addition is governed by the coordination of the potassium enolate to a chiral BOX-type ligand (Scheme 79).

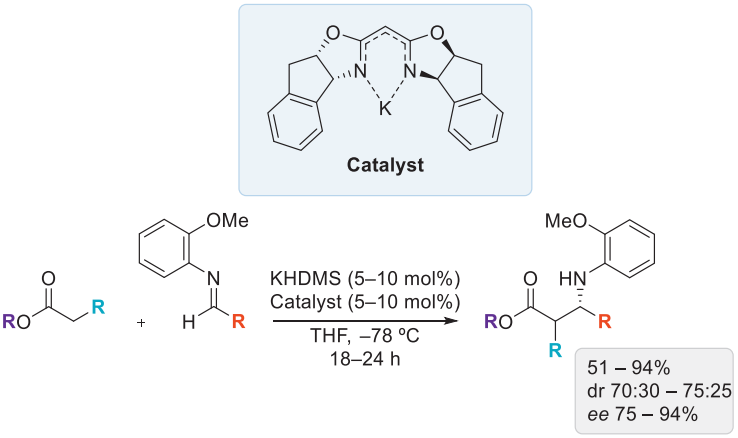

Scheme 79. Reaction of non-activated imines with potassium enolates.

An alternative approach involves the use of imine surrogates that, upon activation by a Brønsted or Lewis acid, generate the imine or iminium ion *in situ*, which then reacts with the nucleophile. For example, Smith reported the addition of β-arylacetic esters to *N,O*-aminals using cooperative isothiourea and HCl Brønsted acid catalysis (Scheme 80).

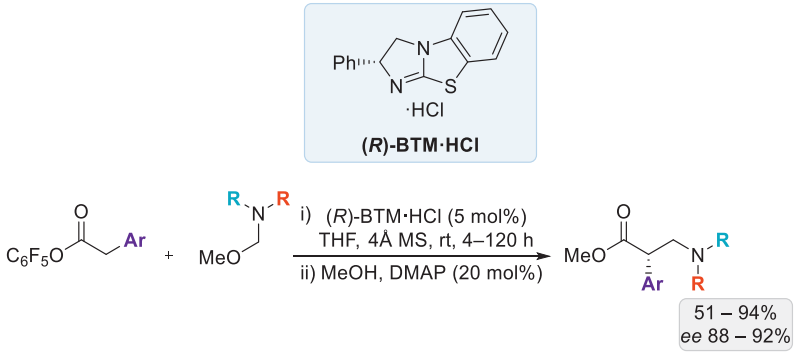

Scheme 80. *N,O*-Aminals in asymmetric Mannich reactions.

In this context, and based on our previous experience in aldol and Michael reactions, we envisaged that our nickel(II) enolates from thioimides could be good candidates to react with these type of preformed *N*-substituted imines or aminals able to provide the required iminium-like intermediates. The activation of such imines or aminals by a Lewis acid would enhance the electrophilicity as occurred with the aldehyde counterparts, which would facilitate the desired Mannich transformation. (Scheme 81)

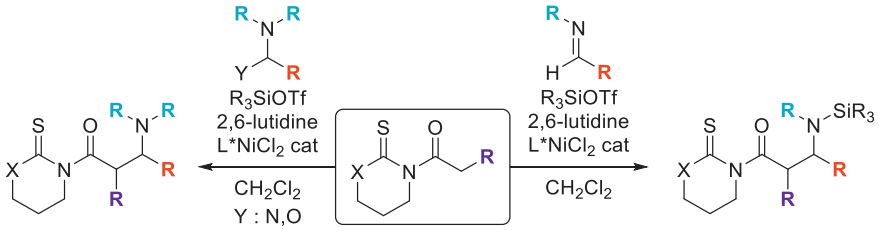

Scheme 81. Reaction of thioimides with activated imines or aminals.

2 Starting materials

2.1 Activated imines

The use of preformed activated imines offers several advantages, such as an enhanced stability towards the nickel(II) complex, a higher concentration of the electrophile, or the avoidance of products associated to the presence of free carbonyl and amine compounds in parallel aldol transformations.

For these reasons, we decided to synthesise imines bearing different protecting groups for the initial trials. These protecting groups could also act as activating agents for the Mannich addition by increasing the electrophilicity of the iminium intermediate. For instance, Ts, Cbz, and Bz groups are electron withdrawing substituents increase the electrophilicity of the C=N bond while furnish the protected amines as Mannich adducts, thereby increasing the value of the overall transformation. We were also interested in assessing the reactivity of alkyl or aryl imines, activated by a Lewis acid species to give tertiary amines after the Mannich reaction. Particularly, the use of a benzyl group furnishes an easily removable and highly valuable protecting group of the amine in the Mannich adduct.

Two primarily methodologies were used for the synthesis of imines. The first one involved the formation of an adduct between the imine and *p*-toluenesulphinate (Table 39, A), which upon treatment with a base formed the desired pure imine.[23] The second methodology consisted of the condensation of the carbonyl compound and the amine to form the corresponding imine in the presence of a dehydrating agent (Table 39, B).[24]

The results shown in Table 39 report non-optimized yields. Importantly, the resulting imines were highly unstable and readily hydrolysed, requiring their immediate use after formation for most substrates.

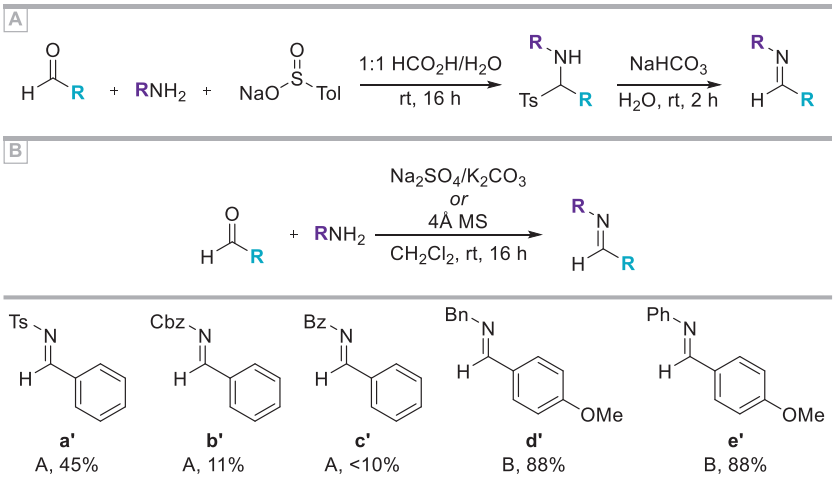

Table 39. Synthesis of imines.

Furthermore, *N*-Dpp protected imines are particularly advantageous for peptide synthesis because their cleavage does not form carbocationic intermediates, thus preventing undesired side reactions. To evaluate the feasibility of their Mannich reactions with our nickel enolates, we synthesized imine **f'** by treatment of diphenylphosphinamide with benzaldehyde catalysed by $TiCl_4$ in the presence of Et_3N (Scheme 82).[25]

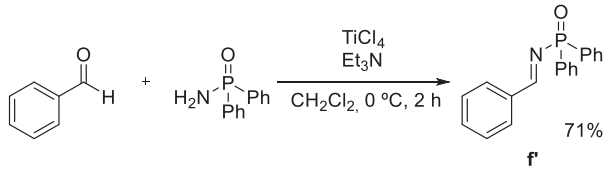

Scheme 82. Synthesis of Dpp-imine.

Finally, benzaldehyde oxime was also synthesized from benzaldehyde by treatment with hydroxylamine, which was then methylated using methyl iodide and NaH to yield the final *O*-methyl oxime **f'** (Scheme 83).[26]

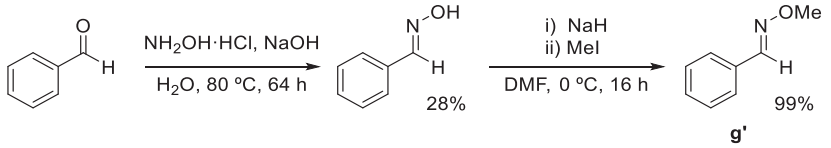

Scheme 83. Synthesis of *O*-methyl oxime of benzaldehyde.

2.2 *N,O*- and *N,N*-aminals

An alternative to activated imines as electrophiles hinges on the use of iminium ion surrogates. The most common imine equivalents are their adducts with alcohols or amines, to form the corresponding *N,O*- and *N,N*-aminals. Upon activation by a Lewis acid, these adducts form an iminium ion, which may participate in a Mannich transformation.

First, a cyclic *N,O*-aminal was synthesized by condensation of 4-methoxybenzaldehyde and ethanolamine using a Dean-Stark apparatus, followed by protection of the resultant free amine to form the desired *N,O*-aminal **j'** (Scheme 84).

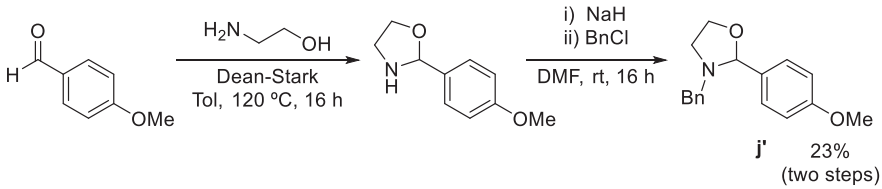

Scheme 84. Synthesis of a cyclic *N,O*-aminal.

In turn, *N,O*-aminal **k'** was synthesized from phthalic anhydride and benzylamine to form *N*-benzyl phthalimide in quantitative yield. Subsequent partial reduction with $NaBH_4$ in MeOH, followed by methylation using NaH and methyl iodide resulted in the formation of the desired *N,O*-aminal **k'** (Scheme 85).

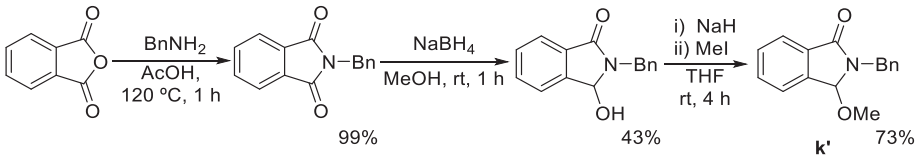

Scheme 85. Synthesis of a phthalimide-derived *N,O*-aminal.

Various aminals were synthesized by reaction of the aldehyde and the amine in the presence of a dehydrating agent followed by the *in situ* addition of an alcohol or an amine to the resultant imine (Table 40).[27]

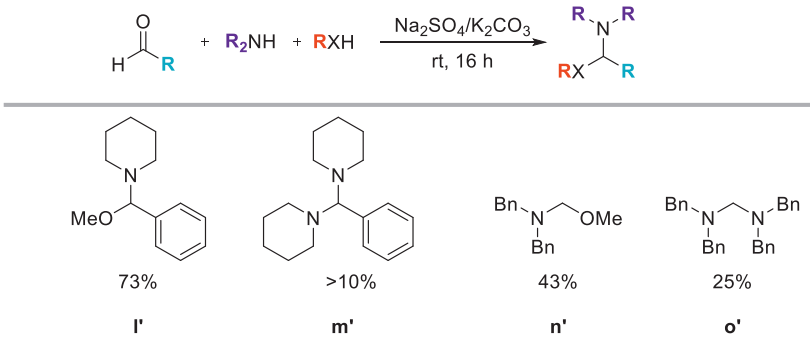

Table 40. Synthesis of aminals by condensation.

The synthesis of *N,N*-aminal **m'** proved to be challenging due to the incomplete formation of the final adduct, which difficulted the purification. To overcome this problem, a mixture of benzaldehyde and piperidine was treated with alumina in THF under reflux, which led to a complete conversion and a 75% yield of the desired pure *N,N*-aminal **m'** (Scheme 86). [28]

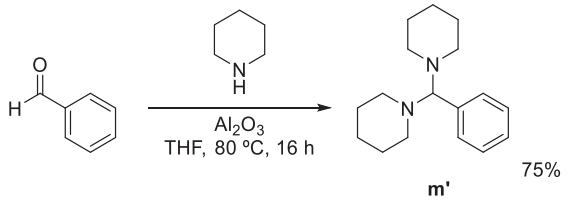

Scheme 86. Synthesis of a piperidine-derived *N,N*-aminal.

An *N,N*-aminal **p'** containing a benzotriazole ring was also synthesized (Scheme 87). These aminals are known to be stable and can be easily purified by recrystallization. Indeed, treatment of benzaldehyde with dibenzyl amine and benzotriazole led to a mixture from which *N,N*-aminal **p'** was recrystallised in a good yield.[29]

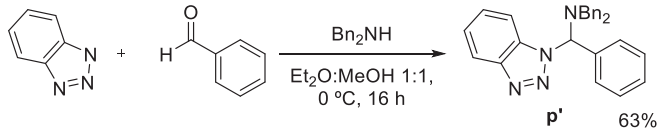

Scheme 87. Synthesis of aminal **p'** from benzotriazole and dibenzylamine.

Finally, in an alternative approach, a nitrone **q'** derived from dibenzylamine was synthesized. Its activation with a trialkylsilyl group would render an iminium ion equivalent. Furthermore, nitrones are known to be bench stable and easy to handle compounds, contrary to several of the previous imine surrogates. The synthesis relied on the oxidation of the

hydroxylamine precursor with H_2O_2, rendering the corresponding nitrone in high yield (Scheme 88).[30]

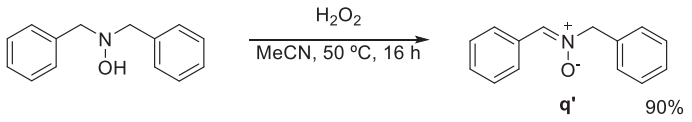

Scheme 88. Synthesis of nitrone **q'.**

3 Additions to imines

We initiated our investigation by using the conditions of the method developed in Chapter I, with achiral $(Me_3P)_2NiCl_2$ complex as catalyst and conducting the reaction at 0 °C. The results revealed that tiny amounts of the desired Mannich adduct were formed (Scheme 89), while, the *N,O*-silyl ketene acetal **30a** was obtained instead as the major product as a 68:32 (*Z:E*) ratio.

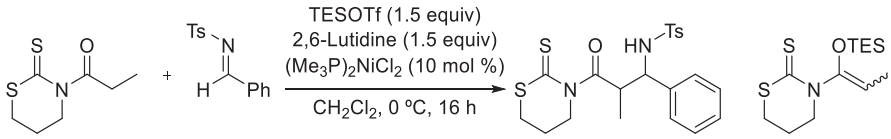

Scheme 89. Mannich reaction with tosyl imine.

Since the reaction without the presence of the imine did not produce the silyl ketene acetal, the tosyl imine must play a key role in its formation (Scheme 90). Presumably, the imine is firstly silylated, and the resultant intermediate acts as a more effective silylating agent compared to TESOTf, which reacts directly with the thioimide rather than through the Mannich addition pathway, to produce the silyl ketene acetal **30a** with 2,6-lutidine acting as a base. This pathway is highly undesirable as the formation of the silyl enol ether may be irreversible, blocking the direct Mannich addition, or undergoing a Mukaiyama-Mannich pathway without any stereochemical control.

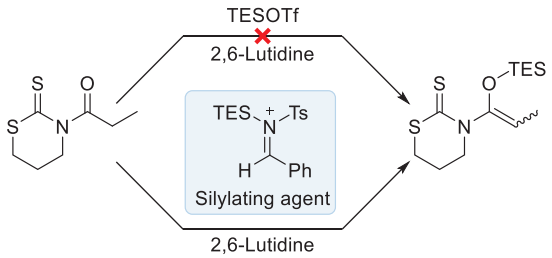

Scheme 90. Formation of the silyl ketene acetal.

This unexpected result led us to explore the impact of the thioimide, aiming to enhance the reaction towards the Mannich adduct while avoiding the silyl ketene acetal formation. The substitution of the endocyclic sulphur atom by an oxygen significantly increased the amount of the Mannich adduct (Table 41, entries 3–4) but the conversion was still poor and the undesired silyl ketene acetal **30** was also formed in comparable yields (Table 41, entries 2 and 4). Other silyl triflates and $BF_3{\cdot}Et_2O$ were also tested in the reaction with **1l** but without success.

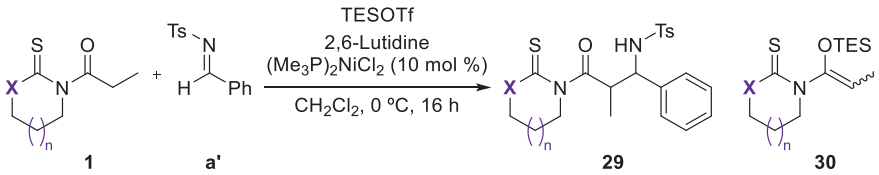

1 a' 29 30

Entry	1	X	n	1 (%)[a]	Mannich (%)[a]	dr[b]	30 (%)[a]
1	**1a**	S	1	53	< 3	-	47
2	**1n**	O	1	51	22	57:42	16
3	**1l**	S	0	42	4	80:20	54
4	**1m**	O	0	42	37	55:44	20

a) Established by ^{1}H NMR analysis using mesitylene as internal standard.
c) dr of the Mannich adduct **29**.

Table 41. Screening of heterocycles for the Mannich addition.

The unsatisfactory results called for a new approach to obtain the desired β-amino carbonyl compounds. Instead of focusing our efforts in the reaction with tosyl imine **a'**, we moved to explore different nitrogen substituents able to facilitate the formation of the iminium ion while avoiding the silyl transfer to the thioimide. Furthermore, we selected different amine protecting groups to activate the C=N bond and obtain directly valuable protected amines.

Unfortunately, the introduction of activating groups such as Cbz, Bz, or Dpp proved to be useless and the expected Mannich adducts were never observed in significant amounts in the reaction mixtures. In turn, the use of *N*-benzyl or *N*-phenyl imines was neither appropriate and gave mixtures of undesired products probably as the result of attacks to the exocyclic sulphur atom of the thioimide.

4 Additions to aminals

Due to the abovementioned poor results, we decided to change the strategy and assess the use of imine equivalents. Initially, we explored the reaction with preformed iminium ions derived from Eschenmoser salts. Surprisingly, these salts were found to be unreactive towards the Mannich addition of our nickel enolates, recovering only the thioimide **1l** (Scheme 91).

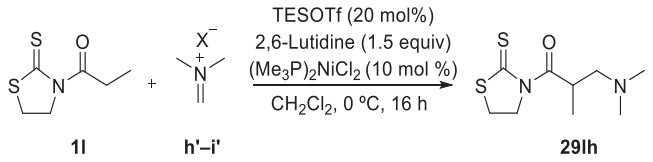

Scheme 91. Mannich reaction using iminium salts.

Thus, we focused our attention to the use of *N,O*-aminals, which upon activation with the Lewis acid TMSOTf were expected to generate the required iminium ion. We first examined the cyclic *N,O* aminal **j',** which resulted unreactive, only recovering the starting thioimide **1l** (Table 42). Next, we assessed the reaction of *N,O*-aminal **l'**, which yielded the Mannich adduct with a 90:10 diastereomeric ratio in low yields (<30%) alongside with several subproducts, as *N*-propanoyl-piperidine which suggests a partial degradation of the starting material, and accounts for the low conversion towards the Mannich adduct obtained. Similarly, the use of *N,N*-aminal counterpart **m'** resulted exclusively in the formation of *N*-propanoyl-piperidine and deacylated thiazolidinethione, preventing the formation of the Mannich adduct.

All the former aminals proved to be highly sensitive and difficult to handle, which posed a significant challenge to the development of the methodology. Therefore, we employed more robust *N,O*-aminals such as **k'** and **p'**. However, the utilization of **k'** only led to the formation of a complex mixture of unknown products. Remarkably, the addition of **p'** to the reaction mixture provoked immediately a colour change from black, typically associated to the nickel(II) complex, to bright yellow, which suggests a rapid catalyst degradation presumably due to the coordination of the benzotriazole moiety.

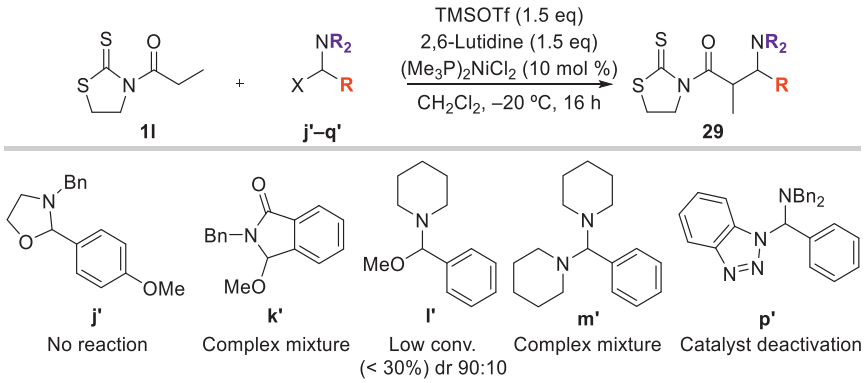

Table 42. Mannich reactions with aminals.

To our delight, the use of *N,O*-aminal **n'** resulted in the formation of the Mannich adduct with a high 85% conversion (Table 43, entry 1). Unfortunately, the reaction was difficult to reproduce, probably due to the low stability of the starting *N,O*-aminal. This low reproducibility could be effectively solved by using the *N,N*-aminal counterpart **o'**, which yielded exclusively the Mannich adduct, with a 68% yield and a 14% *ee* using [(*S*)-BINAP]$NiCl_2$ as catalyst (Table 43, entry 2). In order to improve the enantioselectivity, the reaction was cooled down to –20 °C. The reaction was complete in just 2 h and the selectivity increased up to 56% *ee* (Table 43, entry 3). Further cooling to –40 °C did not improve the selectivity (Table 43, entry 4).

Entry	aminal	L*	t (h)	T (°C)	SM (%)	Conv. (%)[a,b]	Yield (%)[c]	*ee* (%)[d]
1	**n'**	$(Me_3P)_2$	16	0	15	85	-	-
2	**o'**	(*S*)-BINAP	16	0	0	100	54	14
3	**o'**	(*S*)-BINAP	2	–20	0	100	-	56
4	**o'**	(*S*)-BINAP	5	–40	0	100	-	56

a) Established by ^{1}H NMR. b) Conversion. c) Isolated yield. d) Established by ^{1}H NMR of the (*S*)-α-methylbenzylamine derivative.

Table 43. Screening of aminals as imine surrogates.

This modest result showcases the ability of thioimide nickel(II) enolates to react with iminium ions in Mannich-type reactions. Obviously, further studies are required to unveil the most appropriate conditions to attain good enough transformations.

Finally, we explored the utilization of a nitrone **q'** as an imine precursor, which upon *in situ* activation with a silyl triflate, it was expected to generate an iminium intermediate capable of participating in a Mannich addition to give adduct **33lq'**. Unfortunately, the reaction yielded small amounts of the desired adduct, along with a large mixture of unknown products (Scheme 92).

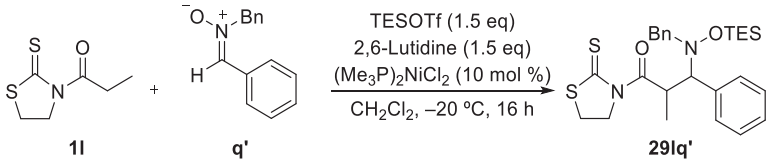

Scheme 92. Nitrone **q'** in direct Mannich addition.

5 A change of perspective

5.1 Cycloaddition reactions

Up to this point, the Thesis has dealt with the reaction of metal enolates from thioimides, particularly chiral nickel (II) complexes, in direct type stereocontrolled C–C bond forming reactions with different electrophiles (Scheme 93, right). Keeping advantage of such experience, we envisaged that α,β-unsaturated thioimides might be excellent platforms from which to carry out cycloaddition type reactions. Indeed, the chiral nickel complex would form the chelate with the α,β-unsaturated thioimide, thereby creating an active electron-deficient olefin able to take part in cycloaddition reactions (Scheme 93, left).

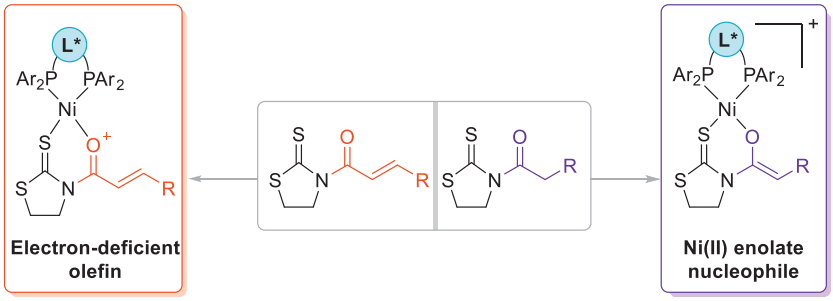

Scheme 93. Nucleophilic enolates and electrophilic electron-poor olefins of thioimides.

Particularly, we hypothesized that nitrones might undergo 1,3 dipolar cycloadditions with α,β-unsaturated thioimides to yield elaborate β-amino carbonyl motifs.[31] Further reduction of the N–O bond of the resultant oxazoline might yield the corresponding β-amino carbonyl compound with up to three new stereocenters (Scheme 94).

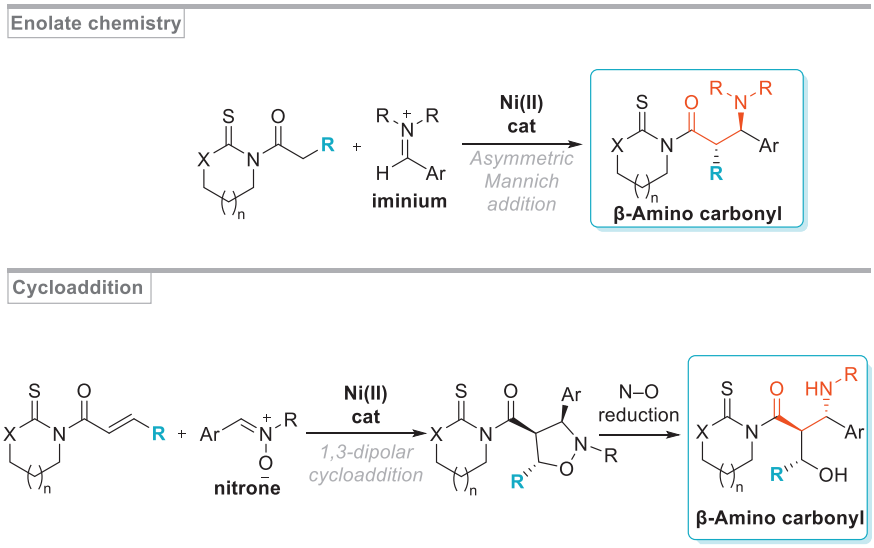

Scheme 94. Access to β-amino carbonyl compounds.

Electron deficient olefins derived from imides and thioimides have been reported to be suitable dienophiles in Diels-Alder reactions or [3+2] dipolar additions to nitrones. Evans provided remarkable approaches in this area and developed highly efficient Diels-Alder reactions using α,β-unsaturated imides catalysed by [(*S,S*)-^{t}BuBOX]Cu(SbF_6) (Scheme 95).[32] This methodology was subsequently utilized in the key step of the synthesis of Δ^1-THC.

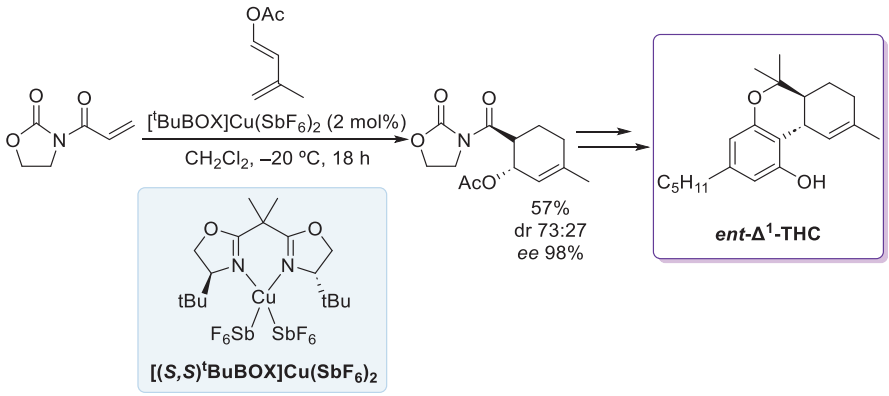

Scheme 95. Diels-Alder reactions of imides.

Furthermore, Evans developed an hetero-Diels-Alder transformation from these imides and silyl enol ethers. Upon treatment of the cycloaddition adduct with an alcohol, the equivalent to a Michael adduct was isolated (Scheme 96).[33]

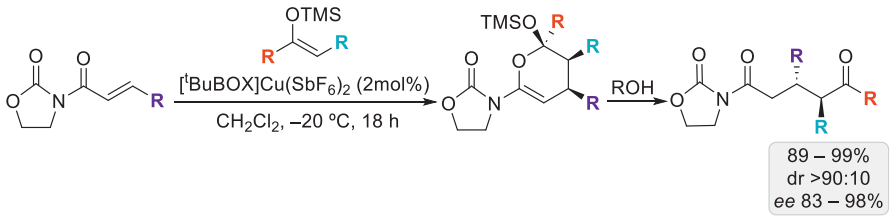

Scheme 96. Hetero-Diels Alder reaction of imide.

5.2 1,3-Dipolar cycloadditions

The 1,3 dipolar reactions are a particular class of [3+2] cycloadditions in which a dipole reacts with a dipolarophile, typically a carbon-carbon multiple bond. They have been extensively used in organic synthesis, which includes classic transformations such as ozonolysis or copper(I)-catalysed cycloaddition of alkynes and azides. The later reaction was key to what is known as click chemistry and was recognized with the 2022 Nobel Prize to Sharpless and Meldal.[34,35]

Other significant dipoles include carbonyl ylides or nitrones. Carbonyl ylides have been widely used for their facile *in situ* generation by rhodium(II) catalysed decomposition of α-diazo carbonyl compounds. For instance, Suga developed a tandem rhodium(II) catalysed carbonyl ylide generation followed by intermolecular 1,3 dipolar cycloaddition with *N*-acryl oxazolidinones catalysed by a chiral ytterbium complex (Scheme 97).[36]

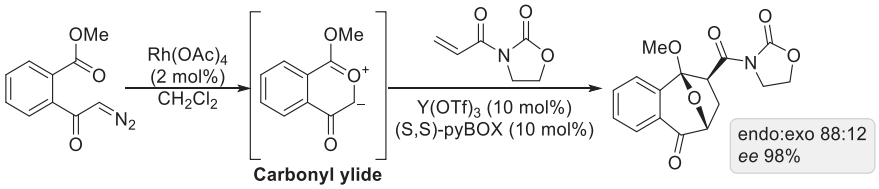

Scheme 97. 1,3-Dipolar reaction of an α-diazido carbonyl ylide.

Interestingly, Suga described a highly *exo*-selective cycloaddition of nitrones and *N*-acryl thiazolidinthiones as dipolarophiles catalysed by a chiral nickel(II) complex, which affords the corresponding *exo* adduct with a remarkable enantiomeric excess (Scheme 98).[37]

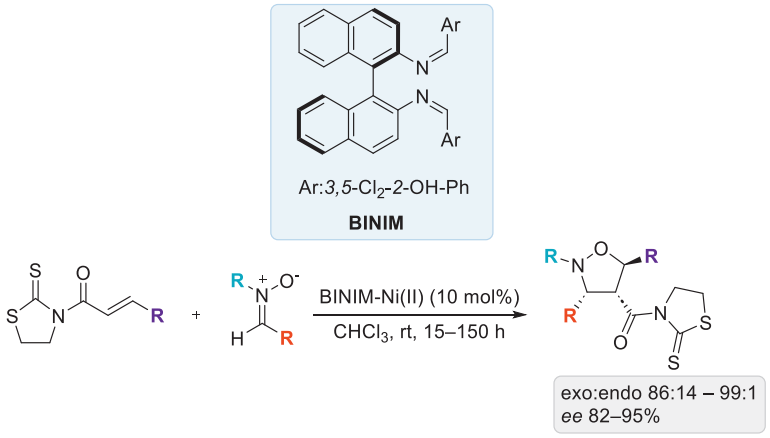

Scheme 98. Reaction of thioimides with nitrones in 1,3 dipolar cycloadditions.

5.3 Stereodivergent 1,3-dipolar cycloadditions

In this context and having explored the Mannich reaction with nitrone **q'**, we tested their 1,3-cycloaddition reactions to generate β-amino carbonyl compounds using our nickel catalyst in a parallel transformation to that reported by Suga. Our first approach used 10 mol% of [(*R*)-DTBM-SEGPHOS]$NiCl_2$ as catalyst, activated with TMSOTf. To our delight, the reaction furnished the *endo* adduct **31sq'** with an excellent dr 97:3, a high 90% ee in a 66% yield (Scheme 99). Additionally, [(*S*)-BINAP]$NiCl_2$ produced the complementary *exo* adduct **31'sq'** in a good dr 21:79 as a single enantiomer with a 47% overall yield (Scheme 99).

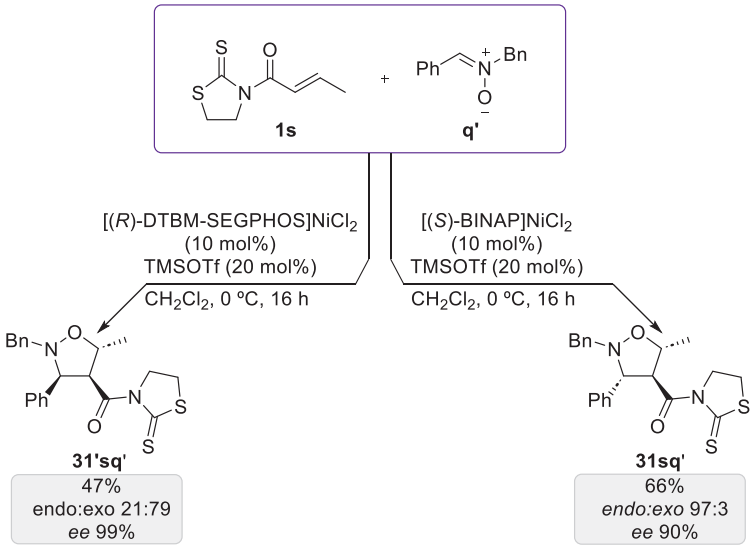

Scheme 99. Stereodivergent 1,3-dipolar cycloaddition of nitrone.

These very preliminary results herald a promising asymmetric stereodivergent method for the formation of five-membered heterocyclic rings and up to three new stereocenters in a highly controlled manner. Subsequent manipulations of these valuable heterocyclic intermediates are expected to provide β-amino carbonyl compounds equivalent to Mannich adducts, which could give access to such challenging motifs.

Beyond the need for a comprehensive analysis of the new stereodivergent paradigm, we hypothesize that acryl thioimides could become a useful platform for a wide array of asymmetric pericyclic reactions, which could encompass 1,3-dipolar cycloadditions as well as Diels-Alder reactions, catalysed by chiral nickel complexes (Scheme 100).

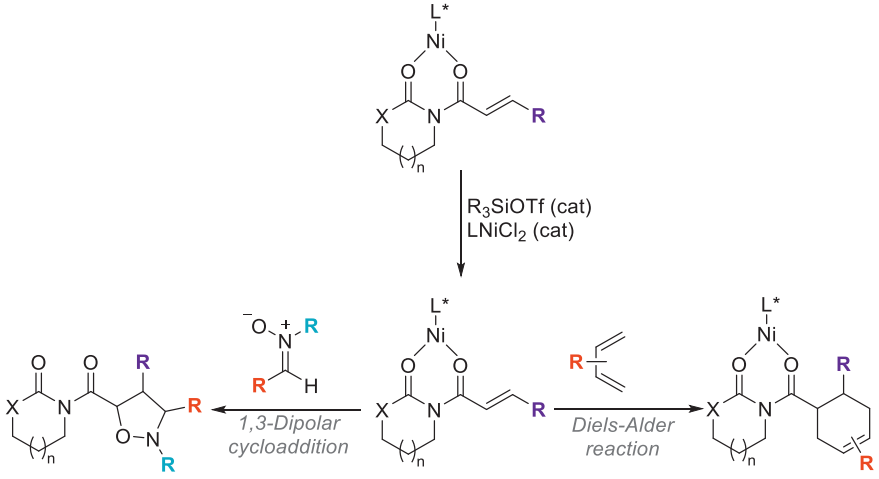

Scheme 100. Cycloaddition reactions from acryl thioimides.

We are aware that the development of such transformations will demand great efforts, but the benefits of would be tremendously worthwhile.

6 Outline

Overall, Chapter IV describes the efforts made towards the development of new methods to obtain β-amino carbonyl compounds.

Direct and asymmetric Mannich additions of thioimides to several activated imines have been attempted without success. Sometimes the imine was not stable enough under the reaction conditions, leading to extensive degradation, other times imines triggered the synthesis of undesired silyl ketene acetals, thus preventing the Mannich addition pathway.

In turn, *N,O*-aminals have proven to be difficult to manipulate, and poor results have been obtained. Instead, the *N,N*,-aminal counterparts are much more promising substrates towards the Mannich addition. The best result has been obtained with *N,N*-dibenzylaminal.

Finally, a stereodivergent approach based on 1,3-dipolar cycloaddition of nitrones have been assayed with excellent results. The addition of nitrones to *N*-acryl thioimides catalysed by either [(*R*)-DTBM-SEGPHOS]$NiCl_2$ or [(*S*)-BINAP]$NiCl_2$ afforded the cycloaddition products with *endo* and *exo* selectivity respectively. Therefore, further efforts in both lines are warranted to develop highly stereocontrolled carbon-carbon bond forming reactions from thioimides catalysed by chiral nickel(II) complexes.

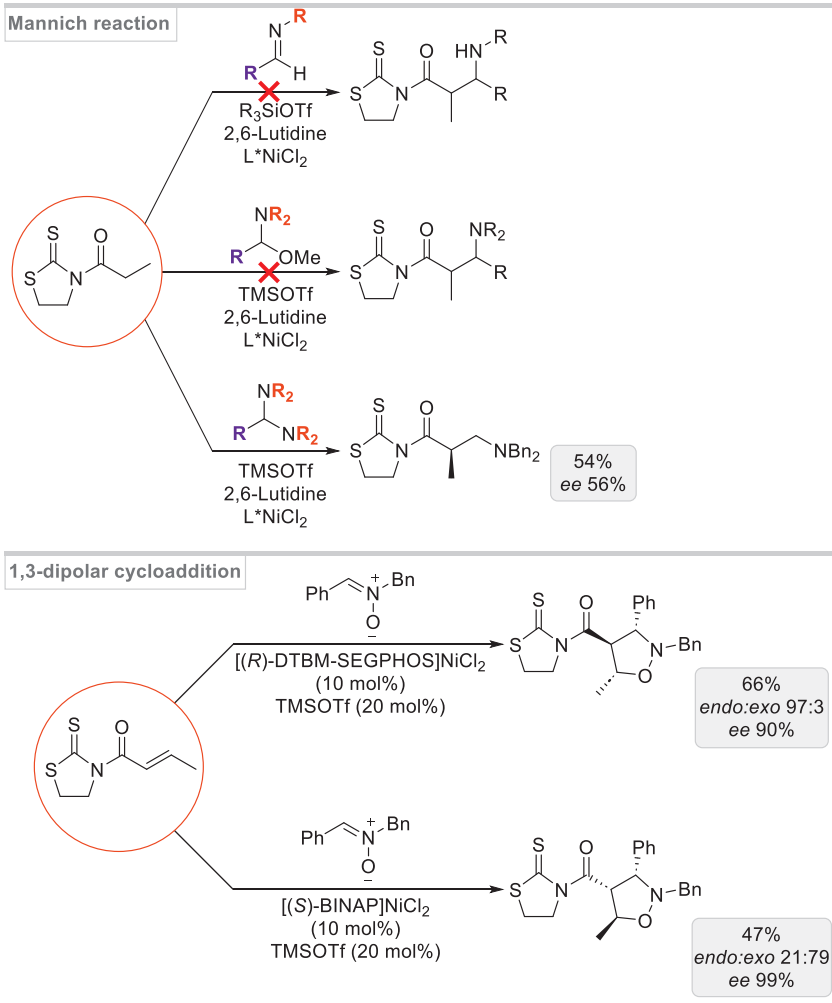

Scheme 101. Summary of Mannich and cycloaddition reactions.

7 References

(1) Ishitani, H.; Ueno, M.; Kobayashi, S. Catalytic Enantioselective Mannich-Type Reactions Using a Novel Chiral Zirconium Catalyst. *J. Am. Chem. Soc.* **1997**, *119* (30), 7153–7154.

(2) Ishitani, H.; Ueno, M.; Kobayashi, S. Enantioselective Mannich-Type Reactions Using a Novel Chiral Zirconium Catalyst for the Synthesis of Optically Active β-Amino Acid Derivatives. *J. Am. Chem. Soc.* **2000**, *122* (34), 8180–8186.

(3) Ferraris, D.; Young, B.; Dudding, T.; Lectka, T. Catalytic, Enantioselective Alkylation of α-Imino Esters Using Late Transition Metal Phosphine Complexes as Catalysts. *J. Am. Chem. Soc.* **1998**, *120* (18), 4548–4549.

(4) Wenzel, A. G.; Jacobsen, E. N. Asymmetric Catalytic Mannich Reactions Catalyzed by Urea Derivatives: Enantioselective Synthesis of *β* -Aryl- *β* -Amino Acids. *J. Am. Chem. Soc.* **2002**, *124* (44), 12964–12965.

(5) Akiyama, T.; Itoh, J.; Yokota, K.; Fuchibe, K. Enantioselective Mannich-Type Reaction Catalyzed by a Chiral Brønsted Acid. *Angew. Chem. Int. Ed.* **2004**, *43* (12), 1566–1568.

(6) Uraguchi, D.; Terada, M. Chiral Brønsted Acid-Catalyzed Direct Mannich Reactions via Electrophilic Activation. *J. Am. Chem. Soc.* **2004**, *126* (17), 5356–5357.

(7) Zhang, H.; Mitsumori, S.; Utsumi, N.; Imai, M.; Garcia-Delgado, N.; Mifsud, M.; Albertshofer, K.; Ha-Yeon Cheong, P.; Houk, K. N.; Tanaka, F.; Barbas, C. F. Catalysis of 3-Pyrrolidinecarboxylic Acid and Related Pyrrolidine Derivatives in Enantioselective Anti-Mannich-Type Reactions: Importance of the 3-Acid Group on Pyrrolidine for Stereocontrol. *J. Am. Chem. Soc.* **2008**.

(8) Shi, S.; Qiu, W.; Miao, P.; Li, R.; Lin, X.; Sun, Z. Three-Component Radical Homo Mannich Reaction. *Nature Commun.* **2021**, *12* (1), 1006.

(9) Juhl, K.; Gathergood, N.; Jørgensen, K. A. Catalytic Asymmetric Direct Mannich Reactions of Carbonyl Compounds Withα-Imino Esters. *Angew. Chem. Int. Ed.* **2001**, *40* (16), 2995–2997.

(10) Matsunaga, S.; Kumagai, N.; Harada, S.; Shibasaki, M. *Anti* -Selective Direct Catalytic Asymmetric Mannich-Type Reaction of

Hydroxyketone Providing β-Amino Alcohols. *J. Am. Chem. Soc.* **2003**, *125* (16), 4712–4713.

(11) Hamashima, Y.; Sasamoto, N.; Hotta, D.; Somei, H.; Umebayashi, N.; Sodeoka, M. Catalytic Asymmetric Addition of β-Ketoesters to Various Imines by Using Chiral Palladium Complexes. *Angew. Chem. Int. Ed.* **2005**, *44* (10), 1525–1529.

(12) Kobayashi, S.; Kiyohara, H.; Yamaguchi, M. Catalytic Silicon-Mediated Carbon-Carbon Bond-Forming Reactions of Unactivated Amides. *J. Am. Chem. Soc.* **2011**, *133* (4), 708–711.

(13) Trost, B. M.; Saget, T.; Lerchen, A.; Hung, C. (Joey). Catalytic Asymmetric Mannich Reactions with Fluorinated Aromatic Ketones: Efficient Access to Chiral β-Fluoroamines. *Angew. Chem. Int. Ed.* **2016**, *128* (2), 791–794.

(14) List, B. The Direct Catalytic Asymmetric Three-Component Mannich Reaction. *J. Am. Chem. Soc.* **2000**, *122* (38), 9336–9337.

(15) Wang, Q.; Van Gemmeren, M.; List, B. Asymmetric Disulfonimide-Catalyzed Synthesis of δ-Amino-β-Ketoester Derivatives by Vinylogous Mukaiyama-Mannich Reactions. *Angew. Chem. Int. Ed.* **2014**, *53* (49), 13592–13595.

(16) Bahmanyar, S.; Houk, K. N. Origins of Opposite Absolute Stereoselectivities in Proline-Catalyzed Direct Mannich and Aldol Reactions. *Org. Lett.* **2003**, *5* (8), 1249–1251.

(17) Šramel, P.; Šebesta, R. Organocatalytic Mannich Type Reactions of Glyoxylate Imines and Related Compounds. *Tetrahedron Lett.* **2024**, *143*, 155129.

(18) Weiner, B.; Szymański, W.; Janssen, D. B.; Minnaard, A. J.; Feringa, B. L. Recent Advances in the Catalytic Asymmetric Synthesis of β-Amino Acids. *Chem. Soc. Rev.* **2010**, *39* (5), 1656.

(19) Córdova, A. The Direct Catalytic Asymmetric Mannich Reaction. *Acc. Chem. Res.* **2004**, *37* (2), 102–112.

(20) Filho, J. F. A.; Lemos, B. C.; de Souza, A. S.; Pinheiro, S.; Greco, S. J. Multicomponent Mannich Reactions: General Aspects, Methodologies and Applications. *Tetrahedron* **2017**, *73* (50), 6977–7004.

(21) Arend, M.; Westermann, B.; Risch, N. Modern Variants of the Mannich Reaction. *Angew. Chem. Int. Ed.* **1998**, *37* (8), 1044–1070.

(22) Sun, B.; Pluta, R.; Kumagai, N.; Shibasaki, M. Direct Catalytic Asymmetric Mannich-Type Reaction en Route to α-Hydroxy-β-Amino Acid Derivatives. *Org. Lett.* **2018**, *20* (3), 526–529.

(23) Yao, W.-W.; Li, R.; Li, J.-F.; Sun, J.; Ye, M. NHC Ligand-Enabled Ni-Catalyzed Reductive Coupling of Alkynes and Imines Using Isopropanol as a Reductant. *Green Chem.* **2019**, *21* (9), 2240–2244.

(24) Lawson, J. R.; Wilkins, L. C.; Melen, R. L. Tris(2,4,6-trifluorophenyl)Borane: An Efficient Hydroboration Catalyst. *Chem. Eur. J.* **2017**, *23* (46), 10997–11000.

(25) Yamada, K.; Harwood, S. J.; Gröger, H.; Shibasaki, M. The First Catalytic Asymmetric Nitro-Mannich-Type Reaction Promoted by a New Heterobimetallic Complex. *Angew. Chem. Int. Ed.* **1999**, *38* (23), 3504–3506.

(26) Ismail, T.; Shafi, S.; Singh, S.; Sidiq, T.; Khajuria, A.; Rouf, A.; Yadav, M.; Saikam, V.; Singh, P. P.; Alam, M. S.; Islam, N.; Sharma, K.; Kumar, H. M. S. Synthesis and Immunopotentiating Activity of Novel Isoxazoline Functionalized Coumarins. *Eur. J. Med. Chem.* **2016**, *123*, 90–104.

(27) Borys, A. M.; Gil-Negrete, J. M.; Hevia, E. Atom-Efficient Transition-Metal-Free Arylation of *N*,*O*-Acetals Using Diarylzinc Reagents through Zn/Zn Cooperativity. *Chem. Commun.* **2021**, *57* (71), 8905–8908.

(28) Hatano, B.; Nagahashi, K.; Kijima, T. Zinc-Mediated Allylation and Alkylation of Aminals in the Presence of TMSCl and Diisopropylamine. *J. Org. Chem.* **2008**, *73* (22), 9188–9191.

(29) Wang, K.; Yu, J.; Shao, Y.; Tang, S.; Sun, J. Forming All-Carbon Quaternary Stereocenters by Organocatalytic Aminomethylation: Concise Access to $\beta^{2,2}$-Amino Acids. *Angew. Chem. Int. Ed.* **2020**, *59* (52), 23516–23520.

(30) Granato, Á. S.; Amarante, G. W.; Adrio, J. Metal-Free Solvent Promoted Oxidation of Benzylic Secondary Amines to Nitrones with H_2O_2. *J. Org. Chem.* **2021**, *86* (19), 13817–13823.

(31) Hashimoto, T.; Maruoka, K. Recent Advances of Catalytic Asymmetric 1,3-Dipolar Cycloadditions. *Chem. Rev.* **2015**, *115* (11), 5366–5412.

(32) Evans, D. A.; Barnes, D. M.; Johnson, J. S.; Lectka, T.; von Matt, P.; Miller, S. J.; Murry, J. A.; Norcross, R. D.; Shaughnessy, E. A.; Campos, K. R. Bis(Oxazoline) and Bis(Oxazolinyl)Pyridine Copper Complexes as

Enantioselective Diels–Alder Catalysts: Reaction Scope and Synthetic Applications. *J. Am. Chem. Soc.* **1999**, *121* (33), 7582–7594.

(33) Evans, D. A.; Willis, M. C.; Johnston, J. N. Catalytic Enantioselective Michael Additions to Unsaturated Ester Derivatives Using Chiral Copper(II) Lewis Acid Complexes. *Org. Lett.* **1999**, *1* (6), 865–868.

(34) Tornøe, C. W.; Christensen, C.; Meldal, M. Peptidotriazoles on Solid Phase: [1,2,3]-Triazoles by Regiospecific Copper(I)-Catalyzed 1,3-Dipolar Cycloadditions of Terminal Alkynes to Azides. *J. Org. Chem.* **2002**, *67* (9), 3057–3064.

(35) Rostovtsev, V. V.; Green, L. G.; Fokin, V. V.; Sharpless, K. B. A Stepwise Huisgen Cycloaddition Process: Copper(I)-Catalyzed Regioselective "Ligation" of Azides and Terminal Alkynes. *Angew. Chem. Int. Ed.* **2002**, *41* (14), 2596–2599.

(36) Suga, H.; Inoue, K.; Inoue, S.; Kakehi, A. Highly Enantioselective 1,3-Dipolar Cycloaddition Reactions of 2-Benzopyrylium-4-Olate Catalyzed by Chiral Lewis Acids. *J. Am. Chem. Soc.* **2002**, *124* (50), 14836–14837.

(37) Suga, H.; Nakajima, T.; Itoh, K.; Kakehi, A. Highly *Exo* -Selective and Enantioselective Cycloaddition Reactions of Nitrones Catalyzed by a Chiral Binaphthyldiimine–Ni(II) Complex. *Org. Lett.* **2005**, *7* (7), 1431–1434.

CONCLUSIONS

This Thesis has explored catalytic asymmetric carbon-carbon bond forming transformations using catalysed by chiral complexes of common and abundant metals, with emphasis on chiral nickel (II) derivatives. Taking advantage of nickel(II) enolates from thioimides, we have made contributions in the fields of asymmetric aldol, Michael and Mannich reactions.

In **Chapter I**, the aldol reaction of thioimides with a wide range of aldehydes was described. During these studies, we successfully developed the aldol reaction between *N*-acyl-1,3-thiazinane-2-thiones and aromatic aldehydes activated by TIPSOTf in the presence of [(*R*)-Tol-BINAP]$NiCl_2$ (2–10 mol%) to furnish the protected *anti* aldol adduct in high yields and diastereoselectivities, along with an excellent enantiomeric excess. Challenging substrates such as α,β-unsaturated aldehydes, propargyl aldehydes and the acetate aldol reaction marked the limits of this novel transformation. Furthermore, other abundant metals such as cobalt and iron could also catalyse the aldol reactions, thus paving the way for future advancements.

In this context, attention should be paid to the introduction of chiral ligands to these metals such as chiral SALEN derivatives or chiral phosphines to achieve control over the enantioselectivity of the process (Scheme 102).

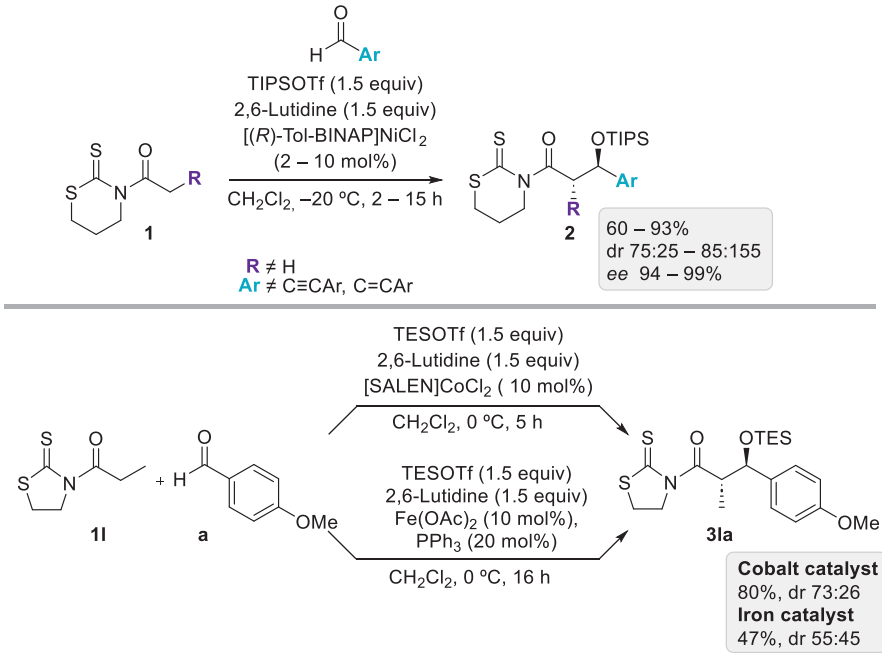

Scheme 102. Aldol reactions of thioimides catalysed by metal enolates.

Part of these results of Chapter I were published in:

"Kennington, S. C. D.; Teloxa, S. F.; Mellado-Hidalgo, M.; Galeote, O.; Puddu, S.; Bellido, M.; Romea, P.; Urpí, F.; Aullón, G.; Font-Bardia, M. Direct and Enantioselective Aldol Reactions Catalyzed by Chiral Nickel(II) Complexes. *Angew. Chem. Int. Ed.* **2021**, *60* (28), 15307–15312."

In **Chapter II**, a stereodivergent Michael addition of *N*-acyl thiazinanethiones to the challenging α,β-unsaturated aldehydes was described. These substrates had not previously been reported in metal-catalysed Michael reactions, due to the inherent tendency towards 1,2 aldol adducts. We surpassed this challenge by the use of bulky TIPSOTf and *N*-acyl thiazinanethiones, which react with aromatic aldehydes in the presence of [(*R*)-DTBM-SEGPHOS]$NiCl_2$ (2–10 mol%) to furnish the *syn* Michael adduct in high yields and diastereoselectivities. Additionally, the reaction in the presence of [(*R*)-BINAP]$NiCl_2$ (2–10 mol%) yielded the complementary *anti* diastereomer in high yields and diastereoselectivities. In both cases, the regioselectivity was complete to the 1,4 addition adduct and the enantioselectivity was outstanding (99% *ee*). So we can prepare any of the potential stereoisomers at will. Importantly, this transformation proved to tolerate the presence of several functional group on the aromatic moiety and the *N*-acyl thiazinanethione (Scheme 103).

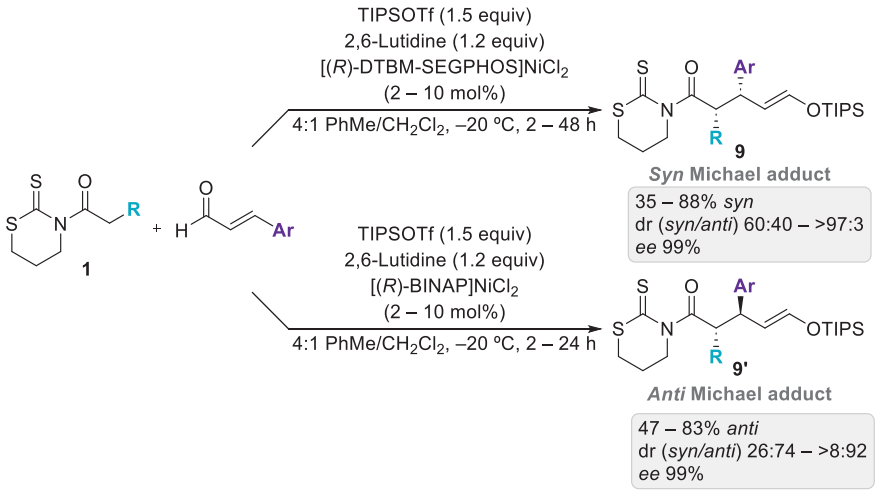

Scheme 103. Stereodivergent Michael addition to α,β unsaturated aldehydes.

Chapter III explores the scale-up and the derivatization of the Michael adduct, demonstrating that the thiazinanethione acts as an active ester and can be readily removed to convert the Michael adduct into a wide variety of useful functional groups. Additionally, the resulting silyl enol ether from the Michael reaction is also an important reacting centre from which several transformations can be carried out. The map of the transformations of the model adduct **9ab** is represented in Scheme 104.

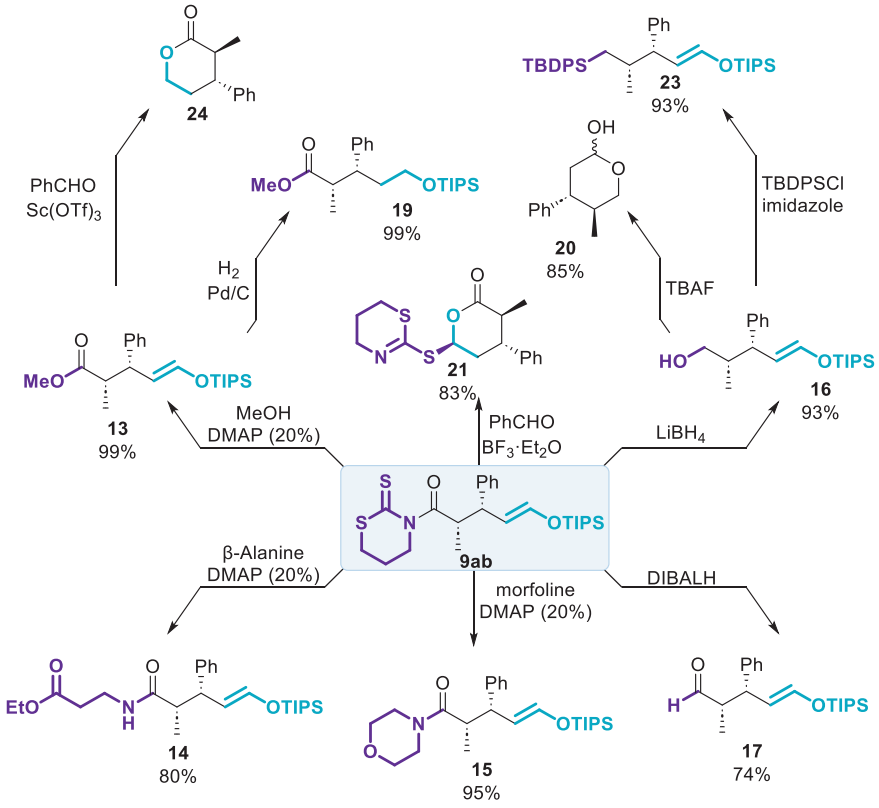

Scheme 104. Transformations from the Michael adduct **9ab.**

Taking advantage of these results, the asymmetric synthesis of (*R,R*)-tapentadol, a commercially available opioid, was achieved in six-steps in high overall yield (45 %) with an excellent stereochemical control. The synthetic sequence is summarised in Scheme 105.

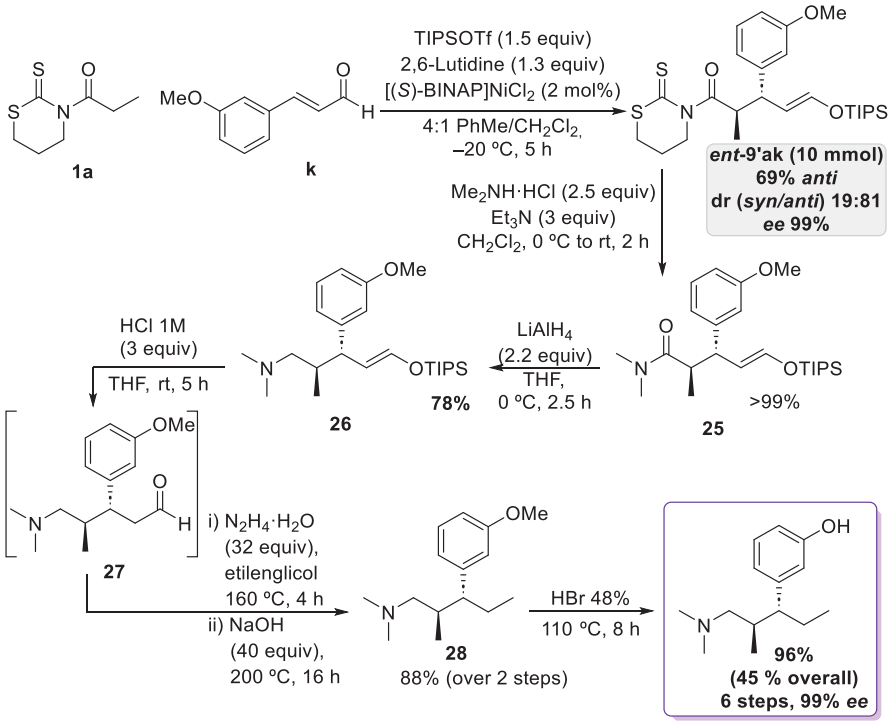

Scheme 105. Total synthesis of (*R,R*)-tapentadol

The results of **Chapter II** and **Chapter III** were published in:

"Galeote, O.; Kennington, S. C. D.; Benedito, G.; Fraedrich, L.; Davies-Howe, E.; Costa, A. M.; Romea, P.; Urpí, F.; Aullón, G.; Font-Bardia, M.; Puigjaner, C. Direct, Stereodivergent, and Catalytic Michael Additions of Thioimides to α,B-Unsaturated Aldehydes – Total Synthesis of Tapentadol. *Angew. Chem. Int. Ed.* 2024, *63* (12)."

In **Chapter IV**, the Mannich reaction between *N*-acyl thioimides and imines or imine surrogates, as *N,O*- and *N,N*-aminals, was explored. In these transformations, the *N*-propanoyl thioimide was treated with the activated imines or iminium ions in the presence of a nickel(II) complex. Unexpectedly, the use of imines mostly furnished the formation of an *N,O*-silyl ketene acetal. Additionally, most of the *N,O* and *N,N*-aminals tested were unstable and difficult to handle. These limitations could be solved by the use of *N,N*-

dibenzyl aminal, but it furnished the corresponding Mannich adduct with a modest enantioselectivity.

In the near future, robust *N,O* or *N,N*-aminals should be tested, looking for the best option to get access to the corresponding Mannich adducts. We expect that the use of substituted aminals could provide two new stereocentres, which would increase the synthetic potential of the reaction.

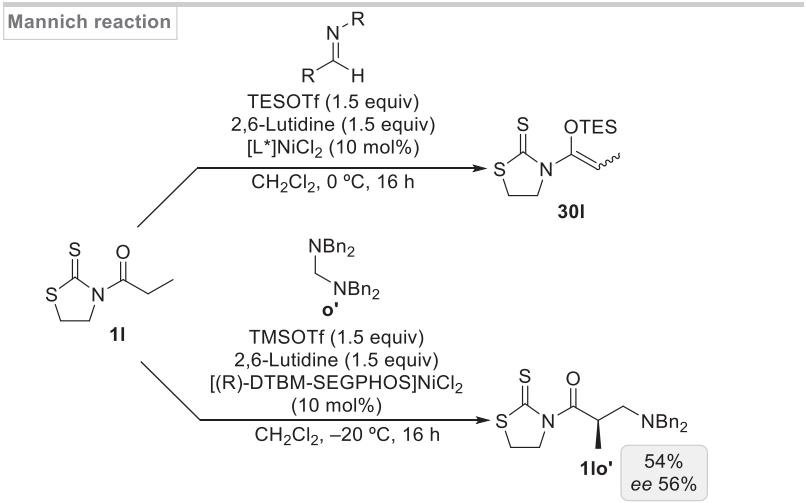

Scheme 106. Mannich reactions of thioimides to imines and aminals.

Furthermore, preliminary studies on the reaction of *N*-acryl-thiazolidinethione and nitrones in 1,3 dipolar cycloadditions in the presence of [(*R*)-DTBM-SEGPHOS]$NiCl_2$ furnished exclusively the *endo* diastereomer with a 90% *ee*, while [(*S*)-BINAP]$NiCl_2$ produced the *exo* counterpart with a dr 79:21 as a single enantiomer. These completely different reactions might open new avenues for the stereoselective construction of carbon-carbon bonds through reaction of thioimides catalysed by chiral nickel(II) complexes.

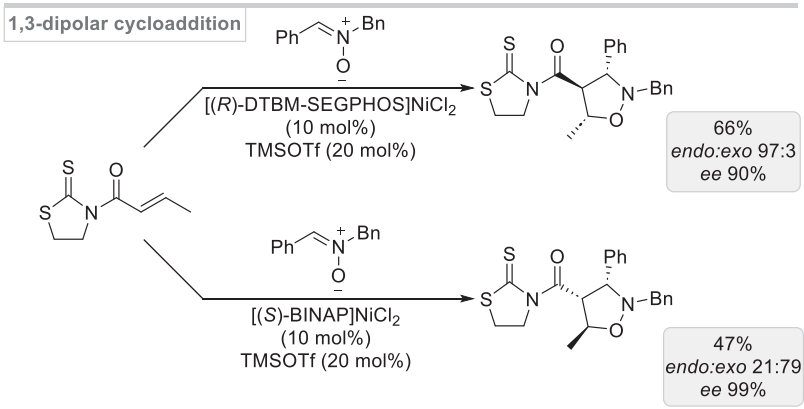
1,3-dipolar cycloaddition
[(R)-DTBM-SEGPHOS]NiCl2
(10 mol%)
TMSOTf (20 mol%)
66%
endo:exo 97:3
ee 90%
[(S)-BINAP]NiCl2
(10 mol%)
TMSOTf (20 mol%)
47%
endo:exo 21:79
ee 99%

EXPERIMENTAL SECTION

Table of Contents

GENERAL PROCEDURES

1 General methods

Unless otherwise noted, reactions were conducted in oven-dried glassware under inert atmosphere of N_2 with anhydrous solvents. The solvents and reagents were dried and purified when necessary according to standard procedures. Commercially available reagents were used as received. Analytical thin-layer chromatographies (**TLC**) were carried out on Merck silica gel 60 F_{254} plates and analysed by UV (254 nm) and stained with phosphomolybdic acid, $KMnO_4$ or 4-methoxybenzaldehyde. Column chromatographies were carried under low pressure (flash) conditions and performed on SDS silica gel 60 (35–70 μm). Eluents are indicated in brackets in each case. $\mathbf{R_f}$ values are approximate. Melting points (**Mp**) were determined with a Stuart SMP10 apparatus and are uncorrected. Specific rotations ($\mathbf{[\alpha]_D}$) were determined at 20 °C on a Perkin-Elmer 241 MC polarimeter equipped with a sodium lamp (λ 589 nm, D-line).

HPLC analyses were conducted on a Shimadzu LC–20 HPLC system, using chiral Phenomenex Lux® columns under isocratic conditions and detected at 254 nm. High performance liquid chromatography–mass spectra (**HPLC-MS**) chromatograms were obtained with a Waters Alliance HT 2795 coupled with a photodiode array Waters PDA 2996 and a Waters ZQ 2000 spectrometer.

IR spectra (Attenuated Total Reflectance, ATR) were recorded on a Nicolet 6700 FT-IR Thermo Scientific spectrometer and only the more representative frequencies (ν) are reported in cm^{-1}.

^{1}H NMR (400 MHz) and **^{13}C NMR** (101 MHz) spectra were recorded at room temperature on a Varian Mercury 400 or a Bruker 400. **^{1}H NMR** (500 MHz) and **^{13}C NMR** (126 MHz) were recorded at room temperature on a Bruker 500. Chemical shifts (δ) are quoted in ppm and referenced to internal TMS (δ 0.00 for ^{1}H NMR) and $CDCl_3$ (δ 77.0 for ^{13}C NMR). Data are reported as follows: chemical shift (number of protons, multiplicity, coupling constants, proton); multiplicity is reported as follows: s, singlet. d, doublet. t, triplet. q, quartet. p, quintet or m, multiplet (and their corresponding combinations); coupling constants (*J*) are quoted in Hz. Where necessary, 2D techniques (NOESY, COSY, HSQC) were also used to assist on structure elucidation.

High resolution mass spectra (HRMS) were obtained with an Agilent 1100 spectrometer by the Unitat d'Espectrometria de Masses, Universitat de Barcelona.

2 Preparations of starting materials

2.1 Preparation of scaffolds

2.1.1 Synthesis of thiazinanethione[1]

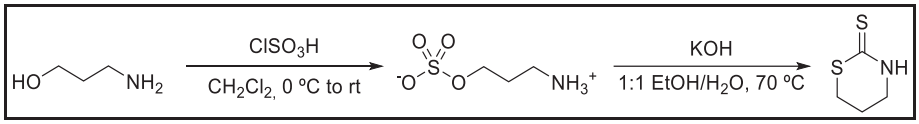

3-Ammoniopropylsulphate

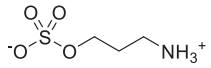

Chlorosulphonic acid (10.5 mL, 159 mmol, 1.06 equiv) was added dropwise to a solution of 3-amino-1-propanol (11.5 mL, 150 mmol, 1.0 equiv) in CH_2Cl_2 (35 mL) under a constant flow of N_2 at 0 °C. The reaction mixture was stirred for 15 h at rt after which the solvent was removed in vacuo to afford a white solid. The white solid was triturated with MeOH and dried under reduced pressure to afford 20.7 g of 3-ammoniopropylsulphate (134 mmol, 89% yield), which was pure enough by ^{1}H NMR and required no further purification.

White solid.
Mp 205–207 °C.
IR (ATR) *v* 3126, 3064, 2976, 1627, 1530, 1195, 1169, 1065, 923, 759, 574 cm^{-1}.
^{1}H NMR (400 MHz, DMSO-d_6) δ 7.64 (br s, 3H, N$\underline{H}_3$), 3.81 (t, *J* = 6.0 Hz, 2H, C$\underline{H}_2SO_3$), 2.76–2.90 (m, 2H, C$\underline{H}_2NH_3$), 1.74–1.86 (m, 2H, C$\underline{H}_2CH_2NH_3$).
^{13}C NMR (100.6 MHz, DMSO-d_6) δ 63.2 (CH_2), 36.7 (CH_2), 27.3 (CH_2).
HRMS (+ESI) *m/z* calcd for $C_3H_{10}NO_4S$ $[M+H]^+$ 156.0325, found 156.0322.

1,3-Thiazinane-2-thione

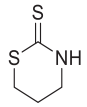

Carbon disulphide (9.6 mL, 160 mmol, 1.3 equiv) was added dropwise to 3-ammoniopropylsulfate (18.70 g, 121 mmol, 1 equiv) under N_2 at rt. Then, a solution of KOH (14.8 g, 265 mmol in 1:1 H_2O/EtOH 200 mL, 2.2 equiv) was added dropwise to the reaction mixture at 0 °C. The resulting solution was then heated to reflux and stirred for 2 h, after which it was further stirred overnight at rt. Then,

it was cooled with an ice/water bath. The white precipitate was filtered and rinsed with cold water. It was dissolved in CH_2Cl_2, dried ($MgSO_4$), and the solvent was removed in vacuo to obtain a white solid. The filtrate was also acidified and extracted with CH_2Cl_2 to recover more product. The combined product was purified by recrystallization in CH_2Cl_2/Hexanes to obtain 10.12 g of 1,3-thiazinane-2-thione (75.6 mmol, 63% yield).

White solid.
Mp 130–133 °C.
R_f 0.20 (CH_2Cl_2).
IR (ATR) ν 3144, 3052, 2917, 1546, 1358, 1335, 1013, 899 cm^{-1}.
^{1}H NMR (400 MHz, $CDCl_3$) δ 8.92 (s, 1H, NH), 3.48 (t, *J* = 5.6 Hz, 2H, NCH$_2$), 3.02–2.99 (m, 2H, SCH$_2$), 2.18 (tt, *J* = 7.6, 4.7 Hz, 2H, NCH$_2$CH$_2$).
^{13}C NMR (100.6 MHz, $CDCl_3$) δ 194.6 (C), 44.3 (CH_2), 30.0 (CH_2), 20.5 (CH_2).
HRMS (+ESI): *m/z* calcd. for $[M+H]^+$ $C_4H_8NS_2$: 134.0093; found: 134.0093.

2.1.2 Synthesis of 1,3-oxazinane-2-thione and 1,3-oxazolidine-2-thione

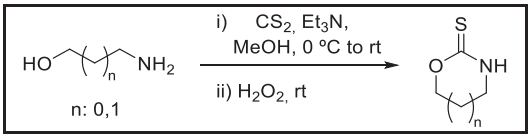

1,3-Oxazinane-2-thione

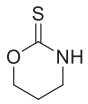

Anhydrous Et_3N (5.6 mL, 40 mmol, 1 equiv) was added dropwise to a solution of 3-amino-1-propanol (3.2 mL, 40 mmol, 1 equiv) in absolute methanol (40 mL) under a nitrogen atmosphere. The mixture was then cooled to 0 °C, followed by the dropwise addition of carbon disulphide (3.6 mL, 60 mmol, 1.5 equiv). After complete addition, the mixture was stirred at 0 °C for 30 min, warmed up to rt and stirred for another 30 min. The resulting pale-yellow solution was then quenched dropwise with 30% (v/v) H_2O_2 (7.0 mL). The yellow suspension was filtered, and the organic layer was concentrated under reduced pressure using a peroxide tramp before the addition of 2 M NaOH (20 mL) and concentrated further. Afterwards, the solution was acidified by the addition of 2 M HCl (ca. 30 mL) to pH 1. The resulting bright yellow solution was extracted with CH_2Cl_2 (3 × 25 mL), and the combined organic layers were dried ($MgSO_4$), filtered, and concentrated under

reduced pressure. The solid obtained was purified by recrystallization (Hexanes/CH_2Cl_2) to yield 3.34 g (29 mmol, 72% yield) of a white crystalline powder.

White solid.
Mp 126–127 °C.
R_f 0.35 (80:20 Hexanes/EtOAc).
IR (ATR) *v* 3162, 2976, 2946, 1567, 1462, 1311, 1227, 1151, 1049, 913, 760, 578 cm^{-1}.
^{1}H NMR (400 MHz, $CDCl_3$) δ 8.82 (1H, br s, N<u>H</u>), 4.42–4.35 (2H, m, OC<u>H</u>$_2$), 3.40 (2H, td, *J* = 6.2, 2.7 Hz, NC<u>H</u>$_2$), 2.16–2.05 (2H, m, NCH$_2$C<u>H</u>$_2$).
^{13}C NMR (100.6 MHz, $CDCl_3$) δ 186.7 (C), 68.0 (CH_2), 40.3 (CH_2), 19.6 (CH_2).
HRMS (+ESI): *m/z* calcd. for $[M+H]^+$ C_4H_8NOS: 118.0321; found 118.0323.

1,3-Oxazolidine-2-thione

Anhydrous Et_3N (5.6 mL, 40 mmol, 1 equiv) was added dropwise to a solution of ethanolamine (2.4 mL, 40 mmol, 1 equiv) in ethanol (40 mL). The mixture was then cooled to 0 °C, followed by the dropwise addition of carbon disulphide (3.6 mL, 60 mmol, 1.5 equiv). After complete addition, the mixture was stirred at 0 °C for 30 min, warmed up to rt and stirred for further 30 min. The resulting yellow solution was then quenched by dropwise addition of 30% (v/v) H_2O_2 (7.5 mL). The pale-yellow suspension was filtered, and the organic layer was concentrated under reduced pressure before the addition of 2 M NaOH (25 mL) and concentrated further. Afterwards, the solution was acidified by the addition of 2 M HCl (ca. 35 mL) to pH 1. The resulting bright yellow solution was extracted with CH_2Cl_2 (3 × 25 mL), and the combined organic layers were dried ($MgSO_4$), filtered, and concentrated under reduced pressure. The solid obtained was purified by recrystallization (Hexanes/CH_2Cl_2) to yield 3.1 g (30 mmol, 74% yield) of pure product.

White solid.
R_f 0.40 (50:50 Hexanes/EtOAc).
Mp 97–99 °C.
IR (ATR) ν 3203, 2923, 1520, 1456, 1398, 1312, 1284, 1203, 1162, 1033 cm^{-1}.
^{1}H NMR (400 MHz, $CDCl_3$) δ 7.80 (1H, br s, NH), 4.73 (2H, t, *J* = 8.8 Hz, OCH_2), 3.85 (2H, t, *J* = 8.8 Hz, NHCH_2).
^{13}C NMR (100.6 MHz, $CDCl_3$) δ 190.1 (C), 70.4 (CH_2), 44.1 (CH_2).
HRMS (+ESI): *m/z* calcd. for C_3H_6NOS $[M+H]^+$: 104.0165; found 104.0167.

2.2 Synthesis of *N*-acyl-thioimides

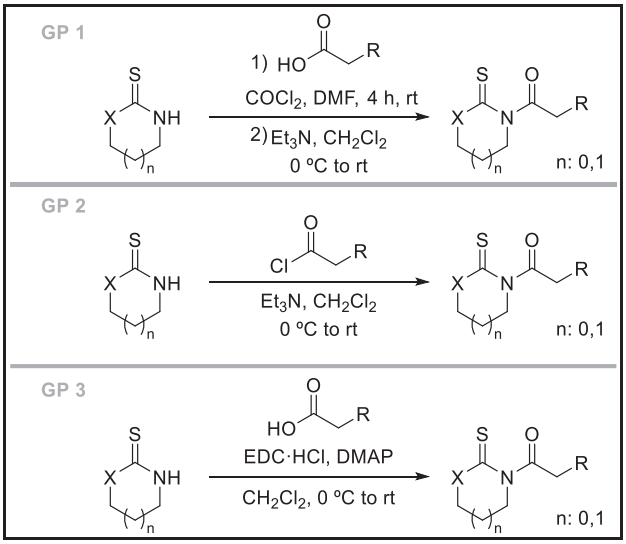

GENERAL PROCEDURE 1

Two drops of DMF were added to a solution of a carboxylic acid (1 equiv) in CH_2Cl_2 (0.25 M) at rt. The solution was cooled in an ice/water bath, oxalyl chloride (1.2 equiv) was added dropwise and the resultant solution was warmed up to rt and stirred for 4 h. Then, removal of the volatiles under reduced pressure afforded the corresponding acyl chloride, which was used directly in the next reaction.

A solution of 1,3-thiazinane-2-thione (1 equiv) in CH_2Cl_2 (0.5 M) was cooled to 0 °C with an ice/water bath and neat Et_3N (1.3 equiv) was added dropwise. Afterwards, a solution of the acid chloride (1.2 equiv) previously prepared in CH_2Cl_2 (1.2 M) was added dropwise with a cannula. The mixture was warmed up to rt and the reaction was followed by TLC. On apparent completion, the reaction mixture was quenched with sat. NH_4Cl (5 mL/10 mmol), rinsed with water (20 mL/10 mmol) and extracted with CH_2Cl_2 (3 × 10 mL/10 mmol). The combined

organic extracts were washed with 2 M NaOH (3 × 25 mL/10 mmol) and 2 M HCl (25 mL/10 mmol), dried ($MgSO_4$) and concentrated under reduced pressure. The resulting residue was purified by flash chromatography to give the desired *N*-acyl-heterocycles.

General Procedure 2

An acyl chloride (1.2 equiv) was added dropwise to a solution of 1,3-thiazinane-2-thione (1 equiv) and Et_3N (1.3 equiv) in CH_2Cl_2 (0.5 M) at 0 °C in an ice/water bath. The mixture was warmed up to rt and the reaction was followed by TLC. On apparent completion, the reaction mixture was quenched with a saturated solution of NH_4Cl (5 mL/10 mmol), rinsed with water (20 mL/ 10 mmol) and extracted with CH_2Cl_2 (3 × 10 mL/ 10 mmol). The combined organic extracts were washed with 2 M NaOH (3 × 25 mL/ 10 mmol) and 2 M HCl (25 mL /10 mmol), dried ($MgSO_4$) and concentrated under reduced pressure. The resulting residue was purified by flash chromatography or recrystallization to give the desired *N*-acyl heterocycle.

General Procedure 3

A carboxylic acid (1.2 equiv) was added dropwise at rt to a solution of 1,3-thiazinane-2-thione (1 equiv), EDC·HCl (1.3 equiv) and DMAP (20 mol%) in CH_2Cl_2 (1.2 M). On apparent completion by TLC, the reaction mixture was partitioned (for 10 mmol) in Et_2O (30 mL) and water (30 mL), washed with sat. NH_4Cl (20 mL), NaOH (3 × 25 mL) and brine (25 mL). The residue was purified by flash chromatography to give the desired *N*-acyl-heterocycles.

N-Propanoyl-1,3-thiazinane-2-thione (1a)

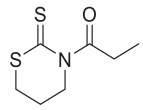

Following the General Procedure 1 , 1,3-thiazinane-2-thione (10.64 g, 80 mmol) was dissolved in CH_2Cl_2 (80 mL). Subsequently, Et_3N (14.5 mL, 104 mmol) and propionyl chloride (8.4 mL, 96 mmol) were added dropwise and the solution was stirred for 2 h. The crude was purified by flash chromatography (90:10 Hexanes/EtOAc) to give 12.7 g (67 mmol, 84% yield) of pure **1a**.

Yellow oil.

R_f 0.4 (80:20 Hexanes/EtOAc).

IR (ATR) ν 2975, 2934, 2877, 1700, 1469, 1374, 1344, 1302, 1198, 1166, 1020, 966, 919 cm^{-1}.

^{1}H NMR (400 MHz, $CDCl_3$) δ 3.95–3.91 (m, 2H, NC$\underline{H}_2$), 3.09 (q, *J* = 7.3 Hz, 2H, OCC$\underline{H}_2$), 3.03 (t, *J* = 6.8 Hz, 2H, SC$\underline{H}_2$), 2.29–2.21 (m, 2H, $NCH_2C\underline{H}_2$), 1.22 (t, *J* = 7.3 Hz, 3H, C$\underline{H}_3$).

^{13}C NMR (101 MHz, $CDCl_3$) δ 202.8 (C), 178.9 (C), 46.4 (CH_2), 32.0 (CH_2), 22.8 (CH_2), 10.0 (CH_3).

HRMS (+ESI) *m/z* calcd for $[M+H]^+$ $C_7H_{12}NOS_2$: 190.0355, found 190.0354.

***N*-Butanoyl-1,3-thiazinane-2-thione (1b)**

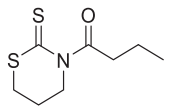

Following the General Procedure 2, 1,3-thiazinane-2-thione (1.33 g, 10 mmol) was dissolved in CH_2Cl_2 (10 mL). Then, Et_3N (1.8 mL, 12 mmol) and butanoyl chloride (1.26 mL, 12 mmol) were added. The resulting mixture was stirred for 3 h. The crude was purified by flash column chromatography (from 40:60 to 60:40 Hexanes/CH_2Cl_2) to afford 689 mg (3.3 mmol, 67% yield) of pure **1b**.

Yellow oil.

R_f 0.3 (80:20 Hexanes/EtOAc).

^{1}H NMR (400 MHz, $CDCl_3$) δ 3.94–3.90 (m, 2H, NC$\underline{H}_2$), 3.09–2.99 (m, 4H, SC$\underline{H}_2$, COC$\underline{H}_2$), 2.29–2.20 (m, 2H, $SCH_2C\underline{H}_2$), 1.81–1.67 (m, 2H, $COCH_2C\underline{H}_2$), 0.95 (t, *J* = 7.4 Hz, 3H, C$\underline{H}_3$).

^{13}C NMR (101 MHz, $CDCl_3$) δ 203.4 (C), 177.9 (C), 46.3 (CH_2), 41.0 (CH_2), 32.1 (CH_2), 23.0 (CH_2), 19.6 (CH_2), 13.6 (CH_3).

HRMS (+ESI) *m/z* calcd. for $[M+H]^+C_8H_{14}NOS_2$: 204.0511; found: 204.0510.

***N*-(4-Methylpentanoyl)-1,3-thiazinane-2-thione (1c)**

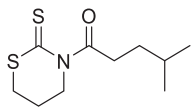

Following the General Procedure 3, 1,3-thiazinane-2-thione (2.67 g, 20 mmol, 1 equiv), EDC·HCl (4.98 g, 26 mmol, 1.3 equiv) and DMAP (490 mg, 4 mmol, 20 mol%) were dissolved in CH_2Cl_2 (40 mL). Subsequently, 4-methylpentanoic acid (3.0 mL, 24 mmol, 1.2 equiv) were added dropwise and the solution was stirred

for 24 h. The crude residue was purified by flash chromatography (1:1 Hexanes/CH_2Cl_2) to give 858 mg (3.8 mmol, 19% yield) of pure **1c**.

Yellow solid.
Mp 32–35 °C.
R_f 0.30 (80:20 Hexanes/EtOAc).
IR (ATR) ν 2953, 2927, 2867, 1702, 1287, 1133, 1107, 1014, 925 cm^{-1}.
^{1}H NMR (400 MHz, $CDCl_3$) δ 3.94–3.88 (2H, m, NC$\underline{H}_2$), 3.10–3.00 (4H, m, SC$\underline{H}_2$, COC$\underline{H}_2$), 2.29–2.21 (2H, m, $NCH_2C\underline{H}_2$), 1.65–1.51 (3H, m, $C\underline{H}_2C\underline{H}(CH_3)_2$), 0.90 (6H d, *J* = 6.4 Hz, $CH(C\underline{H}_3)_2$).
^{13}C NMR (100.6 MHz, CDCl3) δ 203.2 (C), 178.4 (C), 46.4 (CH_2), 37.2 (CH_2), 34.8 (CH_2), 32.0 (CH_2), 27.7 (CH_2), 22.9 (CH_2), 22.3 (CH_3).
HRMS (+ESI): *m/z* calcd for $[M+H]^+$ $C_{10}H_{18}NOS_2$: 232.0824, found: 232.0826.

***N*-(4-Pentenoyl)-1,3-thiazinane-2-thione (1d)**

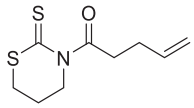

Following the General Procedure 1, 4-pentenoic acid (0.77 mL, 7 mmol) was dissolved in CH_2Cl_2 (25 mL) and two drops of DMF were added. Then, oxalyl chloride (0.72 mL, 8.4 mmol) was added dropwise. After 4 h, volatiles were removed under reduced pressure to obtain 4-pentenoyl chloride, which was used directly in the next reaction without further purification.

Afterwards, Et_3N (0.91 mL, 1.3 mmol) and 5-hexynoyl chloride were added to a solution of 1,3-thiazinane-2-thione (666 mg, 5 mmol) in CH_2Cl_2 (10 mL) at 0 °C, and the resulting mixture was stirred for 2 h. The reaction crude was purified by flash column chromatography (from 40:60 to 60:40 Hexanes/CH_2Cl_2) to afford 358 mg (2.0 mmol, 28% yield) of pure **1d**.

Yellow oil.
R_f 0.4 (70:30 Hexanes/EtOAc).
IR (ATR) ν 3074, 2924, 1703, 1639, 1287, 1124, 1066, 1014, 915 cm^{-1}.
^{1}H NMR (400 MHz, $CDCl_3$) δ 5.82 (ddt, *J* = 16.8, 10.2, 6.5 Hz, 1H, C$\underline{H}$=CH_2), 5.11–4.96 (m, 2H, CH=C$\underline{H}_2$), 3.95–3.88 (m, 2H, NC$\underline{H}_2$), 3.19 (t, *J* = 7.4 Hz, 2H, OCC$\underline{H}_2$), 3.03 (t, *J* = 6.8 Hz, 2H, SC$\underline{H}_2$), 2.52–2.41 (m, 2H, $C\underline{H}_2$CH), 2.28–2.20 (m, 2H, $NCH_2C\underline{H}_2$).
^{13}C NMR (101 MHz, $CDCl_3$) δ 203.76 (C), 177.35 (C), 136.77 (CH), 115.82 (CH_2), 46.50 (CH_2), 38.55 (CH_2), 32.24 (CH_2), 30.25 (CH_2), 23.19 (CH_2).
HRMS (+ESI) calcd. for $[M+H]^+$ $C_9H_{14}NOS_2$: 216.0511; found: 216.0511

N-(5-Hexynoyl)-1,3-thiazinane-2-thione (1e)

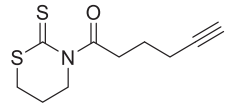

Following the General Procedure 1, 5-hexynoic acid (0.77 mL, 7 mmol) was dissolved in CH_2Cl_2 (25 mL) and two drops of DMF were added. Then, oxalyl chloride (0.72 mL, 8.4 mmol) was added dropwise. After 4 h, volatiles were removed under reduced pressure to obtain 5-hexynoyl chloride.

Afterwards, Et_3N (0.91 mL, 1.3 mmol) and 5-hexynoyl chloride were added to a solution of 1,3-thiazinane-2-thione (666 mg, 5 mmol) in CH_2Cl_2 (10 mL) at 0 °C, and the resulting solution was stirred for 2 h. The reaction crude was purified by flash column chromatography (from 40:60 to 60:40 Hexanes/CH_2Cl_2) to afford 822 mg (3 mmol, 60% yield) of pure **1e**.

Yellow oil.
R_f 0.4 (70:30 Hexanes/EtOAc).
IR (ATR) ν 3284, 3132, 3039, 2922, 1813, 1742, 1702, 1123, 1040, 1009 cm^{-1}.
^{1}H NMR (400 MHz, $CDCl_3$) δ 3.97–3.91 (m, 2H, NC$\underline{H}_2$), 3.20 (t, *J* = 7.3 Hz, 2H, COC$\underline{H}_2$), 3.04 (t, *J* = 6.8 Hz, 2H, SC$\underline{H}_2$), 2.31–2.21 (m, 4H, $SCH_2C\underline{H}_2$, $C\underline{H}_2CCH$), 2.00–1.89 (m, 3H, $COCH_2C\underline{H}_2$, $CC\underline{H}$).
^{13}C NMR (101 MHz, $CDCl_3$) δ 203.96 (C), 177.2 (C), 83.3 (C), 69.4 (CH), 46.4 (CH_2), 37.9 (CH_2), 32.2 (CH_2), 24.8 (CH_2), 23.2 (CH_2), 17.8 (CH_2).
HRMS (+ESI) *m/z* calcd. for $C_4H_8NS_2$ 134.0093; found: 134.0095. *m/z* calcd. for $[M+H]^+$ $C_{10}H_{14}NOS_2$: 228.0511; found: 228.0512.

N-(5-Methoxy-5-oxopentanoyl)-1,3-thiazinane-2-thione (1f)

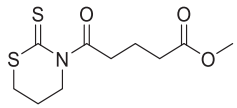

Following General Procedure 2, 1,3-thiazinane-2-thione (803 mg, 5 mmol) was dissolved in CH_2Cl_2 (10 mL). Afterwards, Et_3N (1 mL, 7.8 mmol) and methyl 5-chloro-5-oxopentanoate (1 mL, 7.2 mmol) were added and the solution was stirred for 24 h. The crude residue was purified by flash chromatography (CH_2Cl_2) to give 921 mg (3.0 mmol, 59% yield) of pure **1f**.

Yellow oil.
R_f 0.25 (CH_2Cl_2)
IR (ATR) ν 2948, 2847, 1733, 1470, 1463, 1454, 1437, 1128, 929 cm^{-1}.
^{1}H NMR (400 MHz, CDCl3) δ 3.95–3.91 (m, 2H, NC$\underline{H}_2$), 3.67 (s, 3H, O$\underline{Me}$), 3.14 (t, *J* = 7.3 Hz, 2H, OCC$\underline{H}_2$), 3.03 (t, *J* = 6.8 Hz, 2H, SC$\underline{H}_2$), 2.38 (t, *J* = 7.3 Hz, 2H, C$\underline{H}_2CO_2Me$), 2.30–2.22 (m, 2H, $NCH_2C\underline{H}_2$), 2.09–2.00 (p, *J* = 7.3 Hz, 2H, $OCCH_2C\underline{H}_2$)
^{13}C NMR (CDCl3, 100.6 MHz) δ 203.7 (C), 176.9 (C), 173.4 (C), 51.6 (CH_3), 46.3 (CH_2), 38.1 (CH_2), 33.0 (CH_2), 32.1 (CH_2), 23.0 (CH_2), 21.1 (CH_2).
HRMS (+ESI) *m/z* calcd. for $[M+H]^+$ $C_{10}H_{16}NO_3S_2$: 262.0566; found: 262.0562.

N-(6-Bromohexanoyl)-1,3-thiazinane-2-thione (1g)

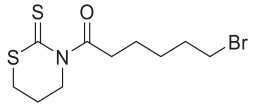

Following the General Procedure 2, 1,3-thiazinane-2-thione (803 mg, 5 mmol) was dissolved in CH_2Cl_2 (10 mL). Afterwards, Et_3N (1 mL, 7.8 mmol) and methyl 5-chloro-5-oxopentanoate (1 mL, 7.2 mmol) were added and the solution was stirred for 24 h. The crude residue was purified by flash chromatography (CH_2Cl_2) to give 902 mg (3.0 mmol, 42% yield) of pure **1g**.

Yellow oil.
R_f 0.3 (80:20 Hexanes/EtOAc).
IR (ATR) ν 2929, 2859, 1703, 1287, 1114, 1014, 925 cm^{-1}.
^{1}H NMR (400 MHz, $CDCl_3$) δ 3.96–3.87 (m, 2H, NC$\underline{H}_2$), 3.41 (t, *J* = 6.7 Hz, 2H, C$\underline{H}_2$Br), 3.11–3.06 (m, 2H, OCC$\underline{H}_2$), 3.04 (t, *J* = 6.8 Hz, 2H, SC$\underline{H}_2$), 2.30–2.21 (m, 2H, $NCH_2C\underline{H}_2$), 1.93–1.83 (m, 2H, C$\underline{H}_2CH_2$Br), 1.75 (p, *J* = 7.5 Hz, 2H, $OCCH_2C\underline{H}_2$), 1.53–1.43 (m, 2H, $OCCH_2CH_2C\underline{H}_2$).
^{13}C NMR (101 MHz, $CDCl_3$) δ 203.78 (C), 177.71 (C), 46.52 (CH_2), 38.93 (CH_2), 33.71 (CH_2), 32.48 (CH_2), 32.25 (CH_2), 27.67 (CH_2), 25.27 (CH_2), 23.16 (CH_2).
HRMS (+ESI) *m/z* calcd. for $[M+H]^+$ $C_{10}H_{17}{}^{79}BrNOS_2$ 309.9929; found: 309.9922.

N-Acetyl-1,3-thiazinane-2-thione (1h)

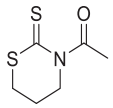

Following the General Procedure 2, 1,3-thiazinane-2-thione (1.33 g, 10 mmol) was dissolved in CH_2Cl_2 (10 mL). Subsequently, Et_3N (1.6 mL, 11.3 mmol) and acetyl chloride (0.86 mL, 12 mmol) were added dropwise and the solution was stirred

for 2 h. The crude was purified by flash chromatography (from 80:20 to 50:50 Hexanes/EtOAc) to give 1.17 g (6.7 mmol, 67% yield) of pure **1h**.

Yellow oil.
R$_f$ 0.4 (50:50 Hexanes/EtOAc).
^{1}H NMR (400 MHz, $CDCl_3$) δ 4.04–3.95 (m, 2H, NC$\underline{H}_2$), 3.03 (t, *J* = 6.9 Hz, 2H, SC$\underline{H}_2$), 2.68 (s, 3H, C$\underline{H}_3$), 2.36–2.18 (m, 2H, NCH$_2$C$\underline{H}_2$).

***N*-Acetyl-1,3-oxazinane-2-thione (1i)**

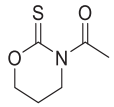

Following the General Procedure 2, 1,3-oxazinane-2-thione (1.15 g, 10 mmol) was dissolved in CH_2Cl_2 (10 mL). Subsequently, Et_3N (1.6 mL, 11.3 mmol) and acetyl chloride (0.86 mL, 12 mmol) were added dropwise and the solution was stirred for 16 h. The crude was purified by flash chromatography (from 70:30 to 50:50 Hexanes/EtOAc) to give 746 mg (4.8 mmol, 48% yield) of pure **1i**.

Pale yellow oil.
R$_f$ 0.5 (30:70 Hexanes/EtOAc).
^{1}H NMR (400 MHz, $CDCl_3$) δ 4.38–4.30 (m, 2H, NC$\underline{H}_2$), 3.77 (t, *J* = 7.1 Hz, 2H, SC$\underline{H}_2$), 2.74 (s, 3H, C$\underline{H}_3$), 2.28–2.15 (m, 2H, NCH$_2$C$\underline{H}_2$).

***N*-Acetyl-1,3-thiazolidine-2-thione (1j)**

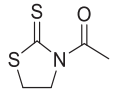

Following the General Procedure 2, 1,3-thiazinane-2-thione (1.19 g, 10 mmol) was dissolved in CH_2Cl_2 (10 mL). Subsequently, Et_3N (1.6 mL, 11.3 mmol) and acetyl chloride (0.86 mL, 12 mmol) were added dropwise and the solution was stirred for 16 h. The crude was purified by flash chromatography (from 80:20 to 60:40 Hexanes/EtOAc) to give 1.35 g (8.4 mmol, 84% yield) of pure **1j**.

Yellow thick oil.
R$_f$ 0.3 (70:30 Hexanes/EtOAc).
^{1}H NMR 4.59 (t, *J* = 7.5 Hz, 2H, NC$\underline{H}_2$), 3.30 (t, *J* = 7.5 Hz, 2H, SC$\underline{H}_2$), 2.79 (s, 3H, C$\underline{H}_3$).

***N*-Acetyl-1,3-oxazolidine-2-thione (1k)**

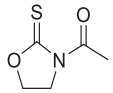

Following the General Procedure 2, 1,3-oxazolidine-2-thione (1.01 g, 10 mmol) was dissolved in CH_2Cl_2 (10 mL). Subsequently, Et_3N (1.6 mL, 11.3 mmol) and acetyl chloride (0.86 mL, 12 mmol) were added dropwise and the solution was stirred for 16 h. The crude was recrystallized (cycloHexanes/ CH_2Cl_2) to give 756 mg (5.3 mmol, 53% yield) of pure **1k**.

White solid.
R_f 0.2 (80:20 Hexanes/EtOAc).
^{1}H NMR (400 MHz, $CDCl_3$) δ 4.55 (t, *J* = 8.6 Hz, 2H, OC$\underline{H}_2$), 4.23 (t, *J* = 8.6 Hz, 2H, NC$\underline{H}_2$), 2.84 (s, 3H, C$\underline{H}_3$).

***N*-Propanoyl-1,3-thiazolidine-2-thione (1l)**

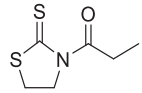

Following the General Procedure 2, 1,3-thiazinane-2-thione (10.6 g, 80 mmol) was dissolved in CH_2Cl_2 (80 mL). Subsequently, Et_3N (14.5 mL, 104 mmol) and propionyl chloride (8.4 mL, 96 mmol) were added dropwise and the solution was stirred for 2 h. The crude was purified by flash chromatography (90:10 Hexanes/EtOAc) to give 9.8 g (55 mmol, 68% yield) of pure **1l.**

Yellow oil.
R_f 0.7 (CH_2Cl_2).
IR (ATR) ν 2979, 2938, 1702, 1365, 1281, 1222, 1157 cm^{-1}.
^{1}H NMR (400 MHz, $CDCl_3$) δ 4.59 (*t*, *J* = 7.6 Hz, 2H, NC$\underline{H}_2$), 3.28 (t, *J* = 7.6 Hz, 2H, SC$\underline{H}_2$), 3.26 (q, *J* = 7.3 Hz, 2H, C$\underline{H}_2$CH$_3$), 1.18 (t, *J* = 7.3 Hz, 3H, CH$_2$C$\underline{H}_3$).
^{13}C NMR (101 MHz, CDCl3) δ 201.5 (C), 175.5 (C), 56.0 (CH_2), 32.2 (CH_2), 28.2 (CH_2), 8.7 (CH_3).

***N*-Propanoyl-1,3-oxazolidine-2-thione (1m)**

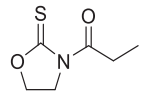

Following the General Procedure 2, 1,3-oxazolidine-2-thione (1.03 g, 10 mmol) was dissolved in CH_2Cl_2 (25 mL). Subsequently, Et_3N (1.8 mL, 13 mmol) and propionyl chloride (1.1 mL, 12 mmol) were added dropwise and the solution was

stirred for 16 h. The crude was purified by flash chromatography (from 90:10 to 70:30 Hexanes/EtOAc) to give 1.27 g (7.8 mmol, 78% yield) of pure **1m**.

White solid.
Mp 47–49 °C.
R_f 0.35 (80:20 Hexanes/EtOAc).
IR (ATR) *v* 2987, 2912, 1697, 1458, 1381, 1156, 930, 648 cm^{-1}.
^{1}H NMR ($CDCl_3$, 400 MHz) δ 4.55 (2H, t, *J* = 8.6 Hz, $OC\underline{H}_2$), 4.24 (2H, t, *J* = 8.6 Hz, $NC\underline{H}_2$), 3.31 (2H, q, *J* = 7.3 Hz, $C\underline{H}_2CH_3$), 1.20 (3H, t, *J* = 7.3 Hz, $CH_2C\underline{H}_3$).
^{13}C NMR ($CDCl_3$, 100.6 MHz) δ 185.5 (C), 175.1 (C), 66.4 (CH_2), 47.1 (CH_2), 31.1 (CH_2), 8.5 (CH_3).
HRMS (+ESI): *m/z* calcd. for $[M+H]^+$ $C_6H_{10}NO_2S$: 160.0427; found 160.0431.

***N*-Propanoyl-1,3-oxazinane-2-thione (1n)**

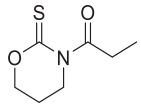

Following the General Procedure 2, 1,3-oxazinane-2-thione (703 mg, 6 mmol) was dissolved in CH_2Cl_2 (25 mL). Subsequently, Et_3N (1.1 mL, 7.8 mmol) and propionyl chloride (0.6 mL, 7.2 mmol) were added dropwise and the solution was stirred for 16 h. The crude was purified by flash chromatography (from 70:30 to 40:60 Hexanes/EtOAc) to give 482 mg (2.8 mmol, 46% yield) of pure **1n**.

White solid.
Mp 59–61 °C.
R_f 0.20 (70:30 Hexanes/EtOAc).
IR (ATR) *v* 2977, 2873, 1712, 1471, 1300, 1250, 1038, 901 cm^{-1}.
^{1}H NMR ($CDCl_3$, 400 MHz) δ 4.34 (2H, t, *J* = 5.5 Hz, $OC\underline{H}_2$), 3.75 (2H, t, *J* = 7.1 Hz, $NC\underline{H}_2$), 3.15 (2H, q, *J* = 7.3 Hz, $C\underline{H}_2CH_3$), 2.26–2.15 (2H, m, $NCH_2C\underline{H}_2$), 1.23 (3H, t, *J* = 7.3 Hz, $CH_2C\underline{H}_3$).
^{13}C NMR ($CDCl_3$, 100.6 MHz) δ 190.1 (C), 179.2 (C), 68.3 (CH_2), 43.9 (CH_2), 32.2 (CH_2), 22.3 (CH_2), 10.2 (CH_3).
HRMS (+ESI): *m/z* calcd. for $[M+H]^+$ $C_7H_{12}NO_2S$: 174.0581; found 174.0581.

***N*-(2-Azidoacetyl)-1,3-thiazolidine-2-thione (1o)**

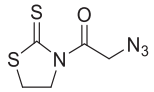

Following the General Procedure 3, 1,3-thiazolidine-2-thione (1.19 g, 10 mmol), EDC·HCl (2.3 g, 12 mmol) and DMAP (244 mg, 2 mmol) were dissolved in CH_2Cl_2 (18 mL). Subsequently, 2-azidoacetic acid (1192 mg, 10 mmol) was dissolved in CH_2Cl_2 (9 mL) and the resulting solution was cooled in an ice/water bath. Then, this solution was added dropwise *via* cannula to the former one and the solution was stirred for 24 h. The crude was purified by flash column chromatography (Hexanes/AcOEt from 80:20 to 60:40) to afford 1.05 g (5 mmol, 52% yield) of pure **1o**.

Yellow oil.
R_f 0.5 (60:40 Hexanes/EtOAc).
IR (ATR) *ν* 2904, 2097, 1698, 1395, 1349, 1264, 1220, 1157, 1043 cm^{-1}.
^{1}H NMR (500 MHz, $CDCl_3$) δ 4.84 (s, 2H, $COC\underline{H}_2$), 4.64 (t, *J* = 7.6 Hz, 2H, $NC\underline{H}_2$), 3.40 (t, *J* = 7.6 Hz, 2H, $SC\underline{H}_2$).
^{13}C NMR (101 MHz, $CDCl_3$) δ 201.5 (C), 169.4 (C), 55.6 (CH_2), 55.4 (CH_2), 29.2 (CH_2).
HRMS (+ESI) *m/z* calcd. For $[M+H]^+$ $C_5H_7N_4OS_2$ 203.0055, found: 203.0061.

3-(4-Methoxyphenoxy)propanenitrile

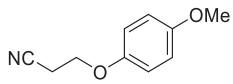

Following a literature procedure,[2] a microwave vial was charged with mequinol (3.1 g, 25 mmol) and acrylonitrile (10 mL, 150 mmol) and dissolved in a 10% solution of Me_4NOH in water (2.5 mL). The mixture was heated under microwave irradiation to 60 °C for 30 min. Afterwards, the mixture was rinsed with water (25 mL) and extracted with Et_2O (3 × 30 mL). The combined organic extracts were washed subsequently with 2 M HCl (25 mL), sat. $NaHCO_3$ (30 mL), and brine (30 mL), dried ($MgSO_4$) and concentrated under reduced pressure to give 2.1 g (12 mmol, 47% yield) of pure product.

White solid.
^{1}H NMR (400 MHz, $CDCl_3$) δ 6.89–6.82 (m, 4H, Ar$\underline{H}$), 4.15 (t, *J* = 6.4 Hz, 2H, $OC\underline{H}_2$), 3.78 (s, 3H, O$\underline{Me}$), 2.80 (t, *J* = 6.4 Hz, 2H, $C\underline{H}_2CN$).

3-(4-Methoxyphenoxy)propanoic acid

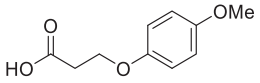

Following a literature procedure,[2] 3-(4-methoxyphenoxy)propanenitrile (2.1 g, 12 mmol) was dissolved in HCl 37% (15 mL) and heated to reflux for 2h. Then, the mixture was cooled to 0 °C to crystalize the acid, which was filtered and washed with water and cold methanol to obtain 778 mg (4.3 mmol, 36% yield) of the pure product.

White solid.
^{1}H NMR (400 MHz, $CDCl_3$) δ 6.88–6.81 (m, 4H, Ar<u>H</u>), 4.21 (t, *J* = 6.3 Hz, 2H, OC<u>H</u>$_2$), 3.77 (s, 3H, O<u>Me</u>), 2.83 (t, *J* = 6.3 Hz, 2H, C<u>H</u>$_2$COOH).

***N*-3-(4-Methoxyphenoxy)propanoyl-1,3-thiazinane-2-thione (1p)**

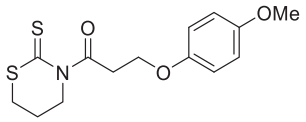

Following the General Procedure 1, 3-(4-methoxyphenoxy)propanoic acid (2.0 g, 10 mmol) was dissolved CH_2Cl_2 (40 mL) and two drops of DMF were added. Then, oxalyl chloride (1.0 mL, 12 mmol) was added dropwise. After 4 h, volatiles were removed under reduced pressure to obtain 3-(4-methoxyphenoxy)propanoyl chloride which was used without further purification.

Afterwards, 1,3-thiazinane-2-thione (1.73 g, 13 mmol) was dissolved in CH_2Cl_2 (10 mL), then Et_3N (1.8 mL, 13 mmol) and the previously prepared 3-(4-methoxyphenoxy)propanoyl chloride were added, and the solution was stirred for 2 h. The crude mixture was purified by flash chromatography (from 80:20 to 70:30 Hexanes/EtOAc) to afford 1.50 g (5.1 mmol, 51% yield) of pure **1p**.

Yellow solid.
Mp 58–61 °C.
R$_f$ 0.4 (70:30 Hexanes/EtOAc).
IR (ATR) ν 3140, 2929, 2835, 1814, 1747, 1733, 1505, 1228, 1193, 1112, 1090, 1023, 984, 824, 733 cm^{-1}.
^{1}H NMR (400 MHz, $CDCl_3$) δ 6.82 (s, 4H, Ar<u>H</u>), 4.26 (t, *J* = 6.1 Hz, 2H, OC<u>H</u>$_2$), 3.98–3.90 (m, 2H, NC<u>H</u>$_2$), 3.77 (s, 3H, O<u>Me</u>), 3.53 (t, *J* = 6.1 Hz, 2H, O=CC<u>H</u>$_2$) 3.02 (t, *J* = 6.8 Hz, 2H, SC<u>H</u>$_2$), 2.30–2.15 (m, 2H, NCH$_2$C<u>H</u>$_2$).

^{13}C NMR (126 MHz, $CDCl_3$) δ 203.5 (C), 175.7 (C), 154.1 (C), 152.5 (C), 115.6 (CH), 114.7 (CH), 65.5 (CH_2), 55.7 (CH_3), 46.6 (CH_2), 39.6 (CH_2), 32.0 (CH_2), 22.9 (CH_2).
HRMS (ESI+) *m/z* calcd for $[M+H]^+$ $C_{14}H_{18}NO_3S_2$: 312.0723, found: 312.0725.

N-(3-Phenylpropanoyl)-1,3-thiazinane-2-thione (1q)

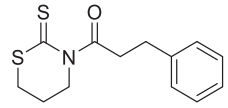

Following the General Procedure 3, 1,3-thiazinane-2-thione (666 mg, 5.0 mmol), EDC·HCl (1.25 g, 6.5 mmol), DMAP (125 mg, 1.0 mmol), and 3-phenylpropanoic acid (915 g, 6.5 mmol) were used. The crude residue was purified by column chromatography (80:20 EtOAc/Hexanes) to give 317 mg (1.2 mmol, 24% yield) of **1q**.

Yellow oil.
R_f 0.40 (80:20 CH_2Cl_2/Hexanes).
IR (ATR) ν 3060, 3026, 2926, 2860, 1755, 1731, 1682, 1603, 1496, 749, 701 cm^{-1}.
^{1}H NMR ($CDCl_3$, 400 MHz) δ 7.30–7.25 (m, 2H, ArH), 7.22–7.18 (m, 3H, ArH), 3.76–3.73 (m, 2H, NCH_2), 3.38 (t, *J* = 7.4 Hz, 2H, $OCCH_2$), 3.04 (t, *J* = 7.4 Hz, 2H, $PhCH_2$), 2.83 (t, *J* = 6.8 Hz, 2H, SCH_2), 2.02–1.96 (m, 2H, NCH_2CH_2).
^{13}C NMR ($CDCl_3$, 100.6 MHz) δ 203.8 (C), 177.4 (C), 140.3 (C), 128.5 (CH), 126.3 (CH), 46.3 (CH_2), 40.7 (CH_2), 32.6 (CH_2), 31.8 (CH_2), 22.8 (CH_2).
HRMS (+ESI) *m/z* calcd. for $[M+H]^+$ $C_{13}H_{16}NOS_2$: 266.0668; found: 266.0669.

N-Phenylacetyl-1,3-thiazinane-2-thione (1r)

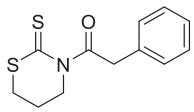

Following the General Procedure 3, 1,3-thiazinane-2-thione (800 mg, 6.0 mmol), EDC·HCl (1.50 g, 7.8 mmol), DMAP (146 mg, 1.2 mmol), and 2-phenylacetic acid (0.95 mL, 7 mmol) were used. The crude residue was purified by column chromatography (from 85:15 to 70:30 Hexanes/EtOAc) to give 265 mg (1.19 mmol, 17% yield) of **1r**.

Thick yellow oil.
R_f 0.30 (70:30 Hexanes/EtOAc)
IR (ATR) ν 3026, 2922, 2872, 1754, 1123, 1060, 1014, 906, 705, 691 cm^{-1}

^{1}H NMR (400 MHz, $CDCl_3$) δ 7.34–7.25 (m, 5H, Ar<u>H</u>), 4.47 (s, 2H, Ar$C\underline{H}_2$), 3.80–3.78 (m, 2H, $NC\underline{H}_2$), 2.89–2.86 (m, 2H, $SC\underline{H}_2$), 2.12–2.06 (m, 2H, $NCH_2C\underline{H}_2$)
^{13}C NMR (101 MHz, $CDCl_3$) δ 203.6 (C), 176.3 (C), 129.5 (CH), 128.7 (CH), 127.4 (CH), 47.3 (CH_2), 45.0 (CH_2), 31.7 (CH_2), 22.7 (CH_2)
HRMS (+ESI) *m/z* calcd for $C_{12}H_{13}NNaOS_2$ $[M+Na]^+$ 274.0331, found 274.0324.

N-(2-*E*-Butenoyl)-1,3-thiazolidine-2-thione (1s)

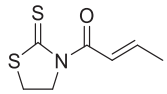

Following General Procedure 3, 1,3-thiazolidine-2-thione (596 mg, 5 mmol), EDC·HCl (1.25 g, 6.5 mmol) and DMAP (122 mg, 1 mmol) were dissolved in CH_2Cl_2 (4 mL). Then, 3-butenoic acid (0.5 mL, 6 mmol) were added dropwise and the resulting mixture was stirred for 3 h. The crude residue was purified by flash column chromatography (from 80:20 to 70:30 Hexanes/EtOAc) to afford 441 mg (2.4 mmol, 47% yield) of pure **1s**.

Yellow oil.
R_f 0.3 (80:20 Hexanes/EtOAc).
^{1}H NMR (500 MHz, $CDCl_3$) δ 7.23 (dq, *J* = 15.0, 1.6 Hz, 1H, $C\underline{H}$=$CHCH_3$), 7.03 (dq, *J* = 15.0, 7.0 Hz, 1H, CH=$C\underline{H}CH_3$), 4.52 (t, *J* = 7.4 Hz, 2H, $NC\underline{H}_2$), 3.33 (t, *J* = 7.4 Hz, 2H, $SC\underline{H}_2$), 1.95 (dd, *J* = 7.0, 1.6 Hz, 3H, $CHC\underline{H}_3$).

2.3 Synthesis of chiral Nickel (II) Catalysts.

A solution of chiral diphosphine ligand (1 equiv) and anhydrous $NiCl_2$ (1 equiv) in acetonitrile (0.05 M) was heated to reflux overnight. Afterwards, the mixture was filtered through Celite® and eluted with acetonitrile. The volatiles were removed under reduced pressure to afford the corresponding chiral Nickel compound which was used without further purification.

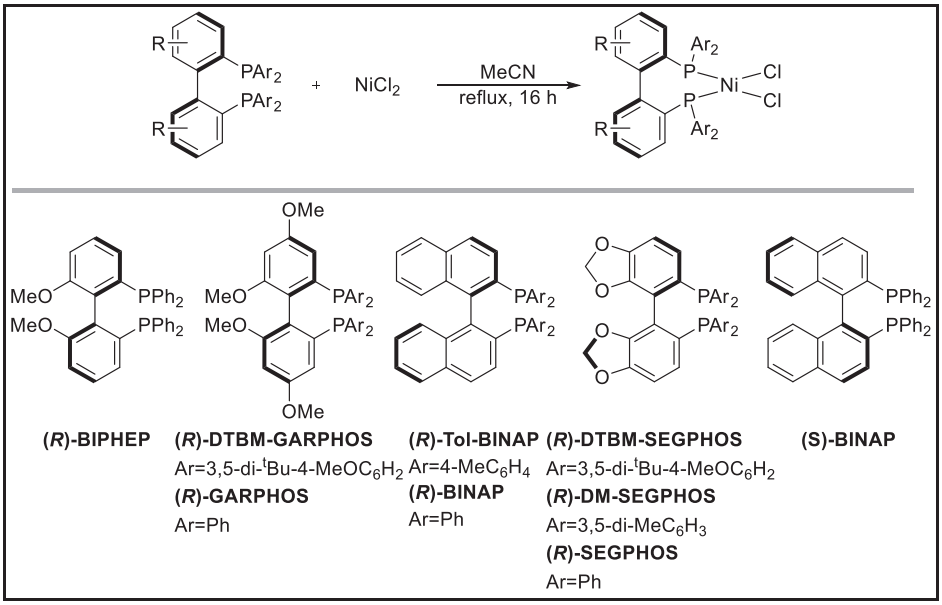

CHAPTER I

The aldol reaction

3 Aldol reactions with aromatic aldehydes

3.1 Synthesis of starting materials

3-Phenylpropiolaldehyde dicobalthexacarbonyl (e)

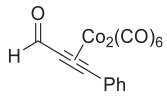

Following a literature procedure,[3] 10% wet with Hexanes dicobalt octacarbonyl (2.28 g, 6 mmol) was dissolved in CH_2Cl_2 (40 mL) and cooled to 0 °C. Then, a solution 3-phenylpropiolaldehyde (0.6 mL, 5 mmol) in CH_2Cl_2 (15 mL) was added dropwise via cannula and the resulting mixture was stirred for 4 h.

Afterwards, the volatiles were removed under reduced pressure (with caution, since the completely dry product is pyrophoric and decomposes eliminating toxic fumes of CO) and the crude product was purified by flash chromatography (from 90:10 to 80:20 Hexanes/EtOAc) to give 1.93 g (4.6 mmol, 93% yield) of **e**. If needed, the aldehyde was further purified by flash chromatography (from 80:20 to 50:50 Hexanes/CH_2Cl_2).

Dark brown solid.
R_f 0.4 (80:20 Hexanes/EtOAc).
IR (ATR) ν 3070, 3024, 2808, 2098, 2059, 2029, 1666, 1573, 1481, 1442 cm^{-1}
^{1}H NMR (400 MHz, $CDCl_3$) δ 10.53 (s, 1H, C<u>H</u>O), 7.59 (s, 2H, Ar<u>H</u>), 7.38 (s, 3H, Ar<u>H</u>).
^{13}C NMR ($CDCl_3$, 100 MHz) δ 197.7 (C), 190.9 (CH), 136.2 (C), 129.7 (CH), 129.1 (CH), 128.9 (CH), 92.1 (C), 85.5 (C).

3.2 Direct, catalytic, and asymmetric *anti* aldol reactions of aromatic aldehydes

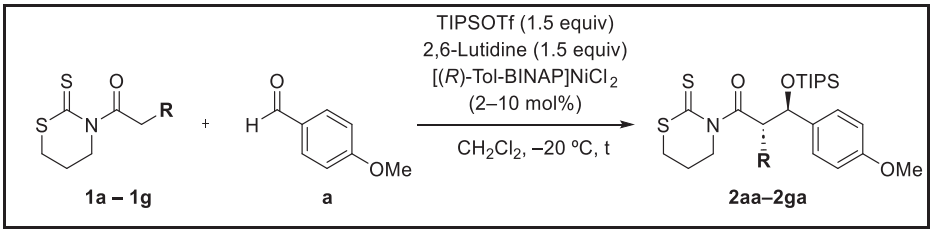

GENERAL PROCEDURE 4

A solution of an *N*-acyl 1,3-thiazinane-2-thione **1** (1.0 mmol, 1.0 equiv), 4-methoxybenzaldehyde (1.1 mmol, 1.1 equiv) and [(*R*)-Tol-BINAP]$NiCl_2$ (2–10 mol%) in CH_2Cl_2 (2 mL) was cooled at –20 °C under N_2. Then, neat TIPSOTf (405 µL, 1.5 mmol, 1.5 equiv) was added followed by 2,6-lutidine (175 µL, 1.5 mmol, 1.5 equiv) and the resultant mixture was stirred at –20 °C.

The reaction mixture was quenched with sat. NH_4Cl (2 mL) and partitioned in CH_2Cl_2 (15 mL) and water (15 mL). The aqueous layer was extracted with CH_2Cl_2 (2 × 15 mL). The combined organic extracts were dried over Na_2SO_4 and concentrated under reduced pressure. The resultant residue was analysed by ^1H NMR (400 MHz) and purified by flash column chromatography to yield the named compound.

N-[(2*S*,3*R*)-3-(4-Methoxyphenyl)-2-Methyl-3-triisopropylsilyloxypropanoyl]-1,3-thiazinane-2-thione (2aa)

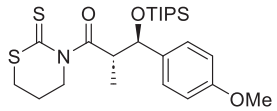

The General Procedure 4 was followed with *N*-propanoyl-1,3-thiazinane-2-thione **1a** (189 mg, 1.0 mmol, 1.0 equiv), [(*R*)-Tol-BINAP]$NiCl_2$ (16.0 mg, 20 µmol, 2 mol%), 4-methoxybenzaldehyde (135 µL, 1.1 mmol, 1.1 equiv), TIPSOTf (405 µL, 1.5 mmol, 1.5 equiv), and 2,6-lutidine (175 µL, 1.5 mmol, 1.5 equiv) at –20 °C for 1 h.

The residue (dr 85:15) was purified by column chromatography (90:10 Hexanes/EtOAc) to give 395 mg (0.82 mmol, 82% yield) of *anti* aldol **2aa**.

Yellow oil.

R_f 0.30 (90:10 Hexanes/EtOAc).

Chiral HPLC (Phenomenex Lux® Cellulose-1 column, 1% i-PrOH in Hexanes, flow rate 1 mL/min): R_t 9.3 min (Major 2*S*,3*R*-enantiomer) R_t 10.7 min (minor 2*R*,3*S*-enantiomer), 99% *ee*.

$[\alpha]_D^{20}$ +281.9 (c 1.00, $CHCl_3$).

IR (ATR) ν 2939, 2866, 1701, 1613, 1514, 1461, 1353, 1302, 1255, 1122, 1036, 875, 831, 679 cm^{-1}.

^{1}H NMR (400 MHz, $CDCl_3$) δ 7.25–7.21 (m, 2H, ArH), 6.85–6.82 (m, 2H, ArH), 4.95 (d, *J* = 8.5 Hz,1H, CHOTIPS), 4.23–4.18 (m, 1H, NCH_xH_y), 4.09 (dq, *J* = 8.5, 6.8 Hz, 1H, $COCHCH_3$), 3.80 (s, 3H, OMe), 3.63 (ddd, *J* = 13.1, 7.1, 5.7 Hz, 1H, NCH_xH_y), 3.02–2.92 (m, 2H, SCH_2), 2.27–2.20 (m, 2H, NCH_2CH_2), 0.99 (d, 3H, *J* = 6.8 Hz, $COCHCH_3$), 0.99–0.97 (m, 9H, OTIPS), 0.91–0.84 (m, 12H, OTIPS).

^{13}C NMR (100.6 MHz, $CDCl_3$) δ 203.8 (C), 180.7 (C), 159.3 (C), 134.7 (C), 128.7 (CH), 113.4 (CH), 79.3 (CH), 55.2 (CH_3), 50.5 (CH), 46.4 (CH_2), 31.9 (CH_2), 23.2 (CH_2), 18.2 (CH_3), 17.9 (CH_3), 16.1 (CH_3), 12.9 (CH).

HRMS (+ESI): *m/z* calcd for $[M–OTIPS]^+$ $C_{15}H_{18}NO_2S_2$: 308.0773, found: 308.0771; *m/z* calcd for $[M+H]^+$ $C_{24}H_{40}NO_3S_2Si$: 482.2213, found: 482.2214.

N-[(2*S*,3*R*)-2-Ethyl-3-(4-methoxyphenyl)-3-triisopropylsilyloxypropanoyl]-1,3-thiazinane-2-thione (2ba)

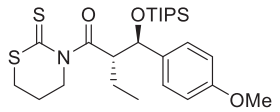

The General Procedure 4 was followed with *N*-butanoyl-1,3-thiazinane-2-thione **1b** (204 mg, 1.0 mmol, 1.0 equiv), [(*R*)-Tol-BINAP]$NiCl_2$ (16.7 mg, 22 μmol, 2 mol%), 4-methoxybenzaldehyde (135 μL, 1.1 mmol, 1.1 equiv), TIPSOTf (405 μL, 1.5 mmol, 1.5 equiv), and 2,6-lutidine (175 μL, 1.5 mmol, 1.5 equiv) at –20 °C for 2 h.

The residue (dr 81:19) was purified by column chromatography (60:40 Hexanes/CH_2Cl_2) to give 389 mg (0.78 mmol, 78% yield) of *anti* aldol **2ba**.

Yellow oil.

R_f 0.50 (60:40 Hexanes/CH_2Cl_2).

Chiral HPLC (Phenomenex Lux® Amylose-3 column, 1% i-PrOH in Hexanes, flow rate 0.5 mL/min): R_t 18.5 min (Major 2*S*,3*R*-enantiomer) R_t 27.7 min (minor 2*R*,3*S*-enantiomer), 99% *ee*.

$[\alpha]_D^{20}$ +42.7 (c 1.00, $CHCl_3$).

IR (ATR) ν 2940, 2864, 1691, 1610, 1511, 1461, 1302, 1171, 1246, 1108, 1086, 1061, 1034, 1012, 910, 882, 836, 731 cm^{-1}.
^{1}H NMR (400 MHz, $CDCl_3$) δ 7.29–7.21 (m, 2H, ArH), 6.86–6.80 (m, 2H, ArH), 5.05 (d, *J* = 7.9 Hz, 1H, CHOTIPS), 4.40–4.32 (m, 1H, COCHEt), 4.08 (dt, *J* = 13.4, 5.8 Hz, 1H, NCH_xH_y), 3.88–3.77 (m, 1H, NCH_xH_y), 3.80 (s, 3H, OMe), 3.02–2.86 (m, 2H, SCH_2), 2.28–2.14 (m, 2H, NCH_2CH_2), 1.54–1.43 (m, 2H, $CHCH_2CH_3$), 1.03–0.85 (m, 21H, OTIPS), 0.73 (t, *J* = 7.5 Hz, 3H, $CHCH_2CH_3$).
^{13}C NMR (100.6 MHz, $CDCl_3$) δ 205.0 (C), 178.0 (C), 159.2 (C), 135.0 (C), 128.6 (CH), 113.3 (CH), 77.2 (CH), 55.2 (CH_3), 46.2 (CH_2), 31.9 (CH_2), 23.3 (CH_2), 23.2 (CH_2), 18.1 (CH_3), 17.9 (CH_3), 12.7 (CH), 11.1 (CH_3).
HRMS (+ESI): *m/z* calcd for $[M–OTIPS]^+$ $C_{16}H_{20}NO_2S_2$: 322.0930, found: 322.0931; *m/z* calcd for $[M+H]^+$ $C_{25}H_{42}NO_3S_2Si$: 496.2370, found: 496.2375.

N-[(2*S*,3*R*)-2-Isobutyl-3-(4-methoxyphenyl)-3-triisopropylsilyloxypropanoyl]-1,3-thiazinane-2-thione (2ca)

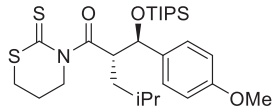

The General Procedure 4 was followed with *N*-(4-methylpentanoyl)-1,3-thiazinane-2-thione **1c** (226 mg, 1.0 mmol, 1.0 equiv), [(*R*)-Tol-BINAP]$NiCl_2$ (41.6 mg, 50 μmol, 5 mol%), 4-methoxybenzaldehyde (135 μL, 1.1 mmol, 1.1 equiv), TIPSOTf (405 μL, 1.5 mmol, 1.5 equiv), and 2,6-lutidine (175 μL, 1.5 mmol, 1.5 equiv) at –20 °C for 2 h.

The residue (dr 75:25) was purified by column chromatography (60:40 Hexanes/CH_2Cl_2) to give 318 mg (0.61 mmol, 60% yield) of *anti* aldol **2ca**.

Yellow oil.
R_f 0.50 (60:40 Hexanes/CH_2Cl_2).
Chiral HPLC (Phenomenex Lux® Cellulose-5 column, 1% i-PrOH in Hexanes, flow rate 0.5 mL/min): R_t 29.8 min (Major 2*S*,3*R*-enantiomer) R_t 13.8 min (minor 2*R*,3*S*-enantiomer), 99% *ee*.
$[\alpha]_D^{20}$ –88.7 (c 1.00, $CHCl_3$).
IR (ATR) ν 2942, 2864, 1691, 1610, 1511, 1462, 1302, 1247, 1171, 1109, 1087, 1064, 1032, 881, 842, 737, 678 cm^{-1}.
^{1}H NMR (400 MHz, $CDCl_3$) δ 7.28–7.22 (m, 2H, ArH), 6.88–6.80 (m, 2H, ArH), 5.05 (d, *J* = 7.2 Hz, 1H, CHOTIPS), 4.67–4.59 (m, 1H, COCH), 4.39 (dt, *J* = 13.3, 5.3 Hz, 1H, NCH_xH_y), 3.81 (s, 3H, OMe), 3.56–3.44 (m, 1H, NCH_xH_y), 3.02–2.85 (m, 2H, SCH_2), 2.28–2.11 (m, 2H, NCH_2CH_2), 1.62–1.49 (m, 1H, $COCHCH_xH_y$), 1.41–1.29 (m, 1H,

C<u>H</u>(CH_3)$_2$), 1.21–1.13 (m, 1H, COCHCH_x<u>H</u>$_y$), 1.00–0.87 (m, 21H, O<u>TIPS</u>), 0.79 (d, *J* = 6.5 Hz, 3H, CHC<u>H</u>$_3$), 0.77 (d, *J* = 6.5 Hz, 3H, CHC<u>H</u>$_3$).
^{13}C NMR (100.6 MHz, $CDCl_3$) δ 205.1 (C), 177.9 (C), 159.0 (C), 134.9 (C), 128.6 (CH), 113.1 (CH), 77.2 (CH), 55.2 (CH_3), 52.0 (CH), 46.2 (CH_2), 39.4 (CH_2), 31.9 (CH_2), 26.1 (CH), 23.6 (CH_3), 23.1 (CH_2), 22.1 (CH_3), 18.0 (CH_3), 17.9 (CH_3), 12.6 (CH).
HRMS (+ESI): *m/z* calcd for $[M–OTIPS]^+$ $C_{18}H_{24}NO_2S_2$: 350.1243, found: 350.1245; *m/z* calcd for $[M+H]^+$ $C_{27}H_{46}NO_3S_2Si$: 524.2683, found: 524.2690.

N-[(2*S*,3R)-2-Allyl-3-(4-methoxyphenyl)-3-triisopropylsilyloxypropanoyl]-1,3-thiazinane-2-thione (2da)

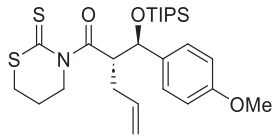

The General Procedure 4 was followed with *N*-(4-pentenoyl)-1,3-thiazinane-2-thione **1d** (220 mg, 1.0 mmol, 1.0 equiv), [(*R*)-Tol-BINAP]$NiCl_2$ (16.7 mg, 22 μmol, 2 mol%), 4-methoxybenzaldehyde (135 μL, 1.1 mmol, 1.1 equiv), TIPSOTf (405 μL, 1.5 mmol, 1.5 equiv), and 2,6-lutidine (175 μL, 1.5 mmol, 1.5 equiv) at –20 °C for 3 h.

The residue (dr 81:19) was purified by column chromatography (from 90:10 to 80:20 Hexanes/EtOAc) to give 394 mg (0.78 mmol, 76% yield) of *anti* aldol **2da**.

Yellow oil.
R_f 0.40 (90:10 Hexanes/EtOAc).
Chiral HPLC (Phenomenex Lux® Cellulose-5 column, 0.5% i-PrOH in Hexanes, flow rate 0.8 mL/min): R_t 40.6 min (Major 2*S*,3*R*-enantiomer) R_t 14.6 min (minor 2*R*,3*S*-enantiomer), 99% *ee*.
$[\alpha]_D^{20}$ +42.4 (c 1.00, $CHCl_3$).
IR (ATR) ν 2940, 2864, 1691, 1611, 1511, 1461, 1246, 1302, 1171, 1107, 1086, 1034, 1012, 933, 882, 836, 733, 678 cm^{-1}.
^{1}H NMR (400 MHz, $CDCl_3$) δ 7.30–7.21 (m, 2H, Ar<u>H</u>), 6.88–6.80 (m, 2H, Ar<u>H</u>), 5.73–5.59 (m, 1H, C<u>H</u>=CH_2), 5.11 (d, *J* = 7.8 Hz, 1H, C<u>H</u>OTIPS), 4.96–4.86 (m, 2H, CH=C<u>H</u>$_2$), 4.57 (ddd, *J* = 8.9, 7.8, 4.7 Hz, 1H, COCHC<u>H</u>$_2$), 4.22–4.12 (m, 1H, NC<u>H</u>$_x$H$_y$), 3.80 (s, 3H, O<u>Me</u>), 3.70–3.59 (m, 1H, NCH_x<u>H</u>$_y$), 3.05–2.85 (m, 2H, SC<u>H</u>$_2$), 2.31 2.04 (m, 4H, NCH_2C<u>H</u>$_2$, COCHC<u>H</u>$_2$), 1.01–0.84 (m, 21H, O<u>TIPS</u>).
^{13}C NMR (100.6 MHz, $CDCl_3$) δ 205.4 (C), 177.3 (C), 159.2 (C), 135.2 (C), 134.6 (CH), 128.7 (CH), 116.8 (CH_2), 113.3 (CH), 77.2 (CH), 55.2 (CH_3), 53.8 (CH), 46.1 (CH_2), 34.8 (CH_2), 31.8 (CH_2), 23.1 (CH_2), 18.0 (CH_3), 17.9 (CH_3), 12.6 (CH).

HRMS (+ESI): *m/z* calcd for $[M–OTIPS]^+$ $C_{17}H_{20}NO_2S_2$: 334.0930, found: 334.0927; *m/z* calcd for $[M+H]^+$ $C_{26}H_{42}NO_3S_2Si$: 508.2370, found: 508.2368.

N-[(2*S*,3*R*)-2-(3-Butynyl)-3-(4-methoxyphenyl)-3-triisopropylsilyloxypropanoyl]-1,3-thiazinane 2-thione (2ea)

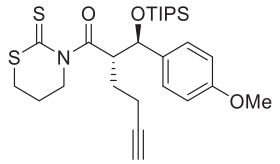

The General Procedure 4 was followed with *N*-(5-hexynoyl)-1,3-thiazinane-2-thione **1e** (273 mg, 1.0 mmol, 1.0 equiv), [(*R*)-Tol-BINAP]$NiCl_2$ (41.2 mg, 55 µmol, 5 mol%), 4-methoxybenzaldehyde (135 µL, 1.1 mmol, 1.1 equiv), TIPSOTf (405 µL, 1.5 mmol, 1.5 equiv), and 2,6-lutidine (175 µL, 1.5 mmol, 1.5 equiv) at –20 °C for 5 h.

The residue (dr 81:19) was purified by column chromatography (from 95:5 to 80:20 Hexanes/EtOAc) to give 425 mg (0.75 mmol, 75% yield) of *anti* aldol **2ea**.

Yellow oil.
R_f 0.50 (80:20 Hexanes/EtOAc).
Chiral HPLC (Phenomenex Lux® Cellulose-5 column, 1.5% i-PrOH in Hexanes, flow rate 0.9 mL/min): R_t 23.3 min (Major 2*S*,3*R*-enantiomer) R_t 11.6 min (minor 2*R*,3*S*-enantiomer), 98% *ee*.
$[\alpha]_D^{20}$ +25.5 (c 1.00, $CHCl_3$).
IR (ATR) ν 3303, 2942, 2865, 1691, 1611, 1511, 1463, 1246, 1204, 1171, 1123, 1087, 1062, 1031, 922, 882, 834, 734, 703, 678, 638 cm^{-1}.
^{1}H NMR (400 MHz, $CDCl_3$) δ 7.28–7.20 (m, 2H, ArH), 6.88–6.80 (m, 2H, ArH), 5.10 (d, *J* = 7.4 Hz, 1H, CHOTIPS), 4.53–4.47 (m, 1H, $COCHCH_2$), 4.08 (dt, *J* = 13.4, 5.8 Hz, 1H, NCH_xH_y), 3.85–3.76 (m, 1H, NCH_xH_y), 3.81 (s, 3H, OMe), 3.07–2.88 (m, 2H, SCH_2), 2.29–2.18 (m, 2H, NCH_2CH_2), 2.17–2.04 (m, 1H, CH_xH_yCCH), 2.02–1.87 (m, 2H, CH_xH_yCCH), 1.83–1.71 (m, 2H, CH_2CH_2CCH), 1.03–0.79 (m, 21H, OTIPS).
^{13}C NMR (100.6 MHz, $CDCl_3$) δ 205.0 (C), 177.4 (C), 159.3 (C), 134.3 (C), 128.5 (CH), 113.4 (CH), 83.5 (C), 77.2 (CH), 69.1 (CH), 55.2 (CH_3), 53.1 (CH), 46.3 (CH_2), 31.8 (CH_2), 28.8 (CH_2), 23.2 (CH_2), 18.1 (CH_3), 17.9 (CH_3), 16.0 (CH_2), 12.7 (CH).
HRMS (+ESI): *m/z* calcd for $[M–OTIPS]^+$ $C_{18}H_{20}NO_2S_2$: 346.0930, found: 346.0925; *m/z* calcd for $[M+H]^+$ $C_{27}H_{42}NO_3S_2Si$: 520.2370, found: 520.2362.

***N*-[(2*S*,3*R*)-2-(3-Methoxy-3-oxopropyl)-3-(4-methoxyphenyl)-3-triisopropylsilyloxy-propanoyl] 1,3-thiazinane-2-thione (2fa)**

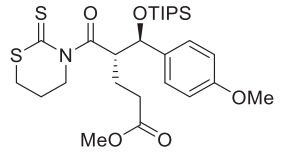

The General Procedure 4 was followed with *N*-(5-methoxy-5-oxopentanoyl)-1,3-thiazinane-2-thione **1f** (250 mg, 0.96 mmol, 1.0 equiv), [(*R*)-Tol-BINAP]$NiCl_2$ (16.3 mg, 20 μmol, 2 mol%), 4-methoxybenzaldehyde (135 μL, 1.1 mmol, 1.1 equiv), TIPSOTf (405 μL, 1.5 mmol, 1.5 equiv), and 2,6 lutidine (175 μL, 1.5 mmol, 1.5 equiv) at –20 °C for 3 h.

The residue (dr 82:18) was purified by column chromatography (from 90:10 to 70:30 Hexanes/EtOAc) to give 330 mg (0.60 mmol, 62% yield) of *anti* aldol **2fa** slightly contaminated by a minor *syn* diastereomer.

Yellow oil.
R_f 0.30 (80:20 Hexanes/EtOAc).
Chiral HPLC (Phenomenex Lux® Cellulose-1 column 1% i-PrOH in Hexanes, flow rate 0.8 mL/min): R_t 23.3 min (Major 2*S*,3*R*-enantiomer) R_t 26.5 min (minor 2*R*,3*S*-enantiomer), 94% *ee*.
IR (ATR) ν 2941, 2864, 1733, 1689, 1610, 1511, 1462, 1302, 1247, 1200, 1171, 1123, 1086, 1062, 1031, 921, 882, 837, 736, 679 cm^{-1}.
^{1}H NMR (400 MHz, $CDCl_3$) δ 7.26–7.20 (m, 2H, ArH), 6.88–6.81 (m, 2H, ArH), 5.05 (d, *J* = 7.5 Hz, 1H, CHOTIPS), 4.54–4.47 (m, 1H, $COCHCH_2$), 3.99–3.88 (m, 2H, NCH_2), 3.80 (s, 3H, ArOMe), 3.59 (s, 3H, CO_2CH_3), 3.03–2.88 (m, 2H, SCH_2), 2.26–2.19 (m, 3H, NCH_2CH_2,$CH_xH_yCO_2Me$), 2.15–2.03 (m, 1H, $CH_xH_yCO_2Me$), 1.89–1.79 (m, 2H, $COCHCH_2$), 1.01–0.86 (m, 21H, OTIPS).
^{13}C NMR (100.6 MHz, $CDCl_3$) δ 205.0 (C), 177.5 (C), 173.4 (C), 159.4 (C), 134.2 (C), 128.5 (CH), 113.5 (CH), 77.4 (CH), 55.2 (CH_3), 53.1 (CH), 51.5 (CH_3), 46.4 (CH_2), 31.9 (CH_2), 31.2 (CH_2), 25.0 (CH_2), 23.1 (CH_2), 18.1 (CH_3), 17.9 (CH_3), 12.7 (CH).
HRMS (+ESI): *m/z* calcd for $[M–OTIPS]^+$ $C_{18}H_{22}NO_4S_2$: 380.0985, found: 380.0981; *m/z* calcd for $[M+H]^+$ $C_{27}H_{44}NO_5S_2Si$: 554.2425, found: 554.2418.

***N*-[(2*S*,3*R*)-2-(4-Bromobutyl)-3-(4-methoxyphenyl)-3-triisopropylsilyloxypropanoyl]-1,3 thiazinane-2-thione (2ga)**

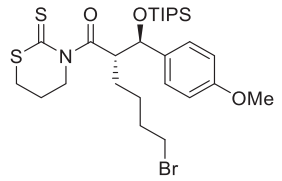

The General Procedure 4 was followed with *N*-(6-bromohexanoyl)-1,3-thiazinane-2-thione **1g** (310 mg, 1.0 mmol, 1.0 equiv), [(*R*)-Tol-BINAP]$NiCl_2$ (16.2 mg, 21 µmol, 2 mol%), 4-methoxybenzaldehyde (135 µL, 1.1 mmol, 1.1 equiv), TIPSOTf (405 µL, 1.5 mmol, 1.5 equiv), and 2,6-lutidine (175 µL, 1.5 mmol, 1.5 equiv) at –20 °C for 15 h.

The residue (dr 79:21) was purified by column chromatography (from 95:5 to 70:30 Hexanes/EtOAc) to give 419 mg (0.70 mmol, 70% yield) of *anti* aldol **2ga**.

Yellow oil.
R_f 0.40 (80:20 Hexanes/EtOAc).
Chiral HPLC (Phenomenex Lux® Cellulose-5 column 1% i-PrOH in Hexanes, flow rate 1 mL/min): R_t 32.9 min (Major 2*S*,3*R*-enantiomer) R_t 13.5 min (minor 2*R*,3*S*-enantiomer), 99% *ee*.
$[\alpha]_D^{20}$ +38.7 (c 1.00, $CHCl_3$).
IR (ATR) ν 2940, 2864, 1691, 1610, 1511, 1462, 1247, 1171, 1118, 1061, 1032, 920, 882, 837, 736, 703, 680 cm^{-1}.
^{1}H NMR (400 MHz, $CDCl_3$) δ 7.28–7.21 (m, 2H, Ar<u>H</u>), 6.89–6.80 (m, 2H, Ar<u>H</u>), 5.04 (d, *J* = 7.7 Hz, 1H, C<u>H</u>OTIPS), 4.44 (td, *J* = 7.7, 5.0 Hz, 1H, COCHC<u>H_2</u>), 4.08 (dt, *J* = 13.5, 5.9 Hz, 1H, NC<u>$H_x$$H_y$</u>), 3.88–3.76 (m, 1H, NCH_x<u>H_y</u>), 3.81 (s, 3H, O<u>Me</u>), 3.27 (t, *J* = 6.7 Hz, 2H, C<u>H_2</u>Br), 3.05–2.88 (m, 2H, SC<u>H_2</u>), 2.27–2.18 (m, 2H, NCH_2C<u>H_2</u>), 1.76–1.58 (m, 2H, C<u>H_2</u>CH_2Br), 1.55–1.39 (m, 2H, COCHC<u>H_2</u>), 1.38–1.28 (m, 1H, C<u>H_x</u>HyCH_2CH_2Br), 1.23–1.11 (m, 1H, CH_x<u>H_y</u>CH_2CH_2Br), 1.01–0.87 (m, 21H, O<u>TIPS</u>).
^{13}C NMR (100.6 MHz, $CDCl_3$) δ 205.2 (C), 177.9 (C), 159.2 (C), 134.7 (C), 128.5 (CH), 113.4 (CH), 77.2 (CH), 55.2 (CH_3), 53.9 (CH), 46.3 (CH_2), 33.7 (CH_2), 32.7 (CH_2), 31.9 (CH_2), 29.3 (CH_2), 25.3 (CH_2), 23.1 (CH_2), 18.1 (CH_3), 17.9 (CH_3), 12.7 (CH).
HRMS (+ESI): *m/z* calcd for $[M–OTIPS]^+$ $C_{18}H_{23}{}^{79}BrNO_2S_2$: 428.0348, found: 428.0341; *m/z* calcd for $[M+H]^+$ $C_{27}H_{45}{}^{79}BrNO_3S_2Si$: 602.1788, found: 602.1771.

4 Acetate aldol reaction

General Procedure 5

A solution of *N*-propanoyl-thioimide (1 equiv) and catalyst (2–10 mol%) in CH_2Cl_2 (0.5 M) was cooled to –20 °C. Then, 4-methoxybenzaldehyde (1.1 equiv), TIPSOTf (1.5 equiv) and 2,6-lutidine (1.5 equiv) were added consecutively, and the mixture was stirred at this temperature for 16 h.

Afterwards, the solution was quenched by addition of sat. NH_4Cl (1 mL), rinsed with water (25 mL) and extracted with CH_2Cl_2 (3 × 10 mL). The combined organic extracts were dried ($MgSO_4$) and concentrated under reduced pressure. The crude mixture was purified by column chromatography to obtain pure products.

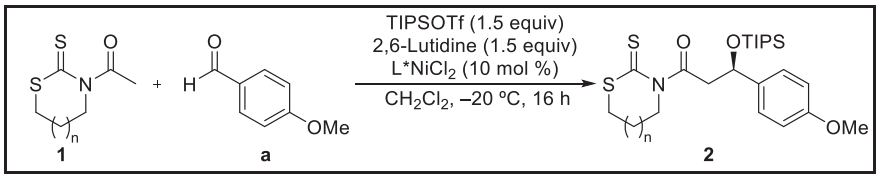

Entry	1	n	L*	Conv (%)[a]	Yield (%)[b]	*ee(%)*[c]
1	**1h**	1	(*S*)-BINAP	72	-	30
2	**1h**	1	(*S*)-Tol-BINAP	54	20	38
3	**1h**	1	(*R*)-SEGPHOS	56	-	28
4[d]	**1h**	1	(*R*)-DTBM-SEGPHOS	67	36	0
5	**1h**	1	(*R*)-BIPHEP	98	-	42
6	**1h**	1	(*R*)-GARPHOS	88	-	30
7	**1h**	1	(*S,S*)-Ph-BPE	0	-	-
8	**1i**	0	(*S*)-BINAP	54	-	42
9	**1i**	0	(*S*)-Tol-BINAP	50	32	40
10	**1i**	0	(*R*)-SEGPHOS	69	-	38
11	**1i**	0	(*R*)-DTBM-SEGPHOS	80	-	0
12	**1i**	0	(*R*)-BIPHEP	99	-	44
13	**1i**	0	(*R*)-GARPHOS	89	-	42

a) Established by ^{1}H NMR analysis. b) Isolated yield. c) Established by chiral HPLC analysis. d) 0 °C

Table 44. Aldol reactions of thioimides **1h** and **1i**.

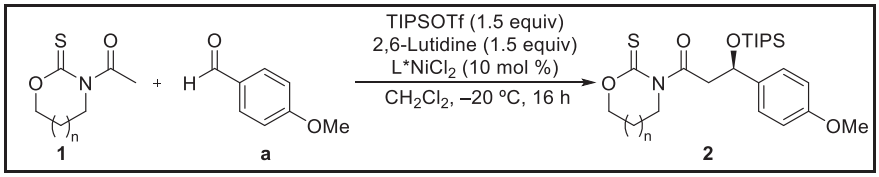

Entry	1	n	L*	Conv (%)[a]	Yield (%)[b]	*ee(%)*[c]
1	**1j**	0	(*S*)-Tol-BINAP	95	93	28
2	**1j**	0	(*R*)-BIPHEP	96	-	20
3	**1j**	0	(*R*)-GARPHOS	82	69	7
4	**1k**	1	(*S*)-BINAP	76	36	28
5	**1k**	1	(*S*)-Tol-BINAP	62	20	40
6	**1k**	1	(*R*)-BIPHEP	93	-	47
7	**1k**	1	(*R*)-GARPHOS	70	54	40

a) Established by ^{1}H NMR analysis. b) Isolated yield. c) Established by chiral HPLC analysis.

Table 45. Aldol reactions of thioimides **1j** and **1k**.

N-[3-(4-Methoxyphenyl)-(3-triisopropylsilyloxy)propanoyl]-1,3-thiazinane-2-thione (2ha)

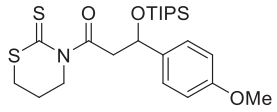

The General Procedure 5 was followed with **1h** (175 mg, 1 mmol), [*(R)*-DTBM-SEGPHOS]$NiCl_2$ (65.6 mg, 100 µmol, 10 mol%), 4-methoxybenzaldehyde (134 µL, 1.1 mmol, 1.1 equiv), TIPSOTf (405 µL, 1.5 mmol, 1.5 equiv), and 2,6-lutidine (87 µL, 1.5 mmol, 1.5 equiv) at 0 °C for 16 h.

The residue was purified by column chromatography (from 90:10 to 70:30 Hexanes/EtOAc) to give 168 mg (0.36 mmol, 36% yield) of aldol adduct **2ha**.

Yellow oil.

R_f 0.4 (80:20 Hexanes/EtOAc).

Chiral HPLC (Phenomenex Lux® Cellulose-5 column, 5% *i*-PrOH in Hexanes, flow rate 1 mL/min): R_t 9.8 min (major isomer) R_t 32.4 min (minor isomer), 0% *ee*.

IR (ATR) ν 2940, 2865, 1693, 1511, 1108, 1086, 1063, 1030, 881, 867, 729, 678 cm^{-1}.

^{1}H NMR (500 MHz, $CDCl_3$) δ 7.29–7.22 (m, 2H, Ar<u>H</u>), 6.86–6.80 (m, 2H, Ar<u>H</u>), 5.21 (dd, *J* = 7.9, 6.1 Hz, 1H, C<u>H</u>OTIPS), 3.79 (s, 3H, O<u>Me</u>), 3.64 (ddd, *J* = 13.3, 6.4, 5.1 Hz,

1H, NC$\underline{H}_x H_y$), 3.55 (dd, *J* = 14.7, 7.9 Hz, 1H, OCC$\underline{H}_x H_y$), 3.49 (ddd, *J* = 13.2, 8.4, 4.8 Hz, 1H, NCH$_x\underline{H}_y$), 3.43 (dd, *J* = 14.7, 6.2 Hz, 1H, OCCH$_x\underline{H}_y$), 2.79 (dt, *J* = 12.4, 6.8 Hz, 1H, SC$\underline{H}_x H_y$), 2.57 (ddd, *J* = 12.4, 7.2, 6.3 Hz, 1H, SCH$_x\underline{H}_y$), 2.03–1.91 (m, 1H, NCH$_2$C$\underline{H}_x H_y$), 1.68–1.58 (m, 1H, NCH$_2$CH$_x\underline{H}_y$), 1.07–0.91 (m, 21H, O$\underline{\text{TIPS}}$).

^{13}C NMR (126 MHz, $CDCl_3$) δ 204.11, 175.38, 159.30, 136.40, 127.94, 113.62, 73.38, 55.46, 51.04, 46.20, 31.48, 22.91, 18.16, 18.04, 12.41.

HRMS (ESI+) *m/z* calcd for $[M+Na]^+$ $C_{23}H_{37}NNaO_3S_2Si$: 490.1876, found: 490.1877.

N-[-3-(4-methoxyphenyl)-(3-triisopropylsilyloxy)propanoyl]-1,3-oxazinane-2-thione (2ia)

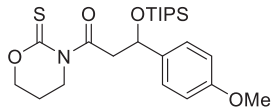

The General Procedure 5 was followed with **1i** (81 mg, 0.5 mmol), [*(R)*-MeO-BIPHEP]$NiCl_2$ (33.7 mg, 26 μmol, 5 mol%), 4-methoxybenzaldehyde (134 μL, 0.55 mmol, 1.2 equiv), TIPSOTf (203 μL, 0.75 mmol, 1.5 equiv), and 2,6-lutidine (87 μL, 0.75 mmol, 1.5 equiv) for 16 h.

The residue was purified by column chromatography (from 90:10 to 70:30 Hexanes/EtOAc) to give 113 mg (0.05 mmol, 50% yield) of aldol adduct **2ia**.

Colorless oil.

R$_f$ 0.2 (80:20 Hexanes/EtOAc).

Chiral HPLC (Phenomenex Lux® Cellulose-5 column, 5% *i*-PrOH in Hexanes, flow rate 1 mL/min): R_t 15.9 min (major isomer) R_t 19.1 min (minor isomer), 40% *ee*.

IR (ATR) ν 2941, 2864, 1701, 1610, 1317, 1180, 1087, 1045, 881, 732, 678 cm^{-1}.

^{1}H NMR (500 MHz, $CDCl_3$) δ 7.29–7.23 (m, 2H, Ar$\underline{H}$), 6.86–6.80 (m, 2H, Ar$\underline{H}$), 5.20 (t, *J* = 6.9 Hz, 1H, C$\underline{H}$OTIPS), 4.20–4.12 (m, 1H, OC$\underline{H}_x H_y$), 3.83–3.75 (m, 1H, OCH$_x\underline{H}_y$), 3.79 (s, 3H, O$\underline{\text{Me}}$), 3.62 (dd, *J* = 14.6, 7.4 Hz, 1H, OCC$\underline{H}_x H_y$), 3.58–3.50 (m, 2H, OCCH$_x\underline{H}_y$, NC$\underline{H}_x H_y$), 3.20 (dt, *J* = 12.6, 7.7 Hz, 1H, NCH$_x\underline{H}_y$), 2.08–1.96 (m, 1H, OCH$_2$C$\underline{H}_x H_y$), 1.98–1.87 (m, 1H, OCH$_2$C$\underline{H}_x H_y$), 1.11–0.90 (m, 21H, O$\underline{\text{TIPS}}$).

^{13}C NMR (126 MHz, $CDCl_3$) δ 190.2 (C), 175.6 (C), 159.1 (C), 136.2 (C), 127.7 (CH), 113.5 (CH), 73.3 (CH), 67.9 (CH_2), 55.3 (CH_3), 50.4 (CH_2), 43.4 (CH_2), 22.1 (CH_2), 18.00 (CH/CH_3), 17.9 (CH/CH_3), 12.3 (CH/CH_3).

HRMS (ESI+) *m/z* calcd for $[M+Na]^+$ $C_{23}H_{37}NNaO_3S_2Si$: 474.2105, found: 474.2104.

N-[3-(4-methoxyphenyl)-(3-triisopropylsilyloxy)propanoyl]-1,3-thiaziolidine-2-thione (2ja)

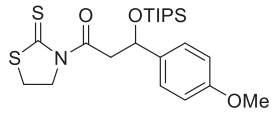

The General Procedure 5 was followed with **1j** (161.5 mg, 1 mmol), [(*R*)-GARPHOS]$NiCl_2$ (28.3 mg, 100 μmol, 10 mol%), 4-methoxybenzaldehyde (134 μL, 1.1 mmol), TIPSOTf (405 μL, 1.5 mmol), and 2,6-lutidine (175 μL, 1.5 mmol) for 16 h.

The residue was purified by column chromatography (from 90:10 to 70:30 Hexanes/EtOAc) to give 460 mg (0.93 mmol, 93% yield) of aldol adduct **2ja**.

Yellow oil.
R_f 0.3 (85:15 Hexanes/EtOAc).
Chiral HPLC (Phenomenex Lux® Cellulose-5 column, 5% *i*-PrOH in Hexanes, flow rate 1 mL/min): R_t 14.3 min (major isomer) R_t 15.6 min (minor isomer), 42% *ee*.
IR (ATR) ν 2940, 2865, 1693, 1511, 1278, 1243, 1221, 1151, 1086, 1052, 735, 678 cm^{-1}.
^{1}H NMR (500 MHz, $CDCl_3$) δ 7.34–7.26 (m, 2H, ArH), 6.84 (d, *J* = 8.7 Hz, 2H, ArH), 5.36–5.28 (m, 1H, CHOTIPS), 4.48–4.34 (m, 2H, NCH_2), 3.80 (s, 3H, OMe), 3.83–3.75 (m, 1H, $OCCH_xH_y$), 3.65 (dd, *J* = 16.0, 6.1 Hz, 1H, $OCCH_xH_y$), 3.23–3.09 (m, 2H, SCH_2), 1.06–0.89 (m, 21H, OTIPS).
^{13}C NMR (126 MHz, $CDCl_3$) δ 201.5 (C), 172.2 (C), 159.0 (C), 136.5 (C), 127.6 (CH), 113.4 (CH), 71.9 (CH), 56.0 (CH_2), 55.2 (CH_3), 49.5 (CH_2), 28.4 (CH_2), 18.0 (CH/CH_3), 17.9 (CH/CH_3), 12.3 (CH/CH_3).
HRMS (ESI+) *m/z* calcd for $[M+H]^+$ $C_{22}H_{36}NO_3S_2Si$: 468.2057, found: 468.2061.

N-[3-(4-methoxyphenyl)-(3-triisopropylsilyloxy)propanoyl]-1,3-oxaziolidine-2-thione (2ka)

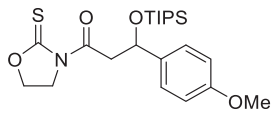

The General Procedure 5 was followed with **1k** (143 mg, 1 mmol), [(*S*)-Tol-BINAP]$NiCl_2$ (80 mg, 100 μmol, 10 mol%), 4-methoxybenzaldehyde (134 μL, 1.1 mmol), TIPSOTf (405 μL, 1.5 mmol), and 2,6-lutidine (175 μL, 1.5 mmol) for 16 h.

The residue was purified by column chromatography (from 90:10 to 75:25 Hexanes/EtOAc) to give 392 mg (0.90 mmol, 90% yield) of aldol adduct **2ka**.

White solid.

R_f 0.3 (80:20 Hexanes/EtOAc).

Chiral HPLC (Phenomenex Lux® Cellulose-4 column, 5% *i*-PrOH in Hexanes, flow rate 1 mL/min): R_t 21.6 min (minor isomer) R_t 30.3 min (major isomer), 9% *ee*.

IR (ATR) ν 2944, 2865, 1699, 1608, 1234, 1154, 1061, 1007, 829 cm^{-1}.

^{1}H NMR (500 MHz, $CDCl_3$) δ 7.38–7.31 (m, 2H, Ar<u>H</u>), 6.88–6.81 (m, 2H, Ar<u>H</u>), 5.37 (dd, *J* = 7.0, 6.0 Hz, 1H, C<u>H</u>OTIPS), 4.52–4.38 (m, 2H, OC<u>H_2</u>), 4.19–4.05 (m, 2H, NC<u>H_2</u>), 3.90 (dd, *J* = 16.1, 7.0 Hz, 1H, OCC<u>H_x</u>H_y), 3.80 (s, 3H, O<u>Me</u>), 3.72 (dd, *J* = 16.1, 6.0 Hz, 1H, OCCH_x<u>H_y</u>), 1.06–0.89 (m, 21H, O<u>TIPS</u>).

^{13}C NMR (126 MHz, $CDCl_3$) δ 185.4 (C), 171.7 (C), 159.0 (C), 136.5 (C), 127.7 (CH), 113.5 (CH), 71.6 (CH), 66.3 (CH_2), 55.2 (CH_3), 48.0 (CH_2), 47.1 (CH_2), 18.00 (CH/CH_3), 17.9 (CH/CH_3), 12.3 (CH/CH_3).

HRMS (ESI+) *m/z* calcd for $[M+Na]^+$ $C_{22}H_{35}NNaO_3S_2Si$: 460.1948, found: 460.1945.

5 Co and Fe catalysed aldol

5.1 Cobalt catalysed aldol reactions

5.1.1 Assessment of cobalt salts as catalysts

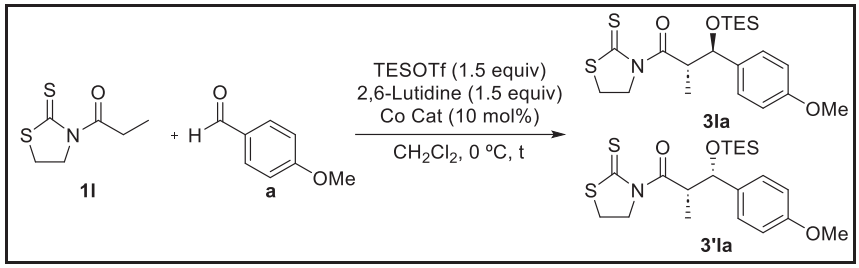

A solution of *N*-propanoyl-1,3-thiazinane-2-thione (35 mg, 0.2 mmol, 1.0 equiv), 4-methoxybenzaldehyde (27 µL, 0.22 mmol, 1.1 equiv) and a cobalt salt (10 mol%) in CH_2Cl_2 (0.4 mL) was cooled at 0 °C under N_2. Then, neat TESOTf (69 µL, 0.3 mmol, 1.5 equiv) was added followed by 2,6-lutidine (35 µL, 1.5 mmol, 1.5 equiv) and the resultant mixture was stirred at 0 °C.

The reaction mixture was quenched with sat. NH_4Cl (1 mL) and a known quantity of methyl 4-nitrobenzoate was added as internal standard (10–20 mg). The mixture was partitioned in CH_2Cl_2 (15 mL) and water (15 mL). The aqueous layer was extracted with CH_2Cl_2 (2 × 10 mL). The combined organic extracts were dried ($MgSO_4$) and concentrated under reduced pressure. The resultant residue was analysed by ^1H NMR and the results are summarized in Table 46.

Entry	Catalyst	2 h (%)[a]	5 h (%)[a]	16 h (%)[a]	dr (*anti:syn*)[b]	Aldol adduct Detected[b]	Yield (%)[c]
1	$NiCl_2$	-	27	38	-	✗	Complex mixture
2	$CoCl_2$	34	55	72	59:41	✓	60
3	CoF_3	0	0	0	-	✗	-
4	$Ni(OAc)_2$	-	25	69	-	✗	0
5	$Co(OAc)_2$	59	71	80	70:30	✓	22
6	$Co(acac)_2$	0	11	23	-	✓	Complex mixture
7	$Co(NO_3)_2$	-	58	69	-	✗	Complex mixture
8	$CoSO_4$	-	-	76	-	✗	Complex mixture
9	Co(SALEN)	-	-	92	70:30	✓	90
10	$(Ph_3P)_3CoCl$	-	-	70	77:23	✓	69
11	$(Ph_3P)_2CoCl_2$	-	-	76	71:29	✓	66
12	$CoCl_2$ + 2 PPh_3	-	-	-	20:80	✓	Complex mixture

a) Conversion based on starting material recovered established by ^1H NMR analysis using methyl 4-nitrobenzoate as internal reference. b) Established by ^1H NMR analysis. c) NMR yield using methyl 4-nitrobenzoate as internal reference.

Table 46. Cobalt catalysed aldol reaction.

N-[((±)*anti)*-3-(4-Methoxyphenyl)-2-methyl-3-triethylsilyloxypropanoyl]-1,3-thiazinane-2 thione (3la)

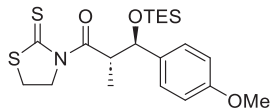

A solution of *N*-propanoyl-1,3-thiazinane-2-thione (88 mg, 0.5 mmol, 1.0 equiv), 4-methoxybenzaldehyde (67 µL, 0.55 mmol, 1.1 equiv) and Co(SALEN) (16.4 mg, 0.05 mmol, 10 mol%) in CH_2Cl_2 (0.1 mL) was cooled at –20 °C under N_2. Then, neat TESOTf (69 µL, 0.3 mmol, 1.5 equiv) was added followed by 2,6-lutidine (35 µL, 1.5 mmol, 1.5 equiv) and the resultant mixture was stirred at –20 °C for 5 h.

The reaction mixture was quenched with sat. NH_4Cl (1 mL) and methyl 4-nitrobenzoate was added as internal standard (17 mg). The mixture was partitioned in CH_2Cl_2 (15 mL) and water (15 mL). The aqueous layer was extracted

with CH_2Cl_2 (2 × 10 mL). The combined organic extracts were dried ($MgSO_4$) and concentrated under reduced pressure. The resultant residue (dr 70:30) was purified by flash chromatography (Hexanes/EtOAc from 95:5 to 85:15) to give 130 mg (0.3 mmol, 64% yield) of **3la** and 40 mg (0.1 mmol, 20% yield) of **3'la**.

Yellow oil.

R_f 0.75 (CH_2Cl_2).

IR (ATR) ν 2958, 2930, 2869, 1701, 1610, 1518, 1460, 1365, 1307, 1255, 1160, 1069, 1038, 956, 940, 833 cm^{-1}.

^{1}H NMR (400 MHz, $CDCl_3$) δ 7.30–7.26 (2H, m, ArH), 6.81–6.79 (2H, m, ArH), 4.99 (1H, dq, *J* = 7.7, 6.7 Hz, COCHCH$_3$), 4.85 (1H, d, *J* = 7.7 Hz, CHOTES), 4.42–4.35 (1H, m, OCH$_x$H$_y$), 4.07–3.98 (2H, m, OCH$_x$H$_y$, NCH$_x$H$_y$), 3.79 (3H, s, OMe), 3.73–3.69 (1H, m, NCH$_x$H$_y$), 1.31 (3H, d, *J* = 6.7 Hz, COCHCH$_3$), 0.85 (9H, t, *J* = 7.9 Hz, SiCH$_2$CH$_3$), 0.50–0.45 (6H, m, O SiCH$_2$CH$_3$).

^{13}C NMR (100.6 MHz, $CDCl_3$) δ 185.1 (C), 176.4 (C), 159.0 (C), 135.1 (C), 127.9 (CH), 113.1 (CH), 76.4 (CH), 66.1 (CH_2), 55.2 (CH_3), 47.3 (CH_2), 47.2 (CH), 13.4 (CH_3), 6.7 (CH_2), 4.7 (CH_3).

HRMS (+ESI): *m/z* calcd for $[M–OTES]^+$ $C_{14}H_{16}NO_3S$: 294.0617, found: 294.0615; calcd for $C_{20}H_{31}NNaO_4SSi$ $[M+Na]^+$: 432.1635, found 432.1644.

***N*-[((±)*syn*)-3-(4-methoxyphenyl)-2-methyl-3-triethylsilyloxypropanoyl]-1,3-thiazinane-2 thione (3'la)**

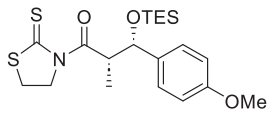

Minor diastereomer:

Yellow oil.

R_f 0.60 (CH_2Cl_2).

IR (ATR) ν 2958, 2930, 2869, 1701, 1610, 1518, 1460, 1365, 1307, 1255, 1160, 1069, 1038, 956, 940, 833 cm^{-1}.

^{1}H NMR (400 MHz, $CDCl_3$) δ 7.30–7.26 (2H, m, ArH), 6.88–6.84 (2H, m, ArH), 5.12 (1H, dq, *J* = 9.5, 6.8 Hz, COCHCH$_3$), 4.76 (1H, d, *J* = 9.5 Hz, CHOTES), 4.57 (1H, td, *J* = 8.6, 6.6 Hz, OCH$_x$H$_y$), 4.49–4.42 (1H, m, OCH$_x$H$_y$), 4.26–4.20 (2H, m, NCH$_2$), 3.81 (3H, s, OMe), 0.89 (3H, d, *J* = 6.8 Hz, COCHCH$_3$), 0.78 (9H, t, *J* = 7.9 Hz, SiCH$_2$CH$_3$), 0.42–0.34 (6H, m, SiCH$_2$CH$_3$).

^{13}C NMR (100.6 MHz, $CDCl_3$) δ 185.6 (C), 177.7 (C), 159.2 (C), 134.4 (C), 128.6 (CH), 113.5 (CH), 78.6 (CH), 66.1 (CH_2), 55.2 (CH_3), 47.4 (CH_2), 46.1 (CH), 14.0 (CH_3), 6.6 (CH_2), 4.7 (CH_3).

HRMS (+ESI): *m/z* calcd for $[M–OTES]^+$ $C_{14}H_{16}NO_3S$: 294.0617, found: 294.0615; calcd for $C_{20}H_{31}NNaO_4SSi$ $[M+Na]^+$: 432.1635, found 432.1644.

5.1.2 Temperature and catalyst assessment

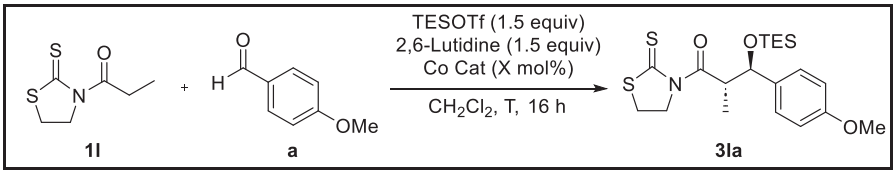

A solution of *N*-propanoyl-1,3-thiazolidine-2-thione (35 mg, 0.2 mmol, 1.0 equiv), 4-methoxybenzaldehyde (27 µL, 0.22 mmol, 1.1 equiv) and cobalt catalyst (10–20 mol%) in CH_2Cl_2 (0.4 mL) was cooled at 0 °C or –20 °C under N_2. Then, neat TESOTf (69 µL, 0.3 mmol, 1.5 equiv) was added followed by 2,6-lutidine (35 µL, 1.5 mmol, 1.5 equiv) and the resultant mixture was stirred at 0 °C or –20 °C.

The reaction mixture was quenched with sat. NH_4Cl (1 mL) and a known quantity of methyl 4-nitrobenzoate was added as internal standard (10–20 mg). The mixture was partitioned in CH_2Cl_2 (15 mL) and water (15 mL). The aqueous layer was extracted with CH_2Cl_2 (2 × 10 mL). The combined organic extracts were dried ($MgSO_4$) and concentrated under reduced pressure. The resultant residue was analysed by ^1H NMR. The results are summarised in Table 47.

Entry	Catalyst	mol%	T (°C)	Conv (%)[a]	dr (anti:syn)[a]	Yield(%)[b]
1	$(Ph_3P)_3CoCl$	10	0	70	77:23	-
2	$(Ph_3P)_3CoCl$	20	–20	23	75:25	-
3	$(Ph_3P)_2CoCl_2$	10	0	81	76:24	-
4	$(Ph_3P)_2CoCl_2$	20	–20	40	80:20	-
5	$(SALEN)CoCl_2$	10	0	>95	75:25	90
6	$(SALEN)CoCl_2$	20	–20	<10	76:24	-

a) Established by ^1H NMR analysis. b) NMR yield using methyl 4-nitrobenzoate as internal reference.

Table 47. Temperature and catalyst assessment.

5.1.3 Thioimide assessment

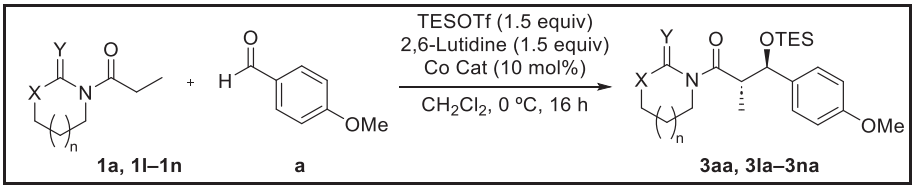

A solution of an *N*-propanoyl-thioimide (0.2 mmol, 1.0 equiv), 4-methoxybenzaldehyde (27 µL, 0.22 mmol, 1.1 equiv) and metal catalyst (10

mol%) in CH_2Cl_2 (0.4 mL) was cooled at 0 °C under N_2. Then, neat TESOTf (69 µL, 0.3 mmol, 1.5 equiv) was added followed by 2,6-lutidine (35 µL, 1.5 mmol, 1.5 equiv) and the resultant mixture was stirred at 0 °C for 16 h.

The reaction mixture was quenched with sat. NH_4Cl (1 mL) and a known quantity of methyl 4-nitrobenzoate was added as internal standard (10–20 mg). The mixture was partitioned in CH_2Cl_2 (15 mL) and water (15 mL). The aqueous layer was extracted with CH_2Cl_2 (2 × 10 mL). The combined organic extracts were dried ($MgSO_4$) and concentrated under reduced pressure. The resultant residue was analysed by ^1H NMR. The results are summarised in Table 48.

Entry	1	X	Y	n	Catalyst	Conv. (%)[a]	dr (anti:syn)[a]	Yield (%)[b]
1	**1l**	S	S	0	$(Ph_3P)_3CoCl$	70	77:23	69
2	**1l**	S	S	0	$(Ph_3P)_2CoCl_2$	80	76:24	80
3	**1l**	S	S	0	$(SALEN)CoCl_2$	81	73:26	80
4	**1a**	S	S	1	$(Ph_3P)_3CoCl$	74	96:4	36
5	**1a**	S	S	1	$(Ph_3P)_2CoCl_2$	81	91:9	32
6	**1a**	S	S	1	$(SALEN)CoCl_2$	83	87:13	14
7	**1m**	O	S	0	$(Ph_3P)_3CoCl$	100	-	0
8	**1m**	O	S	0	$(Ph_3P)_2CoCl_2$	86	63:36	22
9	**1m**	O	S	0	$(SALEN)CoCl_2$	100	62:38	46
10	**1n**	O	S	1	$(Ph_3P)_3CoCl$	100	-	0
11	**1n**	O	S	1	$(Ph_3P)_2CoCl_2$	88	-	0
12	**1n**	O	S	1	$(SALEN)CoCl_2$	93	-	0

a) Established by ^1H NMR analysis. b) NMR yield using methyl 4-nitrobenzoate as internal reference.

Table 48. Thioimide assessment in cobalt catalysed aldol reaction.

5.1.4 Reaction conditions assessment

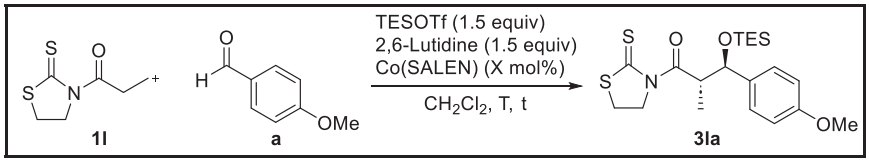

A solution of *N*-propanoyl-1,3-thiazinane-2-thione (35 mg, 0.2 mmol, 1.0 equiv), 4-methoxybenzaldehyde (27 µL, 0.22 mmol, 1.1 equiv) and Co(SALEN) (6.5mg, 20 µmol, 10 mol%) in CH_2Cl_2 was cooled at 0 °C or –20 °C under N_2. Then, neat TESOTf

(69 µL, 0.3 mmol, 1.5 equiv) was added followed by 2,6-lutidine (35 µL, 1.5 mmol, 1.5 equiv) and the resultant mixture was stirred at 0 °C.

The reaction mixture was quenched with sat. NH_4Cl (1 mL) and a known quantity of methyl 4-nitrobenzoate was added as internal standard (10–20 mg). The mixture was partitioned in CH_2Cl_2 (15 mL) and water (15 mL). The aqueous layer was extracted with CH_2Cl_2 (2 × 10 mL). The combined organic extracts were dried ($MgSO_4$) and concentrated under reduced pressure. The resultant residue was analysed by ^1H NMR. The results are summarised in Table 49.

Entry	Catalyst (mol%)	Conc (M)	t (h)	T (°C)	Conv. (%)	dr (Anti:Syn)	Yield (%)
1	10	0.25	16	0	72	70:30	32
2	10	0.5	16	0	83	75:25	46
3	10	1	16	0	>95	73:27	>95
4	10	5	2	0	>95	76:24	>95
5	10	5	16	–20	100	70:30	84
6	20	Solvent free	16	0	87	61:39	-

a) Established by ^1H NMR analysis. b) NMR yield using methyl 4-nitrobenzoate as internal reference.

Table 49. Reaction conditions assessment in cobalt catalysed aldol reaction.

5.2 Iron catalysed aldol reactions

5.2.1 Assessment of iron salts as catalysts

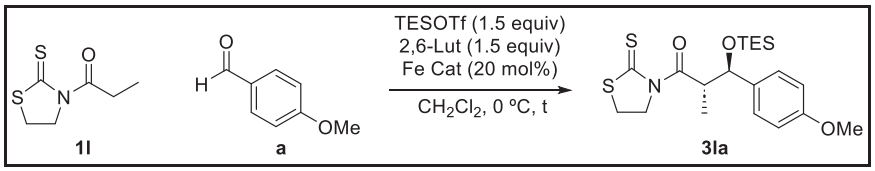

A solution of *N*-propanoyl-1,3-thiazinane-2-thione (35 mg, 0.2 mmol, 1.0 equiv), 4-methoxybenzaldehyde (27 µL, 0.22 mmol, 1.1 equiv) and iron salt (10 mol%) in CH_2Cl_2 (0.4 mL) was cooled at 0 °C under N_2. Then, neat TESOTf (69 µL, 0.3 mmol, 1.5 equiv) was added followed by 2,6-lutidine (35 µL, 1.5 mmol, 1.5 equiv) and the resultant mixture was stirred at 0 °C.

The reaction mixture was quenched with sat. NH_4Cl (1 mL) and a known quantity of methyl 4-nitrobenzoate was added as internal standard (10–20 mg). The mixture was partitioned in CH_2Cl_2 (15 mL) and water (15 mL). The aqueous layer was extracted with CH_2Cl_2 (2 × 10 mL). The combined organic extracts were dried ($MgSO_4$) and concentrated under reduced pressure. The resultant residue was analysed by ^1H NMR.

Entry	Catalyst	Additive	Conv (%)[a]	dr (*anti:syn*)[b]	Yield (%)[c]
1	$FeCl_3$	-	78	78:22	27
2	$Fe(OAc)_2$	-	49	78:22	14
3	$(Phen)FeCl_3$	-	61	-	0
4	$FeCl_3$	Phen	64	-	0
5	$FeCl_3$	2,2'-bipyridine	43	-	0
6	$FeCl_3$	2,2'-biquinoline	52	-	traces
7	$FeCl_3$	PPh_3	57	58:42	17
8	$Fe(OAc)_2$	PPh_3	67	55:45	40

a) Starting material recovered established by ^1H NMR analysis using methyl 4-nitrobenzoate as internal reference b) Established by ^1H NMR analysis c) NMR yield using methyl 4-nitrobenzoate as internal reference

Table 50. Iron salts as catalyst in aldol reaction.

5.3 Aldol reactions with α,β unsaturated aldehydes

5.3.1 Scaffold and Lewis acid assessment

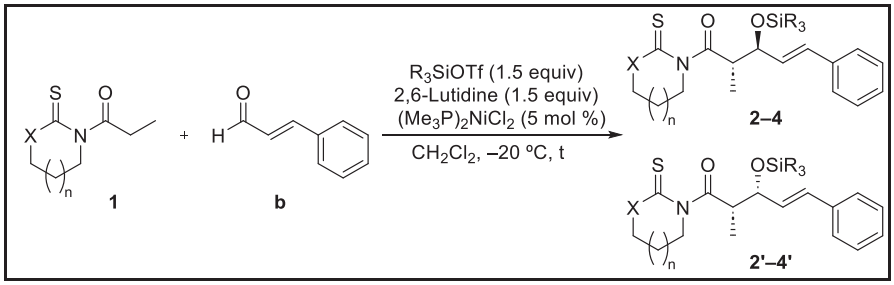

A solution of *N*-propanoyl thioimide **1** (1 mmol, 1.0 equiv), cinnamaldehyde **b** (138 µL, 1.1 mmol, 1.1 equiv), and $(Me_3P)_2NiCl_2$ (14.1 mg, 50 µmol, 5 mol%) in CH_2Cl_2 (0.4 mL) was cooled at –20 °C under N_2. Then, neat R_3SiOTf (1.5 mmol, 1.5 equiv) was added followed by 2,6-lutidine (174 µL, 1.5 mmol, 1.5 equiv) and the resultant mixture was stirred at –20 °C.

The reaction mixture was quenched with sat. NH_4Cl (1 mL) and partitioned in CH_2Cl_2 (10 mL) and water (25 mL). The aqueous layer was extracted with CH_2Cl_2 (2 × 10 mL). The combined organic extracts were dried ($MgSO_4$), and concentrated. The resultant residue was analysed by ^1H NMR (400 MHz). The results are summarized in Table 51.

Entry	1	X	n	R_3SiOTf	t (h)	Conv(%)[a]	rr [a,b]	dr (1,2)[a,c]	dr (1,4) [a]
1	**1a**	S	1	TIPSOTf	5	93	15:85	-	81:19
2	**1a**	S	1	TESOTf	5	88	44:56	84:16	78:22
3	**1a**	S	1	TBSOTf	2	>99	67:33	76:24	78:22
4	**1a**	S	1	TMSOTf	2	>95	74:26	80:20	80:20
5	**1n**	O	1	TIPSOTf	5	94	27:73	-	80:20
6	**1n**	O	1	TESOTf	5	94	62:38	95:5	65:35
7	**1n**	O	1	TBSOTf	16	76	75:25	94:6	52:48
8 [d]	**1n**	O	1	TMSOTf	16	90	82:18	92:8	55:45
9	**1l**	S	0	TIPSOTf	5	90	13:87	-	81:19
10	**1l**	S	0	TESOTf	5	80	48:52	89:11	77:23
11	**1l**	S	0	TMSOTf	2	>99	65:35	86:14	65:35
12	**1m**	O	0	TIPSOTf	5	97	28:72	-	70:30
13	**1m**	O	0	TESOTf	5	80	50:50	96:4	58:42
14	**1m**	O	0	TBSOTf	5	85	52:48	90:10	50:50
15	**1m**	O	0	TMSOTf	2	99	73:27	62:38	43:57

a) Established by ^{1}H NMR analysis. b) 1,2:1,4 ratio. c) Diastereomeric ratios from 1,2 adducts. d) 43% isolated yield of TMS unprotected *anti* aldol adduct.

Table 51. Thioimide and lewis acid assessment in the aldol reaction.

5.3.2 Catalyst and solvent screening

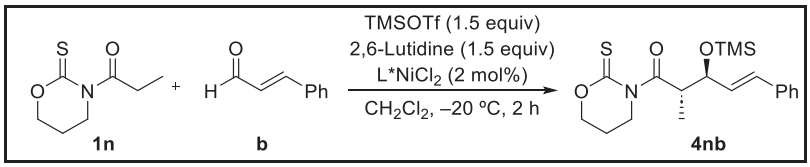

A solution of 1,3-thiazinane-2-thione **1n** (35 mg, 0.2 mmol, 1.0 equiv), cinnamaldehyde **b** (28 µL, 0.22 mmol, 1.1 equiv), and the catalyst (20 µmol, 2 mol%) in CH_2Cl_2 (0.4 mL) was cooled at –20 °C under N_2. Then, neat TMSOTf (54 µL, 0.3 mmol, 1.5 equiv) was added followed by 2,6-lutidine (35 µL, 1.5 mmol, 1.5 equiv) and the resultant mixture was stirred at –20 °C for 2 h.

The reaction mixture was quenched with sat. NH_4Cl (1 mL) and partitioned in CH_2Cl_2 (10 mL) and water (25 mL). The aqueous layer was extracted with CH_2Cl_2 (2 × 10 mL). The combined organic extracts were dried ($MgSO_4$), and concentrated. The resultant residue was analysed by ^{1}H NMR (400 MHz). The results are summarized in Table 52.

Entry	L*	Conv (%)[a]	rr (1,2:1,4)[a]	dr (*syn/anti*)[a,b]
1	(*S*)-BINAP	85	49:51	30:70
2	(*S*)-Tol-BINAP	40	50:50	28:72
3	(*R*)-BIPHEP	0	-	-
4	(*R*)-TM-BIPHEP	<5	-	-
5	(*R*)-SEGPHOS	67	43:57	33:67
6	(*R*)-DM-SEGPHOS	0	-	-
7	(*R*)-DTBM-SEGPHOS	<5	-	-
8	(*R*)-GARPHOS	64	46:54	31:69
9	(*R*)-DMM-GARPHOS	52	58:42	22:78
10	(*R*)-DTBM-GARPHOS	34	51:49	11:89

a) Established by ^{1}H NMR analysis. b) Diastereomeric ratio of aldol adduct

Table 52. Catalyst assessment in the aldol reaction with α,β-unsaturated aldehydes.

5.3.3 Aldol reaction with α-methyl-cinnamaldehyde

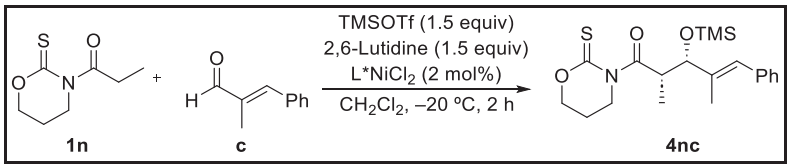

A solution of 1,3-oxazinane-2-thione **1n** (35 mg, 0.2 mmol, 1.0 equiv), α-methyl-cinnamaldehyde **c** (31 µL, 0.22 mmol, 1.1 equiv), and the catalyst (20 µmol, 2 mol%) in CH_2Cl_2 (0.4 mL) was cooled at –20 °C under N_2. Then, neat TMSOTf (54 µL, 0.3 mmol, 1.5 equiv) was added followed by 2,6-lutidine (35 µL, 0.3 mmol, 1.5 equiv) and the resultant mixture was stirred at –20 °C for 2 h.

The reaction mixture was quenched with sat. NH_4Cl (1 mL) and partitioned in CH_2Cl_2 (10 mL) and water (25 mL). The aqueous layer was extracted with CH_2Cl_2 (2 × 10 mL). The combined organic extracts were dried ($MgSO_4$), and concentrated. The resultant residue was analysed by ^{1}H NMR (400 MHz). The results are summarised in Table 53.

Entry	L*	Conv (%)[a]	rr (1,2:1,4)[a]	dr[a,b]
1	(*R*)-BINAP	0	-	-
2	(*R*)-DTBM-SEGPHOS	>95	65:35	>95

a) Established by ^{1}H NMR analysis. b) Diastereomeric ratio of aldol adduct.

Table 53. Aldol reactions with α-methyl-cinnamaldehyde.

N-[2,4-Dimethyl-5-phenyl-3-trimethylsilyloxy-4-pentenoyl]-1,3-oxazinane-2-thione

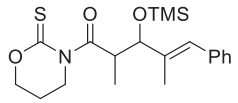

A solution of 1,3-oxazinane-2-thione **1n** (35 mg, 0.2 mmol, 1.0 equiv), **c** (31 μL, 0.22 mmol, 1.1 equiv), and [(*R*)-DTBM-SEGPHOS]$NiCl_2$ (5.2 mg, 20 μmol, 2 mol%) in CH_2Cl_2 (0.4 mL) was cooled at –20 °C under N_2. Then, neat TMSOTf (54 μL, 0.3 mmol, 1.5 equiv) was added followed by 2,6-lutidine (35 μL, 0.3 mmol, 1.5 equiv) and the resultant mixture was stirred at –20 °C for 2 h.

The reaction mixture was quenched with sat. NH_4Cl (1 mL) and partitioned in CH_2Cl_2 (10 mL) and water (25 mL). The aqueous layer was extracted with CH_2Cl_2 (2 × 10 mL). The combined organic extracts were dried ($MgSO_4$), and concentrated. The resultant residue purified by flash chromatography (from 95:5 to 80:20 Hexanes/EtOAc) to give 39 mg (0.1 mmol, 50% yield) of aldol adduct **4nc** with impurities of Michael adduct **5nc**.

Yellow oil.
R_f 0.5 (80:20 Hexanes/EtOAc).
^{1}H NMR (400 MHz, $CDCl_3$) δ 7.38–7.32 (m, 2H, ArH), 7.30–7.23 (m, 3H, ArH), 6.47 (s, 1H, PhCH), 4.50–4.44 (m, 1H, OCH_xH_y), 4.26 (d, *J* = 9.6 Hz, 1H, CHOTMS), 4.21 (td, *J* = 10.4, 3.9 Hz, 1H, OCH_xH_y), 4.01 (dq, *J* = 9.6, 6.7 Hz, 1H, $CHCH_3$), 3.91–3.82 (m, 1H, NCH_xH_y), 3.58 (ddd, *J* = 12.6, 9.8, 8.1 Hz, 1H, NCH_xH_y), 2.27–2.12 (m, 2H, NCH_2CH_2), 1.79 (d, *J* = 1.4 Hz, 3H, CCH_3), 1.21 (d, *J* = 6.7 Hz, 3H, $CHCH_3$), 0.06 (s, 9H, OTMS).

5.4 Aldol reactions with propargyl aldehydes

5.4.1 Initial trials

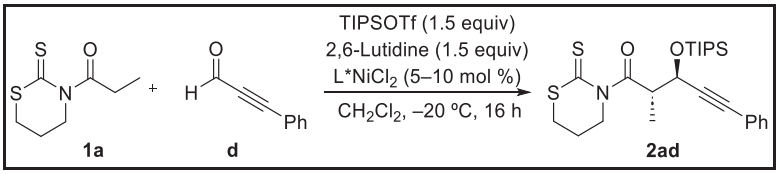

A solution of *N*-propanoyl 1,3-thazinane-2-thione **1a** (0.2 mmol, 1.0 equiv), phenylpropargyl aldehyde **d** (29 µL, 0.24 mmol, 1.2 equiv), and a nickel catalyst (5–10 mol%) in CH_2Cl_2 (0.5 M) was cooled at –20 °C under N_2. Then, neat TIPSOTf (81 µL, 0.3 mmol, 1.5 equiv) was added followed by 2,6-lutidine (30 µL, 0.3 mmol, 1.5 equiv) and the resultant mixture was stirred at –20 °C for 16 h and followed by TLC.

After apparent completion, the reaction mixture was quenched with sat. NH_4Cl (1 mL) and partitioned in CH_2Cl_2 (10 mL) and water (25 mL). The aqueous layer was extracted with CH_2Cl_2 (2 × 10 mL). The combined organic extracts were dried ($MgSO_4$), and concentrated. The resultant residue was analysed by ^1H NMR. The results are summarised in Table 54.

Entry	L*	mol %	Conv(%)	S-alkylation (%)
1	$(Me_3P)_2$	10	45	9
2	(*S*)-BINAP	5	82	26
3	(*R*)-DTBM-SEGPHOS	5	55	10

a) Established by ^1H NMR analysis.

Table 54. Initial trials with phenylpropargyl aldehyde.

S-(3-Oxo-1-phenylpropenyl)-1,3-thiazinane-2-thione (8)

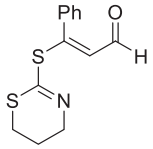

A solution of **1a** (38 mg, 0.2 mmol, 1 equiv), [*(S)*-BINAP]$NiCl_2$ (7.5 mg, 10 µmol, 5 mol%) and **d** (29 mg, 0.24 mmol, 1.2 equiv) in CH_2Cl_2 (0.4 mL) was cooled at –20 °C under N_2. Then, neat TIPSOTf (81 µL, 0.3 mmol, 1.5 equiv) was added followed by 2,6-lutidine (30 µL, 0.3 mmol, 1.5 equiv) and the resulting mixture was stirred at –20 °C for 16 h.

The reaction mixture was quenched with sat. NH_4Cl (1 mL) and partitioned in CH_2Cl_2 (10 mL) and water (25 mL). The aqueous layer was extracted with CH_2Cl_2 (2 × 10 mL). The combined organic extracts were dried ($MgSO_4$), and concentrated. The residue was purified by column chromatography (from 70:30 to 30:70 Hexanes/EtOAc) to give 10 mg of **8** (0.03 mmol, 18% yield).

Colorless oil.
R_f 0.2 (50:50 Hexanes/EtOAc).
^{1}H NMR (400 MHz, $CDCl_3$) δ 9.34 (d, *J* = 7.9 Hz, 1H, C<u>H</u>O), 7.53–7.39 (m, 5H, Ar<u>H</u>) 6.58 (d, *J* = 7.9 Hz, 1H, C<u>H</u>CHO), 3.81–3.75 (m, 2H, NC<u>H</u>$_2$), 3.07–3.00 (m, 2H, SC<u>H</u>$_2$), 1.86–1.75 (m, 2H, NCH$_2$C<u>H</u>$_2$).

5.5 Cobalt-protected propargyl aldehydes

5.5.1 Initial trials in the aldol reaction with Co-protected propargyl aldehydes

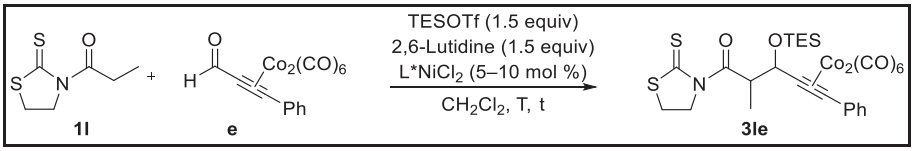

A solution of **1l** (35 mg, 0.2 mmol, 1.0 equiv), **e** (92 mg, 0.22 mmol, 1.1 equiv), and catalyst (0–10 mol%) in CH_2Cl_2 (0.5 M) was cooled at the desired temperature under N_2. Then, neat TESOTf (69 µL, 0.3 mmol, 1.5 equiv) was added followed by 2,6-lutidine (35 µL, 0.3 mmol, 1.5 equiv) and the resultant mixture was stirred and followed by TLC.

Upon apparent completion, the reaction mixture was quenched with sat. NH_4Cl (1 mL) and a known amount of methyl 4-nitrobenzoate (15–40 mg) was added. Then, the mixture was partitioned in CH_2Cl_2 (10 mL) and water (25 mL). The aqueous layer was extracted with CH_2Cl_2 (2 × 10 mL). The combined organic extracts were dried ($MgSO_4$), and concentrated. The resultant residue was analysed by ^{1}H NMR. The results are summarised in Table 55.

Entry	L* (%)	Cat (mol%)	e	t (h)	T (°C)	Conv. (%)[a]	dr[b]	Yield (%)[c]	*ee* (%)
1	(*R*)-DTBM-SEGPHOS	5	Batch 1	16	0	66	85:15	(48)	0
2	(*R*)-DTBM-SEGPHOS	5	Batch 1	16	0	60	83:17	-	-
3	(*R*)-DTBM-SEGPHOS	10	Batch 1	16	0	100	86:14	(38)	-
4	(*R*)-DTBM-SEGPHOS	10	Batch 1	16	0	100	87:13	(35) 34	-
5	$(Me_3P)_2$	10	Batch 1	16	0	65	87:13	-	0
6	(*S*)-BINAP	10	Batch 1	16	0	100	78:22	Comp mix	-
7	(*R*)-DTBM-SEGPHOS	10	Batch 2	5	0	100	>97:3	(54)	-
8[e]	-	-	Batch 2	5	0	100	>97:3	-	-
9	(*R*)-DTBM-SEGPHOS	7.5	Batch 2	5	0	100	>97:3	(60) 44	0
10	(*R*)-DTBM-SEGPHOS	10	Batch 3	16	0	100	>97:3	32	-
11	(*R*)-DTBM-SEGPHOS	10	Batch 3	16	–20	3	>97:3	-	-
12[e]	-	-	Batch 2	5	0	>90	>97:3	-	0
13	(*R*)-DTBM-SEGPHOS	7.5	Batch 3	5	0	100	>97:3	(60)	0
14[e]	-	-	Batch 4[d]	3	0	42	>97:3	-	-
15	(*R*)-DTBM-SEGPHOS	10	Batch 4[d]	5	0	50	>97:3	-	7
16[e]	-	-	Batch 2[d]	16	0	46	>97:3	-	0
17	(*R*)-DTBM-SEGPHOS	10	Batch 2[d]	72	–20	23	>97:3	-	-
18	(*R*)-DTBM-SEGPHOS	10	Batch 2[d]	5	0	0	-	-	-

a) Based on the recovery of **1l** established by ^{1}H NMR analysis using methyl 4-nitrobenzoate as internal reference. b) Established by ^{1}H NMR analysis. c) Isolated yield, (NMR yield established by ^{1}H NMR analysis using methyl 4-nitrobenzoate as internal reference) d) Further purified by column chromatography. e) Reactions carried out without any catalyst.

Table 55. Initial trials in the aldol reaction with protected phenylpropargyl aldehyde.

5.5.2 Scaffold assessment

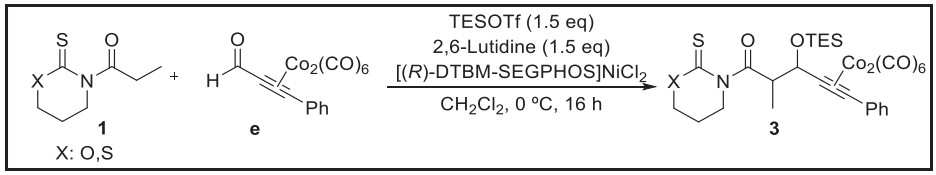

A solution of thioimide **1** (0.2 mmol, 1.0 equiv), **e** (92 mg, 0.22 mmol, 1.1 equiv), and [(*R*)-DTBM-SEGPHOS]$NiCl_2$ (0–10 mol%) in CH_2Cl_2 (0.5 M) was cooled at 0 °C under N_2. Then, neat TESOTf (69 µL, 0.3 mmol, 1.5 equiv) was added followed by 2,6-lutidine (35 µL, 0.3 mmol, 1.5 equiv) and the resultant mixture was stirred at 0 °C for 16 h.

The reaction mixture was quenched with sat. NH_4Cl (1 mL) and a known amount of methyl 4-nitrobenzoate (15–40 mg) was added. Then, the mixture was partitioned in CH_2Cl_2 (10 mL) and water (25 mL). The aqueous layer was extracted with CH_2Cl_2 (2 × 10 mL). The combined organic extracts were dried ($MgSO_4$), and concentrated. The resultant residue was analysed by ^1H NMR. In any case, the mixture turned out to be a complex mixture without the presence of the formation of the desired product.

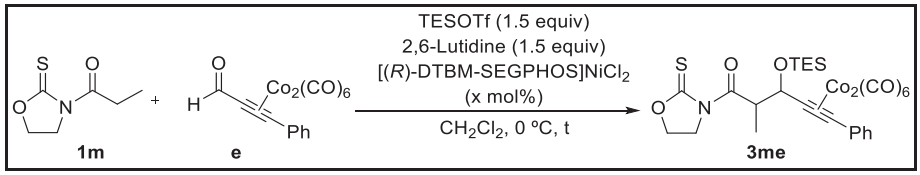

A solution of **1m** (32 mg, 0.2 mmol, 1.0 equiv), **e** (92 mg, 0.22 mmol, 1.1 equiv), and [(*R*)-DTBM-SEGPHOS]$NiCl_2$ (0–10 mol%) in CH_2Cl_2 (0.5 M) was cooled at 0 °C under N_2. Then, neat TESOTf (69 µL, 0.3 mmol, 1.5 equiv) was added followed by 2,6-lutidine (35 µL, 0.3 mmol, 1.5 equiv) and the resultant mixture was stirred at 0 °C for 5–16 h.

The reaction mixture was quenched with sat. NH_4Cl (1 mL) and a known amount of methyl 4-nitrobenzoate (15–40 mg) was added. Then, the mixture was partitioned in CH_2Cl_2 (10 mL) and water (25 mL). The aqueous layer was extracted with CH_2Cl_2 (2 × 10 mL). The combined organic extracts were dried ($MgSO_4$), and concentrated. The resultant residue was analysed by ^1H NMR. The results are summarised in Table 56.

Entry	Cat (mol%)	e	t (h)	Conv. (%)[a]	dr[b]	Yield (%)[c]	*ee* (%)
1	10	Batch 1	16	100	66:33	(53)	-
2	10	Batch 2	5	100	74:26	(84) 68	-
3	10	Batch 2[d]	5	100	80:20	(70)	3
4	0	Batch 2[d]	5	83	77:23	(34)	-
5	10	Batch 5	5	100	87:13	(70)	-

a) Based on the recovery of **1m** established by ^{1}H NMR analysis using methyl 4-nitrobenzoate as internal reference. b) Established by ^{1}H NMR analysis. c) Isolated yield, (NMR yield established by ^{1}H NMR analysis using methyl 4-nitrobenzoate as internal reference) d) further purified by column chromatography.

Table 56. Aldol reaction of thioimide **1m** with different **e** batches.

5.5.3 Lewis acid assessment

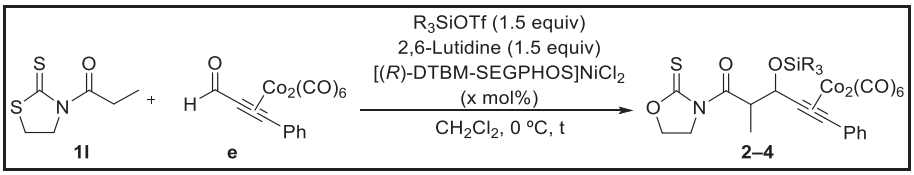

A solution of **1l** (35 mg, 0.2 mmol, 1.0 equiv), **e** (92 mg, 0.22 mmol, 1.1 equiv), and [(*R*)-DTBM-SEGPHOS]$NiCl_2$ (0–10 mol%) in CH_2Cl_2 (0.5 M) was cooled at the desired temperature under N_2. Then, neat TESOTf (69 µL, 0.3 mmol, 1.5 equiv) was added followed by 2,6-lutidine (35 µL, 0.3 mmol, 1.5 equiv) and the resultant mixture was stirred and followed by TLC.

Upon apparent completion, the reaction mixture was quenched with sat. NH_4Cl (1 mL) and a known amount of methyl 4-nitrobenzoate (15–40 mg) was added. Then, the mixture was partitioned in CH_2Cl_2 (10 mL) and water (25 mL). The aqueous layer was extracted with CH_2Cl_2 (2 × 10 mL). The combined organic extracts were dried ($MgSO_4$), and concentrated. The resultant residue was analysed by ^{1}H NMR.

Entry	L* (%)	Lewis acid	e	T (°C)	T (h)	Conv. (%)[a]	dr[b]	Yield (%)[c]	*ee* (%)
1	10	TIPSOTf	Batch 2*	0	5	100	-	<5%	-
2	-	TIPSOTf	Batch 2*	0	5	100	-	<5%	-
3	10	TBSOTf	Batch 2*	0	5	90%	80:20	41	60
4	-	TBSOTf	Batch 2*	0	5	8%	-	-	-
5	10	TBSOTf	Batch 5	0	16	<5%		-	-
6	10	TMSOTf	Batch 2*	0	5	100	88:12	(58)45	77
7	-	TMSOTf	Batch 2*	0	5	80%	90:10	(46)38	-
8	10	TMSOTf	Batch 5	0	5	80%	86:14	-	47
9[d]	10	TMSOTf	Batch 5	–20	16	60%	87:13	-	50

a) Based on the recovery of **1l** established by ^{1}H NMR analysis using methyl 4-nitrobenzoate as internal reference. b) Established by ^{1}H NMR analysis. c) Isolated yield, (NMR yield established by ^{1}H NMR analysis using methyl 4-nitrobenzoate as internal reference) d) Temperature –20 °C.

Table 57. Assessment of different lewis acids.

General Procedure 6

A solution of thioimide **1** (1.0 equiv), **e** (1.1 equiv), and [(*R*)-DTBM-SEGPHOS]$NiCl_2$ (5–10 mol%) in CH_2Cl_2 (0.5 M) was cooled at 0 °C under N_2. Then, neat R_3SiOTf (1.5 equiv) was added followed by 2,6-lutidine (1.5 equiv) and the resultant mixture was stirred at 0 °C and followed by TLC.

After apparent completion, the reaction mixture was quenched with sat. NH_4Cl (1 mL) and partitioned in CH_2Cl_2 (10 mL) and water (25 mL). The aqueous layer was extracted with CH_2Cl_2 (2 × 10 mL). The combined organic extracts were dried ($MgSO_4$), and concentrated. The resultant residue was analysed by ^{1}H NMR.

***N*-[Hexacarbonyl{μ-[η⁴(3-triethylsililoxy-2-methyl-5-phenyl-4-pentynoyl)]dicobalt (Co-Co)}-1,3-thiazolidine-2-thione (3le)**

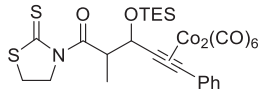

The General Procedure 6 was followed with **1l** (35 mg, 0.2 mmol, 1.0 equiv), [*(R)*-DTBM-SEGPHOS]$NiCl_2$ (19.8 mg, 15 μmol, 10 mol%), **e** (94 mg, 0.55 mmol, 1.2 equiv), TESOTf (162 μL, 0.75 mmol, 1.5 equiv), and 2,6-lutidine (87 μL, 0.75 mmol, 1.5 equiv) at 0 °C for 16 h.

The residue (dr >95:5) was purified by column chromatography (from 95:5 to 80:20 Hexanes/EtOAc) to give 62 mg (0.09 mmol, 44% yield) of **3le**.

Dark brown oil.
R_f 0.25 (90:10 Hexanes/EtOAc).
^{1}H NMR (400 MHz, $CDCl_3$) δ 7.43–7.38 (m, 2H, ArH), 7.36–7.27 (m, 3H, ArH), 5.69 (d, *J* = 6.1 Hz, 1H, CHOTES), 4.63 (dq, *J* = 7.4, 6.1 Hz, 1H, $CHCH_3$), 4.33 (dt, *J* = 12.3, 7.8 Hz, 1H, NCH_xH_y), 4.18 (ddd, *J* = 12.3, 7.8, 6.6 Hz, 1H, NCH_xH_y), 3.12 (ddd, *J* = 11.1, 7.8, 6.6 Hz, 1H, SCH_xH_y), 3.03 (dt, *J* = 11.1, 7.8 Hz, 1H, SCH_xH_y), 1.36 (d, *J* = 7.0 Hz, 3H, $CHCH_3$), 0.96 (t, *J* = 7.4 Hz, 9H, $OSiCH_2CH_3$), 0.66 (q, *J* = 7.7 Hz, 6H, $OSiCH_2CH_3$).
Chiral HPLC (Phenomenex Lux® Cellulose-1 column, 1% *i*-PrOH in Hexanes, flow rate 1 mL/min): R_t 10.2 min, R_t 11.0 min, 0% *ee*.

***N*-[Hexacarbonyl{μ-[η⁴(3-triethylsililoxy-2-methyl-5-phenyl-4-pentynoyl)]dicobalt (Co-Co)}-1,3-oxazolidine-2-thione (3me)**

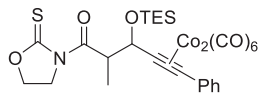

The General Procedure was followed with **1m** (80 mg, 0.5 mmol, 1.0 equiv), **e** (230 mg, 0.55 mmol, 1.2 equiv), [*(R)*-DTBM-SEGPHOS]$NiCl_2$ (65.5 mg, 50 μmol, 10 mol%), TESOTf (162 μL, 0.75 mmol, 1.5 equiv), and 2,6-lutidine (87 μL, 0.75 mmol, 1.5 equiv) at 0 °C for 16 h.

The residue (dr 26:74) was purified by column chromatography (from 95:5 to 70:30 Hexanes/EtOAc) to give 183 mg (0.27 mmol, 53% yield) of **3me** and 51 mg (0.07 mmol, 15% yield) of **3'me**.

Dark brown oil.

R_f 0.5 (70:30 Hexanes/EtOAc).

^{1}H NMR (400 MHz, $CDCl_3$) δ 7.41–7.27 (m, 5H, ArH), 5.68 (d, *J* = 7.1 Hz, 1H, CHOTES), 4.73 (p, *J* = 7.1 Hz, 1H, CHCH$_3$), 4.43–4.35 (m, 1H, OCH$_x$H$_y$), 4.29–4.17 (m, 1H, OCH$_x$H$_y$), 3.97 (ddd, *J* = 11.3, 9.6, 8.1 Hz, 1H, NCH$_x$H$_y$), 3.70 (ddd, *J* = 11.3, 9.6, 6.9 Hz, 1H, NCH$_x$H$_y$), 1.38 (d, *J* = 7.1 Hz, 3H, CHCH$_3$), 0.96 (t, *J* = 7.9 Hz, 9H, OSiCH$_2$CH$_3$), 0.71–0.60 (m, 6H, OSiCH$_2$CH$_3$).

N-[hexacarbonyl{μ-[η^4(3-triethylsililoxy-2-methyl-5-phenyl-4-pentynoyl)]dicobalt (Co-Co)}-1,3-oxazolidine-2-thione (4le)

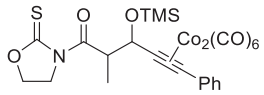

The General Procedure 6 was followed with **1l** (32 mg, 0.2 mmol, 1.0 equiv), [*(R)*-DTBM-SEGPHOS]NiCl$_2$ (26.5 mg, 20 μmol, 10 mol%), **e** (88 mg, 0.22 mmol, 1.2 equiv), TMSOTf (162 μL, 0.75 mmol, 1.5 equiv), and 2,6-lutidine (87 μL, 0.75 mmol, 1.5 equiv) at 0 °C for 16 h.

The residue (dr 95:5) was purified by column chromatography (from 95:5 to 70:30 Hexanes/EtOAc) to give 183 mg (0.27 mmol, 53% yield) of **4le** and 51 mg (0.07 mmol, 15% yield) of **4'le**.

Dark brown oil.

R_f 0.5 (70:30 Hexanes/EtOAc).

^{1}H NMR (400 MHz, $CDCl_3$) δ 7.45–7.38 (m, 2H, ArH), 7.37–7.27 (m, 3H, ArH), 5.62 (d, *J* = 6.9 Hz, 1H, CHOTMS), 4.61 (p, *J* = 6.9 Hz, 1H, CHCH$_3$), 4.29 (dt, *J* = 12.1, 8.0 Hz, 1H, NCH$_x$H$_y$), 4.09 (ddd, *J* = 12.1, 7.8, 6.2 Hz, 1H, NCH$_x$H$_y$), 3.08 (ddd, *J* = 11.1, 7.8, 6.2 Hz, 1H, SCH$_x$H$_y$), 2.98 (dt, *J* = 11.1, 8.0 Hz, 1H, SCH$_x$H$_y$), 1.35 (d, *J* = 6.9 Hz, 3H, CHCH$_3$), 0.15 (s, 9H, OTMS).

Chiral HPLC (Phenomenex Lux® Cellulose-1 column, 1% *i*-PrOH in Hexanes, flow rate 1 mL/min): R_t 6.8 min (minor isomer) R_t 7.4 min (major isomer), 77% *ee*.

5.5.4 Analysis of the enantioselectivity of the reaction

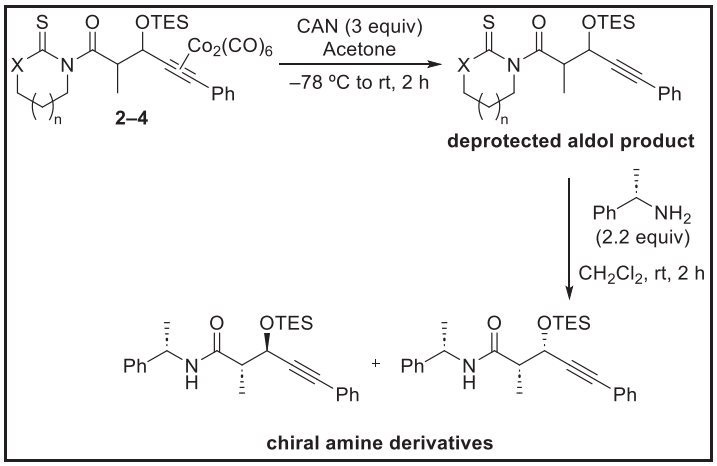

Enantioselectivity was determined either by chiral HPLC of the deprotected alkyne derived from **2–4** or ^{1}H NMR of the derivative chiral amine derivative.

A solution of the corresponding adduct **2–4** in acetone (0.04 M) was added dropwise to a solution of CAN (3 equiv) in acetone (0.4 M) at –78 °C. Then, the mixture is warmed up to rt and controlled by TLC. The resulting purple solution is diluted with water (20 mL) and extracted with CH_2Cl_2 (3 × 10 mL). The combined organic extracts were dried ($MgSO_4$) and concentrated under reduced pressure to give the corresponding deprotected aldol product.

(*S*)-1-Phenylethylamine (2.2 equiv) was added dropwise to a solution of the deprotected aldol adduct (1 equiv) in CH_2Cl_2 (0.3 M) at rt. The mixture was stirred and the reaction was controlled by TLC until apparent completion. Afterwards, the mixture was diluted in water (15 mL) and extracted with CH_2Cl_2 (3 × 10 mL). The combined organic extracts were dried ($MgSO_4$) and concentrated under reduced pressure. The resultant residue was analysed by ^{1}H NMR to determine the dr, which corresponds to the initial *ee*.

CHAPTER II

The Michael reaction

6 Starting materials

6.1 Synthesis of α,β-unsaturated aldehydes

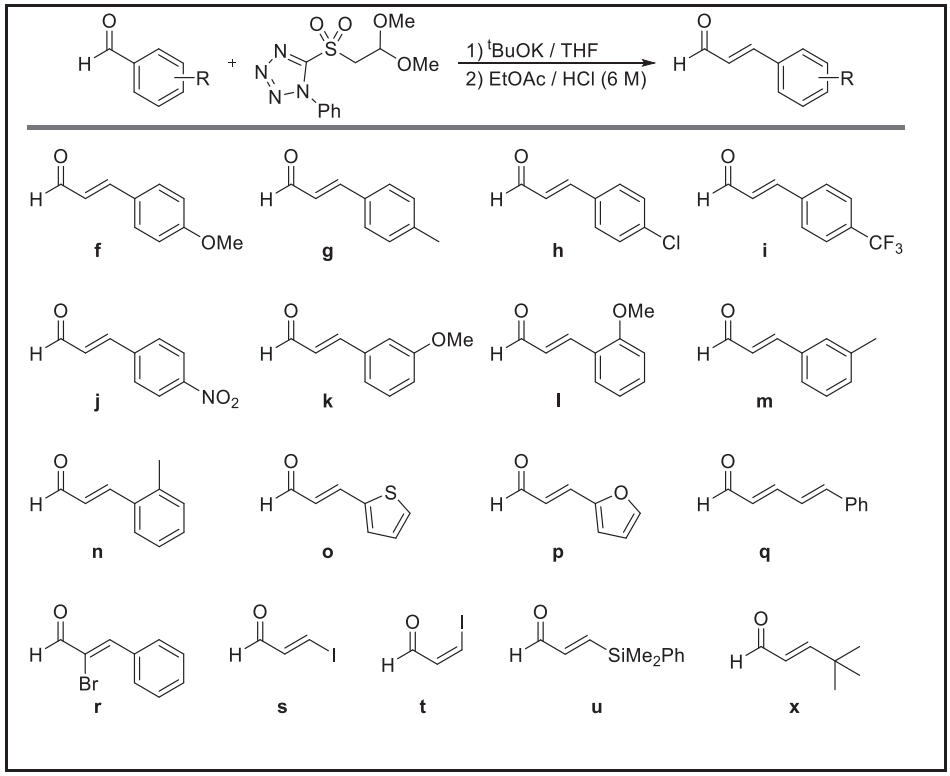

GENERAL PROCEDURE 7

A mixture of *t*-BuOK (3 equiv) in THF (2.25 M) was slowly added to a solution of 2,2-dimethoxyethyl-1-phenyl-1*H*-tetrazol-5-yl sulfone (2 equiv) and the aldehyde (1 equiv) in THF (0.4 M) at 0 °C, and the final mixture was stirred at rt for 1 h.

Next, EtOAc was added to obtain a 1:1 THF/EtOAc mixture, which was cooled to 0 °C. Then, 5 M HCl (30 mL) was added dropwise, and the resultant mixture was stirred for 40 min at rt.

The layers were separated. The aqueous layer was extracted with EtOAc (3 × 40 mL). The combined extracts were washed with 2 M NaOH (40 mL), sat. NH_4Cl (20 mL), and brine (40 mL), dried ($MgSO_4$) and concentrated under reduced pressure. The crude mixture was purified by column chromatography (Hexanes/EtOAc) to give the desired α,β-unsaturated aldehyde.

6.1.1 Synthesis of PT sulphone

5-(2,2-Dimethoxyethylthio)-1-phenyl-1*H*-tetrazole

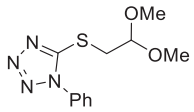

Following a literature procedure,[4] 2-bromoacetaldehyde dimethyl acetal (6.2 mL, 52.5 mmol) was added dropwise to a solution of 2-phenyl-2*H*-tetrazole-5-thiol (8.9 g, 50 mmol) and ^{t}BuOK (6.17g, 55 mmol) in DMF (50 mL) at rt.

Then, the mixture was stirred at 80 °C for 6 h. Afterwards, the mixture was rinsed with water (60 mL) and extracted with EtOAc (2 × 50 mL). The combined organic extracts were washed with water (5 × 50 mL) and brine (50 mL), dried ($MgSO_4$) and concentrated under reduced pressure to give 12.97 g (49 mmol, 97% yield), which needed no further purification.

White solid.
^{1}H NMR (400 MHz, $CDCl_3$) δ 7.62–7.51 (m, 5H, Ar<u>H</u>), 4.72 (t, *J* = 5.3 Hz, 1H, C<u>H</u>OMe), 3.60 (d, *J* = 5.3 Hz, 2H, SC<u>H</u>$_2$), 3.43 (s, 6H, O<u>Me</u>).

5-(2,2-Dimethoxyethyl 1-phenyl-1*H*-tetrazolyl) Sulfone (PT sulphone)

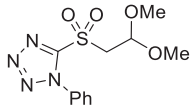

Following a literature procedure,[4] 30% H_2O_2 (47 mL, 460 mmol) was added dropwise to a solution of 5-(2,2-dimethoxyethylthio)-1-phenyl-1*H*-tetrazole (12.97 g, 49 mmol) and $(NH_4)_6Mo_7O_{24}{\cdot}4H_2O$ (6.49 g, 5.25 mmol, 10 mol%) in EtOH (20 mL) at 0 °C and the resulting mixture was stirred at rt for 3 h.

The solution was cooled to 0 °C and sat. Na_2SO_3 was added slowly to quench the reaction until pH ≈ 4. Then, it was neutralized with $NaHCO_3$ (60 mL) and extracted with EtOAc (2 × 60 mL). The combined organic extracts were washed with brine (60 mL), dried ($MgSO_4$) and concentrated under reduced pressure to give 13.6 g (46 mmol, 94% yield) of PT sulphone.

White to pale orange solid.
^{1}H NMR (400 MHz, $CDCl_3$) δ 7.68–7.57 (m, 5H, ArH), 4.93 (t, *J* = 5.5 Hz, 1H, CHOMe), 3.82 (d, *J* = 5.5 Hz, 2H, SCH_2), 3.29 (s, 6H, OMe).

6.1.2 α,β-Unsaturated aldehydes

(*E*)-3-(4-Methoxyphenyl)propenal (f)

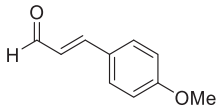

Following the General Procedure 7, 4-methoxybenzaldehyde (1.8 mL, 15 mmol) was used. The crude mixture was purified by flash chromatography (from 90:10 to 85:15 Hexanes/EtOAc) to give 1.90 g (11.9 mmol, 79% yield) of pure **f**.

White solid.
R_f 0.6 (80:20 Hexanes/EtOAc).
^{1}H NMR (400 MHz, $CDCl_3$): δ 9.67 (d, *J* = 7.7 Hz, 1H, CHO), 7.57–7.51 (m, 2H, ArH), 7.45 (d, *J* = 15.6 Hz, 1H, CHCHCHO), 6.97-6.91 (m, 2H, ArH), 6.62 (dd, *J* = 15.6 Hz, 7.7 Hz, 1H, CHCHO), 3.86 (s, 3H, OMe).

(*E*)-3-(4-Methylphenyl)propenal (g)

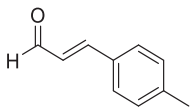

Following the General Procedure 7, 4-methylbenzaldehyde (0.6 mL, 5 mmol) was used. The crude mixture was purified by flash chromatography (from 95:5 to 85:15 Hexanes/EtOAc) to give 619 mg (4.2 mmol, 85% yield) of pure **g**.

Pale yellow solid.
Mp 42–43 °C.
R_f 0.5 (80:20 Hexanes/EtOAc).
IR (ATR) ν 2918, 2821, 2742, 1678, 1625, 1601, 1122, 1108, 979, 804 cm^{-1}.
^{1}H NMR (400 MHz, $CDCl_3$) δ 9.68 (d, *J* = 7.7 Hz, 1H, CHO), 7.49–7.41 (m, 3H, CHCHCHO, ArH), 7.27–7.21 (m, 2H, ArH), 6.68 (dd, *J* = 15.9, 7.7 Hz, 1H, CHCHO), 2.40 (s, 3H, ArMe).
^{13}C NMR (101 MHz, $CDCl_3$) δ 193.8 (CH), 152.9 (CH), 141.9 (C), 131.3 (C), 129.8 (CH), 128.5 (CH), 127.7 (CH), 21.5 (CH_3).
HRMS (ESI+) *m/z* calcd for $[M+H]^+$ $C_{10}H_{11}O$: 147.0804, found: 147.0808.

(*E*)-3-(4-Chlorophenyl)propenal (h)

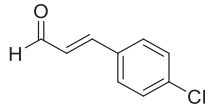

Following the General Procedure 7, 4-chlorobenzaldehyde (2.11 g, 15 mmol) was used. The crude mixture was purified by flash chromatography (from 95:5 to 85:15 Hexanes/EtOAc) to give 2.0 g (12.0 mmol, 80% yield) of pure **h**.

White solid.
Mp 61–62 °C.
R_f 0.3 (90:10 Hexanes/EtOAc).
IR (ATR) *v* 3056, 2994, 2851, 2761, 1694, 1626, 1588, 1489, 1123, 1086, 806 cm^{-1}.
^{1}H NMR (400 MHz, $CDCl_3$) δ 9.71 (d, *J* = 7.6 Hz, 1H, C<u>H</u>O), 7.54–7.48 (m, 2H, Ar<u>H</u>), 7.43–7.39 (m, 3H, C<u>H</u>CHCHO, Ar<u>H</u>), 6.69 (dd, *J* = 16.0, 7.6 Hz, 1H, C<u>H</u>CHO).
^{13}C NMR (101 MHz, $CDCl_3$) δ 193.3 (CH), 151.0 (CH), 137.2 (C), 132.5 (C), 129.6 (CH), 129.4 (CH), 128.9 (CH).
HRMS (ESI+) *m/z* calcd for $[M+H]^+$ $C_9H_8{}^{35}ClO$: 167.0258, found: 167.0261; *m/z* calcd for $[M+H]^+$ $C_9H_8{}^{37}ClO$: 169.0236, found: 169.0235.

(*E*)-3-(4-Trifluoromethylphenyl)propenal (i)

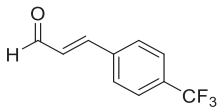

Following the General Procedure 7, 4-(trifluoromethyl)benzaldehyde (2.1 mL, 15 mmol) was used. The crude mixture was purified by flash chromatography (from 95:5 to 85:15 Hexanes/EtOAc) to give 2.34 g (11.7 mmol, 78% yield) of pure **i**.

White solid.
Mp 60–62 °C.
R_f 0.6 (80:20 Hexanes/EtOAc).
IR (ATR) *v* 2821, 2740, 1678, 1317, 1119, 1107, 1063, 981, 819 cm^{-1}.
^{1}H NMR (400 MHz, $CDCl_3$) δ 9.76 (d, *J* = 7.5 Hz, 1H, C<u>H</u>O), 7.73–7.65 (m, 4H, Ar<u>H</u>), 7.51 (d, *J* = 16.0 Hz, 1H, C<u>H</u>CHCHO), 6.78 (dd, *J* = 16.0, 7.5 Hz, 1H, C<u>H</u>CHO).
^{13}C NMR (101 MHz, $CDCl_3$) δ 193.1 (CH), 150.2 (CH), 137.3 (C), 132.6 (q, $^1J_{C-F}$ = 32.8 Hz, CF_3), 130.5 (C), 128.6 (CH), 126.1 (CH), 126.0 (CH).
HRMS (ESI+) *m/z* calcd for $[M+H]^+$ $C_{10}H_8F_3O$: 201.0522, found: 201.0526.

(*E*)-3-(4-Nitrophenyl)propenal (j)

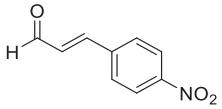

Following the General Procedure 7, 4-nitrobenzaldehyde (2.26 g, 15 mmol) was used. The crude mixture was purified by flash chromatography (from 95:5 to 70:30 Hexanes/EtOAc) to give 1.23 g (6.9 mmol, 46% yield) of pure **j**.

Yellow solid.
Mp 134–136 °C.
R_f 0.3 (70:30 Hexanes/EtOAc).
IR (ATR) ν 3062, 2921, 2825, 1531, 1344, 1313, 1123, 1109, 866, 826, 740 cm^{-1}.
^{1}H NMR (500 MHz, $CDCl_3$) δ 9.79 (d, *J* = 7.4 Hz, 1H, C<u>H</u>O), 8.34–8.27 (m, 2H, Ar<u>H</u>), 7.78–7.71 (m, 2H, Ar<u>H</u>), 7.54 (d, *J* = 16.1 Hz, 1H, C<u>H</u>CHCHO), 6.82 (dd, *J* = 16.1, 7.4 Hz, 1H, C<u>H</u>CHO).
^{13}C NMR (126 MHz, $CDCl_3$) δ 192.8 (C), 149.0 (C), 148.8 (CH), 139.9 (C), 131.7 (CH), 129.0 (CH), 124.3 (CH).
HRMS (ESI–) *m/z* calcd for $[M-H]^-$ $C_9H_6NO_3$: 176.0353, found: 176.0357.

3-Methoxybenzaldehyde

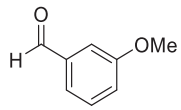

Methyl iodide (2.3 mL, 60 mmol) was added to a solution of 3-hydroxibenzaldehyde (3.66 g, 30 mmol) in acetone (18 mL) at 0 °C. Next, solid K_2CO_3 (8.3 g, 60 mmol) was added and the resultant mixture was stirred for 16 at rt. The mixture was filtrated and the volatiles were removed under reduced pressure. Then, the crude mixture was purified by flash chromatography (85:15 Hexanes/EtOAc) to give 3.89 g (28.5 mmol, 95% yield) of pure 3-methoxybenzaldehyde.

Pale yellow liquid.
R_f 0.4 (85:15 Hexanes/EtOAc).
^{1}H NMR (400 MHz, $CDCl_3$) δ 9.99 (s, 1H, C<u>H</u>O), 7.48–7.44 (m, 2H, Ar<u>H</u>), 7.42–7.38 (m, 1H, Ar<u>H</u>), 7.21–7.15 (m, 1H, Ar<u>H</u>), 3.87 (s, 3H, O<u>Me</u>).

(*E*)-3-(3-Methoxyphenyl)propenal (k)

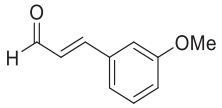

Following the General Procedure 7, 3-methoxybenzaldehyde (4.08 g, 30 mmol) was used. The crude mixture was purified by flash chromatography (from 95:5 to 80:20 Hexanes/EtOAc) to give 3.85 g (23.7 mmol, 79% yield) of pure **k**.

Pale yellow liquid.
R_f 0.4 (85:15 Hexanes/EtOAc).
IR (ATR) ν 2941, 2835, 2737, 1669, 1625, 1271, 1118, 1036, 970, 775, 682 cm^{-1}.
^{1}H NMR (400 MHz, $CDCl_3$) δ 9.71 (d, *J* = 7.7 Hz, 1H, C<u>H</u>O), 7.45 (d, *J* = 16.0 Hz, 1H, C<u>H</u>CHCHO), 7.39–7.31 (m, 1H, Ar<u>H</u>), 7.20–7.14 (m, 1H, Ar<u>H</u>), 7.11–7.06 (m, 1H, Ar<u>H</u>), 7.03–6.95 (m, 1H, Ar<u>H</u>), 6.71 (dd, *J* = 16.0, 7.7 Hz, 1H, C<u>H</u>CHO), 3.85 (s, 3H, O<u>Me</u>).
^{13}C NMR (101 MHz, $CDCl_3$) δ 193.6 (CH), 160.0 (CH), 152.6 (C), 135.3 (C), 130.1 (CH), 128.8 (CH), 121.2 (CH), 117.1 (CH), 113.3 (CH), 55.3 (CH_3).
HRMS (ESI+) *m/z* calcd for $[M+H]^+$ $C_{10}H_{11}O_2$: 163.0754, found: 163.0752.

2-Methoxybenzaldehyde

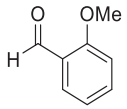

Methyl iodide (2.3 mL, 60 mmol) was added to a solution of 2-hydroxibenzaldehyde (3.66 g, 30 mmol) in acetone (18 mL) at 0 °C. Next, solid K_2CO_3 (8.3 g, 60 mmol) and the mixture was stirred overnight at rt.

The mixture was filtrated and the volatiles removed under reduced pressure. Then, the crude mixture was purified by flash chromatography (85:15 Hexanes/EtOAc) to give 3.54 g (26.0 mmol, 87% yield) of pure 2-methoxybenzaldehyde.

Pale yellow liquid.
R_f 0.4 (85:15 Hexanes/EtOAc).
^{1}H NMR (400 MHz, $CDCl_3$) δ 10.48 (s, 1H, C<u>H</u>O), 7.85–7.82 (m, 1H, Ar<u>H</u>), 7.59–7.53 (m, 1H, Ar<u>H</u>), 7.06–6.98 (m, 2H, Ar<u>H</u>), 3.94 (s, 3H, O<u>Me</u>).

(*E*)-3-(2-Methoxyphenyl)propenal (l)

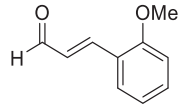

Following the General Procedure 7, 2-methoxybenzaldehyde (2.04 g, 15 mmol) was used. The crude mixture was purified by flash chromatography (from 90:10 to 85:15 Hexanes/EtOAc) to give 2.00 g (12.3 mmol, 82% yield) of pure **l**.

Colorless oil.
R_f 0.5 (80:20 Hexanes/EtOAc).
^{1}H NMR (400 MHz, $CDCl_3$) δ 9.70 (d, *J* = 7.9 Hz, 1H, C<u>H</u>O), 7.85 (d, *J* = 16.1 Hz, 1H, C<u>H</u>CHCHO), 7.56 (dd, *J* = 7.5, 1.6 Hz, 1H, Ar<u>H</u>), 7.42 (ddd, *J* = 8.2, 7.5, 1.7 Hz, 1H, Ar<u>H</u>), 7.01 (t, *J* = 7.5 Hz, 1H, Ar<u>H</u>), 6.96 (d, *J* = 8.2 Hz, 1H, Ar<u>H</u>), 6.80 (dd, *J* = 16.1, 7.9 Hz, 1H, C<u>H</u>CHO), 3.92 (s, 3H, O<u>Me</u>).

(*E*)-3-(3-Methylphenyl)propenal (m)

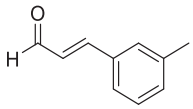

Following the General Procedure 7, 3-methylbenzaldehyde (1.6 mL, 15 mmol) was used. The crude mixture was purified by flash chromatography (from 95:5 to 85:15 Hexanes/EtOAc) to give 0.95 g (6.5 mmol, 43% yield) of pure **m**.

Pale yellow liquid.
R_f 0.6 (Hexanes/EtOAc 80:20).
IR (ATR) ν 2920, 2812, 2732, 1669, 1624, 1604, 1119, 969, 775, 686 cm^{-1}.
^{1}H NMR (400 MHz, $CDCl_3$) δ 9.69 (d, *J* = 7.7 Hz, 1H, C<u>H</u>O), 7.45 (d, *J* = 16.0 Hz, 1H, C<u>H</u>CHCHO), 7.40–7.22 (m, 4H, Ar<u>H</u>), 6.71 (dd, *J* = 16.0, 7.7 Hz, 1H, C<u>H</u>CHO), 2.39 (s, 3H, Ar<u>Me</u>).
^{13}C NMR (101 MHz, $CDCl_3$) δ 193.7 (CH), 153.0 (CH), 138.8 (C), 133.9 (C), 132.1 (CH), 129.1 (CH), 128.9 (CH), 128.4 (CH), 125.7 (CH), 21.3 (CH_3).

(*E*)-3-(2-Methylphenyl)propenal (n)

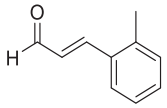

Following the General Procedure 7, 2-methylbenzaldehyde (1.8 mL, 15 mmol) was used. The crude mixture was purified by flash chromatography (from 90:10 to 80:20 Hexanes/EtOAc) to give 1.49 g (10.2 mmol, 68% yield) of pure **n**.

Pale yellow liquid.
R_f 0.6 (80:20 Hexanes/EtOAc).
IR (ATR) ν 2816, 2737, 1671, 1619, 1600, 1126, 1097, 748, 729, 711, 613 cm^{-1}.
^{1}H NMR (400 MHz, $CDCl_3$) δ 9.73 (d, *J* = 7.7 Hz, 1H, C<u>H</u>O), 7.78 (d, *J* = 15.8 Hz, 1H, C<u>H</u>CHCHO), 7.62–7.55 (m, 1H, Ar<u>H</u>), 7.38–7.20 (m, 3H, Ar<u>H</u>), 6.67 (dd, *J* = 15.8, 7.7 Hz, 1H, C<u>H</u>CHO), 2.48 (s, 3H, ArC<u>H</u>$_3$).
^{13}C NMR (101 MHz, $CDCl_3$) δ 193.9 (CH), 150.3 (CH), 137.9 (C), 132.8 (C), 131.0 (CH), 131.0 (CH), 129.6 (CH), 126.8 (CH), 126.6 (CH), 19.7 (CH_3).

(*E*)-3-(2-Thiophenyl)propenal (o)

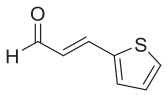

Following the General Procedure 7, thiophene-2-carbaldehyde (1.4 mL, 15 mmol) was used. The crude mixture was purified by flash chromatography (from 95:5 to 80:20 Hexanes/EtOAc) to give 1.60 g (11.5 mmol, 77% yield) of pure **o**.

Brown liquid.
R_f 0.4 (90:10 Hexanes/EtOAc).
IR (ATR) ν 3085, 2814, 2721, 1662, 1606, 1419, 1225, 1112, 1043, 957, 856, 815,703, 561 cm^{-1}.
^{1}H NMR (400 MHz, $CDCl_3$) δ 9.63 (d, *J* = 7.7 Hz, 1H, C<u>H</u>O), 7.59 (dt, *J* = 15.6, 0.7 Hz, 1H, C<u>H</u>CHCHO), 7.53–7.48 (m, 1H, Ar<u>H</u>), 7.39–7.33 (m, 1H, Ar<u>H</u>), 7.14–7.09 (m, 1H, Ar<u>H</u>), 6.51 (dd, *J* = 15.6, 7.7 Hz, 1H, C<u>H</u>CHO).
^{13}C NMR (101 MHz, $CDCl_3$) δ 192.9 (CH), 144.4 (CH), 139.2 (C), 132.0 (CH), 130.4 (CH), 128.5 (CH), 127.3 (CH).
HRMS (ESI+) *m/z* calcd for $[M+H]^+$ C_7H_7OS: 139.0212, found: 139.0212.

(*E*)-3-(2-Furanyl)propenal (p)

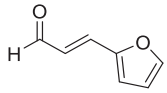

Following the General Procedure 7, furane-2-carbaldehyde (1.44 g, 15 mmol) was used. The crude mixture was purified by flash chromatography (from 95:5 to 85:25 Hexanes/EtOAc) to give 666 mg (5.4 mmol, 36% yield) of pure **p**.

Dark brown liquid.
R$_f$ 0.4 (80:20 Hexanes/EtOAc).
^{1}H NMR (400 MHz, $CDCl_3$) δ 9.63 (d, *J* = 7.9 Hz, 1H, C<u>H</u>O), 7.58–7.56 (m, 1H, Ar<u>H</u>), 7.22 (d, *J* = 15.8 Hz, 1H, ArC<u>H</u>), 6.80–6.75 (m, 1H, Ar<u>H</u>), 6.59 (dd, *J* = 15.8, 7.9 Hz, 1H, C<u>H</u>CHO), 6.55–6.52 (m, 1H, Ar<u>H</u>).

(2*E*,4*E*)-5-Phenyl-2,4-pentadienal (q)

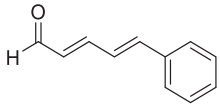

Following the General Procedure 7, cinnamaldehyde (2.4 mL, 19 mmol) was used. The crude mixture was purified by flash chromatography (from 98:2 to 94:6 Hexanes/EtOAc) to give 2.29 g (14.4 mmol, 76% yield) of pure **q**.

Colorless oil.
R$_f$ 0.5 (90:10 Hexanes/EtOAc).
^{1}H NMR (400 MHz, $CDCl_3$) δ 9.63 (d, *J* = 8.0 Hz, 1H, C<u>H</u>O), 7.53–7.48 (m, 2H, Ar<u>H</u>), 7.42–7.34 (m, 3H, Ar<u>H</u>), 7.31–7.24 (m, 2H, C<u>H</u>CHPh, C<u>H</u>CHCHO), 7.01 (d, *J* = 7.3 Hz, 1H, C<u>H</u>Ph), 6.28 (dd, *J* = 15.2, 8.0 Hz, 1H, C<u>H</u>CHO).

(*Z*)-2-Bromo-3-phenylacrylaldehyde (r)

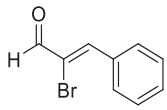

Following a literature procedure,[5] bromine (17 mL, 333 mmol, 1 equiv) was added to a solution of (*E*)-cinnamaldehyde (42 mL, 333 mmol, 1 equiv) in acetic acid (170 mL) at 0 °C. Next, solid K_2CO_3 (23 g, 170 mmol, 0.5 equiv) was added and the mixture was stirred until gas evolution stopped.

Then, the mixture was heated to reflux for 30 min and it was cooled to rt. The mixture was poured in 450 mL of water and the reddish precipitate was filtered

and purified by recrystallization (EtOH) to give 55 g (263 mmol, 79% yield) of pure **r**.

Pale yellow solid.
^{1}H NMR (400 MHz, $CDCl_3$) δ 9.36 (s, 1H, C<u>H</u>O), 8.04–7.98 (m, 2H, Ar<u>H</u>), 7.91 (s, 1H, C<u>H</u>Ph), 7.53–7.46 (m, 3H, Ar<u>H</u>).

(*E*)-3-Iodoacrolein (s)

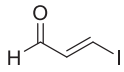

Following a literature report,[6] 3,3-diethoxy-1-propyne (0.72 mL, 5 mmol) was added to a stirring biphasic mixture of 4 M solution of H_2SO_4 (5 mL) and Et_2O (1.2 mL) at 0 °C. Then, powdered NaI (1.12 g, 7.5 mmol) was added and the mixture was closed with a glass stopper [**Caution:** The impurities in rubber stoppers can catalyse the decomposition of the reaction] and it was stirred for 2 h.

The mixture was rinsed with a sat. $NaHCO_3$ (15 mL), and extracted with Et_2O (3 × 10 mL). The combined organic mixture was washed with sat. $Na_2S_2O_3$ (15 mL) and brine (30 mL), dried ($MgSO_4$) and concentrated under reduced pressure to give the compound as a bright pale yellow-green solid, which easily degrades under air to become a useless black oil.

Ethyl (*Z*)-3-iodoacrylate

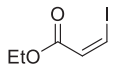

Following a literature procedure,[7] ethyl propiolate (205 μL, 2 mmol) was added dropwise to a stirring solution of NaI (300 mg, 2 mmol) in glacial acetic acid (1 mL) at rt. Then, the mixture was heated to 70 °C and it was stirred for 16 h.

The mixture was rinsed with H_2O (20 mL) and extracted with Et_2O (3 × 10 mL). The combined organic extracts were washed with NaOH (20 mL), dried ($MgSO_4$) and concentrated under reduced pressure. The crude mixture was purified by column chromatography (from 95:5 to 85:15 Hexanes/EtOAc) to give 268 mg (1.2 mmol, 60% yield) of pure compound ethyl (*Z*)-3-iodoacrylate.

Colorless liquid.
^{1}H NMR (400 MHz, $CDCl_3$) δ 7.44 (d, *J* = 8.9 Hz, 1H, C<u>H</u>I), 6.89 (d, *J* = 8.9 Hz, 1H, C<u>H</u>CHI), 4.26 (q, *J* = 7.1 Hz, 2H, C<u>H</u>$_2$CH$_3$), 1.32 (t, *J* = 7.1 Hz, 3H, CH$_2$C<u>H</u>$_3$).

(*Z*)-3-Iodoacrylaldehyde (t)

Following a literature procedure,[7] ethyl (*Z*)-3-iodoacrylate (268 mg, 1.2 mmol) was dissolved in CH_2Cl_2 (5 mL) and cooled to –78 °C. Then, a 1 M solution of DIBAL-H in toluene (1.6 mL, 1.6 mmol) was added dropwise over 10 min and the reaction mixture was stirred at this temperature for 5 min.

Then, the reaction was quenched with MeOH (1 mL), and a sat. solution of sodium potassium tartrate was added (15 mL) and it was stirred for 2 h at rt. The mixture was rinsed with water (10 mL) and extracted with Et_2O (3 × 10 mL). The combined organic extracts were washed with brine (15 mL) and dried (K_2CO_3). The crude mixture was purified by flash chromatography (80:20 Hexanes/EtOAc) to give 102 mg (0.56 mmol, 47% yield) of product **t**.

Pale yellow liquid.
R_f 0.4 (80:20 Hexanes/EtOAc).
^{1}H NMR (400 MHz, $CDCl_3$) δ 9.69 (1H, d, *J* = 6.5 Hz, C<u>H</u>O), 7.79 (1H, d, *J* = 8.2 Hz, IC<u>H</u>CH), 6.75 (1H, dd, *J* = 8.2, 6.5 Hz, ICHC<u>H</u>).

(*E*)-4,4-Dimethyl-2-pentenal (x)

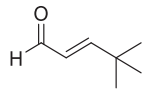

Following the General Procedure 7, pivaldehyde (0.6 mL, 5 mmol) was used. The crude mixture was purified by flash chromatography (from 98:2 to 96:4 Hexanes/EtOAc) to give 75 mg (0.67 mmol, 13% yield) of pure **x**.

Pale yellow oil.
R_f 0.6 (90:10 Hexanes/EtOAc).
^{1}H NMR (400 MHz, $CDCl_3$) δ 9.52 (d, *J* = 7.7 Hz, 1H, C<u>H</u>O), 6.81 (d, *J* = 15.9 Hz, 1H, ^{t}BuC<u>H</u>), 6.05 (dd, *J* = 15.8, 7.8 Hz, 1H, C<u>H</u>CHO), 1.14 (s, 9H, <u>^{t}Bu</u>CH).

7 Michael addition to α,β-unsaturated aldehydes

7.1 Heterocycle and Lewis acid assessment

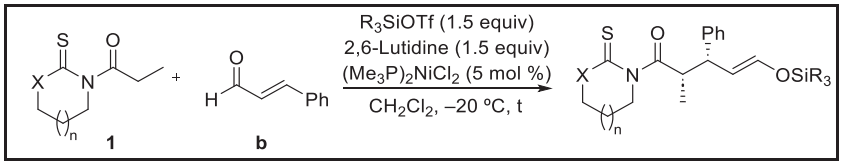

A solution of an *N*-propanoyl thioimide **1** (1.0 mmol, 1.0 equiv), cinnamaldehyde **b** (140 µL, 1.1 mmol, 1.1 equiv), and $(Me_3P)_2NiCl_2$ (14.1 mg, 50 µmol, 5 mol%) in CH_2Cl_2 (2 mL) was cooled at –20 °C under N_2. Then, neat R_3SiOTf (1.5 mmol, 1.5 equiv) was added followed by 2,6-lutidine (175 µL, 1.5 mmol, 1.5 equiv), and the resultant mixture was stirred at –20 °C.

The reaction mixture was quenched with sat. NH_4Cl (1 mL) and partitioned in CH_2Cl_2 (10 mL) and water (25 mL). The aqueous layer was extracted with CH_2Cl_2 (2×10 mL). The combined organic extracts were dried ($MgSO_4$) and concentrated. The resultant residue was analysed by ^1H NMR (400 MHz) and purified by flash column chromatography to give the named compound. These results are summarised in Table 58.

Entry	R_3SiOTf	1	X	n	t (h)	Conv. (%)[a]	rr (1,2:1,4)[a]	dr (1,2)[a,c]	dr (1,4)[a]	*syn* (%)[b]	*anti* (%)[b]
1	TIPSOTf	**1a**	S	1	5	93	15:85	-	81:19	54	15
2	TESOTf	**1a**	S	1	5	88	44:56	84:16	78:22	-	-
3	TBSOTf	**1a**	S	1	2	>99	67:33	76:24	78:22	-	-
4	TMSOTf	**1a**	S	1	2	>95	74:26	80:20	80:20	-	-
5	TIPSOTf	**1n**	O	1	5	94	27:73	-	80:20	-	-
6	TESOTf	**1n**	O	1	5	94	62:38	95:5	65:35	-	-
7	TBSOTf	**1n**	O	1	16	76	75:25	94:6	52:48	-	-
8	TMSOTf	**1n**	O	1	16	90	82:18	92:8	55:45	-	-
9	TIPSOTf	**1l**	S	0	5	90	13:87	-	81:19	62	16
10	TESOTf	**1l**	S	0	5	80	48:52	89:11	77:23	-	-
11	TMSOTf	**1l**	S	0	2	>99	65:35	86:14	65:35	-	-
12	TIPSOTf	**1m**	O	0	5	97	28:72	-	70:30	-	-
13	TESOTf	**1m**	O	0	5	80	50:50	96:4	58:42	-	-
14	TBSOTf	**1m**	O	0	5	85	52:48	90:10	50:50	-	-
15	TMSOTf	**1m**	O	0	2	99	73:27	62:38	43:57	-	-

a) Determined by ^1H NMR analysis of the crude mixture. b) Isolated yield of 1,4 adducts.

Table 58. Heterocycle and Lewis acid assessment in the Michael reaction.

7.2 Catalyst and solvent assessment

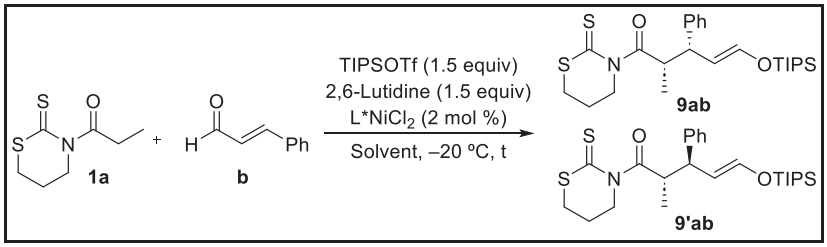

A solution of thioimide **1a** (189 mg, 1.0 mmol, 1.0 equiv), cinnamaldehyde **b** (140 µL, 1.1 mmol, 1.1 equiv), and the nickel catalyst (20 µmol, 2 mol%) in the corresponding solvent (2 mL) was cooled at –20 °C under N_2. Then, neat TIPSOTf (1.5 mmol, 1.5 equiv) was added followed by 2,6-lutidine (175 µL, 1.5 mmol, 1.5 equiv) and the resultant mixture was stirred at –20 °C.

The reaction mixture was quenched with sat. NH_4Cl (1 mL) and partitioned in CH_2Cl_2 (10 mL) and water (25 mL). The aqueous layer was extracted with CH_2Cl_2

(2 × 10 mL). The combined organic extracts were dried ($MgSO_4$), and concentrated. The resultant residue was analysed by ^1H NMR (400 MHz) and purified by flash column chromatography to give **9ab** and **9'ab**. The results are summarised in Table 59.

Entry	L*	Solvent	t (h)	Conv. (%)[a]	rr (1,4:1,2)[a]	dr (*syn/anti*)[a]	*ee* (%)[b]	*syn* (%)[c]	*anti* (%)[c]
1	(*R*)-DTBM-SEGPHOS	CH_2Cl_2	1	>97	98:2	79:21	99	70	19
2	(*R*)-DTBM-SEGPHOS	PhMe/CH_2Cl_2 4:1	1	>97	>99:1	84:16	99	72	16
3	(*R*)-DTBM-SEGPHOS	PhMe/CH_2Cl_2 4:1	5	>97	>99:1	88:12	99	80	11
4	(*R*)-DTBM-SEGPHOS	PhMe	16	94	>99:1	84:16	99	-	-
5	(*R*)-DTBM-SEGPHOS	PhMe/DCE 4:1	5	92	>99:1	87:13	99	-	-
6	(*R*)-DTBM-SEGPHOS	Pentane/CH_2Cl_2 4:1	5	95	>99:1	76:24	99	-	-
7	(*R*)-BINAP	CH_2Cl_2	5	>97	97:3	51:49	-	-	-
8	(*R*)-BINAP	PhMe/CH_2Cl_2 4:1	5	>97	>99:1	15:85	99	15	78
9	(*R*)-Tol-BINAP	CH_2Cl_2	5	>97	98:2	60:40	-	-	-
10	(*R*)-Tol-BINAP	PhMe/CH_2Cl_2 4:1	5	>97	>99:1	15:85	99	15	75
11	(*R*)-SEGPHOS	CH_2Cl_2	1	>97	98:2	55:45	-	46	41
12	(*R*)-SEGPHOS	PhMe/CH_2Cl_2 4:1	5	>97	>99:1	19:81	99	19	74
13	(*R*)-DM-SEGPHOS	PhMe/CH_2Cl_2 4:1	5	>97	>99:1	31:69	99	26	52
14	(*R*)-TM-BIPHEP	PhMe/CH_2Cl_2 4:1	5	16	>99:1	30:70	-	-	-
15	(*R*)-BIPHEP	PhMe/CH_2Cl_2 4:1	5	>97	>99:1	23:77	99	23	75
16	(*R*)-GARPHOS	PhMe/CH_2Cl_2 4:1	5	>97	>99:1	20:80	-	19	79
17	(*S*)-DMM-GARPHOS	PhMe/CH_2Cl_2 4:1	5	47	>99:1	13:87	-	-	-
18	(*R*)-DTBM-GARPHOS	PhMe/CH_2Cl_2 4:1	5	90	>99:1	87:13	99	68	11

a) Determined by ^1H NMR analysis of the crude mixture. b) Determined by chiral HPLC analysis. c) Isolated yield.

Table 59. Catalyst and solvent assessment.

7.3 Michael additions of thioimides to α,β-unsaturated aldehydes

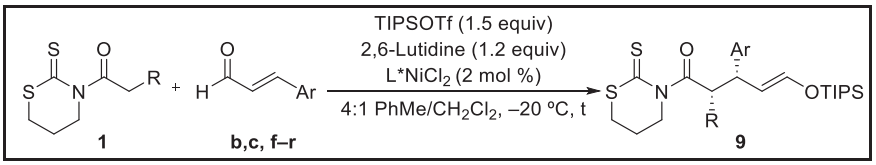

GENERAL PROCEDURE 8

A solution of a thioimide (1.0 mmol, 1.0 equiv), an α,β-unsaturated aldehyde (1.1 mmol, 1.1 equiv), and a chiral nickel (II) complex (2–10 mol%) in 4:1 Toluene/CH_2Cl_2 (2 mL) was cooled at –20 °C under N_2. Then, neat TIPSOTf (1.5 mmol, 1.5 equiv) was added followed by 2,6-lutidine (140 µL, 1.2 mmol, 1.2 equiv) and the resultant mixture was stirred at –20 °C.

The reaction mixture was quenched with sat. NH_4Cl (1 mL) and partitioned in CH_2Cl_2 (10 mL) and water (25 mL). The aqueous layer was extracted with CH_2Cl_2 (2 × 10 mL). The combined organic extracts were dried (Na_2SO_4), and concentrated. The resultant residue was analysed by ^1H NMR (400 MHz) and purified by flash column chromatography to give the named compound.

***N*-[(2*S*,3*R*,4*E*)-2-Methyl-3-phenyl-5-triisopropylsilyloxy-4-pentenoyl]-1,3-thiazinane-2-thione (9ab)**

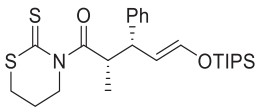

The General Procedure 8 was followed with **1a** (185 mg, 1 mmol, 1.0 equiv), [*(R)*-DTBM-SEGPHOS]$NiCl_2$ (27.5 mg, 21 µmol, 2 mol%), **b** (140 µL, 1.1 mmol, 1.1 equiv), TIPSOTf (405 µL, 1.5 mmol, 1.5 equiv), and 2,6-lutidine (140 µL, 1.2 mmol, 1.2 equiv) at –20 °C for 5 h.

The residue (dr 88:12) was purified by column chromatography (from 98:2 to 90:10 Hexanes/EtOAc) to give 373 mg (0.80 mmol, 80% yield) of *syn* Michael **9ab** and 52 mg (0.11 mmol, 11% yield) of the *anti* Michael **9'ab**.

Yellow oil.
R_f 0.4 (90:10 Hexanes/EtOAc).
$[\alpha]_D^{20}$ +203.9 (*c* 1.0 $CHCl_3$).
Chiral HPLC (Phenomenex Lux® Cellulose-5 column, 2% *i*-PrOH in Hexanes, flow rate 1 mL/min): R_t 13.8 min (2*R*,3*S* minor isomer) R_t 29.8 min (2*S*,3*R* major isomer), 99% *ee*.

IR (ATR) ν 2940, 2891, 2865, 1700, 1656, 1156, 1125, 919, 881, 806, 783, 760, 702, 684, 656 cm^{-1}.
^{1}H NMR (400 MHz, $CDCl_3$) δ 7.32–7.25 (m, 2H, ArH), 7.22–7.16 (m, 1H, ArH), 7.16–7.12 (m, 2H, ArH), 6.32 (d, *J* = 11.6 Hz, 1H, CHOTIPS), 5.18 (dd, *J* = 11.6, 10.4 Hz, 1H, CHCHOTIPS), 4.19 (dt, *J* = 13.1, 5.2 Hz, 1H, NCH_xH_y), 4.11 (dq, *J* = 10.4, 6.6 Hz, 1H,O=CCH), 3.37 (ddd, *J* = 13.1, 7.6, 6.6 Hz, 1H, NCH_xH_y), 3.23 (t, *J* = 10.4 Hz, 1H, PhCH), 3.08–2.88 (m, 2H, SCH_2), 2.22–2.12 (m, 2H, SCH_2CH_2), 1.11 (d, *J* = 6.6 Hz, 3H, CH_3), 1.09–0.96 (m, 21H,OTIPS).
^{13}C NMR (101 MHz, $CDCl_3$) δ 204.1 (C), 183.0 (C), 142.8 (C), 141.7(CH), 128.6 (CH), 127.5 (CH), 126.5 (CH), 112.2 (CH), 51.0 (CH), 48.4 (CH), 46.7 (CH_2), 31.6 (CH_2), 22.9 (CH_2), 17.7 (CH/CH_3), 17.6 (CH/CH_3) 16.8 (CH/CH_3), 12.3 (CH/CH_3) 11.8(CH/CH_3).
HRMS (ESI+) *m/z* calcd for $[M+H]^+$ $C_{25}H_{40}NO_2S_2Si$: 478.2264, found: 478.2262.

N-[(2*S*,3*R*,4*E*)-3-(4-Methoxyphenyl)-2-methyl-5-triisopropylsilyloxy-4-pentenoyl]-1,3-thiazinane-2-thione (9af)

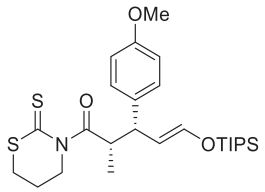

The General Procedure 8 was followed with **1a** (187 mg, 1.0 mmol, 1.0 equiv), [*(R)*-DTBM-SEGPHOS]$NiCl_2$ (26.7 mg, 21 μmol, 2 mol%), **f** (178 mg, 1.1 mmol, 1.1 equiv), TIPSOTf (405 μL, 1.5 mmol, 1.5 equiv), and 2,6-lutidine (140 μL, 1.2 mmol, 1.2 equiv) at –20 °C for 5 h.
The residue (dr 80:20) was purified by column chromatography (from 97:3 to 90:10 Hexanes/EtOAc) to give 296 mg (0.58 mmol, 58% yield) of *syn* Michael **9af** and 97 mg (0.19 mmol, 19% yield) of the *anti* Michael **9'af**.

Yellow thick oil.
R_f 0.6 (80:20 Hexanes/EtOAc).
$[\alpha]_D^{20}$ +203.3 (*c* 1.0 $CHCl_3$).
Chiral HPLC (Phenomenex Lux® Cellulose-5 column, 4% *i*-PrOH in Hexanes, flow rate 1 mL/min): R_t 8.3 min (2*R*,3*S* minor isomer) R_t 31.7 min (2*S*,3*R* major isomer), 99% *ee*.
IR (ATR) ν 2942, 2865, 1711, 1655, 1609, 1510, 1249, 1163, 1120, 1033, 986, 925, 881, 824, 795, 736, 681, 663 cm^{-1}.
^{1}H NMR (400 MHz, $CDCl_3$) δ 7.07–7.03 (m, 2H, ArH), 6.85–6.80 (m, 2H, ArH), 6.30 (d, *J* = 11.6 Hz, 1H, CHOTIPS), 5.14 (dd, *J* = 11.6, 10.4 Hz, 1H, CHCHOTIPS), 4.20 (dt, *J* = 13.2, 5.2 Hz, 1H, NCH_xH_y), 4.04 (dq, *J* = 10.4, 6.5 Hz, 1H, O=CCH), 3.78 (s, 3H,

OMe), 3.37 (ddd, *J* = 13.1, 7.4, 6.6 Hz, 1H, NCH_xH_y), 3.18 (t, *J* = 10.4 Hz, 1H, ArCH), 3.08–2.89 (m, 2H, SCH_2), 2.25–2.13 (m, 2H, NCH_2CH_2), 1.10 (d, *J* = 6.5 Hz, 3H, $CHCH_3$), 1.08–0.97 (m, 21H, OTIPS).

^{13}C NMR (101 MHz, $CDCl_3$) δ 204.0 (C), 183.1 (C), 158.1 (C), 141.4 (CH), 134.9 (C), 128.4 (CH), 113.9 (CH), 112.5 (CH), 55.2 (CH_3), 50.2 (CH), 48.7 (CH), 46.7 (CH_2), 31.6 (CH_2), 22.9 (CH_2), 17.7 (CH/CH_3), 17.7 (CH/CH_3), 17.6 (CH/CH_3), 16.8 (CH_3), 11.8 (CH/CH_3).

HRMS (ESI+) *m/z* calcd for $[M+H]^+$ $C_{26}H_{42}NO_3S_2Si$: 508.2370, found: 508.2370.

N-[(2*S*,3*R*,4*E*)-2-Methyl-3-(4-methylphenyl)-5-triisopropylsilyloxy-4-pentenoyl]-1,3-thiazinane-2-thione (9ag)

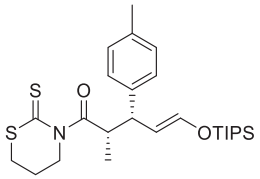

The General Procedure 8 was followed with **1a** (189 mg, 1.0 mmol, 1.0 equiv), [*(R)*-DTBM-SEGPHOS]$NiCl_2$ (26.3 mg, 20 µmol, 2 mol%), **g** (160 mg, 1.1 mmol, 1.1 equiv), TIPSOTf (405 µL, 1.5 mmol, 1.5 equiv), and 2,6-lutidine (140 µL, 1.2 mmol, 1.2 equiv) a –20 °C for 5 h.

The residue (dr 88:12) was purified by column chromatography (from 100:1 to 100:2 (80:20 Hexanes/toluene)/EtOAc) to give 355 mg (0.72 mmol, 72% yield) of *syn* Michael **9ag** and 51 mg (0.10 mmol, 10% yield) of the *anti* Michael **9'ag**.

Yellow oil.

R_f 0.6 [90:10 (80:20 Hexanes/toluene)/EtOAc].

$[\alpha]_D^{20}$ +246.6 (*c* 1.0 $CHCl_3$).

Chiral HPLC (Phenomenex Lux® Cellulose-5 column, 5% *i*-PrOH in Hexanes, flow rate 1 mL/min): R_t 6.0 min (2*R*,3*S* minor isomer) R_t 19.8 min (2*S*,3*R* major isomer), 99% *ee*.

IR (ATR) ν 2942, 2865, 1712, 1655, 1297, 1163, 1120, 986, 926, 881, 811, 794, 682, 663 cm^{-1}.

^{1}H NMR (400 MHz, $CDCl_3$) δ 7.11–7.06 (m, 2H, ArH), 7.05–6.99 (m, 2H, ArH), 6.31 (d, *J* = 11.6 Hz, 1H, CHOTIPS), 5.15 (dd, *J* = 11.6, 10.4 Hz, 1H, CHCHOTIPS), 4.19 (dt, *J* = 13.1, 5.2 Hz, 1H, NCH_xH_y), 4.06 (dq, *J* = 10.4, 6.5 Hz, 1H, O=CCH), 3.37 (dt, *J* = 13.1, 7.0 Hz, 1H, NCH_xH_y), 3.19 (t, *J* = 10.4 Hz, 1H, ArCH), 3.07–2.90 (m, 2H, SCH_2), 2.31 (s, 3H, $ArCH_3$), 2.22–2.13 (m, 2H, NCH_2CH_2), 1.10 (d, *J* = 6.5 Hz, 2H, $CHCH_3$), 1.09–0.97 (m, 21H, OTIPS).

^{13}C NMR (101 MHz, $CDCl_3$) δ 204.0 (C), 183.1 (C), 141.5 (CH), 139.7 (C), 135.9 (C), 129.2 (CH), 127.4 (CH), 112.3 (CH), 50.6 (CH), 48.6 (CH), 46.7 (CH_2), 31.6 (CH_2),

22.9 (CH_2), 21.0 (CH_3), 17.7 (CH/CH_3), 17.6 (CH/CH_3), 16.8(CH/CH_3), 11.8 (CH/CH_3).
HRMS (ESI+) *m/z* calcd for $[M+H]^+$ $C_{26}H_{42}NO_2S_2Si$: 492.2421, found: 492.2420.

N-[(2*S*,3*R*,4*E*)-3-(4-Chlorophenyl)-2-methyl-5-triisopropylsilyloxy-4-pentenoyl]-1,3-thiazinane-2-thione (9ah)

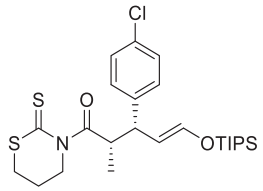

The General Procedure 8 was followed with **1a** (188 mg, 1.0 mmol, 1.0 equiv), [*(R)*-DTBM-SEGPHOS]$NiCl_2$ (66.3 mg, 51 μmol, 5 mol%), **h** (182 mg, 1.1 mmol, 1.1 equiv), TIPSOTf (405 μL, 1.5 mmol, 1.5 equiv), and 2,6-lutidine (140 μL, 1.2 mmol, 1.2 equiv) at –20 °C for 5 h.
The residue (dr 85:15) was purified by column chromatography (from 98:2 to 90:10 Hexanes/EtOAc) to give 340 mg (0.67 mmol, 67% yield) of *syn* Michael **9ah** and 64 mg (0.12 mmol, 12% yield) of the *anti* Michael **9'ah**.

Yellow thick oil.
R_f 0.5 (85:15 Hexanes/EtOAc).
$[\alpha]_D^{20}$ +212.0 (*c* 1.0 $CHCl_3$).
Chiral HPLC (Phenomenex Lux® Cellulose-5 column, 4% *i*-PrOH in Hexanes, flow rate 1 mL/min): R_t 6.2 min *(2R,3S* minor isomer) R_t 17.6 min (3*S,*2*R* major isomer), 99% *ee*.
IR (ATR) ν 2941, 2891, 2865, 1707, 1655, 1165, 1121, 1013, 987, 926, 881, 818, 783, 683, 652 cm^{-1}.
^{1}H NMR (400 MHz, $CDCl_3$) δ 7.29–7.22 (m, 2H, ArH), 7.10–7.04 (m, 2H, ArH), 6.31 (d, *J* = 11.6 Hz, 1H, CHOTIPS), 5.11 (dd, *J* = 11.6, 10.5 Hz, 1H, CHCHOTIPS), 4.21 (dt, *J* = 13.2, 5.2 Hz, 1H, NCH_xH_y), 4.06 (dq, *J* = 10.5, 6.5 Hz, 1H, O=CCH), 3.39 (ddd, *J* = 13.2, 7.5, 6.5 Hz, 1H, NCH_xH_y), 3.22 (t, *J* = 10.5 Hz, 1H, ArCH), 3.09–2.91 (m, 2H, SCH_2), 2.25–2.14 (m, 2H, NCH_2CH_2), 1.09 (d, *J* = 6.5 Hz, 3H, $CHCH_3$), 1.12–0.97 (m, 21H, OTIPS).
^{13}C NMR (101 MHz, $CDCl_3$) δ 204.3 (C), 182.6 (C), 142.0 (CH), 141.3 (C), 132.2 (C), 128.8 (CH), 128.7(CH), 111.8 (CH), 50.4 (CH), 48.3 (CH), 46.7 (CH_2), 31.7 (CH_2), 22.9 (CH_2), 17.6 (CH/CH_3), 17.6 (CH/CH_3), 16.7 (CH_3), 12.3 (CH/CH_3), 11.8 (CH/CH_3).
HRMS (ESI+) *m/z* calcd for $[M+H]^+$ $C_{25}H_{39}ClNO_2S_2Si$: 512.1875, found: 512.1877.

***N*-[(2*S*,3*R*,4*E*)-2-Methyl-3-(4-trifluoromethylphenyl)-5-triisopropylsilyloxy-4-pentenoyl]-1,3-thiazinane-2-thione (9ai)**

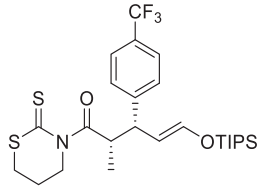

The General Procedure 8 was followed with **1a** (187 mg, 1.0 mmol, 1.0 equiv), [*(R)*-DTBM-SEGPHOS]$NiCl_2$ (131.0 mg, 100 μmol, 10 mol%), **i** (193 mg, 1.1 mmol, 1.1 equiv), TIPSOTf (405 μL, 1.5 mmol, 1.5 equiv), and 2,6-lutidine (140 μL, 1.2 mmol, 1.2 equiv) at –20 °C for 48 h.

The residue (dr 67:33) was purified by column chromatography (from 90:10 to 60:40 Hexanes/CH_2Cl_2) to give 284 mg (0.53 mmol, 53% yield) of *syn* Michael **9ai** and 141 mg (0.26 mmol, 26% yield) of the *anti* Michael **9'ai** as a mixture of diastereomers.

Yellow oil.
R_f 0.75 (50:50 Hexanes/CH_2Cl_2).
IR (ATR) *ν* 2942, 2867, 1966, 1699, 1655, 1324, 1163, 1115, 1066, 1015, 926, 831, 735, 685 cm^{-1}.
^{1}H NMR (400 MHz, $CDCl_3$) δ 7.57–7.52 (m, 2H, ArH), 7.28–7.23 (m, 2H, ArH), 6.34 (d, *J* = 11.5 Hz, 1H, CHOTIPS), 5.14 (dd, *J* = 11.5, 10.5 Hz, 1H, CHCHOTIPS), 4.23 (dt, *J* = 13.2, 5.3 Hz, 1H, NCH_xH_y), 4.13 (dq, *J* = 10.5, 6.6 Hz, 1H, O=CCH), 3.40 (ddd, *J* = 13.2, 8.5, 5.3 Hz, 1H, NCH_xH_y), 3.31 (t, *J* = 10.5 Hz, 1H, ArCH), 3.09–2.91 (m, 2H, SCH_2), 2.26–2.11 (m, 2H, SCH_2CH_2), 1.12–1.08 (m, 3H, $CHCH_3$), 1.06–0.97 (m, 21H, OTIPS).
^{13}C NMR (101 MHz, $CDCl_3$) δ 204.4 (C), 183.0 (C), 147.0 (C), 142.4 (CH), 128.8 (q, $^1J_{C-F}$ = 32.5 Hz, CF_3), 128.1 (C), 127.8 (CH), 125.6 (CH), 111.3 (CH), 50.8 (CH), 48.1 (CH), 46.7 (CH_2), 31.7 (CH_2), 23.0 (CH_2), 17.6 (CH/CH_3), 16.8 (CH_3), 11.8 (CH/CH_3).
HRMS (ESI+) *m/z* calcd for $[M+H]^+$ $C_{26}H_{38}F_3NO_2S_2Si$: 546.2138, found: 546.2252.

***N*-[(2*S*,3*R*,4*E*)-2-Methyl-3-(4-nitrophenyl)-5-triisopropylsilyloxy-4-pentenoyl]-1,3-thiazinane-2-thione (9aj)**

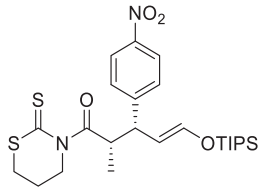

The General Procedure 8 was followed with **1a** (187 mg, 1.0 mmol, 1.0 equiv), [*(R)*-DTBM-SEGPHOS]$NiCl_2$ (131.6 mg, 100 μmol, 10 mol%), ***J*** (192 mg, 1.1 mmol, 1.1 equiv), TIPSOTf (405 μL, 1.5 mmol, 1.5 equiv), and 2,6-lutidine (140 μL, 1.2 mmol, 1.2 equiv) at –20 °C for 48 h.

The residue (86% conversion, dr 60:40) was purified by column chromatography (from 95:5 to 85:15 Hexanes/EtOAc) to give 179 mg (0.35 mmol, 35% yield) of *syn* Michael **9aj** and 113 mg (0.22 mmol, 22% yield) of the *anti* Michael **9'aj**.

Yellow solid.
Mp 91–93 °C.
R_f 0.6 (80:20 Hexanes/EtOAc).
$[\alpha]_D^{20}$ +49.7 (*c* 1.0 $CHCl_3$).
Chiral HPLC (Phenomenex Lux® Cellulose-5 column, 10% *i*-PrOH in Hexanes, flow rate 1 mL/min): R_t 14.4 min (2*R*,3*S* minor isomer) R_t 38.8 min (2*S*,3*R* major isomer), 99% *ee*.
IR (ATR) ν 2939, 2864, 1726, 1655, 1608, 1345, 1168, 1135, 1125, 994, 928, 843, 710, 683 cm^{-1}.
^{1}H NMR (400 MHz, $CDCl_3$) δ 8.21–8.13 (m, 2H, Ar<u>H</u>), 7.35–7.27 (m, 2H, Ar<u>H</u>), 6.37 (d, *J* = 11.6 Hz, 1H, C<u>H</u>OTIPS), 5.11 (dd, *J* = 11.6, 10.5 Hz, 1H, C<u>H</u>CHOTIPS), 4.26 (dt, *J* = 13.2, 5.2 Hz, 1H, NC<u>H</u>$_x$H$_y$), 4.16 (dq, *J* = 10.6, 6.6 Hz, 1H, O=CC<u>H</u>), 3.48–3.33 (m, 2H, NCH$_x$<u>H</u>$_y$, ArC<u>H</u>), 3.14–2.94 (m, 2H, SC<u>H</u>$_2$), 2.28–2.17 (m, 2H, NCH$_2$C<u>H</u>$_2$), 1.13–0.95 (m, 24H, CHC<u>H</u>$_3$, O<u>TIPS</u>).
^{13}C NMR (101 MHz, $CDCl_3$) δ 204.5 (C), 181.9 (C), 150.5 (C), 146.7 (C), 142.8 (CH), 128.32 (CH), 124.1 (CH), 111.0 (CH), 50.9 (CH), 47.8 (CH), 46.7 (CH_2), 31.7 (CH_2), 23.0 (CH_2), 17.6 (CH/CH_3), 17.5 (CH/CH_3), 16.7(CH/CH_3), 11.8 (CH/CH_3).
HRMS (ESI+) *m/z* calcd for $[M+H]^+$ $C_{25}H_{39}N_2O_4S_2Si$: 523.2115, found: 523.2117.

***N*-[(2*S*,3*R*,4*E*)-3-(3-Methoxyphenyl)-2-methyl-5-triisopropylsilyloxy-4-pentenoyl]-1,3-thiazinane-2-thione (9ak)**

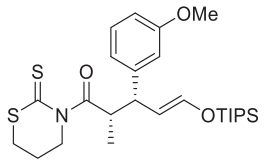

The General Procedure 8 was followed with **1a** (188 mg, 1.0 mmol, 1.0 equiv), [*(R)*-DTBM-SEGPHOS]$NiCl_2$ (26.2 mg, 20 μmol, 2 mol%), **k** (178 mg, 1.1 mmol, 1.1 equiv), TIPSOTf (405 μL, 1.5 mmol, 1.5 equiv), and 2,6-lutidine (140 μL, 1.2 mmol, 1.2 equiv) at –20 °C for 5 h.

The residue (dr 85:15) was purified by column chromatography (from 96:4 to 90:10 Hexanes/EtOAc) to give 308 mg (0.61 mmol, 61% yield) of *syn* Michael **9ak** and 30 mg (0.06 mmol, 6% yield) of the *anti* Michael **9'ak**.

Yellow oil.
R_f 0.6 (80:20 Hexanes/EtOAc).
$[\alpha]_D^{20}$ +213.3 (*c* 1.0 $CHCl_3$).
Chiral HPLC (Phenomenex Lux® Cellulose-5 column, 4% *i*-PrOH in Hexanes, flow rate 1 mL/min): R_t 8.7 min (2*R*,3*S* minor isomer) R_t 32.3 min (2*S*,3*R* major isomer), 99% *ee.*
IR (ATR) ν̃ 2941, 2863, 1720, 1644, 1606, 1580, 1461, 1434, 1389, 1348, 1302, 1284, 1219, 1204, 1120, 1064, 1150, 988, 942, 881, 777, 706, 684, 669 cm^{-1}.
^{1}H NMR (500 MHz, $CDCl_3$) δ 7.23–7.17 (m, 1H, ArH), 6.77–6.66 (m, 3H, ArH), 6.32 (d, *J* = 11.6 Hz, 1H, CHOTIPS), 5.16 (dd, *J* = 11.6, 10.4 Hz, 1H, CHCHOTIPS), 4.18 (dt, *J* = 13.2, 5.2 Hz, 1H, NCH_xH_y), 4.09 (dq, *J* = 10.4, 6.5 Hz, 1H, O=CCH), 3.79 (s, 3H, OMe), 3.38 (ddd, *J* = 13.1, 7.7, 6.3 Hz, 1H, NCH_xH_y), 3.20 (t, *J* = 10.4 Hz, 1H, ArCH), 3.06–2.98 (m, 1H, SCH_xH_y), 2.98–2.90 (m, 1H, SCH_xH_y), 2.21–2.13 (m, 2H, NCH_2CH_2), 1.12 (d, *J* = 6.5 Hz, 3H, $CHCH_3$), 1.12–0.96 (m, 21H, OTIPS).
^{13}C NMR (126 MHz, $CDCl_3$) δ 204.0 (C), 182.9 (C), 159.7 (C), 144.5 (C), 141.8 (CH), 129.6 (CH), 119.8 (CH), 113.3 (CH), 112.0 (CH), 111.7 (CH), 55.2 (CH_3), 51.0 (CH), 48.3 (CH), 46.7 (CH_2), 31.6 (CH_2), 22.9 (CH_2), 17.7 (CH/CH_3) (CH_3), 17.6 (CH_3), 16.8 (CH_3), 11.8 (CH).
HRMS (ESI+) *m/z* calcd for $[M+H]^+$ $C_{26}H_{42}NO_3S_2Si$: 508.2370, found 508.2365.

***N*-[(2*S*,3*R*,4*E*)-3-(2-Methoxyphenyl)-2-methyl-5-triisopropylsilyloxy-4-pentenoyl]-1,3-thiazinane-2-thione (9al)**

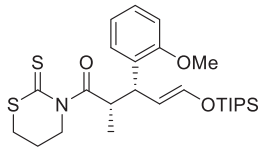

The General Procedure 8 was followed with **1a** (189 mg, 1.0 mmol, 1.0 equiv), [*(R)*-DTBM-SEGPHOS]$NiCl_2$ (65.7 mg, 50 μmol, 5 mol%), **l** (178 mg, 1.1 mmol, 1.1 equiv), TIPSOTf (405 μL, 1.5 mmol, 1.5 equiv), and 2,6-lutidine (140 μL, 1.2 mmol, 1.2 equiv) at –20 °C for 5 h.

The residue (dr 93:7) was purified by column chromatography (from 96:4 to 90:10 Hexanes/EtOAc) to give 272 mg (0.54 mmol, 54% yield) of *syn* Michael **9al** and 22 mg (40 μmol, 4% yield) of the *anti* Michael **9'al**.

Yellow oil.
R_f 0.6 (80:20 Hexanes/EtOAc).
$[\alpha]_D^{20}$ +129.2(*c* 1.0 $CHCl_3$).
Chiral HPLC (Phenomenex Lux® Cellulose-5 column, 4% *i*-PrOH in Hexanes, flow rate 1 mL/min): R_t 8.0 min (2*R*,3*S* minor isomer) R_t 47.8 min (2*S*,3*R* major isomer), 99% *ee.*
IR (ATR) ν 2943, 2865, 1704, 1653, 1490, 1452, 1350, 1281, 1264, 1213, 1050, 984, 863, 779, 703, 591, 558 cm^{-1}.
^{1}H NMR (500 MHz, $CDCl_3$) δ 7.20–7.14 (m, 1H, ArH), 7.09–7.06 (m, 1H, ArH), 6.90–6.86 (m, 1H, ArH), 6.85–6.81 (m, 1H, ArH), 6.35 (d, *J* = 11.6 Hz, 1H, CHOTIPS), 5.25 (dd, *J* = 11.7, 10.4 Hz, 1H, CHCHOTIPS), 4.36 (dq, *J* = 10.4, 6.6 Hz, 1H, O=CCH), 4.13 (dt, *J* = 13.2, 5.3 Hz, 1H, NCH_xH_y), 3.81 (s, 3H, OMe), 3.63 (t, *J* = 10.4 Hz, 1H, ArCH), 3.35 (ddd, *J* = 13.2, 8.3, 5.6 Hz, 1H, NCH_xH_y), 2.98–2.86 (m, 2H, SCH_2), 2.15–2.07 (m, 2H, NCH_2CH_2), 1.12 (d, *J* = 6.6 Hz, 3H, $CHCH_3$), 1.10–0.98 (m, 21H, OTIPS).
^{13}C NMR (126 MHz, $CDCl_3$) δ 204.1 (C), 183.4 (C), 157.1 (C), 142.0 (CH), 131.0 (C), 128.1 (CH), 127.4 (CH), 120.6 (CH), 111.1 (CH), 110.7 (CH), 55.3 (CH_3), 46.6 (CH_2), 46.1 (CH), 31.6 (CH_2), 23.0 (CH_2), 18.1 (CH_3), 17.8 (CH_3), 17.7 (CH_3) 16.7 (CH_3), 13.4 (CH), 12.3 (CH), 11.9 (CH).
HRMS (ESI+) *m/z* calcd for $[M+H]^+$ $C_{26}H_{42}NO_3S_2Si$: 508.2370, found 508.2366.

***N*-[(2*S*,3*R*,4*E*)-2-Methyl-3-(3-methylphenyl)-5-triisopropylsilyloxy-4-pentenoyl]-1,3-thiazinane-2-thione (9am)**

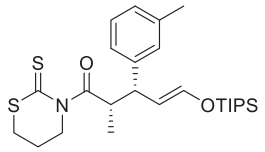

The General Procedure 8 was followed with **1a** (192 mg, 1.0 mmol, 1.0 equiv), [*(R)*-DTBM-SEGPHOS]$NiCl_2$ (65.7 mg, 50 μmol, 5 mol%), **m** (160 mg, 1.1 mmol, 1.1 equiv), TIPSOTf (405 μL, 1.5 mmol, 1.5 equiv), and 2,6-lutidine (140 μL, 1.2 mmol, 1.2 equiv) at –20 °C for 5 h.

The residue (dr 80:20) was purified by column chromatography (from 98:2 to 94:6 Hexanes/EtOAc) to give 366 mg (0.74 mmol, 74% yield) of *syn* Michael **9am** and 38 mg (0.07 mmol, 7% yield) of the *anti* Michael **9'am**.

Yellow oil.
R_f 0.7 (80:20 Hexanes/EtOAc).
$[\alpha]_D^{20}$ +189.5 (*c* 1.0 $CHCl_3$).
Chiral HPLC (Phenomenex Lux® Cellulose-5 column, 3% *i*-PrOH in Hexanes, flow rate 1 mL/min): R_t 6.7 min (2*R*,3*S* minor isomer) R_t 18.7 min (2*S*,3*R* major isomer), 99% *ee.*
IR (ATR) ν 2941, 2891, 2864, 1655, 1627, 1462, 1382, 1366, 1345, 1253, 1217, 1049, 1012, 835, 592, 561 cm^{-1}.
^{1}H NMR (400 MHz, $CDCl_3$) *δ* 7.19–7.13 (m, 1H, ArH), 7.03–6.98 (m, 1H, ArH), 6.95–6.90 (m, 2H, ArH), 6.31 (d, *J* = 11.6 Hz, 1H, CHOTIPS), 5.16 (dd, *J* = 11.6, 10.3 Hz, 1H, CHCHOTIPS), 4.18 (dt, *J* = 13.2, 5.2 Hz, 1H, NCH_xH_y), 4.08 (dq, *J* = 10.3, 6.5 Hz, 1H, O=CCH), 3.37 (ddd, *J* = 13.2, 7.2, 6.2 Hz, 1H, NCH_xH_y), 3.19 (t, *J* = 10.3 Hz, 1H, ArCH), 2.99–2.90 (m, 2H, SCH_2), 2.32 (s, 3H, $ArCH_3$), 2.20–2.10 (m, 2H,NCH_2CH_2), 1.11 (d, *J* = 6.6 Hz, 3H, $CHCH_3$), 1.11–0.98 (m, 21H, OTIPS).
^{13}C NMR (101 MHz, $CDCl_3$) *δ* 204.0 (C), 183.1 (C), 142.7 (C), 141.6 (CH), 138.1 (C), 128.4 (CH), 128.1 (CH), 127.2 (CH), 124.6 (CH), 112.2 (CH), 50.9 (CH), 48.5 (CH), 46.7 (CH_2), 31.6 (CH_2), 22.9 (CH_2), 21.5 (CH_3), 17.7 (CH_3), 17.6 (CH_3), 16.9 (CH_3), 11.8 (CH).
HRMS (ESI+) *m/z* calcd for $[M+H]^+$ $C_{26}H_{42}NO_2S_2Si$: 492.2421, found 492.2410.

***N*-[(2*S*,3*R*,4*E*)-2-Methyl-3-(2-methylphenyl)-5-triisopropylsilyloxy-4-pentenoyl]-1,3-thiazinane-2-thione (9an)**

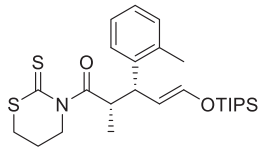

The General Procedure 8 was followed with **1a** (189 mg, 1.0 mmol, 1.0 equiv), [*(R)*-DTBM-SEGPHOS]$NiCl_2$ (65 mg, 50 μmol, 5 mol%), **n** (160 mg, 1.1 mmol, 1.1 equiv), TIPSOTf (405 μL, 1.5 mmol, 1.5 equiv), and 2,6-lutidine (140 μL, 1.2 mmol, 1.2 equiv) at –20 °C for 16 h.

The residue (dr 90:10) was purified by column chromatography (from 98:2 to 96:4 Hexanes/EtOAc) to give 291 mg (0.60 mmol, 60% yield) of *syn* Michael **9an** and 41 mg (80 μmol, 8% yield) of the *anti* Michael **9'an**.

Yellow oil.
R_f 0.7 (80:20 Hexanes/EtOAc).
$[\alpha]_D^{20}$ +170,5 (*c* 1.0 $CHCl_3$).
Chiral HPLC (Phenomenex Lux® Cellulose-5 column, 3% *i*-PrOH in Hexanes, flow rate 1 mL/min): R_t 6.3 min (2*R*,3*S* minor isomer) R_t 13.7 min (2*S*,3*R* major isomer), 99% *ee.*
IR (ATR) ν 2943, 2865, 1705, 1653, 1490, 1462, 1350, 1282, 1264, 1213, 1050, 1253, 984, 863, 796, 591, 558 cm^{-1}.
^{1}H NMR (400 MHz, $CDCl_3$) *δ* 7.21–7.04 (m, 4H, ArH), 6.31 (d, *J* = 11.6 Hz, 1H, CHOTIPS), 5.05 (dd, *J* = 11.6, 10.4 Hz, 1H, CHCHOTIPS), 4.28 (dt, *J* = 13.2, 5.2 Hz, 1H, NCH_xH_y), 4.21 (dq, *J* = 10.4, 6.5 Hz, 1H, O=CCH), 3.54 (t, *J* = 10.4 Hz, 1H, ArCH), 3.38 (ddd, *J* = 13.1, 8.6, 5.6 Hz, 1H, NCH_xH_y), 3.06 (dt, *J* = 12.6, 6.5 Hz, 1H, SCH_xH_y), 2.96 (dt, *J* = 12.6, 7.1 Hz, 1H, SCH_xH_y), 2.31 (s, 3H, $ArCH_3$), 2.25–2.16 (m, 2H, NCH_2CH_2), 1.10 (d, *J* = 6.5 Hz, 3H, $CHCH_3$), 1.16–0.96 (m, 21H, OTIPS).
^{13}C NMR (101 MHz, $CDCl_3$) *δ* 204.4 (C), 183.2 (C), 141.5 (CH), 140.5 (C), 135.8 (C), 130.5 (CH), 126.5 (CH), 126.1 (CH), 126.0 (CH), 112.3 (CH), 48.2 (CH), 46.7 (CH_2), 46.0 (CH), 31.7 (CH_2), 23.1 (CH_2), 19.8 (CH_3), 17.7 (CH_3), 17.6 (CH_3), 16.4 (CH_3), 11.8 (CH).
HRMS (ESI+) *m/z* calcd for $[M+H]^+$ $C_{26}H_{42}NO_2S_2Si$: 492.2421, found 492.2412.

***N*-[(2*S*,3*R*,4*E*)-2-Methyl-3-(2-thiophenyl)-5-triisopropylsilyloxy-4-pentenoyl]-1,3-thiazinane-2-thione (9ao)**

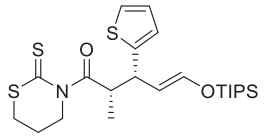

The General Procedure 8 was followed with **1a** (189 mg, 1.0 mmol, 1.0 equiv), [*(R)*-DTBM-SEGPHOS]$NiCl_2$ (26.1 mg, 20 μmol, 2 mol%), **o** (152 mg, 1.1 mmol, 1.1 equiv), TIPSOTf (405 μL, 1.5 mmol, 1.5 equiv), and 2,6-lutidine (140 μL, 1.2 mmol, 1.2 equiv) at –20 °C for 2 h.

The residue (dr 94:6) was purified by column chromatography (from 97:3 to 80:20 Hexanes/EtOAc) to give 418 mg (0.86 mmol, 86% yield) of *syn* Michael **9ao** and 25 mg (50 μmol, 5% yield) of the *anti* Michael **9'ao**.

Yellow oil.
R_f 0.7 (80:20 Hexanes/EtOAc).
$[\alpha]_D^{20}$ +168.7 (*c* 1.0 $CHCl_3$).
Chiral HPLC (Phenomenex Lux® Cellulose-5 column, 1% *i*-PrOH in Hexanes, flow rate 1 mL/min): R_t 11.8 min (2*R*,3*S* minor isomer) R_t 45.5 min (2*S*,3*R* major isomer), 99% *ee*.
IR (ATR) ν 2942, 2865, 2360, 2342, 1717, 1684, 1659, 1166, 1145, 1122, 1010, 881, 801, 684 cm^{-1}.
^{1}H NMR (400 MHz, $CDCl_3$) δ 7.19–7.10 (m, 1H, ArH), 6.96–6.88 (m, 1H, ArH), 6.83–6.80 (m, 1H, ArH), 6.36 (dd, *J* = 11.6, 0.5 Hz, 1H, CHOTIPS), 5.14 (dd, *J* = 11.6, 10.2 Hz, 1H, CHCHOTIPS), 4.15–4.03 (m, 2H, NCH_xH_y, O=CCH), 3.56 (t, *J* = 10.2 Hz, 1H, ArCH), 3.36 (ddd, *J* = 13.2, 9.2, 4.8 Hz, 1H, NCH_xH_y), 3.04–2.87 (m, 2H, SCH_2), 2.20–2.01 (m, 2H, NCH_2CH_2), 1.24 (d, *J* = 6.6 Hz, 3H, $CHCH_3$), 1.20–0.98 (m, 21H, OTIPS).
^{13}C NMR (101 MHz, $CDCl_3$) δ 203.8 (C), 182.2 (C), 146.8 (C), 142.5 (CH), 126.7 (CH), 123.8 (CH), 123.6 (CH), 111.6 (CH), 49.3 (CH), 46.7 (CH_2), 45.8 (CH), 31.6 (CH_2), 22.8 (CH_2), 17.7 (CH_3/CH), 17.6 (CH_3/CH), 17.0 (CH_3), 12.3 (CH_3/CH), 11.8 (CH_3/CH).
HRMS (ESI+) *m/z* calcd for $[M+H]^+$ $C_{23}H_{38}NO_2S_3Si$: 484.1828, found: 484.1834.

***N*-[(2*S*,3*R*,4*E*) 3-(2-Furanyl)-2-methyl-5-triisopropylsilyloxy-4-pentenoyl]-1,3-thiazinane-2-thione (9ap)**

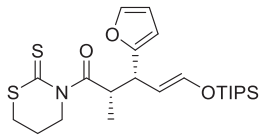

The General Procedure 8 was followed with **1a** (188 mg, 1.0 mmol, 1.0 equiv), [*(R)*-DTBM-SEGPHOS]$NiCl_2$ (65.5 mg, 50 μmol, 5 mol%), **p** (135 mg, 1.1 mmol, 1.1 equiv), TIPSOTf (405 μL, 1.5 mmol, 1.5 equiv), and 2,6-lutidine (140 μL, 1.2 mmol, 1.2 equiv) at –20 °C for 16 h.

The residue (dr 91:9) was purified by column chromatography (from 97:3 to 90:10 Hexanes/EtOAc) to give 384 mg (0.83 mmol, 83% yield) of *syn* Michael **9ap** and 37 mg (80 μmol, 8% yield) of the *anti* Michael **9'ap**.

Yellow oil.
R_f 0.5 (75:20:5 Hexanes/toluene/EtOAc).
$[\alpha]_D^{20}$ +238.0 (*c* 1.0 $CHCl_3$).
Chiral HPLC (Phenomenex Lux® Cellulose-5 column, 3% *i*-PrOH in Hexanes, flow rate 1 mL/min): R_t 7.2 min (2*R*,3*S* minor isomer) R_t 20.7 min (2*S*,3*R* major isomer), 99% *ee*.
IR (ATR) ν̃ 2941, 2891, 2864, 1713, 1658, 1165, 1128, 1009, 881, 801, 730, 676 cm^{-1}.
^{1}H NMR (500 MHz, $CDCl_3$) δ 7.33–7.28 (m, 1H, ArH), 6.35 (d, *J* = 11.7 Hz, 1H, CHOTIPS), 6.29–6.23 (m, 1H, ArH), 6.04–5.99 (m, 1H, ArH), 5.11 (dd, *J* = 11.8, 10.4 Hz, 1H, CHCHOTIPS), 4.18–4.07 (m, 2H, NCH_xH_y, O=CCH), 3.43–3.32 (m, 2H, NCH_xH_y, ArCH), 3.04 (dt, *J* = 12.6, 6.5 Hz, 1H, SCH_xH_y), 2.94 (dt, *J* = 12.6, 7.0 Hz, 1H, SCH_xH_y), 2.21–2.13 (m, 2H, NCH_2CH_2), 1.19 (d, *J* = 6.6 Hz, 3H, $CHCH_3$), 1.16–1.00 (m, 21H, OTIPS).
^{13}C NMR (126 MHz, $CDCl_3$) δ 203.8 (C), 182.3 (C), 155.6 (C), 142.9 (CH), 141.3 (CH), 110.1 (CH), 109.0 (CH), 105.8 (CH), 46.9 (CH), 46.7 (CH_2), 44.0 (CH), 31.6 (CH_2), 22.9 (CH_2), 17.7 (CH_3), 17.6 (CH_3), 16.6 (CH_3), 12.3 (CH), 11.9 (CH).
HRMS (ESI+) *m/z* calcd for $[M+H]^+$ $C_{23}H_{38}NO_3S_2Si$: 468.2057, found: 468.2063.

_N_-[(2_S_,3_R_,4_E_)-2-Methyl-3-[(_E_)-2-phenylethenyl)-5-triisopropylsilyloxy-4-pentenoyl]-1,3-thiazinane-2-thione (9aq)

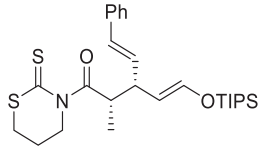

The General Procedure 8 was followed with **1a** (184 mg, 1.0 mmol, 1.0 equiv), [*(R)*-DTBM-SEGPHOS]$NiCl_2$ (26.4 mg, 20 µmol, 2 mol%), **q** (173 mg, 1.1 mmol, 1.1 equiv), TIPSOTf (405 µL, 1.5 mmol, 1.5 equiv), and 2,6-lutidine (140 µL, 1.2 mmol, 1.2 equiv) at –20 °C for 16 h.

The residue (dr 92:8) was purified by column chromatography (from 98:2 to 90:10 Hexanes/EtOAc) to give 353 mg (0.72 mmol, 72% yield) of *syn* Michael **9aq** and 42 mg (70 µmol, 7% yield) of the *anti* Michael **9'aq**.

Yellow oil.
R_f 0.5 (90:10 Hexanes/EtOAc).
$[\alpha]_D^{20}$ +275.1 (*c* 1.0 $CHCl_3$).
Chiral HPLC (Phenomenex Lux® Cellulose-4 column, 0.5% *i*-PrOH in Hexanes, flow rate 1 mL/min): R_t 19.9 min (2*R*,3*S* minor isomer) R_t 42.3 min (2*S*,3*R* major isomer), 99% *ee*.
IR (ATR) ν 2942, 285, 1713, 1655, 1165, 1124, 983, 965, 926, 881, 790, 736, 690, 663 cm^{-1}.
^{1}H NMR (500 MHz, $CDCl_3$) δ 7.36–7.28 (m, 4H, ArH), 7.24–7.19 (m, 1H, ArH), 6.38 (dd, *J* = 15.8, 1.0 Hz, 1H, PhCH), 6.32 (d, *J* = 11.7 Hz, 1H, CHOTIPS) 6.05 (dd, *J* = 15.8, 7.9 Hz, 1H, PhCHCH), 4.95 (dd, *J* = 11.7, 9.8 Hz, 1H, CHCHOTIPS), 4.19 (dt, *J* = 13.1, 5.2 Hz, 1H, NCH_xH_y), 3.78 (dq, *J* = 9.8, 6.6 Hz, 1H, O=CCH), 3.38 (ddd, *J* = 13.1, 9.2, 4.7 Hz, 1H, NCH_xH_y), 3.04 (dt, *J* = 12.7, 6.4 Hz, 1H, SCH_xH_y), 2.98–2.84 (m, 2H, SCH_xH_y, O=CCHCH), 2.28–2.12 (m, 2H, NCH_2CH_2), 1.31 (d, *J* = 6.6 Hz, 3H, $CHCH_3$), 1.19–1.00 (m, 21H, OTIPS).
^{13}C NMR (126 MHz, $CDCl_3$) δ 203.7 (C), 182.9 (C), 142.1 (CH), 137.2 (C), 131.0 (CH), 130.9 (CH), 128.5 (CH), 127.3 (CH), 126.1 (CH), 110.7 (CH), 48.3 (CH), 47.7 (CH), 46.8 (CH_2), 31.6 (CH_2), 22.9 (CH_2), 17.7 (CH_3), 16.5 (CH_3), 11.9 (CH).
HRMS (ESI+) *m/z* calcd for $[M+H]^+$ $C_{27}H_{41}NNaO_2S_2Si$: 526.2240, found: 526.2231.

***N*-[(2*S*,3*R*,4*Z*)-4-Bromo-2-methyl-3-phenyl-5-triisopropylsilyloxy-4-pentenoyl]-1,3-thiazinane-2-thione (9ar)**

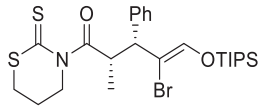

The General Procedure 8 was followed with **1a** (187 mg, 1.0 mmol, 1.0 equiv), [*(R)*-DTBM-SEGPHOS]$NiCl_2$ (65.8 mg, 50 μmol, 5 mol%), **r** (233 mg, 1.1 mmol, 1.1 equiv), TIPSOTf (405 μL, 1.5 mmol, 1.5 equiv), and 2,6-lutidine (140 μL, 1.2 mmol, 1.2 equiv) at –20 °C for 5 h.

The residue (95% conversion, dr >97:3) was purified by column chromatography (from 98:2 to 96:4 Hexanes/EtOAc) to give 473 mg (0.86 mmol, 86% yield) of *syn* Michael **9ar**.

Yellow solid.
Mp 97–100 °C.
R_f 0.5 (80:20 Hexanes/EtOAc).
$[\alpha]_D^{20}$ +295.9 (*c* 1.0 $CHCl_3$).
Chiral HPLC (Phenomenex Lux® Cellulose-5 column, 4% *i*-PrOH in Hexanes, flow rate 1 mL/min): R_t 7.2 min (2*R*,3*S* minor isomer) R_t 19.6 min (2*S*,3*R* major isomer), 99% *ee*.
IR (ATR) *ν* 2923, 2863, 1690, 1643, 1118, 988, 879, 795, 758, 699, 684, 669, 605 cm^{-1}.
^{1}H NMR (500 MHz, $CDCl_3$) δ 7.33–7.28 (m, 2H, ArH), 7.26–7.20 (m, 3H, ArH), 6.76 (s, 1H, CHOTIPS), 4.65 (dq, *J* = 11.1, 6.5 Hz, 1H, O=CCH), 4.28 (dt, *J* = 13.2, 5.4 Hz, 1H, NCH_xH_y), 3.64 (d, *J* = 11.1 Hz, 1H, PhCH), 3.43 (ddd, *J* = 13.2, 9.4, 4.5 Hz, 1H, NCH_xH_y), 3.26 (ddd, *J* = 12.4, 7.0, 6.1 Hz, 1H, SCH_xH_y), 2.93 (dt, *J* = 12.4, 7.0 Hz, 1H, SCH_xH_y), 2.43–2.32 (m, 1H, $NCH_2CH_xH_y$), 2.22–2.12 (m, 1H, $NCH_2CH_xH_y$), 1.19 (d, *J* = 6.5 Hz, 3H, $CHCH_3$), 1.18–1.01 (m, 21H, OTIPS).
^{13}C NMR (126 MHz, $CDCl_3$) δ 205.0 (C), 182.3 (C), 138.9 (C), 137.9 (CH), 128.5 (CH), 128.3 (CH), 127.1 (CH), 110.6 (C), 55.2 (CH), 46.7 (CH_2), 44.1 (CH), 31.8 (CH_2), 22.6 (CH_2), 17.6 (CH_3), 17.5 (CH_3), 16.6 (CH_3), 11.8 (CH).
HRMS (ESI+) *m/z* calcd for $[M+Na]^+$ $C_{25}H_{38}BrNNaO_2S_2Si$: 578.1189, found: 578.1184.

***N*-[(2*S*,3*R*,4*E*)-2,4-Dimethyl-3-phenyl-5-triisopropylsilyloxy-4-pentenoyl]-1,3-thiazinane-2-thione (9ac)**

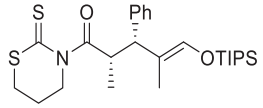

The General Procedure 8 was followed with **1a** (192 mg, 1.0 mmol, 1.0 equiv), [*(R)*-DTBM-SEGPHOS]$NiCl_2$ (26.9 mg, 21 μmol, 2 mol%), **c** (185 μL, 1.1 mmol, 1.1 equiv), TIPSOTf (405 μL, 1.5 mmol, 1.5 equiv), and 2,6-lutidine (140 μL, 1.2 mmol, 1.2 equiv) at –20 °C for 5 h.
The residue (dr > 97:3) was purified by column chromatography (from 98:2 to 90:10 Hexanes/EtOAc) to give 434 mg (0.88 mmol, 88% yield) of *syn* Michael **9ac**.

Yellow solid.
Mp 78–79 °C.
R_f 0.5 (90:10 Hexanes/EtOAc).
$[\alpha]_D^{20}$ +228.1 (*c* 1.0 $CHCl_3$).
Chiral HPLC (Phenomenex Lux® Cellulose-5 column, 2% *i*-PrOH in Hexanes, flow rate 1 mL/min): R_t 7.1 min (2*R*,3*S* minor isomer) R_t 27.5 min (2*S*,3*R* major isomer), 99% *ee*.
IR (ATR) ν 2942, 2865, 1705, 1656, 1462, 1164, 1124, 986, 880, 755, 663 cm^{-1}.
^{1}H NMR (500 MHz, $CDCl_3$) δ 7.31–7.24 (m, 2H, ArH), 7.22–7.16 (m, 1H, ArH), 7.13–7.07 (m, 2H, ArH), 6.33 (q, *J* = 1.4 Hz, 1H, CHOTIPS), 4.58 (dq, *J* = 11.5, 6.5 Hz, 1H, O=CCH), 4.19 (dt, *J* = 13.3, 5.3 Hz, 1H, NCH_xH_y), 3.45 (ddd, *J* = 13.3, 9.1, 4.4 Hz, 1H, NCH_xH_y), 3.33 (d, *J* = 11.5 Hz, 1H, PhCH), 3.09–2.93 (m, 2H, SCH_2), 2.29–2.14 (m, 2H, NCH_2CH_2), 1.46 (d, *J* = 1.4 Hz, 3H, CCH_3), 1.17 (d, *J* = 6.5 Hz, 3H, $CHCH_3$), 1.15–1.00 (m, 21H, OTIPS).
^{13}C NMR (126 MHz, $CDCl_3$) δ 203.3 (C), 183.5 (C), 140.6 (C), 136.1 (CH), 128.2 (CH), 128.2 (CH), 126.3 (CH), 117.4 (C), 56.0 (CH), 47.0 (CH_2), 43.6 (CH), 31.9 (CH_2), 22.5 (CH_2), 17.7 (CH_3), 17.6 (CH_3), 16.4 (CH_3), 11.8 (CH), 9.2 (CH_3).
HRMS (ESI+) *m/z* calcd for $[M+H]^+$ $C_{26}H_{42}NO_2S_2Si$: 492.2421, found: 492.2412.

***N*-[(2*S*,3*S*,4*E*)-2-Methyl-3-phenyl-5-triisopropylsilyloxy-4-pentenoyl]-1,3-thiazinane-2-thione (9'ab)**

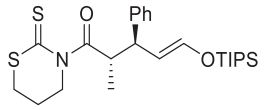

The General Procedure 8 was followed with **1a** (185 mg, 1 mmol, 1.0 equiv), [*(R)*-BINAP]$NiCl_2$ (16.8 mg, 21 μmol, 2 mol%), **b** (140 μL, 1.1 mmol, 1.1 equiv), TIPSOTf (405 μL, 1.5 mmol, 1.5 equiv), and 2,6-lutidine (140 μL, 1.2 mmol, 1.2 equiv) at –20 °C for 5 h.

The residue (dr 15:85) was purified by column chromatography (from 98:2 to 90:10 Hexanes/EtOAc) to give 74 mg (0.15 mmol, 15% yield) of *syn* Michael **9ab** and 370 mg (0.78 mmol, 78% yield) of the *anti* Michael **9'ab**.

Yellow thick oil.
R_f 0.3 (90:10 Hexanes/EtOAc).
$[\alpha]_D^{20}$ +223.1 (*c* 1.0 $CHCl_3$).
Chiral HPLC (Phenomenex Lux® Cellulose-5 column, 2% *i*-PrOH in Hexanes, flow rate 1 mL/min): R_t 10.8 min (2*R*,3*R* minor isomer) R_t 15.1 min (2*S*,3*S* major isomer), 99% *ee*.
IR (ATR) ν 2940, 2891, 2865, 1700, 1656, 1156, 1125, 919, 881, 806, 783, 760, 702, 684, 656 cm^{-1}.
^{1}H NMR (500 MHz, $CDCl_3$) δ 7.29–7.24 (m, 2H, ArH), 7.20–7.15 (m, 3H, ArH), 6.39 (d, *J* = 11.7 Hz, 1H, CHOTIPS), 5.06 (dd, *J* = 11.7, 10.5 Hz, 1H, CHCHOTIPS), 4.01 (dq, *J* = 10.5, 6.5 Hz, 1H, O=CCH), 3.44–3.37 (m, 1H, NCH_xH_y), 3.25 (t, *J* = 10.5 Hz, 1H, PhCH), 3.10–3.02 (m, 1H, NCH_xH_y), 2.64–2.55 (m, 1H, SCH_xH_y), 2.34–2.25 (m, 1H, SCH_xH_y), 1.79–1.67 (m, 1H, $NCH_2CH_xH_y$), 1.40 (d, *J* = 6.5 Hz, 3H, $CHCH_3$), 1.17–1.02 (m, 22H, $NCH_2CH_xH_y$, OTIPS).
^{13}C NMR (126 MHz, $CDCl_3$) δ 204.1 (C), 182.4 (C), 144.1 (C), 142.7 (CH), 128.7 (CH), 127.8 (CH), 126.5 (CH), 112.3 (CH), 51.6 (CH), 47.8 (CH), 46.2 (CH_2), 31.3 (CH_2), 22.2 (CH_2), 17.7 (CH_3), 11.9 (CH).
HRMS (ESI+) *m/z* calcd for $[M+H]^+$ $C_{25}H_{40}NO_2S_2Si$: 478.2264, found: 478.2262.

***N*-[(2*S*,3*S*,4*E*)-3-(4-Methoxyphenyl)-2-methyl-5-triisopropylsilyloxy-4-pentenoyl]-1,3-thiazinane-2-thione (9'af)**

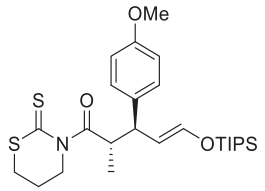

The General Procedure 8 was followed with **1a** (169 mg, 0.9 mmol, 1.0 equiv), [*(R)*-BINAP]$NiCl_2$ (16.8 mg, 21 μmol, 2 mol%), **f** (178 mg, 0.99 mmol, 1.1 equiv), TIPSOTf (363 μL, 1.35 mmol, 1.5 equiv), and 2,6-lutidine (125 μL, 1.1 mmol, 1.2 equiv) at –20 °C for 5 h.

The residue (dr 25:75) was purified by column chromatography (from 95:5 to 85:15 Hexanes/EtOAc) to give 89 mg (0.17 mmol, 20% yield) of *syn* Michael **9af** and 250 mg (0.49 mmol, 50% yield) of the *anti* Michael **9'af**.

Yellow solid.
Mp 70–72 °C.
R_f 0.5 (80:20 Hexanes/EtOAc).
$[\alpha]_D^{20}$ +219.5 (*c* 1.0 $CHCl_3$).
Chiral HPLC (Phenomenex Lux® Cellulose-5 column, 4% *i*-PrOH in Hexanes, flow rate 1 mL/min): R_t 9.1 min (2*R*,3*R* minor isomer) R_t 11.3 min (2*S*,3*S* major isomer), 99% *ee*.
IR (ATR) ν 2942, 2865, 1711, 1655, 1609, 1510, 1249, 1163, 1120, 1033, 986, 925, 881, 825, 795, 736, 682, 663 cm^{-1}.
^{1}H NMR (400 MHz, $CDCl_3$) δ 7.11–7.05 (m, 2H, ArH), 6.84–6.78 (m, 2H, ArH), 6.37 (dd, *J* = 11.6, 0.6 Hz, 1H, CHOTIPS), 5.03 (dd, *J* = 11.6, 10.5 Hz, 1H, CHCHOTIPS), 3.97 (dq, *J* = 10.5, 6.5 Hz, 1H, O=CCH), 3.76 (s, 3H, OMe), 3.44 (dt, *J* = 13.3, 5.5 Hz, 1H, NCH_xH_y), 3.21 (t, *J* = 10.5 Hz, 1H, ArCH), 3.09 (ddd, *J* = 13.3, 9.1, 4.5 Hz, 1H, NCH_xH_y), 2.64 (dt, *J* = 12.4, 6.7 Hz, 1H, SCH_xH_y), 2.40–2.32 (m, 1H, SCH_xH_y), 1.84–1.71 (m, 1H, $NCH_2CH_xH_y$), 1.38 (d, *J* = 6.5 Hz, 3H, $CHCH_3$), 1.27–1.14 (m, 1H, $NCH_2CH_xH_y$), 1.14–0.98 (m, 21H, OTIPS).
^{13}C NMR (101 MHz, $CDCl_3$) δ 203.9 (C), 182.6 (C), 158.3 (C), 142.4 (CH), 136.2 (C), 128.7 (CH), 114.0 (CH), 112.4 (CH), 55.4 (CH_3), 50.7 (CH), 48.0 (CH), 46.2 (CH_2), 31.3 (CH_2), 22.2 (CH_2), 17.7 (CH_3), 11.9 (CH/CH_3).
HRMS (ESI+) *m/z* calcd for $[M+H]^+$ $C_{26}H_{42}NO_3S_2Si$: 508.2370, found 508.2370.

***N*-[(2*S*,3*S*,4*E*)-2-Methyl-3-(4-methylphenyl)-5-triisopropylsilyloxy-4-pentenoyl]-1,3-thiazinane-2-thione (9'ag)**

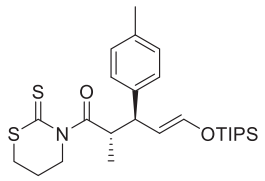

The General Procedure 8 was followed with **1a** (190 mg, 1.0 mmol, 1.0 equiv), [*(R)*-BINAP]$NiCl_2$ (15.4 mg, 20 μmol, 2 mol%), **g** (161 mg, 1.1 mmol, 1.1 equiv), TIPSOTf (405 μL, 1.5 mmol, 1.5 equiv), and 2,6-lutidine (140 μL, 1.2 mmol, 1.2 equiv) at –20 °C for 5 h.

The residue (dr 17:83) was purified by column chromatography (from 80:20:1 to 80:20:3 Hexanes/Toluene/EtOAc) to give 71 mg (0.14 mmol, 14% yield) of *syn* Michael **9ag** and 364 mg (0.74 mmol, 74% yield) of the *anti* Michael **9'ag**.

Yellow oil.
R_f 0.5 (72:18:10 Hexanes/toluene/EtOAc).
$[\alpha]_D^{20}$ +147.9 (*c* 1.0 $CHCl_3$).
Chiral HPLC (Phenomenex Lux® Cellulose-5 column, 4% *i*-PrOH in Hexanes, flow rate 1 mL/min): R_t 7.5 min (2*R*,3*R* minor isomer) R_t 9.1 min (2*S*,3*S* major isomer), 99% *ee*.
IR (ATR) ν 2942, 2865, 1712, 1655, 1297, 1163, 1120, 986, 926, 881, 811, 794, 682, 663 cm^{-1}.
^{1}H NMR (400 MHz, $CDCl_3$) δ 7.10–7.03 (m, 4H, ArH), 6.38 (dd, *J* = 11.7, 0.6 Hz, 1H, CHOTIPS), 5.04 (dd, *J* = 11.7, 10.6 Hz, 1H, CHCHOTIPS), 3.98 (dq, *J* = 10.6, 6.5 Hz, 1H, O=CCH), 3.41 (dt, *J* = 13.3, 5.5 Hz, 1H, NCH_xH_y), 3.20 (t, *J* = 10.6 Hz, 1H, ArCH), 3.07 (ddd, *J* = 13.3, 9.1, 4.6 Hz, 1H, NCH_xH_y), 2.61 (dt, *J* = 12.3, 6.8 Hz, 1H, SCH_xH_y), 2.29 (s, 3H, $ArCH_3$), 1.82–1.68 (m, 1H, SCH_xH_y), 1.38 (d, *J* = 6.5 Hz, 3H, $CHCH_3$), 1.22–0.99 (m, 21H, OTIPS).
^{13}C NMR (101 MHz, $CDCl_3$) δ 204.0 (C), 182.6 (C), 142.5 (CH), 141.1 (C), 136.1 (C), 129.1 (CH), 127.6 (CH), 112.3 (CH), 51.2 (CH), 48.0 (CH), 46.2 (CH_2), 31.2 (CH_2), 22.1 (CH_2), 21.0 (CH_3), 17.7 (CH/CH_3), 12.3 (CH/CH_3), 11.9 (CH/CH_3).
HRMS (ESI+) *m/z* calcd for $[M+H]^+$ $C_{26}H_{42}NO_2S_2Si$: 492.2421, found: 492.2420.

***N*-[(2*S*,3*S*,4*E*)- 3-(4-Chlorophenyl)-2-methyl-5-triisopropylsilyloxy-4-pentenoyl]-1,3-thiazinane-2-thione (9'ah)**

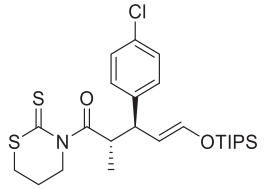

The General Procedure 8 was followed with **1a** (187 mg, 1.0 mmol, 1.0 equiv), [*(R)*-BINAP]$NiCl_2$ (37.6 mg, 51 μmol, 5 mol%), **h** (181 mg, 1.1 mmol, 1.1 equiv), TIPSOTf (405 μL, 1.5 mmol, 1.5 equiv), and 2,6-lutidine (140 μL, 1.2 mmol, 1.2 equiv) at –20 °C for 5 h.

The residue (dr 17:83) was purified by column chromatography (from 98:2 to 90:10 Hexanes/EtOAc) to give 63 mg (0.12 mmol, 12% yield) of *syn* Michael **9ah** and 288 mg (0.57 mmol, 57% yield) of the *anti* Michael **9'ah**.

Yellow oil.
R_f 0.4 (85:15 Hexanes/EtOAc).
$[\alpha]_D^{20}$ +148.9 (*c* 1.0 $CHCl_3$).
Chiral HPLC (Phenomenex Lux® Cellulose-5 column, 0.5% *i*-PrOH in Hexanes, flow rate 1 mL/min): R_t 22.8 min (2*R*,3*S* minor isomer) R_t 32.4 min (2*S*,3*R* isomer), 99% *ee*.
IR (ATR) *ν* 2941, 2891, 2865, 1707, 1655, 1165, 1121, 1013, 987, 926, 881, 818, 783, 683, 652 cm^{-1}.
^{1}H NMR (400 MHz, $CDCl_3$) δ 7.28–7.23 (m, 2H, ArH), 7.14–7.09 (m, 2H, ArH), 6.40 (d, *J* = 11.6, 1H, CHOTIPS), 5.01 (dd, *J* = 11.6, 10.5 Hz, 1H, CHCHOTIPS), 4.00 (dq, *J* = 10.5, 6.6 Hz, 1H, O=CCH), 3.54 (dt, *J* = 13.3, 5.5 Hz, 1H, NCH_xH_y), 3.25 (t, *J* = 10.5 Hz, 1H, ArCH), 3.11 (ddd, *J* = 13.4, 9.1, 4.5 Hz, 1H, NCH_xH_y), 2.69 (dt, *J* = 12.5, 6.8 Hz, 1H, SCH_xH_y), 2.34 (ddd, *J* = 12.5, 7.4, 5.9 Hz, 1H, SCH_xH_y), 1.90–1.77 (m, 1H, $NCH_2CH_xH_y$), 1.38 (d, *J* = 6.6 Hz, 3H, $CHCH_3$), 1.24–1.17 (m, 1H, $NCH_2CH_xH_y$), 1.16–0.99 (m, 21H, OTIPS).
^{13}C NMR (101 MHz, $CDCl_3$) δ 204.4 (C), 181.8 (C), 143.0 (CH), 142.7 (C), 132.3 (C), 129.1 (CH), 128.7 (CH), 111.5 (CH), 50.8 (CH), 47.7 (CH), 46.1 (CH_2), 31.4 (CH_2), 22.2 (CH_2), 17.6 (CH/CH_3), 11.9 (CH/CH_3).
HRMS (ESI+) *m/z* calcd for $[M+H]^+$ $C_{25}H_{39}ClNO_2S_2Si$: 512.1875, found: 512.1877.

***N*-[(2*S*,3*S*,4*E*)-2-Methyl-3-(4-trifluoromethylphenyl)-5-triisopropylsilyloxy-4-pentenoyl]-1,3-thiazinane-2-thione (9'ai)**

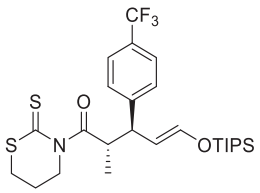

The General Procedure 8 was followed with **1a** (187 mg, 1.0 mmol, 1.0 equiv), [*(R)*-BINAP]$NiCl_2$ (131 mg, 100 µmol, 10 mol%), **i** (193 µL, 1.1 mmol, 1.1 equiv), TIPSOTf (405 µL, 1.5 mmol, 1.5 equiv), and 2,6-lutidine (140 µL, 1.2 mmol, 1.2 equiv) at –20 °C for 16 h.

The residue (dr 18:82) was purified by column chromatography (from 79:20:1 to 78:19:3 Hexanes/toluene/EtOAc) to give 96 mg (0.17 mmol, 17% yield) of *syn* Michael **9ai** and 362 mg (0.66 mmol, 66% yield) of the *anti* Michael **9'ai** as a mixture of diastereomers.

Yellow oil.
R_f 0.75 (50:50 Hexanes/CH_2Cl_2).
IR (ATR) ν 2942, 2867, 1966, 1699, 1655, 1324, 1163, 1115, 1066, 1015, 926, 831, 735, 685 cm^{-1}.
^{1}H NMR (400 MHz, $CDCl_3$) δ 7.58–7.52 (m, 2H, ArH), 7.34–7.28 (m, 2H, ArH), 6.43 (dd, *J* = 11.6, 0.5 Hz, 1H, CHOTIPS), 5.04 (dd, *J* = 11.6, 10.6 Hz, 1H, CHCHOTIPS), 4.06 (dq, *J* = 10.6, 6.6 Hz, 1H, O=CCH), 3.55 (dt, *J* = 13.2, 5.5 Hz, 1H, NCH_xH_y), 3.35 (t, *J* = 10.6 Hz, 1H, ArCH), 3.12–3.02 (m, 1H, NCH_xH_y), 2.64 (ddd, *J* = 12.5, 7.1, 6.7 Hz, 1H, SCH_xH_y), 2.28–2.14 (m, 1H, SCH_xH_y), 1.86–1.72 (m, 1H, $NCH_2CH_xH_y$), 1.40 (d, *J* = 6.6 Hz, 3H, $CHCH_3$), 1.19–0.96 (m, 22H, $NCH_2CH_xH_y$, OTIPS).
^{13}C NMR (101 MHz, $CDCl_3$) δ 204.6 (C), 181.4 (C), 148.4 (C), 143.4 (CH), 129.0 (q, $^1J_{C-F}$ = 32.4 Hz, CF_3), 128.1 (CH), 127.8 (CH), 125.6 (CH), 125.5 (CH), 111.1 (CH), 51.2 (CH), 47.6 (CH), 46.0 (CH_2), 31.3 (CH_2), 22.1 (CH_2), 17.6 (CH_3), 11.9 (CH).
HRMS (ESI+) *m/z* calcd for $[M+H]^+$ $C_{26}H_{38}F_3NO_2S_2Si$: 546.2138, found: 546.2252.

***N*-[(2*S*,3*S*,4*E*)-2-Methyl-3-(4-nitrophenyl)-5-triisopropylsilyloxy-4-pentenoyl]-1,3-thiazinane-2-thione (9'aj)**

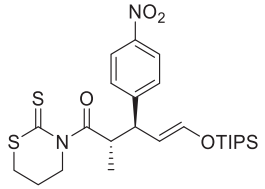

The General Procedure 8 was followed with **1a** (191 mg, 1.0 mmol, 1.0 equiv), [*(R)*-BINAP]$NiCl_2$ (75.2 mg, 100 μmol, 10 mol%), ***J*** (195 mg, 1.1 mmol, 1.1 equiv), TIPSOTf (405 μL, 1.5 mmol, 1.5 equiv), and 2,6-lutidine (140 μL, 1.2 mmol, 1.2 equiv) a_t –20 °C for 24 h.

The residue (dr 26:74) was purified by column chromatography (from 95:5 to 90:10 Hexanes/EtOAc) to give 96 mg (0.18 mmol, 18% yield) of *syn* Michael **9aj** and 268 mg (0.51 mmol, 51% yield) of the *anti* Michael **9'aj**.

Yellow thick oil.
R_f 0.5 (80:20 Hexanes/EtOAc).
$[\alpha]_D^{20}$ +94.3 (*c* 1.0 $CHCl_3$).
Chiral HPLC (Phenomenex Lux® Cellulose-5 column, 10% *i*-PrOH in Hexanes, flow rate 1 mL/min): R_t 10.7 min (*2R,3R* isomer) R_t 12.8 min (*2S,3S* isomer), 99% *ee*.
IR (ATR) ν 2939, 2864, 1726, 1655, 1608, 1345, 1168, 1135, 1125, 994, 928, 843, 710, 683 cm^{-1}.
^{1}H NMR (400 MHz, $CDCl_3$) δ 8.17–8.11 (m, 2H, ArH), 7.40–7.30 (m, 2H, ArH), 6.44 (d, *J* = 11.6 Hz, 1H, CHOTIPS), 5.00 (dd, *J* = 11.6, 10.5 Hz, 1H, CHCHOTIPS), 4.14 (dq, *J* = 10.5, 6.6 Hz, 1H, O=CCH), 3.60 (ddd, *J* = 13.4, 6.0, 5.2 Hz, 1H, NCH_xH_y), 3.46 (t, *J* = 10.5 Hz, 1H, ArCH), 3.17 (ddd, *J* = 13.4, 9.0, 4.5 Hz, 1H, NCH_xH_y), 2.71 (dt, *J* = 12.6, 6.9 Hz, 1H, SCH_xH_y), 2.36–2.26 (m, 1H, SCH_xH_y), 1.92–1.78 (m, 1H, $NCH_2CH_xH_y$), 1.40 (d, *J* = 6.6 Hz, 3H, $CHCH_3$), 1.31–0.96 (m, 22H, OTIPS, $NCH_2CH_xH_y$).
^{13}C NMR (101 MHz, $CDCl_3$) δ 204.6 (C), 180.7 (C), 151.9 (C), 146.6 (C), 143.8 (CH), 128.6 (CH), 123.8 (CH), 110.5 (CH), 50.8 (CH), 47.0 (CH), 46.0 (CH_2), 31.6 (CH_2), 22.4 (CH_2), 17.6 (CH_3), 11.9 (CH).
HRMS (ESI+) *m/z* calcd for $[M+Na]^+$ $C_{25}H_{38}N_2NaO_4S_2Si$: 545.1934, found: 545.1931. *m/z* calcd for $[M+H]^+$ $C_{25}H_{39}N_2O_4S_2Si$: 523.2115, found: 523.2117.

***N*-[(2*S*,3*S*,4*E*)-3-(3-Methoxyphenyl)-2-methyl-5-triisopropylsilyloxy-4-pentenoyl]-1,3-thiazinane-2-thione (9'ak)**

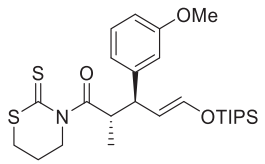

The General Procedure 8 was followed with **1a** (188 mg, 1.0 mmol, 1.0 equiv), [*(R)*-BINAP]$NiCl_2$ (15.1 mg, 20 μmol, 2 mol%), **k** (180 mg, 1.1 mmol, 1.1 equiv), TIPSOTf (405 μL, 1.5 mmol, 1.5 equiv), and 2,6-lutidine (140 μL, 1.2 mmol, 1.2 equiv) at –20 °C for 5 h.

The residue (dr 13:87) was purified by column chromatography (from 96:4 to 90:10 Hexanes/EtOAc) to give 64 mg (0.10 mmol, 10% yield) of *syn* Michael **9ak** and 278 mg (0.55 mmol, 55% yield) of the *anti* Michael **9'ak**.

Yellow oil.
R_f 0.4 (80:20 Hexanes/EtOAc).
$[\alpha]_D^{20}$ +242.7 (*c* 1.0 $CHCl_3$).
Chiral HPLC (Phenomenex Lux® Cellulose-5 column, 4% *i*-PrOH in Hexanes, flow rate 1 mL/min): R_t 8.7 min (2*R*,3*R* minor isomer) R_t 11.1 min (2*S*,3*S* major isomer), 99% *ee*.
IR (ATR) ν 2941, 2863, 1720, 1644, 1606, 1580, 1461, 1434, 1389, 1348, 1302, 1284, 1219, 1204, 1120, 1064, 1150, 988, 942, 881, 777, 706, 684, 669 cm^{-1}.
^{1}H NMR (500 MHz, $CDCl_3$) δ 7.19–7.15 (m, 1H, ArH), 6.77–6.68 (m, 3H, ArH), 6.40 (d, *J* = 11.7 Hz, 1H, CHOTIPS), 5.04 (dd, *J* = 11.7, 10.5 Hz, 1H, CHCHOTIPS), 4.05 (dq, *J* = 10.5, 6.5 Hz, 1H, O=CCH), 3.79 (s, 3H, OMe), 3.43 (dt, *J* = 13.2, 5.6 Hz, 1H, NCH_xH_y), 3.22 (t, *J* = 10.5 Hz, 1H, ArCH), 3.11 (ddd, *J* = 13.2, 8.9, 4.6 Hz, 1H, NCH_xH_y), 2.63 (dt, *J* = 12.4, 6.7 Hz, 1H, SCH_xH_y), 2.36 (ddd, *J* = 12.4, 7.5, 5.8 Hz, 1H, SCH_xH_y), 1.83–1.73 (m, 1H, $NCH_2CH_xH_y$), 1.39 (d, *J* = 6.5 Hz, 3H, $CHCH_3$), 1.27–1.16 (m, 1H, $NCH_2CH_xH_y$), 1.16–0.98 (m, 21H, OTIPS).
^{13}C NMR (126 MHz, $CDCl_3$) δ 204.1 (C), 182.3 (C), 159.8 (C), 145.7 (C), 142.7 (CH), 129.7 (CH), 120.1 (CH), 112.7 (CH), 112.5 (CH), 112.1 (CH), 55.3 (CH_3), 51.7 (CH), 47.5 (CH), 46.3 (CH_2), 31.3 (CH_2), 22.3 (CH_2), 17.7 (CH_3), 17.6 (CH_3), 11.9 (CH).
HRMS (ESI+) *m/z* calcd for $[M+H]^+$ $C_{26}H_{42}NO_3S_2Si$: 508.2370, found 508.2365.

***N*-[(2*S*,3*S*,4*E*)-3-(2-Methoxyphenyl)-2-methyl-5-triisopropylsilyloxy-4-pentenoyl]-1,3-thiazinane-2-thione (9'al)**

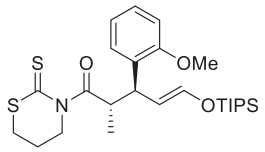

The General Procedure 8 was followed with **1a** (189 mg, 1.0 mmol, 1.0 equiv), [*(R)*-BINAP]$NiCl_2$ (37.8 mg, 50 μmol, 5 mol%), **l** (179 mg, 1.1 mmol, 1.1 equiv), TIPSOTf (405 μL, 1.5 mmol, 1.5 equiv), and 2,6-lutidine (140 μL, 1.2 mmol, 1.2 equiv) at –20 °C for 5 h.

The residue (dr 26:74) was purified by column chromatography (from 96:4 to 90:10 Hexanes/EtOAc) to give 97 mg (0.19 mmol, 19% yield) of *syn* Michael **9'al** and 217 mg (0.43 mmol, 43% yield) of the *anti* Michael **9'al**.

Yellow oil.
R_f 0.4 (80:20 Hexanes/EtOAc).
$[\alpha]_D^{20}$ +189.7 (*c* 1.0 $CHCl_3$).
Chiral HPLC (Phenomenex Lux® Cellulose-5 column, 4% *i*-PrOH in Hexanes, flow rate 1 mL/min): R_t 10.8 min (2*S*,3*S* isomer) R_t 28.4 min (2*R*,3*R* isomer), 99% *ee.*
IR (ATR) ν 2943, 2865, 1704, 1653, 1490, 1452, 1350, 1281, 1264, 1213, 1050, 984, 863, 779, 703, 591, 558 cm^{-1}.
^{1}H NMR (500 MHz, $CDCl_3$) δ 7.18–7.13 (m, 1H, ArH), 7.07–7.02 (m, 1H, ArH), 6.86–6.80 (m, 2H, ArH), 6.42 (d, *J* = 11.9 Hz, 1H, CHOTIPS), 5.24 (dd, *J* = 11.9, 10.5 Hz, 1H, CHCHOTIPS), 4.48–4.40 (m, 1H, O=CCH), 3.84 (s, 3H, OMe), 3.43 (t, *J* = 10.5 Hz, 1H, ArCH), 3.28–3.21 (m, 1H, NCH_xH_y), 3.18–3.11 (m, 1H, NCH_xH_y), 2.68–2.60 (m, 1H, SCH_xH_y), 2.46–2.38 (m, 1H, SCH_xH_y), 1.80–1.70 (m, 1H, $NCH_2CH_xH_y$), 1.34 (d, *J* = 6.6 Hz, 3H, $CHCH_3$), 1.12–1.00 (m, 22H, $NCH_2CH_xH_y$, OTIPS).
^{13}C NMR (126 MHz, $CDCl_3$) δ 203.1 (C), 183.2 (C), 157.4 (C), 142.7 (CH), 131.6 (C), 129.7 (CH), 127.7 (CH), 120.7 (CH), 111.2 (CH), 110.8 (CH), 55.1 (CH_3), 46.6 (CH), 46.3 (CH), 44.7 (CH_2), 31.4 (CH_2), 22.1 (CH_2), 17.7 (CH/CH_3), 11.9 (CH_3).
HRMS (ESI+) *m/z* calcd for $[M+H]^+$ $C_{26}H_{42}NO_3S_2Si$: 508.2370, found 508.2366.

***N*-[(2*S*,3*R*,4*E*)-2-Methyl-3-(3-methylphenyl)-5-triisopropylsilyloxy-4-pentenoyl]-1,3-thiazinane-2-thione (9'am)**

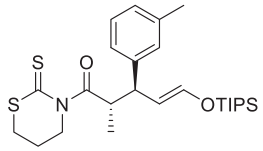

The General Procedure 8 was followed with **1a** 191 mg, 1.0 mmol, 1.0 equiv), [*(R)*-BINAP]$NiCl_2$ (37.7 mg, 50 μmol, 5 mol%), **m** (161 mg, 1.1 mmol, 1.1 equiv), TIPSOTf (405 μL, 1.5 mmol, 1.5 equiv), and 2,6-lutidine (140 μL, 1.2 mmol, 1.2 equiv) at –20 °C for 5 h.

The residue (dr 11:89) was purified by column chromatography (from 98:2 to 90:10 Hexanes/EtOAc) to give 26 mg (50 μmol, 5% yield) of *syn* Michael **9am** and 246 mg (0.50 mmol, 50% yield) of the *anti* Michael **9'am**.

Yellow oil.
R_f 0.6 (80:20 Hexanes/EtOAc).
$[\alpha]_D^{20}$ +242.2 (*c* 1.0 $CHCl_3$).
Chiral HPLC (Phenomenex Lux® Cellulose-5 column, 1.5% *i*-PrOH in Hexanes, flow rate 1 mL/min): R_t 17.3 min (2*R*,3*R* minor isomer) R_t 48.0 min (2*S*,3*S* major isomer), 99% *ee.*
IR (ATR) ν 2941, 2891, 2864, 1655, 1627, 1462, 1382, 1366, 1345, 1253, 1217, 1049, 1012, 835, 592, 561 cm^{-1}.
^{1}H NMR (400 MHz, $CDCl_3$) δ 7.17–7.11 (m, 1H, ArH), 7.01–6.92 (m, 3H, ArH), 6.39 (d, *J* = 11.7 Hz, 1H, CHOTIPS), 5.04 (dd, *J* = 11.7, 10.5 Hz, 1H, CHCHOTIPS), 4.01 (dq, *J* = 10.5, 6.5 Hz, 1H, O=CCH), 3.40 (dt, *J* = 13.2, 5.6 Hz, 1H, NCH_xH_y), 3.20 (t, *J* = 10.5 Hz, 1H, ArCH), 3.08 (ddd, *J* = 13.3, 8.9, 4.6 Hz, 1H, NCH_xH_y), 2.60 (dt, *J* = 12.3, 6.6 Hz, 1H, SCH_xH_y), 2.31 (s, 3H, $ArCH_3$), 2.30–2.23 (m, 1H, SCH_xH_y), 1.79–1.67 (m, 1H, $NCH_2CH_xH_y$), 1.38 (d, *J* = 6.5 Hz, 3H, $CHCH_3$), 1.17–0.99 (m, 22H, $NCH_2CH_xH_y$, OTIPS).
^{13}C NMR (101 MHz, $CDCl_3$) δ 204.1 (C), 182.5 (C), 144.0 (C), 142.5 (CH), 138.2 (C), 128.6 (CH), 128.4 (CH), 127.3 (CH), 124.9 (CH), 112.4 (CH), 51.6 (CH), 47.7 (CH), 46.2 (CH_2), 31.3 (CH_2), 22.2 (CH_2), 21.4 (CH_3), 17.7 (CH_3/CH), 17.6 (CH_3/CH), 11.9 (CH_3/CH).
HRMS (ESI+) *m/z* calcd for $[M+H]^+$ $C_{26}H_{42}NO_2S_2Si$: 492.2421, found 492.2410.

***N*-[(2*S*,3*S*,4*E*)-2-Methyl-3-(2-methylphenyl)-5-triisopropylsilyloxy-4-pentenoyl]-1,3-thiazinane-2-thione (9'an)**

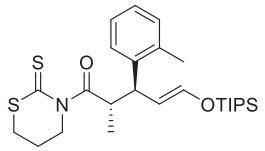

The General Procedure 8 was followed with **1a** (193 mg, 1.0 mmol, 1.0 equiv), [*(R)*-BINAP]$NiCl_2$ (37.8 mg, 50 μmol, 5 mol%), **n** (163mg, 1.1 mmol, 1.1 equiv), TIPSOTf (405 μL, 1.5 mmol, 1.5 equiv), and 2,6-lutidine (140 μL, 1.2 mmol, 1.2 equiv) at –20 °C for 16 h.

The residue (dr 17:83) was purified by column chromatography (from 98:2 to 94:6 Hexanes/EtOAc) to give 53 mg (0.11 mmol, 11% yield) of *syn* Michael **9an** and 281 mg (0.57 mmol, 56% yield) of the *anti* Michael **9'an**.

Yellow oil.
R_f 0.6 (80:20 Hexanes/EtOAc).
$[\alpha]_D^{20}$ +135.7 (*c* 1.0 $CHCl_3$).
Chiral HPLC (Phenomenex Lux® Cellulose-5 column, from 1 to 5% *i*-PrOH in Hexanes, flow rate 1 mL/min): R_t 17.3 min (2*S*,3*S* major isomer) R_t 49.1 min (2*R*,3*R* minor isomer), 99% *ee.*
IR (ATR) ν 2943, 2865, 1705, 1653, 1490, 1462, 1350, 1282, 1264, 1213, 1050, 1253, 984, 863, 796, 591 cm^{-1}.
^{1}H NMR (400 MHz, $CDCl_3$) δ 7.27–7.23 (m, 1H, ArH) 7.20–7.14 (m, 1H, ArH), 7.09–7.04 (m, 2H, ArH), 6.39 (d, *J* = 11.6 Hz, 1H, CHOTIPS), 4.94 (dd, *J* = 11.6, 10.1 Hz, 1H, CHCHOTIPS), 4.12 (dq, *J* = 10.6, 6.5 Hz, 1H, O=CCH), 3.57 (t, *J* = 10.6 Hz, 1H, ArCH), 3.22–3.07 (m, 2H, NCH_2), 2.67–2.58 (m, 1H, SCH_xH_y), 2.45–2.37 (m, 1H, SCH_xH_y), 2.27 (s, 3H, $ArCH_3$), 1.78–1.68 (m, 1H, $NCH_2CH_xH_y$), 1.41 (d, *J* = 6.5 Hz, 3H, $CHCH_3$), 1.15–1.00 (m, 22H, OTIPS, $NCH_2CH_xH_y$).
^{13}C NMR (101 MHz, $CDCl_3$) δ 203.3 (C), 182.9 (C), 142.4 (CH), 142.0 (C), 135.6 (C), 130.6 (CH), 126.9 (CH), 126.4 (CH), 126.2 (CH), 112.4 (CH), 46.7 (CH), 46.3 (CH_2), 46.2 (CH), 31.5 (CH_2), 22.0 (CH_2), 19.6 (CH_3), 17.7 (CH_3/CH), 12.3 (CH_3/CH), 11.9 (CH_3/CH).
HRMS (ESI+) *m/z* calcd for $[M+H]^+$ $C_{26}H_{42}NO_2S_2Si$: 492.2421, found 492.2412.

***N*-[(2*S*,3*S*,4*E*)-2-Methyl-3-(2-thiophenyl)-5-triisopropylsilyloxy-4-pentenoyl]-1,3-thiazinane-2-thione (9'ao)**

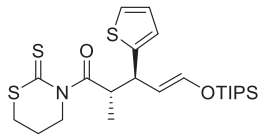

The General Procedure 8 was followed with **1a** (187 mg, 1.0 mmol, 1.0 equiv), [*(R)*-BINAP]$NiCl_2$ (38.4 mg, 51 μmol, 5 mol%), **o** (155 mg, 1.1 mmol, 1.1 equiv), TIPSOTf (405 μL, 1.5 mmol, 1.5 equiv), and 2,6-lutidine (140 μL, 1.2 mmol, 1.2 equiv) at –40 °C for 5 h.

The residue (dr 26:74) was purified by column chromatography (from 97:3 to 90:10 Hexanes/EtOAc) to give 104 mg (0.22 mmol, 22% yield) of *syn* Michael **9ao** and 302 mg (0.63 mmol, 63% yield) of the *anti* Michael **9'ao**.

Yellow solid.
Mp 75–78 °C.
R_f 0.4 (80:20 Hexanes/EtOAc).
$[\alpha]_D^{20}$ +288.4 (*c* 1.0 $CHCl_3$).
Chiral HPLC (Phenomenex Lux® Cellulose-5 column, 1% *i*-PrOH in Hexanes, flow rate 1 mL/min): R_t 13.2 min (2*R*,3*R* minor isomer) R_t 19.3 min (2*S*,3*S* major isomer), 99% *ee*.
IR (ATR) ν 2942, 2865, 2360, 2342, 1717, 1684, 1659, 1166, 1145, 1122, 1010, 881, 801, 684 cm^{-1}.
^{1}H NMR(500 MHz, $CDCl_3$) δ 7.17–7.12 (m, 1H, ArH), 6.91–6.85 (m, 1H, ArH), 6.79–6.74 (m, 1H, ArH), 6.42 (d, *J* = 11.7 Hz, 1H, CHOTIPS), 5.01 (dd, *J* = 11.7, 10.3 Hz, 1H, CHCHOTIPS), 3.94 (dq, *J* = 10.3, 6.6 Hz, 1H, O=CH), 3.73 (dt, *J* = 13.3, 5.5 Hz, 1H, NCH_xH_y), 3.64 (t, *J* = 10.3 Hz, 1H, ArCH), 3.16 (ddd, *J* = 13.3, 9.2, 4.7 Hz, 1H, NCH_xH_y), 2.70 (dt, *J* = 12.4, 6.8 Hz, 1H, SCH_xH_y), 2.51 (ddd, *J* = 12.4, 7.5, 6.0 Hz, 1H, SCH_xH_y), 1.94–1.83 (m, 1H, $NCH_2CH_xH_y$), 1.50–1.38 (m, 1H, $NCH_2CH_xH_y$), 1.38 (d, *J* = 6.6 Hz, 3H, $CHCH_3$), 1.18–0.98 (m, 21H, OTIPS).
^{13}C NMR (126 MHz, $CDCl_3$) δ 204.5 (C), 181.9 (C), 148.0 (C), 143.0 (CH), 126.6 (CH), 123.9 (CH), 123.7 (CH), 112.2 (CH), 49.2 (CH), 46.3 (CH), 46.2 (CH_2), 31.4 (CH_2), 22.5 (CH_2), 17.8 (CH_3), 17.7 (CH_3), 11.9 (CH).
HRMS (ESI+) *m/z* calcd for $[M+H]^+$ $C_{23}H_{38}NO_2S_3Si$: 484.1828, found: 484.1834.

_N_-[(2_S_,3_S_,4_E_)-3-(2-Furanyl)-2-methyl-5-triisopropylsilyloxy-4-pentenoyl]-1,3-thiazinane-2-thione (9'ap)

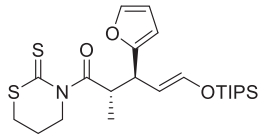

The General Procedure 8 was followed with **1a** (189, 1.0 mmol, 1.0 equiv), [*(R)*-BINAP]$NiCl_2$ (37.8 mg, 50 µmol, 5 mol%), **p** (132 mg, 1.1 mmol, 1.1 equiv), TIPSOTf (405 µL, 1.5 mmol, 1.5 equiv), and 2,6-lutidine (140 µL, 1.2 mmol, 1.2 equiv) at –20 °C for 16 h.

The residue (dr 47:53) was purified by column chromatography (from 79:20:1 to 78:20:2 Hexanes/toluene/EtOAc) to give 184 mg (0.39 mmol, 39% yield) of *syn* Michael **9ap** and 188 mg (0.40 mmol, 40% yield) of the *anti* Michael **9'ap**.

Yellow oil.
R_f 0.3 (75:20:5 Hexanes/toluene/EtOAc).
$[\alpha]_D^{20}$ +124.7 (*c* 1.0 $CHCl_3$).
Chiral HPLC (Phenomenex Lux® Cellulose-5 column, 3% *i*-PrOH in Hexanes, flow rate 1 mL/min): R_t 9.9 min (2*R*,3*R* minor isomer) R_t 17.2 min (2*S*,3*S* major isomer), 99% *ee*.
IR (ATR) ν 2941, 2891, 2864, 1713, 1658, 1165, 1128, 1009, 881, 801, 730, 676 cm^{-1}.
^{1}H NMR (500 MHz, $CDCl_3$) δ 7.33–7.29 (m, 1H, ArH), 6.41 (d, *J* = 11.8 Hz, 1H, CHOTIPS), 6.28–6.24 (m, 1H, ArH), 6.03–5.92 (m, 1H, ArH), 5.02 (dd, *J* = 11.8, 10.3 Hz, 1H, CHCHOTIPS), 4.01 (dq, *J* = 10.3, 6.6 Hz, 1H, O=CCH), 3.89–3.78 (m, 1H, NCH_xH_y), 3.46 (t, *J* = 10.3 Hz, 1H, ArCH), 3.27 (ddd, *J* = 13.5, 9.0, 4.7 Hz, 1H, NCH_xH_y), 2.80 (dt, *J* = 12.3, 6.7 Hz, 1H, SCH_xH_y), 2.71 (ddd, *J* = 12.3, 7.5, 5.9 Hz, 1H, SCH_xH_y), 2.06–1.95 (m, 1H, $NCH_2CH_xH_y$), 1.82–1.72 (m, 1H, $NCH_2CH_xH_y$), 1.35 (d, *J* = 6.6 Hz, 3H, $CHCH_3$), 1.20–0.99 (m, 21H, OTIPS).
^{13}C NMR (126 MHz, $CDCl_3$) δ 204.2 (C), 182.2 (C), 156.7 (C), 143.4 (CH), 141.2 (CH), 110.3 (CH), 109.2 (CH), 105.3 (CH), 46.4 (CH_2), 46.1 (CH), 44.2 (CH), 31.4 (CH_2), 22.6 (CH_2), 17.7 (CH_3), 17.6 (CH_3), 17.3 (CH_3), 12.3 (CH), 11.9 (CH).
HRMS (ESI+) *m/z* calcd for $[M+H]^+$ $C_{23}H_{38}NO_3S_2Si$: 468.2057, found: 468.2063.

***N*-[(2*S*,3*S*,4*E*)-2-Methyl-3-[(*E*)-2-phenylethenyl]-5-triisopropylsilyloxy-4-pentenoyl]-1,3-thiazinane-2-thione (9'aq)**

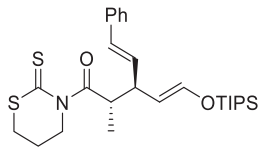

The General Procedure 8 was followed with **1a** (187 mg, 1.0 mmol, 1.0 equiv), [*(R)*-BINAP]$NiCl_2$ (15.5 mg, 21 μmol, 2 mol%), **q** (172 mg, 1.1 mmol, 1.1 equiv), TIPSOTf (405 μL, 1.5 mmol, 1.5 equiv), and 2,6-lutidine (140 μL, 1.2 mmol, 1.2 equiv) at –20 °C for 16 h.

The residue (rr 1,4/1,2 70:30, dr 1,4 17:83) was purified by column chromatography (from 98:2 to 90:10 Hexanes/EtOAc) to give 30 mg (0.07 mmol, 7% yield) of *syn* Michael **9'aq**, 242 mg (0.49 mmol, 49% yield) of the *anti* Michael **9'aq** and 101 mg (0.20 mmol, 20% yield) of 1,6-adducts **12**.

Yellow solid.
Mp 45–48 °C.
R_f 0.4 (90:10 Hexanes/EtOAc).
$[\alpha]_D^{20}$ +68.5 (*c* 1.0 $CHCl_3$).
Chiral HPLC (Phenomenex Lux® Cellulose-5 column, 5% *i*-PrOH in Hexanes, flow rate 1 mL/min): R_t 8.4 min (2*R*,3*R* minor isomer) R_t 20.4 min (2*S*,3*S* major isomer), 99% *ee*.
IR (ATR) ν 2942, 285, 1713, 1655, 1165, 1124, 983, 965, 926, 881, 790, 736, 690, 663 cm^{-1}.
^{1}H NMR ^{1}H NMR (500 MHz, $CDCl_3$) δ 7.35–7.25 (m, 4H, ArH), 7.23–7.16 (m, 1H, ArH), 6.40 (d, *J* = 11.8 Hz, 1H, CHOTIPS), 6.30 (d, *J* = 15.8 Hz, 1H, PhCH), 6.05 (dd, *J* = 15.8, 9.1 Hz, 1H, PhCHCH), 4.86 (dd, *J* = 11.8, 9.4 Hz, 1H, CHCHOTIPS), 4.02 (dt, *J* = 13.3, 5.3 Hz, 1H, NCH_xH_y), 3.73 (dq, *J* = 9.9, 6.6 Hz, 1H, O=CCH), 3.27 (ddd, *J* = 13.3, 9.4, 4.5 Hz, 1H, NCH_xH_y), 2.94 (q, *J* ≈ 9.5 Hz, 1H, PhCHCHCH), 2.75–2.59 (m, 2H, SCH_2), 1.84–1.74 (m, 1H, $NCH_2CH_xH_y$), 1.70–1.59 (m, 1H, $NCH_2CH_xH_y$), 1.31 (d, *J* = 6.6 Hz, 3H, $CHCH_3$), 1.20–1.03 (m, 21H, OTIPS).
^{13}C NMR (126 MHz, $CDCl_3$) δ 203.8 (C), 182.9 (C), 142.9 (CH), 137.0 (C), 131.3 (CH), 130.0 (CH), 128.6 (CH), 127.5 (CH), 126.0 (CH), 110.6 (CH), 49.0 (CH), 47.7 (CH), 46.6 (CH_2), 31.6 (CH_2), 22.5 (CH_2), 17.7 (CH_3), 16.7 (CH_3), 11.9 (CH).
HRMS (ESI+) *m/z* calcd for $[M+H]^+$ $C_{27}H_{41}NNaO_2S_2Si$: 526.2240, found: 526.2231.

***N*-[(2*S*,3*S*,4*Z*)-4-Bromo-2-methyl-3-phenyl-5-triisopropylsilyloxy-4-pentenoyl]-1,3-thiazinane-2-thione (9'ar)**

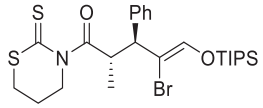

The General Procedure 8 was followed with **1a** (188 mg, 1.0 mmol, 1.0 equiv), [*(R)*-BINAP]$NiCl_2$ (38 mg, 51 μmol, 5 mol%), **r** (231 mg, 1.1 mmol, 1.1 equiv), TIPSOTf (405 μL, 1.5 mmol, 1.5 equiv), and 2,6-lutidine (140 μL, 1.2 mmol, 1.2 equiv) at –20 °C for 5 h.

The residue (dr 17:83) was purified by column chromatography (from 98:2 to 90:10 Hexanes/EtOAc) to give 98 mg (0.16 mmol, 16% yield) of *syn* Michael **9ar** and 414 mg (0.75 mmol, 75% yield) of the *anti* Michael **9'ar**.

Yellow solid.
Mp 100–104 °C.
R_f 0.3 (80:20 Hexanes/EtOAc).
$[\alpha]_D^{20}$ +157.4 (*c* 1.0 $CHCl_3$).
Chiral HPLC (Phenomenex Lux® Cellulose-4 column, 1% *i*-PrOH in Hexanes, flow rate 1 mL/min): R_t 10.3 min (2*S*,3*S* major isomer) R_t 12.4 min (2*R*,3*R* major isomer), 99% *ee*.
IR (ATR) ν 2923, 2863, 1690, 1643, 1118, 988, 879, 795, 758, 699, 684, 669, 605 cm^{-1}.
^{1}H NMR (500 MHz, $CDCl_3$) δ 7.41–7.35 (m, 2H, ArH), 7.31–7.25 (m, 2H, ArH), 7.25–7.20 (m, 1H, ArH), 6.86 (s, 1H, CHOTIPS), 4.54 (dq, *J* = 11.0, 6.5 Hz, 1H, O=CCH), 3.61 (d, *J* = 11.0 Hz, 1H, PhCH), 3.42 (ddd, *J* = 13.2, 6.0, 5.0 Hz, 1H, NCH_xH_y), 3.12 (ddd, *J* = 13.2, 9.1, 4.3 Hz, 1H, NCH_xH_y), 2.67 (dt, *J* = 12.5, 6.9 Hz, 1H, SCH_xH_y), 2.45 (ddd, *J* = 12.5, 7.1, 6.0 Hz, 1H, NCH_xH_y), 1.81–1.71 (m, 1H, $NCH_2CH_xH_y$), 1.36 (d, *J* = 6.5 Hz, 3H, $CHCH_3$), 1.21–1.03 (m, 22H, $NCH_2CH_xH_y$, OTIPS).
^{13}C NMR (126 MHz, $CDCl_3$) δ 204.0 (C), 181.6 (C), 140.7 (C), 138.5 (CH), 128.4 (CH), 127.2 (CH), 109.4 (C), 55.4 (CH), 46.3 (CH_2), 44.2 (CH), 31.5 (CH_2), 21.9 (CH_2), 17.6 (CH_3), 17.4 (CH_3), 11.9 (CH).
HRMS (ESI+) *m/z* calcd for $[M+Na]^+$ $C_{25}H_{38}BrNNaO_2S_2Si$: 578.1189, found: 578.1184.

_N_-[(2_S_,3_S_,4_E_)-2,4-Dimethyl-3-phenyl-5-triisopropylsilyloxy-4-pentenoyl]-1,3-thiazinane-2-thione (9'ac)

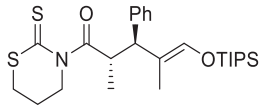

The General Procedure 8 was followed with **1a** (187 mg, 1.0 mmol, 1.0 equiv), [*(R)*-BINAP]$NiCl_2$ (15.8 mg, 21 μmol, 2 mol%), **c** (185 μL, 1.1 mmol, 1.1 equiv), TIPSOTf (405 μL, 1.5 mmol, 1.5 equiv), and 2,6-lutidine (140 μL, 1.2 mmol, 1.2 equiv) at –20 °C for 16 h.

The residue (dr 8:92) was purified by column chromatography (from 99:1 to 90:10 Hexanes/EtOAc) to give 35 mg (70 μmol, 7% yield) of *syn* Michael **9'ac** and 401 mg (0.83 mmol, 83% yield) of the *anti* Michael **9'ac**.

Yellow solid.
Mp 46–47 °C.
R_f 0.3 (90:10 Hexanes/EtOAc).
$[\alpha]_D^{20}$ +275.4 (*c* 1.0 $CHCl_3$).
Chiral HPLC (Phenomenex Lux® Cellulose-5 column, 0.8% *i*-PrOH in Hexanes, flow rate 1 mL/min): R_t 15.8 min (2*R*,3*R* minor isomer) R_t 19.0 min (2*S*,3*S* major isomer), 99% *ee*.
IR (ATR) ν 2942, 2865, 1705, 1656, 1462, 1164, 1124, 986, 880, 755, 663 cm^{-1}.
^{1}H NMR (500 MHz, $CDCl_3$) δ 7.30–7.14 (m, 2H, Ar<u>H</u>), 6.44 (q, *J* = 1.4 Hz, 1H, C<u>H</u>OTIPS), 4.46 (dq, *J* = 11.4, 6.5 Hz, 1H, O=CC<u>H</u>), 3.29 (d, *J* = 11.4 Hz, 1H, PhC<u>H</u>), 3.30–3.22 (m, 1H, NC<u>H</u>$_x$H$_y$), 3.16 (ddd, *J* = 13.2, 8.9, 4.2 Hz, 1H, NCH$_x$<u>H</u>$_y$), 2.69 (ddd, *J* = 12.4, 7.5, 6.4 Hz, 1H, SC<u>H</u>$_x$H$_y$), 2.52 (ddd, *J* = 12.4, 7.1, 5.7 Hz, 1H, SCH$_x$<u>H</u>$_y$) 1.81–1.70 (m, 1H, NCH_2C<u>H</u>$_x$H$_y$), 1.49 (d, *J* = 1.4 Hz, 3H, CC<u>H</u>$_3$), 1.30 (d, *J* = 6.5 Hz, 3H, CHC<u>H</u>$_3$), 1.17–1.01 (m, 22H, NCH_2CH_x<u>H</u>$_y$, O<u>TIPS</u>).
^{13}C NMR (126 MHz, $CDCl_3$) δ 203.3 (C), 183.1 (C), 142.3 (C), 137.0 (CH), 128.3 (C), 128.2 (CH), 126.5 (CH), 116.3 (C), 56.6 (CH), 46.5 (CH_2), 43.1 (CH), 31.7 (CH_2), 21.9 (CH_2), 17.7 (CH/CH_3), 17.3 (CH_3), 11.9 (CH/CH_3), 9.3 (CH_3).
HRMS (ESI+) *m/z* calcd for $[M+H]^+$ $C_{26}H_{42}NO_2S_2Si$: 492.2421, found: 492.2412.

***N*-[(2*S*,3*R*,4*E*)-2-Ethyl-3-phenyl-5-triisopropylsilyloxy-4-pentenoyl]-1,3-thiazinane-2-thione (9bb)**

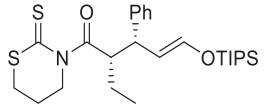

The General Procedure 8 was followed with **1b** (102 mg, 0.5 mmol, 1.0 equiv), [*(R)*-DTBM-SEGPHOS]$NiCl_2$ (65.46 mg, 50 μmol, 10 mol%), **b** (70 μL, 0.55 mmol, 1.1 equiv), TIPSOTf (200 μL, 0.75 mmol, 1.5 equiv), and 2,6-lutidine (70 μL, 0.6 mmol, 1.2 equiv) at –20 °C for 16 h.

The residue (dr 76:24) was purified by column chromatography (from 98:2 to 96:4 Hexanes/EtOAc) to give 101 mg (0.2 mmol, 38% yield) of *syn* Michael **9bb** and 23 mg (50 μmol, 9% yield) of the *anti* Michael **9'bb**.

Yellow oil.
R_f 0.5 (90:10 Hexanes/EtOAc).
$[\alpha]_D^{20}$ +190.1 (c 1.0 $CHCl_3$).
Chiral HPLC (Phenomenex Lux® Cellulose-5 column, 2% *i*-PrOH in Hexanes, flow rate 1 mL/min): R_t 8.7 min (2*R*,3*S* minor isomer), R_t 18.9 min (2*S*,3*R* major isomer), > 99% *ee*.
IR (ATR) ν 2940, 2864, 1684, 1654, 1459, 1288, 1237, 1209, 1163, 1123, 1065, 1043, 1013 cm^{-1}.
^{1}H NMR (500 MHz, $CDCl_3$) δ 7.30–7.26 (m, 2H, ArH), 7.20–7.16 (m, 3H, ArH), 6.33 (d, *J* = 11.8 Hz, 1H, CHOTIPS), 5.30 (dd, *J* = 11.8, 10.5 Hz, 1H, CHCHOTIPS), 4.44–4.39 (m, 1H, O=CCH), 4.03 (dt, *J* = 13.2, 5.7 Hz, 1H, NCH_xH_y), 3.49–3.43 (m, 1H, NCH_xH_y), 3.37 (dd, *J* = 10.5, 9.0 Hz, 1H, PhCH), 2.87–2.77 (m, 2H, CH_2CH_3), 2.11–2.02 (m, 1H, SCH_xH_y), 2.01–1.90 (m, 1H, SCH_xH_y), 1.78–1.67 (m, 1H, $NCH_2CH_xH_y$), 1.63–1.54 (m, 1H, $NCH_2CH_xH_y$), 1.14–0.99 (m, 21H, OTIPS), 0.85 (t, *J* = 7.4 Hz, 3H, CH_2CH_3).
^{13}C NMR (126 MHz, $CDCl_3$) δ 205.4 (C), 180.1 (C), 143.5 (C) 141.7 (CH), 128.4 (CH), 127.4 (CH), 111.7 (CH), 51.8 (CH), 46.3 (CH_2), 48.2 (CH), 31.4 (CH_2), 24.4 (CH_2), 22.6 (CH_2), 11.0 (CH_3).
HRMS (ESI+) *m/z* calcd. for $[M+H]^+$ $C_{26}H_{41}NO_2S_2Si$: 492.2431, found 492.2421.

_N_-[(2_S_,3_R_,4_E_)-2-(3-Butynyl)-3-phenyl-5-triisopropylsilyloxy-4-pentenoyl]-1,3-thiazinane-2-thione (9eb)

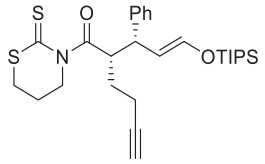

The General Procedure 8 was followed with **1e** (114 mg, 0.5 mmol, 1.0 equiv), [*(R)*-DTBM-SEGPHOS]$NiCl_2$ (65.5 mg, 50 μmol, 10 mol%), **b** (70 μL, 0.55 mmol, 1.1 equiv), TIPSOTf (200 μL, 0.75 mmol, 1.5 equiv), and 2,6-lutidine (70 μL, 0.6 mmol, 1.2 equiv) at –20 °C for 16 h.

The residue (dr 71:29) was purified by column chromatography (from 98:2 to 96:4 Hexanes/EtOAc) to give 120 mg (0.2 mmol, 53% yield) of *syn* Michael **9eb** and 51 mg (90 μmol, 23% yield) of the *anti* Michael **9'eb**.

Yellow oil.
R_f 0.4 (80:20 Hexanes/EtOAc).
$[\alpha]_D^{20}$ +196.0 (c 1.0 $CHCl_3$).
Chiral HPLC (Phenomenex Lux® Cellulose-5 column, 1% *i*-PrOH in Hexanes, flow rate 1 mL/min): R_t 18.4 min (2*R*,3*S* enatiomer), R_t 37.1 min (2*S*,3*R* isomer), >99% *ee*.
IR (ATR) ν 2941, 2864, 1695, 1654, 1462, 1287, 1161, 1124, 1050, 1013 cm^{-1}.
^{1}H NMR (500 MHz, $CDCl_3$) δ 7.31–7.26 (m, 2H, ArH), 7.22–7.17 (m, 3H, ArH), 6.32 (d, *J* = 11.7 Hz, CHOTIPS), 5.29 (dd, *J* = 11.7, 10.6 Hz, CHCHOTIPS), 4.60–4.55 (m, 1H, O=CCH), 4.01 (dt, *J* = 13.2, 5.7 Hz, 1H, NCH_xH_y), 3.47–3.41 (m, 1H, NCH_xH_y), 3.36 (dd, *J* =10.6, 8.8 Hz, PhCH), 2.83–2.78 (m, 2H, SCH_2), 2.22–2.17 (m, 2H, $CHCH_2CH_2$), 2.10–1.92 (m, 3H, $CHCH_xH_y$, NCH_2CH_2), 1.91 (t, *J* = 2.6 Hz, 1H, CCH), 1.82–1.71 (m, 1H, $CHCH_xH_y$), 1.15–0.98 (m, 21H, OTIPS).
^{13}C NMR (126 MHz, $CDCl_3$) δ 205.8 (C), 54 179.5 (C), 143.0 (C), 126.6 (C), 83.7 (C), 142.1 (CH), 128.7 (CH), 127.7 (CH), 111.0 (CH), 68.8. (CH), 50.3 (CH), 48.5 (CH), 46.4 (CH_2), 31.3 (CH_2), 30.1 (CH_2), 22.75 (CH_2), 16.04 (CH_2).
HRMS (ESI+) *m/z* calcd. for $[M+H]^+$ $C_{28}H_{42}NO_2S_2Si$ 516.2421, found 516.2423.

_N_-[(2_S_,3_R_,4_E_)-2-(3-Methoxy-3-oxopropyl)-3-phenyl-5-triisopropylsilyloxy-4-pentenoyl]-1,3-thiazinane-2-thione (9fb)

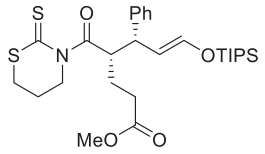

The General Procedure 8 was followed with **1f** (132 mg, 0.5 mmol, 1.0 equiv), [*(R)*-DTBM-SEGPHOS]$NiCl_2$ (33.2 mg, 25 μmol, 5 mol%), **b** (70 μL, 0.55 mmol, 1.1 equiv), TIPSOTf (200 μL, 0.75 mmol, 1.5 equiv), and 2,6-lutidine (70 μL, 0.6 mmol, 1.2 equiv) at –20 °C for 16 h.

The residue (80% conversion, dr 85:15) was purified by column chromatography (from 95:5 to 80:20 Hexanes/EtOAc) to give 149 mg (0.27 mmol, 54% yield) of *syn* Michael **9fb** and 30 mg (50 μmol, 11% yield) of the *anti* Michael **9'fb**.

Yellow oil.
R_f 0.6 (80:20 Hexanes/EtOAc).
$[\alpha]_D^{20}$ +193.3 (c 1.0 $CHCl_3$).
Chiral HPLC (Phenomenex Lux® Cellulose-4 column, 5% *i*-PrOH in Hexanes, flow rate 1 mL/min): R_t 15.5 min (2*S*,3*R* major isomer) R_t 20.2 min (2*R*,3*S* minor isomer), 99% *ee*.
IR (ATR) ν 2943, 2865, 1735, 1654, 1162, 1124, 1045, 881, 761, 685 cm^{-1}.
^{1}H NMR (400 MHz, $CDCl_3$) δ 7.33–7.24 (m, 2H, ArH), 7.23–7.13 (m, 3H, ArH), 6.32 (d, *J* = 11.7 Hz, 1H, CHOTIPS), 5.21 (dd, *J* = 11.7, 10.6 Hz, 1H, CHCHOTIPS), 4.62–4.53 (m, 1H, O=CCH), 4.13 (dt, *J* = 13.2, 5.7 Hz, 1H, NCH_xH_y), 3.60 (s, 3H, COOMe), 3.41 (ddd, *J* = 13.2, 8.7, 5.2 Hz, 1H, NCH_xH_y), 3.32 (dd, *J* = 10.6, 9.4 Hz, 1H, PhCH), 2.95–2.79 (m, 2H, SCH_2), 2.42–2.26 (m, 2H, $O{=}CCHCH_2$), 2.15–1.95 (m, 3H, CH_2COOCH_3, $NCH_2CH_xH_y$), 1.90–1.79 (m, 1H, $NCH_2CH_xH_y$), 1.15–0.93 (m, 21H, OTIPS).
^{13}C NMR (101 MHz, $CDCl_3$) δ 205.9 (C), 179.7 (C), 173.5 (C), 142.7 (C), 141.8 (CH), 128.7 (CH), 127.4 (CH), 126.6 (CH), 111.5 (CH), 51.5 (CH_3), 50.0 (CH), 49.3 (CH), 46.4 (CH_2), 31.3 (CH_2), 26.3 (CH_2), 22.8 (CH_2), 17.6 (CH_3), 11.8 (CH).
HRMS (ESI+) *m/z* calcd for $[M+H]^+$ $C_{28}H_{44}NO_4S_2Si$: 550.2476, found: 550.2471.

***N*-[(2*S*,3*S*,4*E*)-2-Azido-3-phenyl-5-triisopropylsilyloxy-4-pentenoyl]-1,3-thiazolidine-2-thione (9ob)**

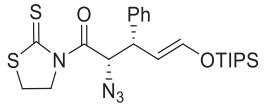

The General Procedure 8 was followed with **1o** (100 mg, 0.5 mmol, 1.0 equiv), [*(R)*-DTBM-SEGPHOS]$NiCl_2$ (65.4 mg, 50 μmol, 10 mol%), **b** (70 μL, 0.55 mmol, 1.1 equiv), TIPSOTf (200 μL, 0.75 mmol, 1.5 equiv), and 2,6-lutidine (70 μL, 0.6 mmol, 1.2 equiv) at –20 °C for 16 h.

The residue (dr 90:10) was purified by column chromatography (from 90:10 to 80:20 Hexanes/EtOAc) to give 162 mg (0.3 mmol, 66% yield) of *syn* Michael **9ob** and 18 mg (30 μmol, 7% yield) of the *anti* Michael **9'ob**.

Yellow solid.
Mp 141–145 °C (decomposition).
R_f 0.4 (80:20 Hexanes/EtOAc).
$[\alpha]_D^{20}$ +123.2 (*c* 1.0 $CHCl_3$).
Chiral HPLC (Phenomenex Lux® Cellulose-5 column, 6% *i*-PrOH in Hexanes, flow rate 1 mL/min): R_t 6.5 min (2*R*,3*S* minor isomer), R_t 7.0 min (2*S*,3*R* major isomer), 99% *ee*.
IR (ATR) ν 2921, 2863, 2095, 1688, 1653, 1456, 1360, 1269, 1234, 1222, 1184, 1153, 1046, 1014 cm^{-1}.
^{1}H NMR (500 MHz, $CDCl_3$) δ 7.36–7.32 (m, 2H, ArH), 7.29–7.24 (m, 3H, ArH) 6.45 (d, *J* = 11.7 Hz, 1H, CHOTIPS), 6.39 (d, *J* = 10.0 Hz, 1H, O=CCH), 5.27 (dd, *J* = 11.7, 10.0 Hz, 1H, CHCHOTIPS), 4.55–4.43 (m, 2H, NCH_2), 3.79 (t, *J* = 10.0 Hz, PhCH), 3.34–3.23 (m, 2H, SCH_2), 1.16–0.99 (m, 21H, OTIPS).
^{13}C NMR (126 MHz, $CDCl_3$) δ 143.9 (CH), 140.5 (C), 128.9 (CH), 127.7 (CH), 127.3 (C), 108.6 (CH), 63.9 (CH), 56.0 (CH_2), 47.9 (CH), 28.7 (CH_2).
HRMS (ESI+) *m/z* calcd for $[M+H]^+$ $C_{23}H_{34}N_4O_2S_2Si$: 490.1789, found 490.1785.

***N*-[(2*S*,3*S*,4*E*)-2-Ethyl-3-phenyl-5-triisopropylsilyloxy-4-pentenoyl]-1,3-thiazinane-2-thione (9'bb)**

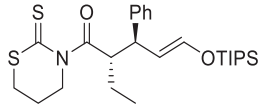

The General Procedure 8 was followed with **1b** (102 mg, 0.5 mmol, 1.0 equiv), [*(R)*-BINAP]$NiCl_2$ (18.82 mg, 25 μmol, 5 mol%), **b** (70 μL, 0.55 mmol, 1.1 equiv), TIPSOTf (200 μL, 0.75 mmol, 1.5 equiv), and 2,6-lutidine (70 μL, 0.6 mmol, 1.2 equiv) at –20 °C for 5 h.

The residue (dr 20:80) was purified by column chromatography (from 98:2 to 96:4 Hexanes/EtOAc) to give 31 mg (60 μmol, 12% yield) of *syn* Michael **9bb** and 150 mg (0.3 mmol, 57% yield) of the *anti* Michael **9'bb**.

Yellow oil.
R_f 0.5 (90:10 Hexanes/EtOAc).
$[\alpha]_D^{20}$ +244.8 (c 1.0 $CHCl_3$).
Chiral HPLC (Phenomenex Lux® Cellulose-5 column, 2% *i*-PrOH in Hexanes, flow rate 1 mL/min): R_t 15.1 min (2*R*,3*R* minor isomer), R_t 17.7 min (2*S*,3*S* major isomer), >99% *ee*.
IR (ATR) ν 2940, 2864, 1684, 1654, 1459, 1288, 1237, 1209, 1163, 1123, 1065, 1043, 1013 cm^{-1}.
^{1}H NMR (500 MHz, $CDCl_3$) δ 7.28–7.24 (m, 2H, ArH), 7.19–7.15 (m, 3H, ArH), 6.38 (d, *J* = 11.7 Hz, 1H, CHOTIPS), 5.07 (dd, *J* = 11.7, 10.5 Hz,1H, CHCHOTIPS) 4.29 (ddd, *J* = 10.5, 6.5, 4.7 Hz, 1H, O=CCH), 3.73 (dt, *J* = 13.3, 5.4 Hz, 1H, NCH_xH_y), 3.35 (t, *J* = 10.5 Hz, 1H, PhCH), 3.08 (ddd, *J* = 13.3, 9.3, 4.5 Hz, 1H, NCH_xH_y), 2.56 (dt, *J* = 12.4, 6.9 Hz, 1H, SCH_xH_y), 2.19 (ddd, *J* = 12.4, 7.2, 6.3 Hz, SCH_xH_y), 1.99–1.89 (m, 1H, $NCH_2CH_xH_y$), 1.90–1.80 (m, 2H, CH_2CH_3), 1.80–1.70 (m, 1H, $NCH_2CH_xH_y$), 1.15–0.97 (m, 25H, OTIPS, CH_2CH_3, $NCH_2CH_xH_y$).
^{13}C NMR (126 MHz, $CDCl_3$) δ 205.1 (C), 179.8 (C), 144.1 (C), 141.9 (CH), 128.7 (CH), 127.7 (CH), 112.3 (CH), 51.3 (CH_2), 50.3 (CH), 46.0 (CH_2), 31.4 (CH_2), 24.9 (CH_2), 22.2 (CH), 11.1 (CH_3).
HRMS (ESI+) *m/z* calcd for $[M+H]^+$ $C_{26}H_{41}NO_2S_2Si$: 492.2431, found 492.2421.

_N_-[(2_S_,3_R_,4_E_)-2-(3-Butynyl)-3-phenyl-5-triisopropylsilyloxy-4-pentenoyl]-1,3-thiazinane-2-thione (9'eb)

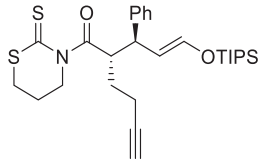

The General Procedure 8 was followed with **1e** (114 mg, 0.5 mmol, 1.0 equiv), [*(R)*-BINAP]$NiCl_2$ (18.8 mg, 25 µmol, 5 mol%), **b** (70 µL, 0.55 mmol, 1.1 equiv), TIPSOTf (200 µL, 0.75 mmol, 1.5 equiv), and 2,6-lutidine (70 µL, 0.6 mmol, 1.2 equiv) at –20 °C for 16 h.

The residue (dr 18:82) was purified by column chromatography (from 95:5 to 85:15 Hexanes/EtOAc) to give 34 mg (70 µmol, 13% yield) of *syn* Michael **9eb** and 139 mg (0.2 mmol, 53% yield) of the *anti* Michael **9'eb**.

Yellow oil.
R_f 0.5 (80:20 Hexanes/EtOAc).
$[\alpha]_D^{20}$ +204.94 (*c* 1.0 $CHCl_3$).
Chiral HPLC (Phenomenex Lux® Cellulose-1 column, 2% *i*-PrOH in Hexanes, flow rate 1 mL/min): R_t 7.9 min (2*R*,3*S* minor isomer), R_t 8.6 min (2*S*,3*R* major isomer), > 99% *ee*.
IR (ATR) ν 2941, 2864, 1695, 1654, 1462, 1287, 1161, 1124, 1050, 1013 cm^{-1}.
^{1}H NMR (500 MHz, $CDCl_3$) δ 7.39–7.25 (m, 2H, ArH), 7.24–7.15 (m, 3H, ArH), 6.41 (d, *J* = 11.7 Hz, 1H, CHOTIPS), 5.06 (dd, *J* = 11.7, 10.5 Hz, 1H, CHCHOTIPS), 4.39 (ddd, *J* = 10.5, 6.9, 4.7 Hz, O=CCH), 3.70 (dt, *J* = 13.2, 5.4 Hz, 1H, NCH_xH_y), 3.31 (t, *J* = 10.5 Hz, 1H, PhCH), 3.09 (ddd, *J* = 13.4, 9.2, 4.5 Hz, 1H, NCH_xH_y), 2.62–2.48 (m, 2H, $CHCH_2$), 2.39–2.30 (m, 1H, SCH_xH_y), 2.23–2.02 (m, 3H, $CHCH_2CH_2$, SCH_xH_y), 1.92 (t, 1H, *J* = 2.6 Hz, CCH), 1.84–1.66 (m, 1H, $NCH_2CH_xH_y$), 1.17–0.99 (m, 22H, $NCH_2CH_xH_y$, OTIPS).
^{13}C NMR (126 MHz, $CDCl_3$) δ 205.3 (C), 179.2 (C), 143.7 (C), 126.6 (C), 84.2 (C), 142.5 (CH), 128.9 (CH), 127.7 (CH), 111.8 (CH), 68.1 (CH), 50.7 (CH), 49.9 (CH), 46.4 (CH_2), 31.3 (CH_2), 29.5 (CH_2), 22.8 (CH_2), 16.0 (CH_2).
HRMS (ESI+) *m/z* calcd for $[M+H]^+$ $C_{28}H_{42}NO_2S_2Si$ 516.2421, found 516.2423.

***N*-[(2*S*,3*S*,4*E*)-2-(3-Methoxy-3-oxopropyl)-3-phenyl-5-triisopropylsilyloxy-4-pentenoyl]-1,3-thiazinane-2-thione (9'fb)**

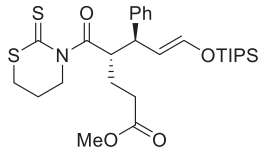

The General Procedure 8 was followed with **1f** (129 mg, 0.5 mmol, 1.0 equiv), [*(R)*-BINAP]$NiCl_2$ (19.3 mg, 26 μmol, 5 mol%), **b** (70 μL, 0.55 mmol, 1.1 equiv), TIPSOTf (200 μL, 1.5 mmol, 1.5 equiv), and 2,6-lutidine (70 μL, 1.2 mmol, 1.2 equiv) at –20 °C for 16 h.

The residue (dr 20:80) was purified by column chromatography (from 95:5 to 80:20 Hexanes/EtOAc) to give 49 mg (90 μmol, 18% yield) of *syn* Michael **9fb** and 193 mg (0.35 mmol, 70% yield) of the *anti* Michael **9'fb**.

Yellow solid.
Mp 53–55 °C.
R_f 0.5 (80:20 Hexanes/EtOAc).
$[\alpha]_D^{20}$ +220.4 (*c* 1.0 $CHCl_3$).
Chiral HPLC (Phenomenex Lux® Cellulose-5 column, 10% *i*-PrOH in Hexanes, flow rate 1 mL/min): R_t 13.5 min (2*S*,3*S* major isomer) R_t 35.4 min (2*R*,3*R* minor isomer), 99% *ee*.
^{1}H NMR (400 MHz, $CDCl_3$) δ 7.31–7.23 (m, 2H, ArH), 7.23–7.13 (m, 3H, ArH), 6.40 (d, *J* = 11.7 Hz, 1H, CHOTIPS), 5.07 (dd, *J* = 11.7, 10.5 Hz, 1H, CHCHOTIPS), 4.45 (ddd, *J* = 10.5, 7.6, 4.3 Hz, 1H, O=CCH), 3.72 (dt, *J* = 13.3, 5.4 Hz, 1H, NCH_xH_y), 3.65 (s, 3H, COOMe), 3.29 (t, *J* = 10.5 Hz, 1H, PhCH), 3.07 (ddd, *J* = 13.4, 9.3, 4.5 Hz, 1H, NCH_xH_y), 2.71 (ddd, *J* = 16.6, 11.1, 5.7 Hz, 1H, CH_xH_yCOOMe), 2.61–2.42 (m, 2H, SCH_xH_y, CH_xH_yCOOMe), 2.35–2.20 (m, 1H, $O=CCHCH_xH_y$), 2.20–2.05 (m, 2H, $O=CCHCH_xH_y$, SCH_xH_y), 1.82–1.68 (m, 1H, $NCH_2CH_xH_y$), 1.17–0.94 (m, 22H, $NCH_2CH_xH_y$, OTIPS).
^{13}C NMR (101 MHz, $CDCl_3$) δ 205.5 (C), 179.4 (C), 173.6 (C), 143.7 (C), 142.4 (CH), 128.8 (CH), 128.7 (CH), 127.6 (CH), 126.6 (CH), 112.0 (CH), 51.4 (CH_3), 50.7 (CH), 49.4 (CH), 46.1 (CH_2), 31.4 (CH_2), 31.2 (CH_2), 26.8 (CH_2), 22.1 (CH_2), 17.6 (CH_3), 11.9 (CH).
HRMS (ESI+) *m/z* calcd for $[M+H]^+$ $C_{28}H_{44}NO_4S_2Si$: 550.2476, found: 550.2471.

***N*-[(2*S*,3*R*,4*E*)-2-Azido-3-phenyl-5-triisopropylsilyloxy-4-pentenoyl]-1,3-thiazolidine-2-thione (9'ob)**

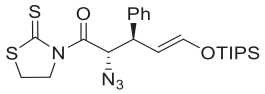

The General Procedure 8 was followed with **1o** (96 mg, 0.5 mmol, 1.0 equiv), [*(R)*-BINAP]$NiCl_2$ (17.0 mg, 50 μmol, 5 mol%), **b** (70 μL, 0.55 mmol, 1.1 equiv), TIPSOTf (200 μL, 0.75 mmol, 1.5 equiv), and 2,6-lutidine (70 μL, 0.6 mmol, 1.2 equiv) at –20 °C for 16 h.

The residue (dr 50:50) was purified by column chromatography (from 95:5 to 85:15 Hexanes/EtOAc) to give 105 mg (0.21 mmol, 45% yield) of *syn* Michael **9ob** and 105 mg (0.21 mmol, 45% yield) of the *anti* Michael **9'ob**.

Yellow thick oil.
R_f 0.3 (80:20 Hexanes/EtOAc).
$[\alpha]_D^{20}$ +76.2 (*c* 1.0 $CHCl_3$).
Chiral HPLC (Phenomenex Lux® Cellulose-5 column, 6% iPrOH in Hexanes, flow rate 1 mL/min): R_t 12.6 min (2*S*,3*R* major isomer), R_t 15.9 min (2*R*,3*S* minor isomer), 99% *ee*.
IR (ATR) ν 2921, 2863, 2095, 1688, 1653, 1456, 1360, 1269, 1234, 1222, 1184, 1153, 1046, 1014 cm^{-1}.
^{1}H NMR (500 MHz, $CDCl_3$) δ 7.35–7.28 (m, 2H, ArH), 7.30–7.21 (m, 3H, ArH), 6.57 (dd, *J* = 11.7, 0.7 Hz, 1H, CHOTIPS), 6.08 (d, *J* = 9.7 Hz, 1H, O=CCH), 5.30 (dd, *J* = 11.7, 9.7 Hz, 1H, CHCHOTIPS), 4.08 (ddd, *J* = 12.4, 11.7, 7.4 Hz, 1H, NCH_xH_y), 3.88 (ddd, *J* = 11.7, 7.4, 2.0 Hz, 1H, NCH_xH_y), 3.69 (t, *J* = 9.7 Hz, 1H, PhCH), 2.89 (ddd, *J* = 10.8, 7.4, 2.0 Hz, 1H, SCH_xH_y), 2.59 (ddd, *J* = 12.4, 10.8, 7.4 Hz, 1H, SCH_xH_y), 1.21–1.01 (m, 21H, OTIPS).
^{13}C NMR (126 MHz, $CDCl_3$) δ 201.9 (C), 173.0 (C), 144.2 (CH), 139.8 (C), 128.8 (CH), 127.8 (CH), 127.4 (CH), 108.9 (CH), 64.5 (CH), 55.9 (CH_2), 49.2 (CH), 28.8 (CH_2), 17.6 (CH_3), 11.9 (CH).
HRMS (ESI+) *m/z* calcd. for $[M+H]^+$ $C_{23}H_{34}N_4O_2S_2Si$: 490.1789, found 490.1785.

***N*-[(2*R*,3*S*,4*E*)-2-(4-Methoxyphenoxymethyl)-3-phenyl-5-triisopropylsilyloxy-4-pentenoyl]-1,3-thiazinane-2-thione (9'pb)**

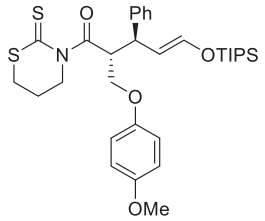

The General Procedure 8 was followed with **1p** (311 mg, 0.5 mmol, 1.0 equiv), [*(R)*-BINAP]$NiCl_2$ (37.6 mg, 50 μmol, 10 mol%), **b** (70 μL, 0.55 mmol, 1.1 equiv), TIPSOTf (200 μL, 0.75 mmol, 1.5 equiv), and 2,6-lutidine (70 μL, 0.6 mmol, 1.2 equiv) at –20 °C for 5 h.

The residue (dr 10:90) was purified by column chromatography (from 95:5 to 85:15 Hexanes/EtOAc) to give 30 mg (50 μmol, 10% yield) of *syn* Michael **9pb** and 183 mg (0.3 mmol, 61% yield) of the *anti* Michael **9'pb**.

Yellow oil.
R_f 0.5 (80:20 Hexanes/EtOAc).
$[\alpha]_D^{20}$ +144.56 (*c* 1.0 $CHCl_3$).
Chiral HPLC (Phenomenex Lux® Cellulose-5 column, 4% *i*-PrOH in Hexanes, flow rate 1 mL/min): R_t 17.9 min (2*R*,3*S* major isomer), R_t 27.2 min (2*S*,3*R* minor isomer), > 99% *ee*.
IR (ATR) ν 2922, 1703, 1657, 1507, 1458, 1347, 1307, 1233, 1208, 1187, 1152, 1121, 1066, 1039, 1028, 1013 cm^{-1}.
^{1}H NMR (500 MHz, $CDCl_3$) δ 7.29–7.26 (m, 5H, ArH), 6.87–6.71 (m, 4H, ArH), 6.42 (d, *J* = 11.7 Hz, 1H, CHOTIPS), 5.15 (dd, *J* = 11.7, 10.4 Hz, 1H, CHCHOTIPS), 4.69 (ddd, *J* = 10.4, 5.3, 3.7 Hz, 1H, O=CCH), 4.37–4.28 (m, 2H, CH_2OAr), 3.82 (t, *J* = 10.4 Hz , 1H, PhCH), 3.76 (s, 3H, OMe), 3.62 (ddd, *J* = 13.3, 6.5, 5.0 Hz, 1H, NCH_xH_y), 3.34 (ddd, *J* = 13.3, 8.4, 4.6 Hz, 1H, NCH_xH_y), 2.67 (dt, *J* = 12.4, 6.8 Hz,1H, SCH_xH_y), 2.39 (ddd, *J* = 12.4, 7.3, 6.3 Hz, 1H, SCH_xH_y), 1.88–1.78 (m, 1H, $NCH_2CH_xH_y$), 1.43–1.31 (m, 1H, $NCH_2CH_xH_y$), 1.10–0.88 (m, 21H, OTIPS).
^{13}C NMR (126 MHz, $CDCl_3$) δ 204.5 (C), 177.2 (C), 153.7 (C), 152.6 (C), 143.5 (C), 142.5 (CH), 128.6 (CH), 127.8 (CH), 126.4 (CH), 115.6 (CH), 114.3 (CH), 111.0 (CH), 68.6 (CH_2), 55.8 (CH_3), 51.0 (CH), 46.5 (CH_2), 46.1 (CH), 31.6 (CH_2), 22.4 (CH_2), 17.5 (CH/CH_3), 11.9 (CH/CH_3).
HRMS (ESI+) *m/z* calcd for $[M+H]^+$ $C_{32}H_{46}NO_4S_2Si$: 600.2632, found 600.2633.

***N*-[(2*S*,3*S*,4*E*)-2-Benzyl-3-phenyl-5-triisopropylsilyloxy-4-pentenoyl]-1,3-thiazinane-2-thione (9'qb)**

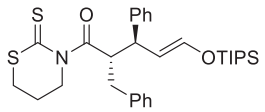

The General Procedure 8 was followed with **1q** (130 mg, 0.5 mmol, 1.0 equiv), [*(R)*-BINAP]$NiCl_2$ (8.0 mg, 11 μmol, 2 mol%), **b** (70 μL, 0.55 mmol, 1.1 equiv), TIPSOTf (405 μL, 1.5 mmol, 1.5 equiv), and 2,6-lutidine (70 μL, 0.6 mmol, 1.2 equiv) at –20 °C for 16 h.

The residue (dr 15:85) was purified by column chromatography (from 98:2 to 94:6 Hexanes/EtOAc) to give 25 mg (50 μmol, 10% yield) of *syn* Michael **9qb** and 123 mg (0.24 mmol, 47% yield) of the *anti* Michael **9'qb**.

Yellow solid.
Mp 69–72 °C.
R_f 0.5 (80:20 Hexanes/EtOAc).
$[\alpha]_D^{20}$ +62.1 (*c* 1.0 $CHCl_3$).
Chiral HPLC (Phenomenex Lux® Cellulose-5 column, 1% *i*-PrOH in Hexanes, flow rate 1 mL/min): R_t 8.4 min (2*R*,3*R* minor isomer) R_t 19.9 min (2*S*,3*S* major isomer), 99% *ee*.
IR (ATR) ν 2920, 2862, 1687, 1658, 1172, 1159, 920, 882, 822, 696 cm^{-1}.
^{1}H NMR (400 MHz, $CDCl_3$) δ 7.29–7.12 (m, 10H, ArH), 6.38 (d, *J* = 11.7 Hz, 1H, CHOTIPS), 5.22 (dd, *J* = 11.7, 10.3 Hz, 1H, CHCHOTIPS), 4.83–4.76 (m, 1H, O=CCH), 3.65 (dd, *J* = 10.3, 8.6 Hz, 1H, PhCH), 3.45 (ddd, *J* = 13.3, 7.1, 5.1 Hz, 1H, NCH_xH_y), 3.34 (ddd, *J* = 13.3, 7.7, 4.8 Hz, 1H, NCH_xH_y), 3.15–3.00 (m, 2H, $PhCH_2$), 2.41–2.22 (m, 2H, SCH_2), 1.61–1.50 (m, 1H, $NCH_2CH_xH_y$), 1.43–1.29 (m, 1H, $NCH_2CH_xH_y$), 1.17–0.96 (m, 21H, OTIPS).
^{13}C NMR (101 MHz, $CDCl_3$) δ 205.1 (C), 178.8 (C), 143.6 (C), 142.7 (CH), 139.3 (C), 129.6 (CH), 128.5 (CH), 128.1 (CH), 127.9 (CH), 126.4 (CH), 126.1 (CH), 111.5 (CH), 52.5 (CH), 49.2 (CH), 46.1 (CH_2), 37.6 (CH_2), 31.4 (CH_2), 22.2 (CH_2), 17.7 (CH_3), 11.9 (CH).
HRMS (ESI+) *m/z* calcd for $[M+H]^+$ $C_{31}H_{44}NO_2S_2Si$: 554.2577, found: 554.2573.

***N*-[(2*R*,3*S*,4*E*)-2,3-Diphenyl-5-triisopropylsilyloxy-4-pentenoyl]-1,3-thiazinane-2-thione (9'rb)**

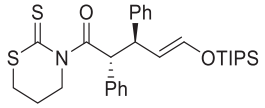

The General Procedure 8 was followed with **1r** (130 mg, 0.5 mmol, 1.0 equiv), [*(R)*-BINAP]$NiCl_2$ (8 mg, 11 μmol, 2 mol%), **b** (70 μL, 0.55 mmol, 1.1 equiv), TIPSOTf (200 μL, 0.75 mmol, 1.5 equiv), and 2,6-lutidine (70 μL, 0.6 mmol, 1.2 equiv) at –20 °C for 16 h.

The residue (dr 15:85) was purified by column chromatography (from 98:2 to 94:6 Hexanes/EtOAc) to give 25 mg (0.05 mmol, 10% yield) of *syn* Michael **9rb** and 123 mg (0.24 mmol, 47% yield) of the *anti* Michael **9'rb**.

Yellow solid.
Mp 66–69 °C.
R_f 0.4 (90:10 Hexanes/EtOAc)
$[\alpha]_D^{20}$ +37.5 (*c* 1.0 $CHCl_3$).
Chiral HPLC (Phenomenex Lux® Cellulose-5 column, 5% *i*-PrOH in Hexanes, flow rate 1 mL/min): R_t 17.2 min (2*R*,3*S* major isomer) R_t 38.4 min (2*S*,3*R* minor isomer), 99% *ee*.
IR (ATR) ν 2942, 2865, 1676, 1655, 1160, 1127, 757, 728, 696, 666 cm^{-1}.
^{1}H NMR ^{1}H NMR (500 MHz, $CDCl_3$) δ 7.56–7.50 (m, 2H, ArH), 7.36–7.28 (m, 6H, ArH), 7.24–7.19 (m, 2H, ArH), 5.89 (d, *J* = 11.7 Hz, 1H, CHOTIPS), 5.36 (d, *J* = 11.1 Hz, 1H, O=CCH), 4.89 (dd, *J* = 11.7, 9.5 Hz, 1H, CHCHOTIPS), 3.84 (dd, *J* = 11.1, 9.5 Hz, 1H, CHCHCHOTIPS), 3.50 (ddd, *J* = 13.1, 6.7, 5.3 Hz, 1H, NCH_xH_y), 3.26 (ddd, *J* = 13.1, 7.9, 4.9 Hz, 1H, NCH_xH_y), 2.45 (dt, *J* = 12.5, 6.8 Hz, 1H, SCH_xH_y), 2.32 (dt, *J* = 12.5, 6.8 Hz, 1H, SCH_xH_y), 1.71–1.61 (m, 1H, $NCH_2CH_xH_y$), 1.35–1.27 (m, 1H, $NCH_2CH_xH_y$), 0.91–0.80 (m, 21H, OTIPS).
^{13}C NMR (126 MHz, $CDCl_3$) δ 205.4 (C), 177.3 (C), 143.5 (C), 142.6 (CH), 138.1 (C), 129.4 (CH), 128.6 (CH), 128.2 (CH), 128.1 (CH), 127.1 (CH), 126.6 (CH), 111.9 (CH), 57.7 (CH), 51.9 (CH), 46.4 (CH_2), 31.1 (CH_2), 22.2 (CH_2), 17.6 (CH/CH_3), 11.6 (CH/CH_3).
HRMS (ESI+) *m/z* calcd for $[M+H]^+$ $C_{30}H_{41}NO_2S_2Si$: 540.2428, found: 540.2421.

8 Other α,β-unsaturated compounds

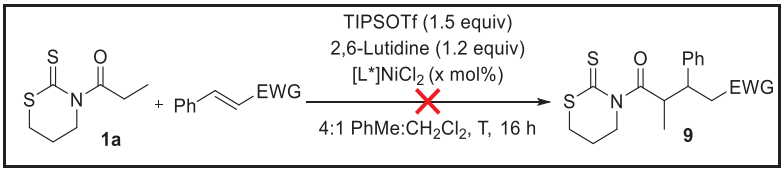

The General Procedure 8 was followed with **1a** (189 mg, 1 mmol, 1.0 equiv), the nickel catalyst (5–10 mol%), and the corresponding electrophile (1.1 mmol, 1.1 equiv), TIPSOTf (405 µL, 1.5 mmol, 1.5 equiv), and 2,6-lutidine (140 µL, 1.2 mmol, 1.2 equiv) for 16 h. The results are summarised in Table 60.

Entry	EWG	L*	Mol%	T (°C)	Conv. (%)[a]
1	COPh	$(Me_3P)_2$	5	–20	59
2	COPh	(*R*)-Tol-BINAP	5	0	86
3	COPh	(*R*)-DTBM-SEGPHOS	5	0	20
4	COPh	(*R*)-Tol-BINAP	5	0	100
5	COOMe	$(Me_3P)_2$	10	rt	0
6	NO_2	$(Me_3P)_2$	5	–20	0

a) Established by ^{1}H NMR analysis.

Table 60. Michael addition to different α,β-unsaturated compounds.

Non-aromatic α,β-unsaturated aldehydes

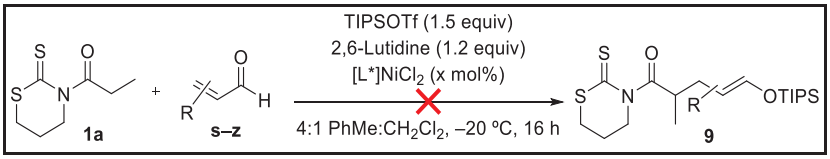

The General Procedure 8 was followed with **1a** (189 mg, 1.0 mmol, 1.0 equiv), the nickel catalyst (5–10 mol%), the corresponding aldehyde (1.1 mmol, 1.1 equiv), TIPSOTf (405 µL, 1.5 mmol, 1.5 equiv), and 2,6-lutidine (140 µL, 1.2 mmol, 1.2 equiv) at –20 °C for 16 h. The results are summarised in Table 61.

Entry	aldehyde	L*	mol%	Conv. (%)
1	**s**	$(Me_3P)_2$	10	Complex mix
2	**t**	$(Me_3P)_2$	10	Complex mix
3	**u**	$(Me_3P)_2$	10	0
4	**v**	$(Me_3P)_2$	5	0
5	**w**	$(Me_3P)_2$	5	0
6	**x**	$(Me_3P)_2$	5	0
7	**y**	$(Me_3P)_2$	5	0
8	**z**	$(Me_3P)_2$	10	Complex mix
9	**z**	(R)-BINAP	5	Complex mix

a) Established by ^{1}H NMR analysis.

Table 61. Michael addition to non-aromatic α,β-unsaturated aldehydes.

9 Michael additions catalysed by cobalt salts

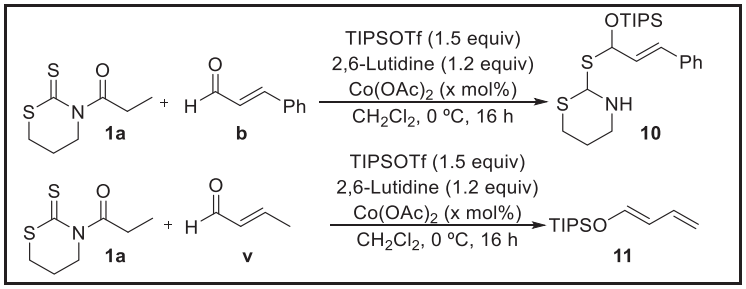

General Procedure 9

A solution of **1a** (95 mg, 0.5 mmol, 1.0 equiv), an aldehyde (0.55 mmol, 1.1 equiv), and $Co(OAc)_2$ (17.7 mg, 10 μmol, 20 mol%) in CH_2Cl_2 (1 mL) was cooled at 0 °C under N_2. Then, neat TIPSOTf (200 μL, 0.75 mmol, 1.5 equiv) was added followed by 2,6-lutidine (70 μL, 1.2 mmol, 1.2 equiv) and the resultant mixture was stirred at 0 °C for 16 h.

The reaction mixture was quenched with sat. NH_4Cl (1 mL) and partitioned in CH_2Cl_2 (10 mL) and water (25 mL). The aqueous layer was extracted with CH_2Cl_2 (2 × 10 mL). The combined organic extracts were dried ($MgSO_4$), and concentrated. The resultant residue was analysed by ^{1}H NMR (400 MHz) and purified by flash column chromatography to give the named compound.

S-[(*E*)-1-Phenyl-3-triisopropylsilyloxy-2-propenylthio]-1,3-thiazinane

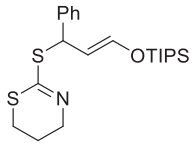

10

The General Procedure 9 was followed with aldehyde **b** (69 μL, 0.55 mmol, 1.1 equiv). The residue was purified by flash chromatography (from 98:2 to 80:20 Hexanes/EtOAc) to give 43 mg (0.12 mmol, 24% yield) of **10**.

Colorless oil.

^{1}H NMR (400 MHz, $CDCl_3$) δ 7.86 (dd, *J* = 3.9, 1.7 Hz, 1H, PhC<u>H</u>), 7.48–7.28 (m, 5H, Ar<u>H</u>), 6.94 (d, *J* = 16.0 Hz, 1H, C<u>H</u>OTIPS), 6.22 (dd, *J* = 16.0, 3.9 Hz, 1H, C<u>H</u>CHOTIPS), 3.64 (ddd, *J* = 14.0, 7.6, 3.3 Hz, 1H, NC<u>H</u>$_x$H$_y$), 3.37 (ddd, *J* = 14.0, 7.5, 3.3 Hz, 1H, NCH$_x$<u>H</u>$_y$), 2.92 (t, *J* = 6.1 Hz, 2H, SC<u>H</u>$_2$), 2.25–2.13 (m, 2H, NCH$_2$C<u>H</u>$_2$), 1.14–1.04 (m, 21H, O<u>TIPS</u>).

(1*E*,3*E*)-Triisopropylsilyloxy-1,3-butadiene (11)

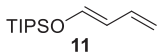

11

The General Procedure 9 was followed with aldehyde **v** (45 μL, 0.55 mmol, 1.1 equiv). The residue purified by flash chromatography (Hexanes/EtOAc from 95:5 to 85:15) to give 28 mg (0.12 mmol, 22% yield) of **11**.

Colorless oil.

^{1}H NMR (400 MHz, $CDCl_3$) δ 6.65 (dd, *J* = 11.8, 0.8 Hz, 1H, C<u>H</u>OTIPS), 6.23 (dddd, *J* = 16.9, 11.0, 10.2, 0.7 Hz, 1H, C<u>H</u>CHCHOTIPS), 5.75 (ddd, *J* = 11.8, 11.0, 0.8 Hz, 1H, C<u>H</u>CHOTIPS), 4.98 (ddd, *J* = 16.9, 1.8, 0.9 Hz, 1H, CHC<u>H</u>$_x$H$_y$), 4.80 (dd, *J* = 10.4, 1.6 Hz, 1H, CHCH$_x$<u>H</u>$_y$), 1.24–1.03 (m, 21H, O<u>TIPS</u>).

10 1,6-Michael additions to α,β-γ,δ-unsaturated aldehydes

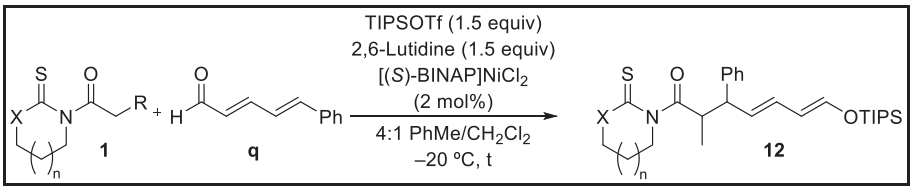

A solution of a thioimide **1** (0.2 mmol, 1.0 equiv), aldehyde **q** (35 mg, 0.22 mmol, 1.1 equiv), and [(*S*)-BINAP]$NiCl_2$ (3.0 mg, 4 μmol, 2 mol%) in CH_2Cl_2 (0.4 mL) was cooled at –20 °C under N_2. Then, neat TIPSOTf (81 μL, 0.3 mmol, 1.5 equiv) was added, followed by 2,6-lutidine (35 μL, 0.24 mmol, 1.2 equiv) and the resultant mixture was stirred at –20 °C.

The reaction mixture was quenched with sat. NH_4Cl (1 mL) and a known quantity of methyl 4-nitrobenzoate was added as internal standard (10–20 mg). The mixture was partitioned in CH_2Cl_2 (15 mL) and water (15 mL). The aqueous layer was extracted with CH_2Cl_2 (2 × 10 mL). The combined organic extracts were dried ($MgSO_4$) and concentrated under reduced pressure. The results are summarised in Table 62.

Entry	Scaffold	X	n	R	t(h)	Conv(%)[a]	rr(1,2:,1,4:1,6)[a]	dr (1,6)[a]
1	**1a**	S	1	Me	1	>99	0:70:30	55:45
2	**1l**	S	0	Me	0.5	>99	0:58:42	45:55
3	**1m**	O	0	Me	0.5	>99	4:53:43	42:58
4	**1n**	O	1	Me	0.5	>99	1:53:46	50:50
5	**1o**	O	0	N_3	0.5	>99	1:53:46	44:56
6	**1t**	O	0	N_3	0.5	>99	1:63:37	35:65

a) Established by ^1H NMR analysis of the crude mixture.

Table 62. Scaffold assessment for the 1,6-Michael addition.

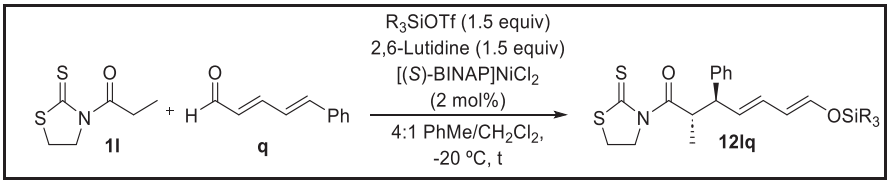

A solution of *N*-propanoyl-1,3-thiazolidine-2-thione **1l** (0.2 mmol, 1.0 equiv), aldehyde **q** (35 mg, 0.22 mmol, 1.1 equiv), and [(*S*)-BINAP]$NiCl_2$ (3.0 mg, 4 µmol, 2 mol%) in CH_2Cl_2 (0.4 mL) was cooled at –20 °C under N_2. Then, neat R_3SiOTf (0.3 mmol, 1.5 equiv) was added, followed by 2,6-lutidine (35 µL, 0.24 mmol, 1.2 equiv) and the resultant mixture was stirred at –20 °C.

The reaction mixture was quenched with sat. NH_4Cl (1 mL) and a known quantity of methyl 4-nitrobenzoate was added as internal standard (10–20 mg). The mixture was partitioned in CH_2Cl_2 (15 mL) and water (15 mL). The aqueous layer was extracted with CH_2Cl_2 (2 × 10 mL). The combined organic extracts were dried ($MgSO_4$) and concentrated under reduced pressure. The results are summarised in Table 63.

Entry	Lewis acid	t (h)	Conv (%)[a]	rr(1,2:,1,4:1,6)[a]	dr (1,6)[a]
1	TIPSOTf	1	>99	1:53:46	55:45
2	TESOTf	2	>99	10:63:27	34:66
3	TMSOTf	2	>99	39:35:26	37:63

a) Established by ^1H NMR analysis of the crude mixture.

Table 63. Lewis acid assessment for 1,6-Michael addition.

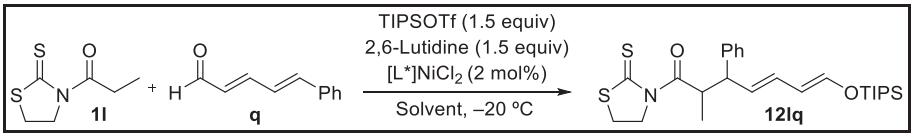

A solution of *N*-propanoyl-1,3-thiazolidine-2-thione **1l** (0.2 mmol, 1.0 equiv), aldehyde **q** (35 mg, 0.22 mmol, 1.1 equiv), and a chiral nickel (II) complex (4 µmol, 2 mol%) in solvent (0.4 mL) was cooled at –20 °C under N_2. Then, neat TIPSOTf (81 µL, 0.3 mmol, 1.5 equiv) was added, followed by 2,6-lutidine (35 µL, 0.24 mmol, 1.2 equiv) and the resultant mixture was stirred at –20 °C.

The reaction mixture was quenched with sat. NH_4Cl (1 mL) and a known quantity of methyl 4-nitrobenzoate was added as internal standard (10–20 mg). The mixture was partitioned in CH_2Cl_2 (15 mL) and water (15 mL). The aqueous layer was extracted with CH_2Cl_2 (2 × 10 mL). The combined organic extracts were dried ($MgSO_4$) and concentrated under reduced pressure. The results are summarised in Table 64.

Entry	L*	Solvent	t (h)	Conv(%)[a]	rr (1,2:,1,4:1,6)[a]	dr (1,6)[a]
1	[(*S*)-BINAP]	CH_2Cl_2	0.5	>99	1:53:46	45:55
2	[(*S*)-BINAP]	PhMe: CH_2Cl_2 4:1	3	>99	7:32:61	39:61
3	[(*R*)-DTBM-SEGPHOS]	CH_2Cl_2	0.5	>99	0:84:16	39:61
4	[(*R*)-DTBM-SEGPHOS]	PhMe: CH_2Cl_2 4:1	3	>99	0:82:18	32:68

a) Established by ^{1}H NMR analysis of the crude mixture.

Table 64. Solvent and catalyst assessment for 1,6-Michael addition.

CHAPTER III

Transformations of the Michael adducts. Total synthesis of Tapentadol

11 Derivatization of Michael adducts

11.1 Scale up of *syn* Michael adduct 9ab

_N_-[(2_S_,3_R_,4_E_)-2-Methyl-3-phenyl-5-triisopropylsilyloxy-4-pentenoyl]-1,3-thiazinane-2-thione (9ab)

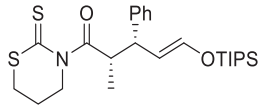

The General Procedure was followed with **1** (1.89 g, 10 mmol, 1.0 equiv), [*(R)*-DTBM-SEGPHOS]$NiCl_2$ (262 mg, 0.2 mmol, 2 mol%), **a** (1.4 mL, 11 mmol, 1.1 equiv), TIPSOTf (4.0 mL, 15 mmol, 1.5 equiv), and 2,6-lutidine (1.4 mL, 12 mmol, 1.2 equiv) at –20 °C for 5 h.

The residue (dr 84:16) was purified by column chromatography (from 98:2 to 90:10 Hexanes/EtOAc) to give 3.45 g (7.3 mmol, 73% yield) of *syn* Michael **2a** and 580 mg (1.2 mmol, 12% yield) of the *anti* Michael **3a**.

11.2 Synthesis of Michael adduct derivatives

Methyl (2_S_,3_R_,4_E_)-2-methyl-3-phenyl-5-triisopropylsilyloxy-4-pentenoate (13)

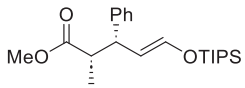

A solution of **9ab** (237 mg, 0.5 mmol, 1 equiv) and DMAP (12.3 mg, 0.1 mmol, 0.2 equiv) in MeOH (2 mL) was stirred at rt under N_2 for 16 h.

The volatiles were removed under reduced pressure and the residue was purified by column chromatography (from 98:2 to 90:10 Hexanes/EtOAc) to give 156 mg (0.5 mmol, 99% yield) of methyl ester **13** and 59 mg (0.44 mmol, 90% yield) of recovered 1,3-thiazinane-2-thione.

Colorless oil.
R_f 0.3 (95:5 Hexanes/EtOAc).
$[\alpha]_D^{20}$ +40.9 (*c* 1.0 $CHCl_3$).
IR (ATR) ν 2944, 2866, 1736, 1655, 1170, 1072, 996, 882, 870, 762, 683, 663 cm^{-1}.
^{1}H NMR (500 MHz, $CDCl_3$) δ 7.32–7.24 (m, 2H, ArH), 7.21–7.13 (m, 3H, ArH), 6.35 (dd, *J* = 11.7, 0.7 Hz, 1H, CHOTIPS), 5.20 (dd, *J* = 11.7, 10.0 Hz, 1H, CHCHOTIPS),

3.66 (s, 1H, O<u>Me</u>) 3.30 (t, *J* = 10.0 Hz, 1H, C<u>H</u>Ph), 2.76 (dq, *J* = 10.0, 6.9 Hz, 1H, O=CC<u>H</u>), 1.14–1.00 (m, 21H, O<u>TIPS</u>), 0.94 (d, *J* = 6.9 Hz, 3H, CHC<u>H</u>$_3$).
^{13}C NMR (126 MHz, $CDCl_3$) δ 176.2 (C), 142.8 (C), 141.9 (CH), 128.5 (CH), 127.8 (CH), 126.4 (CH), 112.2 (CH), 51.4 (CH_3), 48.1 (CH), 46.2 (CH), 17.7 (CH_3), 16.1 (CH_3), 11.9 (CH).
HRMS (ESI+) *m/z* calcd for $[M+H]^+$ $C_{22}H_{37}O_3Si$: 377.2506, found: 377.2507.

Methyl *N*-[(2*S*,3*R*,4*E*)-2-methyl-3-phenyl-5-triisopropylsilyloxy-4-pentenoyl]-β-alaninate (14)

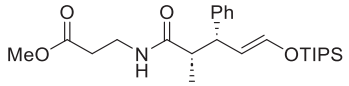

A solution of **9ab** (238 mg, 0.5 mmol, 1 equiv), DMAP (12.6 mg, 0.1 mmol, 0.2 equiv) and β-alanine (175 mg, 1.25 mmol, 2.5 equiv) in CH_2Cl_2 (3.5 mL) was cooled at 0 °C. Then, neat Et_3N (210 μL, 1.5 mmol, 3 equiv) was added dropwise and the resultant mixture was stirred for 16 h at rt.

The mixture was diluted with Et_2O (50 mL) and washed with 2 M HCl (2 × 25 mL), NaOH (3 × 25 mL), and brine (25 mL). The organic layer was dried ($MgSO_4$) and concentrated under reduced pressure to give pure ester **14** (190 mg, 80% yield).

White solid.
Mp 75–77 °C.
R_f 0.3 (70:30 Hexanes/EtOAc).
$[\alpha]_D^{20}$ +40.9 (*c* 1.0 $CHCl_3$).
IR (ATR) ν 3340, 2940, 2863, 2356,1732, 1647, 1152, 881, 762, 704, 680 cm^{-1}.
^{1}H NMR (400 MHz, $CDCl_3$) δ 7.33–7.23 (m, 2H, Ar<u>H</u>), 7.22–7.10 (m, 3H, Ar<u>H</u>), 6.32 (dd, *J* = 11.7, 0.7 Hz, 1H, C<u>H</u>OTIPS), 5.99 (t, *J* = 6.1 Hz, 1H, N<u>H</u>), 5.18 (dd, *J* = 11.7, 9.6 Hz, 1H, C<u>H</u>CHOTIPS), 3.69 (s, 3H, O<u>Me</u>), 3.56–3.40 (m, 2H, C<u>H</u>$_2$N), 3.33 (t, *J* = 9.6 Hz, 1H, PhC<u>H</u>), 2.58–2.46 (m, 2H, MeO_2CC<u>H</u>$_2$), 2.39 (dq, *J* = 9.6, 6.8 Hz, 1H, C<u>H</u>CH_3), 1.14–0.99 (m, 21H, O<u>TIPS</u>), 0.92 (d, *J* = 6.8 Hz, 3H, CHC<u>H</u>$_3$).
^{13}C NMR (101 MHz, $CDCl_3$) δ 175.0 (C), 173.3 (C), 143.2 (C), 142.2 (CH), 128.5 (CH), 127.8 (CH), 126.3 (CH), 111.8 (CH), 51.7 (CH_3), 48.1 (CH), 47.9 (CH), 34.5 (CH_2), 33.9 (CH_2), 17.7 (CH_3), 16.4 (CH_3), 11.9 (CH).
HRMS (ESI+) *m/z* calcd for $[M+H]^+$ $C_{25}H_{42}NO_4Si$: 448.2878, found: 448.2880.

N-[(2*S*,3*R*,4*E*)-2-Methyl-3-phenyl-5-triisopropylsilyloxy-4-pentenoyl]morpholine (15)

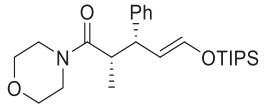

Neat morpholine (105 μL, 1.2 mmol, 2.4 equiv) was added to a solution of **9ab** (239 mg, 0.5 mmol, 1 equiv) and DMAP (12.3 mg, 0.1 mmol, 0.2 equiv) in CH_2Cl_2 (2 mL) at 0 °C, and the resultant mixture was stirred for 16 h at rt.

The reaction mixture was diluted with Et_2O (25 mL) and washed with NaOH (3 × 10 mL). The organic layer was dried ($MgSO_4$) and concentrated under reduced pressure to give pure amide **15** (175 mg, 95% yield).

Colorless oil.
R_f 0.6 (60:40 Hexanes/EtOAc).
$[\alpha]_D^{20}$ +51.3 (*c* 1.0 $CHCl_3$).
IR (ATR) ν 2942, 2864, 1655, 1638, 1165, 731, 699, 681, 667, 645 cm^{-1}.
^{1}H NMR (500 MHz, $CDCl_3$) δ 7.32–7.27 (m, 2H, ArH), 7.22–7.15 (m, 3H, ArH), 6.32 (dd, *J* = 11.6, 0.7 Hz, 1H, CHOTIPS), 5.15 (dd, *J* = 11.7, 9.8 Hz, 1H, CHCHOTIPS), 3.68–3.62 (m, 6H, 2 × OCH_2, OCH_2CH_2), 3.57–3.52 (m, 2H, OCH_2CH_2), 3.44 (t, *J* = 9.8 Hz, 1H, CHPh), 3.01 (dq, *J* = 9.8, 6.8 Hz, 1H, O=CCH), 1.13–0.98 (m, 21H, OTIPS), 0.89 (d, *J* = 6.8 Hz, 3H, $CHCH_3$).
^{13}C NMR (126 MHz, $CDCl_3$) δ 174.2 (C), 143.2 (C), 142.4 (CH), 128.5 (CH), 128.0 (CH), 126.4 (CH), 112.1 (CH), 67.0 (CH_2), 66.8 (CH_2), 48.2 (CH), 46.3 (CH_2), 42.2 (CH_2), 40.9 (CH), 17.7 (CH_3), 16.7 (CH_3), 11.9 (CH).
HRMS (ESI+) *m/z* calcd for $[M+H]^+$ $C_{25}H_{42}NO_3Si$: 432.2928, found: 432.2927.

(2*S*,3*S*,4*E*)-2-Methyl-3-phenyl-5-triisopropylsilyloxy-4-penten-1-ol (16)

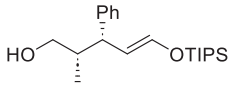

A solution of **9ab** (1.414 g, 3 mmol, 1 equiv) in THF (12 mL) was cooled to 0 °C. Then, a 2 M solution of $LiBH_4$ in THF (3 mL, 6 mmol, 2 equiv) was added dropwise and the resulting solution was stirred at rt under N_2 for 2 h.

The crude was quenched with MeOH (3 mL) and diluted with Et_2O (70 mL). The organic layer was washed with 2 M NaOH (50 mL), sat. NH_4Cl (50 mL) and brine (50 mL). The resulting organic layer was dried ($MgSO_4$) and concentrated under reduced pressure to give 956 mg (93% yield) of pure alcohol **16**.

Colorless oil.
R_f 0.4 (80:20 Hexanes/EtOAc).
$[\alpha]_D^{20}$ +45.5 (*c* 1.0 $CHCl_3$).
IR (ATR) *v* 3410, 3025, 2943, 2865, 1655, 1164, 881, 682, 662 cm^{-1}.
^{1}H NMR (500 MHz, $CDCl_3$) δ 7.30–7.26 (m, 2H, ArH), 7.19–7.13 (m, 3H, ArH), 6.39 (d, *J* = 11.7 Hz, 1H, CHOTIPS), 5.26 (dd, *J* = 11.7, 10.2 Hz, 1H, CHCHOTIPS), 3.68 (dd, *J* = 10.8, 4.9 Hz, 1H, $HOCH_xH_y$), 3.55 (dd, *J* = 10.8, 5.9 Hz, 1H, $HOCH_xH_y$), 3.03 (dd, *J* = 10.2, 8.9 Hz, 1H, CHPh), 2.01–1.92 (m, 1H, $HOCH_2CH$), 1.16–0.98 (m, 21H, OTIPS), 0.80 (d, *J* = 6.8 Hz, 3H, $CHCH_3$).
^{13}C NMR (126 MHz, $CDCl_3$) δ 144.4 (C), 141.3 (CH), 128.4 (CH), 127.8 (CH), 126.0 (CH), 113.2 (CH), 66.6 (CH_2), 47.7 (CH), 40.9 (CH), 17.7 (CH_3), 15.4 (CH_3), 12.0 (CH).
HRMS (ESI+) *m/z* calcd for $[M+H]^+$ $C_{21}H_{37}O_2Si$: 349.2557, found: 349.2542.

(2*S*,3*R*,4*E*)-2-Methyl-3-phenyl-5-triisopropylsilyloxy-4-pentenal (17)

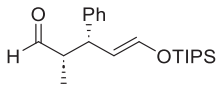

A solution of **9ab** (239 mg, 0.5 mmol, 1 equiv) in CH_2Cl_2 (5 mL) was cooled to –78 °C. Then, a 1 M solution of DIBALH in toluene (0.85 mL, 0.85 mmol, 1.7 equiv) was added dropwise and the resulting solution was stirred at –78 °C under N_2 for 5 h.

The reaction mixture was quenched with MeOH (1 mL). Then, a sat. solution of sodium potassium tartrate (10 mL) was added and the resultant mixture was stirred for 30 min. The mixture was extracted with CH_2Cl_2 (3 × 10 mL) and the combined organic extracts were dried ($MgSO_4$) and concentrated. The residue was purified by column chromatography (from 98:2 to 94:6 Hexanes/EtOAc) to give 128 mg (0.37 mmol, 75% yield) of aldehyde **17**.

Colorless oil.
R_f 0.5 (90:10 Hexanes/EtOAc).
$[\alpha]_D^{20}$ +41.2 (*c* 1.0 $CHCl_3$).
IR (ATR) *v* 2943, 2892, 2866, 1724, 1655, 1459, 1168, 882, 759, 683, 662 cm^{-1}.
^{1}H NMR (500 MHz, $CDCl_3$) δ 9.69 (d, *J* = 3.0 Hz, 1H, CHO), 7.33–7.28 (m, 2H, ArH), 7.23–7.19 (m, 1H, ArH), 7.19–7.15 (m, 2H, ArH), 6.40 (dd, *J* = 11.8, 0.7 Hz, 1H, CHOTIPS), 5.24 (dd, *J* = 11.8, 9.5 Hz, 1H, CHCHOTIPS), 3.39 (t, *J* = 9.5 Hz, 1H, PhCH), 2.76–2.67 (m, 1H, O=CCH), 1.14–1.02 (m, 21H, OTIPS), 0.91 (d, *J* = 6.9 Hz, 3H, $CHCH_3$).
^{13}C NMR (126 MHz, $CDCl_3$) δ 204.9 (C), 142.5 (C+CH), 128.6 (CH), 127.8 (CH), 126.5 (CH), 111.7 (CH), 51.4 (CH), 46.1 (CH), 17.7 (CH_3), 12.8 (CH_3), 11.9 (CH).
HRMS (ESI+) *m/z* calcd for $[M+H]^+$ $C_{21}H_{35}O_2Si$: 347.2401, found: 347.2401.

Methyl (2*S*,3*R*,4*E*)-2-methyl-3-phenyl-5-triisopropylsilyloxypentanoate (19)

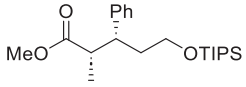

A solution of **13** (140 mg, 0.45 mmol, 1 equiv) and 20% Pd/C (96mg, 0.045 mmol, 10 mol%) in EtOH (3 mL) under N_2 atm was bubbled with H_2 and after 10 min a H_2 balloon was attached to the flask and it was stirred overnight. Afterwards, N_2 was bubbled throught the solution for 15 min and then it was filtered throught Celite® to give 142 mg (0.45 mmol, 99% yield) of pure **19.**

Colorless oil.
R_f. 0.3 (95:5 Hexanes/EtOAc)
$[\alpha]_D^{20}$: + 21.4
IR (ATR) ν 3028, 2941, 2864, 2361, 1933, 1736, 1603, 1161, 1101, 1067, 881, 764, 701, 678 cm^{-1}.
^{1}H NMR (400 MHz, $CDCl_3$) δ 7.31–7.25 (m, 2H, ArH), 7.23–7.17 (m, 1H, ArH), 7.16–7.11 (m, 2H, ArH), 3.71 (s, 3H, OMe), 3.48–3.32 (m, 2H, CH_2OTIPS), 2.97 (td, *J* = 10.5, 4.0 Hz, 1H, PhCH), 2.68 (dq, *J* = 10.1, 6.9 Hz, 1H, CHCH_3), 1.94–1.75 (m, 2H, CH_2CH_2OTIPS), 1.01–0.96 (m, 21H, OTIPS), 0.91 (d, *J* = 6.9 Hz, 3H, CHCH_3).
^{13}C NMR ^{13}C NMR (101 MHz, $CDCl_3$) δ 176.6 (C), 141.7 (C), 128.4 (CH), 128.3 (CH), 126.6 (CH), 61.1 (CH_2), 51.5 (CH_3), 45.9 (CH), 45.4 (CH), 37.7 (CH_2), 17.9 (CH/CH_3), 15.9 (CH/CH_3), 11.9 (CH/CH_3).
HRMS (ESI+) *m/z* calcd for $[M+H]^+$ $C_{22}H_{39}O_3Si$: 379.2663, found: 379.2655.

(4*R*,5*S*)-5-Methyl-4-phenyl-2-tetrahydro-2*H*-pyranol (20)

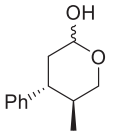

A 1 M solution of TBAF in THF (0.75 mL, 0.75 mmol, 1.5 equiv) was added dropwise to a solution of aldehyde **17** (172 mg, 0.5 mmol, 1 equiv) in THF (5 mL) at 0 °C, and the resultant mixture was stirred at rt for 1 h.

The mixture was rinsed with Et_2O (30 mL) and washed with water (4 × 25 mL). The organic layer was dried ($MgSO_4$) and concentrated under reduced pressure. The residue was purified by flash column chromatography (from 80:20 to 60:40 Hexanes/EtOAc) to give 81 mg (0.41 mmol, 85% yield) of tetrahydropyrane **20** as a 54:46 mixture of diastereomers.

Pale yellow oil.
R_f 0.6 (60:40 Hexanes/EtOAc).
IR (ATR) ν 3372 (br), 3027, 2950, 2924, 2870, 1737, 1602, 1118, 1048, 1008, 754, 698 cm^{-1}.
^{1}H NMR (400 MHz, $CDCl_3$) δ 7.38–7.26 (m, 4H, ArH diast A, B), 7.26–7.13 (m, 6H, ArH, diast A, B), 5.41 (q, *J* = 2.4 Hz, 1H,CHOH, diast A), 4.84 (ddd, *J* = 9.4, 6.1, 2.1 Hz, 1H, CHOH diast B), 4.02 (dd, *J* = 11.7, 4.4 Hz, 1H, OCH_xH_y diast B), 3.79 (t, *J* = 11.2 Hz, 1H, OCH_xH_y diast A), 3.63 (dd, *J* = 11.2, 4.6 Hz, 1H, OCH_xH_y diast A), 3.44 (d, *J* = 6.3 Hz, 1H, OH diast B), 3.27 (dd, *J* = 11.7, 10.9 Hz, 1H, OCH_xH_y diast B), 2.86 (t, *J* = 2.3 Hz, 1H, OH diast A), 2.77 (td, *J* = 11.1, 5.5 Hz, 1H, PhCH diast A), 2.36 (ddd, *J* = 12.6, 10.9, 3.8 Hz, 1H, PhCH diast B), 2.06 (ddd, *J* = 13.0, 3.8, 2.1 Hz, 1H, CH_xH_yCHOH diast B), 2.01–1.81 (m, 4H, CH_2CHOH diast A, $CHCH_3$ diast A, $CHCH_3$ diast B), 1.73–1.60 (m, 1H, CH_xH_yCHOH), 0.63 (d, *J* = 6.6 Hz, 3H, CH_3 diast A), 0.61 (d, *J* = 6.6 Hz, 3H, CH_3 diast B).
^{13}C NMR (101 MHz, $CDCl_3$) δ 144.0 (C), 143.3 (C), 128.6 (CH), 128.5 (CH), 127.6 (CH), 127.5 (CH), 126.6 (CH), 126.4 (CH), 96.5 (CH), 91.8 (CH), 72.1 (CH_2), 65.6 (CH_2), 48.5 (CH), 42.6 (CH), 41.0 (CH_2), 38.2 (CH_2), 36.0 (CH), 35.7 (CH), 14.8 (CH_3), 14.1 (CH_3).
HRMS (ESI+) *m/z* calcd for $[M+Na]^+$ $C_{12}H_{16}NaO_2$: 215.1043, found: 215.1038.

12 Cyclization reactions

12.1 Assessment of the aldehyde

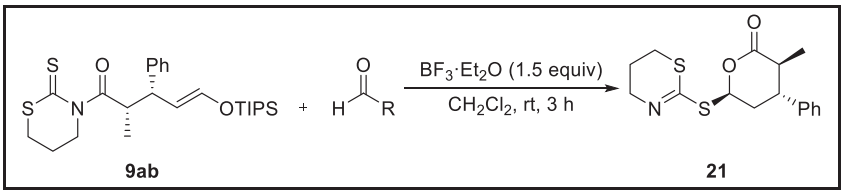

A solution of Michael adduct **9ab** (48 mg, 0.1 mmol, 1 equiv) in CH_2Cl_2 (0.75 mL) was added dropwise to a stirring solution of an aldehyde (0.2 mmol, 2 equiv) and $BF_3{\cdot}Et_2O$ (19 µL, 0.2 mmol, 1.5 equiv) in CH_2Cl_2 (0.75 mL) at 0 °C. The resulting mixture was stirred until apparent completion by TLC.

The mixture was rinsed with water (25 mL), extracted with CH_2Cl_2 (4 × 5 mL) and concentrated under reduced pressure. The combined organic extracts were dried ($MgSO_4$) and concentrated under reduced pressure and the crude mixture was analysed by ^{1}H NMR.

Entry	R	Conv (%)[a]	Purity (%)[a,b]
1[c]	-	96	56
2	4-MeO-C_6H_4	83	Complex mixture
3	4-Me-C_6H_4	92	40
4	Ph	100	90
5	4-Cl-C_6H_4	100	80
6[d,e]	Et	70	44

a) Established by ^{1}H NMR analysis. b) Established by ^{1}H NMR comparing the ratio of product **21** vs all other subproducts. d) Reaction temperature 0 °C. e) Reaction time 4 h

Table 65. Aldehyde screening.

12.2 Assessment of reaction conditions

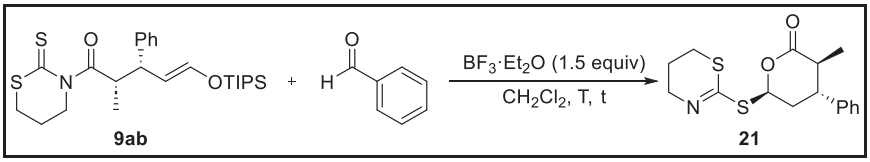

A solution of Michael adduct **9ab** (48 mg, 0.1 mmol, 1 equiv) in CH_2Cl_2 was added dropwise to a stirring solution of benzaldehyde (101 µL, 0.2 mmol, 2 equiv) and $BF_3{\cdot}Et_2O$ (19 µL, 0.2 mmol, 1.5 equiv) in CH_2Cl_2 at 0 °C. The resulting mixture was stirred until apparent completion by TLC. After, the mixture was rinsed with water (25 mL), extracted with CH_2Cl_2 (4 × 5 mL) and concentrated under reduced pressure.

The combined organic extracts were dried ($MgSO_4$) and concentrated under reduced pressure and the crude mixture was analysed by ^{1}H NMR.

Entry	Scale (mmol)	Conc (M)	t (h)	T (°C)	Conv(%)[a]	Yield (%)[b]	Purity(%)[a]
1	0.1	0.07	3.5	–78 to 0	100	63	100
2	0.5	0.07	3	0 to rt	92	-	33
3	0.9	0.07	3	rt	95	-	58
4	0.2	0.04	3	0	100	98	91
5	0.1	0.01	1.5	0	100	-	91
6	0.5	0.01	1	0	95	83	100

a) Established by ^{1}H NMR analysis. b) isolated yield.

Table 66. Assessment of reaction conditions.

(3*S*,4*R*,6*R*)-6-((5,6-Dihydro-4*H*-1,3-thiazin-2-yl)thio)-3-methyl-4-phenyltetrahydro-2*H*-pyran-2-one (21)

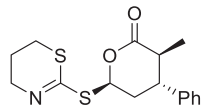

A solution of Michael adduct **9ab** (239 mg, 0.5 mmol, 1 equiv) in CH_2Cl_2 (25 mL) was added dropwise to a stirring solution of benzaldehyde (101 µL, 0.2 mmol, 2 equiv) and $BF_3{\cdot}Et_2O$ (93 µL, 0.75 mmol, 1.5 equiv) in CH_2Cl_2 (25 mL) at 0 °C. The resulting mixture was stirred for 1 h. After, the mixture was rinsed with water (50 mL) and extracted with CH_2Cl_2 (3 × 25 mL), dried ($MgSO_4$) and concentrated under reduced pressure.

The residue was purified by column chromatography (from 80:20 to 60:40 Hexanes/EtOAc) to give 139 mg (0.41 mmol, 83% yield) of pure product **21**.

Colorless oil.
Rf 0.2 (70:30 Hexanes/EtOAc).
$[\alpha]_D^{20}$ = +117.4 (*c* 1.0 $CHCl_3$).
IR (ATR) 2925, 2850, 1740, 1599, 1094, 952, 930, 907, 842, 727, 700 cm^{-1};
^{1}H NMR (500 MHz, $CDCl_3$) δ 7.39–7.33 (m, 2H, ArH), 7.32–7.25 (m, 1H, Ar<u>H</u>), 7.24–7.16 (m, 2H, Ar<u>H</u>), 6.67 (t, *J* = 4.9 Hz, 1H, OC<u>H</u>), 3.81–3.71 (m, 2H, NC<u>H</u>$_2$), 3.09 (t, *J* = 6.0 Hz, 2H, SC<u>H</u>$_2$) 2.95 (td, *J* = 11.0, 5.0 Hz, 1H, PhC<u>H</u>), 2.75 (dq, *J* = 11.0, 6.8 Hz, 1H, C<u>H</u>CH$_3$), 2.50 (ddd, *J* = 14.4, 11.0, 4.9 Hz, 1H, PhCHC<u>H</u>$_x$H$_y$), 2.35 (dt, *J* = 14.4, 4.9 Hz, 1H, PhCHCH$_x$<u>H</u>$_y$), 2.00–1.87 (m, 2H, NCH$_2$C<u>H</u>$_2$), 1.16 (d, *J* = 6.9 Hz, 3H, CHC<u>H</u>$_3$).
^{13}C NMR (126 MHz, $CDCl_3$) δ 172.9 (C), 152.0 (C), 142.0 (C), 129.0 (CH), 127.4 (CH), 127.1 (CH), 80.0 (CH), 48.6 (CH_2), 43.7 (CH), 41.9 (CH), 36.4 (CH_2), 27.8 (CH_2), 20.3 (CH_2), 14.7 (CH_3).
HRMS (ESI+) *m/z* calcd for $[M+H]^+$ $C_{16}H_{20}NO_2S_2$: 322.0930, found: 322.0929.

12.3 Cyclization of the *anti* Michael adduct

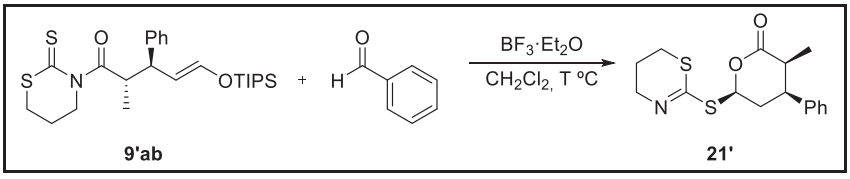

A solution of Michael adduct **9'ab** (48 mg, 0.1 mmol, 1 equiv) in CH_2Cl_2 (0.75 mL) was added dropwise to a stirring solution of benzaldehyde (101 µL, 0.2 mmol, 2 equiv) and $BF_3{\cdot}Et_2O$ (19 µL, 0.2 mmol, 1.5 equiv) in CH_2Cl_2 at 0 °C. The resulting mixture was stirred until apparent completion by TLC. The mixture was rinsed with water (25 mL), extracted with CH_2Cl_2 (4 × 5 mL) and concentrated under reduced pressure.

The combined organic extracts were dried ($MgSO_4$) and concentrated under reduced pressure and the crude mixture was analysed by ^1H NMR. The results are summarised in Table 67.

Entry	Conc (M)	t (h)	T (°C)	Conv(%)[a]	Purity(%)[a,b]
1	0.06	3.5	rt	100%	30
2	0.01	16	0	83%	30

a) Established by ^1H NMR analysis. b) Established by ^1H NMR comparing the ratio of product **21'** vs all other subproducts

Table 67. *Anti* Michael adduct cyclization.

12.4 Attempts for a Mukaiyama aldol addition

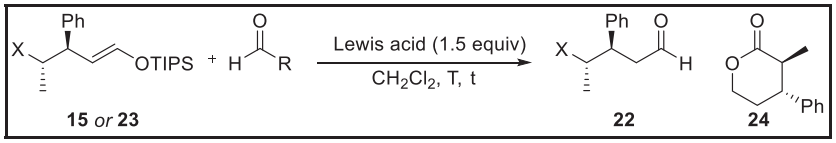

GENERAL PROCEDURE 10

A solution of Michael adduct derivative **13**, **15** or **23** (1 equiv) in CH_2Cl_2 (0.13M) was added dropwise to a stirring solution of benzaldehyde (2 equiv) and Lewis acid (1.5 equiv) in the same amount of CH_2Cl_2. The resulting mixture was stirred until apparent completion by TLC. After, the mixture was rinsed with water (25 mL), extracted with CH_2Cl_2 (4 × 5 mL) and concentrated under reduced pressure.

The combined organic extracts were dried ($MgSO_4$) and concentrated under reduced pressure and the crude mixture was analysed by ^1H NMR.

GENERAL PROCEDURE 11

$TiCl_4$ (0.15 mmol, 1.5 equiv)was added dropwise to a solution of Michael adduct derivative **13** (38 mg, 0.1 mmol, 1 equiv) and benzaldehyde (101 μL, 0.2 mmol, 2 equiv) in CH_2Cl_2 (1.5 mL) at –78 °C. The resulting mixture was stirred at 0 °C until apparent completion by TLC. After, the mixture was rinsed with water (25 mL), extracted with CH_2Cl_2 (4 × 5 mL) and concentrated under reduced pressure.

The combined organic extracts were dried ($MgSO_4$) and concentrated under reduced pressure and the crude mixture was analysed by ^1H NMR. The results are summarised in Table 68.

Entry	SM	GP[a]	Scale (mmol)	Lewis acid	R	t (h)	T (°C)	Conv (%)[b]	Yield (%)[c]	Major product
1	**23**	9	0.1	$BF_3{\cdot}Et_2O$	Ph	3	–78 to 0	100	62	22b
2	**23**	9	0.5	$BF_3{\cdot}Et_2O$	Ph	3	–78 to 0	100	43	22b
3	**23**	9	0.5	$BF_3{\cdot}Et_2O$	Et	3	–78 to 0	100	-	22b
4	**23**	9	0.1	$TiCl_4$	Et	3	–78 to 0	100		Complex mix
5	**15**	9	0.1	$TiCl_4$	Et	5	–78 to 0	100	-	22c
6	**13**	9	0.1	$BF_3{\cdot}Et_2O$	Ph	4	–78 to 0	100	-	22d
7	**13**	9	0.5	$TiCl_4$	Et	4	–78 to 0	100	-	24
8	**13**	10	0.1	$TiCl_4$	Et	5	–78 to 0	100	-	Complex mix
9	**13**	9	0.5	$Sc(OTf)_3$	Et	48	rt	100	-	24

a) General Procedure. b) Established by ^{1}H NMR analysis. c) Isolated yield of product **24**.

Table 68. Assessment of conditions for the obtention of **24.**

(3*R*,4*S*)-5-((tert-butyldiphenylsilyl)oxy)-4-methyl-3-phenylpentanal (22b)

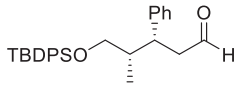

A solution of **23** (37 mg, 0.1 mmol, 1 equiv) in CH_2Cl_2 (0.75 mL) was added dropwise to a stirring solution of propanal (14 µL, 0.2 mmol, 2 equiv) and $BF_3{\cdot}Et_2O$ (19 µL, 0.15 mmol, 1.5 equiv) in CH_2Cl_2 (25 mL) at –78 °C. The resulting mixture was stirred for 1 h. After, the mixture was rinsed with water (50 mL) and extracted with CH_2Cl_2 (3 × 25 mL) and concentrated under reduced pressure to give a mixture of aldehyde **22b** and TIPSOH.

Colorless oil.

^{1}H NMR (400 MHz, $CDCl_3$) δ 9.57 (t, *J* = 2.3 Hz, 1H, C<u>H</u>O), 7.74–7.60 (m, 5H, Ar<u>H</u>), 7.47–7.32 (m, 6H, Ar<u>H</u>), 7.23–7.12 (m, 4H, Ar<u>H</u>), 3.57–3.42 (m, 3H, O<u>CH</u>$_2$, Ph<u>CH</u>), 2.75 (dd, *J* = 7.7, 2.3 Hz, 2H, <u>CH</u>$_2$CHO), 1.94–1.84 (m, 1H, <u>CH</u>CH$_3$), 1.10 (s, 9H, OSi<u>t</u><u>Bu</u>Ph$_2$), 0.71 (d, *J* = 6.9 Hz, 3H, CH<u>CH</u>$_3$).

***N*-[(2*S*,3*R*)-2-Methyl-5-oxo-3-phenylpentanoyl]morpholine (22c)**

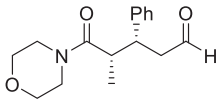

A solution of **15** (59 mg, 0.1 mmol, 1 equiv) in CH_2Cl_2 (0.75 mL) was added dropwise to a stirring solution of propanal (14 µL, 0.2 mmol, 2 equiv) and $TiCl_4$ (17 µL, 0.15 mmol, 1.5 equiv) in CH_2Cl_2 (25 mL) at –78 °C. The resulting mixture was stirred for 1 h. The mixture was rinsed with water (50 mL) and extracted with CH_2Cl_2 (3 × 25 mL) and concentrated under reduced pressure to give a mixture of aldehyde **22c** and TIPSOH.

Colorless oil.

^{1}H NMR (400 MHz, $CDCl_3$) δ 9.57 (dd, *J* = 2.6, 1.9 Hz, 1H, C<u>H</u>O), 7.35–7.29 (m, 2H, Ar<u>H</u>), 7.26–7.18 (m, 3H, Ar<u>H</u>), 3.72–3.53 (m, 7H, NC<u>H</u>$_x$H$_y$C<u>H</u>$_2$O, PhC<u>H</u>), 3.50–3.44 (m, 2H, NCH$_x$<u>H</u>$_y$), 2.97 (dq, *J* = 9.4, 6.9 Hz, 1H, C<u>H</u>CH$_3$), 2.84–2.66 (m, 2H, C<u>H</u>$_2$CHO), 0.94 (d, *J* = 6.9 Hz, 3H, CHC<u>H</u>$_3$).

(2*S*,3*S*,4*E*)-1-*tert*-Butyldiphenylsilyloxy-2-Methyl-3-phenyl-5-triisopropylsilyloxy-4-pentene (23)

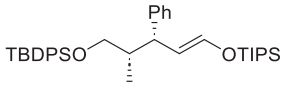

A solution of **9ab** (956 mg, 2.7 mmol, 1 equiv) and imidazole (451 mg, 6.6 mmol) in THF (20 mL) was cooled to 0 °C. Then, TBDPSCl (0.93 mL, 3.6 mmol) was added dropwise and the resulting solution was stirred at rt for 16 h.

The mixture was diluted with CH_2Cl_2 (20 mL) and washed with sat. NH_4Cl (30 mL) and brine (30 mL). The resulting organic layer was dried ($MgSO_4$) and concentrated under reduced pressure to give 1.41 g (2.4 mmol, 88% yield) of pure protected alcohol **23**.

Colorless oil.

R_f 0.4 (90:10 Hexanes/EtOAc).

$[\alpha]_D^{20}$ +17.4 (*c* 1.0 $CHCl_3$).

IR (ATR) ν 3028, 2942, 2864, 1740, 1655, 1166, 1110, 1068, 738, 698, 612 cm^{-1}.

^{1}H NMR (400 MHz, $CDCl_3$) δ 7.69–7.62 (m, 4H, Ar<u>H</u>), 7.45–7.32 (m, 6H, Ar<u>H</u>), 7.29–7.21 (m, 2H, Ar<u>H</u>), 7.20–7.08 (m, 3H, Ar<u>H</u>), 6.27 (d, *J* = 11.8, 1H, C<u>H</u>OTIPS), 5.17 (dd, *J* = 11.8, 9.9 Hz, 1H, C<u>H</u>CHOTIPS), 3.70 (dd, *J* = 9.9, 4.7 Hz, 1H, TBDPSOC<u>H</u>$_x$H$_y$), 3.54–3.46 (m, 1H, TBDPSOCH$_x$<u>H</u>$_y$), 3.13 (dd, *J* = 9.9, 8.5 Hz, 1H, PhC<u>H</u>), 2.00–1.88 (m, 1H,C<u>H</u>CH$_3$), 1.09–0.94 (m, 30H, OSi<u>^{t}Bu</u>Ph$_2$, O<u>TIPS</u>), 0.78 (d, *J* = 6.7 Hz, 3H, CH$_3$).

^{13}C NMR (101 MHz, $CDCl_3$) δ 144.4 (C), 141.2 (CH), 135.6 (CH), 134.1 (C), 134.0 (C), 129.5 (CH), 129.5 (CH), 128.1 (CH), 128.0 (CH), 127.6 (CH), 125.7 (CH), 113.5 (CH), 66.9 (CH_2), 46.7 (CH), 41.0 (CH), 26.9 (CH_3), 19.3 (C) 17.7 (CH), 15.4 (CH_3), 11.9 (CH_3).
HRMS (ESI+) *m/z* calcd for $[M+H]^+$ $C_{37}H_{55}O_2Si_2$: 587.3735, found: 587.3739.

(3*S*,4*R*,6*R*)-6-((5,6-Dihydro-4*H*-1,3-thiazin-2-yl)thio)-3-methyl-4-phenyltetrahydro-2*H*-pyran-2-one (24)

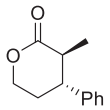

Propanal (72 µL, 1 mmol, 10 equiv) was added dropwise to a solution of **13** (31 mg, 0.1 mmol, 1 equiv) and $Sc(OTf)_3$ (14.8 mg, 0.03 mmol, 30 mol%) in CH_2Cl_2 (1.5 mL) at rt and the resulting mixture was stirred for 48 h.

The mixture was rinsed with water (20 mL) and extracted with CH_2Cl_2 (3 × 25 mL), dried ($MgSO_4$) and concentrated under reduced pressure to give a mixture of **24** and TIPSOH.

Colorless oil.
R_f 0.2 (70:30 Hexanes/EtOAc).
IR (ATR): 2928, 2863, 1724, 1110, 1083, 882, 831, 755, 731, 700, 674 cm^{-1}.
^{1}H NMR (400 MHz, $CDCl_3$) δ 4.52 (ddd, *J* = 11.4, 5.2, 4.3 Hz, 1H, OCH_xH_y), 4.40 (ddd, *J* = 11.4, 8.6, 4.6 Hz, 1H, OCH_xH_y), 2.85–2.68 (m, 2H, CHPh, $CHCH_3$), 2.22–2.06 (m, 2H, OCH_2CH_2), 1.14 (d, *J* = 6.6 Hz, 3H, $CHCH_3$).
^{13}C NMR (101 MHz, $CDCl_3$) δ 174.4 (C), 143.0 (C), 129.0 (CH), 127.1 (CH), 127.2 (CH), 68.0 (CH_2), 45.34 (CH), 41.88 (CH), 31.5 (CH_2), 14.89 (CH_3).
MS (ESI$^+$): *m/z* calcd for $[M+H]^+$ $C_{12}H_{15}O_2$: 191.1, found: 191.1.

13 Tapentadol total synthesis

***N*-[(2*S*,3*S*,4*E*)-3-(3-Methoxyphenyl)-2-methyl-5-triisopropylsilyloxy-4-pentenoyl]-1,3-thiazinane-2-thione (*ent*-9'ak)**

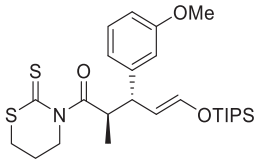

The general procedure was followed with **1a** (1.90 g, 10 mmol, 1.0 equiv), [*(S)*-BINAP]$NiCl_2$ (150 mg, 0.2 mmol, 2 mol%), **k** (1.79 g, 11 mmol, 1.1 equiv), TIPSOTf (4 mL, 15 mmol, 1.5 equiv), and 2,6-lutidine (1.4 mL, 12 mmol, 1.2 equiv) at –20 °C for 5 h.

The residue (dr 19:81) was purified by column chromatography (from 96:4 to 90:10 Hexanes/EtOAc) to give 284 mg (0.56 mmol, 6% yield) of *syn* Michael ***ent*-9ak** and 3.49 g (6.9 mmol, 69% yield) of the *anti* Michael ***ent*-9'ak**.

Yellow oil.

R_f 0.4 (80:20 Hexanes/EtOAc).

$[\alpha]_D^{20}$ –243.1 (*c* 1.0 $CHCl_3$).

Chiral HPLC (Phenomenex Lux® Cellulose-5 column, 4% *i*-PrOH in Hexanes, flow rate 1 mL/min): R_t 9.5 min (2*R*,3*R* major isomer) R_t 11.9 min (2*S*,3*S* minor isomer), 99% *ee.*

IR (ATR) ν 2941, 2863, 1720, 1644, 1606, 1580, 1461, 1434, 1389, 1348, 1302, 1284, 1219, 1204, 1120, 1064, 1150, 988, 942, 881, 777, 706, 684, 669 cm^{-1}.

^{1}H NMR (500 MHz, $CDCl_3$) δ 7.19–7.15 (m, 1H, ArH), 6.77–6.68 (m, 3H, ArH), 6.40 (d, *J* = 11.7 Hz, 1H, CHOTIPS), 5.04 (dd, *J* = 11.7, 10.5 Hz, 1H, CHCHOTIPS), 4.05 (dq, *J* = 10.5, 6.5 Hz, 1H, O=CCH), 3.79 (s, 3H, OMe), 3.43 (dt, *J* = 13.2, 5.6 Hz, 1H, NCH_xH_y), 3.22 (t, *J* = 10.5 Hz, 1H, ArCH), 3.11 (ddd, *J* = 13.2, 8.9, 4.6 Hz, 1H, NCH_xH_y), 2.63 (dt, *J* = 12.4, 6.7 Hz, 1H, SCH_xH_y), 2.36 (ddd, *J* = 12.4, 7.5, 5.8 Hz, 1H, SCH_xH_y), 1.83–1.73 (m, 1H, $NCH_2CH_xH_y$), 1.39 (d, *J* = 6.5 Hz, 3H, $CHCH_3$), 1.27–1.16 (m, 1H, $NCH_2CH_xH_y$), 1.16–0.98 (m, 21H, OTIPS).

^{13}C NMR (126 MHz, $CDCl_3$) δ 204.1 (C), 182.3 (C), 159.8 (C), 145.7 (C), 142.7 (CH), 129.7 (CH), 120.1 (CH), 112.7 (CH), 112.5 (CH), 112.1 (CH), 55.3 (CH_3), 51.7 (CH), 47.5 (CH), 46.3 (CH_2), 31.3 (CH_2), 22.3 (CH_2), 17.7 (CH_3), 17.6 (CH_3), 11.9 (CH).

HRMS (ESI+) *m/z* calcd for $[M+H]^+$ $C_{26}H_{42}NO_3S_2Si$: 508.2370, found 508.2370.

(2*R*,3*R*,4*E*)-3-(3-Methoxyphenyl)-*N*,*N*,2-trimethyl-5-triisopropylsilyloxy-4-pentenamide (25)

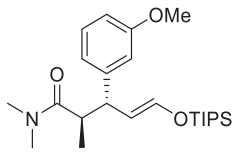

A solution of ***ent*-9'ak** (1.442 g, 2.85 mmol, 1 equiv), DMAP (70 mg, 0.57 mmol, 0.2 equiv) and $Me_2NH{\cdot}HCl$ (583 mg, 7.1 mmol, 2.5 equiv) in CH_2Cl_2 (20 mL) was cooled at 0 °C. Then, neat Et_3N (1.2 mL, 1.5 mmol, 3 equiv) was added dropwise and the mixture was stirred for 2 h at rt.

Afterwards, the crude mixture was diluted with Et_2O (70 mL) and washed with 2 M HCl (2 × 50 mL), 2 M NaOH (2 × 50 mL), and brine (50 mL). The resulting organic layer was dried ($MgSO_4$) and concentrated under reduced pressure to give pure amide **25** (1.192 g, 99% yield) which was used in the next step without further purification.

Colorless oil.
R_f 0.3 (70:30 Hexanes/EtOAc).
$[\alpha]_D^{20}$ +5.7 (*c* 1.0 $CHCl_3$).
IR (ATR) ν 2942, 2865, 1640, 1599, 1463, 1260, 1164, 1045, 923, 881, 803, 781, 685, 662 cm^{-1}.
^{1}H NMR (500 MHz, $CDCl_3$) δ 7.14 (t, *J* = 7.9 Hz, 1H, ArH), 6.79–6.66 (m, 3H, ArH), 6.44 (d, *J* = 11.6 Hz, 1H, CHOTIPS), 5.15 (dd, *J* = 11.6, 10.6 Hz, 1H, CHCHOTIPS), 3.77 (s, 3H, OMe), 3.38 (t, *J* = 10.5 Hz, 1H, ArCH), 2.96 (dq, *J* = 10.4, 6.7 Hz, 1H, $CHCH_3$), 2.71 (s, 3H, NCH_3), 2.69 (s, 3H, NCH_3), 1.16 (d, *J* = 6.7 Hz, 3H, $CHCH_3$), 1.14–1.02 (m, 21H, OTIPS).
^{13}C NMR (126 MHz, $CDCl_3$) δ 175.7 (C), 159.4 (C), 146.2 (C), 142.4 (CH), 129.1 (CH), 119.7 (CH), 113.0 (CH), 111.6 (CH), 55.1 (CH_3), 48.2 (CH), 41.4 (CH), 37.1 (CH_3), 35.4 (CH_3), 17.7 (CH_3), 16.9 (CH_3), 11.9 (CH).
HRMS (ESI+) *m/z* calcd for $[M+H]^+$ $C_{24}H_{42}NO_3Si$: 420.2928, found: 420.2917.

(2*R*,3*S*,4*E*)-3-(3-Methoxyphenyl)-*N*,*N*,2-trimethyl-5-triisopropylsilyloxypentylamine (26)[8]

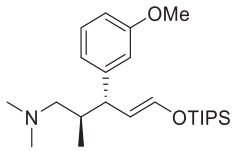

A mixture of $LiAlH_4$ (89 mg, 2.2 mmol, 2.2 equiv) in THF (5 mL) was cooled to 0 °C. Then, a solution of **25** (419 mg, 1 mmol, 1 equiv) in THF (5 mL) was added dropwise and the resulting mixture was stirred at 0 °C for 3 h.
The reaction was quenched with 2 M NaOH (5 mL), further rinsed with 2 M NaOH (20 mL) and extracted with CH_2Cl_2 (3 × 10 mL). The combined organic extracts were dried ($MgSO_4$) and concentrated under reduced pressure. The resultant residue was purified by column chromatography (from 98:2 to 90:10 CH_2Cl_2/MeOH) to give 318 mg (0.78 mmol, 78% yield) of pure amine **26**.

Colorless oil.
R_f 0.5 (CH_2Cl_2/MeOH 90:10).
$[\alpha]_D^{20}$ +11.2 (*c* 1.0 $CHCl_3$).
IR (ATR) *ν* 2942, 2866, 2816, 2762, 1655, 1461, 1259, 1047, 881, 847, 776, 755, 684, 663 cm^{-1}.
^{1}H NMR (500 MHz, $CDCl_3$) δ 7.19 (t, *J* = 7.9 Hz, 1H, ArH), 6.82–6.68 (m, 3H, ArH), 6.36 (d, *J* = 11.7 Hz, 1H, CHOTIPS), 5.23 (dd, *J* = 11.7, 10.4 Hz, 1H, CHCHOTIPS), 3.79 (s, 3H, OMe), 3.22 (dd, *J* = 10.4, 4.9 Hz, 1H, ArCH), 2.20 (s, 6H, $N(CH_3)_2$), 2.18–2.12 (m, 1H, NCH_xH_y), 2.03–1.91 (m, 2H, NCH_xH_y, $CHCH_3$), 1.20–1.05 (m, 21H, OTIPS), 0.84 (d, *J* = 6.4 Hz, 3H, $CHCH_3$).
^{13}C NMR (126 MHz, $CDCl_3$) δ 159.5 (C), 147.3 (C), 142.2 (CH), 129.1 (CH), 120.2 (CH), 113.8 (CH), 110.7 (CH), 109.7 (CH), 65.0 (CH_2), 55.1 (CH_3), 46.5 (CH), 45.8 (CH_3), 36.7 (CH), 17.8 (CH_3), 14.5 (CH_3), 12.0 (CH).
HRMS (ESI+) *m/z* calcd for $[M+H]^+$ $C_{24}H_{44}NO_2Si$: 406.3136, found: 406.3130.

(3*R*,4*R*)-5-Dimethylamino-3-(3-methoxyphenyl)-4-methylpentanal (27)[9]

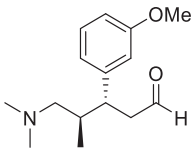

Amine **26** (405 mg, 1 mmol, 1 equiv) was dissolved in a HCl (1 M, 3 mL) and the mixture was stirred at rt for 8 h.

The crude mixture was diluted with Et_2O (50 mL) and washed with 2 M HCl (3 × 15 mL). The aqueous layer was basified with 2 M NaOH (70 mL) and extracted with CH_2Cl_2 (3 × 20 mL). The combined organic extracts were dried (K_2CO_3) and concentrated under reduced pressure. The crude mixture of aldehyde **27** was used without further purification.

(2*R*,3*R*)-3-(3-Methoxyphenyl)-*N*,*N*,2-trimethylpentylamine (28)

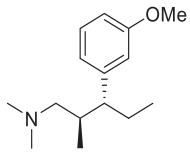

A solution of the crude mixture of aldehyde **27** and $N_2H_4{\cdot}H_2O$ (1.6 mL, 32 mmol, 32 equiv) in ethylene glycol (8 mL) was heated at 160 °C for 4 h. Afterwards, the flask was opened for 5 min and NaOH (1.58 g, 40 mmol, 40 equiv) was added. The resulting mixture was heated at 200 °C for 16 h.

The crude mixture was cooled to rt, diluted with 2 M NaOH (50 mL) and extracted with CH_2Cl_2 (3 × 20 mL). The combined organic extracts were dried ($MgSO_4$) and concentrated under reduced pressure to give 206 mg (0.88 mmol, 88% yield) of amine **28**.

Colorless oil.
R_f 0.2 (90:10 CH_2Cl_2/MeOH).
$[\alpha]_D^{20}$ –30.4 (*c* 1.0 $CHCl_3$).
IR (ATR) ν 2960, 2934, 2872, 2815, 2762, 1582, 1453, 1436, 1258, 1153, 1043, 774, 700 cm^{-1}.
^{1}H NMR (500 MHz, $CDCl_3$) δ 7.23–7.17 (m, 1H, ArH), 6.75–6.71 (m, 2H, ArH), 6.70–6.67 (m, 1H, ArH), 3.80 (s, 3H, OMe), 2.33 (ddd, *J* = 10.8, 6.7, 3.8 Hz, 1H, ArCH), 2.14 (s, 6H, N(CH_3)$_2$), 2.06–1.93 (m, 2H, NCH_2), 1.89–1.80 (m, 1H, $CHCH_3$), 1.80–1.72 (m, 1H, $CH_xH_yCH_3$), 1.64–1.51 (m, 1H, $CH_xH_yCH_3$), 0.97 (d, *J* = 6.6 Hz, 3H, $CHCH_3$), 0.73 (t, *J* = 7.4 Hz, 3H, CH_2CH_3).
^{13}C NMR (126 MHz, $CDCl_3$) δ 159.4 (C), 146.2 (C), 128.9 (CH), 121.0 (CH), 114.6 (CH), 110.6 (CH), 64.8 (CH_2), 55.1 (CH_3), 51.5 (CH), 45.8 (CH_3), 36.6 (CH), 24.0 (CH_2), 15.9 (CH_3), 12.3 (CH_3).
HRMS (ESI+) *m/z* calcd for $[M+H]^+$ $C_{15}H_{26}NO$: 236.2009, found: 236.2007.

(2*R*,3*R*)-Tapentadol [10]

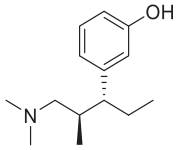

A solution of amine **28** (168 mg, 0.7 mmol, 1 equiv) in HBr 48% (3.5 mL) was heated to reflux for 5 h.

After cooling, the mixture was rinsed with $NaHCO_3$ (50 mL) and washed with CH_2Cl_2 (5 × 20 mL). The combined organic extracts were dried (K_2CO_3) and concentrated under reduced pressure to give pure **Tapentadol** (153 mg, 0.67 mmol, 96% yield).

Brown oil.
R_f 0.2 (90:10 CH_2Cl_2/MeOH).
$[\alpha]_D^{20}$ –23.2 (*c* 1.0 $CHCl_3$); **$[\alpha]_D^{20}$** –30.3 (*c* 1.0 MeOH); lit.[34] **$[\alpha]_D^{20}$** –28.8 (*c* 1.0 MeOH).
IR (ATR) ν 2961, 2872, 2816, 1731, 1699, 1458, 1156, 1013, 778, 736, 702 cm^{-1}.
^{1}H NMR (400 MHz, $CDCl_3$) δ 7.13 (t, *J* = 7.8 Hz, 1H, Ar<u>H</u>), 6.69–6.62 (m, 2H, Ar<u>H</u>), 6.59 (s, 1H, Ar<u>H</u>), 2.32 (ddd, *J* = 10.7, 6.5, 3.8 Hz, 1H, ArC<u>H</u>), 2.18 (s, 6H, N(C<u>H</u>$_3$)$_2$), 2.16–2.10 (m, 1H, NC<u>H</u>$_x$H$_y$), 2.04 (ddd, *J* = 12.0, 9.1, 2.0 Hz, 1H, NCH$_x$<u>H</u>$_y$), 1.94–1.80 (m, 1H, C<u>H</u>CH$_3$), 1.80–1.67 (m, 1H, C<u>H</u>$_x$H$_y$CH$_3$), 1.62–1.48 (m, 1H, CH$_x$<u>H</u>$_y$CH$_3$), 0.97 (d, *J* = 6.6 Hz, 3H, CHC<u>H</u>$_3$), 0.70 (t, *J* = 7.3 Hz, 3H, CH$_2$C<u>H</u>$_3$).
^{13}C NMR (101 MHz, $CDCl_3$) δ 156.1 (C), 146.1 (C), 129.1 (CH), 120.5 (CH), 115.5 (CH), 113.1 (CH), 64.7 (CH_2), 51.2 (CH), 45.7 (CH_3), 36.5 (CH), 23.7 (CH_2), 16.0 (CH_3), 12.3 (CH_3).
HRMS (ESI+) *m/z* calcd for $[M+H]^+$ $C_{14}H_{24}NO$: 222.1852, found: 222.1862.

CHAPTER IV

The Mannich reaction

14 Synthesis of *N*-electrophiles

14.1 Synthesis of imines

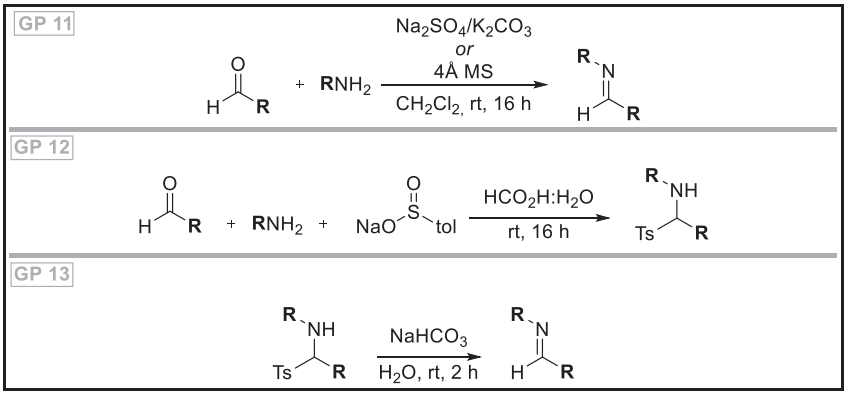

General Procedure 12[11]

Amine (1 equiv) was added dropwise to a solution of the corresponding aldehyde (1 equiv) in CH_2Cl_2 (1 M) in the presence of a dehydrating agent, which could be anhydrous Na_2SO_4 (2 equiv) and anhydrous K_2CO_3 (2 equiv) or 4Å MS. The resulting mixture was stirred at rt for 16 h. Then, the solids were removed by filtration, and the volatiles removed under reduced pressure to obtain the corresponding crude product, which was purified by either recrystallization or distillation of the remaining aldehyde.

General Procedure 13[12]

Aldehyde (1 equiv) was added dropwise to a solution of *p*-Toluenesulphonamide (1 equiv) and sodium *p*-toluenesulphinate (1 equiv) in H_2O/HCOOH 1:1 (0.33 M) at rt and the resulting mixture was stirred for 16 h. Afterwards, the resulting white solid was filtered and washed with water (100 mL/10 mmol) and Hexanes (100 mL/10 mmol) to give pure tosyl-imine adduct.

General Procedure 14[12]

A mixture of tosyl-imine adduct and sat. $NaHCO_3$ or K_2CO_3 (100 mL/10 mmol) was dissolved in CH_2Cl_2 (100 mL/10 mmol), and the biphasic mixture was vigorously stirred at rt for 2–16 h.

The organic layer was separated, dried with K_2CO_3 and concentrated under reduced pressure. The resultant crude solid was recrystallised to obtain pure imine.

(*E*)-*N*-Tosyl benzimine (a')

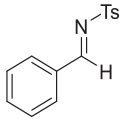

Following General Procedure 13, benzaldehyde (1.0 mL, 10 mmol), *p*-toluenesulphonamide (1.71 g, 10 mmol) and sodium *p*-toluenesulphinate (1.79 g, 10 mmol) were used. The resulting solid was directly used without futher purification and treated as described in General Procedure 14 using CH_2Cl_2 and sat. $NaHCO_3$ (100 mL). The resulting imine was recrystallised from EtOAc/Hexanes to give 1.18 g (4.5 mmol, 45 % yield) of pure **a'**.

White solid.

^{1}H NMR (400 MHz, $CDCl_3$) δ 9.03 (s, 1H, NC<u>H</u>), 7.96–7.86 (m, 4H, Ar<u>H</u>), 7.65–7.59 (m, 1H, Ar<u>H</u>), 7.52–7.46 (m, 2H, Ar<u>H</u>), 7.38–7.32 (m, 2H, Ar<u>H</u>), 2.44 (s, 3H, ArC<u>H</u>$_3$).

***O*-Benzyl *N*-(phenyl(tosyl)methyl)carbamate**

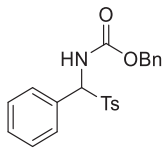

Following General Procedure 13, benzaldehyde (1.0 mL, 10 mmol) was added dropwise to a solution of benzyl carbamate (1.51 g, 10 mmol) and sodium *p*-toluenesulphinate (1.78 g, 10 mmol) were used to give 3.90 g (10 mmol, 99% yield) of pure *O*-benzyl *N*-(phenyl(tosyl)methyl)carbamate.

White solid.

^{1}H NMR (400 MHz, $CDCl_3$) δ 7.70 (d, *J* = 8.3 Hz, 2H, Ar<u>H</u>), 7.46–7.30 (m, 10H, Ar<u>H</u>), 7.26 (s, 2H, Ar<u>H</u>), 5.99–5.85 (m, 2H, N<u>H</u>C<u>H</u>), 5.03–4.89 (m, 2H, C<u>H</u>$_2$Ph), 2.43 (s, 3H, ArC<u>H</u>$_3$).

Benzyl (*E*)-benzylidenecarbamate (b')

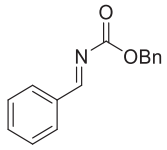

Following General Procedure 14, a mixture of **b''** (890 mg, 2.25 mmol) in CH_2Cl_2 (35 mL) and sat. solution of K_2CO_3 in water (35 mL) was vigorously stirred for 16 h. The remaining crude mixture was recrystallized with CH_2Cl_2/Hexanes to obtain 63 mg (0.24 mmol, 11% yield)of pure **b'**.

White solid.

^{1}H NMR (400 MHz, $CDCl_3$) δ 8.95 (s, 1H, NC<u>H</u>), 7.97–7.88 (m, 2H, Ar<u>H</u>), 7.62–7.55 (m, 1H, Ar<u>H</u>), 7.52–7.27 (m, 7H, Ar<u>H</u>), 5.32 (s, 2H, C<u>H</u>$_2$Ph).

***N*-(Phenyl(tosyl)methyl)benzamide**

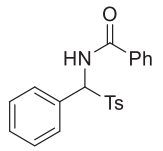

Following General Procedure 13, benzaldehyde (1.0 mL, 10 mmol), benzamide (1.21 g, 10 mmol) and sodium *p*-toluenesulphinate (1.78 g, 10 mmol) were used to give 959 mg (2.6 mmol, 26% yield) of pure *N*-(phenyl(tosyl)methyl)benzamide.

White solid.

^{1}H NMR (400 MHz, $CDCl_3$) δ 7.76 (d, *J* = 8.3 Hz, 1H, Ar<u>H</u>), 7.68 (d, *J* = 6.9 Hz, 2H, Ar<u>H</u>), 7.58–7.50 (m, 3H, Ar<u>H</u>), 7.46–7.39 (m, 5H, Ar<u>H</u>), 7.31–7.23 (m, 2H, Ar<u>H</u>), 7.14 (d, *J* = 10.3 Hz, 1H, N<u>H</u>), 6.45 (d, *J* = 10.3 Hz, 1H NHC<u>H</u>) 2.41 (s, 3H, ArC<u>H</u>$_3$).

(*E*)-*N*-Benzylidenebenzamide (c')

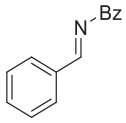

Following General Procedure 14, a mixture of **c''** (365 mg, 1 mmol) in CH_2Cl_2 (16 mL) and sat. solution of K_2CO_3 in water (16 mL) was vigorously stirred for 16 h. Afterwards, the organic layer was separated, dried (K_2CO_3) and concentrated under reduced pressure (high vacuum) at 40 °C to eliminate remaining

benzaldehyde and give **c'**, which was directly used in the next reaction without further purification

(*E*)-*N*-Benzyl benzimine (d')

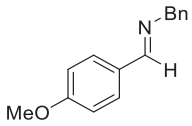

Following General Procedure 12, 4Å MS were used alongside with 4-methoxybenzaldehyde (1.2 mL, 10 mmol) and benzylamine (1.1 mL, 10 mmol). The crude product **d'** (1.99 g, 8.8 mmol, 88% yield) was sufficiently pure to use in further steps.

White solid.

^{1}H NMR (400 MHz, $CDCl_3$) δ 8.33 (s, 1H, NC<u>H</u>), 7.76–7.70 (m, 2H, Ar<u>H</u>), 7.37–7.30 (m, 4H, Ar<u>H</u>), 7.29–7.22 (m, 1H, Ar<u>H</u>), 6.97–6.90 (m, 2H, Ar<u>H</u>), 4.79 (d, *J* = 1.3 Hz, 3H, C<u>H</u>$_2$Ph), 3.84 (s, 3H, O<u>Me</u>).

(*E*)-*N*-Phenyl 4-methoxybenzimine (e')

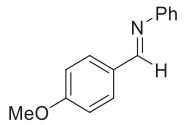

Following General Procedure 12, 4Å MS were used alongside with 4-methoxybenzaldehyde (1.2 mL, 10 mmol) and aniline (0.9 mL, 10 mmol). The crude product **e'** (1.89 g, 8.9 mmol, 89% yield) was sufficiently pure to use in further steps.

Pale brown solid.

^{1}H NMR (400 MHz, $CDCl_3$) δ 8.38 (s, 1H, NC<u>H</u>), 7.90–7.81 (m, 2H, Ar<u>H</u>), 7.43–7.34 (m, 2H, Ar<u>H</u>), 7.25–7.16 (m, 3H, Ar<u>H</u>), 7.02–6.95 (m, 2H, Ar<u>H</u>), 3.87 (s, 3H, O<u>Me</u>).

P,P-Diphenylphosphiniamide

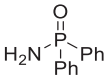

Anhydrous NH_3, which was generated by adding dropwise a sat. solution of NaOH to solid NH_4Cl and dried by passing the gas through an anhydrous $CaCl_2$ tube, was bubbled through a solution of diphenylphosphinic chloride (1.9 mL, 10 mmol) in THF (60 mL) and the resulting solution was stirred for 16 h at rt.

Afterwards, water (60 mL) was added to the mixture and it was concentrated under reduced pressure. Then, the mixture was extracted with CH_2Cl_2 (3 × 20 mL) and the combined organic layers were dried ($MgSO_4$) and concentrated under reduced pressure to give pure diphenylphosphinamide as a white solid (1.66 g, 7.6 mmol, 76% yield).

White solid.
^{1}H NMR (500 MHz, $CDCl_3$) δ 7.97–7.90 (m, 4H, ArH), 7.55–7.48 (m, 2H, ArH), 7.48–7.41 (m, 4H, ArH), 3.07 (s, 2H, NH_2).

(*E*)-*N*-Benzylidene-*P,P*-diphenylphosphinic amide (f')[13]

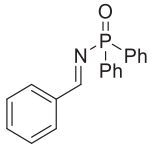

Neat Et_3N (1.25 mL, 9 mmol) and benzaldehyde (0.61 mL, 6 mmol) were added dropwise sequentially to a solution of diphenylphosphinamide (652 mg, 3 mmol) in CH_2Cl_2 (15 mL) and the mixture was cooled to 0 °C. Subsequently, $TiCl_4$ (180 µL, 1.65 mmol) was added dropwise and the resulting mixture was stirred at rt for 2 h.

Afterwards, the mixture was diluted with toluene (100 mL) and filtered through Celite®. The crude mixture was recrystallized from CH_2Cl_2/Hexanes to give 652 mg (2.1 mmol, 71% yield) of product **f'**.

White solid.
^{1}H NMR (400 MHz, $CDCl_3$) δ 9.33 (d, *J* = 32.0 Hz, 1H, NCH), 8.05–7.86 (m, 5H, ArH), 7.55–7.41 (m, 10H, ArH).

14.2 Synthesis of an *O*-methyl oxime

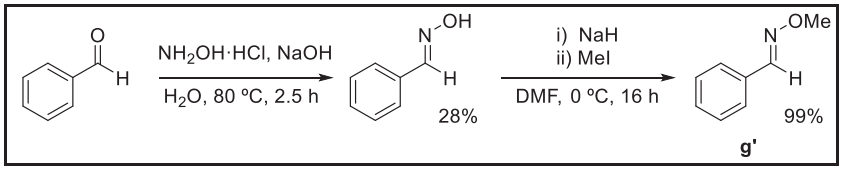

(*E*)-*N*-benzaldehyde oxime[14]

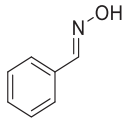

Benzaldehyde (1.0 mL, 10 mmol) was added to a solution of hydroxylamine hydrochloride (1.04 g, 15 mmol) in 2 M NaOH (30 mL, 15 mmol) and the mixture was stirred at 80 °C for 2.5 h.

Afterwards, the mixture was cooled to rt and extracted with EtOAc (60 mL). The organic extract was dried (K_2CO_3), and the volatiles were removed under reduced pressure to obtain 340 mg (2.8 mmol, 28% yield) of pure oxime.

White solid.
^{1}H NMR (500 MHz, $CDCl_3$) δ 8.15 (s, 1H, NC<u>H</u>), 8.01–7.72 (m, 1H, NO<u>H</u>), 7.62–7.54 (m, 2H, Ar<u>H</u>), 7.42–7.36 (m, 3H, Ar<u>H</u>).

(*E*)-*N*-Benzaldehyde *O*-methyloxime (g')[14]

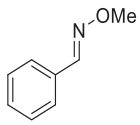

Neat methyl iodide (227 μL, 3.6 mmol) was added dropwise to a solution of *N*-benzaldehyde oxime (340 mg, 2.8 mmol) and NaH 60% in mineral oil (170 mg, 4.4 mmol) in DMF (30 mL) at 0 °C and the mixture was stirred for 16 h at rt. Then, the mixture was diluted in EtOAc (60 mL) and washed with $NaHCO_3$ (4 × 50 mL), dried (K_2CO_3) and concentrated under reduced pressure to give pure *O*-methyl oxime **g'**.

White solid.
^{1}H NMR (500 MHz, $CDCl_3$) δ 8.06 (s, 1H, NC<u>H</u>), 7.65–7.55 (m, 2H, Ar<u>H</u>), 7.45–7.34 (m, 3H, Ar<u>H</u>), 3.98 (d, *J* = 1.7 Hz, 3H, O<u>Me</u>).

14.3 Synthesis of *N,O* and *N,N* aminals

GENERAL PROCEDURE 15[15]

To a solution of K_2CO_3 (2 equiv) and Na_2SO_4 (2 equiv) in MeOH (2 M) was added the corresponding amine (1 equiv for *N,O* or 2 equiv for *N,N*) and aldehyde (1 equiv) at rt and the mixture was stirred at rt for 16 h. Afterwards, the mixture was filtered and the volatiles were removed under reduced pressure to give a crude product, which was purified by recrystallization or used without further purification.

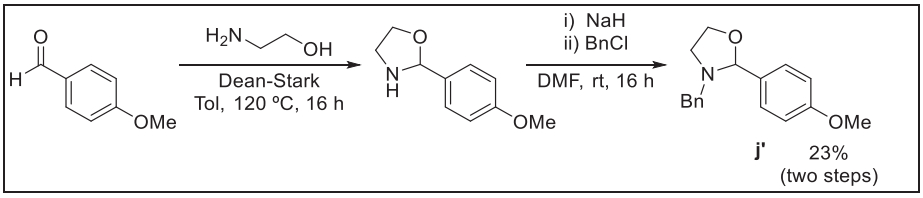

4-methoxybenzaldehyde *N*-benzyl-ethanolamine *N,O*-aminal (j')

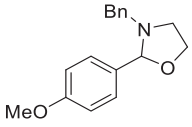

A round bottomed flask was charged with benzaldehyde (1.0 mL, 10 mmol) and ethanolamine (0.66 mL, 11 mmol), equipped with a Dean Stark apparatus. Toluene (60 mL) was added and the resultant mixture was heated to reflux for 16 h. Afterwards, the volatiles were removed, and the crude mixture was directly used in the next step without further purification.

A solution of the previously prepared hemiaminal in DMF (5 mL) was added dropwise to a suspension of NaH 60% in mineral oil (520 mg, 13 mmol) in DMF (15 mL) at 0 °C. Then, benzyl chloride (1.7 mL, 15 mmol) was added dropwise and the mixture stirred at rt for 16 h.

Afterwards, the mixture was cooled to 0 °C and it was carefully quenched with water, diluted with EtOAc (40 mL) and washed with water (4 × 40 mL) and brine (40 mL). The crude mixture was further purified by flash chromatography (from 90:10 to 70:30 Hexanes/EtOAc with 5% Et_3N). Then, the purified fraction was further purified by distillation under vacuum to obtain 547 mg (2.3 mmol, 23% yield) of pure product **j'**.

Colorless oil.

^{1}H NMR (400 MHz, $CDCl_3$) δ 8.33 (s, 1H, NC<u>H</u>O), 7.79–7.70 (m, 2H, Ar<u>H</u>), 7.46–7.38 (m, 3H, Ar<u>H</u>), 7.34–7.23 (m, 4H, Ar<u>H</u>), 4.57 (s, 2H, C<u>H</u>$_2$Ph), 3.88–3.76 (m, 4H, OC<u>H</u>$_2$C<u>H</u>$_2$).

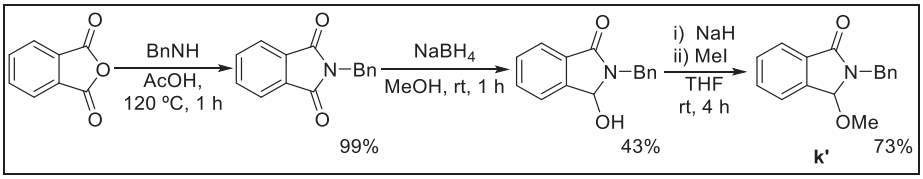

***N*-Benzylphtalimide**

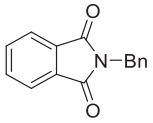

Following a literature procedure,[16] a solution of phtalic anhydride (2.96 g, 20 mmol) and benzylamine (3.3 mL, 30 mmol) in glacial acetic acid (15 mL) was heated to reflux for 1 h. Afterwards, the mixture was poured into ice/water and the resultant white solid was filtered and recrystallized (EtOH) to obtain 4.70 g (20 mmol, 99% yield) of pure *N*-benzylphtalimide.

White solid.

^{1}H NMR (500 MHz, $CDCl_3$) δ 7.85 (dd, *J* = 5.5, 3.0 Hz, 2H, Ar<u>H</u>), 7.73–7.68 (m, 2H, Ar<u>H</u>), 7.45–7.41 (m, 2H, Ar<u>H</u>), 7.34–7.29 (m, 2H, Ar<u>H</u>), 7.28–7.24 (m, 1H, Ar<u>H</u>), 4.85 (s, 2H, C<u>H</u>$_2$Ph).

2-Benzylisoindolin-1-one

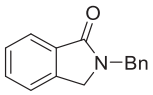

A mixture of tin powder (1.19 g, 10 mmol) and *N*-benzylphtalimide (1.19 g, 5 mmol) in a 5:1 glacial AcOH/37% HCl (10 mL) was stirred at rt for 16 h. Afterwards, the volatiles were removed under reduced pressure with a $NaHCO_3$ trap, and the resulting aqueous layer was extracted with EtOAc (3 × 20 mL). The combined organic extracts were dried ($MgSO_4$) and the volatiles were removed under reduced pressure to give 629 mg (2.81 mmol, 56% yield) of pure product.

White solid.

R_f 0.3 (70:30 Hexanes/EtOAc).

^{1}H NMR (400 MHz, $CDCl_3$) δ 7.90 (d, *J* = 7.3 Hz, 1H, ArH), 7.56–7.44 (m, 2H, ArH), 7.42–7.28 (m, 6H, ArH), 4.81 (s, 2H, CH_2Ph), 4.27 (s, 2H, NCH_2Ar).

***N*-Benzyl-3-hydroxyisoindolin-1-one**

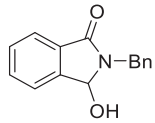

Solid $NaBH_4$ (57 mg, 1.5 mmol) was added slowly to a solution of *N*-benzyl phtalimide (474 mg, 1 mmol) in MeOH (10 mL) in an open flask and the resultant mixture was stirred at rt for 1.5 h. Then, the mixture was diluted with water (20 mL) and MeOH was removed under reduced pressure. The resulting aqueous layer was extracted with CH_2Cl_2 (3 × 20 mL), the combined organic extracts were dried ($MgSO_4$) and concentrated under reduced pressure. The crude mixture was purified by flash chromatography (from 80:20 to 60:40 Hexanes/EtOAc) to give 102 mg (0.43 mmol, 43% yield) of *N*-Benzyl-3-hydroxyisoindolin-1-one.

White solid.

R_f 0.5 (70:30 Hexanes/EtOAc).

^{1}H NMR (500 MHz, $CDCl_3$) δ 7.86–7.79 (m, 1H, ArH), 7.62–7.49 (m, 3H, ArH), 7.41–7.29 (m, 5H, ArH), 5.65 (d, *J* = 11.6 Hz, 1H, NCH), 5.10 (d, *J* = 14.8 Hz, 1H, CH_xH_yPh), 4.40 (d, *J* = 14.8 Hz, 1H, CH_xH_yPh), 2.30 (d, *J* = 11.6 Hz, 1H, OH).

***N*-Benzyl-3-methoxyisoindolin-1-one (k')**

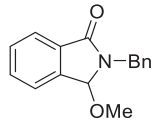

Methyl iodide (40 μL, 0.65 mmol) was added dropwise to a solution of *N*-benzyl-3-methoxyisoindolin-1-one (102 mg, 0.43 mmol) and NaH 60% in mineral oil (22 mg, 0.56 mmol) in THF (1 mL) at 0 °C and the mixture was stirred for 4 h at rt.

Afterwards, the reaction was quenched carefully with water (10 mL) at 0 °C and extracted with CH_2Cl_2 (3 × 10 mL). The combined organic extracts were dried ($MgSO_4$) and concentrated under reduced pressure. The crude mixture was purified by flash chromatography (from 90:10 to 70:30 Hexanes/EtOAc) to give 80 mg (0.31 mmol, 73% yield) of pure **k'**.

White solid.

R_f 0.6 (80:20 Hexanes/EtOAc).

^{1}H NMR (500 MHz, $CDCl_3$) 7.90–7.85 (m, 1H), 7.60–7.46 (m, 3H, ArH), 7.39–7.27 (m, 5H, ArH), 5.71 (s, 1H, CHOMe), 5.19 (d, *J* = 14.7 Hz, 1H, CH_xH_yPh), 4.21 (d, *J* = 14.7 Hz, 1H, CH_xH_yPh), 2.89 (s, 3H, OMe).

N-(1-methoxy(phenyl)methyl)piperidine (l')

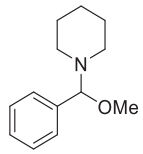

Following the General Procedure 15, benzaldehyde (0.5 mL, 5 mmol), K_2CO_3 (1.4 g, 10 mmol), Na_2SO_4 (1.4 g, 10 mmol), piperidine (0.5 mL, 5 mmol) and MeOH (2.5 mL) were used to give 745 mg (3.6 mmol, 73% yield) of pure **l'**.

White solid.

^{1}H NMR (400 MHz, $CDCl_3$) δ 7.37–7.27 (m, 5H, ArH), 4.73 (s, 1H, NCH), 3.38 (s, 3H, OMe), 2.54 (t, *J* = 5.4 Hz, 4H, NCH_2), 1.57–1.47 (m, 4H, NCH_2CH_2), 1.44–1.36 (m, 2H, $NCH_2CH_2CH_2$).

Benzaldehyde dipiperidine *N,N*-aminal (m')

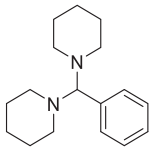

Following a reported procedure,[17] piperidine (3.80 mL, 20 mmol) and benzaldehyde (1.0 mL, 10 mmol) were added sequentially to a suspension of chromatographic Al_2O_3 (3.2 g) in THF (6 mL) and the mixture was heated to reflux for 16 h. Afterwards, the mixture was filtered through Al_2O_3 and the volatiles were removed under reduced pressure. The crude solid was recrystallized from anhydrous acetonitrile and washed with Hexanes to give 1.93 g (7.5 mmol, 75% yield) of **m'**.

White solid

^{1}H NMR (400 MHz, $CDCl_3$) δ 7.35–7.28 (m, 2H, ArH), 7.27–7.23 (m, 1H, ArH), 7.22–7.17 (m, 2H), 3.56 (s, 1H, NCH), 2.50–2.19 (m, 8H, NCH_2), 1.57–1.46 (m, 8H, NCH_2CH_2), 1.41–1.31 (m, 4H, $NCH_2CH_2CH_2$).

Formaldehyde *N,N*-dibenzyl-*O*-methyl *N,O*-aminal (n')

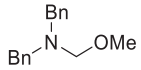

Following the General Procedure 15, *N,N*-dibenzylamine (1.92 mL, 10 mmol), paraformaldehyde (333 mg, 10 mmol), K_2CO_3 (2.8 g, 20 mmol), Na_2SO_4 (2.8 g, 20 mmol) and MeOH (5 mL) were used. The crude product was distilled under reduced pressure at 114 °C to obtain 1.05 g (4.4 mmol, 43% yield) of **n'**.

Colorless liquid.
^{1}H NMR (400 MHz, $CDCl_3$) δ 7.40–7.21 (m, 10H, ArH), 4.03 (s, 2H, NCH_2), 3.83 (s, 4H, CH_2Ph), 3.24 (s, 3H, OMe).

Formaldehyde *N,N*-dibenzyl *N,N*-aminal (o')

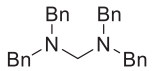

Following the General Procedure 15, *N,N*-dibenzylamine (3.80 mL, 20 mmol), paraformaldehyde (333 mg, 10 mmol), K_2CO_3 (2.8 g, 20 mmol), Na_2SO_4 (2.8 g, 20 mmol) and CH_2Cl_2 (20 mL) were used. The mixture was diluted with $NaHCO_3$ (30 mL) and extracted with CH_2Cl_2 (3 × 20 mL). The resulting solid was recrystallized from CH_2Cl_2/Hexanes to give 1.02 g (2.5 mmol, 25% yield) of **o'**.

White solid.
^{1}H NMR (400 MHz, $CDCl_3$) δ 7.36–7.19 (m, 20H, ArH), 3.61 (s, 8H, CH_2Ph), 3.10 (s, 2H, NCH_2N).

Benzaldehyde dibenzylamine 1-benzotriazole *N,N*-aminal (p')

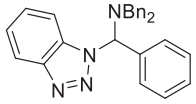

Following a literature procedure,[18] dibenzylamine (1.92 mL, 10 mmol) and benzaldehyde (1.0 mL, 10 mmol) were added sequentially to a solution of benzotriazole (1.2 g, 10 mmol) in 1:1 Et_2O/MeOH at rt. The mixture was stirred for 10 min to dissolve all products and it was stirred at 0 °C for 16 h resulting in the precipitation of a white solid.

Afterwards, the mixture was filtered and the solid was washed with Et_2O to give 2.55 g (6.3 mmol, 63 % yield) **p'** as a 3:1 mixture of isomers (1-benzotriazole/2-benzotriazole).

White solid.
^{1}H NMR major isomer (500 MHz, $CDCl_3$) δ 8.22–8.12 (m, 1H, ArH), 7.45–7.23 (m, 17H, ArH), 6.94–6.90 (m, 1H, ArH) 6.84 (s, 1H, CHPh), 4.25 (d, *J* = 14.1 Hz, 2H, CH_xH_yPh), 3.50 (d, *J* = 14.1 Hz, 2H, CH_xH_yPh).
^{1}H NMR minor isomer (500 MHz, $CDCl_3$) δ 7.45–7.22 (m, 17H, ArH), 7.17–7.13 (m, 2H, ArH), 6.96 (s, 1H, CHPh), 4.24 (d, *J* = 14.2 Hz, 2H, CH_xH_yPh), 3.55 (d, *J* = 14.2 Hz, 2H, CH_xH_yPh).

14.4 Synthesis of a nitrone

***N*-Benzyl-α-phenylnitrone (q')**

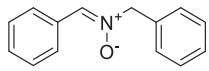

Following a literature procedure,[19] a solution of 30% H_2O_2 (1.2 mL, 12 mmol) was added to a solution of dibenzylhydroxylamine (640 mg, 3 mmol) in acetonitrile (9 mL) and the mixture was stirred at 50 °C for 16 h.

Then, the volatiles were removed under reduced pressure. The crude mixture was purified by flash chromatography (from 80:20 to 60:40 Hexanes/EtOAc) to give 568 mg (2.7 mmol, 90% yield) of **q'**.

White solid.

R_f 0.3 (70:30 Hexanes/EtOAc).

^{1}H NMR (500 MHz, $CDCl_3$) δ 8.25–8.17 (m, 2H, ArH), 7.53–7.46 (m, 2H, ArH), 7.46–7.34 (m, 7H, ArH, NCH), 5.06 (s, 2H, CH_2Ph).

15 Mannich addition of thioimides to imines

15.1 Assessment of the scaffold

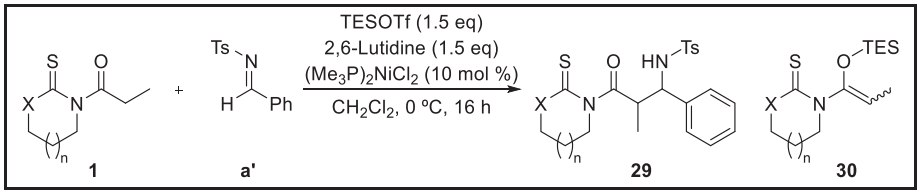

Neat TESOTf (35 µL, 0.15 mmol, 1.5 equiv) and 2,6-lutidine (17 µL, 0.15 mmol, 1.5 equiv) were added sequentially to a solution of a *N*-propanoyl-thioimide **1** (0.1 mmol), **a'** (29 mg, 0.11 mmol, 1.1 equiv), and $(Me_3P)_2NiCl_2$ (2.8 mg, 10 µmol, 10 mol%) in CH_2Cl_2 (0.2 mL) at 0 °C. The resultant mixture was stirred at this temperature for 16 h.

The reaction was quenched with water (15 mL), and extracted with CH_2Cl_2 (3 × 10 mL). The combined organic extracts were dried (Na_2SO_4) and concentrated under reduced pressure. Mesitylene (14 µL, 0.1 mmol) was added to the crude mixture and it was analysed by ^{1}H NMR. The results are summarised in Table 69.

Entry	1	X	n	t (h)	T (°C)	1 (%)[a]	Mannich (%)[a]	dr[b,c]	34 (%)[a]	Ratio 34 (*Z*:*E*)[b]
1	**1a**	S	1	16	0	53	< 3	-	47	68:32
2	**1n**	O	1	16	0	51	22	57:42	16	50:50
3	**1l**	S	0	16	0	42	4	80:20	54	72:28
4	**1m**	O	0	16	0	42	37	55:44	20	-

a) Established by ^{1}H NMR analysis using mesitylene as internal standard b) Established by ^{1}H NMR analysis. c) dr of the Mannich adduct **29**.

Table 69. Assessment of the scaffold.

15.2 Assessment of the Lewis acid

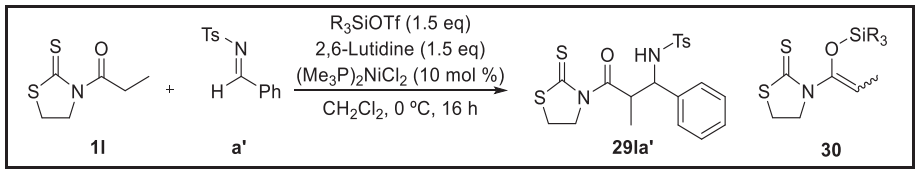

Neat R_3SiOTf (0.15 mmol, 1.5 equiv) and 2,6-lutidine (17 µL, 0.15 mmol, 1.5 equiv) were added sequentially to a solution of **1l** (0.1 mmol, 1 equiv), **a'** (29 mg, 0.11 mmol, 1.1 equiv), and $(Me_3P)_2NiCl_2$ (2.8 mg, 10 µmol, 10 mol%) in CH_2Cl_2 (0.2 mL) at 0 °C and the resultant mixture was stirred at this temperature for 16 h.

The reaction was quenched with water (15 mL) and extracted with CH_2Cl_2 (3 × 10 mL). The combined organic extracts were dried (Na_2SO_4) and concentrated under reduced pressure. Mesitylene (14 µL, 0.1 mmol) was added to the crude mixture and it was analysed by ^1H NMR. The results are summarized in Table 70.

Entry	Lewis acid	1 (%)[a]	Mannich (%)[a]	dr[b]	30l–32l (%)[a]	Ratio 30l–32l (*Z*:*E*)[b]
1	TIPSOTf	75	6	-	6	-
2	TESOTf	16	5	90:10	75	76:24
3	TMSOTf	16	21	88:12	68	57:43
4	$BF_3{\cdot}Et_2O$ TIPSOTf (20 mol%)	93	-	-	-	-

a) Established by ^1H NMR analysis using mesitylene as internal standard b) Established by ^1H NMR analysis.

Table 70. Assessment of the Lewis acid.

15.3 Assessment of the imine activating group

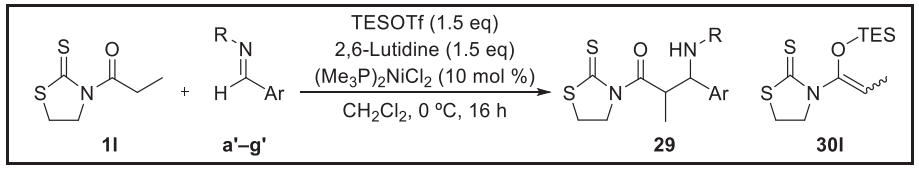

Neat TESOTf (35 µL, 0.15 mmol, 1.5 equiv) and 2,6-lutidine (17 µL, 0.15 mmol, 1.5 equiv) were added sequentially to a solution of **1l** (0.1 mmol), the corresponding imine (1.1 equiv), and $(Me_3P)_2NiCl_2$ (2.8 mg, 10 µmol, 10 mol%) in CH_2Cl_2 (0.2 mL) at 0 °C and the resultant mixture was stirred for 16 h at this temperature.

The reaction was quenched with water (15 mL) and extracted with CH_2Cl_2 (3 × 10 mL). The combined organic extracts were dried (Na_2SO_4) and concentrated under reduced pressure. Mesitylene (14 μL, 0.1 mmol) was added to the crude mixture and it was analysed by ^1H NMR. The results are summarized Table 71.

Entry	imine	SM (%)	Mannich (%)	dr	34(%)
1	**a'**	16	5	90:10	75
2	**b'**	68	-	-	-
3	**c'**	90	-	-	3
4	**d'**	46	< 10	-	0
5	**e'**	25	17		13
6	**f'**	60	-	-	-
7	**g'**	10	-	-	83

a) Established by ^1H NMR analysis using mesitylene as internal standard b) Established by ^1H NMR analysis.

Table 71. Assessment of the imine activating group for the Mannich reaction.

16 The Mannich reaction with *N,O* and *N,N*-Aminals as imine equivalents

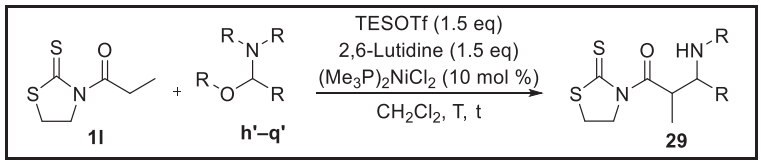

Neat TMSOTf (27 µL, 0.15 mmol, 1.5 equiv) and 2,6-lutidine (17 µL, 0.15 mmol, 1.5 equiv) were added sequentially to a solution of **1l** (18 mg, 0.1 mmol, 1 equiv), the corresponding aminal (0.11 mmol, 1.1 equiv), and $(Me_3P)_2NiCl_2$ (2.8 mg, 10 µmol, 10 mol%) in CH_2Cl_2 (0.2 mL) and the mixture was stirred for 2–16 h.

The reaction was quenched with water (15 mL) and extracted with CH_2Cl_2 (3 × 10 mL). The combined organic extracts were dried (Na_2SO_4) and concentrated under reduced pressure. Mesitylene (14 µL, 0.1 mmol) was added to the crude mixture and it was analysed by ^{1}H NMR. The results are summarized in Table 72.

Entry	imine	t (h)	T (°C)	SM (%)[a]	Mannich (%)[a]	Yield (%)[a]	dr[b]	*er*[c]
1	**h'**	16	0	100	-	-	-	-
2	**i'**	16	0	100	-	-	-	-
3	**j'**	16	0	>90	traces	-	-	-
4	**k'**	16	0	24	-	-	-	-
5	**l'**	16	0	33	29	-	89:11	-
6	**m'**	16	–20	0	-	-	-	-
7	**n'**	16	0	0	85	-	-	-
8	**o'**	16	0	0	100	68	-	57:43
9	**o'**	2	–20	0	100	-	-	78:22
10	**o'**	5	–40	0	100	-	-	78:22
11	**p'**	16	0	25	-	-	-	-

a) Established by ^{1}H NMR analysis using mesitylene as internal standard b) Established by ^{1}H NMR analysis. c) Established by ^{1}H NMR after derivatization with (*S*)-α-methylbenzylamine.

Table 72. Aminals in the Mannich reaction.

_N_-[3-(_N,N_-dibenzylamino)-2-methylpropanoyl]-1,3-thiazolidine-2-thione (29lo')

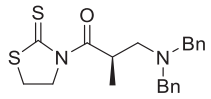

Neat TMSOTf (81 µL, 0.45 mmol, 1.5 equiv) and 2,6-lutidine (52 µL, 0.45 mmol, 1.5 equiv) were added sequentially to a solution of **1l** (53 mg, 0.3 mmol), Formaldehyde **o'** (134 mg, 0.33 mmol) and [(*S*)-BINAP]$NiCl_2$ (11.3 mg, 15 µmol, 5 mol%) in CH_2Cl_2 (0.6 mL) at 0 °C and the resultant mixture was stirred at this temperature for 2 h.

The reaction was quenched with water (15 mL) and extracted with CH_2Cl_2 (3 × 10 mL). The combined organic extracts were dried (Na_2SO_4) and concentrated under reduced pressure. The crude mixture was purified by flash chromatography (from 90:10 to 70:30 Hexanes/EtOAc with 10% Et_3N) to give 67 mg (0.17 mmol, 54% yield) of pure **29lo'**.

Yellow oil

R_f 0.3 (80:20 Hexanes/EtOAc)

^{1}H NMR (400 MHz, $CDCl_3$) δ 7.40–7.20 (m, 10H, Ar<u>H</u>), 4.75 (dp, *J* = 8.6, 6.7 Hz, 1H, C<u>H</u>CH_3), 4.54 (ddd, *J* = 12.0, 7.7, 4.3 Hz, 1H, $SCH_2C\underline{H}_xH_y$), 4.39 (ddd, *J* = 12.0, 10.2, 7.7 Hz, 1H, $SCH_2NCH_x\underline{H}_y$), 3.60 (d, *J* = 13.8 Hz, 2H, $PhC\underline{H}_xH_y$), 3.54 (d, *J* = 13.8 Hz, 2H, $PhCH_x\underline{H}_y$), 3.26 (ddd, *J* = 11.0, 10.2, 7.7 Hz, 1H, $SC\underline{H}_xH_y$), 3.17 (ddd, *J* = 11.0, 7.7, 4.3 Hz, 1H, $SCH_x\underline{H}_y$), 2.94 (dd, *J* = 12.5, 8.6 Hz, 1H, $CHC\underline{H}_xH_y$), 2.48 (dd, *J* = 12.5, 6.7 Hz, 1H, $CHCH_x\underline{H}_y$), 1.15 (d, *J* = 6.7 Hz, 3H, $CHC\underline{H}_3$).

^{13}C NMR (101 MHz, $CDCl_3$) δ 201.5 (C), 178.9 (C), 139.2 (C), 129.6 (CH), 128.8 (CH), 128.2 (CH), 127.0 (CH), 58.6 (CH_2), 56.5 (CH_2), 38.0 (CH), 28.47 (CH_2), 15.5 (CH_3).

Chiral HPLC (Phenomenex Lux® Cellulose-2 column, 5% *i*-PrOH in Hexanes, flow rate 1 mL/min): R_t 13.5 min (minor isomer) R_t 17.9 min (major isomer), 14% *ee*.

MS (ESI+) m/z calcd for $[M+H]^+$ $C_{21}H_{25}N_2OS_2$: 385.1; found: 385.1.

3-(1-Trimethylsilyloxy-1-propenyl)thiazolidine-2-thione (30l)

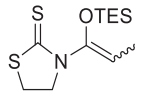

Neat TESOTf (35 µL, 0.15 mmol, 1.5 equiv) and 2,6-lutidine (17 µL, 0.15 mmol, 1.5 equiv) were added sequentially to a solution of **1l** (18 mg, 0.1 mmol, 1 equiv), *(E)*-*N*-benzaldehyde *O*-methyloxime (15 mg, 0.11 mmol, 1.1 equiv) and $(Me_3P)_2NiCl_2$

(2.8 mg, 0.01 mmol, 10 mol%) in CH_2Cl_2 (0.2 mL) at 0 °C and the resultant mixture was stirred at this temperature for 16 h.
The reaction was quenched with sat. NH_4Cl (0.5 mL), diluted with water (15 mL) and extracted with CH_2Cl_2 (3 × 10 mL). The combined organic extracts were dried (Na_2SO_4) and concentrated under reduced pressure. Mesitylene (14 μL, 0.1 mmol) was added to the crude mixture and it was analysed by ^{1}H NMR.

Yellow oil.

Major isomer:

^{1}H NMR (400 MHz, $CDCl_3$ δ 4.90 (q, *J* = 6.9 Hz, 1H, C<u>H</u>CH_3), 4.21 (dd, *J* = 8.1, 7.4 Hz, 2H, NC<u>H</u>$_2$), 3.29 (dd, *J* = 8.1, 7.4 Hz, 2H, SC<u>H</u>$_2$), 1.67 (d, *J* = 6.9 Hz, 3H, CHC<u>H</u>$_3$), 0.93 (t, *J* = 7.9 Hz, 9H, O<u>TES</u>), 0.55–0.48 (m, 6H, O<u>TES</u>).

Minor isomer:

^{1}H NMR (400 MHz, $CDCl_3$) δ 4.79 (q, *J* = 7.0 Hz, 1H, C<u>H</u>CH_3), 4.21 (dd, *J* = 8.1, 7.4 Hz, 2H, NC<u>H</u>$_2$), 3.29 (dd, *J* = 8.1, 7.4 Hz, 2H, SC<u>H</u>$_2$), 1.53 (d, *J* = 7.0 Hz, 3H, CHC<u>H</u>$_3$), 1.06–0.98 (m, 9H, O<u>TES</u>), 0.81–0.72 (m, 6H, O<u>TES</u>).

17 Nickel catalysed 1,3 dipolar cycloaddition reactions

***N*-[(*exo*)-*N*-benzyl-5-methyl-3-phenylisoxazolidin-4-yl]carbonyl-1,3-thiazolidine-2-thione (31sq')**

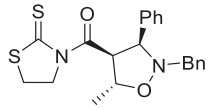

Neat TMSOTf (4 µL, 20 µmol, 20 mol%) was added to a solution of **1s** (19 mg, 0.1 mmol, 1.0 equiv), **q'** (32 mg, 0.15 mmol, 1.5 equiv) and [(*S*)-BINAP]$NiCl_2$ (7.5 mg, 10 µmol, 10 mol%) in CH_2Cl_2 (0.6 mL) at 0 °C and the mixture was stirred at this temperature for three days.

The reaction was quenched with NH_4Cl (0.5 mL), diluted with water (15 mL) and extracted with CH_2Cl_2 (3 × 10 mL). The combined organic extracts were dried ($MgSO_4$) and concentrated under reduced pressure. Mesitylene (14 µL, 0.1 mmol) was added to the crude mixture and it was analysed by ^{1}H NMR (dr *exo/endo* 79:21), Then, it was purified through a silica plug eluted with CH_2Cl_2 to give 19 mg, (47 µmol, 47% yield) of a 80:20 *exo/endo* mixture of the resultant oxazolidinones. The NMR data of the main diastereomer **31sq'** matches the *exo* compound reported in the literature. [20]

Yellow oil.
Chiral HPLC (Phenomenex Lux® Cellulose-1 column, 5% *i*-PrOH in Hexanes, flow rate 1 mL/min): R_t 11.8 min (major isomer) R_t 16.4 min (minor isomer), 99% *ee.*
^{1}H NMR (400 MHz, $CDCl_3$) δ 7.46–7.38 (m, 2H, ArH), 7.33–7.17 (m, 8H, ArH), 5.46 (dd, *J* = 11.0, 8.5 Hz, 1H, OCCH), 4.87 (dq, *J* = 8.5, 6.1 Hz, 1H, CHCH$_3$), 4.29 (d, *J* = 11.0 Hz, 1H, NCH), 4.01 (td, *J* = 12.0, 7.6 Hz, 1H, SCH$_2$CH$_x$H$_y$), 3.90 (d, *J* = 14.4 Hz, 1H, PhCH$_x$H$_y$), 3.81 (d, *J* = 14.4 Hz, 1H, PhCH$_x$H$_y$), 3.76 (ddd, *J* = 12.0, 7.6, 2.4 Hz, 1H, SCH$_2$CH$_x$H$_y$), 2.72 (ddd, *J* = 10.8, 7.6, 2.4 Hz, 1H, SCH$_x$H$_y$), 2.35–2.23 (m, 2H, SCH$_x$H$_y$), 1.36 (d, *J* = 6.1 Hz, 3H, CHCH$_3$).
^{13}C NMR (101 MHz, $CDCl_3$) δ 201.5 (C), 171.5 (C), 137.6 (C), 137.4 (C), 128.7 (CH), 128.6 (CH), 128.2 (CH), 128.1 (CH), 128.1 (CH), 127.1 (CH), 75.4 (CH), 72.8 (CH), 60.5 (CH), 59.8 (CH_2), 56.4 (CH_2), 27.7 (CH_2), 17.8 (CH_3).
MS (ESI+) *m/z* calcd for $[M+H]^+$ $C_{21}H_{23}N_2O_2S_2$: 399.1, found 399.1.

***N*-[(*endo*)-*N*-benzyl-5-methyl-3-phenylisoxazolidin-4-yl]carbonyl-1,3-thiazolidine-2-thione (31'sq')**

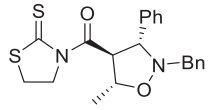

Neat TMSOTf (4 μL, 20 μmol, 20 mol%) was added to a solution of **1s** (19 mg, 0.1 mmol, 1.0 equiv), **q'** (32 mg, 0.15 mmol, 1.5 equiv) and [(*R*)-DTBM-SEGPHOS]$NiCl_2$ (7.5 mg, 10 μmol, 10 mol%) in CH_2Cl_2 (0.6 mL) at 0 °C, and the mixture was stirred for three days at this temperature.

The reaction was quenched with NH_4Cl (0.5 mL), diluted with water (15 mL) and extracted with CH_2Cl_2 (3 × 10 mL). The combined organic extracts were dried ($MgSO_4$) and concentrated under reduced pressure. Mesitylene (14 μL, 0.1 mmol) was added to the crude mixture and it was analysed by ^1H NMR (dr *endo/exo* 97:3) and purified through a silica plug eluted with CH_2Cl_2 to give 24 mg (66 μmol, 66% yield) of the slightly unstable endo diastereomer **31'sq'**.

Yellow oil.
Chiral HPLC (Phenomenex Lux® Cellulose-1 column, 5% *i*-PrOH in Hexanes, flow rate 1 mL/min): R_t 25.3 min (major isomer) R_t 33.4 min (minor isomer), 90% *ee.*
^{1}H NMR ^1H NMR (500 MHz, $CDCl_3$) δ 7.50–7.25 (m, 10H, ArH), 5.54 (dd, *J* = 8.0, 6.0 Hz, 1H, OCC<u>H</u>), 4.54 (p, *J* = 6.0 Hz, 1H, C<u>H</u>CH_3), 4.49–4.37 (m, 2H, $SCH_2C\underline{H}_2$), 4.25 (d, *J* = 8.0 Hz, 1H, NC<u>H</u>), 4.04 (d, *J* = 14.3 Hz, 1H, PhC<u>H</u>$_x$H$_y$), 3.90 (d, *J* = 14.3 Hz, 1H, PhC<u>H</u>$_x$H$_y$), 3.15 (ddd, *J* = 11.1, 7.2, 5.9 Hz, 1H, SC<u>H</u>$_x$H$_y$), 3.06 (ddd, *J* = 11.1, 8.6, 7.6 Hz, 1H, SC<u>H</u>$_x$H$_y$), 1.54 (d, *J* = 6.2 Hz, 3H, CHC<u>H</u>$_3$).
MS (ESI+) *m/z* calcd for $[M+H]^+$ $C_{21}H_{23}N_2O_2S_2$: 399.1, found 399.1.

18 References

(1) Kennington, S. C. D. Synthesis and Acylation of 1,3-Thiazinane-2-Thione. *Org. Synth.* 2021, *98*, 374–390.

(2) Iida, H.; Akatsu, Y.; Mizukami, K.; Natori, S.; Matsukawa, M.; Takahashi, K. Efficient and Rapid Synthesis of Phenolic Analogs of 4-Phenylbutanoic Acid Using Microwave-Assisted Michael Addition as a Key Reaction. *Synth Commun* 2016, *46* (7), 581–585.

(3) Balduzzi, S.; Brook, M. A.; McGlinchey, M. J. Diastereoselective Addition of Allyl- and Crotylstannanes to Dicobalt-Complexed Acetylenic Aldehydes. *Organometallics* 2005, *24* (11), 2617–2627.

(4) Ando, K.; Watanabe, H.; Zhu, X. One-Pot Preparation of (*E*)-α,β-Unsaturated Aldehydes by a Julia–Kocienski Reaction of 2,2-Dimethoxyethyl PT Sulfone Followed by Acid Hydrolysis. *J. Org. Chem.* 2021, *86* (9), 6969–6973.

(5) Allen, C. F. H.; Edens Jr, C. O. Phenylpropargyl Aldehyde. *Org. Synth.* 1945, *25*, 92.

(6) Zheng, K.; Shen, D.; Hong, R. Biomimetic Synthesis of Lankacidin Antibiotics. *J. Am. Chem. Soc.* 2017, *139* (37), 12939–12942.

(7) Paterson, I.; Paquet, T. Total Synthesis and Configurational Validation of (+)-Phorbaside A. *Org. Lett.* 2010, *12* (9), 2158–2161.

(8) Zhang, Q.; Zhang, R.; Tian, J.; Li, J.; Zhu, F.; Jiang, X.; Shen, J. Substituted *n*-Pentanamide Compounds, Preparation Methods and Uses Thereof. *EP2671878 A1* 2016.

(9) Nicolaou, K. C.; Li, A.; Edmonds, D. J.; Tria, G. S.; Ellery, S. P. Total Synthesis of Platensimycin and Related Natural Products. *J. Am. Chem. Soc.* 2009, *131* (46), 16905–16918.

(10) Srivari, chandrasekhar; Prathama, S. M.; Ramagonolla, K. K.; Genji, S. Process for the Preparation of Tapentadol and Analogs Thereof. *US20220177413 A1* 2022.

(11) Lawson, J. R.; Wilkins, L. C.; Melen, R. L. Tris(2,4,6-trifluorophenyl)Borane: An Efficient Hydroboration Catalyst. *Chem. Eur. J.* 2017, *23* (46), 10997–11000.

(12) Yao, W.-W.; Li, R.; Li, J.-F.; Sun, J.; Ye, M. NHC Ligand-Enabled Ni-Catalyzed Reductive Coupling of Alkynes and Imines Using Isopropanol as a Reductant. *Green Chem.* 2019, *21* (9), 2240–2244.

(13) Yamada, K.; Harwood, S. J.; Gröger, H.; Shibasaki, M. The First Catalytic Asymmetric Nitro-Mannich-Type Reaction Promoted by a New Heterobimetallic Complex. *Angew. Chem. Int. Ed.* 1999, *38* (23), 3504–3506.

(14) Ismail, T.; Shafi, S.; Singh, S.; Sidiq, T.; Khajuria, A.; Rouf, A.; Yadav, M.; Saikam, V.; Singh, P. P.; Alam, M. S.; Islam, N.; Sharma, K.; Kumar, H. M. S. Synthesis and Immunopotentiating Activity of Novel Isoxazoline Functionalized Coumarins. *Eur. J. Med. Chem.* 2016, *123*, 90–104.

(15) Borys, A. M.; Gil-Negrete, J. M.; Hevia, E. Atom-Efficient Transition-Metal-Free Arylation of *N*,*O*-Acetals Using Diarylzinc Reagents through Zn/Zn Cooperativity. *Chem. Commun.* 2021, *57* (71), 8905–8908.

(16) Bottle, S.; Blinko, J.; George, G.; Micallef, A.; Wade, T. Profluorescent Nitroxide Compounds. *WO2007/124543A1* 2007.

(17) Hatano, B.; Nagahashi, K.; Kijima, T. Zinc-Mediated Allylation and Alkylation of Aminals in the Presence of TMSCl and Diisopropylamine. *J. Org. Chem.* 2008, *73* (22), 9188–9191.

(18) Wang, K.; Yu, J.; Shao, Y.; Tang, S.; Sun, J. Forming All-Carbon Quaternary Stereocenters by Organocatalytic Aminomethylation: Concise Access to β2,2-Amino Acids. *Angew. Chem. Int. Ed.* 2020, *59* (52), 23516–23520.

(19) Granato, Á. S.; Amarante, G. W.; Adrio, J. Metal-Free Solvent Promoted Oxidation of Benzylic Secondary Amines to Nitrones with H2O2. *J. Org. Chem.* 2021, *86* (19), 13817–13823.

(20) Suga, H.; Nakajima, T.; Itoh, K.; Kakehi, A. Highly *Exo* -Selective and Enantioselective Cycloaddition Reactions of Nitrones Catalyzed by a Chiral Binaphthyldiimine−Ni(II) Complex. *Org. Lett.* 2005, *7* (7), 1431–1434.

Acronyms

$(DHQ)_2PHAL$ – Hydroquinine 1,4-phthalazinediyl diether

$(DHQD)_2PHAL$ –Hydroquinidine 1,4-phthalazinediyl diether

4Å MS – 4 Angstrom molecular sieves

9-BBN – 9-Borabicyclo[3.3.1]nonane

acac – Acetylacetonate

ACDC – Asymmetric counteranion directed catalysis

ACN – Acetonitrile

ALB – AlLi bis(Binaphthoxide)

ATP – Adenosine triphosphate

BINAP – 2,2′-Bis(diphenylphosphino)-1,1′-binaphthyl

BINOL – 1,1′-Bi(2-naphthol)

BIPHEP – 2,2'-Bis(diphenylphosphino)-1,1'-biphenyl

Bn – Benzyl

Boc – *tert*-Butyloxycarbonyl

BOX – Bisoxazoline

BPE – 1,2-Bis(2,5-diphenylphospholano)ethane

BTM – Benzotetramisole

BVMO – Baeyer-Villiger monooxygenase

Bz – Benzoyl

CBD – Cannabidiol

Cbz – Benzyloxycarbonyl

COD – Cyclooctadiene

CSA – Camphorsulphonic acid

DCC – *N,N'*-Dicyclohexylcarbodiimide

DCE – 1,2-dichloroethane

DCM – Dichloromethane

DIBAL-H – Diisobutylaluminium hydride

DIPAMP – Diphenyanisylmethylphosphine

DM – 3,5-Dimethylphenyl

DMAP – 4-Dimethylaminopyridine

DMF – Dimethylformamide

DMP – Dess-Martin periodinane

DMSO – Dimethylsulphoxide

DNBA 2,4-Dinitrobenzoic acid

DPMS – Diphenylmethylsilyl

Dpp – Diphenylphosphinic

dr – Diastereomeric ratio

DTBM – 3,5-Di-tert-butyl-4-methoxyphenyl

E – Electrophile

EDC – 1-Ethyl-3-(3-dimethylaminopropyl)carbodiimide

ee – enantioselective excess

EMA – European medicines agency

EWG – Electron withdrawing group

FDA – Food and drugs administration (United States)

GARPHOS – 2,2'-Bis(diphenylphosphino)-4,4',6,6'-tetramethoxy)-1,1'-biphenyl

HIV – Human immunodeficiency virus

HOBt – Hydroxybenzotriazole

HOMO – Highest occupied molecular orbital

HWE – Horner-Wadsworth-Emmons

IDPi – Imidodiphosphorimidate

IPA – Isopropyl alcohol or Isopropanol

LDA – Lithium diisopropylamide

LLB – $LaLi_3$tris(Binaphthoxide)

LUMO – Lowest unoccupied molecular orbital

mCPBA – *meta*-Chloroperoxybenzoic Acid

MW – Microwave irradiation

NADP –Nicotinamide adenine dinucleotide phosphate

NFSI – *N*-Fluorobenzenesulfonimide

NIS – *N*-Iodosuccinimide

NMM – *N*-Methylmorpholine

NMO – 4-Methylmorpholine-4-oxide

PCC – Pyridinium chlorochromate

PG – Protecting group

pin – Pinacol

PMB – *para*-Methoxybenzyl

PMP – *para*-Methoxyphenyl

PPTS – Pyridinium *para*-Toluenesulfonate

ProPhenol – 2,6-Bis[2-(hydroxydiphenylmethyl)-1-pyrrolidinyl-methyl]-4-methylphenol

PT – 5-phenyl-1*H*-tetrazole

PTSA – *para*-Toluenesulphonic Acid

pyBOX – 2,6-bis(4,5-dihydrooxazol-2-yl)pyridine

rr – regioselective ratio

rt – Room temperature

SALEN – *N,N′*-Bis(salicylidene)ethylenediamino

SEGPHOS – 5,5′-Bis(diphenylphosphino)-4,4′-bi-1,3-benzodioxol

SET – Single electron transfer

SOMO – Single occupied molecular orbital

TBAF – tetrabutylammonium fluoride

TBDPS -*tert*-butyldiphenylsilyl

TBS – *tert*-Butyldimethylsilyl

TES –Triethylsilyl

Tf – Trifluoromethanesulphonate

TFA – Trifluoroacetic acid

THC – Tetrahydrocannabinol

TIPS – Triisopropylsilyl

TMS – Trimethylsilyl

Tol – Tolyl

Ts – *para*-toluenesulphonyl

ANNEX

Asymmetric Catalysis Hot Paper

How to cite: *Angew. Chem. Int. Ed.* **2021**, *60*, 15307–15312
International Edition: doi.org/10.1002/anie.202104352
German Edition: doi.org/10.1002/ange.202104352

Direct and Enantioselective Aldol Reactions Catalyzed by Chiral Nickel(II) Complexes

Stuart C. D. Kennington, Saul F. Teloxa, Miguel Mellado-Hidalgo, Oriol Galeote, Sabrina Puddu, Marina Bellido, Pedro Romea, Fèlix Urpí,* Gabriel Aullón, and Mercè Font-Bardia*

Dedicated to Professor David A. Evans on the occasion of his 80th birthday

Abstract: *A direct and asymmetric aldol reaction of N-acyl thiazinanethiones with aromatic aldehydes catalyzed by chiral nickel(II) complexes is reported. The reaction gives the corresponding O-TIPS-protected anti-aldol adducts in high yields and with remarkable stereocontrol and atom economy. Furthermore, the straightforward removal of the achiral scaffold provides enantiomerically pure intermediates of synthetic interest, which involve precursors for anti-α-amino-β-hydroxy and α,β-dihydroxy carboxylic derivatives. Theoretical calculations explain the observed high stereocontrol.*

The enantioselective construction of the carbon backbone of chiral molecules has been at the forefront of organic synthesis in the last decades. It is therefore hardly surprising that classical transformations such as aldol and Michael reactions or Diels–Alder cycloadditions still hold a prominent position among the most important synthetic methods.[1] In this context, the continuing demand for increasingly more efficient procedures in accordance with the premises dictated by selectivity and economy in synthesis[2,3] has given rise to the development of a plethora of catalytic methods for the enantioselective construction of carbon–carbon bonds.[4] Unfortunately, the scope of most of them is rather narrow, which hampers further development and prevents a comprehensive exploitation of their possibilities. Thus, considering the benefits arising from a general approach, we envisaged that metal enolates from a single platform might participate in a number of direct, enantioselective, and catalytic transformations provided that the appropriate electrophiles are generated in the reaction mixture and evolve through similar open transition states (Scheme 1).

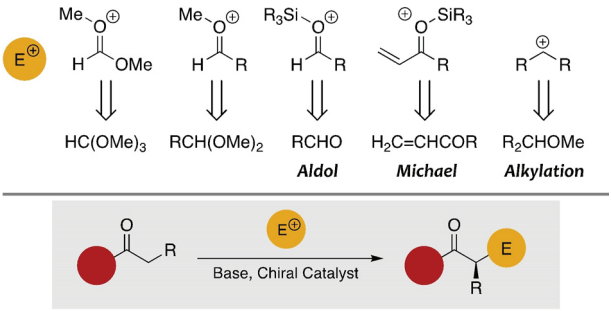

Scheme 1. Direct and enantioselective carbon–carbon bond-forming reactions from carbonylic compounds.

In this context, the activated aldehydes shown in Scheme 1 might react with carbonylic species in the presence of a base and a chiral catalyst to undergo direct and stereocontrolled aldol reactions.[5] With this aim, we have identified *N*-acyl thiazinanethiones as worthy substrates for our purposes and we now describe our findings on the direct and highly enantioselective aldol reactions of aromatic aldehydes catalyzed by chiral nickel(II) complexes in which the resultant protected aldol compounds are obtained selectively with remarkable atom economy. Importantly, this reaction gives access in a single step to protected *anti*-aldol adducts and supplements the *syn*-methods previously described by the groups of Evans,[6] and Kumagai and Shibasaki (Scheme 2).[7,8] Furthermore, the reaction shows a wide scope for the nucleophilic partner, which also permits the obtention of enantiomerically pure protected α-azido-β-hydroxy and α,β-dihydroxy derivatives in high yields under mild conditions (Scheme 2).

[*] Dr. S. C. D. Kennington, Dr. S. F. Teloxa, M. Mellado-Hidalgo, O. Galeote, S. Puddu, M. Bellido, Prof. P. Romea, Prof. F. Urpí
Department of Inorganic and Organic Chemistry
Section of Organic Chemistry
Universitat de Barcelona
Carrer Martí i Franqués 1–11, 08028 Barcelona (Spain)
E-mail: pedro.romea@ub.edu
felix.urpi@ub.edu
Prof. G. Aullón
Department of Inorganic and Organic Chemistry
Section of Inorganic Chemistry
Universitat de Barcelona
Carrer Martí i Franqués 1–11, 08028 Barcelona (Spain)
Dr. M. Font-Bardia
X-ray Diffraction Unity, CCiTUB, Universitat de Barcelona
Carrer Solé i Sabarís 1–3, 08028 Barcelona (Spain)
Supporting information and the ORCID identification numbers for some of the authors of this article can be found under: https://doi.org/10.1002/anie.202104352.

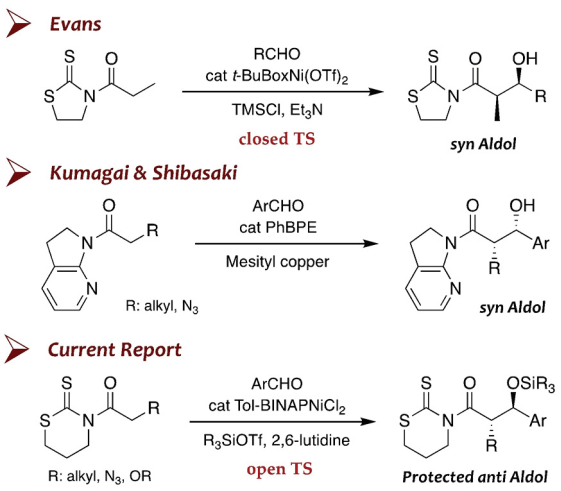

Scheme 2. Direct and enantioselective aldol reactions catalyzed by chiral metal complexes.

Exploratory experiments using *N*-propanoyl derivatives of several achiral heterocycles, triethylsilyltrifluoromethane sulfonate (TESOTf), and $(Me_3P)_2NiCl_2$ proved the feasibility of our approach for a direct and stereocontrolled aldol reaction as well as the advantage of thiazolidinethione and thiazinanethione over other heterocyclic scaffolds. In this respect, and despite both scaffolds producing similar results, the slower kinetics observed with the thiazolidinethione made the thiazinanethione counterpart the best choice for further developments (see Table S1 in the Supporting Information).[9]

We then examined the stereocontrol provided by different chiral nickel(II) complexes. It is important to highlight that these complexes are robust, easy to handle and prepare from the corresponding chiral ligands and $NiCl_2$, and are activated in the reaction mixture at the same time as the aldehyde by simple treatment with a silyl triflate.[10] Therefore, the role of the silyl triflate is twofold, since it activates the aldehyde as well as converting the nickel(II) chloride complex into the true catalytic species.[11] The results summarized in Table 1 show that *N*-propanoyl thiazinanethione **1** reacts with 4-methoxybenzaldehyde (**a**) in the presence of minute amounts of a large array of nickel(II) complexes, with the exception of $DIOPNiCl_2$ (Table 1, entry 2). Indeed, achiral $(Me_3P)_2NiCl_2$ provided a mixture of silyl aldol adducts with a remarkable diastereomeric ratio (dr 88:12) from which the racemic *anti*-adduct **2a** was isolated in 79% yield (Table 1, entry 1), whereas other chiral complexes also catalyzed the desired aldol reaction with full conversion. Interestingly, the steric hindrance of the chiral ligands plays a key role in the stereochemical outcome of the reaction. Indeed, the DTBM-SEGPHOS diphosphine gave an equimolar mixture of *anti* and *syn* diastereomers, whereas the less bulky SEGPHOS ligand performed much better and afforded an 80:20 *anti*/*syn* mixture (Table 1, entries 3 and 4); in addition, the absolute stereocontrol was outstanding and enantiomerically pure (≥ 98% *ee*) aldol adduct **2a** was isolated in both cases. Furthermore, the BINAP family gave much more consistent results, although the stereochemical outcome of the reaction slightly depended on the bulk of the ligand, with the Tol-BINAP ligand being the most appropriate in terms of stereocontrol and yield (Table 1, entries 5–7).

The impact of the bulk of ligands on the reaction led us to explore the influence of the activating Lewis acid. We thus assessed commercially available TMS, TBS, TES, and TIPS triflates. In the reaction with $(Me_3P)_2NiCl_2$, all these silyl triflates—except TMSOTf, which produced similar diastereomeric ratios but larger amounts of deprotection—can be used interchangeably (see Table S2). In contrast, we observed a significant change in the selectivity when [(*R*)-Tol-BINAP]-$NiCl_2$ was used instead. Indeed, the stereoselectivity depends upon the silyl triflate: less bulky TMSOTf and TBSOTf gave lower diastereoselectivities than TESOTf, whereas the bulkiest TIPSOTf increased the diastereomeric ratio up to 85:15 (Table 2, entries 1–4). Furthermore, the enantiocontrol was excellent for all these reagents.

We also evaluated other variables. The temperature had a modest positive effect on the diastereomeric ratio on cooling to −40 °C but duly decreased the rate of reaction, so −20 °C was used as the reaction temperature. Finally,

Table 1: Influence of the chiral nickel(II) complex on the stereochemical outcome of the aldol reaction.

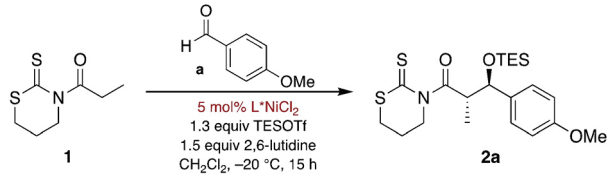

Entry	L*	*anti*/*syn*[a]	*ee* **2a** [%][b]	Yield **2a** [%][c]
1	$(Me_3P)_2NiCl_2$	88:12	–	79
2	(+)-$DIOPNiCl_2$	88:12	< 5	< 10
3	(*R*)-SEGPHOS	80:20	98	67
4	(*R*)-DTBM-SEGPHOS	50:50	99	43
5	(*R*)-BINAP	80:20	97	75
6	(*R*)-Tol-BINAP	80:20	98	76
7	(*R*)-Xyl-BINAP	83:17	83	71

[a] Established by ^{1}H NMR (400 MHz) spectroscopic analysis. [b] Established by chiral HPLC analysis. [c] Yield of isolated product.

Table 2: Influence of the Lewis acid in the stereochemical outcome of the aldol reaction.

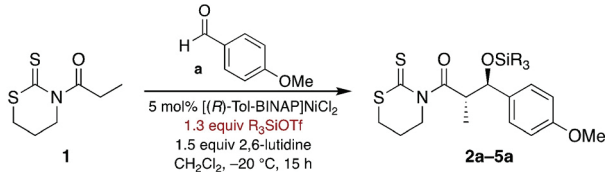

Entry	R_3SiOTf[e]	*anti* Adduct	dr[a]	*ee anti* [%][b]	Yield *anti* [%][c]
1	TESOTf	**2a**	80:20	98	76
2	TMSOTf	**3a**	73:27	nd[d]	nd[d]
3	TBSOTf	**4a**	75:25	99	67
4	TIPSOTf	**5a**	85:15	99	80

[a] *anti*/*syn* ratio established by ^{1}H NMR (400 MHz) spectroscopic analysis. [b] Established by chiral HPLC analysis. [c] Yield of isolated product. [d] Not determined. [e] TES = triethylsilyl, TMS = trimethylsilyl, TBS = *tert*-butyldimethylsilyl, TIPS = triisopropylsilyl.

Table 3: TIPSOTf-mediated aldol reaction of **1** with aromatic aldehydes.

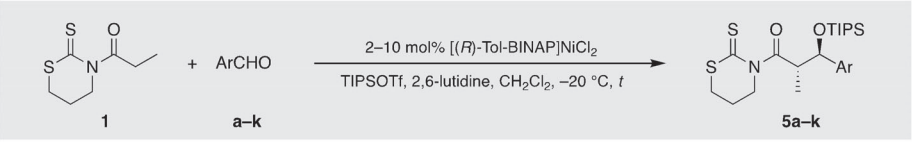

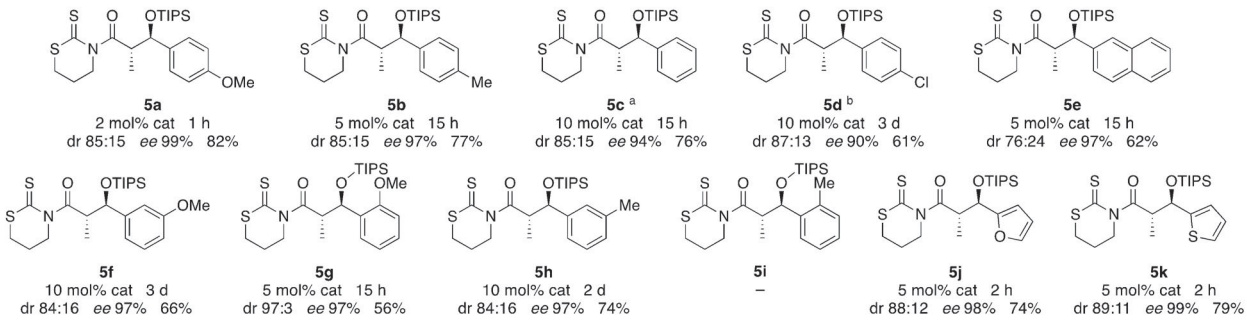

a. A 70% conversion is attained using 5 mol% of the catalyst after 15 h.
b. The reaction gives **5d** in dr 88:12, *ee* 90%, and 49% yield after 2 days at –20 °C, and dr 80:20, *ee* 90%, and 49% yield after 15 h at 0 °C

a comprehensive evaluation of the different variables considered together indicated that the reaction of *N*-propanoyl thiazinanethione **1** with **a** in the presence of 2 mol% [(*R*)-Tol-BINAP]$NiCl_2$, 1.3 equiv TIPSOTf, and 1.5 equiv 2,6-lutidine for only 1 h at −20 °C afforded the protected *anti*-aldol adduct **5a** in 82% yield with excellent stereocontrol (dr 85:15, 99% *ee*).

With the reaction conditions optimized for **a**, we moved to evaluate the scope of the reaction with other aromatic aldehydes.[12] The results summarized in Table 3 prove that the reaction is sensitive to both the electronic character and the steric hindrance of the substituents on the aromatic aldehyde. Indeed, electron-donating groups at the *para* position enabled highly stereocontrolled aldol reactions (dr 85:15 and up to 99% *ee*) and permitted the isolation of enantiomerically pure *anti*-adducts **5a** and **5b** in yields of 82% and 77%, respectively. Benzaldehyde (**c**) required an increase in the catalyst loading to 10 mol% to attain similar results, whereas the more deactivated 4-chlorobenzaldehyde (**d**) only provided *anti*-adduct **5d** in 61% yield after three days at −20 °C or a modest 49% yield when the reaction was carried out at 0 °C for 15 h, as a result of the formation of a by-product arising from the attack of the nucleophilic exo sulfur atom on the activated aldehyde. In turn, the more-electron-rich 2-naphthaldehyde (**e**) gave adduct **5e** in a remarkable 62% yield and 97% *ee* on using 5 mol% of the catalyst. Other isomers of **a** were also assessed and gave satisfactory results. As expected, the 3-methoxy derivative (**f**) turned out to be less reactive, but gave the corresponding *anti*-adduct **5f** in 66% yield after three days when 10 mol% of the catalyst was used. More surprisingly, 2-methoxybenzaldehyde (**g**) led to **5g** as a single stereoisomer (dr 97:3 and 97% *ee*) in 56% yield when using 5 mol% of the catalyst. A parallel aldol reaction of *meta*-tolyl aldehyde **h** proceeded efficiently, but the *ortho* counterpart **i** was found to be completely inactive and did not afford the desired adduct **5i**. This indicates that bulky groups close to the carbonyl group hinder approach to the enolate; we speculate that the outstanding results from **g** may be due to the formation of a chelated oxocarbenium intermediate in which the *ortho* substituent remains far from the carbonyl center. Finally, aromatic aldehydes containing π-electron-rich heterocycles, such as furan **j** and thiophene **k**, afforded the *anti*-aldol adducts **5j** and **5k** in high yields after 2 h when using 5 mol% of the nickel(II) complex.

Once the feasibility of the enantioselective *anti* aldol reaction had been demonstrated, we assessed the influence of the substituents of the acyl group on the addition of *N*-acyl thiazinanethiones **6–13** to **a**. The results shown in Table 4 highlight the key role of steric bulk in the stereochemical outcome of the aldol reaction. Indeed, the enantioselectivity is consistently excellent for the *N*-acyl thiazinanethiones **6–8**, but the diastereoselectivity and consequently the yield are eroded from **5a** (R = Me: dr 85:15, 82%) to **17a** (R = Et: dr 81:19, 78%) and **18a** (R = *i*Bu: dr 75:25, 60%) and the catalyst loading needed to be increased from 2 mol% to 5 mol%. Moreover, the chemoselectivity is excellent and the presence of common functional groups such as alkenes, alkynes, halides, or esters does not have a noticeable influence, so enantiomerically pure (94–99% *ee*) protected *anti*-adducts **19a–22a** were isolated in good to high yields (62–76%). Finally, the presence of a strong electron-withdrawing α-CF_3 group inhibits the reaction, but the α-benzyloxy derivative affords the *anti*-adduct **24a** in a highly efficient manner, which provides straightforward access to protected *anti*-α,β-dihydroxy compounds. At this stage, we tested introducing an azido group at the α-position. Unfortunately, all our attempts failed, and we were obliged to consider the use of the thiazolidinethione scaffold. As previously mentioned, such a heterocycle enables aldol reactions but with slower kinetics than the thiazinanethione counterpart. To our delight, thiazolidinethione-based substrates **14–16** ($m = 0$ in Table 4) also gave excellent results. Indeed, and despite requiring a longer reaction time, *N*-propanoyl thiazolidinethione **14** (R = Me) and the more bulky derivative **15** (R =

Table 4: TIPSOTf-mediated aldol reaction of *N*-acyl-1,3-thiazinane-2-thiones with 4-methoxybenzaldehyde (**a**).

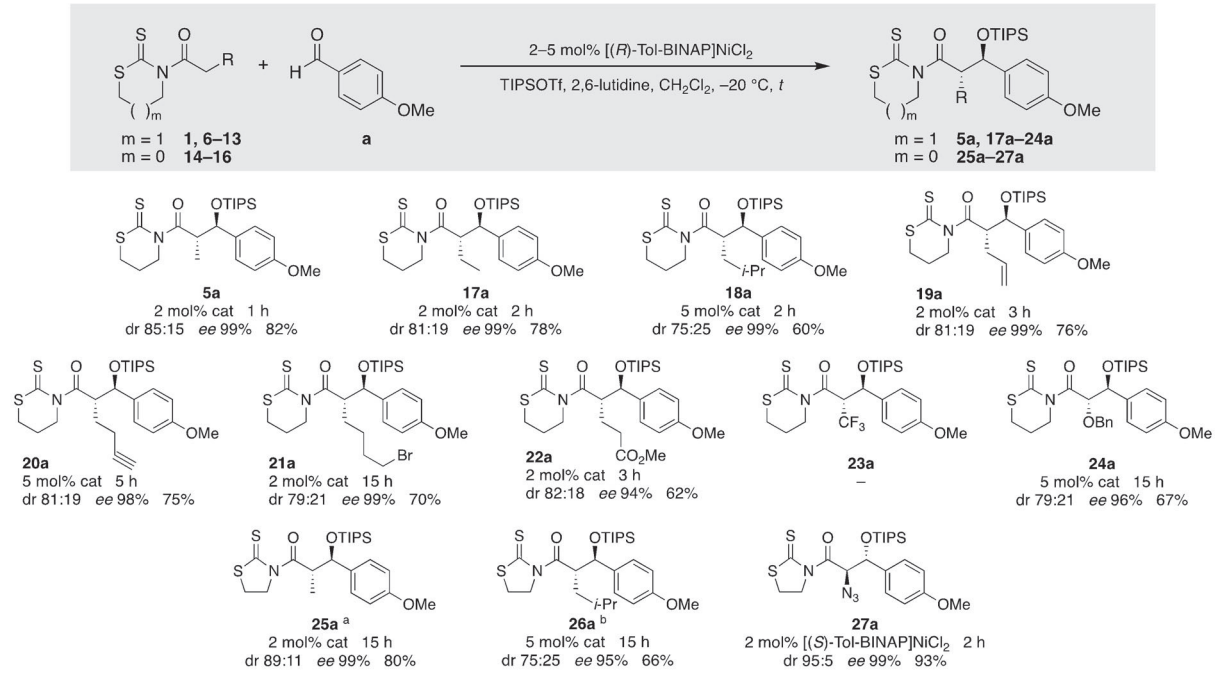

a. The conversion in 1 h was 20%. b. The conversion in 5 h was 35%.

CH_2CHMe_2) also afforded the corresponding aldol adducts **25a** and **26a** with high yields and enantioselectivity (99% and 95% *ee*, respectively). Finally, the azido thiazolidinethione **16** (R = N_3) proved especially successful and afforded in just 2 h the α-azido-β-silyloxy adduct **27a** virtually as a single stereoisomer (dr 95:5, 99% *ee*) in a yield of 93%.[13]

The configuration of **5a** was established as the (2*S*,3*R*)-*anti*-adduct through X-ray analysis of the benzyl amide derivative **28**,[14] which was easily prepared by nucleophilic displacement of the scaffold of **5a** with (*S*)-1-phenyl-1-ethylamine (Scheme 3).[15] Furthermore, amides **29** and **30** were isolated in up to 99% yield after reaction with morpholine and *N*-methoxy-*N*-methylamine, respectively. In addition, aldol **5a** was also converted into a wide array of enantiomerically pure derivatives of synthetic interest. As shown in Scheme 3, treatment of **5a** with $LiBH_4$ gave alcohol **31** in 85% yield, methyl ester **32** was obtained in 95% yield by simply stirring **5a** in methanol, whereas the sodium enolate of ethyl acetate was used to deliver the β-keto ester **33** in a remarkable 78% yield. All together, these transformations prove the easy removal of the thiazinanethione scaffold and the synthetic utility of the aldol adducts.

Having demonstrated the wide scope and synthetic interest of the aldol reaction, we focused our attention on its mechanism. The proposed catalytic cycle is depicted in Scheme 4, where the TIPSOTf plays a dual role as the trigger for the generation of the catalytic species as well as the activating Lewis acid for the aldehyde. We carried out

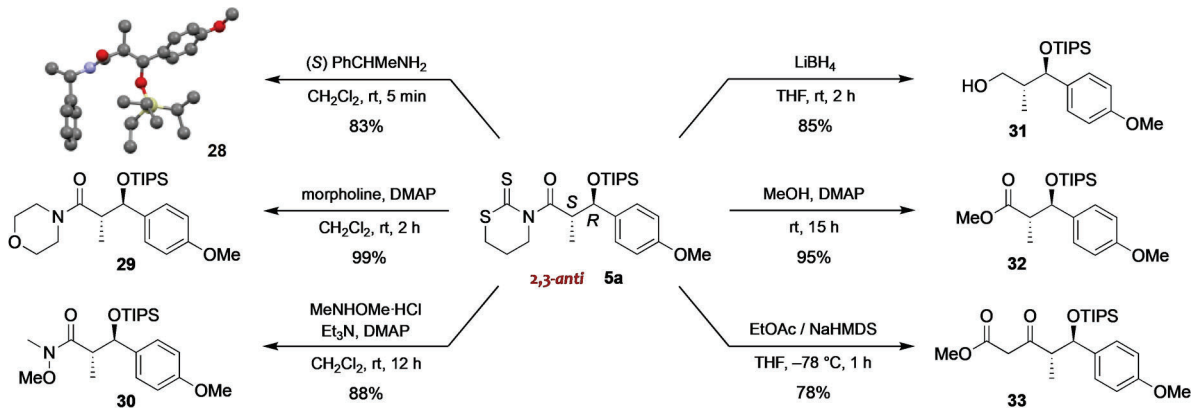

Scheme 3. Removal of the scaffold and conversion of aldol adducts into enantiomerically pure compounds.

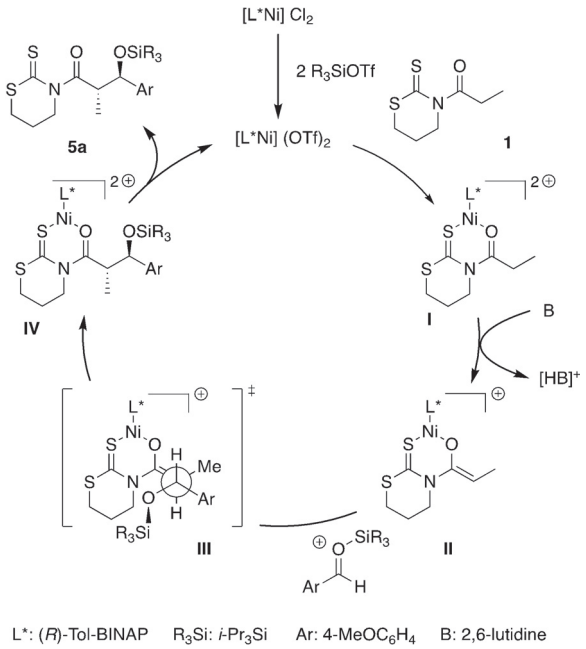

Scheme 4. Mechanistic hypothesis.

a comprehensive computational study of the carbon–carbon bond-forming step.[16] These calculations indicated that the reaction evolves through an open transition state **III**, in which the activated aldehyde approaches the *Re* π-face of the square-planar nickel(II) enolate **II** (Scheme 4). Importantly, the approach to the opposite *Si* π-face is about 3 kcal mol^{-1} less stable, which accounts for the excellent enantiocontrol achieved in all the reactions.

In summary, we have developed a direct and asymmetric aldol reaction of *N*-acyl thiazinanethiones and thiazolidinethiones with aromatic aldehydes in the presence of TIPSOTf and promoted by [(*R*)-Tol-BINAP]$NiCl_2$. This reaction gives the corresponding *O*-TIPS-protected *anti*-aldol adducts in high yields and diastereoselectivity as well as with an excellent enantiocontrol up to 99% *ee*. The wide scope of the reaction permits the use of *N*-acyl groups containing alkenes, alkynes, halides, or esters, as well as α-azido and α-hydroxy substituents, which provides a simple and quick access to *anti*-α-azido-β-silyloxy and α-alkoxy-β-silyloxy moieties. Furthermore, the heterocyclic scaffold can be easily removed to give enantiomerically pure intermediates. Finally, theoretical studies indicate that the carbon–carbon bond-forming step proceeds through an open transition state, in which the steric interactions play a crucial role.

Acknowledgements

Financial support from the Spanish Ministerio de Ciencia, Innovación y Universidades (MCIU)/Agencia Estatal de Investigación (AEI)/Fondo Europeo de Desarrollo Regional (FEDER, UE) (Grant No. PGC2018-094311-B-I00, and Grant No. PGC2018-093863-B-C21), and the Generalitat de Catalunya (2017SGR 271 and 2017SGR 1289) as well as doctorate studentships to S.C.D.K. (FI, Generalitat de Catalunya) and S.F.T. (CONACYT-México, Grant Number 438357) is gratefully acknowledged.

Conflict of interest

The authors declare no conflict of interest.

Keywords: aldol reaction · asymmetric catalysis · direct reaction · nickel · thiazinanethiones

[1] E. M. Carreira, L. Kvaerno, *Classics in Stereoselective Synthesis*, Wiley-VCH, Weinheim, **2009**.
[2] a) B. M. Trost, *Science* **1991**, *254*, 1471 – 1477; b) P. A. Wender, B. L. Miller, *Nature* **2009**, *460*, 197 – 201; c) N. Z. Burns, P. S. Baran, R. W. Hoffmann, *Angew. Chem. Int. Ed.* **2009**, *48*, 2854 – 2867; *Angew. Chem.* **2009**, *121*, 2896 – 2910; d) Y. Hayashi, *Chem. Sci.* **2016**, *7*, 866 – 880.
[3] T. Newhouse, P. S. Baran, R. W. Hoffmann, *Chem. Soc. Rev.* **2009**, *38*, 3010 – 3021.
[4] For leading references, see a) D. W. C. MacMillan, *Nature* **2008**, *455*, 304 – 308; b) J. T. Mohr, M. R. Krout, B. M. Stoltz, *Nature* **2008**, *455*, 323 – 332; c) M. Silvi, P. Melchiorre, *Nature* **2018**, *554*, 41 – 49.
[5] a) B. M. Trost, C. S. Brindle, *Chem. Soc. Rev.* **2010**, *39*, 1600 – 1632; b) B. M. Trost, C.-I. Hung, G. Mata, *Angew. Chem. Int. Ed.* **2020**, *59*, 4240 – 4261; *Angew. Chem.* **2020**, *132*, 4268 – 4291.
[6] a) D. A. Evans, C. W. Downey, J. L. Hubbs, *J. Am. Chem. Soc.* **2003**, *125*, 8706 – 8707; b) D. A. Evans, R. J. Thomson, *J. Am. Chem. Soc.* **2005**, *127*, 10506 – 10507.
[7] a) K. Weidner, N. Kumagai, M. Shibasaki, *Angew. Chem. Int. Ed.* **2014**, *53*, 6150 – 6154; *Angew. Chem.* **2014**, *126*, 6264 – 6268; b) Z. Liu, T. Takeuchi, R. Pluta, F. A. Arteaga, N. Kumagai, M. Shibasaki, *Org. Lett.* **2017**, *19*, 710 – 713.
[8] a) N. Kumagai, M. Shibasaki, *Chem. Eur. J.* **2016**, *22*, 15192 – 15200; b) N. Kumagai, M. Shibasaki, *Synthesis* **2019**, *51*, 185 – 193.
[9] For related studies on the key role of the 1,3-thiazinane-2-thione scaffold, see S. C. D. Kennington, A. J. Taylor, P. Romea, F. Urpí, G. Aullón, M. Font-Bardia, L. Ferré, J. Rodrigalvarez, *Org. Lett.* **2019**, *21*, 305 – 309.
[10] T. Suzuki, Y. Hamashima, M. Sodeoka, *Angew. Chem. Int. Ed.* **2007**, *46*, 5435 – 5439; *Angew. Chem.* **2007**, *119*, 5531 – 5535.
[11] For other examples, see a) J. M. Romo, E. Gálvez, I. Nubiola, P. Romea, F. Urpí, M. Kindred, *Adv. Synth. Catal.* **2013**, *355*, 2781 – 2786; b) J. Fernández-Valparís, J. M. Romo, P. Romea, F. Urpí, H. Kowalski, M. Font-Bardia, *Org. Lett.* **2015**, *17*, 3540 – 3543.
[12] Aliphatic aldehydes reacted sluggishly under the reaction conditions. In turn, α,β-unsaturated aldehydes afforded complex mixtures.
[13] Metal enolates from α-azido carbonyl compounds are rarely used because of their lack of stability. For leading examples, see a) J. Patel, G. Clavé, P.-Y. Renard, X. Franck, *Angew. Chem. Int. Ed.* **2008**, *47*, 4224 – 4227; *Angew. Chem.* **2008**, *120*, 4292 – 4295; b) K. Weidner, Z. Sun, N. Kumagai, M. Shibasaki, *Angew. Chem. Int. Ed.* **2015**, *54*, 6236 – 6240; *Angew. Chem.* **2015**, *127*, 6334 – 6338.
[14] For the X-ray data, see the Supporting Information. Deposition Number 2062607 (for **28**) contains the supplementary crystallographic data for this paper. These data are provided free of charge by the joint Cambridge Crystallographic Data Centre and Fachinformationszentrum Karlsruhe Access Structures service www.ccdc.cam.ac.uk/structures.

[15] The minor isomer was confirmed as the (2*S*,3*S*)-*syn*-aldol product by chemical correlation.
[16] ONIOM calculations were carried out using the Gaussian09 package. High quantum layer B3LYP/TZPV was applied to nickel, phosphorus, and the *N*-acyl thiazinanethione together with the electrophile in the reaction pathway, while low layer including organic substituents of the diphosphane ligand was treated by universal field force. For further details, see the Supporting Information.

Manuscript received: March 29, 2021
Revised manuscript received: April 12, 2021
Accepted manuscript online: April 19, 2021
Version of record online: June 7, 2021

How to cite: *Angew. Chem. Int. Ed.* **2024**, *63*, e202319308
doi.org/10.1002/anie.202319308

Asymmetric catalysis

Direct, Stereodivergent, and Catalytic Michael Additions of Thioimides to α,β-Unsaturated Aldehydes – Total Synthesis of Tapentadol

Oriol Galeote, Stuart C. D. Kennington, Gabriela Benedito, Lena Fraedrich, Evan Davies-Howe, Anna M. Costa, Pedro Romea,* Fèlix Urpí,* Gabriel Aullón, Mercè Font-Bardia, and Cristina Puigjaner*

Dedicated to Professor Jaume Vilarrasa.

Abstract: Direct and stereodivergent Michael additions of *N*-acyl 1,3-thiazinane-2-thiones to α,β-unsaturated aldehydes catalyzed by chiral nickel(II) complexes are reported. The reactions proceed with a remarkable regio-, diastereo-, and enantioselectivity, so access to any of the four potential Michael stereoisomers is granted through the appropriate choice of the chiral ligand of the nickel(II) complex. Simple removal of the heterocyclic scaffold furnishes a wide array of either *syn* or *anti* enantiomerically pure derivatives, which can be exploited for the asymmetric synthesis of biologically active compounds, as demonstrated in a new approach to tapentadol. In turn, a mechanism, based on theoretical calculations, is proposed to account for the stereochemical outcome of these transformations.

[*] O. Galeote, Dr. S. C. D. Kennington, G. Benedito, L. Fraedrich, E. Davies-Howe, Prof. A. M. Costa, Prof. P. Romea, Prof. F. Urpí
Department of Inorganic and Organic Chemistry, Section of Organic Chemistry, and Institut de Biomedicina de la Universitat de Barcelona, Universitat de Barcelona
Carrer Martí i Franqués 1-11, 08028 Barcelona (Spain)
E-mail: amcosta@ub.edu
pedro.romea@ub.edu
felix.urpi@ub.edu

Prof. G. Aullón
Department of Inorganic and Organic Chemistry, Section of Inorganic Chemistry and Institut de Química Teòrica i Computacional de la Universitat de Barcelona, Universitat de Barcelona
Carrer Martí i Franqués 1-11, 08028 Barcelona (Spain)

Dr. M. Font-Bardia, Dr. C. Puigjaner
X-Ray Diffraction Unity, CCiTUB
Universitat de Barcelona
Carrer Solé i Sabarís 1-3, 08028 Barcelona (Spain)

Introduction

It is certainly the case that, at present, new methods in Organic Synthesis must be devised with the compelling need for *selectivity*, since they are expected to act in a masterful manner to produce the desired transformation at a specific site without affecting other parts of the molecule.[1,2] In this scenario, the simultaneous control over the *regio-* and *stereoselectivity* of a particular reaction often presents a formidable challenge. A case in point involves conjugated carbonyl compounds. Indeed, they may undergo nucleophilic attacks at either the carbonyl or the conjugated position, namely 1,2- versus 1,4-additions, which usually entail the installation of up to two stereocenters.[3,4] Faced with the complexity of satisfying both selective requirements, the importance of substrate choice has been empirically acknowledged. Actually, traditional wisdom contends that α,β-unsaturated ketones or esters predominantly participate in 1,4-additions, while the more reactive aldehyde counterparts are prone to evolve through the alternative 1,2-pathway.[5–8] Therefore, it should be no surprise that, despite undeniable interest, just a small number of reports describe regio- and stereoselective Michael additions of acyclic carbonyl compounds to α,β-unsaturated aldehydes. So far, none of the currently reported methods take advantage of metal enolates[9,10] and contrarily hinge on organocatalytic approaches, proceeding through the iminium mode of action, in which the carbonyl bond of the electrophile is temporarily replaced by the iminium counterpart. Indeed, pioneering studies by Palomo on the intermolecular *anti* Michael addition of aldehydes to enals catalyzed by a proline derivative demonstrated the feasibility of such a strategy.[11,12] A little later, Barbas reported a comprehensive study on the addition of activated thioesters of aryl acetic acids to cinnamaldehyde, catalyzed by the Jørgensen-Hayashi amine to provide the *anti* Michael adducts with diastereoselectivities up to 3:1 and variable enantiocontrol.[13,14] Consequently, the development of new methods to successfully achieve 1,4-additions in both a regio- and stereoselective manner to provide both *anti* and *syn* Michael adducts is still necessary to grant access to new valuable molecular architectures, unattainable with current methodologies.[15]

In this context and beyond the abovementioned challenges, the interest in a particular stereoselective carbon-carbon bond forming reaction is nowadays increasingly associated to the ability to provide any of the potential stereoisomers,[16] ideally under the premises of Atom Economy[17] and Green Chemistry.[18] In this context, stereodivergent dual catalysis[19,20] has recently emerged as an engaging option for obtaining any stereoisomer in transformations in which up to two new stereocenters are installed.[21] In principle, such a conceptual framework requires the use of distinct chiral catalysts acting on a single set of precursors to exercise independent control on the absolute configuration of the stereocenters formed. Lee has recently demonstrated the gains and opportunities of such an approach in a highly regio- and stereoselective Michael addition of pentafluorophenyl aryl acetates to α,β-unsaturated aldehydes through the appropriate combination of a proline derivative and a chiral Lewis base (see Eq 1 in Scheme 1).[22] Unfortunately, the profile of the nucleophilic partner is once again restricted to relatively acidic aryl acetic esters,[13] so new approaches are needed to enable the enantioselective formation of carbon-carbon bonds through the addition of a wide array of carbonyl compounds to the conjugated position of α,β-unsaturated aldehydes.

Considering the benefits of a process with a wider scope and the lack of *regio-* and *stereoselective* Michael additions of metal enolates to α,β-unsaturated aldehydes, we envisaged that a close, but less stringent version, of the aforementioned stereodivergent dual catalytic model might be successful. This would entail a single transition-metal catalytic model in such a way that the simple change of the chiral ligand would give access to all the potential stereoisomers in a highly regio- and stereocontrolled manner.[16,23]

Herein, we report that direct and asymmetric Lewis acid-mediated Michael additions of *N*-acyl 1,3-thiazinane-2-thiones to α,β-unsaturated aldehydes catalyzed by nickel(II) complexes, containing chiral diphosphines 5,5′-bis[di(3,5-di-*tert*-butyl-4-methoxyphenyl)phosphino]-4,4′-bi-1,3-benzodioxole (DTBM-SEGPHOS) or 2,2′-bis(diphenylphosphino)-1,1′-binaphthyl (BINAP), produce, at will, enantiomerically pure *syn* or *anti* stereoisomers in good to high yields (Eq 2 in Scheme 1). Importantly, the aldehyde group is transformed through its activation and becomes a protected silyl enol ether in the resultant Michael adduct, which facilitates further transformations and thus enhances the synthetic usefulness of the method.

Results and Discussion

Preliminary Studies and Optimization

During our studies on the direct, asymmetric, and silyl triflate-mediated aldol reactions from *N*-acyl thiazinanethiones catalyzed by chiral nickel(II) complexes,[24] mixtures of aldol and Michael adducts and other unidentified byproducts were obtained when cinnamaldehyde (**a**) was used as the electrophilic partner. In turn, parallel theoretical calculations showed that the participation of C1 and C3 for the LUMO of the silyl-activated cinnamaldehyde were similar (Figure 1). All in all, these signs encouraged us to make further efforts towards the search of selective 1,4-additions.

Therefore, we first explored the regiochemical outcome of the Michael additions using the achiral $(Me_3P)_2NiCl_2$ complex under differing conditions. To our surprise, the silyl triflate proved to be crucial. Indeed, the use of a sterically hindered silyl triflate such as triisopropylsilyl triflate (TIPSOTf) produced the desired Michael adduct with remarkable regioselectivity, while less bulky trimethylsilyl triflate

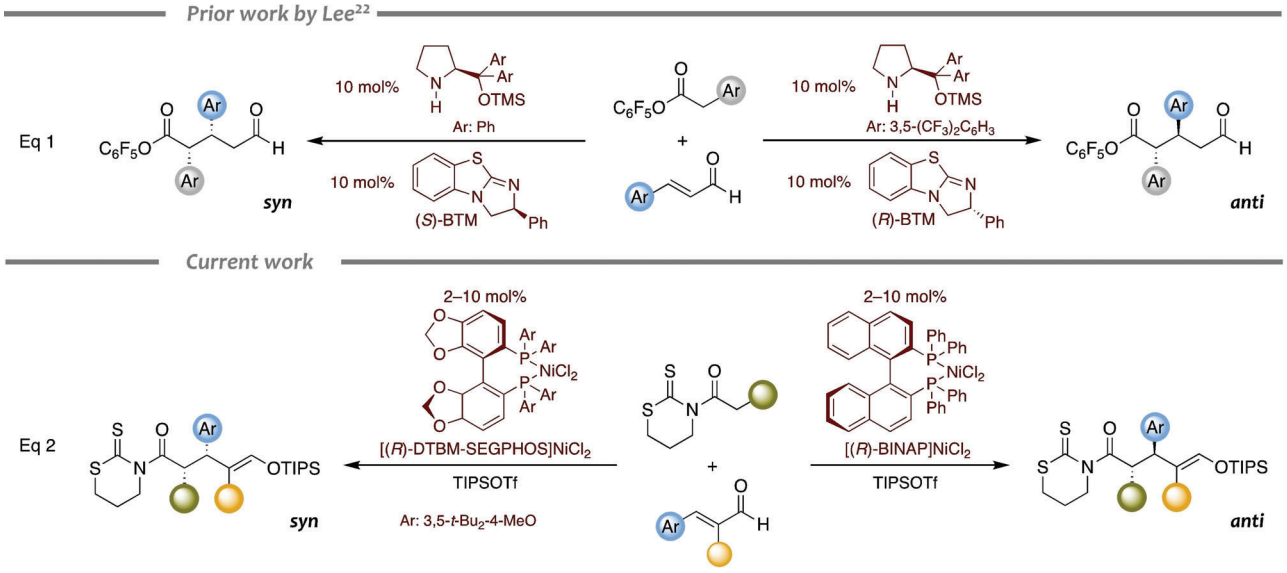

Scheme 1. Direct and Stereodivergent Michael Additions to α,β-Unsaturated Aldehydes. TMS = trimethylsilyl, TIPS = triisopropylsilyl, TIPSOTf = triisopropylsilyl triflate.

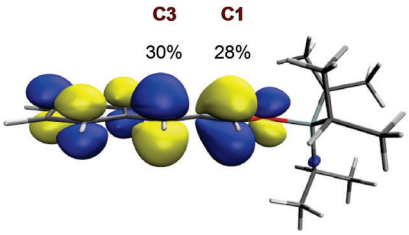

Figure 1. LUMO of [PhCH=CHCHO-TIPS]$^+$.

(TMSOTf) showed opposing selectivity (see Table S1). The scaffold turned out to play a key role too; the thiazinanethione[25] and thiazolidinethione adducts proved to be the most selective, with the former being more efficient in terms of the kinetics of the process (see Table S1).[26] Having identified the pairing of thiazinanethione/TIPSOTf as the best combination for obtaining Michael adducts, we next assessed the influence of chiral nickel(II) catalysts. We were pleased to observe that all chiral catalysts examined produced the desired 1,4-addition with absolute regioselectivity. Furthermore, the diastereoselectivity heavily depended both on the solvent and the ligand (see Table S2) to such an extent that [DTBM-SEGPHOS]$NiCl_2$ in 4:1 toluene/CH_2Cl_2 gave the *syn* Michael adduct (*syn*/*anti* 88:12). Such a solvent mixture also turned out to be the most appropriate when [BINAP]$NiCl_2$ was used; but however, this catalyst led to the *anti* counterpart instead (*syn*/*anti* 15:85). Finally, and most importantly, both the *syn* and *anti* diastereomers were obtained enantiomerically pure (*ee* 99%). All together, these results proved that we could access at will, in a highly stereoselective manner, any of the four possible Michael stereoisomers, with absolute regiocontrol, by just switching between [DTBM-SEGPHOS]$NiCl_2$ and [BINAP]$NiCl_2$ and choosing the appropriate enantiomer of the ligand (Eq 2 in Scheme 1).

Scope

Having established an unusual, direct, and stereodivergent Michael addition to cinnamaldehyde (**a**), we moved to examine the scope of the reaction catalyzed by [(*R*)-DTBM-SEGPHOS]$NiCl_2$ (Scheme 2). Unfortunately, α,β-unsaturated aldehydes containing an alkyl group, a heteroatom, or an ester group at the β position proved unsuitable.[27] On the contrary, β-aryl-α,β-unsaturated aldehydes **a**–**o** turned out to be excellent substrates and all the corresponding *syn* diastereomers **2a**–**o** were easily isolated in enantiomerically pure form by column chromatography except for trifluoromethyl-derived aldehyde **e**.

Indeed, most of these aldehydes, with the single exception of *ortho* methoxy aldehyde **i**, reacted with

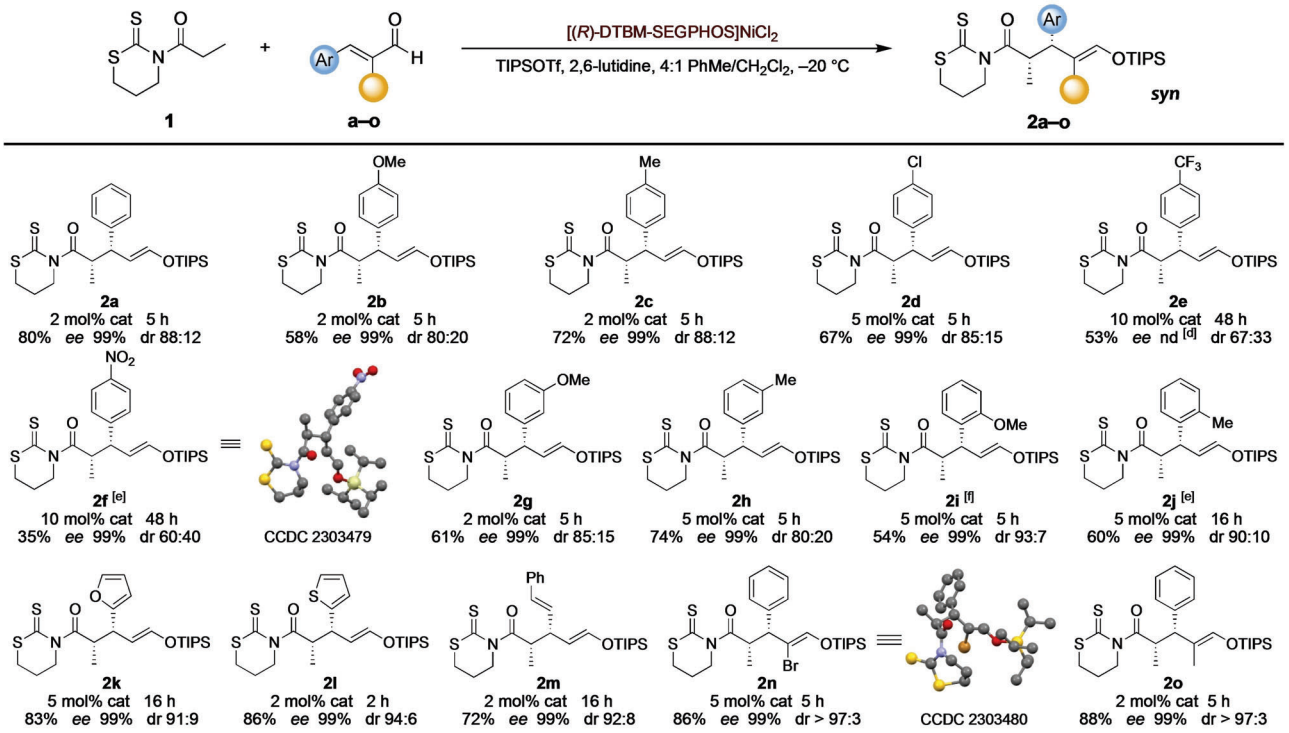

Scheme 2. TIPSOTf-Mediated Michael additions of *N*-propanoyl thiazinanethione **1** to α,β-unsaturated aldehydes catalyzed by [(*R*)-DTBM-SEGPHOS]$NiCl_2$.[a–c]

[a] Isolated yields of the enantiomerically pure **2a**–**o** *syn* adducts are shown. [b] Enantiomeric excess established by chiral HPLC. [c] Diastereomeric ratio (*syn*/*anti*) established by ^{1}H NMR analysis. [d] It was impossible to determine the ee by chiral HPLC. [e] Conversion: 85–90%. [f] rr (1,4:1,2) 87:13.

absolute regiocontrol (rr 1,4:1,2 > 99:1) to provide enantiomerically pure (*ee* 99 %) *syn* Michael adducts **2a–o** in good to high yields. As shown in Scheme 2, the electronic character of the substituents at the *para* position of the aromatic ring has a profound effect on the kinetics of the process. Indeed, electron-donating groups seen in **a–c** required a low catalyst loading of 2 mol % to reach completion in 5 h. Aldehyde **d**, containing chlorine as a slightly electron-withdrawing group, required 5 mol % of the catalyst, while the stronger trifluoromethyl or nitro groups, in **e** and **f** respectively, demanded 10 mol % of the catalyst and reaction times up to 48 h. Even better results were achieved with aldehydes **k** and **l** containing an heteroaromatic ring of furane or thiophene, which allowed for the isolation of enantiomerically pure *syn* adducts **2k** and **2l** in yields of 83–86 %. Noteworthily, the method tolerated the placement of substituents at the *meta* and even the *ortho* position and adducts **2g–j** were obtained under similar conditions and with results close to the corresponding *para* substituted counterparts **2b** and **2c**. Eventually, α,β-γ,δ-unsaturated aldehyde **m**, which could potentially undergo 1,4- and 1,6-attacks, proved to be an excellent substrate since it led to a single regioisomer **2m** with outstanding stereocontrol (dr 92:8, *ee* 99 %) in a 72 % yield. Finally, α-substituted aldehydes **n** and **o** also participated in totally stereocontrolled reactions and provided diastereomerically and enantiomerically pure (dr > 97:3, *ee* 99 %) *syn* Michael products **2n** and **2o** in yields of 86–88 %. It is worth highlighting that the absolute configuration of Michael adducts **2** was firmly established through X-ray analysis of crystals from **2f** and **2n**.[28]

An analogous study was carried out using [(*R*)-BINAP]$NiCl_2$. Results summarized in Scheme 3 show that both the regio- and the enantiocontrol provided by this complex are as good as those imparted by the former. Furthermore, these reactions proved to be faster than those catalyzed by [DTBM-SEGPHOS]$NiCl_2$ and, for instance, the addition to the reluctant aldehyde **f** was, this time, complete in 24 h. The diastereoselectivities were high and close to those of the *syn* series, while the isolated yields of the enantiomerically pure *anti* diastereomers **3a–o** ranged from moderate to high. From a general point of view, the access to the enantiomerically pure *anti* configuration utilizing [BINAP]$NiCl_2$ combines perfectly with that provided by the [DTBM-SEGPHOS]$NiCl_2$ complex and makes the overall method a stereodivergent strategy for Michael additions to α,β-unsaturated aldehydes (Eq 2 in Scheme 1).

Finally, we met the challenge of expanding both procedures to other *N*-acyl thiazinanethiones. Results summarized in Scheme 4 indicate that the reaction catalyzed by [DTBM-SEGPHOS]$NiCl_2$ generally provides the expected *syn* stereoisomers but is highly sensitive to the steric hindrance of the Cα group. A case in point was *N*-butanoyl thiazinanethione **4**, which required a fivefold increase of the

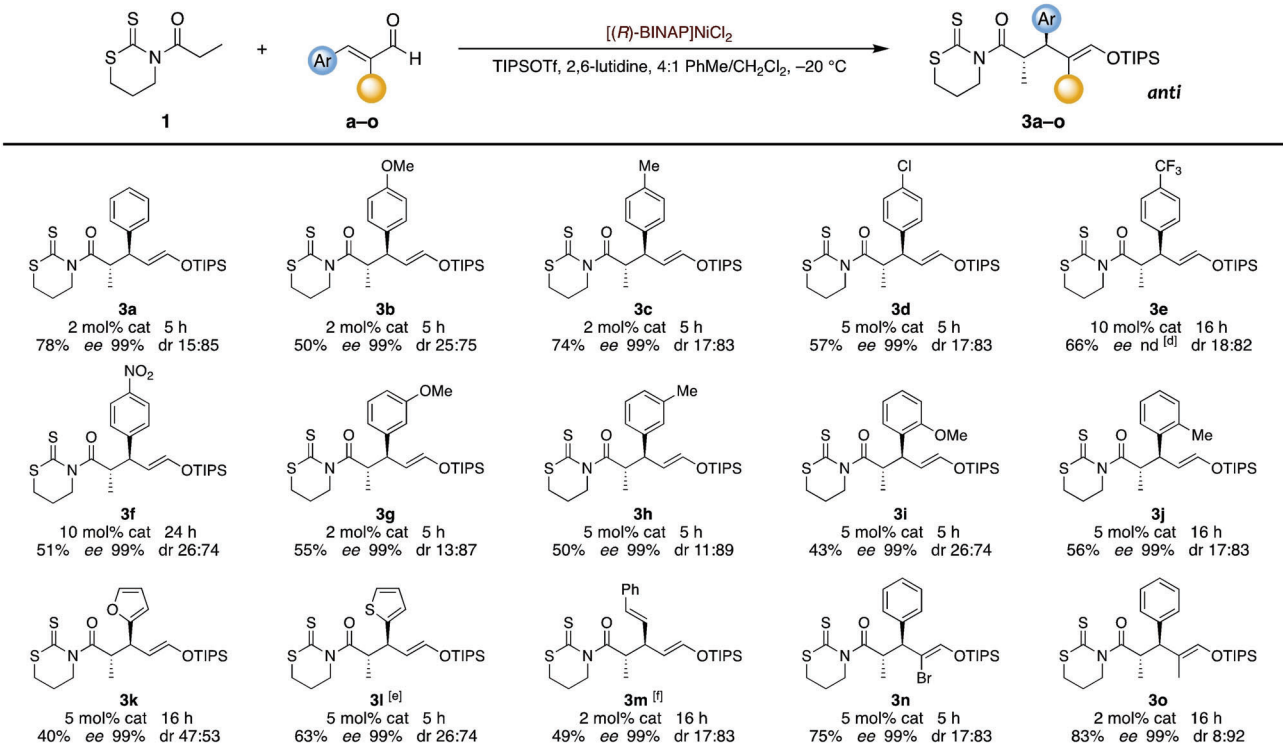

Scheme 3. TIPSOTf-Mediated Michael additions of *N*-propanoyl thiazinanethione **1** to α,β-unsaturated aldehydes catalyzed by [(*R*)-BINAP]$NiCl_2$.[a–c] [a] Isolated yields of the enantiomerically pure **3a–o** *anti* adducts are shown. [b] Enantiomeric excess established by chiral HPLC. [c] Diastereomeric ratio (*syn*/*anti*) established by ^{1}H NMR analysis. [d] It was impossible to determine the ee by chiral HPLC. [e] Reaction temperature of −40 °C. [f] rr (1,4:1,6): 70:30.

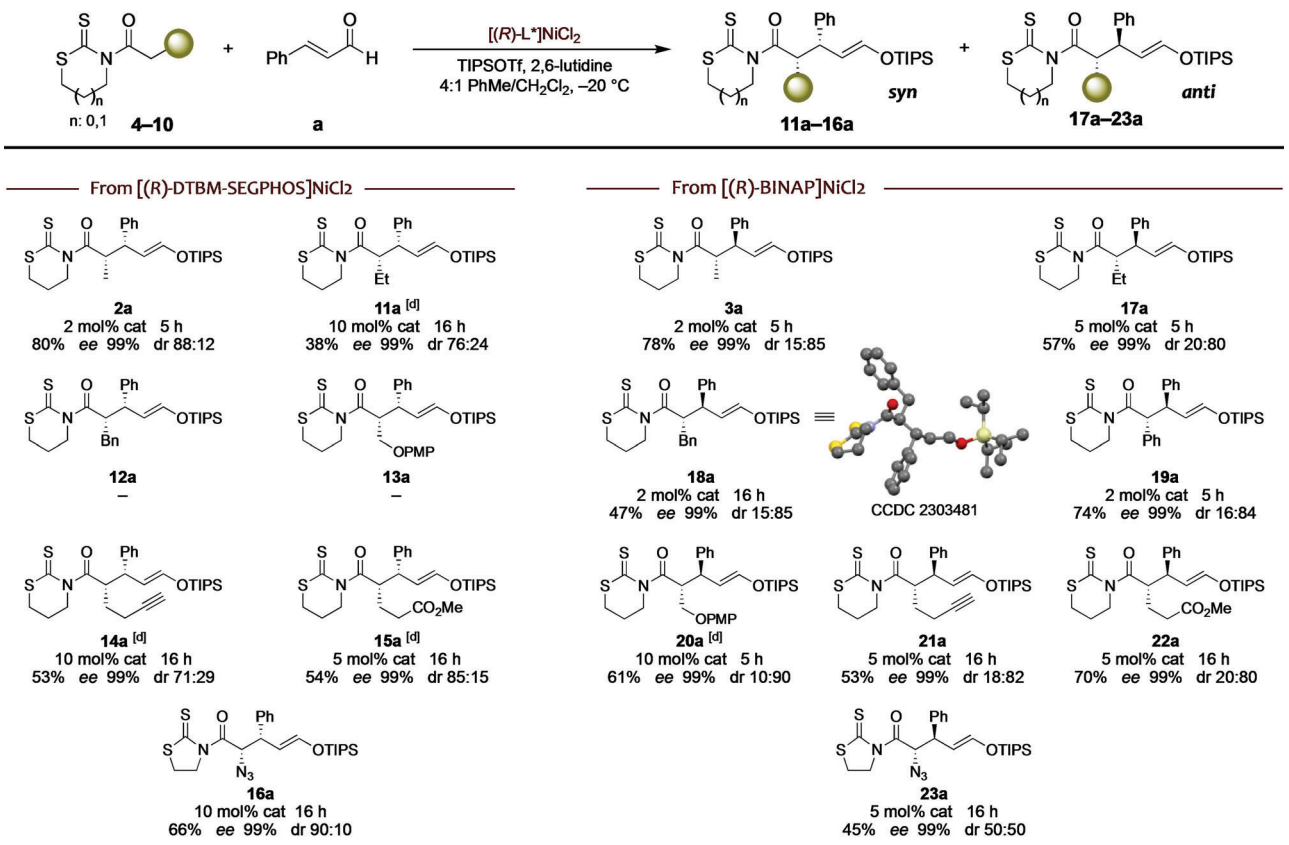

Scheme 4. TIPSOTf-Mediated Michael additions of *N*-acyl thiazinanethiones **4**–**10** to cinnamaldehyde (**a**) catalyzed by chiral nickel(II) complexes.[a–c] [a] Isolated yields of the enantiomerically pure *syn* or *anti* adducts are shown. [b] Enantiomeric excess established by chiral HPLC. [c] Diastereomeric ratio (*syn*/*anti*) established by ^{1}H NMR analysis. [d] rr (1,4:1,2): ca 90:10.

catalyst loading with respect to *N*-propanoyl thiazinanethione **1**, to produce *syn* Michael adduct **11a** with a poorer regioselectivity (rr 1,4:1,2 90:10) and a lower diastereoselectivity (dr 76:24) in a much lower 38% yield. In turn *syn* adducts **12a** and **13a** possessing bulky groups were not obtained, whereas *N*-phenylacetic thioimide **6** surprisingly gave *anti* **19a** as the major stereoisomer. Other substrates with less sterically hindered substituents performed better and gave the corresponding enantiomerically pure *syn* stereoisomers **14a**–**15a** in good yields. In turn, the results achieved with α-azidoacetyl thiazolidinethione **10**[29] were particularly noteworthy, as the expected *syn* diastereomer **16a** was obtained with excellent stereocontrol (dr 90:10, *ee* 99%) and an isolated yield of 66%.

Parallel reactions catalyzed by [BINAP]$NiCl_2$ were less dependent on the steric bulk of the substrate and using 2–5 mol% of catalyst, enantiomerically pure *anti* adducts **17a**–**23a** were isolated in yields of 50–75% with high selectivity except in the case of α-azido thiazolidinethione **10**, which produced an equimolar mixture of *syn* and *anti* stereoisomers, and thioimide **7**, which produced a slight erosion of the regioselectivity of *anti* **20a**. Importantly, the absolute configuration of *anti* adduct **18a** was corroborated through X-ray analysis.[28]

Synthetic Applications

With two fully optimized procedures in hand, we next assessed the removal of the heterocyclic scaffold to yield a variety of chiral intermediates. Initially, the reaction catalyzed by [(*R*)-DTBM-SEGPHOS]$NiCl_2$ was scaled up to get large quantities of model *syn* stereoisomer **2a** in order to test the transformations represented in Part A of Scheme 5. We were pleased to observe that the Michael addition of **1** to cinnamaldehyde (**a**) worked perfectly at a 10 mmol scale, allowing the isolation of enantiomerically pure **2a** in a 77% yield, which proves the robustness of the method. Then, its reduction with $LiBH_4$ or diisobutylaluminium hydride (DIBALH) afforded alcohol **24** or aldehyde **25** respectively in high yields. In turn, secondary and tertiary amides **26** and **27** or methyl ester **28** were easily prepared by simple treatment with the required amines or methanol in the presence of 4-dimethylaminopyridine (DMAP). Finally, the resultant silyl enol moiety turned out to be strategic and its appropriate manipulation afforded hemiacetal **29** (dr 54:46) and the saturated and protected δ-hydroxy ester **30** in excellent yields.

As part of these efforts, we also considered the application of the *anti* procedure to the synthesis of commercially available tapentadol **31** (Part B of Scheme 5), an opioid drug with strong analgesic effects used for the

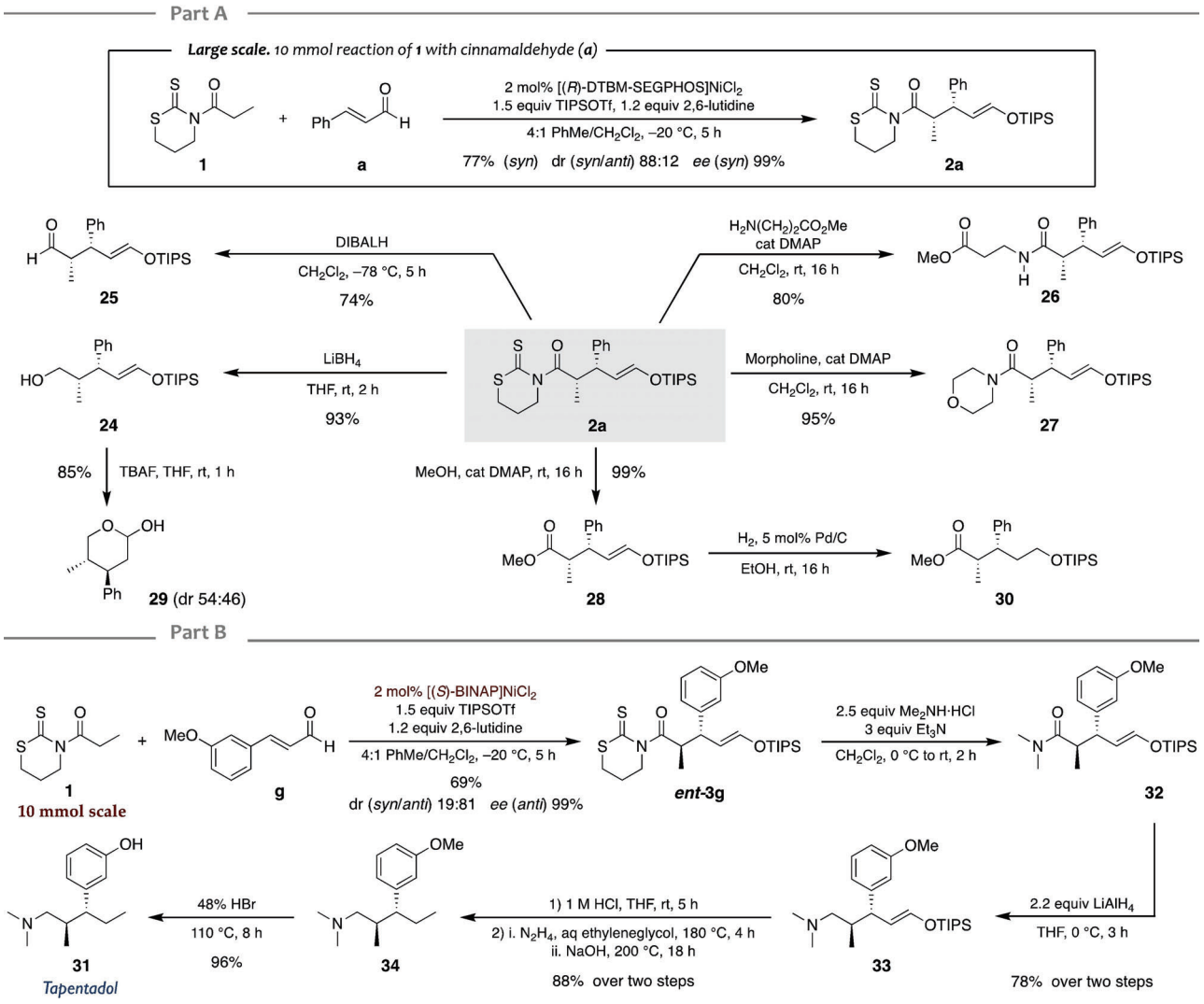

Scheme 5. Transformations of Michael adducts. Synthesis of tapentadol. TBAF = tetrabutylammonium fluoride.

treatment of pain in several diseases.[30] Our retrosynthetic analysis hinged on the strategic disconnection of both stereocenters through a Michael reaction.[31,32]

Thus, the first step involved the stereocontrolled Michael addition of thioimide **1** to (*E*)-3-(3-methoxyphenyl)-2-propenal (**g**) catalyzed by 2 mol % of [(*S*)-BINAP]$NiCl_2$ at a 10 mmol scale (Part B of Scheme 5). Interestingly, the scale was important and enantiomerically pure *anti* ***ent*-3g** was isolated in this case with a similar diastereomeric ratio (dr *syn*/*anti* 19:81) and a significantly higher yield of 69 % than those obtained at 1 mmol scale (see Scheme 3). Smooth removal of the heterocycle in ***ent*-3g** with dimethylamine gave amide **32** in a quantitative yield. Then, it was reduced with $LiAlH_4$ to provide amine **33** in a 78 % yield. Treatment of the silyl enol ether with 1 M HCl for 5 h led to the corresponding aldehyde, which was immediately submitted to a Wolff–Kishner reduction using the Huang-Minlon modification[33] to obtain deoxygenated amine **34** in an 88 % two-step yield. Eventually, demethylation of **34** with 48 % HBr under standard conditions led to tapentadol **31** in a 96 % yield, whose spectroscopic and physical data matched those reported in the literature. Importantly, our synthetic sequence takes advantage of a highly stereocontrolled Michael addition to furnish enantiomerically pure tapentadol with an overall yield of 45 % in six steps.[34,35]

Theoretical Calculations. Mechanism

Once the wide scope and the synthetic interest of the Michael addition had been established, we focused our attention to unraveling the mechanistic basis of such a stereodivergent transformation.

With this idea in mind, we initially evaluated the potential reacting centers of the triisopropylsilyl (TIPS)-activated cinnamaldehyde (**a**), a suitable model of the putative electrophilic partner. Interestingly, contributions of both the C1 and C3 carbons turned out be almost identical (Figure 1), which indicated that the outstanding regioselectivity observed within the present study must rely mostly on

the steric bulk of the TIPS group, which is in accordance with the trend summarized in Table S1.

Building on this initial information, we then carried out a comprehensive analysis of the transition states involved in the addition of the chiral nickel enolates from thioimide **1** to the TIPS-activated cinnamaldehyde.

Initially, we optimized the molecular geometry of the singlet state of [{(*R*)-Diphos}Ni(thiazinanethione)]$^+$ enolates in which the Diphos ligands are the chiral chelating disphosphines (DTBM-SEGPHOS or BINAP). Four conformations were optimized for the *S*,*O*-chelate and the thiazinane rings (see Figure S1). All the conformations from the BINAP-derived enolate were in a range of 3 kcal mol^{-1}, the two most stable resulting in a slightly distorted square-planar geometry for nickel ($S_{SQ\text{-}4}$ < 3.0). However, a completely different energetic ordering was found for the DTBM-SEGPHOS counterpart, likely due to the large steric character of the diphosphine substituents, which suggests that other factors may play an important role in stabilizing each conformation.

Following previous results, the four minima for each catalyst were taken into account to compute the transition states of the additions to the activated cinnamaldehyde, [(*i*-Pr$_3$Si)O=CHCH=CHPh]$^+$. The approach of such an oxocarbenium intermediate generated four transition states for each conformation considering the two π diastereotopic faces of the nickel enolate and the relative arrangement of the groups at the β position of the electrophile.

Then, sixteen transition states for the nickel enolate containing the DTBM-SEGPHOS ligand were calculated (see Figure S2). Interestingly, the most stable among them involves the approach of the *Re* π face of the enolate to the *Si* π face of the activated cinnamaldehyde (namely **TS-D3** in Figure 2, top), in which the TIPS group is directed towards the thiazinane ring. This leads to the *syn* **2a** stereoisomer. In turn, the alternative approach giving access to the *anti* **3a** diastereomer (**TS-C1**, see Figure S2) places the phenyl group close to the heterocycle and turns out to be disfavored by +0.9 kcal mol^{-1}. Other transition states engaging the opposite *Si* π-face of the enolate are higher in energy (from +2.5 to +3.4 kcal mol^{-1}) and exhibit a different conformation of the nickel-chelate ring. The Boltzmann distribution of all these transition states indicates that only two of them truly participate in the reaction, **TS-D3** and **TS-C1**, which predicts a *syn*/*anti* diastereomeric ratio of 85:14 (**2a**/**3a**) at −20 °C with others which would lead to the opposing enantiomer contributing less than 1 %. These results nicely match the experimental results summarized in Scheme 2 (dr 88:12, *ee* 99 %).

In turn, a parallel study for the BINAP-derived enolate predicted that the major stereoisomer should be *anti* **3a**, opposite to that obtained from DTBM-SEGPHOS. The molecular geometries of the resultant transition states along with their relative Gibbs free energies in solution in a range of 20 kcal mol^{-1} are shown in Figure S3. In this case, the most favorable transition state (namely **TS-A1** in Figure 2, bottom) involves the approach of the *Re* π face of the enolate to the *Re* π face of the activated cinnamaldehyde in which the thiazinane ring is close to the phenyl group and

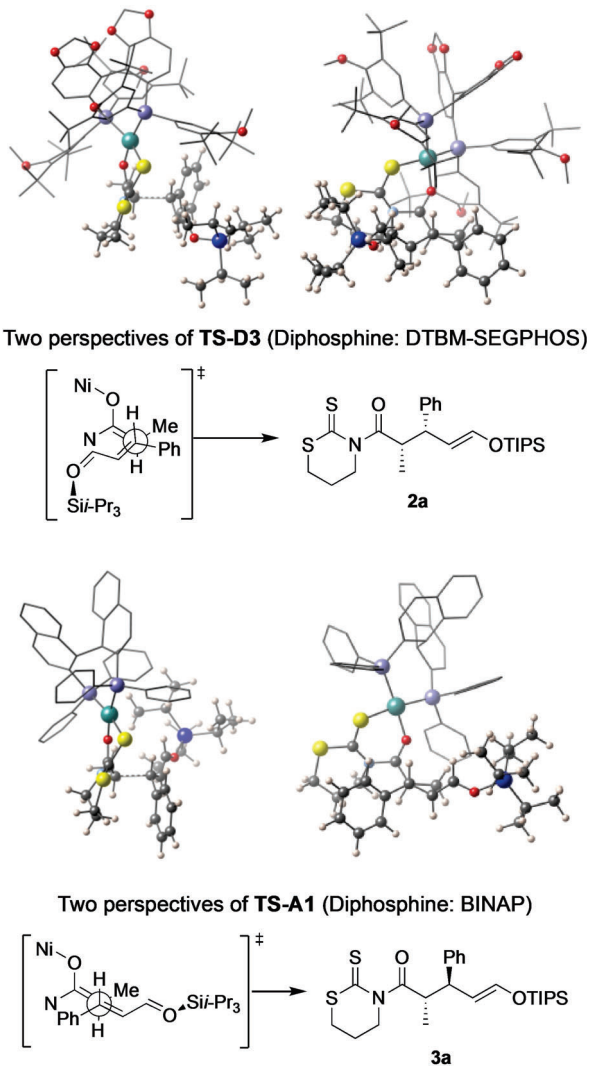

Figure 2. Transition states leading to the *syn* and the *anti* stereoisomers.

far from the bulky TIPS group of the electrophile. This produces the *anti* **3a** stereoisomer in full accordance with the experimental results. Surprisingly, other transition states show energies too high to participate in the stereochemical outcome of the reaction, so *anti* **3a** is expected to be the only stereoisomer. These results account for the amazing enantiocontrol observed throughout these reactions, but the lack of prediction for the minor *syn* **2a** counterpart indicates that minor influences should be also considered.

Despite the fact that the reasons accounting for the stereochemical outcome of the reaction are manifold, the analysis of the transition states of the carbon-carbon bond forming step provide clues for a better understanding of the overall process. Indeed, assuming that the reaction proceeds through an open transition state involving a chelated enolate in which the nickel geometry is mostly square planar, conformations of the thiazinane heterocycle may be of paramount importance to determine distinct approaches to the activated electrophile; this is particularly crucial for the

DTBM-SEGPHOS enolate. Furthermore, chiral ligands containing phosphines with bulky *tert*-butyl groups, such as the DTBM-SEGPHOS and the related 2,2′-bis[bis(4-methoxy-3,5-di-*tert*-butylphenyl)phosphino]-4,4′,6,6′-tetramethoxy-1,1′-biphenyl (DTBM-GARPHOS, see Table S2), play a crucial role to steer the stereochemical outcome towards the *syn* **2a** stereoisomer, through a transition state in which, in a counterintuitive manner, the thiazinane ring is close to the TIPS group (Figure 2, top).

The abovementioned transition states are consistent with a mechanism represented in Scheme 6 in which a silyl-activated cinnamaldehyde approaches a chelated nickel(II) enolate from thioimide **1** through the open transition states shown in Figure 2. Indeed, taking advantage of Sodeoka's findings[36] on the activation of nickel(II) chloride complexes with silyl triflates, the chiral nickel(II) chloride complexes employed in this study generate in situ nickel(II) triflate **I**, the real catalytic species. Coordination of **I** with **1** produces chelate **II**, which can be deprotonated by 2,6-lutidine to produce the nickel(II) enolate **III**. Then, the *Re* π-face of **III** approaches the activated aldehyde through the open transition states **IV** in which the distribution of the substituents determines the configuration of the new β stereocenter in **V**. Eventually, release of the L*Ni group gives the desired Michael adduct (**2a** or **3a**) and the nickel(II) triflate **I** necessary for a new catalytic cycle.

Conclusion

We have developed a direct and asymmetric TIPSOTf-mediated Michael addition of thioimides to α,β-unsaturated aldehydes catalyzed by chiral nickel(II) complexes possessing DTBM-SEGPHOS or BINAP ligands. The reaction shows remarkable regio- and stereochemical control, and delivers at will any of the potential *syn* or *anti* stereoisomers, depending on the chiral ligand, in a highly efficient stereodivergent manner. In turn, the resultant adducts can be smoothly converted into a wide array of enantiomerically pure derivatives that can be used for the synthesis of biologically active compounds, as demonstrated in a new approach to tapentadol. Finally, theoretical studies clarify the mechanistic intricacies of such a transformation and provide arguments for a proper understanding of the observed stereodivergency.

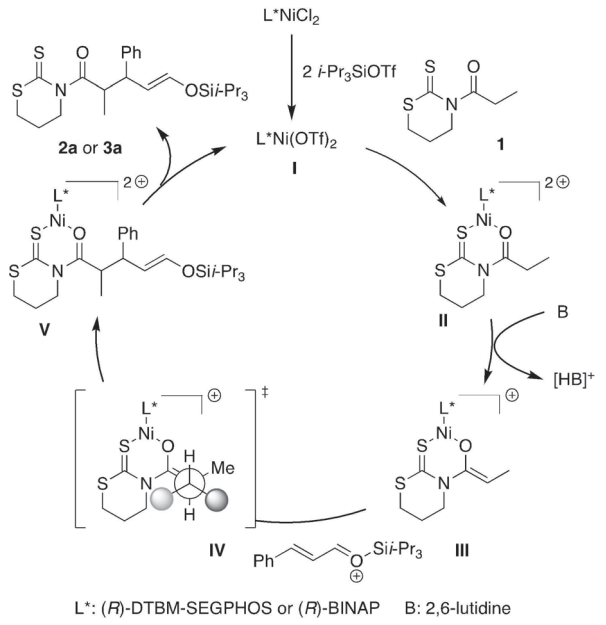

Scheme 6. Proposed mechanism.

Supporting Information

The authors have cited additional references within the Supporting Information.[37–48]

Acknowledgements

Financial support from the Spanish Ministerio de Ciencia e Innovación (MCIN/AEI/10.13039/501100011033/FEDER, UE, Grant PID2021-126251NB-I00 and Grant PGC2018-093863-B-C21), including Spanish Structures of Excellence Maria de Maeztu Program (CEX2021-001202-M), and the Generalitat de Catalunya (2021SGR 268 and 2021SGR 286), as well as doctorate studentships to O. G. and S. C. D. K. (FI, Generalitat de Catalunya), and Erasmus+Programme Grants to L. F. and E. D.-H. are gratefully acknowledged.

Conflict of Interest

The authors declare no conflict of interest.

Data Availability Statement

If our manuscript is accepted, a copy of a preprinted version will be available in the repository of the Universitat de Barcelona

Keywords: Michael addition · asymmetric catalysis · nickel complexes · stereodivergent synthesis · tapentadol

[1] a) T. Newhouse, P. S. Baran, R. W. Hoffmann, *Chem. Soc. Rev.* **2009**, *38*, 3010–3021; b) D. S. Peters, C. R. Pitts, K. S. McClymont, T. P. Stratton, C. Bi, P. S. Baran, *Acc. Chem. Res.* **2021**, *54*, 605–617.

[2] K. C. Nicolaou, J. S. Chen, *Classics in Total Synthesis III*, Wiley-VCH, Weinheim, **2011**.

[3] For enantioselective and catalytic aldol additions, see: Y. Yamashita, T. Yasukawa, W.-J. Yoo, T. Kitanosono, S. Kobayashi, *Chem. Soc. Rev.* **2018**, *47*, 4388–4480.

[4] For enantioselective and catalytic Michael Reactions, see: a) E. Reyes, U. Uria, J. L. Vicario, L. Carrillo, in *Organic Reactions*, *Vol. 90* (Ed.-in-Chief: S. E. Denmark), John Wiley & Sons, Hoboken, **2016**, pp. 1–898; b) K. Zheng, X. Liu, X. Feng, *Chem. Rev.* **2018**, *118*, 7586–7656.

[5] J. Clayden, N. Greeves, S. Warren, in *Organic Chemistry*, Oxford University Press, Oxford, **2012**.

[6] P. Perlmutter, in *Conjugate Addition Reactions in Organic Synthesis*, Pergamon Press, Oxford, **2013**.

[7] E. M. Carreira, L. Kvaerno, in *Classics in Stereoselective Synthesis*, Wiley-VCH, Weinheim, **2009**.

[8] For an insightful switch of regioselectivity in the asymmetric addition of aldehydes to enals, see: T. Kano, H. Maruyama, R. Sakamoto, K. Maruoka, *Chem. Commun.* **2015**, *51*, 10062–10065.

[9] For rare examples of Michael additions of metal enolates of activated carbonylic compounds to acrolein, see: a) M. Sawamura, H. Hamashima, Y. Ito, *J. Am. Chem. Soc.* **1992**, *114*, 8295–8296; b) Y. Motoyama, Y. Koga, K. Kobayashi, K. Aoki, H. Nishiyama, *Chem. Eur. J.* **2002**, *8*, 2968–2975.

[10] A few examples of Michael additions of cyclic β-keto esters to acrolein and crotonaldehyde have been described, see: Y. Hamashima, D. Hotta, N. Umebayashi, Y. Tsuchiya, T. Suzuki, M. Sodeoka, *Adv. Synth. Catal.* **2005**, *347*, 1576–1586.

[11] C. Palomo, A. Landa, A. Mielgo, M. Oiarbide, A. Puente, S. Vera, *Angew. Chem. Int. Ed.* **2007**, *46*, 8431–8435.

[12] For an early report on Michael additions of cyclic β-keto esters to α,β-unsaturated aldehydes catalyzed by cinchona derivatives, see: F. Wu, R. Hong, J. Khan, X. Liu, L. Deng, *Angew. Chem. Int. Ed.* **2006**, *45*, 4301–4305.

[13] D. A. Alonso, S. Kitagaki, N. Utsumi, C. F. Barbas III, *Angew. Chem. Int. Ed.* **2008**, *47*, 4588–4591.

[14] For other studies on organocatalytic Michael additions to enals, see: a) S. Cabrera, E. Reyes, J. Alemán, A. Milelli, S. Kobbelgaard, K. A. Jørgensen, *J. Am. Chem. Soc.* **2008**, *130*, 12031–12037; b) S. Duce, I. Alonso, A. M. Lamsabhi, E. Rodrigo, S. Morales, J. L. G. Ruano, A. Poveda, P. Mauleón, M. B. Cid, *ACS Catal.* **2018**, *8*, 22–34, and references therein.

[15] For other organocatalytic approaches based on preformed enolates, see: a) S. P. Brown, N. C. Goodwin, D. W. C. MacMillan, *J. Am. Chem. Soc.* **2003**, *125*, 1192–1194; b) W. Wang, H. Li, J. Wang, *Org. Lett.* **2005**, *7*, 1637–1639.

[16] a) L. Lin, X. Feng, *Chem. Eur. J.* **2017**, *23*, 6464–6482; b) M. Bihani, J. C.-G. Zhao, *Adv. Synth. Catal.* **2017**, *359*, 534–575; c) I. P. Beletskaya, C. Nájera, M. Yus, *Chem. Rev.* **2018**, *118*, 5080–5200.

[17] B. M. Trost, *Science* **1991**, *254*, 1471–1477.

[18] a) P. T. Anastas, M. M. Kirchhoff, *Acc. Chem. Res.* **2002**, *35*, 686–694; b) B. M. Trost, *Acc. Chem. Res.* **2002**, *35*, 695–705.

[19] S. Krautwald, E. M. Carreira, *J. Am. Chem. Soc.* **2017**, *139*, 5627–5639.

[20] X. Huo, G. Li, X. Wang, W. Zhang, *Angew. Chem. Int. Ed.* **2022**, *61*, e202210086.

[21] For a milestone report, see: S. Krautwald, D. Sarlah, M. A. Schafroth, E. M. Carreira, *Science* **2013**, *340*, 1065–1068.

[22] B. Kim, Y. Kim, S. Y. Lee, *J. Am. Chem. Soc.* **2021**, *143*, 73–79.

[23] For a recent example on aldol reaction, see: M. A. Rahman, T. Cellnik, B. B. Ahuja, L. Li, A. R. Healy, *Sci. Adv.* **2023**, *9*, eadg8776.

[24] S. C. D. Kennington, S. F. Teloxa, M. Mellado-Hidalgo, O. Galeote, S. Puddu, M. Bellido, P. Romea, F. Urpí, G. Aullón, M. Font-Bardia, *Angew. Chem. Int. Ed.* **2021**, *60*, 15307–15312.

[25] S. C. D. Kennington, O. Galeote, M. Mellado-Hidalgo, P. Romea, F. Urpí, *Org. Synth.* **2021**, *98*, 374–390.

[26] For other examples showing the key role of the heterocycle, see: a) S. C. D. Kennington, A. J. Taylor, P. Romea, F. Urpí, G. Aullón, M. Font-Bardia, L. Ferré, J. Rodrigalvarez, *Org. Lett.* **2019**, *21*, 305–309; b) M. Mellado-Hidalgo, E. A. Romero-Cavagnaro, S. Nageswaran, S. Puddu, S. C. D. Kennington, A. M. Costa, P. Romea, F. Urpí, G. Aullón, M. Font-Bardia, *Org. Lett.* **2023**, *25*, 659–664.

[27] Starting materials were recovered in these cases, which suggests that such α,β-unsaturated aldehydes are not properly activated with TIPSOTf under the reaction conditions.

[28] Deposition numbers 2303479 (for **2f**), 2303480 (for **2n**), and 2303481 (for **18a**) contain the supplementary crystallographic data for this paper. These data are provided free of charge by the joint Cambridge Crystallographic Data Centre and Fachinformationszentrum Karlsruhe Access Structures service.

[29] Thiazolidinethione was employed because of the unexpected instability of the *N*-azidoacetyl thiazinanethione counterpart, see: S. F. Teloxa, M. Mellado-Hidalgo, S. C. D. Kennington, P. Romea, F. Urpí, G. Aullón, M. Font-Bardia, *Chem. Eur. J.* **2022**, *28*, e202200671.

[30] a) T. M. Tzschentke, T. Christoph, B. Kögel, K. Schiene, H.-H. Hennies, W. Englberger, M. Haurand, U. Jahnel, T. I. F. H. Cremers, E. Friderichs, J. De Vry, *J. Pharmacol. Exp. Ther.* **2007**, *323*, 265–276; b) S. M. Hoy, *Drugs* **2012**, *72*, 375–393; c) U. Freo, P. Romualdi, H. G. Kress, *J. Pain. Res.* **2019**, *12*, 1537–1551; d) J. Santos, J. Alarcão, F. Fareleira, A. Vaz-Carneiro, J. Costa, *Cochrane Database Syst. Rev.* **2015**, CD009923; e) P. J. Wiffen, S. Derry, K. Naessens, R. F. Bell, *Cochrane Database Syst. Rev.* **2015**, CD011460.

[31] For a review on metal-catalyzed asymmetric Michael additions in natural products synthesis, see: C. Hui, F. Pu, J. Xu, *Chem. Eur. J.* **2017**, *23*, 4023–4036.

[32] For an overview on synthetic approaches to tapentadol, see: P. P. Graczyk, O. Zbrojkiewicz, S. Nerdinger, *Tetrahedron: Asymmetry* **2017**, *28*, 387–400.

[33] Huang-Minlon, *J. Am. Chem. Soc.* **1946**, *68*, 2487–2488.

[34] For a recent and highly efficient total synthesis of tapentadol (eight steps, 47 %) based on the asymmetric coupling of 1,3-dienes with pentafluorophenyl acetates, see: Q. Zhang, M. Zhu, W. Zi, *Chem.* **2022**, *8*, 2784–2796.

[35] For a recent formal synthesis of tapentadol based on an asymmetric hydrogenation of an α-methyl-β-ketoamide, see: L. Zhang, Z. Wang, Z. Han, K. Ding, *Angew. Chem. Int. Ed.* **2020**, *59*, 15565–15569.

[36] T. Suzuki, Y. Hamashima, M. Sodeoka, *Angew. Chem. Int. Ed.* **2007**, *46*, 5435–5439.

[37] C. F. H. Allen, C. O. Edens Jr, *Org. Synth.* **1945**, *25*, 92–94.

[38] K. Ando, H. Watanabe, X. Zhu, *J. Org. Chem.* **2021**, *86*, 6969–6973.

[39] H. Iida, Y. Akatsu, K. Mizukami, S. Natori, M. Matsukawa, K. Takahashi, *Synth. Commun.* **2016**, *46*, 581–585.

[40] Q. Zhang, R. Zhang, G. Tian, J. Li, F. Zhu, X. Jiang, J. Shen, EP2671878-A1 **2016**.

[41] K. C. Nicolaou, A. Li, D. J. Edmonds, G. S. Tria, S. P. Ellery, *J. Am. Chem. Soc.* **2009**, *131*, 16905–16918.

[42] C. Srivari, S. M. Prathama, K. K. Ramagonolla, S. Genji, US20220177413-A1, **2022**.

[43] M. J. Frisch, G. W. Trucks, H. B. Schlegel, G. E. Scuseria, M. A. Robb, J. R. Cheeseman, G. Scalmani, V. Barone, B. Mennucci, G. A. Petersson, H. Nakatsuji, M. Caricato, X. Li, H. P. Hratchian, A. F. Izmaylov, J. Bloino, G. Zheng, J. L. Sonnenberg, M. Hada, M. Ehara, K. Toyota, R. Fukuda, J. Hasegawa, M. Ishida, T. Nakajima, Y. Honda, O. Kitao, H. Nakai, T. Vreven, J. A. Montgomery, Jr., J. E. Peralta, F. Ogliaro, M. Bearpark, J. J. Heyd, E. Brothers, K. N. Kudin, V. N. Staroverov, T. Keith, R. Kobayashi, J. Normand, K. Raghavachari, A. Rendell, J. C. Burant, S. S. Iyengar, J. Tomasi, M. Cossi, N. Rega, J. M. Millam, M. Klene, J. E. Knox, J. B. Cross, V. Bakken, C. Adamo, J. Jaramillo, R. Gomperts, R. E. Stratmann, O. Yazyev, A. J. Austin, R. Cammi, C. Pomelli, J. W. Ochterski, R. L. Martin, K. Morokuma, V. G. Zakrzewski, G. A. Voth, P. Salvador, J. J. Dannenberg, S. Dapprich, A. D. Daniels, O. Farkas, J. B. Foresman,

J. V. Ortiz, J. Cioslowski, D. J. Fox, *Gaussian 09 (Revission D.1)*; Gaussian Inc.: Wallingford CT **2010**.
[44] a) F. Maseras, K. Morokuma, *J. Comput. Chem.* **1995**, *16*, 1170–1179; b) S. Dapprich, I. Komáromi, K. S. Byun, K. Morokuma, M. J. Frisch, *J. Mol. Struct.-Theochem.* **1999**, *462*, 1–21.
[45] a) A. D. Becke, *J. Chem. Phys.* **1993**, *98*, 5648–5652; b) C. Lee, W. Yang, R. G. Parr, *Phys. Rev. B* **1988**, *37*, 785–789.
[46] A. Schäfer, C. Huber, R. Ahlrichs, *J. Chem. Phys.* **1994**, *100*, 5829–5835.
[47] J. Tomasi, B. Mennucci, R. Cammi, *Chem. Rev.* **2005**, *105*, 2999–3094.
[48] M. Llunell, D. Casanova, J. Cirera, P. Alemany, S. Alvarez, *SHAPE* (version 2.0), Barcelona, **2010**.

Manuscript received: December 14, 2023
Accepted manuscript online: January 17, 2024
Version of record online: February 15, 2024

RESUM

Esta tesis presenta nuevas metodologías para la formación asimétrica de enlaces C–C, centrándose en catalizadores basados en complejos quirales de níquel(II).

En el **Capítulo I**, se introduce un enfoque innovador para reacciones aldólicas asimétricas directas utilizando tioimidas, logrando aductos *anti*-aldólicos con un control estereoquímico excepcional (hasta 99% *ee*) mediante el complejo [(*R*)-Tol-BINAP]$NiCl_2$. También se exploran metales alternativos como cobalto e hierro, con potencial para catalizadores sostenibles. Se estudiaron también los límites de esta metodología, como el control regioselectivo en aldehídos α,β-insaturados y la pobre enantioselectividad en sustratos difíciles como las reacciones aldólicas de acetato (Esquema 1).

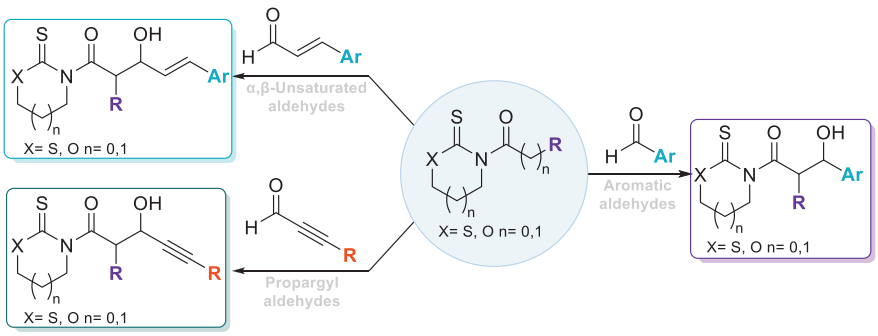

Esquema 1. Reacciones aldólicas asimétricas.

El **Capítulo II** destaca un logro importante: el desarrollo de una adición de Michael asimétrica a aldehídos α,β-insaturados, catalizada por complejos quirales de níquel(II). Este método muestra alta regioselectividad y enantioselectividad (99% *ee*) en una amplia gama de sustratos. El complejo [(*R*)-DTBM-SEGPHOS]$NiCl_2$ resultó ser el más eficaz para obtener aductos *sin* con alta diastereoselectividad, mientras que [(*R*)-BINAP]$NiCl_2$ fue más adecuado para aductos *anti* (Esquema 2).

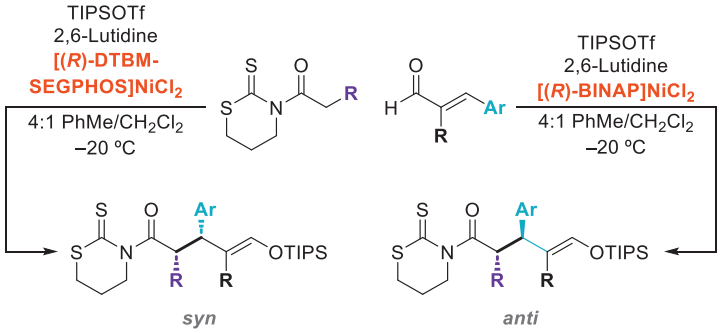

Esquema 2. Reacciones de Michael asimétricas.

En el **Capítulo III**, los aductos de Michael se convierten en diversos grupos funcionales como ésteres, amidas, aldehídos o alcoholes, demostrando versatilidad de estos intermedios. Además, se aplicó esta metodología en la síntesis del opioide comercial (*R,R*)-tapentadol con un rendimiento global del 45% y obteniendo un solo isómero, logrando un proceso eficiente y escalable (Esquema 3).

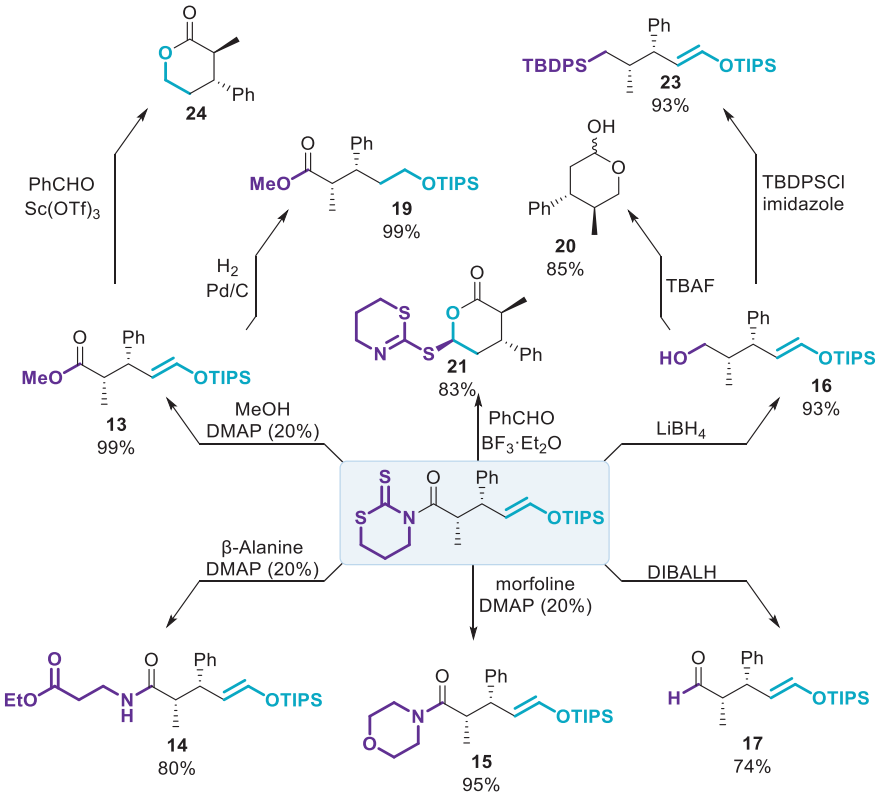

Esquema 3. Transformaciones del aducto de Michael quiral.

El **Capítulo IV** aborda la síntesis de compuestos β-amino carbonílicos mediante adiciones asimétricas de Mannich, aunque enfrentó problemas con la inestabilidad de las iminas. No obstante, se lograron resultados prometedores utilizando *N,N*-dibenzilaminales como sustitutos de iminas y a través de cicloadiciones 1,3-dipolares de nitronas, abriendo nuevas vías para el desarrollo de reacciones estereocontroladas impulsadas por complejos de níquel(II) (Esquema 4).

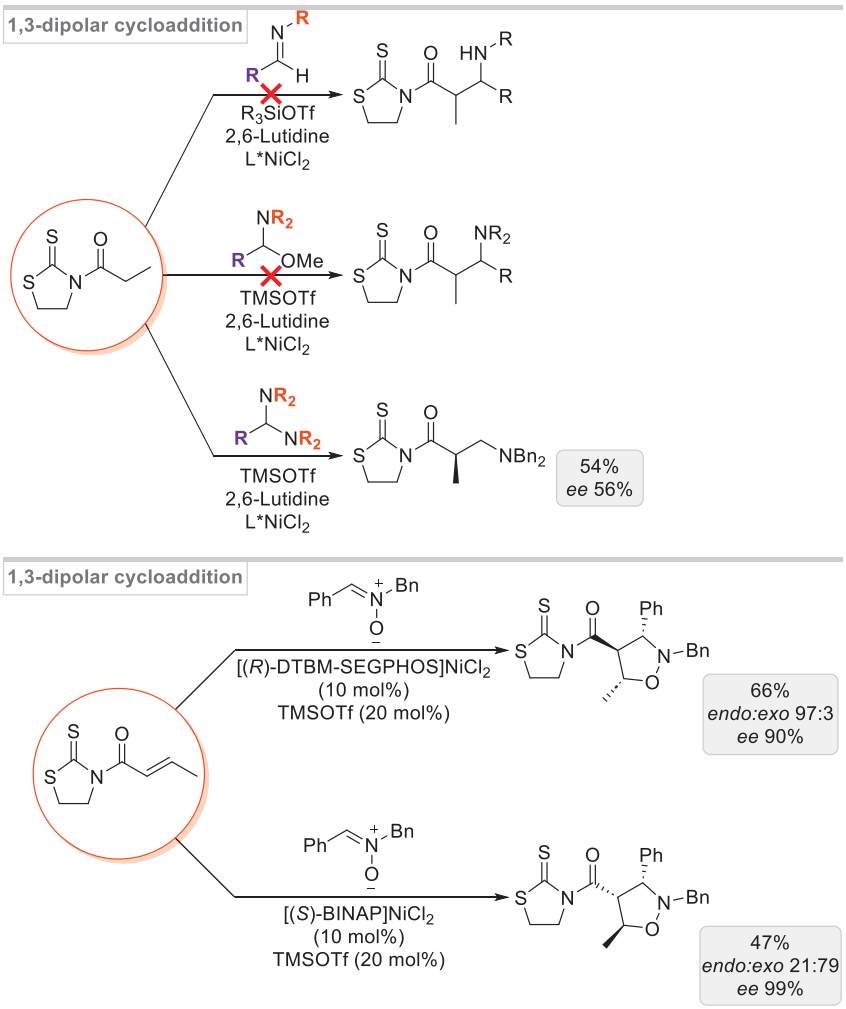

Esquema 4. Reacciones de cicloadición 1,3 dipolar estereodivergentes.